This work is protected by copyright and other intellectual property rights and duplication or sale of all or part is not permitted, except that material may be duplicated by you for research, private study, criticism/review or educational purposes. Electronic or print copies are for your own personal, non-commercial use and shall not be passed to any other individual. No quotation may be published without proper acknowledgement. For any other use, or to quote extensively from the work, permission must be obtained from the copyright holder/s.

Development of water-soluble tetravalent glycoclusters based around a calix[4]resorcinarene core

Keele University

By

Tahani Waleed Jihad Jihad

A thesis submitted in partial fulfilment of the requirements of Keele University for the degree of Doctor of Philosophy at the School of Pharmacy

March 2020

Abstract

Calix[4]resorcinarenes functionalised with glycosidic ligands on their lower rim have received little interest compared to analogues bearing carbohydrates on the upper rim. In this study, series of novel macrocyclic glycoclusters bearing mono- or disaccharides on the lower rim of a calix[4]resorcinarene core were prepared. Calix[4]resorcinarenes can exist as conformational isomers so each glycocluster was isolated and characterised as the pure conformer, where possible.

Amongst the distinct features of this work is that Lewis acid catalysis was used for the synthesis of calix[4]resorcinarenes by condensation of resorcinol, or its 2-substitued analogues, with an aldehyde. Also, rather than linking the glycosidic moieties to the pre-formed calix[4]resorcinarene, the glycosidic aldehydes were assembled prior to condensation with the resorcinols. Significantly, acylation of the glycoclusters facilitated separation of each conformational isomer.

Amongst the aldehydes used for condensation were glycosylated derivatives of hydroxybenzaldehydes, compounds with a short alkyl spacer between the glycosidic aryl moiety and the aldehydic carbonyl group, and a number with an alkyl or polyether spacer that did not contain any aryl group. Following a study of the condensation products from the reaction of each series of aldehydes with resorcinol, 2-methylresorcinol or pyrogallol it became clear that the distribution of conformational isomers could be predicted, influenced greatly by the properties of the starting materials.

Finally, it was demonstrated that deprotection of a conformational isomer obtained during the initial studies gave a glycosylated calix[4]resorcinarene

which is fully soluble in aqueous media. Such compounds may have great potential in solubilisation and the formulation of hydrophobic drugs.

“This thesis is the result of the author's original research. The copyright of this thesis belongs to the author under the terms of the United Kingdom Copyright Acts as qualified by Keele University. Due acknowledgement must always be made of the use of any material contained in, or derived from, this thesis.”

Acknowledgements

I would like to express my sincere thankfulness to my supervisor Dr Anthony Curtis for his continuous support and patience, his guidance helped me during the research and writing my thesis. Thank you for the immense knowledge and advice to make my PhD thesis seems by this appearance.

Also, I would like to thank my sponsor, the Higher Committee for Education Development in Iraq (HCED), for their finical support and giving me the opportunity to study my PhD.

Special thanks should go to all my family, my mom, my dad, my sisters (Tamara and Revan), my brothers (Ziyad and Karam), my nephew (Yousif) and my niece (Marium). Words do not express how grateful I am towards all their thoughts and prayers that were raise to me, despite the far distances between us but their hearts and souls were with me so far.

A thank go to my advisor Dr. David Morgan at the same time to Dr. Russell Pearson and Patricia Ragazzon. Also, special mention to my cosupervisor Dr. Clare Hoskins.

I am also grateful to my friend Huda Abid for her helping over a long time during my living in the UK. A huge thank you to John Clews, who has never hesitated to help me at any occasion when I needed chemicals, glassware or fixing the NMR. He was always available as a resource. I am grateful to Lisa Blackburn and Aisling Ni cheallaigh for their helping and kindness. I personally would like to acknowledge my colleague Ali Alsuraifi for his helping in analysing the solubility data.

Tahani

Table of Contents

Table of Schemes

Table of Figures

Table of tables

Table of appendices

Abbreviation

µm	micromolar
AcOH	Acetic acid
$AlCl_3$	Aluminium(III) chloride
$BF_3.Et_2O$	Boron trifluoride diethyl etherate
br	broad
CCL_4	Carbon tetrachloride
d	doublet
DCM	Dichloromethane
dd	double doublet
ddd	double double doublet
DEPT-135	Distortionless Enhancement of Polarisation Transfer
DIPE	Diisopropyl ether
DLS	Dynamic light scattering
DMP	Dess-Martin periodinane
DMSO	Dimethyl sulfoxide
Et_2O	Diethyl ether
EtOAc	Ethyl acetate
EtOH	Ethanol
g	grams
hr	hours
HSQC	Heteronuclear Single Quantum Correlation
IR	Infrared
J	Coupling constant
M	Molar

m	multiplet
MeCN	Acetonitrile
MeOH	Methanol
MHz	mega hertz
min	minute
mL	millilitres
mmol	millimoles
Mp	melting point
MS	Mass spectrum
NMR	Nuclear Magnetic Resonance
PCC	Pyridinium chlorochromate
PCS	Photon correlation spectroscopy
PDI	Polydispersity index
Pet. ether	Petroleum ether (40-60 ^{0}C)
$PhNO_2$	Nitrobenzene
q	quartet
r.t	Room temperature
s	singlet
t	triplet
TEA	Triethylamine
THF	Tetrahydrofuran
$TiCl_4$	Titanium(IV) chloride
TLC	Thin Layer Chromatography
UV	Ultra Violet
$ZnCl_2$	Zinc(II) chloride
ZP	Zeta potential

CHAPTER 1: INTRODUCTION

1.1 Supramolecular Chemistry

Supramolecular chemistry has been defined as the chemistry beyond the molecule, while a 'supermolecule' is formed by intermolecular interactions between two or more covalently bonded molecules or ions. These non-covalent bonding interactions include hydrophobic effects, π–π interactions, hydrogen bonding, electrostatic interactions and dispersion interactions (Williams and Westwell 1998).

Supramolecular chemistry can be classified into two principal streams, host-guest chemistry and self-assembly. Donald Cram established the term of host-guests chemistry: his definition was that the host is a molecule, larger than the guest, which possesses a cavity and binding sites which can associate with or envelope around the smaller guest molecule, whose binding sites diverge in the complex (Figure 1) (Cram 1986).

Whereas self-assembly is the non-covalent aggregation between two or more molecules, they are equal in size and no species acts as a host for the other. This process is spontaneous but may be affectted by solvation or templating effects (Li *et al*., 2018).

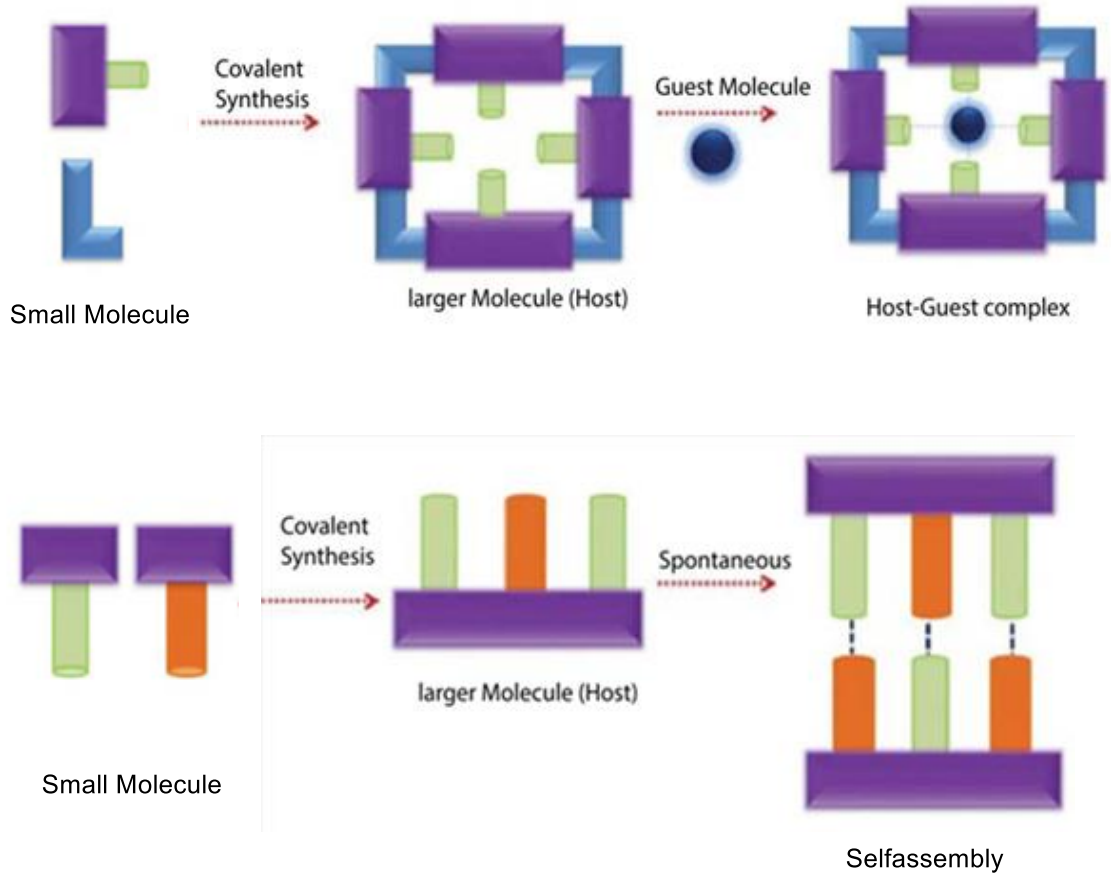

Figure 1: The formation of a supramolecular system (Host-guest interaction) and (self-assembly) from small building blocks (adapted from Tiwari and Uzun 2015)

1.2 Types of host molecules

Host molecules consist of two main classes: acyclic (podands) or cyclic (macrocyclic, macrobicyclic, *etc*). A podand is an acyclic or branching host contain a number of binding sites that are located at intervals along the length of the molecule or around a common spacer (Ali *et al*., 2018).

A macrocyclic host is cyclic compound contain a number of binding sites that are coordinated round the closed system. Macrocyclic organic host molecules consist of major classes such as: crown ethers, cyclodextrins, cucurbiturils, calix[n]arenes and calix[4]resorcinarenes. The latter are well-characterised

building blocks for the creation of supramolecular assemblies (Sherman 2003). Calix[n]arenes and calix[4]resorcinarenes can be functionalised readily and their hydrophobic cavities can be exploited as hosts for sensing and drug delivery applications (Delbianco *et al*., 2015). However, studies of the behaviour of most synthetic macrocycle compounds have taken place in non-polar organic solvents, whereas all of the host-guest interaction events in nature occur in water (Murray *et al*., 2017). This provides two main challenges for supramolecular chemistry in aqueous media: to make the host molecules soluble in aqueous media whilst retaining their gross shape and cavity size and/or to exploit the influence of water in non-covalent interactions (Liu *et al*., 2019). The synthesis of receptors for use in aqueous media presents challenges also: the availability of building blocks for their construction is limited, certain interactions with the guest must be targeted to avoid the competitive effect of water and encapsulation and/or molecular recognition in aqueous media must be achievable with the desired guest molecules (Murray *et al*., 2017).

1.2.1 Calix[n]arenes

Calix[n]arenes comprise of four phenol units linked *via* methylene or bridges at the 2- and 6-positions relative to the hydroxyl group. Calix[n]arenes can adopt several conformations due to two possible modes for inversion of the phenol unit: the oxygen through the annulus rotation and the 4-substituent through the annulus rotation, should there be a substituent in the 4-position relative to the phenolic hydroxyl group. These conformations are: cone, partial-cone, 1,2-alternate and 1,3-alternate (Figure 2) (Otsuka and Shinkai 1996; Arnott 2018). The cone conformation is the most favourable conformation for calix[4]arenes

due to stabilisation of the structure by intramolecular hydrogen bonding interactions between the hydroxy groups (Sardjono and Rachmawati 2017).

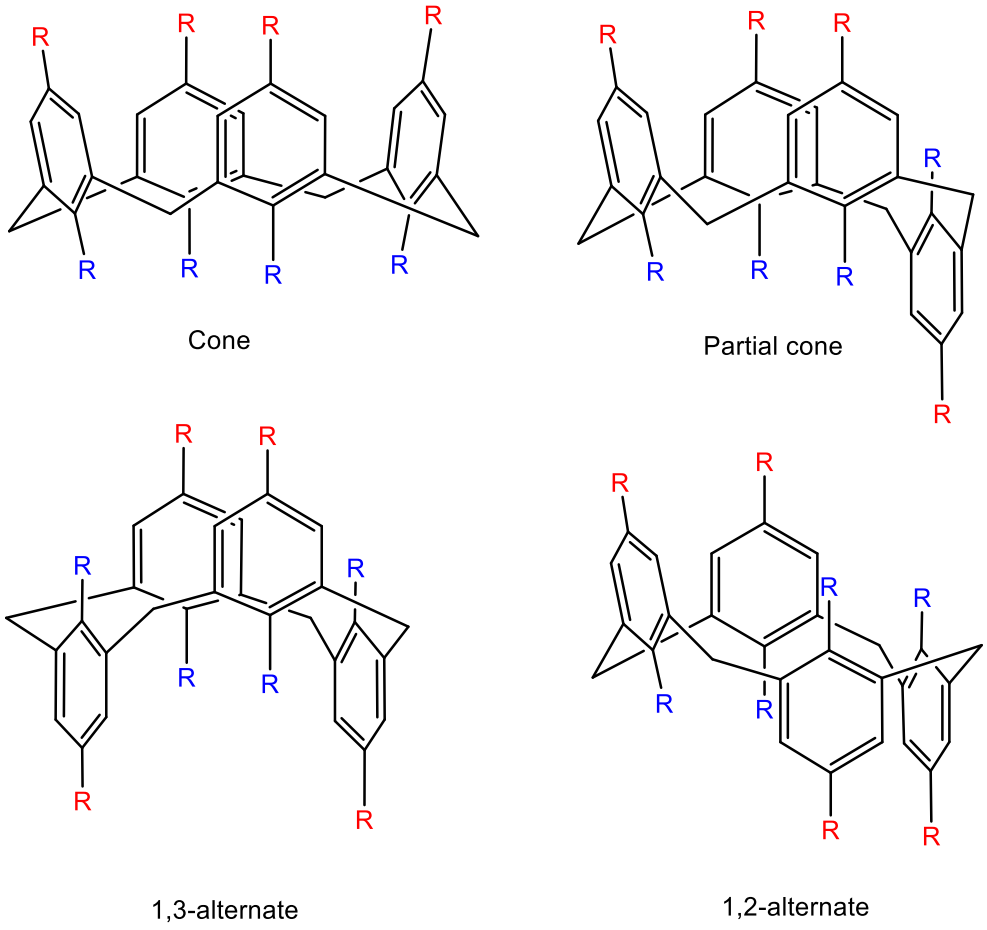

Figure 2: The conformations of calix[4]arenes (Hoskins & Curtis 2015)

Structural studies using X-ray analysis, ^{1}H-NMR spectroscopy and theoretical calculations showed that the cone conformation between calix[n]arenes of different sizes are slightly different depending on the size of the macrocyclic ring. For example, homooxacalix[3]arenes adopt a cone conformation but the ring is more flexible than calix[4]arenes (Araki *et al*., 1993). Calix[4]arenes and calix[5]arenes adopt a high symmetry cone conformation *via* the intramolecular hydrogen bonds between neighbouring hydroxy groups, whereas the calix[6]arenes adopt a winged or hinged conformation due to a slight

deformation of the ring. Calix[7]arenes and calix[8]arenes adopt a pleated-loop conformation because of the increase in deformation of the ring and disruption of the intramolecular hydrogen-bonds (Gutsche and Bauer 1985).

In 1981 Gutsche *et al*. suggested the one-pot synthesis of calix[n]arenes by condensation of 4-*tert*-butylphenol with aqueous formaldehyde under basic conditions (KOH, NaOH), leading to the formation of calix[4]arenes, calix[6]arenes and calix[8]arenes dependent on the reaction conditions used (Scheme 1) (Gutsche *et al*., 1981).

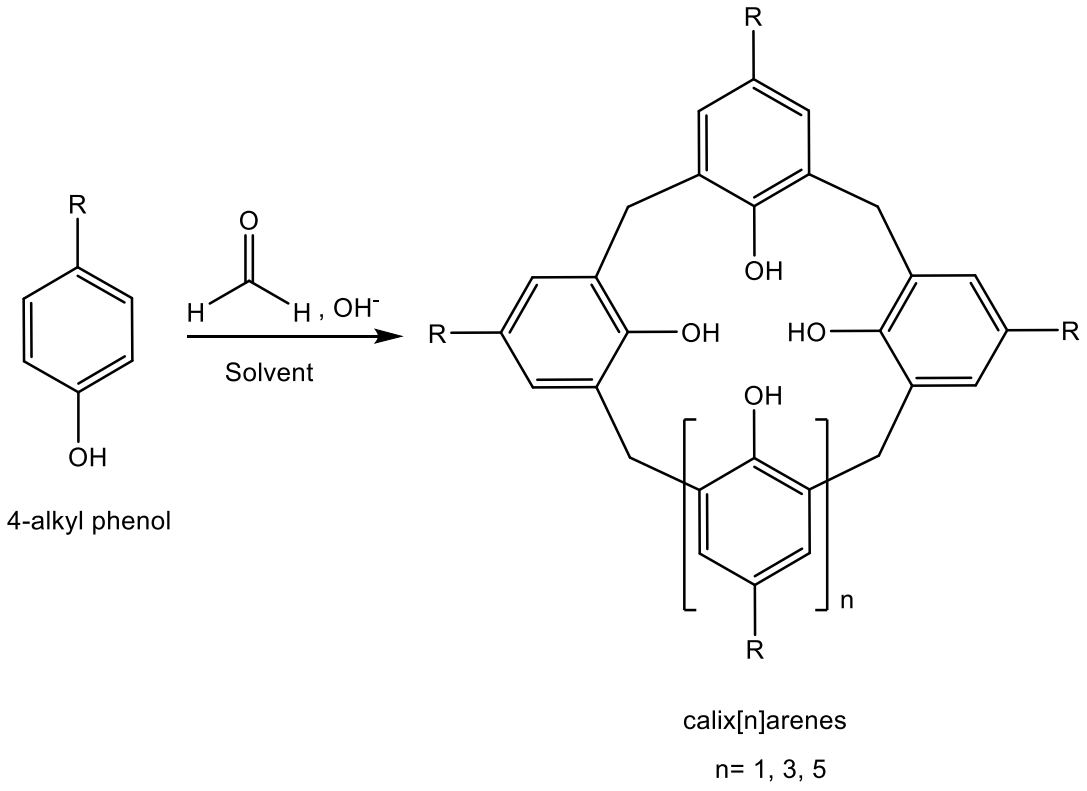

Scheme 1: Conventional synthesis of calix[n]arenes (Sardjono and Rachmawati 2017)

Calix[n]arenes are inherently hydrophobic and are typically insoluble in water. Also, conformational flexibility in the larger calix[n]arenes limits their practical use as solubilising agents in drug delivery. The introduction of polar moieties on the upper or lower rim of the calix[n]arene core can increase the affinity of calix[n]arenes towards guest molecules through additional interactions (Madasamy *et al*., 2017; Athar *et al*., 2018). Indeed, the synthesis of functionalised calix[n]arenes which are stable in water may provide candidate host molecules for use in the pharmaceutical field (Moussa *et al*., 2018).

Attachment of polar functional groups to the upper or lower rim either directly or by using a linker enables calix[n]arenes to construct supramolecular amphiphiles by forming host-guest inclusion complexes dependent upon non-covalent interactions. This may lead to a change in the affinity of guest molecules towards water, stabilisation of a formulation, physical isolation of components from a mixture of compounds and aid in monitoring the physicochemical properties of the guest. Such modifying groups are sulfonates (Fahmy *et al*., 2018), amines (Granata *et al*., 2017), phosphonates (Mo *et al*., 2016), amino acids (Gasparello *et al*., 2019), saccharides (Aleandri *et al*., 2013), peptides (Mutihac *et al*., 2011), guanidinium groups (Samanta *et al*., 2017) and poly (ethylene oxide) (PEG groups) (Yu *et al*., 2009).

1.2.1.1 Synthesis of calix[n]arene which are soluble in water

The 4-*tert*-butyl calix[4]arene **1** was used to prepare a series of amphiphilic 4-phosphonic acid calix[n]arenes **2a-g** with an alkyl chain at the lower rim; these compounds were soluble in water and in DMSO at high pH (>10), with certain compounds (n= 4, R= H, C_6H_{13}, C_8H_{17} and n= 5, R= H) were soluble at neutral

pH. The C_{4v} symmetrical cone conformation predominated in the synthesis of these phospholipid analogues (Scheme 2).

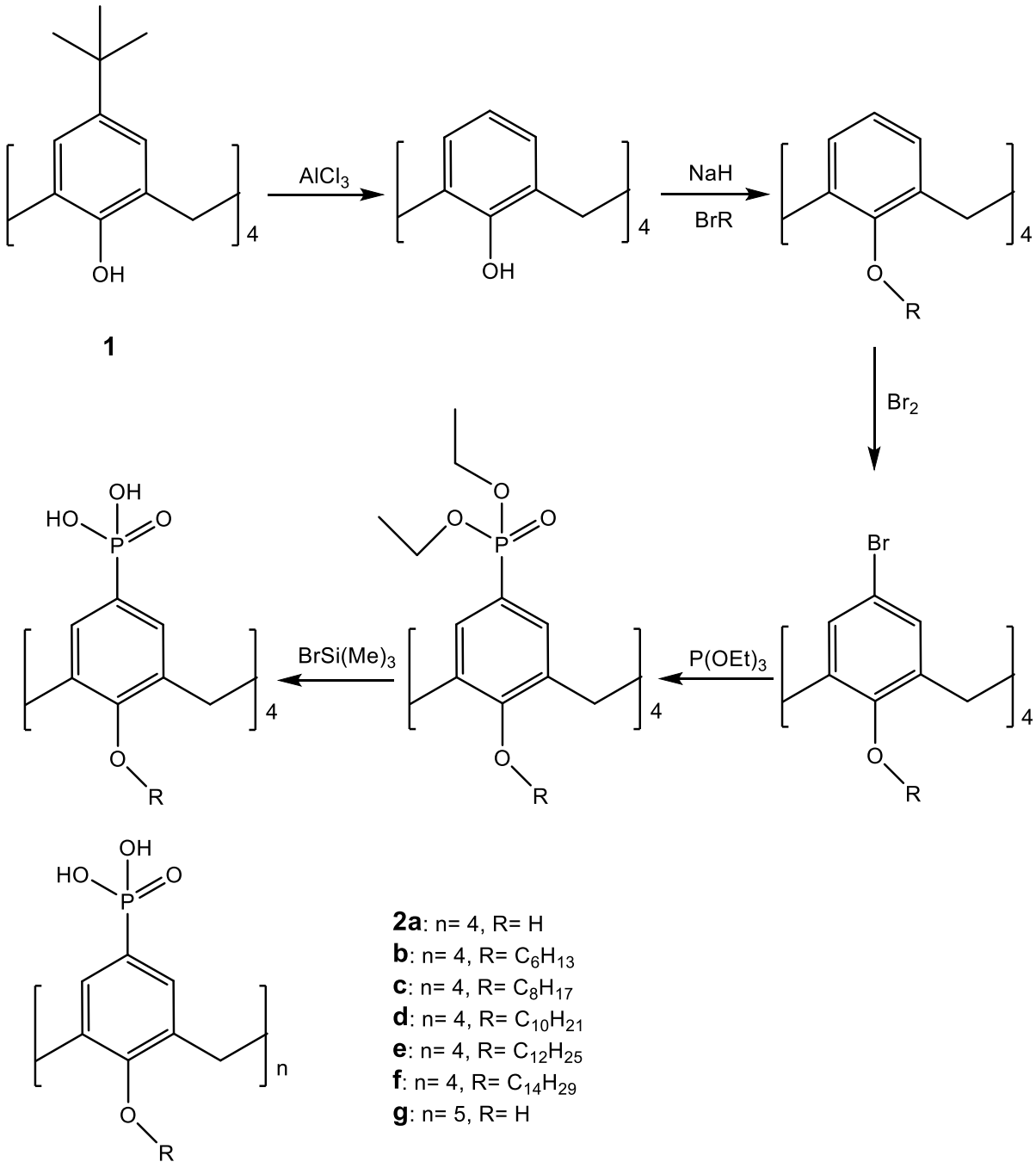

Scheme 2: Synthesis of 4-phosphonic acid calix[4]arenes (Martin *et al*., 2012)

The toxicity of 4-phosphonic acid calix[n]arenes **2a-g** has been examined: mixed retinal cells proved to be more sensitive than rat pheochromocytoma cells to the toxic effect related to these compounds. 4-Phosphonic acid calix[n]arenes with hydroxyl group at the lower rim, showed reduced toxicity with pheochromocytoma cells can tolerate to at least 1.0 mg mL^{-1} concentrations for **2a** and **2g**. In addition, the aggregation of these phospholipids has been studied and showed that 4-phosphonic acid calix[4]arenes (n= 4, R= C_8H_{17}) could form micelles with a diameter of 4-5 nm which offer stability over a wide range of pH values and also able to incorporate the antioxidant curcumin. Also, these micelles showed reduced toxicity towards pheochromocytoma cells compared to **2c** in monomeric form, thereby making them potential compounds for targeted drug delivery (Martin *et al*., 2012).

1.2.1.2 Calix[n]arene biocompatibility and use in drug delivery

Calix[n]arenes have structural characteristics that are favourable for design and development of components in drug delivery systems: a variety of different conformations of each calix[n]arene are available which can be readily functionalised on both upper- and lower rims. They possess a hydrophobic cavity capable of forming complexes with small guest molecules and ions and a number of calix[n]arene molecules can aggregate to create inclusion complexes with larger molecules. Additionally, several calix[n]arenes with antiviral (HIV), antifungal, antibacterial, antimicrobial agents, antithrombotic and anticancer activity have been reported (Perret *et al*., 2006; Athar *et al*., 2017; Consoli *et al*., 2017).

When the host-guest complex encounters the target cells, the drug molecule is released and interacts with the affected cell, whilst the host leaves the body without any side effect (Rodik *et al*., 2009; Perret and Coleman 2011).

Calix[n]arenes are relatively non-toxic and do not evoke immune responses (Yang and de Villiers 2004). Their applications in the pharmaceutical field have not been approved yet by the Food and Drug administration (FDA) but the lack of toxicity enhances attention on their use in medicines and other proposed applications in biological systems. For example: for the encapsulation of neutral organic guests by water soluble calix[4]arenes, as enzyme mimics, as ligands for the molecular recognition of cell surface proteins, as scaffolds for magnetic resonance imaging agents, as gene transfection vectors and in drug delivery (Bagnacani *et al*., 2008; Khan *et al*., 2017; Bonaccorso *et al*., 2017; Alex *et al*., 2018).

Several types of nanostructures, such as micelles, vesicles and nanotubes, result from self-assembly of amphiphilic calixarenes because of the substituent groups, molecular structure and experimental conditions used. Shinkai *et al*. explained that the conformation of calix[n]arenes plays a key role in their aggregation behaviour and the cone conformation typically forms globular micelles in aqueous media (Shinkai *et al*., 1986; Arimori *et al*., 1995).

In addition, Strobel *et al*. found that the nature of ionic functional groups on the calix[n]arene also play a crucial role in controlling the aggregation behaviour of amphiphilic calix[n]arenes: for example, trimethylammonium-substituted calix[4]arenes form micelles, whereas calix[4]arenes with carboxyl groups tend to form vesicles. Such dominance of the size and the shape of aggregates and

associated properties are very important for creating systems for drug and gene therapy (Strobel *et al*., 2006).

Although a few studies into the capability of calix[n]arenes to solubilise drugs have been reported these mostly relate to the commercially available or readily prepared anionic sulfonated derivatives, 4-sulfonatocalix[4]arenes for example (Chen *et al*., 2016; Athar *et al*., 2017).

1.2.1.2.1 Sulfonatocalix[n]arenes

This class of cyclooligomers are widely used as host molecules for different organic and inorganic compounds: 4-sulfonatocalix[n]arenes have attracted great attention in the last two decades because of their solubility in aqueous media (> 0.1 mol/L) (Khokhar *et al*., 2017) and low toxicity (Da Silva *et al*., 2004; Lazar *et al*., 2004). Also investigated are their catalytic properties, selective binding ability, biological compatibility and their role as a carrier in drug delivery. Another possible pharmaceutical application that has been examined is their ability to increase the therapeutic effect of a drug moiety (Perret and Coleman 2011; Ostos *et al*., 2017).

The highly water-soluble 4-sulfonatocalix[4]arene **3** has been used in a study into the aggregation properties of *α*-tocopherol (*α*-T) **4** due to the biological significance of vitamin E. *α*-Tocopherol, works as a natural antioxidant, represents the main form of vitamin E, and exists in the cellular concentration and the blood than other forms of vitamin E. It has been established that vitamin E acts as radical scavenging by delaying or preventing the chronic disease related to free radicals. *α*-Tocopherol with hydrophilic phenol moiety

and long alkyl chain conducts as an amphiphile, therefore it places beneath aqueous insoluble vitamins (Figure 3).

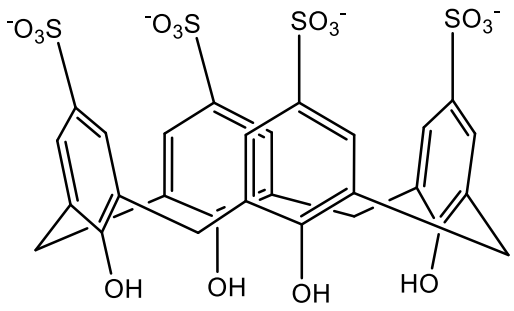

4-sulfonatocalix[4]arene **3**

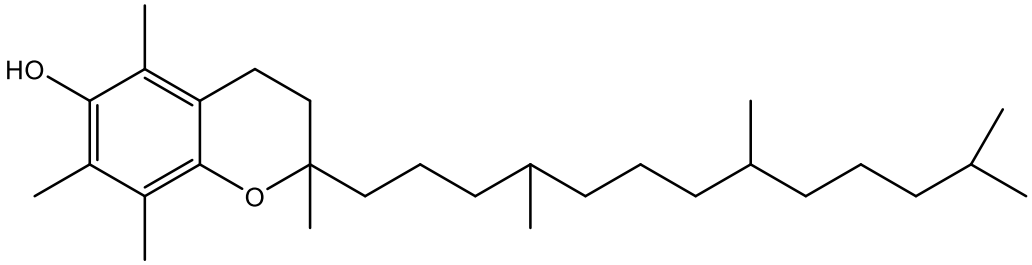

Vitamin E (alpha-T)

4

Figure 3: Structures of 4-sulfonatocalix[4]arene and Vitamin E (Ashwin *et al*., 2018)

The encapsulation of (*α*-T) within 4-sulfonatocalix[4]arene in solution has been studied by employing cyclic voltammetry (CV) and fluorescence spectroscopic techniques. The critical aggregation concentration value (CAC) of pure vitamin E is reduced a half in the presence of 4-sulfonatocalix[4]arene. The measured quenching (10^7 $M^{-1}s^{-1}$) and binding constant (10^3 M^{-1}) values showed good binding tendency of vitamin E with 4-sulfonatocalix[4]arene. The Job's plot method has also confirmed the (1:1) binding stoichiometry of 4-sulfonatocalix[4]arene and (*α*-T). The host-guest inclusion complex in the solid state has been successfully prepared and proved the cavity packed with lipid

soluble (*α*-T) inside the cavity of 4-sulfonatocalix[4]arene using CV, FT-IR, SEM, XRD and ^{1}H-NMR characterization (Ashwin *et al*., 2018).

Supramolecular host-guest chemistry has attracted increased attention due to the reversible nature of complex formation (complexation and decomplexation) (Figure 4) (Yang *et al*., 2014). In 2009, Wheate *et al*. used 4-sulfonatocalix[4]arene as a nanocarrier for the dinuclear platinum anticancer drug, trans-[{PtCl$(NH_3)_2$}$_2$μ-dpzm]$^{2+}$ (di-Pt; where dpzm= 4,4'-dipyrazolylmethane). It was noticed that 4-sulfonatocalix[4]arene binds to di-Pt in 1:1 ratio, it is low binding constant or partial encapsulation does not provide steric hindrance to prevent binding the metal complex to guanosine. The system releases the platinum species upon *in vivo* administration due to blood serum content is high in the body (Wheate *et al*., 2009).

Liu *et al*. reported the stoichiometric inclusion complexes between 4-sulfonatocalix[4]arene with anticancer drugs topotecan and irinotecan. One- and two-dimensional NMR and UV-vis spectroscopies and DSC were used to confirm complex formation (Wang *et al*., 2011; Wang *et al*., 2011).

The binding between 4-sulfonatocalix[6]arene and vitamin B_6 was investigated by Song *et al*. in an acidic or basic media. Release of the guest molecule could be triggered by a change in pH (Song *et al*., 2012).

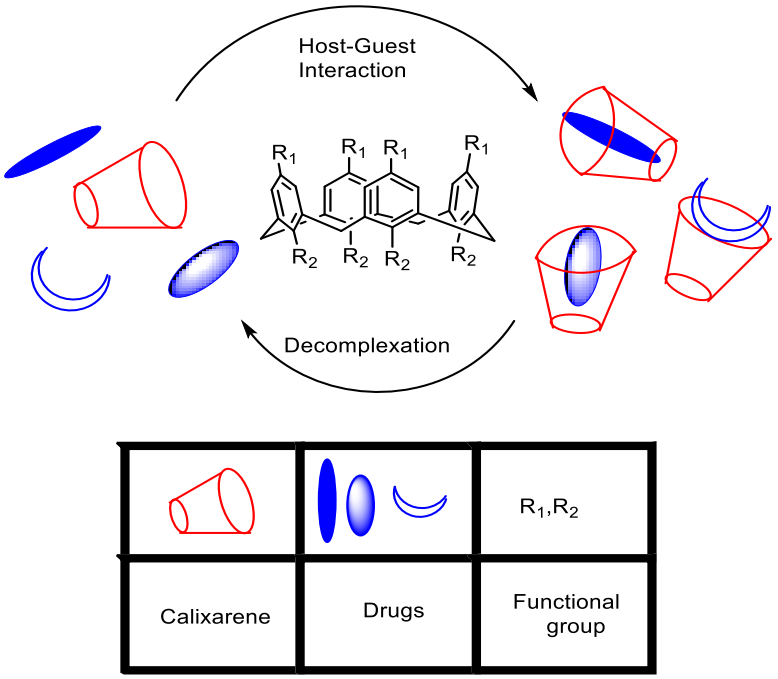

Figure 4: Presentation of the formation of inclusion complexes based on calix[n]arenes and their decomplexation (Zhou *et al*., 2015)

Coleman and Perret showed that any modifications on the parent calix[n]arene structure, such as mono-substitution of 4-sulfonatocalix[n]arenes, can evoke surprising changes in their complexation with biomolecules, particularly, they showed an increased performance to bind the aspartic acid and the glutamic acid groups which will have reflections in the recognition of protein (Perret and Coleman 2011).

Contrary to other reports in the literature, Da Silva *et al*. reported the haemolytic properties of a number of 4-sulfonato-calix[n]arene derivatives having pendant groups at the lower rim (Figure 5): they found that the haemolytic effect rises with the size of the macrocyclic ring. For example, 30% haemolysis of human erythrocytes was observed for 4-sulfonatocalix[8]arene at a concentration of 200 mM. The haemolysis effect was lower for 4-sufonatocalix[6]arene and 4-

sulfonatocalix[4]arene, at 8% and 0.5% respectively at the same 200 mM concentration.

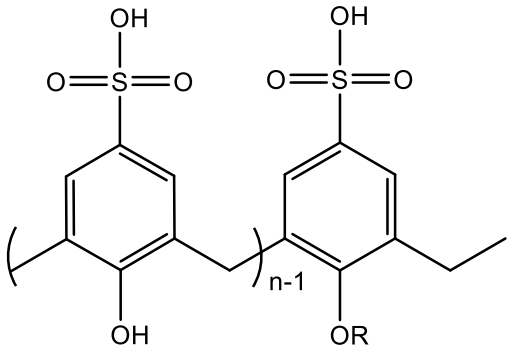

5: n= 4, **6**: n= 6, **7**: n= 8

5a, **6a**, **7a**: R= H
5b, **6b**, **7b**: R= CH_2COOH
5c, **6c**, **7c**: R= CH_2CONH_2
5d, **6d**, **7d**: R= $CH_2CH_2NH_2$

Figure 5: Presentation of different water soluble 4-sulfonatocalix[n]arenes (Da Silva *et al*., 2004)

In all cases, introduction of a methoxy-carboxylate function on the lower rim leads to a decrease in haemolytic behaviour at 50 mM concentration and above. The presence of an ethoxy-amine function on the lower rim enhanced the haemolytic effect for 4-sulfonatocalix[4]arene **5d** and 4-sulfonatocalix[6]arene **6d** at all concentrations but decreases the impact for 4-sufonatocalix[8]arene **7d** derivatives (Da Silva *et al*., 2004).

Amphoteric calix[8]arene **8** presenting negatively charged sulfonate groups on the upper rim and positively charged quaternary ammonium groups on the lower rim has been reported by Xiao *et al*. (Xue *et al*., 2013). It displayed pH-sensitive loading and release of the hydrophobic drug ciprofloxacin into the cavity of the calix[8]arene (Figure 6).

It was proposed that the calix[8]arenes load the drug at neutral pH by self-assembly of calix[8]arene molecules through the electrostatic bonds between both rims. At higher or lower pH, the amphoteric calix[8]arene complexes disassemble and can evoke drug release (Xue *et al*., 2013).

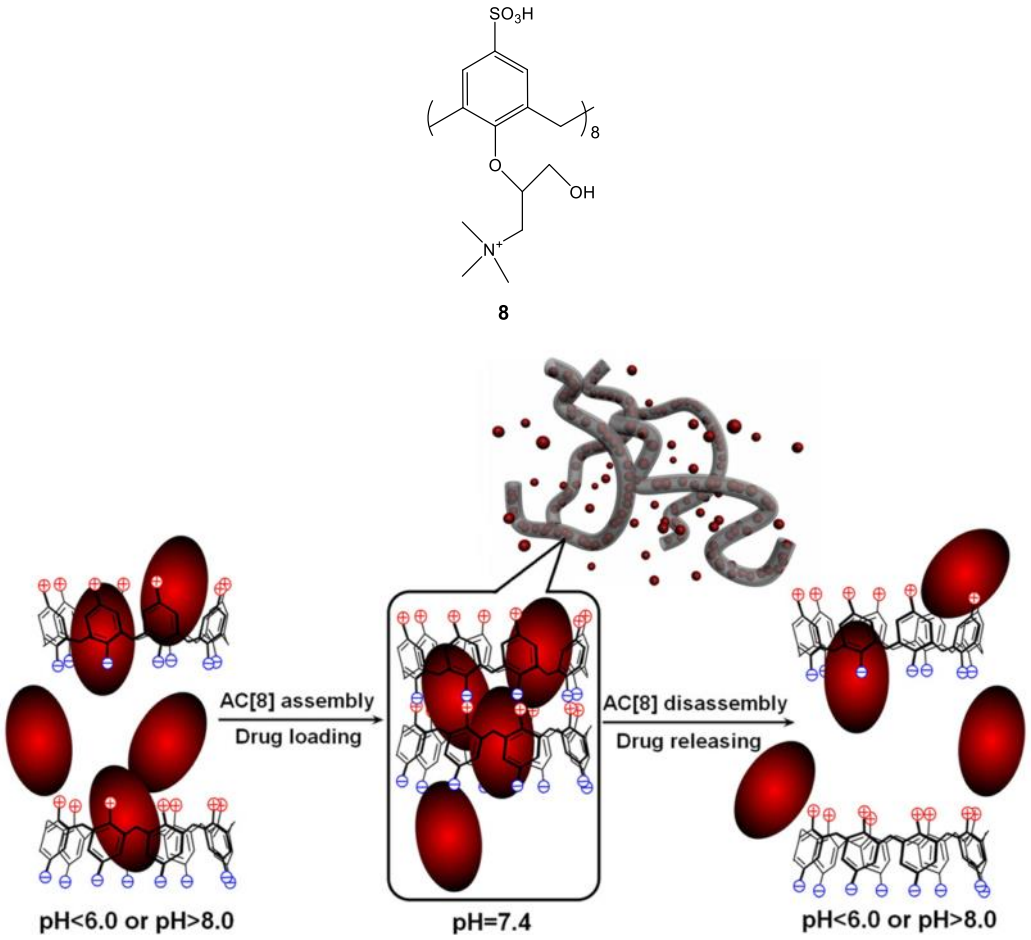

Figure 6: Drug loading and releasing procedure depended on pH (Xue *et al*., 2013)

1.2.1.2.2 Aminocalix[n]arenes

The ability of cationic calix[n]arenes to solubilise and deliver drugs across biological membranes has not been investigated in depth. Aminocalix[n]arenes have been investigated for their ability to self-assemble and for molecular interaction with DNA (Shahgaldian *et al*., 2008).

Ukhatskaya *et al*. studied the solubilising effect and complexing ability of cationic aminocalix[4]arene (Figure 7): they reported that the calix[4]arene enhanced the solubility of paracetamol, lidocaine and ketoprofen in aqueous media, notably more effectively when compared to cyclodextrins. The highest increase in solubility was noticed for steroidal drugs, 17β-estradiol for example. Results from dynamic light scattering (DLS) and transmission electron microscopy (TEM) showed that the calix[4]arene perhaps exists in vesicles aggregates of two diverse size populations. Correlation data of the relationship between physical and physio-chemical properties of the drugs and the solubilising effect of aminocalix[4]arene **9** supports the suggestion that the mechanism of solubilisation depends on the interaction between the drug and aggregates of **9** rather than forming inclusion complexes of drug/aminocalix[4]arene (Ukhatskaya *et al*., 2010).

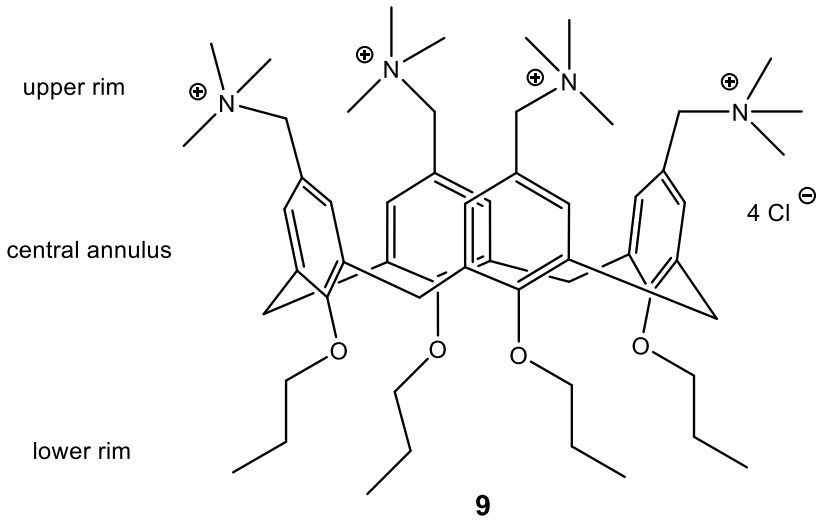

9

Figure 7: The structure of trimethylammniomethylcalix[4]arene (Ukhatskaya *et al*., 2010)

1.2.1.2.3 Phosphorylated calix[4]arene

Curcumin, like other natural products, has been found to reduce the risk of developing different types of cancers (Chen *et al*., 2017). The employment of curcumin in drug design is also appealing due to the fluorescence spectrum and can be tracked simply *in vitro* and *in vivo*. However, the clinical application of curcumin is still challenging due to its low stability and bioavailability. By delivering it in nanoparticulate carriers it is likely to be effective against various cancers, but against therapeutically aggressive and highly heterogeneous disease like Triple-negative breast cancer (TNBC). Development of nanocarrier could assist to increase curcumin efficiency against this form of cancer.

Phosphorylated calix[4]arene amphiphile **10**, which contain hydrophilic phosphate moieties on the upper rim and hydrophobic chains on the lower rim (Figure 8), has been developed to improve the solubility, stability and anti-tumour activity of curcumin (Chen *et al*., 2017).

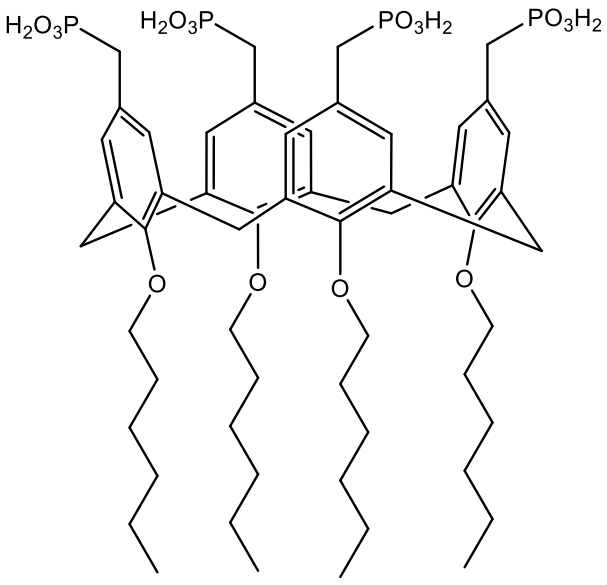

10

Figure 8: Phosphorylated calix[4]arene (Chen *et al*., 2017)

Curcumin-loaded phosphorylated calix[4]arene micelles were generated utilising a thin-film dispersion method. These loaded micelles showed a shell-core structure, small particle size (3.86±0.32 nm) with small size distribution (PDI) (0.125±0.078). The micelles displayed high curcumin loading capacity (loading ratio, 17.10±1.25%) as determined by HPLC coupled to a tandem MS in positive ESI mode by examining the retention time and peak area for curcumin.

Cell culture studies indicated that phosphorylated calix[4]arenes can release curcumin or other payload in response to a change in pH and hence can effectively inhibit (TNBC) *in vitro* and *in vivo*. These micelles assist the capability of curcumin to inhibit proliferation, migration, and invasion. In addition to their ability of increasing apoptosis and reducing the nuclear activity of *β*-catenin and androgen receptor and destroy breast cancer stem cells (BCSCs). These effects reflected the strong capability to reduce the growth of tumour sphere by BT-549 in mice without causing clear side effects within 14 days of treatment (Chen *et al*., 2017).

1.2.1.2.4 PEGylated calix[5]arenes

Two classes of amphiphilic PEGylated calix[5]arenes **13** and **14** were prepared directly from 4-methylcalix[5]arene **11** and 4-*tert*-butylcalix[5]arene **12** (Scheme 3). Their aggregation properties were examined in water and the possibility of compound **13** to act as drug delivery system was also investigated using Rose Bengal, a fluorescent dye use for spectrophotometric determination and is also employed clinically (Pisagatti *et al*., 2018).

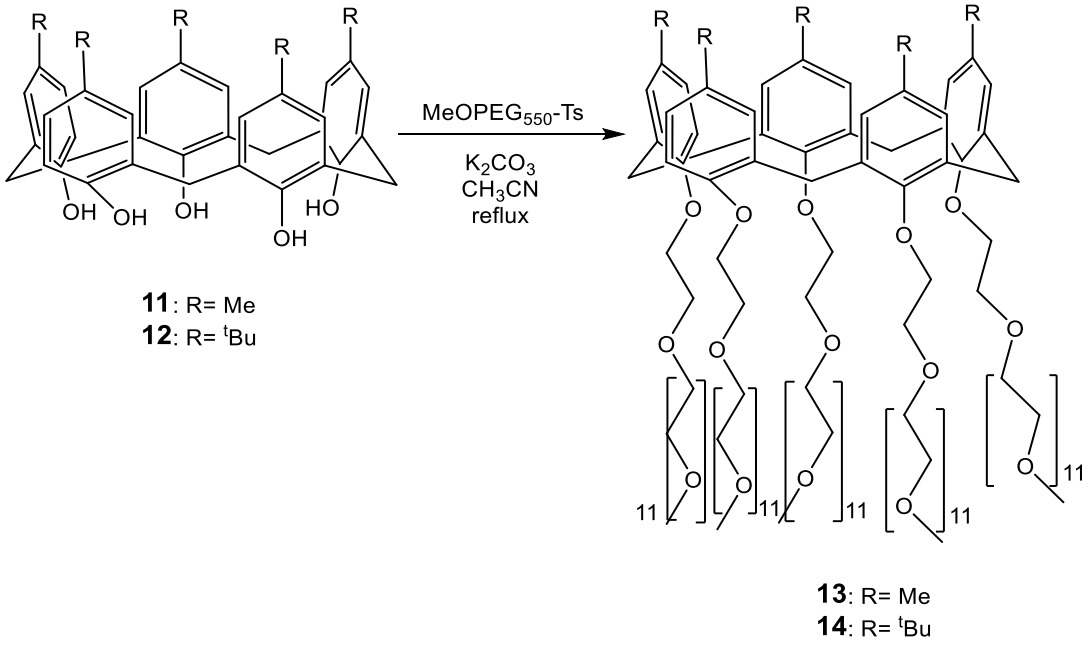

Scheme 3: Synthesis of 4-substituted PEGylated calix[5]arenes

(Pisagatti *et al*., 2018)

The aggregation behaviour of the two derivatives was studied using ^{1}H or DOSY NMR and AFM. The ^{1}H-NMR spectra of compound **13** and compound **14** in D_2O showed broad signals indicating that the aggregation process is happening in this solvent due to their amphiphilic character. Diffusion Ordered NMR spectroscopy, (DOSY) analysis using 0.4 mM of both derivatives, showed diffusion coefficients of low values (D_{obs} = 1.17 × 10^{-10} and 0.73 × 10^{-10} m^2s^{-1} for compound **13** and **14** respectively). The critical micellar concentrations (CMC) values were determined to be low also (4.5 µM (14.7 mg/L) and 0.5 µM (1.7 mg/L) for compound **13** and compound **14** respectively). The AFM topography images showed different aggregation features: compound **13** forms relatively small-sized assemblies, but by contrast compound **14** predominately assemblies into large circular aggregates. These differences in morphologies and CMC values are possibly ascribed to the differences in conformational mobility of the two calix[5]arenes, which in turn can be attributed to the size of

substituents present on the upper rim. The thermal release of Rose Bengal from the micellar environment of PEGylated calix[5]arene **13** was tested by increasing the temperature of the solution, it was seen that λ_{max} of Rose Bengal shifted back from 563 nm to 553 nm referring to the release of the drug from the micellar core (Pisagatti *et al*., 2018).

1.2.1.2.5 Carboxylated calix[6]arene

Carboxylated calix[6]arenes (Figure 9) have been investigated for their capability to form 1:1 inclusion complexes with esters of aminoacids, tryptophan for example, in a liquid-liquid extraction system. The interaction between the ammonium cation of the guest molecule and the oxygen atoms of the calix[6]arene was the driving force for complexation. The structure and the stoichiometry of the complexes formed were elucidated by spectroscopic analysis and systematic studies of liquid-liquid extraction method using a Job plot and slope analysis (Oshima *et al*., 2002).

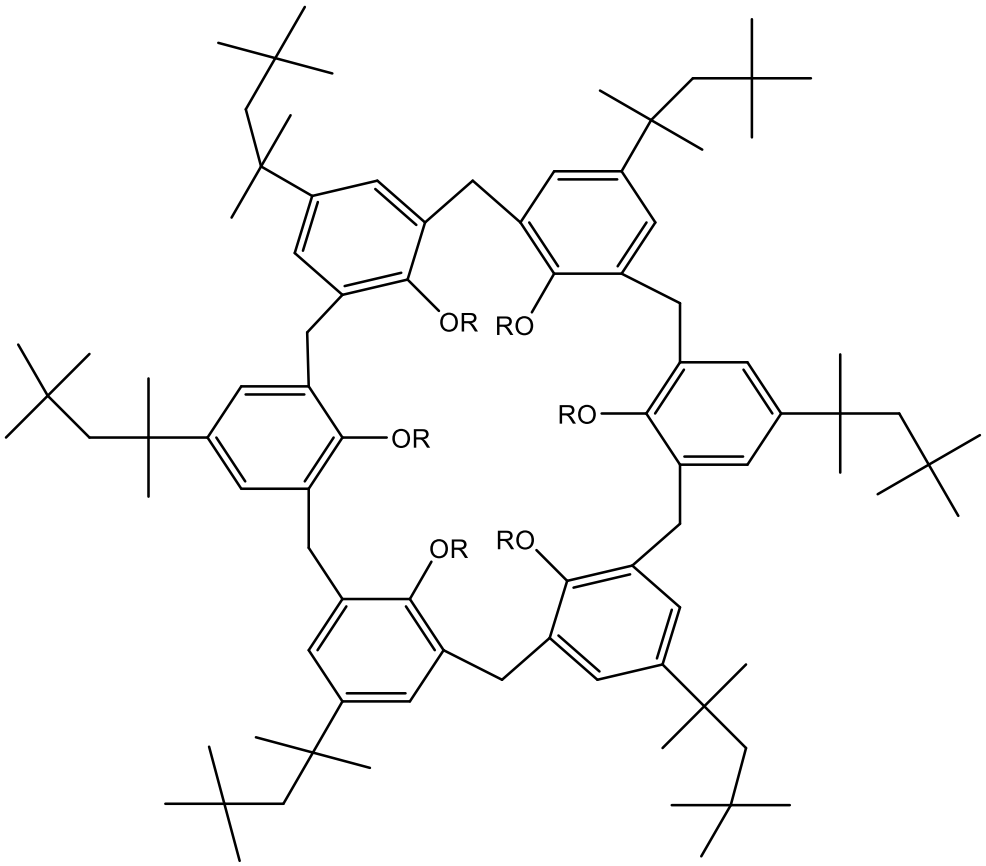

15

Figure 9: Molecular structure of 4-*tert*-octylcalix[6]arene hexacarboxylic acid derivative (Oshima *et al*., 2002)

Induced circular dichroism (ICD) spectrum of 4-*tert*-octylcalix[6]arene **15** was observed when the guest molecule was complexed, such phenomenon is based on the asymmetric rearrangement of the host by including the amino acid guest within the cavity (Oshima *et al*., 2002).

1.3 Glycoclusters and glycodendrimers

Dendrimers refer to a class of complex and branched structures with a symmetric and regular spherical shape. Whereas, clusters are small compounds with fewer repeating arms. The first dendrimers were described by Vogtle in 1978 (Buhleier *et al*., 1978), then the field exploded in the early 1980s (Tomalia and Fréchet 2002).

Glycodendrimers are scaffolds functionalised with carbohydrate chains based on different cores such as cyclodextrins, fullerenes, calix[n]arenes, calix[4]resorcinarenes and neo-glycopeptides (Figure 10) (Reina and Rojo 2015; Delbianco *et al*., 2015; Bojarová and Křen 2016).

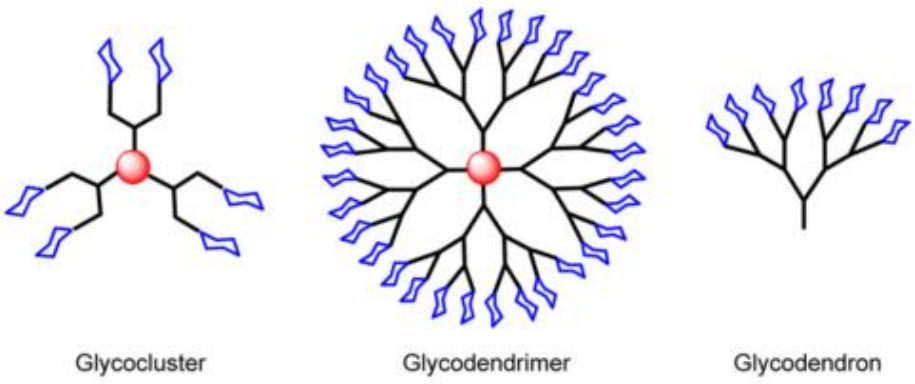

Figure 10: General structures of glycodendrimers, glycoclusters and glycodendrons (Delbianco *et al*., 2015)

These systems, modulated with carbohydrates provide valuable platforms for the synthesis of multivalent frameworks, allowing conjunction of a multiple number of peripheral functional groups for biological recognition purposes (carbohydrate-protein interaction (Cousin and Cloninger 2016; Denavit *et al*., 2018) or preventing infections from pathogens (Shchelik *et al*., 2015), as examples).

The inner sphere of a dendrimer can be used as a container for gene or drug delivery (Svenson and Tomalia 2012). These systems have been used as vaccines, anticancer drugs, antibacterial agents and imaging reporters (Shiao and Roy 2012).

1.2.1.2.6 Glycosylated calix[n]arenes

Glycocalixarenes are a subclass of calix[n]arenes bearing at least one saccharide unit anchored to their structure; glycocalix[n]arenes that possess two or more saccharide units are called multivalent glycocalix[n]arenes (Baldini *et al*., 2007; Dondoni and Marra 2010). These compounds have received great attention in bioorganic and supramolecular chemistry due to their ability to interact with biologically active macromolecules. As a consequence of this association they may be beneficial in hindering a number of adhesion phenomena, such as toxin adhesion to cells, infection by pathogenic viruses and bacteria and tumour progression and migration (Varki 1993; Lee and Lee 1995; Lis and Sharon 1998; Gabius *et al*., 2011).

Glycocalixarenes have been shown to recognise and associate with proteins due to multivalent interactions between the protein and the saccharide residues on the glycocalixarene. In nanomedicine, glycocalixarenes could be potentially useful, *via* covalent or noncovalent binding processes (Figure 11): they can load many type of cargo, such as drugs, fluorescent labels, radioactive or paramagnetic probes and immunoadjuvant units like tripalmitoyl-*S*-glycerylcysteinyl-serine for potential applications extending from diagnosis to therapy. Anticancer vaccine was synthesised by clustering of four glycomimetic antigen units onto calix[4]arene matrix conjucated with an immunoadjuvant unti. This unit determines the extent of immune response of vaccine candidate

(Geraci *et al*., 2008). On the other hand, these macrocycles can form supramolecular formulations to detect ovarian and other gynecologic cancers at the early stages by forming host-gust recognition with the biomarker, Lysophosphatidic acid (LPA) exists in different concentrations in plasma for healthy and patients posses gynecologic cancers (Yu and Chen 2019). Due to their lipophilic cavity, calixarenes can complex with small molecules in aqueous media through the hydrophobic effect (Figure 11a). Besides, upper or lower rim functionalisation with polar groups permits association with polar guests, anions and cations (Casnati *et al*., 2003; Baldini *et al*., 2012).

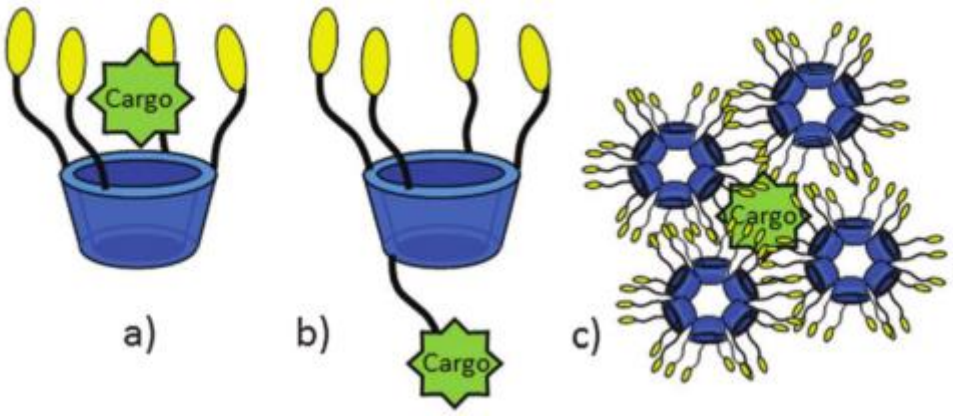

Figure 11: Noncovalent (a and c) and covalent (b) interactions of the glycocalixarene load with the cargo *via* complexation (a), bond formation (b) and self-assembly (c) (Sansone and Casnati 2013)

The synthesis of calix[4]arene based glycoconjugates at the upper and the lower rim with four saccharide units can convert the lipophilic calixarene structure into a water soluble species, thereby providing a multivalent agent for molecular interaction (Dondoni and Marra 2010).

1.2.1.2.6.1 Upper rim glycosylation

1.2.1.2.6.1.1 Synthesis of calix[4]arene *O*-glycoside

Calix[4]arene glycosides with four carbohydrates at the upper rim have been prepared starting from calix[4]arene **16**, which was converted to tetrahydroxymethylated calix[4]arene **19** *via* the tetrapropoxy derivative **17** and the tetraaldehyde **18** (Scheme 4).

Glycosylation of compound **19** by using thioethyl galactoside **20** afforded the water soluble (up to 5 mM) tetrakis-*O*-galactosyl calixarene **21** together with the ether-bridged by-product bis-*O*-galactosyl calixarene **22** in a very low yield. Coupling of compound **19** with thioethyl lactoside **23** afforded the capped glycocalix[4]arene **24** (intramolecular ether bridge) in low yield as the only product (Dondoni *et al*., 1997).

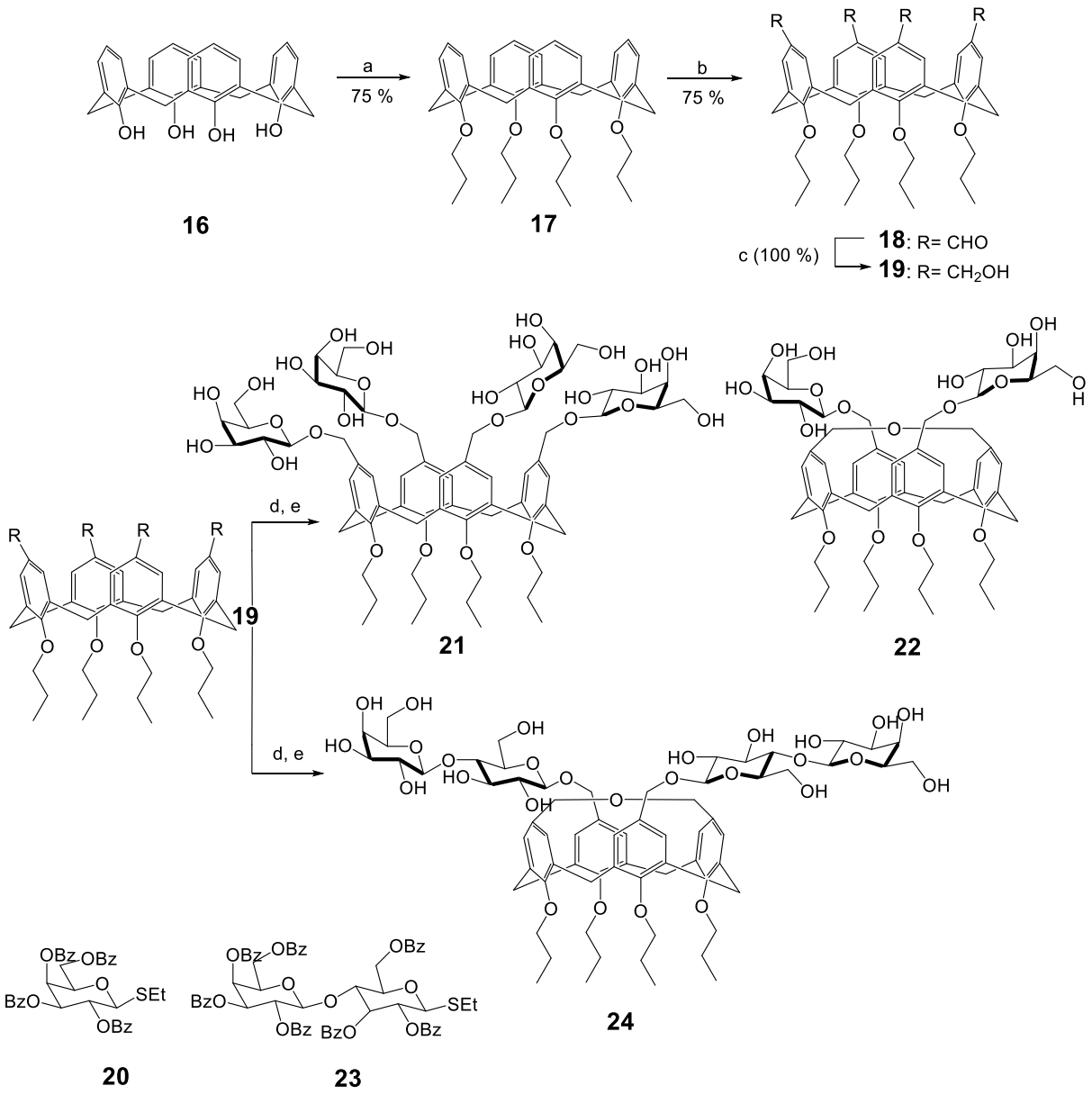

Reagents a) *n*-PrI, NaH; b) $(CH_2)_6N_4$, TFA; c) $NaBH_4$; d) $Cu(OTf)_2$, CH_3CN; e) MeONa, MeOH

Scheme 4: Synthesis of tetrakis-*O*-galactosyl calixarene and ether bridge bis-*O*-lactosyl calix[4]arene (Dondoni *et al*., 1997)

1.2.1.2.6.1.2 Synthesis of calix[n]arenes *N*-glycosides

Four glycocalix[n]arenes having *α*-mannoside groups at the upper rim have been synthesised as multivalent ligands for DC-SIGN (Dendritic Cell-Specific ICAM-3 Grabbing Nonintegrin). However, the conformational mobility, the valency of the scaffold and the spacer between the scaffold and the ligating units were different in order to estimate the possible effect of these glycocalix[n]arenes towards receptor.

Tetramannosylthioureidocalix[4]arenes **27a** and **27b** (Scheme 5) bearing propyl groups at the lower rim and the mannosides units linked to the upper rim by ethylthioureido linker, are locked in the cone and 1,3-alternate conformation, respectively.

Hexamannosylcalix[6]arene **27c** with methyl units at the lower rim, displays a multivalency and is conformationally mobile. Mannosylcalix[4]arene **27d** is analogous to compound **27a** but the mannosyl residues are connected to the macrocycle through the thiourea unit (Scheme 5).

The behaviour of deprotected mannosyl products **29a-d** in water was recorded by ^{1}H-NMR spectra in D_2O solution and as expected they showed different solubility in water. Compounds **29a** and **29d** showed very low solubility in water and very broad signals were noticed in the spectra at room temperature, probably due to strong self-assembly in solution. Conversely, compound **29b**, which is locked in the 1,3-alternate conformation, was highly soluble in water and sharp ^{1}H NMR signals appeared in the spectrum at room temperature. Compound **29c** showed similar behaviour to compound **29a** in water with broad signals in the spectrum at room temperature. The relative diversity in the behaviour of these compounds in solution can be related to the relative

configuration of hydrophilic and lipophilic sites in the structures (Morbioli *et al*., 2017).

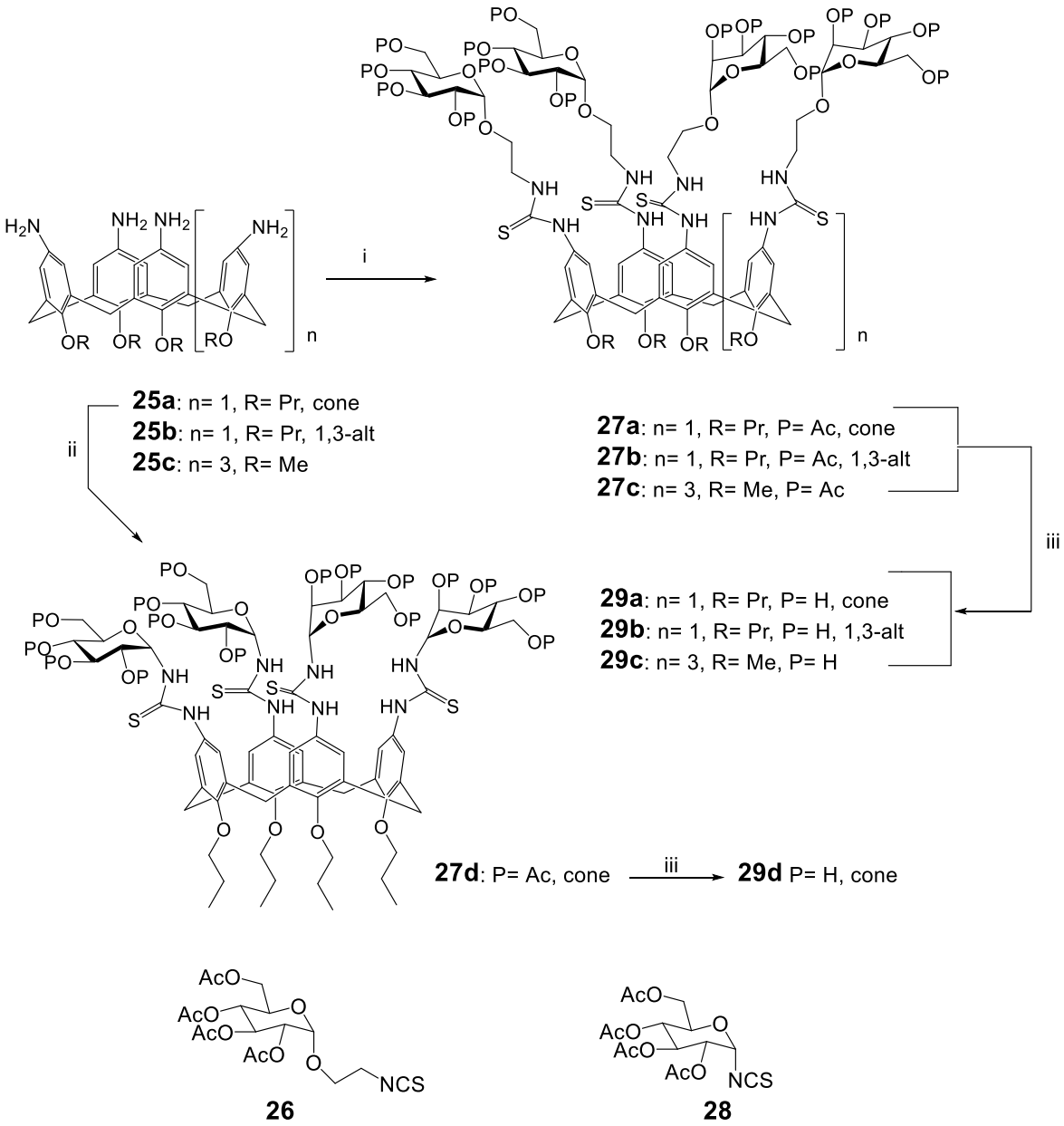

Reagents and conditions : i) **26**, Et_3N, dry DCM, rt, overnight to obtain compound **27a**, 40% yield; **26**, Et_3N, dry DMF, MW, 50 ^{0}C, 200 W,1h (x3) to obtain compounds **27b**,**c**, 45 and 19% yield respectively; ii) **28**, Et_3N, dry DMF, MW, 50 ^{0}C, 200 W,1h (x3), 60 % yield; iii)1.NaOMe, MeOH,0 ^{0}C, 24h; 2. Amberlite IR-120 (H^+), rt, 30 min, 65% **29a**, 85% **29b**, 72% **29c** and 82% **29d** yield

Scheme 5: Synthesis of mannosylcalix[n]arenes (Morbioli *et al*., 2017)

1.2.1.2.6.2 Lower rim glycosylation

Calix[4]arene **16** was reacted with tetra-*O*-acetyl-*α*,*β*-D-glucopyranose **30** by Mitsunobu reaction: this gave a mixture of two compounds, *α*,*α*-bisglucoside **31** and *α*,*β*-bisglucoside **32** in 1:1 ratio (Scheme 6). The ^{1}H and ^{13}C NMR analysis clearly confirmed the cone conformation of the glycocalixarenes. Also, the ^{13}C NMR spectra demonstrated the diametrical 1,3-substitution in **31**. The hydrolysis of both compounds afforded the unprotected calix[4]arene glycosides **33** and **34**, but these compounds exhibited low water solubility which consequently limits their use in processes which rely upon molecular recognition interactions (Marra *et al*., 1995).

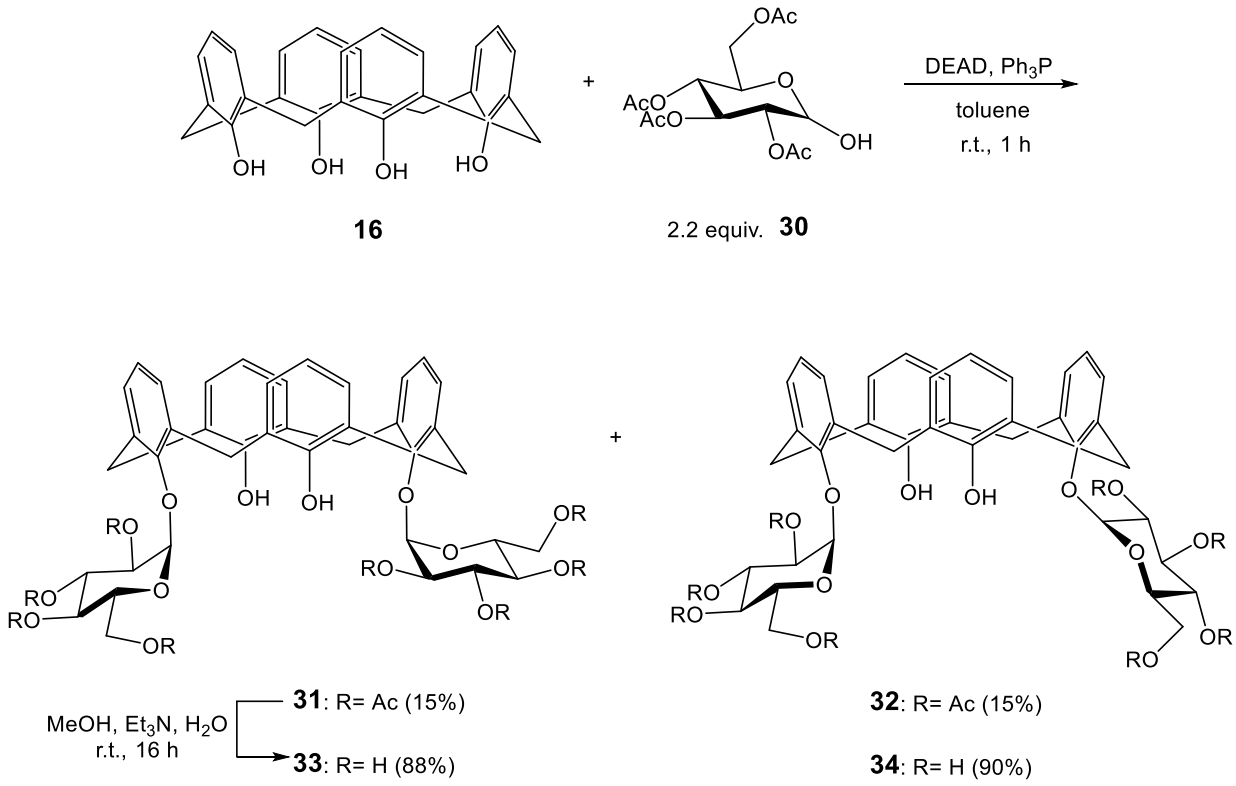

Scheme 6: Synthesis of calix[4]arene-*O*-glycoside (Dondoni and Marra 2010)

1.2.2 Calix[4]resorcinarenes

In 1872 Baeyer reported that a crystalline product can be formed by the addition of sulfuric acid to a mixture of resorcinol and benzaldehyde (Baeyer 1872). Afterwards, Michael reported that these compounds were produced by the condensation of an equal ratio of resorcinol and benzaldehyde with the lost of an equal number of water molecules (Michael 1883). In 1940, Niederl and Vogel proposed the cyclic tetrameric structure of these compounds when they found the ratio between the resorcinol- and the aldehyde-derived residues is 4:4 by molecular weight determination (Niederl and Vogel 1940). In 1968, Erdtman finally proved the structure of these compounds by single crystal X-ray analysis (Erdtman *et al*., 1968).

Calix[4]resorcinarenes are cyclic oligomers that can serve as building blocks for a variety of applications, including nanocapsule formation (Pan *et al*., 2015), nanoparticle formation (Shalaeva *et al*., 2018), catalysis (Jose *et al*., 2017), dendrimers in biological systems (Mendoza-Cardozo *et al*., 2019), as NMR solvating agents (Wenzel 2014), in the synthesis of cavitands (Moussaoui *et al*., 2017), carcerands (Warmuth 2012). They have also attracted special interest in the fields of biotechnology, microelectronics and others.

Calix[4]resorcinarenes can exist predominantly in five isomeric conformations (Hogberg 1980; Hogberg 1980; Tunstad *et al*., 1989): crown (C_{4v}), boat (C_{2v}), chair (C_{2h}), diamond (C_s) and saddle (D_{2d}) (Figure 12).

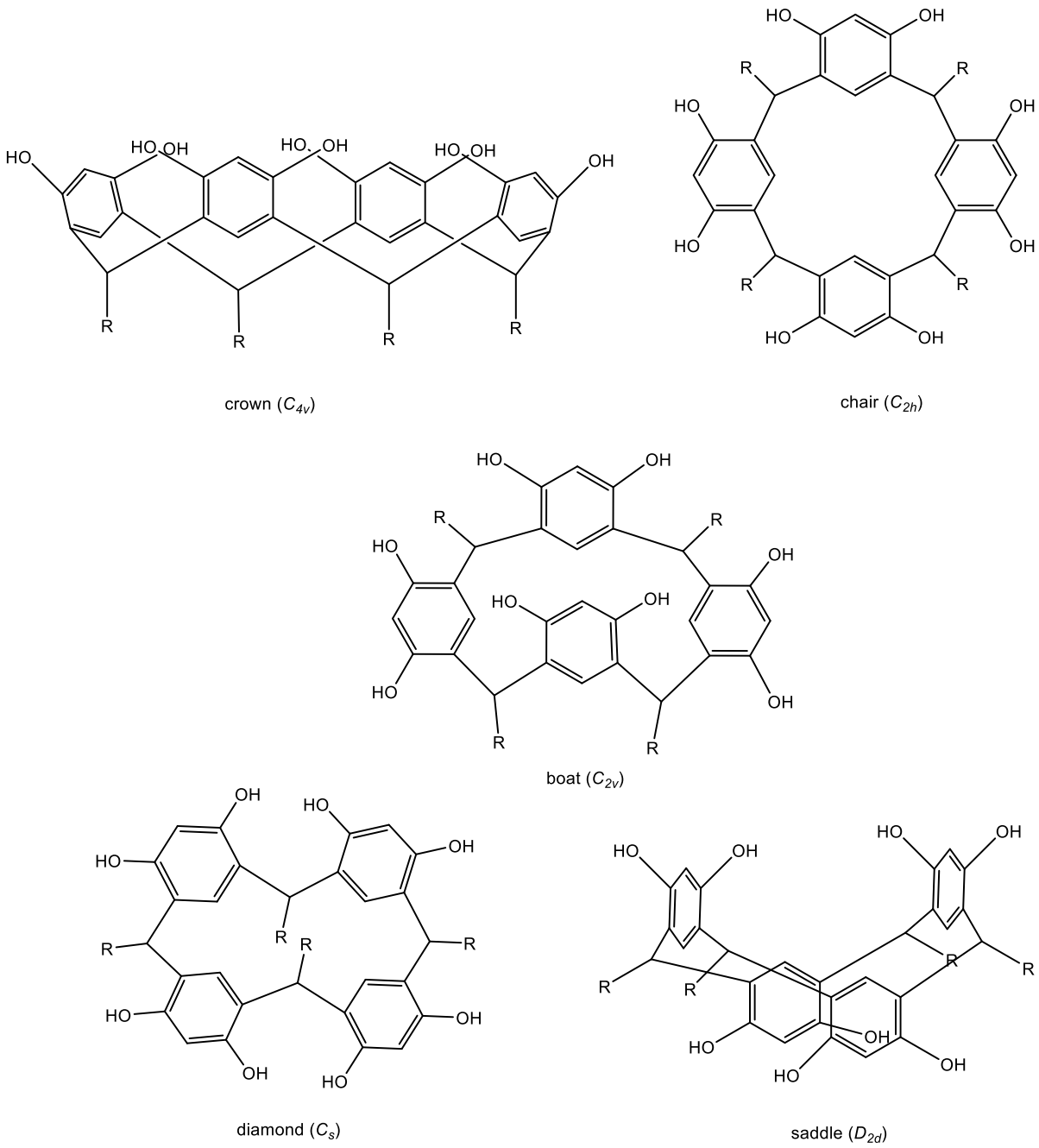

Figure 12: The conformation of calix[4]resorcinarene (Jain and Kanaiya 2011)

The relative configuration of the residues at CH-bridges can also be used to denote the stereoisomeric forms: all-*cis* (*rccc*), *cis-cis-trans* (*rcct*), *cis-trans-trans* (*rctt*) and *trans-cis-trans* (*rtct*) (Figure 13).

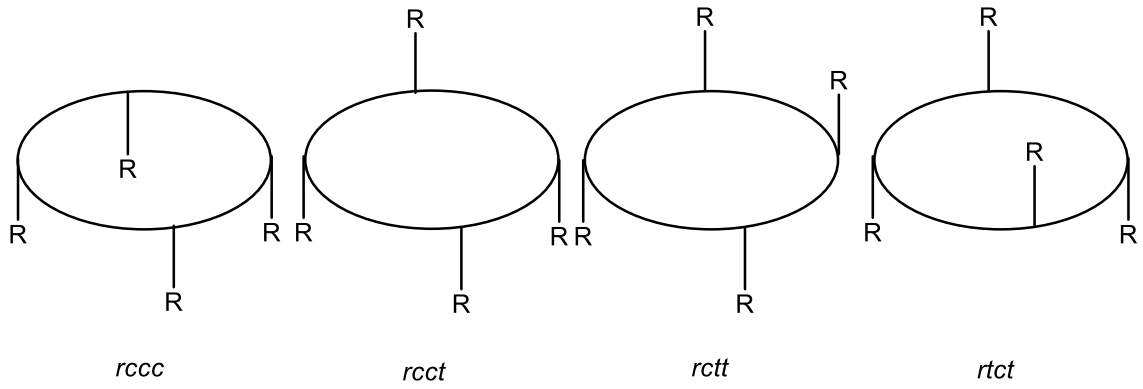

Figure 13: The configuration of calix[4]resorcinarene (Patil *et al*., 2016)

The individual configuration of substituents on the methylene bridges can adopt either ‘axial’ or ‘equatorial’ positions within *C* symmetric resorcinarenes. The integration of these criteria leads to a clear descriptions of the stereoisomeric calix[4]resorcinarenes. Experimentally, the all-*cis* isomers have been found to adopt either C_4 symmetry (crown conformation) or C_{2v} symmetry (boat conformation) predominantly.

Generally, the boat conformation is determined as a crown conformation due to the rapid interconversion between the two boat isomers gives a time averaged crown conformation (Figure 14). But, the interconversion between the boat and other isomers doesn’t happen because covalent bonds would need to be cleaved and then reformed.

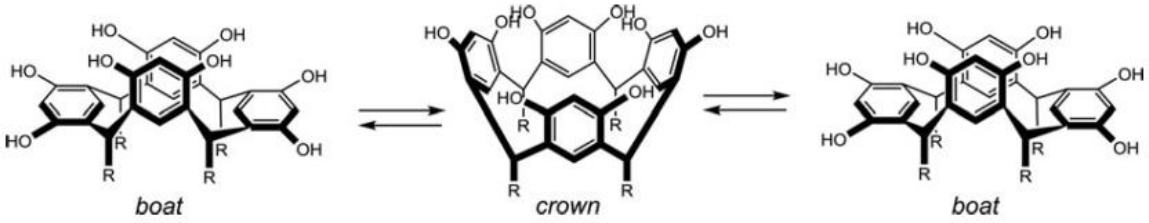

Figure 14: (boat-crown-boat) interconversion of *rccc* calix[4]resorcinarene (Glushko *et al*., 2017)

All these confomers are expected to form in a reaction to prepare a calix[4]resorcinarene, with the ratio of different isomers being mainly dependent on the reaction conditions used. Under homogenous acidic conditions, the product ratio depends on the thermodynamic stability of isomers due to the reversible condensation reaction under these conditions (Weinelt and Schneider 1991). Under heterogeneous conditions, the product ratio is determined by the relative solubility of various isomers in the reaction solvent used (Hogberg 1980).

Isolation and purification of calix[4]resorcinarenes can be difficult because their synthesis can deliver different conformations (Figure 12) and also because they can form supramolecular complexes with solvents (Payne and Oliver 2018).

Studies have showed that calix[4]resorcinarenes in which the hydroxyl groups are unsubstituted and the substituents on the methylene bridge are in the *rccc* arrangement exist solely in the crown conformation in both solid and solution phases. Usually the conformation obtained is determined by the hydrogen bonding between adjacent hydroxyl groups (Murayama and Aoki 1998; Rose *et al*., 1998).

1.2.2.1 Synthesis of calix[4]resorcinarenes

The most common synthetic route to calix[4]resorcinarenes remains heating the starting materials in a mixture of aqueous mineral acid and an alcohol to allow the formation of the thermodynamically stable product which possesses a cone-like 'crown' conformation (Scheme 7) (Högberg 1980; Egberink *et al*., 1992). And there is no point for condensation of formaldehyde with resorcinol under these conditions because of it is high reactivity, formaldehyde lead to the formation a copolymer with resorcinol.

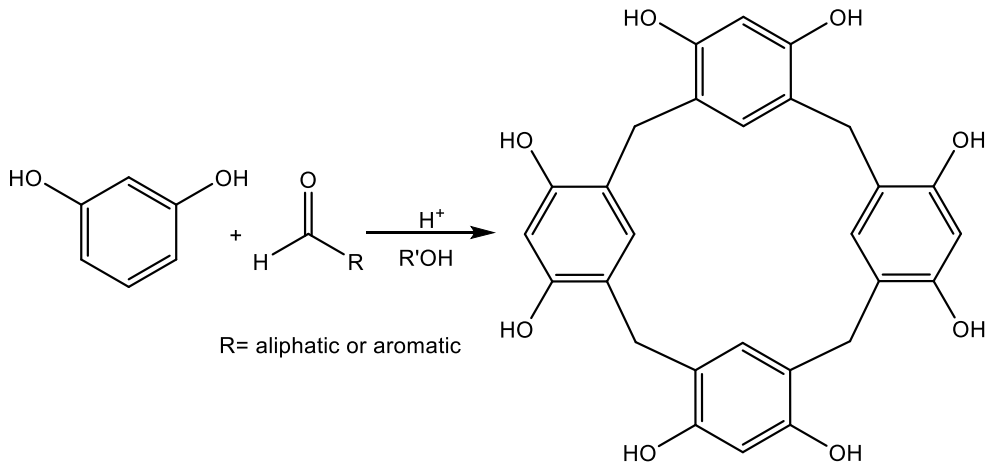

Resorcinol (1 equiv.), aldehyde (1 equiv.), H^+ (1 equiv.), alchoholic solvent (R'OH), T= 0 ^{0}C to reflux, overnight

Scheme 7: Synthesis of calix[4]resorcinarene (Castillo-Aguirre *et al*., 2017)

The acid-catalysed synthesis of substituted calix[4]resorcinarenes from the reaction of 2-nitroresorcinol, 2,6-dihydroxybenzoic acid and 2-acetylresorcinol with formaldehyde only yields dimeric or polymeric compounds. An alkaline medium is more appropriate for condensation of resorcinols bearing an electron-withdrawing group between the phenolic hydroxyl groups **35a-c**; this method also permits the synthesis of the completely unsubstituted calix[4]resorcinarene **36d** (Scheme 8) (Bourgeois and Stoeckli-evans 2005).

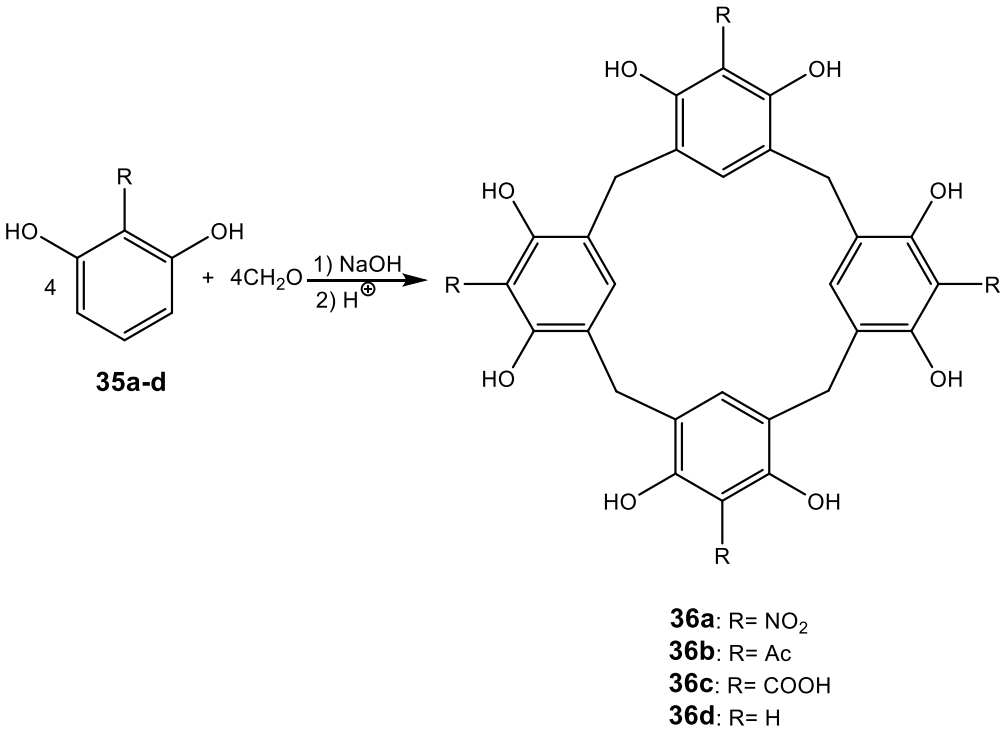

Scheme 8: Synthesis of calix[4]resorcinarenes from 2-substituted resorcinols and formaldehyde (Bourgeois and Stoeckli-Evans 2005)

Deleersnyder *et al*. have showed that lanthanide(III), iron(III), and copper(II) 4-toluenesufonates and lanthanide(III) nitrobenzenesulfonate can be used as efficient catalysts for the reaction of resorcinol with aromatic or aliphatic aldehydes to form calix[4]resorcinarenes. They observed that two diastereoisomers, the all-*cis* (*rccc*) and the *cis-trans-trans* (*rctt*) isomers are formed in the reaction of resorcinol with benzaldehyde. Moreover, the ratio of each isomer depends on the reaction conditions used (the time and the metal ion) and a good yield is gained after 24 h with only a catalytic 0.1 mol% of La(III) salts (Deleersnyder *et al*., 2007).

Barrett *et al*. reported the use of ytterbium(III) triflate nonahydrate as a catalyst in the synthesis of calix[4]resorcinarenes to avoid the problems encountered with Bronsted and other Lewis acids. Under these conditions, it was found that the reaction of resorcinol with a number of aliphatic aldehydes under standard conditions (48 h) afforded the desired all-*cis* isomers in high yields. In contrast, reaction of resorcinol with benzaldehyde gave the kinetically favoured *rctt* diastereoisomer **37b** and the thermodynamically favoured *rccc* isomer **37a** in 89% yield overall and an *rctt:rccc* ratio of 0.7:1.0. Following a longer reaction time (216 h) the reaction mixture was shown to be composed only of the all-*cis* isomer (Scheme 9) (Barrett *et al*., 1999).

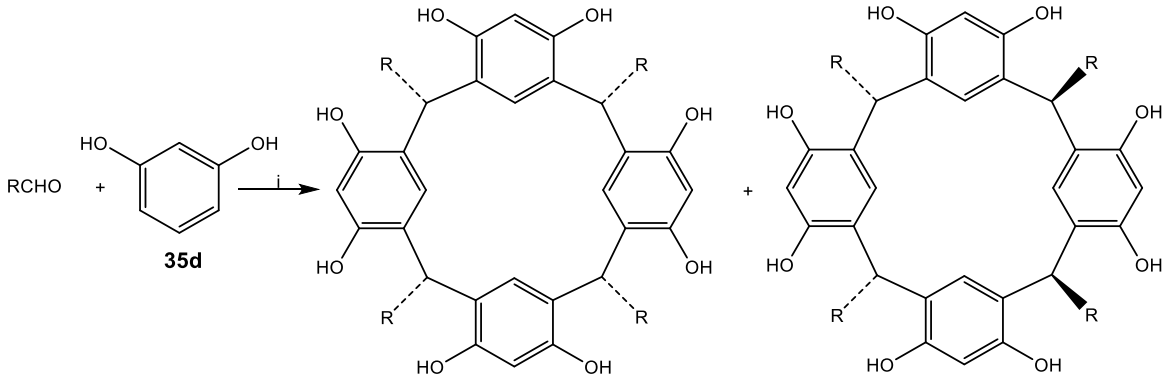

37a: R= Ph (52%)
38: R= Et (71%)
39: R= C_5H_{11} (94%)
40: R= C_9H_{19} (94%)
41: R= $C_{11}H_{23}$ (93%)

37b: R= Ph (37%)

i: $[Yb(H_2O)_9](OTf)_3$, EtOH, reflux for 48 h

Scheme 9: Ytterbium(III) triflate catalysed synthesis of calix[4]resorcinarenes (Barrett *et al*., 1999)

The use of bismuth triflate $Bi(OTf)_3$ (5 mol%) has been shown to be an efficient catalyst for calix[4]resorcinarene synthesis from aliphatic and aromatic aldehydes conducted in ethanol giving calix[4]resorcinarenes in good yields.

The condensation of resorcinol with aliphatic aldehydes required up to a day and gave only the thermodynamically favoured the all-*cis* (*rccc*) isomer **39a** and **40a**: with benzaldehyde only 75 min was needed for completion, the product obtained was a mixture of (*rccc*) **37a** and (*rctt*) **37b** isomers in a ratio (**37a**: **37b**= 0.78:1.0) (Scheme 10).

When the reaction was allowed to continue for 8 days, the product was only the all-*cis* isomer **37a** and no other isomer was found by ^{1}H-NMR spectroscopy. When the diastereomeric mixture obtained from 75 min reaction time was resubjected to the reaction conditions for 10 days, the product was a mixture which consisted mostly of the (*rccc*) isomer **37a** (**37a**: **37b**=1.0:0.11) (Peterson *et al*., 2003).

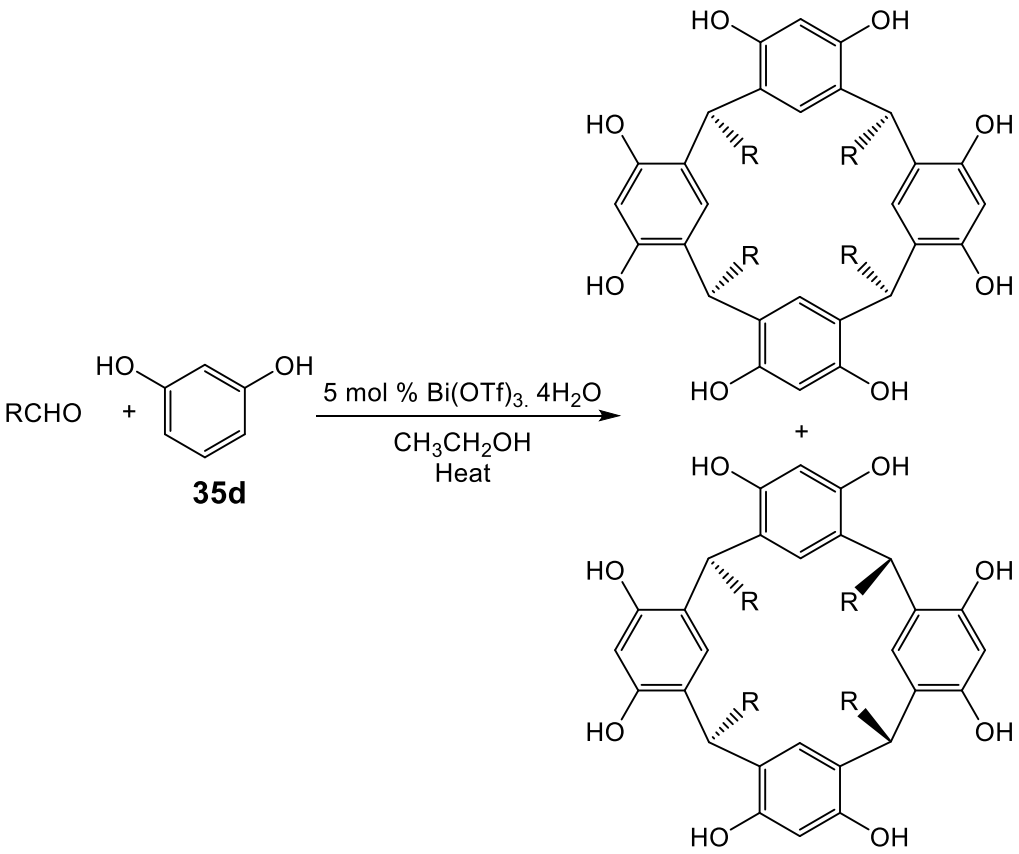

37: R= Ph, t= 75 min, Yield= 66% (**37a**: **37b**= 0.78:1.0)
37: R= Ph, t= 8 days, Yield= 89% (**37a**: **37b**= 1:0)
39: R= C_5H_{11}, t= 4 h, Yield= 84% (**39a**: **39b**= 1:0)
40: R= C_9H_{19}, t= 24 h, Yield= 91% (**40a**: **40b**= 1:0)

Scheme 10: Bismuth triflate $Bi(OTf)_3$ catalysed synthesis of calix[4]resorcinarenes (Peterson *et al*., 2003)

A range of Lewis acids were used by Iwanek and co-workers as catalysts for the condensation of 1,3-dimethoxybenzene **42** and isovaleraldehyde **43** in chloroform solvent. Among them, only $SnCl_4$ catalysed this reaction selectively and enhanced the formation of all-*cis* isomer **44a** in a high yield. However, three conformers were obtained with other Lewis acids, the cone (*rccc*) and diamond (*rcct*) predominating over the chair (*rctt*) isomer in all cases (Scheme 11). Only branched chain aldehydes undergo reaction in chloroform; changing the solvent to diethyl ether for the reaction of 1,3-dimethoxy benzene with

straight-chain aldehydes led to the formation of the crown conformer of octamethoxycalix[4]resorcinarene with only small amounts of other isomers being found (Iwanek and Syzdol 1999).

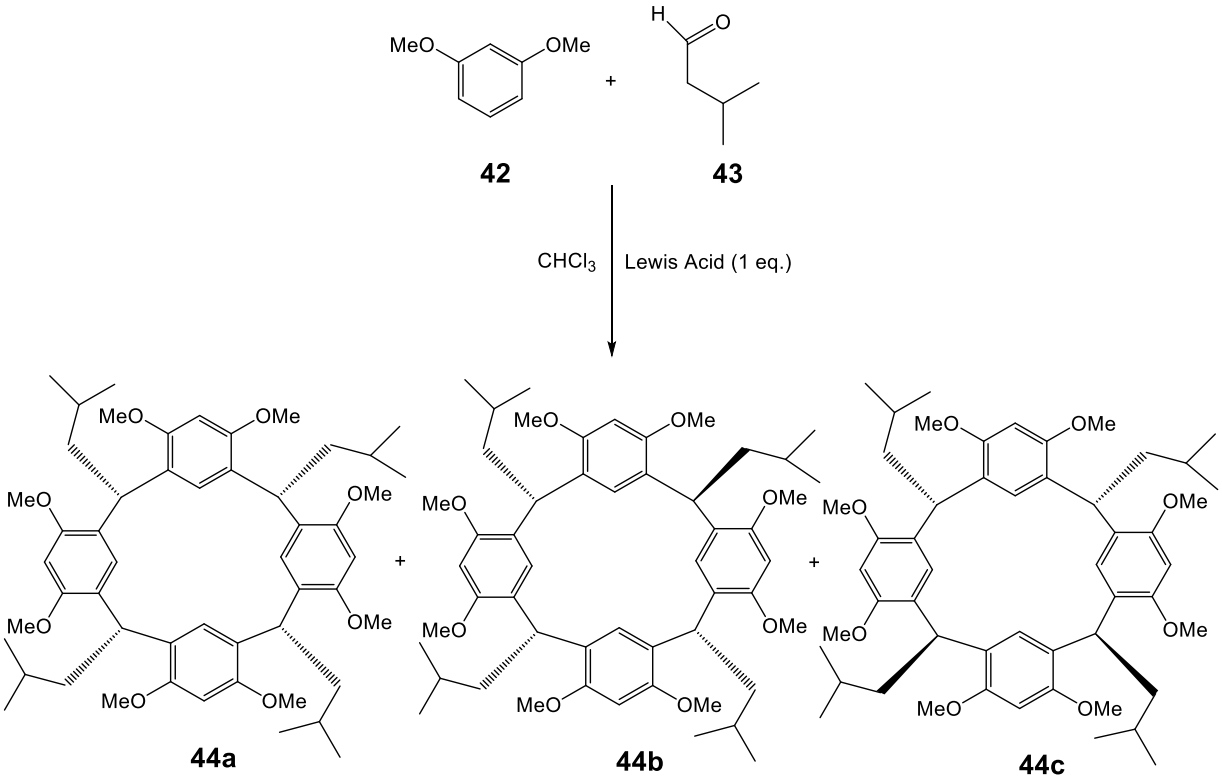

$SnCl_4$	100%		
$SOCl_2$	40%	55%	5%
$POCl_3$	35%	62%	3%
$AlCl_3$	30%	60%	10%
$SiCl_2Me_2$	50%	43%	7%
$SiClMe_3$	50%	45%	5%

Scheme 11: Lewis acid catalysed synthesis of octamethoxy calix[4]resorcinarene (Moore and Matthews 2009)

It has been reported that partially alkylated resorcinol does not produce cyclooligomeric products by reaction with aldehydes in an alcoholic acidic medium (Weinelt and Schneider 1991; Timmerman *et al*., 1996). However, octamethylcalix[4]resorcinarenes have been synthesised by using a Lewis acid catalyst (Iwanek and Syzdol 1999; Morikawa *et al*., 2006), this was the incentive to employ Lewis acids in the condensation reaction of resorcinol monoethers **45** and **46** with octanal **47** and dodecanal **48** (Scheme 12) (McIldowie *et al*., 2000).

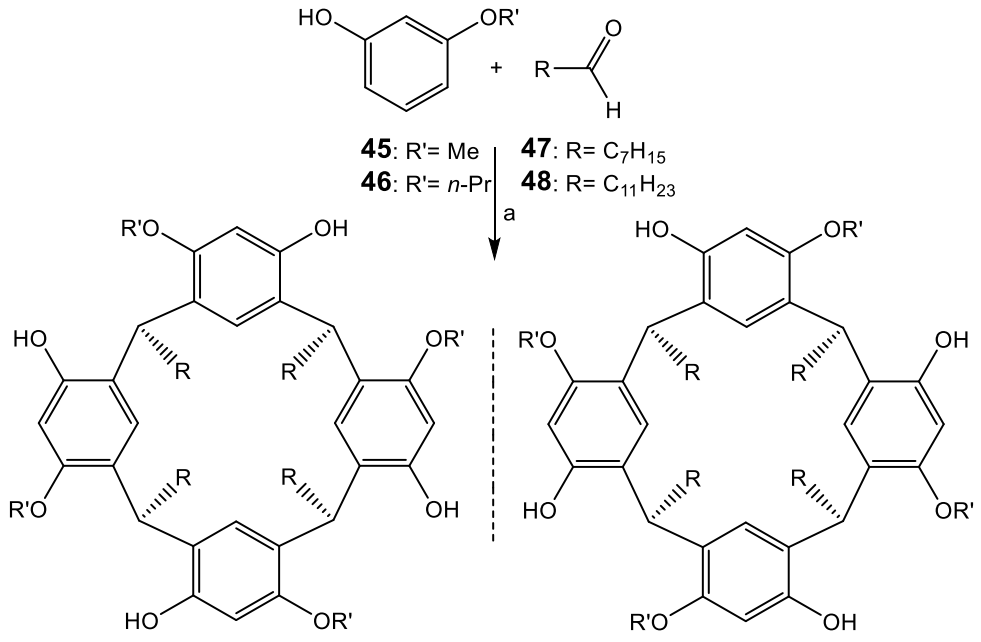

Scheme 12: Lewis acid catalysed the reaction of partially alkylated resorcinol with octanal and dodecanal (McIldowie *et al*., 2000)

Yttrium(III) nitrate hexahydrate has also been shown to be an efficient and safe Lewis acid for the synthesis of some calix[4]resorcinarenes derived from aromatic aldehydes as a mixture of two diastereoisomers (Scheme 13). The reaction was carried out at 120 ^{0}C in a preheated oil bath under solvent free conditions. They found that this method not only gave a high yield but was also fast, cheap and facile (Arami *et al*., 2015).

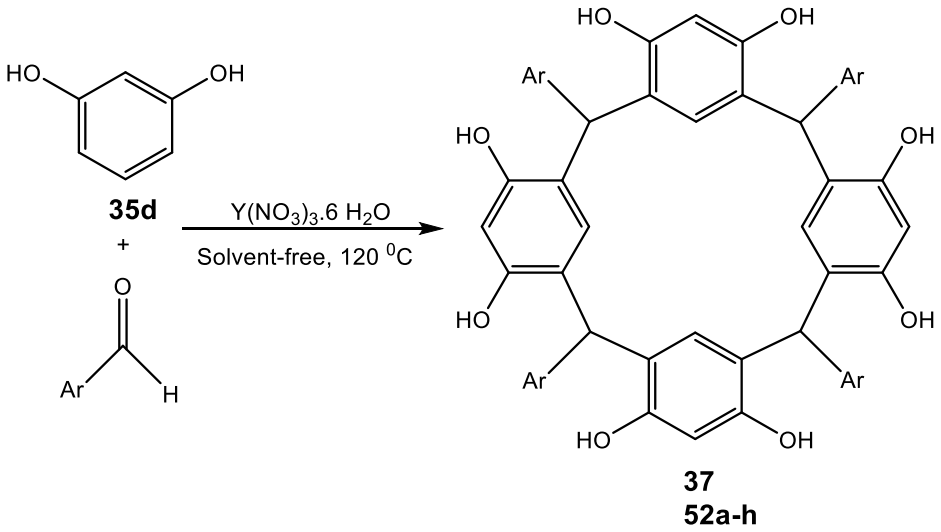

37: Ar= C_6H_5, **52a**: Ar= 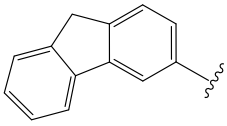 , **b**: Ar= 2-OH-3MeO-C_6H_3, **c**: Ar= 2-ClC_6H_4, **d**: Ar= 4-MeOC_6H_4, **e**: Ar= 4-Cl-C_6H_4, **f**: Ar= 3-Br-C_6H_4, **g**: Ar= 2-NO_2-C_6H_4, **h**: Ar= 4-Me-C_6H_4

Scheme 13: Synthesis of calix[4]resorcinarenes using Yttrium(III) nitrate (Arami *et al*., 2015)

Roberts *et al*. prepared a number of calix[4]resorcinarenes from the reaction of resorcinol and aldehydes using 4-toluenesulfonic acid as a catalyst by grinding the starting materials in a mortar and pestle for a few minutes (Roberts *et al*., 2001). Calix[4]resorcinarenes prepared in this way are generally isolated in two isomeric forms, C_{4v} *rccc* and C_{2h} *rctt* isomers. For *C*-methyl and *C*-C_6H_4-4'-*O*-

octyl-calix[4]resorcinarenes the *rccc* isomer predominates, whilst for *C*-C_6H_4-2'-OH-calix[4]resorcinarene the C_{2h} isomer predominates and for *C*-C_6H_4-4'-*O*$(CH_2)_4$Br calix[4]resorcinarene both isomers are produced. This method is simple, gives high yields and can be applied to reactions of resorcinol with a wide range of aldehydes (Scheme 14) (Cave *et al*., 2001).

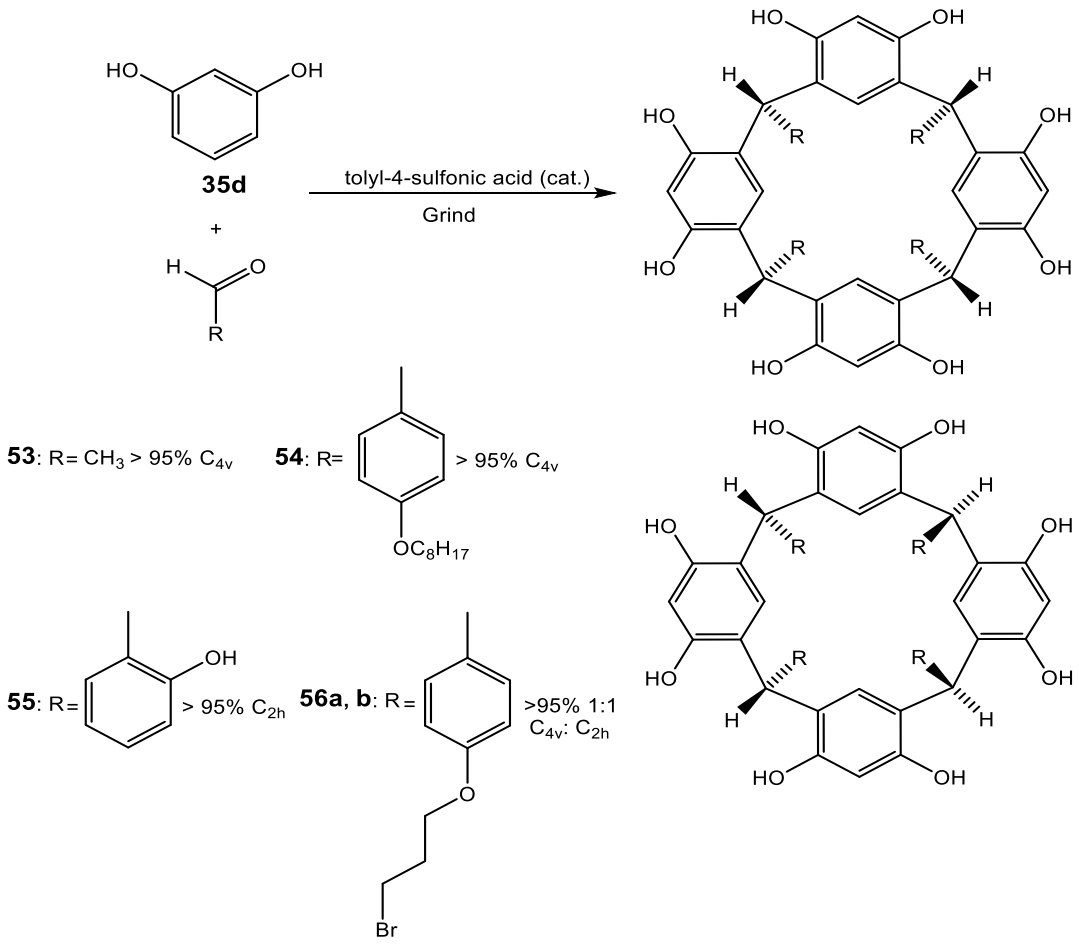

Scheme 14: Reaction of resorcinol and aldehyde under solvent-free conditions (Cave *et al*., 2001)

Microwaves have also been used as a tool for the synthesis of organic compounds. The use of microwaves provides rapid heating, reduces the reaction time in addition to reducing the amount of acid catalyst required to give high yields of calix[4]resorcinarenes. Sardjono *et al*. reported the synthesis of *C*-3,7-dimethyl-7-hydroxycalix[4]resorcinarene **58** by using resorcinol and 7-hydroxycitronellal **57** under 4-toluenesulfonic acid catalysis using microwave irradiation (Scheme 15). The reaction conditions gave higher yields in short reaction times (<3-7 minutes) compared to the same reaction but under acidic conditions (Sardjono *et al*., 2018).

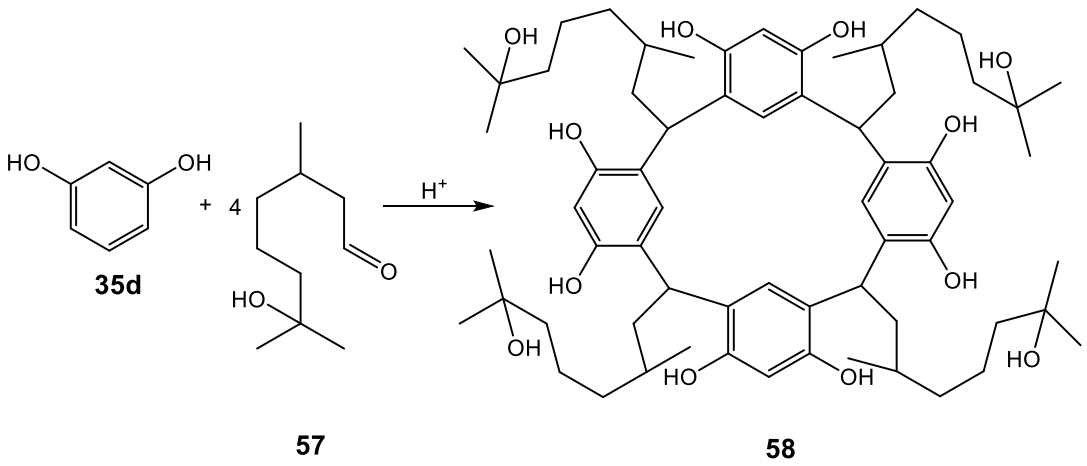

Scheme 15: Synthesis of *C*-3,7-dimethyl-7-hydroxycalix[4]resorcinarene (Sardjono *et al*., 2018)

As mentioned beforehand, amphiphilic cyclophanes have a specific association style which is different from conventional surfactants which can be considered as being between that for classical surfactants and biological molecules. Analogues of these cyclophanes have been synthesised by modifying the macrocyclic scaffolds. Calix[n]arene molecules open the field to extend the range of intermolecular interactions leading to association by attaching functional groups on both rims of calix[n]arenes. Therefore, calix[n]arenes

present enormous possibility for the design of supramolecular assemblies. It is also worth noting that the introduction of different substituents onto calix[4]resorcinarene scaffolds modulates their capacity and selectivity for complexing ions (Hidayat *et al*., 2007), organic molecules (Pollok *et al*., 2017; Puttreddy *et al*., 2017), heavy metals (Jumina *et al*., 2019) and increased antioxidant activity (Li *et al*., 2017). Alongside this, different types of nanostructures such as micelles, vesicles, fibers and capsules can be formed (Ryzhkina *et al*., 2004; Kazakova *et al*., 2004; McKinlay *et al*., 2005; Sun *et al*., 2008; Syakaev *et al*., 2008).

1.2.2.2 Synthesis of water soluble calix[4]resorcinarene

Functionalisation of calix[4]resorcinarenes *via* reaction with hydroxyl groups on the upper rim increases the size of the calix[4]resorcinarene cavity, thus developing the ability and selectivity to form complexes with guest compounds. The introduction of hydroxyethyl groups into the molecular structure of a calix[4]resorcinarene amphiphile may also simplify the hydrogen bonding contribution to the self-assembly. Thus, the formation of supramolecular architectures can change dependent on the equilibrium between the hydrophilic and lipophilic properties of calix[4]resorcinarenes.

The synthesis of octa-2-hydroxyethyl calix[4]resorcinarenes **60a-f** has been achieved by the acid catalysed reaction of 1,3-di(2-hydroxyethoxy) benzene **59** with different alkyl aldehydes (Scheme 16). Their association properties in mixed water-organic solvent systems and their ability to solubilise a model dye and drugs have been explored. It was found that the association behaviour and surface properties of calix[4]resorcinarenes is depended on their structure and the co-solvent nature. Only pentyl substituted calix[4]resorcinarene shows

surface activity in water-DMSO and water-DMF mixtures, while no surface activity happens in the mixed water-THF solution. Calix[4]resorcinarenes of poor hydrophobicity associate *via* open pattern and form large aggregates (D_H ca. 300–400 nm), while, calix[4]resorcinarene of higher hydrophobicity associate through closed pattern with formation small micelle-like aggregates (ca.10–20 nm) (Pashirova *et al*., 2014).

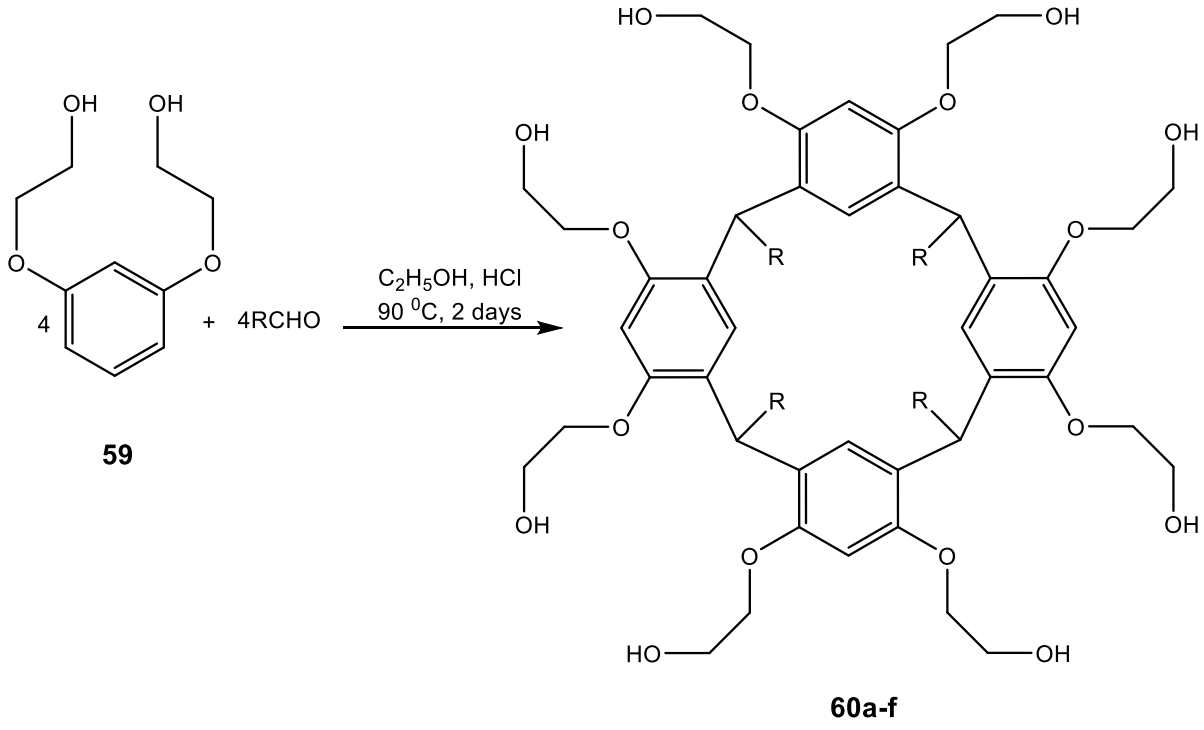

a: R= C_2H_5; **b**: R= *n*-C_5H_{11}; **c**: R= *n*-C_7H_{15}; **d**: R= *n*-C_8H_{17}; **e**: R= *n*-C_9H_{19} and **f**: R= *n*-$C_{11}H_{23}$

Scheme 16: Synthesis of octa-2-hydroxyethyl calix[4]resorcinarenes **60a-f** (Pashirova *et al*., 2014)

It has been shown that the interaction between Fe(II) or Fe(III) ions with *π*-faces of aromatic biomolecules, plays a crucial role in physiological processes (Ma and Dougherty 1997). On this basis, the synthesis of a host molecule and the ability to complex a phenol (guest) by the assistance of Fe(II) ions has been investigated in aqueous solvents using quantum-chemical and

photoluminescence (PL) methods (Kunsági-Máté *et al*., 2004). The host *C*-methyl calix[4]resorcinarene octacarboxylate **62** has been prepared by the hydrolysis of the octaester-*C*-methyl calix[4]resorcinarene **61** in refluxing alcoholic potassium hydroxide (Scheme 17) (Iwanek 1998).

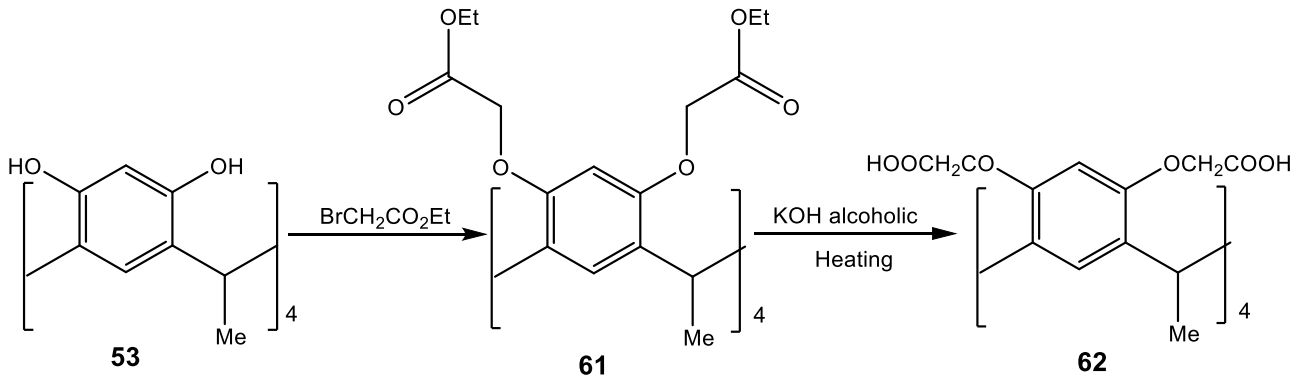

Scheme 17: Synthesis of *C*-methyl calix[4]resorcinarene octacarboxylate (Iwanek 1998; Kunsági-Máté *et al*., 2004)

The result showed that calix[4]resorcinarene octacarboxylate forms 1:2 stoichiometric complexes with phenols in aqueous media at room temperature, and the strength of complexation reduces in solvents which possess high permittivity. However, previous investigations suggested that Fe(II) ions prefer coordination to the aromatic ring of compound **62** *via* cation-π interactions rather than the carboxylate units of the molecule (Kunsági-Máté *et al*., 2003), thus, they are able to raise slightly the weak (π-π) interaction between the host and the guest. Consequently, the aqueous soluble calix[4]resorcinarene octacarboxylate constitute stable complex (sandwich-like) with the phenol by the aid of Fe(II) ions (Kunsági-Máté *et al*., 2004).

Three water soluble *N*-Alkyl ammonium calix[4]resorcinarene chloride receptors **66**, **68** and **70** bearing four terminal hydroxyl groups at the lower rims were prepared *via* Mannich condensation reaction of calix[4]resorcinarene **64** with amines (ethanolamine, cyclohexyl amine and benzyl amine) in the presence of an excess of formaldehyde to form tetrabenzoxazines **65**, **67** and **69**. Ring opening of the tetrabenzoxazines under reflux in an acidic medium gave **66**, **68** and **70** (Scheme 18). The receptor **66** is also functionalised with four terminal hydroxyl groups at the upper rims, rendering it more water soluble (35 mg/mL). The receptor **68** possesses four rigid cyclohexyl fragments at the upper rims, and the other receptor **70** is functionalised with four benzyl fragments at the upper rims.

These receptors with varying hydrophilicity of the substituents on the upper rim exist in the crown conformation (C_{4v}) as noticed from their ^{1}H-NMR spectra. The study also demonstrated stabilisation of these compounds in water by possessing a hydrophobic cavities and hydrophilic (cation-anion) interaction on the upper rim.

The complexation properties of receptors with three water soluble viologen derivative guests were investigated using Isothermal Titration Calorimetry (ITC), NMR and fluorescence studies in water. ITC analyses showed binding constants of 10^{3} M^{-1}. The hosts showed higher affinity towards guests with acetylmethyl group over the methyl viologen guest due to the hydrogen bonding interaction between (cation-anion) of the host and carbonyl groups of the guest (Beyeh *et al*., 2017).

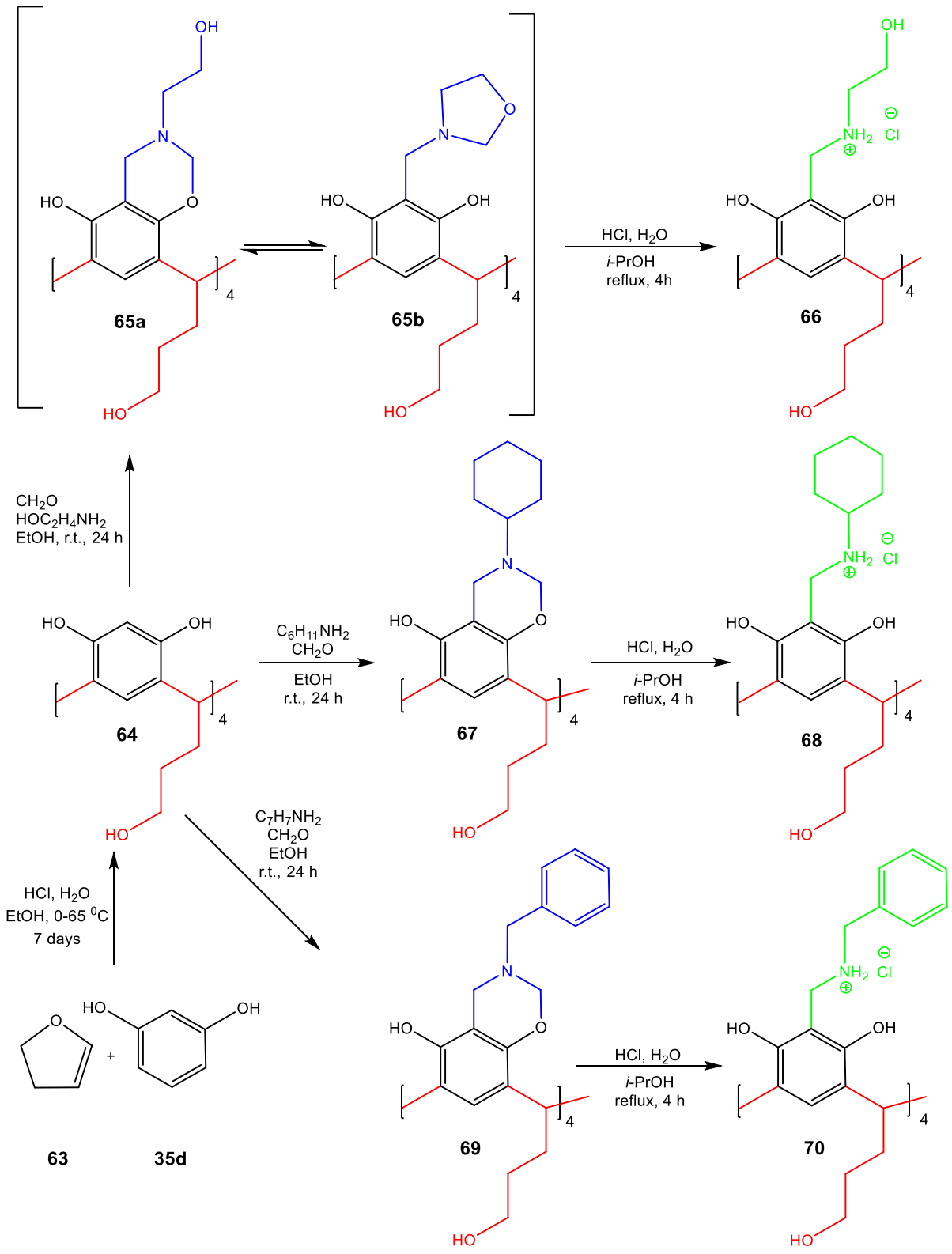

Scheme 18: Synthesis of water soluble *N*-Alkyl ammonium calix[4]resorcinarene chlorides (**66**, **68** and **70**) (Beyeh *et al*., 2017)

1.2.2.3 Calix[4]resorcinarenes in drug delivery and biocompability

Nanotechnology not only has shown a great promise in different fields of science and technology, it also has biomedical relevance in the therapy and diagnosis of varied disease states (Banerjee 2018). Nanotechnology in drug delivery has opened new field of nanosized carriers of size ≤100 nm with various abilities and applications. Drug delivery systems are used to enhance the solubility, alter the biodistribution of their drug loads or particularly to monitor the period and rate of drug loading and release (Valand *et al*., 2015).

Drug carriers are specifically synthesised for targeting specific tissues, cells or organs of the human organism and to trigger release of the cargo such as drug, diagnostic reporter or gene molecule upon arrival to their target site (Sinha *et al*., 2006). These carriers work in a stimulus reactive manner depending on external or internal stimuli (pH or temperature variation) that can alter the ability of the carrier to release the cargo (Morozova *et al*., 2016). Drug delivery systems have also been created to improve the efficacy and safety of administration of toxic therapies, especially anticancer drugs. Integration of cage-like molecules in nanoparticle drug carriers is expected to increase their capability to efficiently combine drugs by creating strong host-guest inclusion, and minimize premature drug release due to absence the affinity among the carrier and the drug molecule (Zangabad *et al*., 2017).

Nanocontainers based upon amphiphilic molecules incorporate these features and are able to enhance the solubility of poorly soluble drugs in aqueous media. At increased concentrations, micelles form spontaneously from the self-aggregation of amphiphilic molecules, the hydrophobic part of amphiphilic

molecule forming the micelle core, while the hydrophilic parts form the shell of the micelle. When used as a drug carrier, the micelle solubilises nonpolar drugs *via* encapsulation within the micelle core, whereas the hydrophilic part ensures the system retains stability in solution (Morozova *et al*., 2018).

A series of amphiphilic carboxycalix[4]resorcinarenes **71a-f** with varying hydrophobicity was made with different substituents at the lower rim (Figure 15) and used to investigate the solubility of an azo-derivative of isatin **72** bearing an ammonium group in aqueous solution. It was observed that the isatin derivative has antimicrobial activity (Syakaev *et al*., 2018).

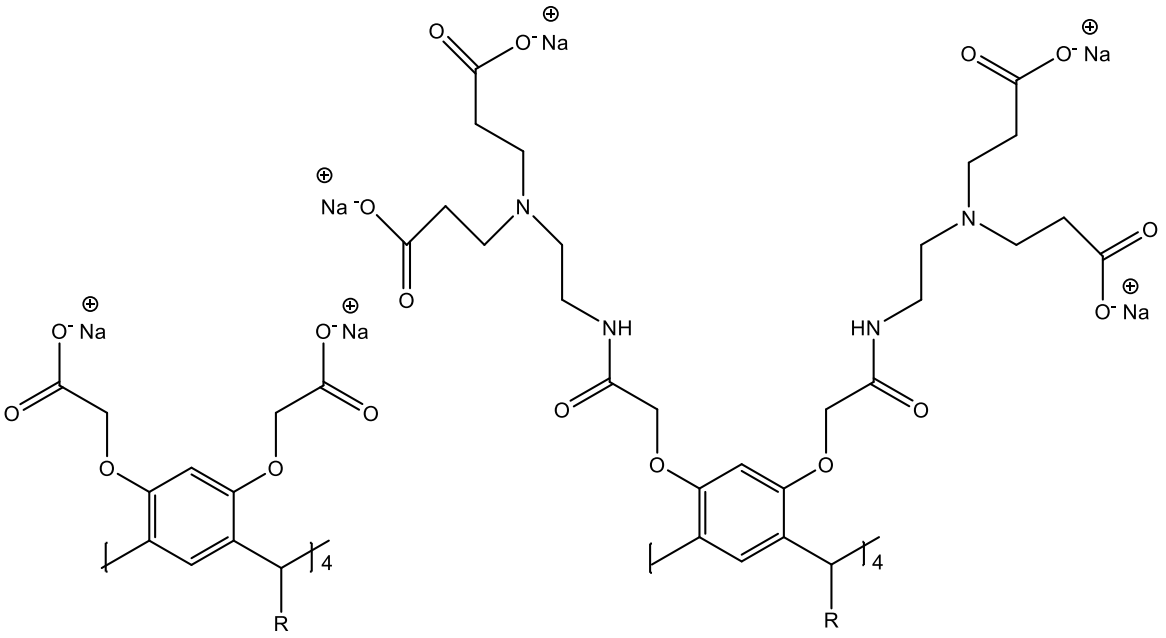

Cn-CR

71a: C_5-CR R= C_5H_{11}
71b: C_5OPh-CR R= 4-C_6H_4-*O*-C_5H_{11}
71c: C_8-CR R= C_8H_{17}
71d: C_{11}-CR R= $C_{11}H_{23}$
71e: C_{12}OPh-CR R= 4-C_6H_4-*O*-$C_{12}H_{25}$

71f: C_5-*N*-CR R= C_5H_{11}

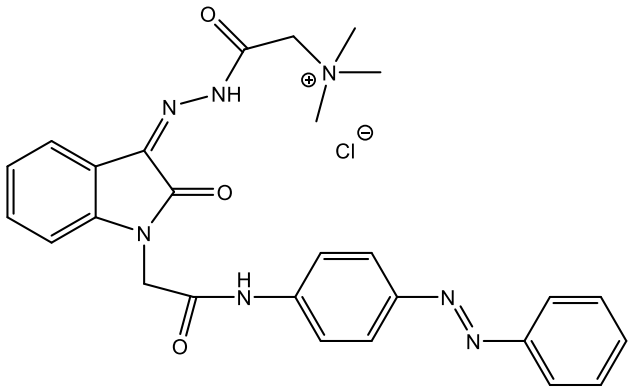

72

Figure 15: Structures of carboxycalix[4]resorcinarenes and the isatin drug

(Syakaev *et al*., 2018)

The toxicity of the macrocycles **71a-f** is characterised by low haemotoxicity at a solution concentration of 0.5 mM, with the exception of C_8-carboxyresorcinarene which showed reduced toxicity with dilution. The low haemolytic toxicity of carboxyl-substituted calix[4]resorcinarenes is probably due to the existence of the ionic head groups in the structure. As a consequence of this low toxicity, such calix[4]resorcinarenes can be used for the construction of supramolecular systems for solubilisation of therapeutic agents (Syakaev *et al*., 2018).

In aqueous solution, the macrocycles self-associated and solubilised the isatin derivative by inclusion of it into the hydrophobic part of the molecule (amongst the lower rim substituents). It was observed that the solubilisation effect increases with changing the structure and length of hydrophobic part of macrocycles. In the case of C_5-carboxyresorcinarene **71a** and compound **71f**, the macrocycle cannot provide enough hydrophobic microenvironment for the isatin and the existence of ions in solution hinders the efficient interaction and solubilisation. The most significant self-association was observed for the C_{11}-carboxyresorcinarene, which increased the solubility of substrate only slightly due to more dense surface charge which reduced the permeability of the substrate into the hydrophobic part. The C_{12}-*O*-Ph-carboxy calix[4]resorcinarene self-associates due to the presence of oxy-phenylene groups at the lower rim, increasing the solubility of isatin by additional π-π interaction. Finally, C_8-carboxyresorcinarene and C_5-*O*-Ph-carboxyresorcinarene showed the highest loading ability for the isatin derivative; the increased hydrophobicity in the co-associates of the macrocycles with substrate led to the formation of a large supramolecular system through a clustering effect (Syakaev *et al*., 2018).

Calix[4]resorcinarene substituted with *N*-methylethanolamine residues on the upper rim and ethylsulfonate groups on the lower rim (Figure 16) was used to facilitate the release hydrophobic drugs, including antitumour drug 2,2'-bibenzimidazole (BBI) and Sudan I from ionic surfactant cetyltrimethylammonium bromide (CTAB) micelles.

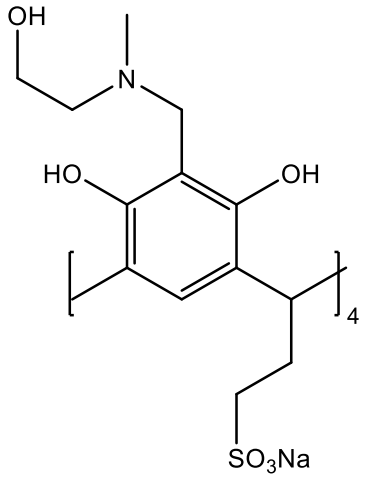

73

Figure 16: Molecular structure of calix[4]resorcinarene (Kashapov *et al*., 2016)

In aqueous solution, calix[4]resorcinarene self-assembles into vesicles of different shapes and sizes. The driving force for the self-assembly is probably due to noncovalent interactions and π-stacking of the aromatic walls, together with the strong hydrogen bonding interaction between the hydroxyl groups and the methylated ethanolamine.

The addition of calix[4]resorcinarene **73** to surfactant micellar solution of CTAB results in the electrostatic interaction between lower rim substituents of the calix[4]resorcinarene and surfactant head group, which may trigger the transformation from spherical micellar to vesicles structure. It was noticed that the small globular micelles convert into vesicles upon the addition of a small amount of calix[4]resorcinarene, which enhances the rapid and complete

release of the sequestered hydrophobic drugs from CTAB in response to **73** (Kashapov *et al*., 2016).

Generally, calix[4]resorcinarenes with long alkyl chains on the lower rim exist in the cone or boat conformation of the macrocycle, which leads to self-association of calix[4]resorcinarene into micelle-like aggregates. One of the ways to increase the aqueous solubility of calix[4]resorcinarene and to reduce its toxicity is by introducing hydrophilic substituents such as polyethyleneglycol, polycaprolactone and polylactic acid residues which are known to be biocompatible. The modulation of calix[4]resorcinarenes with such groups leads to formulation hyperbranched three-dimensional structures with higher aqueous solubility and low viscosity.

Polyethyleneglycol has good water solubility and low toxicity which in turn makes it the most employed polymer in the production of different therapeutic agents and nanomaterials. Thus, conjugation of polyethyleneglycol and calix[4]resorcinarene will produce an amphiphilic structure with increased binding features and hence lead to increase in the time to release the drug captured by calix[4]resorcinarene-PEG conjugated micelles, tetraundecylcalix[4]resorcinarene **74** bearing methoxy polyethyleneglycol chains at the upper rim has been synthesised to investigate this purpose (Figure 17) (Ermakova *et al*., 2018).

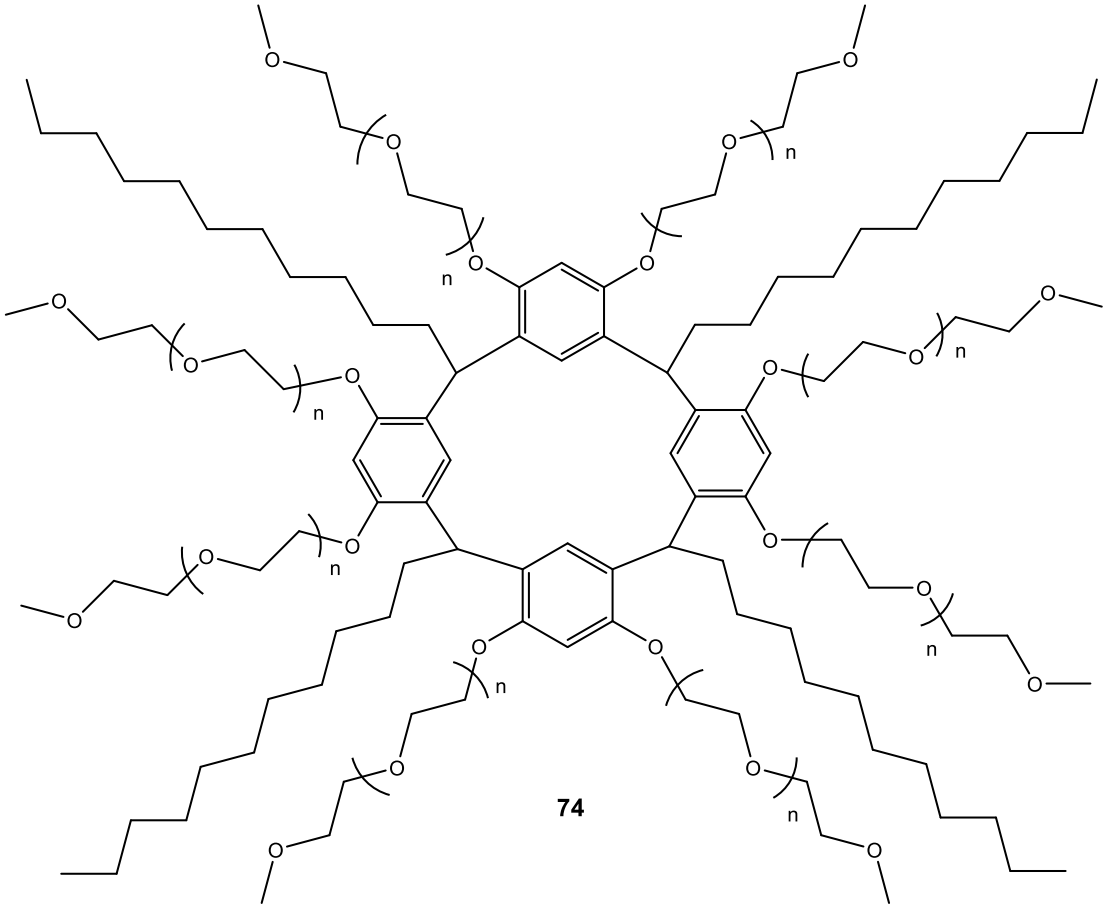

Figure 17: Tetraundecylcalix[4]resorcinarene–methoxy PEG conjugate

(Ermakova *et al*., 2018)

In aqueous solution, they are able to self-associate and form small micellar structures with average diameters of 9-18 nm. In phosphate-buffered saline solution or in physiological sodium chloride solution, these compounds form multimicellar associations with averaged diameters of 142-164 nm and become thermo-responsive (Figure 18). The obtained macrocycle exhibits low haemolytic toxicity. It is able to encapsulate various hydrophobic organic substrates, including drugs (naproxen, doxorubicin, ibuprofen and quercetin). The encapsulation occurs by permeation of the drug molecule into the micelles and further interaction with the aromatic hydrophobic wall of the macrocycle. This leads to slow release of substrate *in vitro*. Temperature-dependent release

of doxorubicin from the micelles was demonstrated by heating the supramolecular drug container in 0.9% NaCl solution (Ermakova *et al*., 2018).

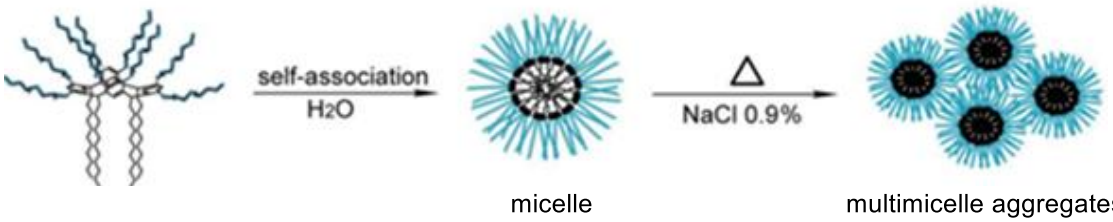

Figure 18: Proposed scheme of macrocycle self-association (Ermakova *et al*., 2018)

Sulfonatomethylated calix[4]resorcinarenes with various lengths of hydrophobic chains on the lower rim (methyl, pentyl, heptyl) act as hosts to a number of biologically active compounds with different physico-chemical properties (Figure 19). Aliphatic, aromatic and cationic guests were chosen to study the effect of sizes, polarities, shapes, charge character and symmetry on the aggregation process with the influence of solvent on these systems. The guests used included dimephosphon, xymedon, tetramethylammonium bromide, choline, tyramine, neurotransmitters theophylline, tetrabutylammonium chloride, 1-methyl-4,4'-bipyridinium phosphorus hexafluoride and methylviologen (Syakaev *et al*., 2012).

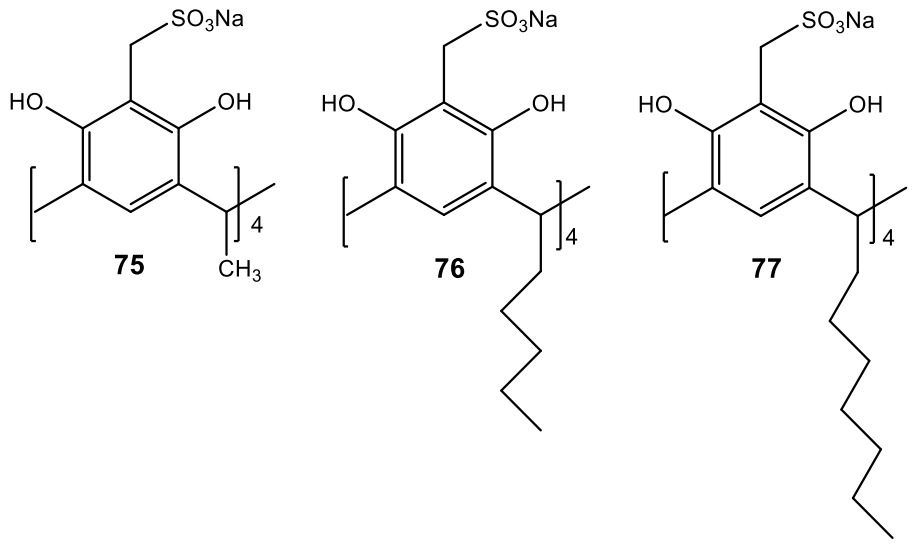

Figure 19: The chemical structures of sulfonatomethylated calix[4]resorcinarenes (Syakaev *et al*., 2012)

It was noticed that quite small changes in the length of the hydrophobic chain on the lower rim of calix[4]resorcinarene can alter their aggregation properties. While calix[4]resorcinarene with pentyl moieties form head to tail structures when packed, calix[4]resorcinarene with heptyl substituent is aggregated into micelle-like structures in water and water-methanol solutions. There was no evidence of aggregation of sulfonatomethylated calix[4]resorcinarene with a methyl group on the lower rim. The solubilising of guest molecules was more efficient by aggregation of calix[4]resorcinarene with pentyl moieties due, in this case, to two calix[4]resorcinarenes forming a capsule for inclusion of the guest molecules. The association with guest molecules by the aggregation of the host with pentyl tail on the lower rim was increased for uncharged guests, whereas there was nearly complete binding of the ammonium cation. The formation of host-guest complex may lead to an increase or decrease in the size of the aggregates with preservation of the head to tail packing mode of calix[4]resorcinarenes **76** (Syakaev *et al*., 2012).

Mycophenolate mofetil (MMF) is an effective immunosuppressive agent that does not cause reduction of bone marrow activity and is important in treatment of inflammatory glomerular disease. The drug is practically insoluble in water (43 µg mL^{-1}). Sulfonatocalix[4]resorcinarene **78** was chosen to interact with MMF in order to improve its solubility and dissolution rate in aqueous media with changing the bioavailability. In the solid state the inclusion complexes was proved using aqueous phase solubility studies, HPLC, Thermal analysis, Powder X-ray diffraction studies, UV-Vis and FT-IR spectroscopy (Menon *et al*., 2011).

The result referred to the formation of an inclusion complex between MMF: Sulfonatocalix[4]resorcinarene at a 1:2 ratio with stability constant 2285 M^{-1} in aqueous solution (Scheme 19). FT-IR studies did not show any significant differences indicating that no new chemical bond was produced in the complex. Differential Scanning Calorimetry and X-ray studies showed reduced crystallinity of the complex (drug: sulfonatocalix[4]resorcinarene). This was apparent from the absence of an endotherm in the DSC thermogram and no diffraction peaks in the X-ray diffractogram as compared to those in the physical mixture of each substrate alone. *In vivo* studies showed reduced toxicity of the pure drug MMF after complexation with an increase in the LD_{50} value of the complex as compared with the reported LD_{50} value of the free drug (Menon *et al*., 2011).

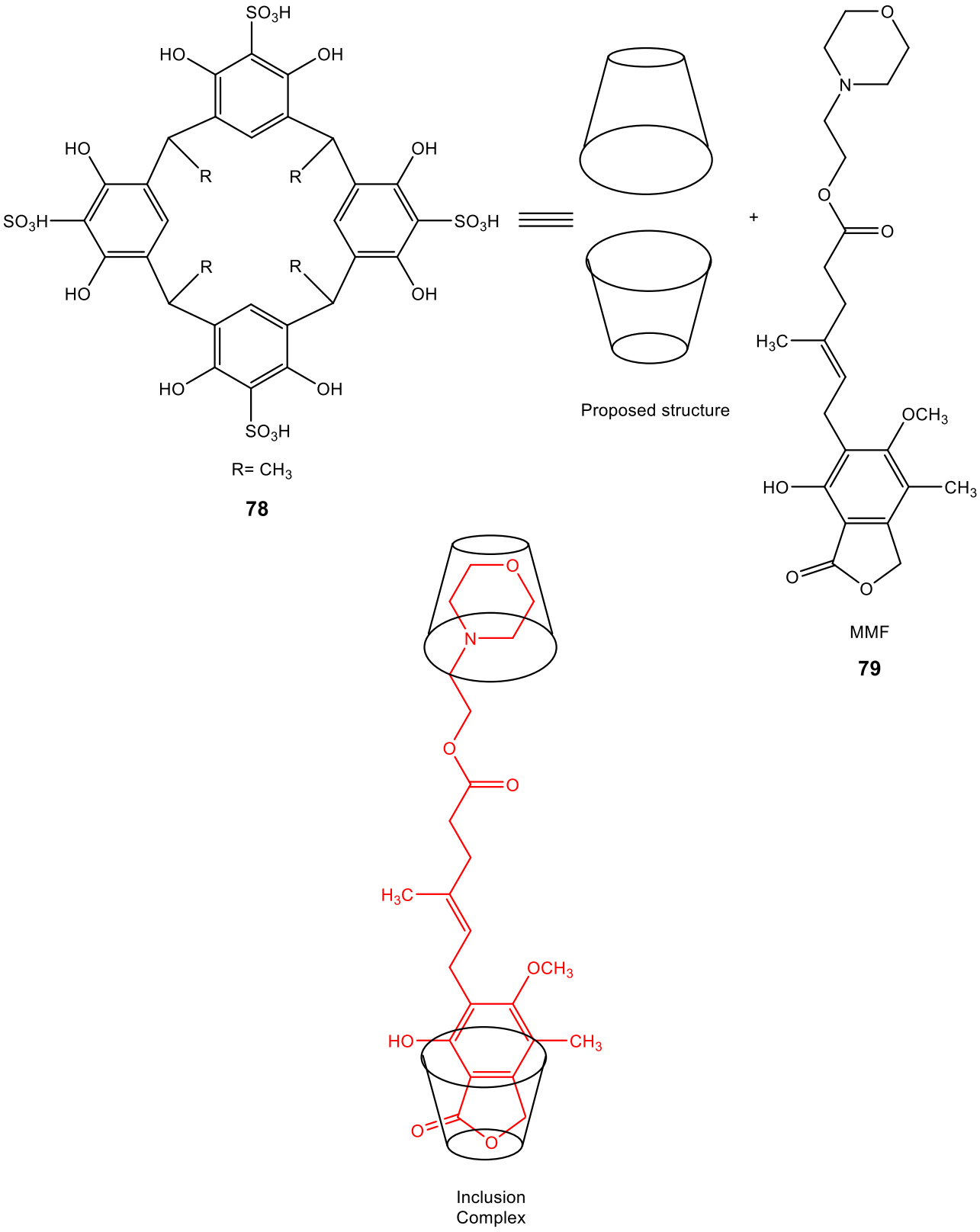

Scheme 19: Inclusion complex of mycophenolate mofetil: sulfonatocalix[4]resorcinarene (1:2) (Menon *et al*., 2011)

Patel *et al*. prepared the inclusion complex between the anticonvulsant drug lamotrigine **80** with sulfonatocalix[4]resorcinarene **78** and investigated the dissolution properties of the drug in the complex. The inclusion complex in the solid state was studied by various analytical techniques comprising PXRD, FT-IR and DSC. Studies also included the solubility of the drug *versus* the complexed species in the aqueous phase, and *in vitro* and *in vivo* release of the drug was studied (Patel *et al*., 2013).

The result of their studies showed the formation (1:1) inclusion complex of sulfonato calix[4]resorcinarene: lamotrigine with a stability constant of 854.1 M^{-1} in water (Scheme 20). The FT-IR spectra showed the absence the free amino groups of the drug and formation intermolecular hydrogen bonding between the drug and the carrier. The X-ray diffractogram studies showed reduced crystallinity of the drug in the complex as compared with those in the physical mixture of each pure compound. The acute toxicity studies showed that after complexation the toxicity of the pure drug lamotrigine decreased and the inclusion complex did not show any mortality up to 450 mg kg^{-1} in mice (Patel *et al*., 2013).

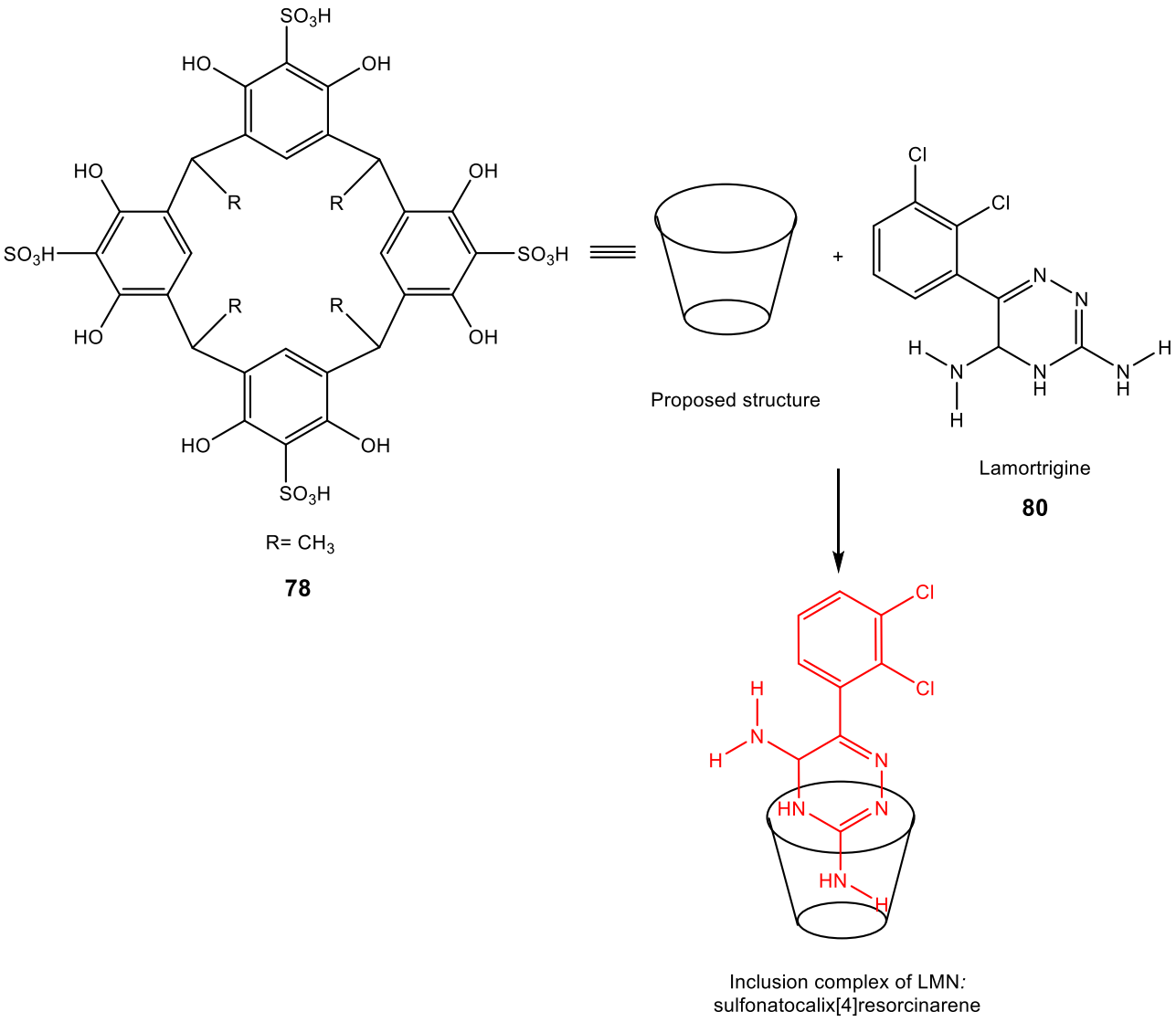

Scheme 20: Inclusion complex of sulfonatocalix[4]resorcinarene: lamotrigine

(Patel *et al*., 2013)

1.2.2.4 Calix[4]resorcinarene glycosides

Various drug delivery systems have been evaluated and developed to enhance the therapeutic efficiency of cancer treatments, but there remain challenges associated with limited transportation efficacy of drugs to the target tissues and also some types of cancer have progressed resistance towards anticancer therapies (Pillai 2014; Soni *et al*., 2017).

Many strategies have been recognised to improve drug delivery systems that preferentially and selectivity deliver the dosage to the target cells and reduce the delivery to non-target sites (Jain *et al*., 2017). For this objective, one of the more obvious methods for drug targeting is the use of ligands that will overcome the undesirable toxic effects related to the conventional drug carriers. Glycosidic ligand structures have been combined with different nanocarriers to investigate tumour-targetting due to aberrant glycosylation in tumour cells (Cai *et al*., 2018). Besides targetting the drug, carbohydrates conjugated with different carriers like dendrimers, liposomes, nanoparticles, *etc.* may also offer other varied beneficial features, including biostability, bioadhesion, enhanced aqueous solubility as well as reduced toxicity (Latxague *et al*., 2018).

Calix[4]resorcinarenes appended with monosaccharides on the upper rim and long alkyl chain on the lower rim were introduced in the late 1990s (Fujimoto *et al*. 1997). These compounds form (1:1) stable inclusion complexes with guests in water. Such guests include fluorescent dyes and 8-anilinonaphthalene-1-sulfonate (ANS). The carbohydrate residues form hydrogen bonds with ConA-Sepharose gel and allow absorbance of the complex on a silica surface (Figure 20). The uptake system of calix[4]resorcinarene galactoside with a fluorescent dye as a guest can be delivered to hepatocytes that contain asialoglycoprotein

receptors on the surface which recognize the terminal galactose; the specific binding was confirmed by fluorescent microscopy (Fujimoto *et al*., 2000).

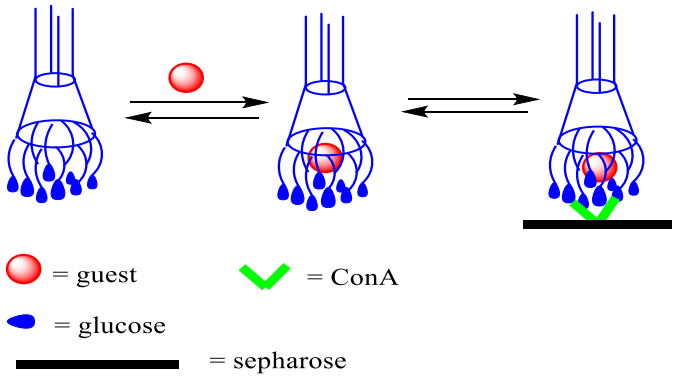

Figure 20: The use of calix[4]resorcinarene glucosides to deliver guest molecule to the surface of sepharose gel immobilised Con A *via* forming a ternary complex between the host/guest with the Con A-immobilised on the gel (Delbianco *et al*., 2015)

In general, the success of gene treatments depends upon the evolution of new effective gene delivery vehicles. The groups of Aoyama (Aoyama *et al*., 2003; Aoyama 2004) and Ungaro (Sansone *et al*., 2006) have developed calix[4]arenes and calix[4]resorcinarenes as gene delivery vectors (Ortiz Mellet *et al*., 2010).

Aoyama and co-workers (Aoyama 2005) synthesised calix[4]resorcinarene amphiphiles **81-83** having eight disaccharide units (lactose, cellobiose or maltose) and long hydrophobic chains (Figure 21a). In water, these compounds **81-83** were found to undergo irreversible aggregation into micellar nanoparticles of size 4.3-4.8 nm and an aggregation number about of 6 molecules per micelle (Aoyama *et al*., 2003; Nakai *et al*., 2003). The driving force for the formation these micellar glycol-nanoparticles was ascribed to the

hydrophobic interactions among the multiple undecanoic moieties in conjunction with H-bonding between the saccharide residues (Figure 21b).

Addition of sodium phosphate led to aggregation these micellar into larger structures of diameter 50-300 nm resembling saccharide wrapped micelles. The complexation between phosphate ions and glyco-nanoparticles highlights their potential applications as gene carriers. According to gel electrophoresis data, these compounds **81-83** are able to bind DNA molecules at a ratio of 0.2-0.3 molecules per DNA molecule. This refers to a stoichiometry of two GNPs (glyco-nanoparticles) per DNA helical pitch. Glyco-nanoparticles **82** with cellobiose units in the presence of plasmid DNA can form artificial glycoviruses of about 54 nm in diameter. In contrast, glyco-nanoparticles **81** and **83** with lactose and maltose fragments form larger particles (200-300 nm). Notably, the zeta potential of glyco-nanoparticle **81-83** complexes with DNA was about 0 mV, indicating cluster saccharide residues with charge masking (Aoyama 2005).

Transfection trials on HeLa and HepG2 cells showed that cellobiose glycoviruses with a viral size up to 20 nm performed as efficient gene carriers for HeLa cells and was 1000-fold more active than maltose- and lactose-glycoviruses. In contrast, the transfection ability of lactose-coating glycoviruses was good into HepG2 cells which bear the galactose receptor (Aoyama 2009).

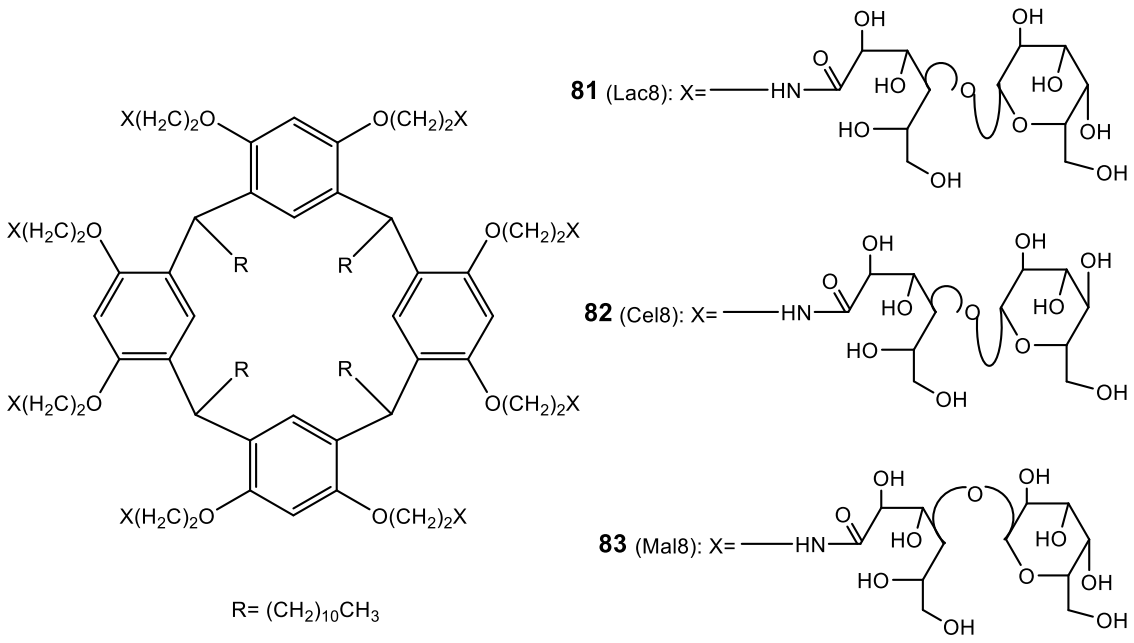

(a)

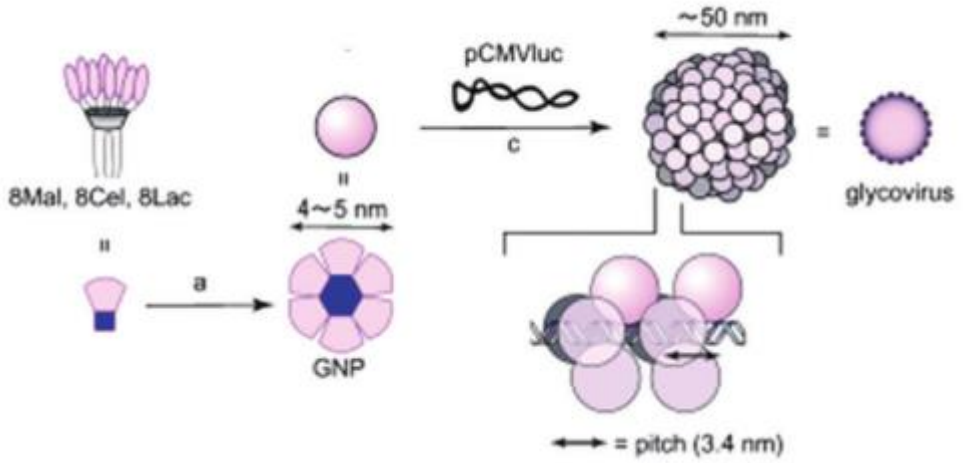

(b)

Figure 21: (a) Structures of calix[4]resorcinarene glycosides and (b) Hierarchical growth of amphiphilic calix[4]resorcinarene bearing disaccharides over glycol-nanoparticles to glycovirus (Matsuura 2018)

1.2.2.4.1 Synthesis of glycosylated calix[4]resorcinarenes

1.2.2.4.1.1 Upper rim glycosylation

Calix[4]resorcinarene glucosides with C_8-C_{13} hydrophobic alkyl chains at the lower rim and eight glucose moieties on the upper rim, in which each phenolic hydroxyl group is conjugated to the glucose residue through an ethoxy group have been synthesised (Scheme 21). The calix[4]resorcinarene glucosides thus prepared possessed enhanced scaffold flexibility and several of these amphiphiles were tested for their ability to increase the stability of four specific proteins, including a G-protein coupled receptor. All of these compounds were highly soluble in water (>10 % (w/v)) and showed micelle stability as a result of elongating the alkyl chain length, especially for calix[4]resorcinarene with C_{13} alkyl chain **86f**, the compound was completely water soluble even at 10%. These compounds were also characterised in terms of their critical micelle concentrations (CMC) and the hydrodynamic radius measured by using dynamic light scattering. The CMC values changed from 2 μM to 10 μM, these values were dropped with elongating the alkyl chain length, referring to depending CMC values on the macrocycles hydrophobicity. It was also observed that micellar formation of these glucosides of small micelle size which may also related to their flexibility (Hussain *et al*., 2017).

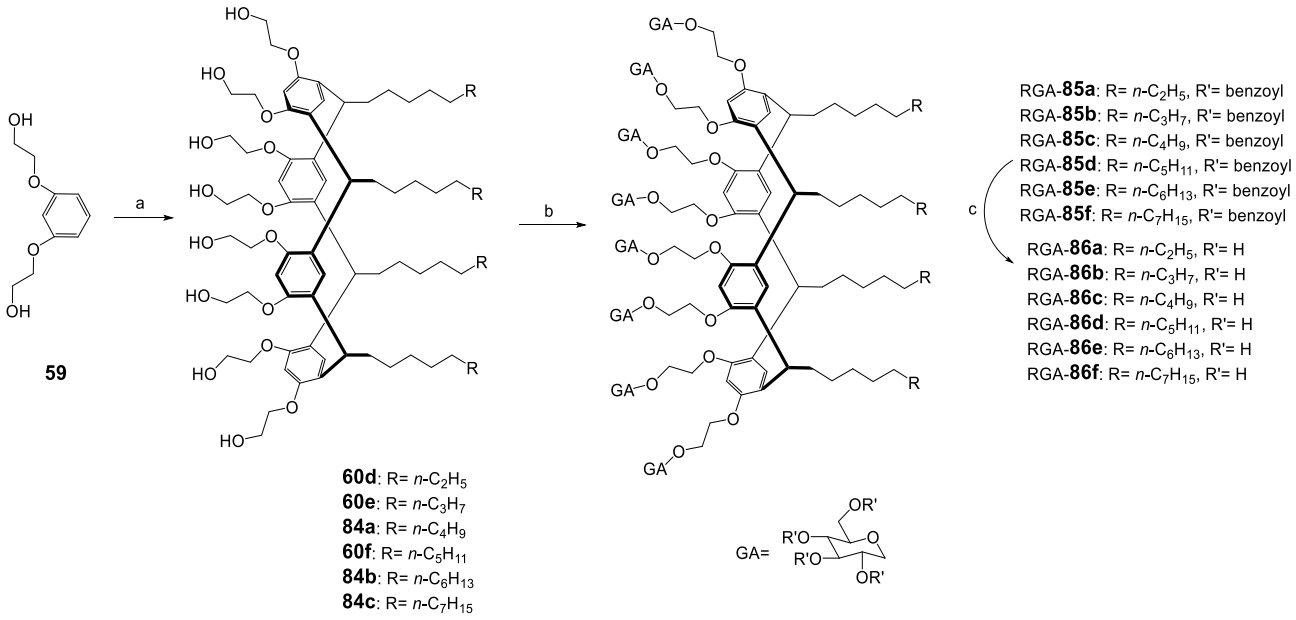

a) Aldehyde, ethanol/ HCl, 80 ^{0}C; b) AgOTf, 2,4,6-collidine, DCM, perbenzoylated glucosylbromide, 0 ^{0}C to RT; c) NaOMe, MeOH, RT

Scheme 21: Synthesis of octa-2-glucoseethoxytetraalkyl calix[4]resorcinarenes (Hussain *et al*., 2017)

1.2.2.4.1.2 Lower rim glycosylation

The synthesis of two specific topologies of tetravalent glycoclusters of calix[4]resorcinarene, the chair *rctt* and boat *rccc* stereoisomers has been reported by Soomro and co-workers (Soomro *et al*., 2011). The introduction of carbohydrate groups at the lower rim was conducted through the synthesis of calix[4]resorcinarene bearing alkynyl residues **88a** and **88b** (Scheme 22) suitable for conjugation with azide functionalised galactoside **89a** and lactoside **89b** through Cu-catalysed azide-alkyne click chemistry (CuAAC) (Scheme 23). The deprotection of the acetate groups was then carried out under methanolysis conditions to produce the desired calix[4]resorcinarene glycoclusters.

Although the glycoclusters **91** possessed limited solubility a range of techniques were used to measure the binding affinity towards lectins. The Enzyme-linked lectin assays (ELLA) results produced for the galactose glycoclusters **91aG** and **91bG** showed high affinity for *Pseudomonas aeruginosa* (PA-IL) and the topology of these glycoclusters could not cause any difference in binding features (Soomro *et al*., 2011).

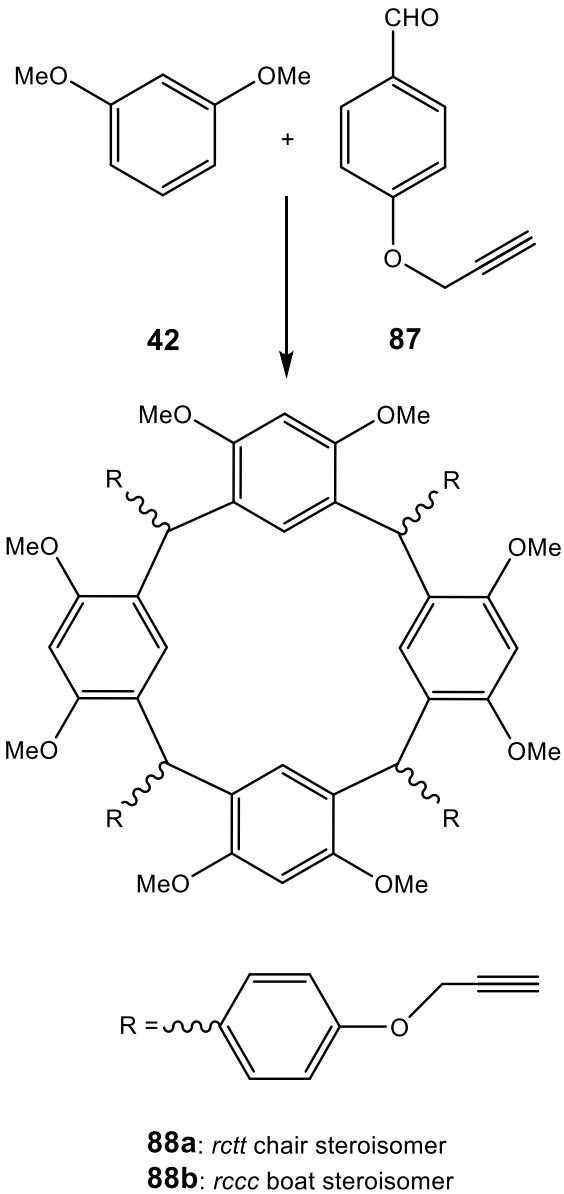

88a: *rctt* chair steroisomer
88b: *rccc* boat steroisomer

Scheme 22: Synthesis of tetrapropargylated calix[4]resorcinarenes (Soomro *et al*., 2011)

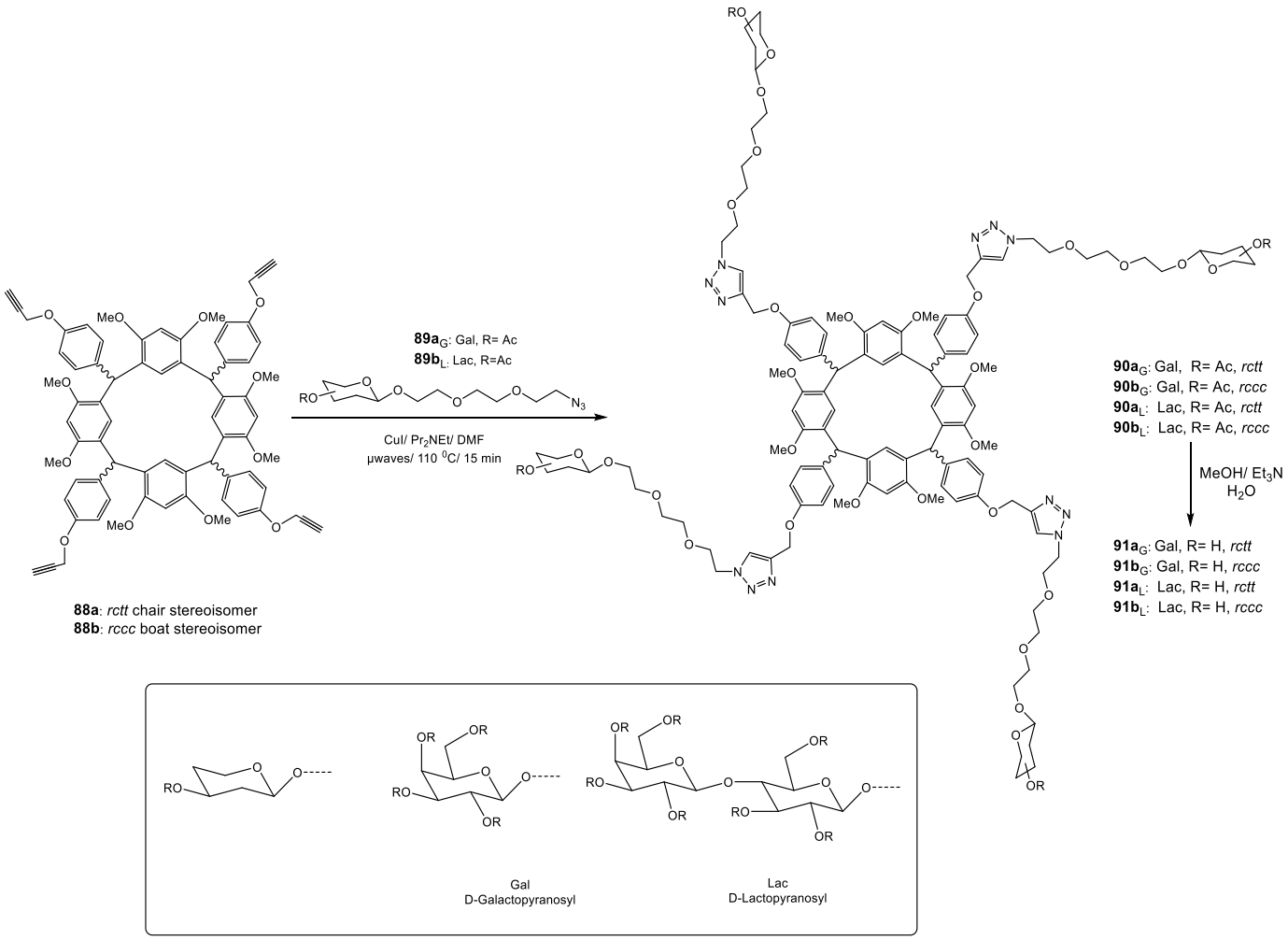

Scheme 23: Synthesis of isomeric calix[4]resorcinarene-based glycoclusters

(Soomro *et al*., 2011)

1.2.3 Calix[4]pyrogallolarenes

Calix[4]pyrogallolarene or hydroxyresorc[4]arene can be easily prepared by acid catalysed condensation of aldehydes with pyrogallol (Negin *et al*., 2014). Usually, the result is the all-*cis* (*rccc*) bowl-like cyclic oligomer, though other studies showed that the all-*cis* (boat/cone) are the kinetically stable conformers and *rctt* (chair) is the thermodynamically more stable conformer for calix[4]pyrogallolarenes. The formation of specific conformer is affected by many factors including reaction conditions, type of substituent and conformer solubility in certain solvents (Maerz *et al*., 2010; Patil *et al*., 2016).

Calix[4]pyrogallolarenes can be functionalised by changing the nature of the substituent on the aldehyde starting materials, which may later assist modification of the lower rim of the cyclic tetramer. On the upper rim, hydroxyl groups are the obvious site for chemical reactions: they can be modified with phosphoryl groups (Nikolelis *et al*., 2009), acetyl hydrazine groups (Podyachev *et al*., 2007), carboxymethyl groups (Pod *et al*., 2004) and imidazolium groups (Kim *et al*., 2004). It is noteworthy that studies involving the *O*-acetylation of calix[4]pyrogallolarenes with acetic anhydride in pyridine showed that the chair conformation is the main product of the reaction and the reaction conditions do not induce conformational changes if the conformation is originally fixed in chair conformer (Han *et al*., 2007; Yan *et al*., 2007; Waidely *et al*., 2015). However, in these studies there is no evidence to the formation crown conformer from these reactions.

In order to prove what happens to the crown conformation, Casas-Hinestroza and Maldonado, in their studies showed that the resulting acid catalysed condensation reaction an equal amounts of benzaldehyde and pyrogallol in

ethanol, *C*-tetra(phenyl)calix[4]pyrogallolarene was obtained as a mixture of two conformations in the ratio of 43% crown to 57% chair (Scheme 24), Acetylation of a mixture of *C*-terta(phenyl)calix[4]pyrogallolarene crown and chair conformers, showed that the chair conformer keeps its conformation, while the cone changed to boat conformation. ^{1}H-NMR experiments at different temperatures showed that increased conformational changes reduce the ability to separate the conformers. Alterations of substituents on the lower rim provides different conformer ratios due to differing interactions, with considerable differences in the nature of substituents on calix[4]pyrogallolarene lower rim providing equally considerable variation in conformer ratios (Casas-Hinestroza and Maldonado 2018).

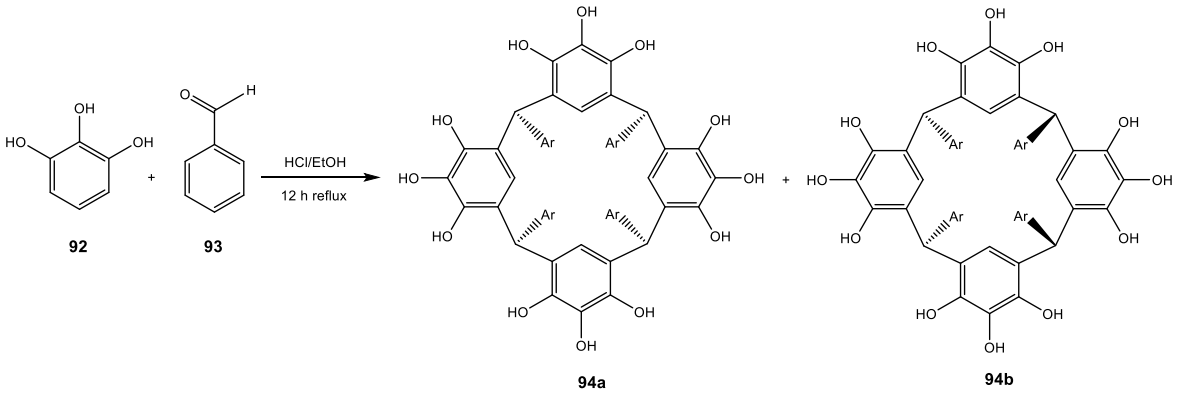

Scheme 24: Synthesis of *C*-tetra(phenyl)calix[4]pyrogallolarene (Casas-Hinestroza and Maldonado 2018)

The presence of twelve hydroxyl group on the upper rim exhibits high polarity, π-rich cavity and their favourable structure has led to calix[4]pyrogallolarenes being widely used as a starting material in the synthesis of carcerands (Chopra and Sherman 1997), in complexation studies (Pfeiffer *et al*., 2014) and in the synthesis of liquid-crystal material (Cometti *et al*., 1990).

Calix[4]pyrogallolarenes self-assembled into large nano-capsules or supramolecular structures have been studied in the solid state and in solution based on inter- or intramolecular hydrogen bonding (Journey *et al*., 2017; Wang *et al*., 2018). Generally, the twelve hydroxyl groups lead to stabilisation of calix[4]pyrogallolarene assembly by hydrogen bonds and consequently a number of guests such as solvents, ammonium salts, hydrocarbons, metal ions and other organic molecules can be entrapped in to the large cavity (Bowley *et al*., 2014; Beyeh *et al*., 2015; Galan and Ballester 2016; Zhang *et al*., 2017).

Calix[4]pyrogallolarenes have been used for stabilisation of active species by using cocrystallisation method. Stabilisation of these species has attracted increased attention, by which not only confer us to store and characterise these active species but also to their potential applications as catalysis reactions and as drug delivery. For example, a pharmaceutical gabapentin largely used in the treatment of neuropathic pain and epilepsy, has been employed in such cocrystallisation process with calix[4]pyrogallolarenes as both compounds have hydrogen bond donating and accepting regions result in the formation of cocrystals with increased pharmaceutical properties to assist targeted drug delivery, improve bioavailability, solubility, staibility and dissolution rates compared to that of the drug alone (Fowler *et al*., 2011; Fujisawa *et al*., 2018; Spiel *et al*., 2018).

1.2.4 Cavitands and carcerands

Cavitands are synthetic molecules that possessing enforced cavities, molecular vessels with a large size able to accommodate other organic molecules, ions or atoms inside their cavity and then trigger them in a dynamic balance with the solvent (Figure 22). In the early 1980s, Cram prepared cavitand from calix[4]resorcinarene by linking the hydroxy groups of relative aromatic rings of one or two atoms with covalent linkages giving rigid receptor, has been widely studied in supramolecular chemistry (Cram 1983; Nguyen *et al*., 2018).

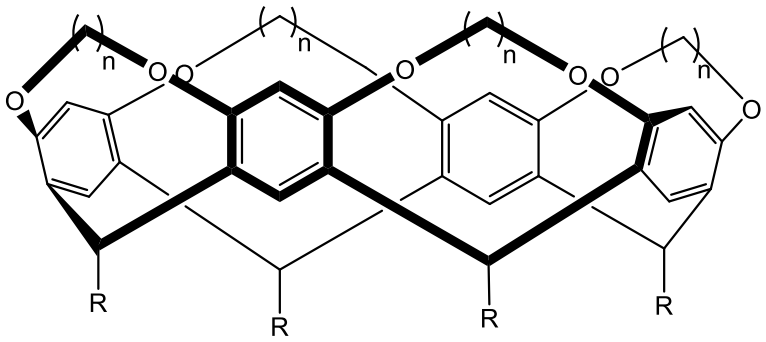

n= 1, 2

Figure 22: Calix[4]resorcinarene cavitand structure

The chemical linking of two cavitand molecules *via* the substituents existed in 2-position to the main resorcinol hydroxyl lead to formation rigid three-dimensional structures called either carcerands (Figure 23) or hemicarcerands relying on the number of bridges created among the two cavitands and present or absence the pores in the hollow structure by which the guest molecules are able to enter or release (Cram 1988; Cram 1983).

Carceplexes are the inclusion complexes of one or two guest molecules of the solvent used in the last step of the carcerand synthesis because the dimensions of the cavity opening are too small making strong steric hindrances for guest escaping. While carcerands formed by coupling two cavitand

molecules of four bridges, Hemicarcerands are missing one or more bridges of the carcerand molecule, guests are more freely for mobile exchange in solution, thus, the chemical properties of hemicarcerands similar to cavitands more than to carcerands (Nuwaysir *et al*., 1992).

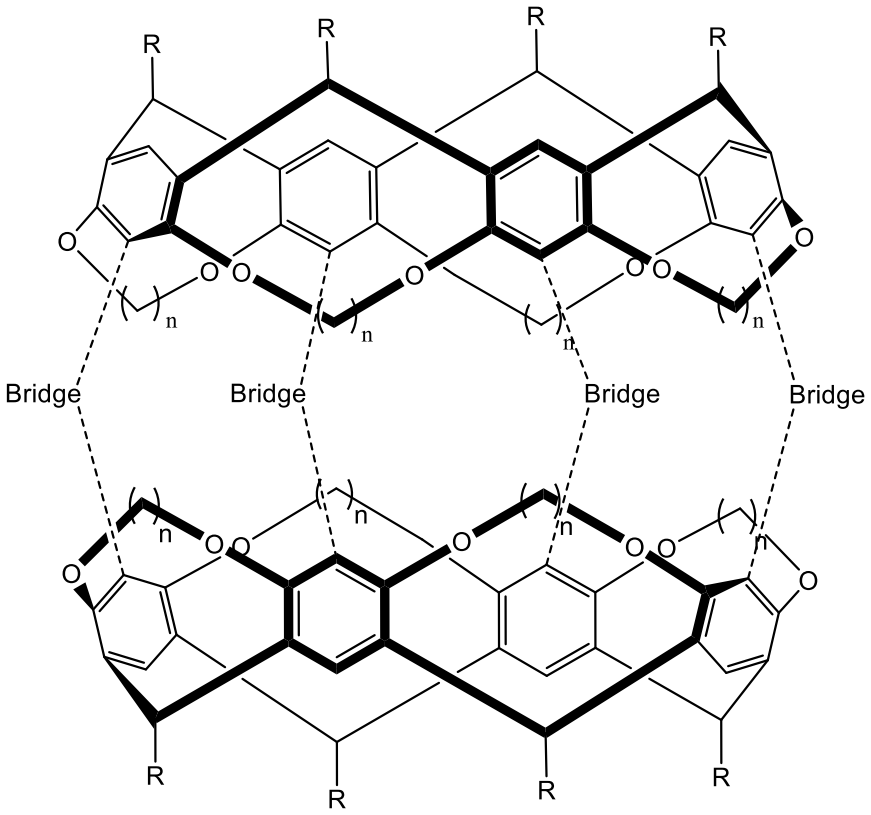

Figure 23: Carcerand structure

The parent cavitands are insoluble in aqueous media; water solubility was investigated by attachment hydrophilic or charged groups to the upper or lower rim of calix[4]resorcinarene-based cavitands, the solubility of cavitands relying on the nature and the number of attached moieties. The hydrophobic force is also expected to have a great effect on the complexation process of cavitands towards guest molecules (Hillyer *et al*., 2016; Bibal 2018).

1.2.4.1 Synthesis of water soluble cavitands

Hydroxyl group footed methylene bridged cavitands **97** was prepared by selective bridging of chlorobromomethane with dodecol **96**, afforded by the acid catalysed condensation of 2-methylresorcinol **95** and 2,3-dihydrofuran **63** (Mezo and Sherman 1998). Sherman *et al*. reported the synthesis of a water soluble cavitands by conversion the hydroxyl groups into the feet of cavitands to phosphonate group (Scheme 25). Binding studies of these cavitands towards various organic guests ($(CH_3)_2CO$, CH_3CN, Toluene, Benzene, $CHCl_3$, $CH_3CH_2CO_2CH_3$, $CH_3CO_2CH_2CH_3$, $CH_3CO_2CH_3$), were investigated in water using the general methods with binding constants are in range 10-10^3 and subjected to rapid exchange on the ^{1}H-NMR timescale. Solutions were prepared with different host concentrations and constant guest concentrations in D_2O (50 mM $(NH_4)_2CO_3$, pD= 9.4), the chemical shift of guest protons were obtained from the ^{1}H-NMR spectra gave an indication to 1:1 complexing ratio (Gui and Sherman 2001).

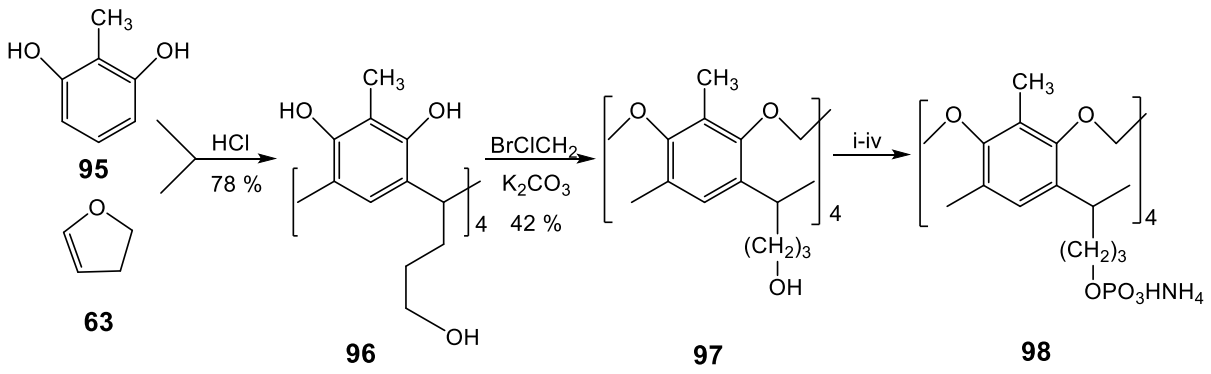

(i) Diphenyl-*N*,*N*-diethylphosphoramidite, tetrazole, THF, rt (ii) 30% H_2O_2, 278 °C, 65% (iii) H_2/Pd/C, rt, 86%. (iv) 0.1 M $(NH_4)_2CO_3$, 100%

Scheme 25: Synthesis of water soluble cavitand (Mezo and Sherman 1998; Gui and Sherman 2001)

Two cavitand molecules, octaamine **99** and octa acid **100** are soluble in water under acidic or basic conditions (Figure 24), respectively and form capsule with the hydrophobic organic guests, capsule formation is dependent only on the pH of the solution, under acidic solution in case of ocata amine cavitand and under basic conditions with the octaacid cavitand.

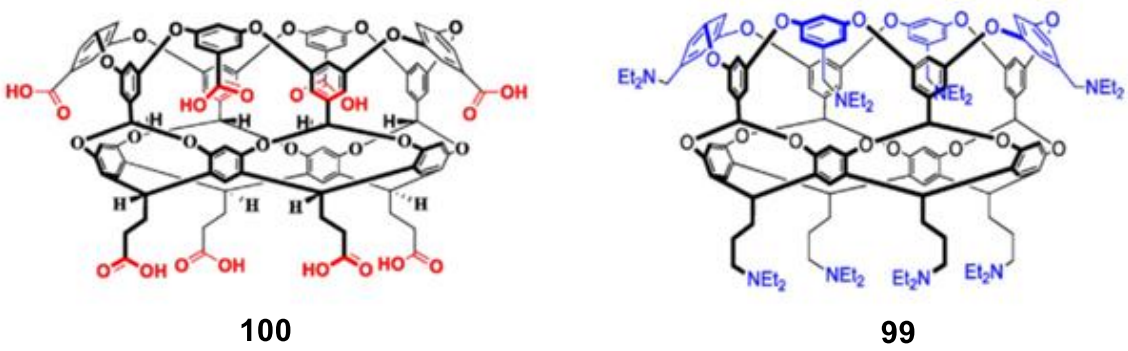

Figure 24: Structures of octa amino and octa acid cavitands (Raj *et al*., 2018)

Octaacid cavitand are able to form different complexes with guests of various sizes or shapes at pH>8.5 in water. It was noticed that octa acid cavitand form 1:1 complexes with the organic guest of hydrophobic frame and hydrophilic head substituent. It forms 1:2 or 2:2 host-guest complexes with other hydrophobic guest molecules relying on the size and shape, such guests naphthalene, pyrene, anthracene and tetracene. The dynamic of the capsular assembly-disassembly and the equilibrium behaviour could be controlled by changing the acidity or basicity of the solution. It was noticed that the hydrophobicity of the guest can alter the rate of the disassembling, the rate slow down with guest of more hydrophobicity, while, guests of less hydrophobicity, the disassembling completely occur of cavitand **100** at pH 4.9. This event has been monitored using three fluorescence hydrophobic guests: coumarin-1, coumarin-153 or coumarin-480 that showed that emission and

absorption spectral properties are dependent on solvent polarity, thus the capsule opening (polar) and closed capsule (non-polar) (Raj *et al*., 2018).

1.2.4.2 Glycosylated cavitands

Calix[4]resorcinarene based malotoside amphiphiles with four hydrophilic groups at the upper rim and four alkyl chains of various lengths at the lower rims have been prepared by attaching maltoside substituents to the central calix[4]resorcinarene scaffold either directly or by linking to the ethylene glycol and the hydroxyl groups of each resorcinol subunit have been linked by methylene group (Scheme 26). All the calix[4]resorcinarene amphiphiles expect for amphiphiles with C_{5-} alkyl chain, showed water solubility in a medium range (1-5% w/v) and headed to precipitate after a short time, referred to limited solubility and stability of these micelles in water. Calix[4]resorcinarene based maltoside with C5-alkyl chain at the lower rim was poorly soluble in water (<1% w/v), but for those with ethylene glycol linker and same alkyl chain were slightly higher than the calix[4]resorcinarene cavitand without linker. Generally, the micelles formed by these compounds were unstable due to rigid structure did not allow conformational changes in solution (Hussain *et al*., 2017).

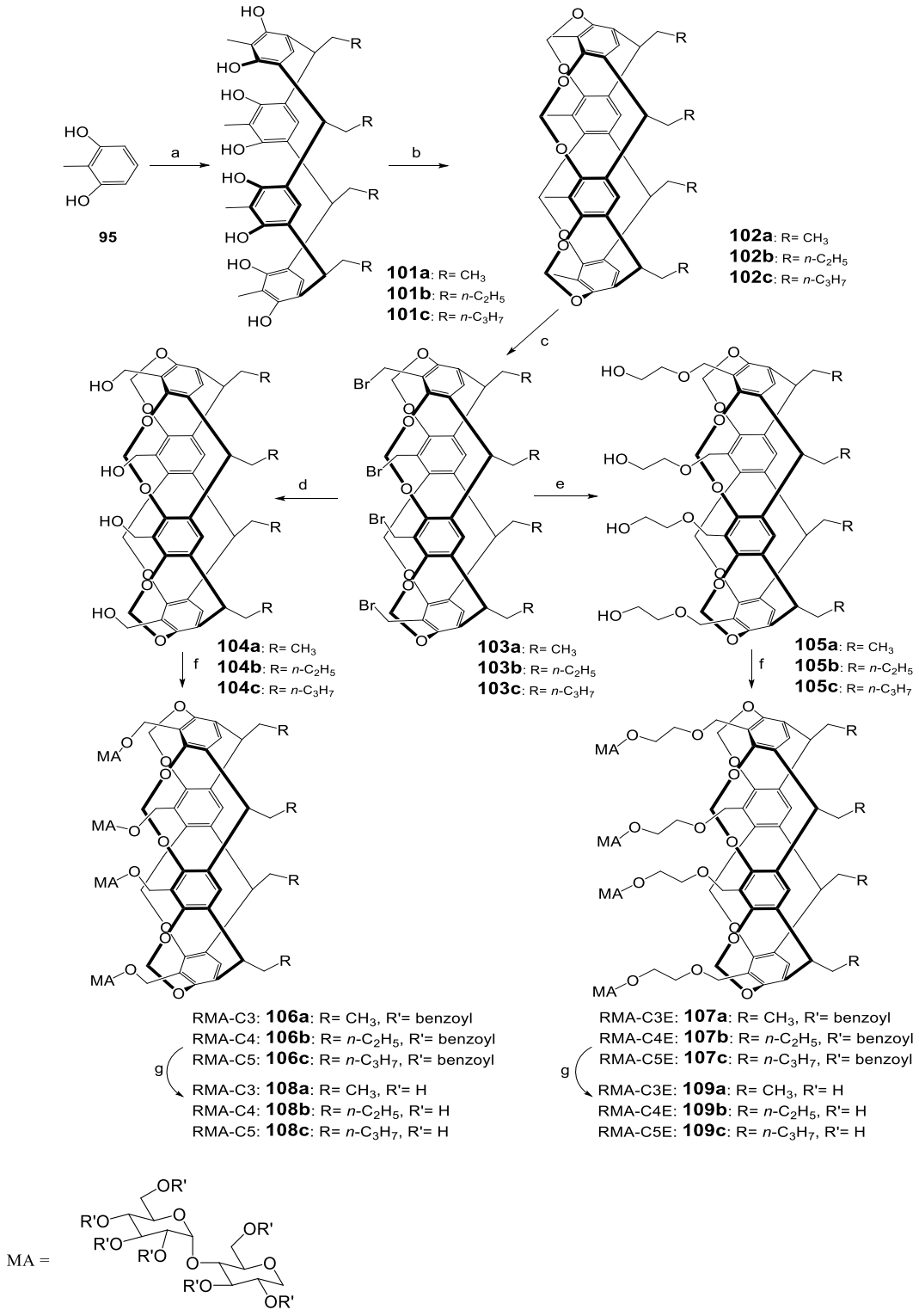

a) Aldehyde, ethanol/HCl, 80 ^{0}C; b) bromochloromethane, DMF, 80 ^{0}C; c) AIBN, NBS, benzene, 80 ^{0}C; d) K_2CO_3, acetone/H_2O, 80 ^{0}C; e) NaH, ethylene glycol, DMF, 80 ^{0}C; f) AgOTf, 2,4,6-collidine, DCM, perbenzoylated maltosylbromide, 0 ^{0}C to RT; g) NaOMe, MeOH, RT

Scheme 26: Synthesis of calix[4]resorcinarene cavitand based maltoside (Hussain *et al*., 2017)

1.4 Aims and objectives

The aim of this research involved the synthesis of a library of novel calix[4]resorcinarene glycosides that bear carbohydrate residues on the bottom rim of the hydrophobic box-like cavity. Calix[4]resorcinarene glycosides can be synthesised by reacting resorcinol or it is derivatives (2-methylresorcinol and pyrogallol) with differently functionalised aldehydes which contain protected carbohydrate units in the presence of Lewis acid catalysis. As calix[4]resorcinarene synthesis is affected directly by the starting material and the reaction conditions used, a series of glycosylated aldehydes was used to react with resorcinols to study their effects on the conformation, configuration and isomer ratios. In this context, a series of glycosylated derivatives of hydroxybenzaldehydes was used to prepare calix[4]resorcinarene glycosides bearing mono or disaccharides containing units at the methine bridges. Another series of calix[4]rersorcinarenes characterised by having different functional groups in 2-positions of resorcinol units was also prepared.

Glycosidic aldehydes bearing an alkyl spacer to separate the arylglucoside from the aldehyde group or alkyl spacer without aromatic unit were also used in calix[4]resorcinarene synthesis.

The conformational isomers of these glycoclusters was determined in most cases by acylation of the product calix[4]resorcinarenes, isolation and characterisation of all the configurational isomers. The results of this research may be used to identify isomers to provide new agents that have potential for drug solubilisation.

Finally, one of the requirements of a calix[4]resorcinarene glycocluster that will be used for drug delivery is that it must be soluble in aqueous media. This was investigated by solvolysis of all the protecting acyl groups from one

butyrated calix[4]resorcinarene glycoside isolated during this research. This was partially characterised and provides opportunity for future research.

CHAPTER 2: SYNTHESIS AND CHARACTERISATION OF NOVEL CALIX[4]RESORCINARENE GLYCOSIDES

2.1 Background

Carbohydrates play a vital role in many biological processes. Many pathological and physiological events, such as cell trafficking, intercellular connection, immune response and tumour cell growth, occur as a result of the interaction of carbohydrate groups with lectins, cell surface proteins which lack enzymatic and immunogenic activity (Geissner and Seeberger 2016). The interaction between monovalent saccharide probes and lectins is usually weak but presentation of a large number of glycoside moieties to the receptor ensures a better or specific association. Molecules which display a large number of carbohydrate residues available for protein interactions are called glycoclusters (Laaf *et al*., 2018), a particular group of multivalent neoglycoconjugates (Jebali *et al*., 2017). Multivalency is related to the capability of a molecule to bind another molecule *via* noncovalent interactions. In this case, the valency is the number of ligating residues displayed by a molecule which are available for non-covalent interaction with complementary residues on another, separate molecular species.

The concept of multivalency in interaction with biologically important molecules has been applied to supramolecular chemistry, with the aim of gaining a better understanding of the multivalent effect (Cecioni *et al*., 2012). Whilst multivalent ligands are different in their topologies, they generally consist of a core which is covalently linked to the peripheral ligating moieties, perhaps *via* linkers (spacers).

A variety of molecules can be used as the core scaffold for a multivalent ligand, from those with low valency such as monosaccharides, benzene derivatives, cyclodextrins, fullerenes, calix[n]arenes and calix[4]resorcinarenes to

compounds with high valency, such as dendrimers, liposomes and nanoparticles (Delbianco *et al*., 2016; Compostella *et al*., 2017; Latxague *et al*., 2018).

Glycoconjugates based on calix[n]arenes or calix[4]resorcinarenes consist of carbohydrate residues bonded on to a functionalised scaffold that displays a defined number of phenolic hydroxyl groups for further decoration. There are several reports in the literature of the conjugation of calix[n]arene or calix[4]resorcinarene matrices with carbohydrate units in order to enhance the solubility of these compounds in aqueous media, hence increasing their binding potential to lectins (Cecioni *et al*., 2009; Cecioni *et al*., 2011). Furthermore, calix[n]arenes are considered as suitable scaffolds for multivalent glycoclusters due to the availability of different scaffold sizes and conformations. This affects the valency and the spatial orientation of the carbohydrate residues in the glycocalix[n]arenes (Giuliani *et al*., 2015).

Calix[4]resorcinarenes are related to calix[n]arenes and are formed from the condensation of resorcinol with an aldehyde to form a ‘container’ oligomer with analogous structural, conformational and binding features to those of calix[n]arenes. Calix[4]resorcinarenes have been widely used for the creation and implementation of novel architectures due to their rigid structure, highly symmetrical concave cavities and aromatic groups capable of further reaction (Sanabria *et al*., 2018).

Calix[4]resorcinarenes display eight phenolic hydroxyl units on their upper rims that provide useful handles for additional chemical modulation of these matrices. In addition, the presence of four pendant groups on their lower rims, defined by the aldehyde used in the synthesis, make them more generally

applicable in supramolecular chemistry than calix[n]arenes. These structural characteristics, amongst others, have enabled further studies into calix[4]resorcinarenes as important scaffolds for decoration with carbohydrate residues.

Much work on the synthesis and biological employment of calix[4]resorcinarene-based glycoclusters which bear carbohydrates on the upper rim was done in Aoyama's laboratory in Japan beginning from mid 1990s. Since then, further reports of calix[4]resorcinarene based glycoconjugates with mono- or disaccharide residues on either the upper rim or the lower rim have appeared.

In 1999, Fujimoto *et al*. reported the synthesis of calix[4]resorcinarene glycoside possessing sialic acid residues at the upper rim and four undecyl alkyl chains at the lower rim **113** (Fujimoto *et al*., 1999). Calix[4]resorcinarene octaamine **110** was converted into the octa(chloroacetamide) **111**, which was then reacted with the protected sialyl thiol **112**. The target glycocluster was afforded after hydrolysis of the protecting groups in 84% overall yield (Scheme 27).

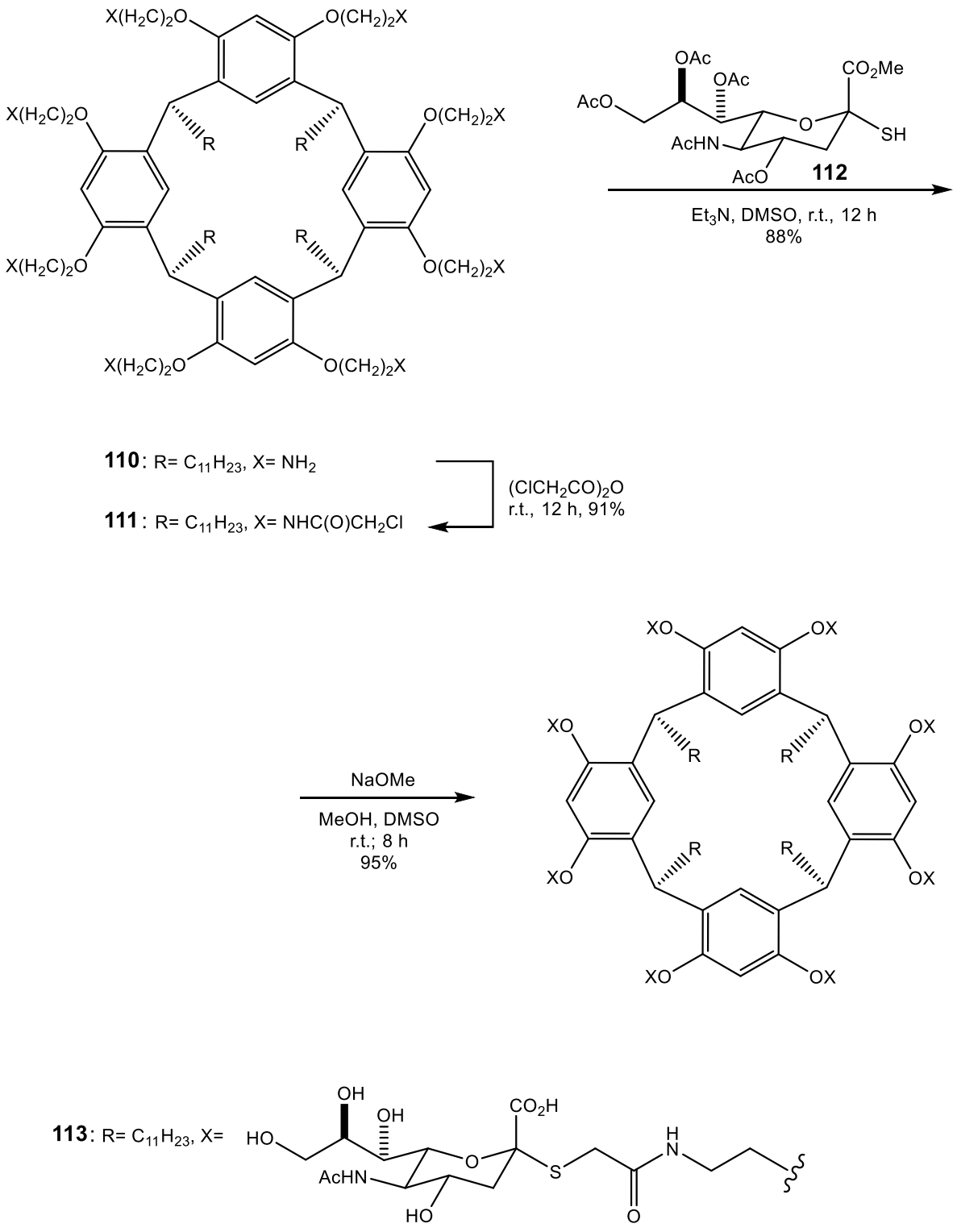

Scheme 27: Synthesis of calix[4]resorcinarene sialic acid cluster (Dondoni and Marra 2010)

Other calix[4]resorcinarene based cluster glycosides (Scheme 28) were prepared in three-step strategies starting from the corresponding calix[4]resorcinarenes. These were converted to ethyl calixarylacetate **114a** and **114b** by alkylation with ethylbromoacetate and heating with acetone/K_2CO_3. An amidation reaction was later performed using an excess of diamines to convert the ester group in **114a** and **114b** to amide group **115a-d** with free terminal amine groups, which in turn reacted with glycosyl isothiocyanate **116** in refluxing DMSO/DCM mixture to give the corresponding thiourea-bridged cluster glycoside **117a-d** (Ge *et al*., 2005).

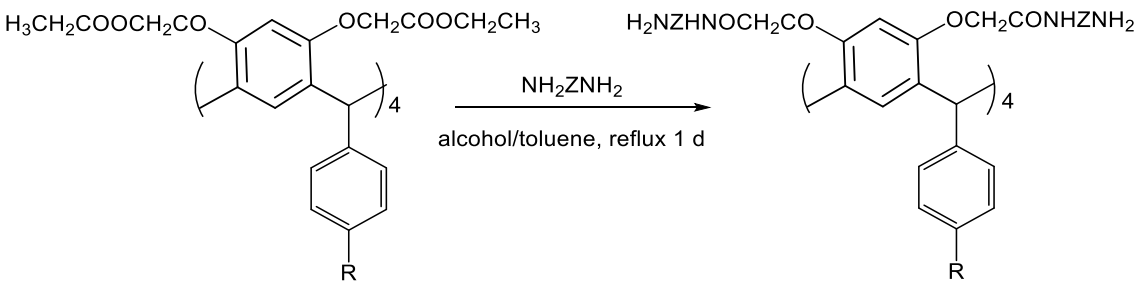

114a: R= H
114b: R= $OCH_2COOCH_2CH_3$

115a: Z= $(CH_3)CHCH_2$, R= H
115b: Z= $(CH_3)CHCH_2$, R= $OCH_2CONH(CH_3)CHCH_2NH_2$
115c: Z= $(CH_2)_4$, R= H
115d: Z= $(CH_2)_4$, R= $OCH_2CONH(CH_2)_2NH_2$

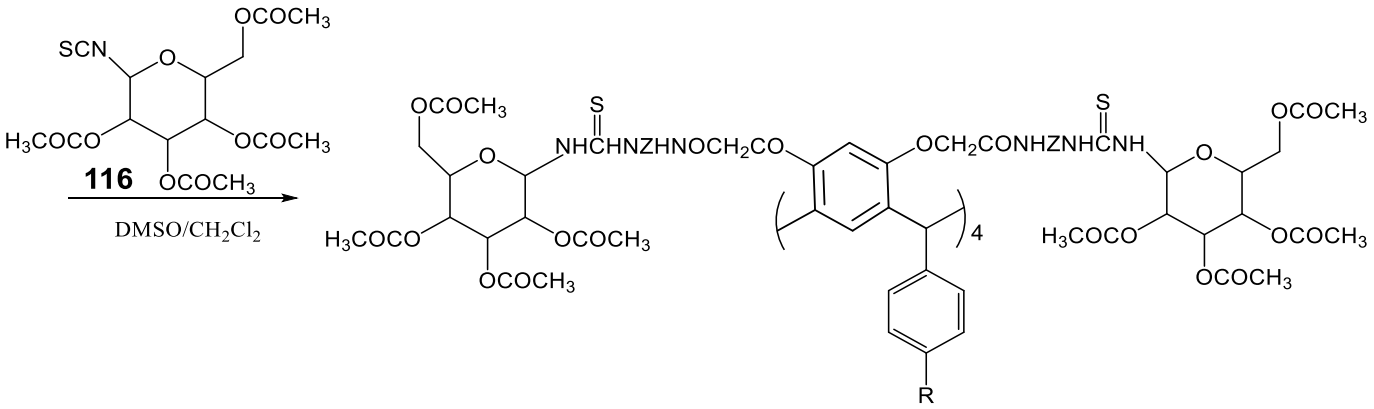

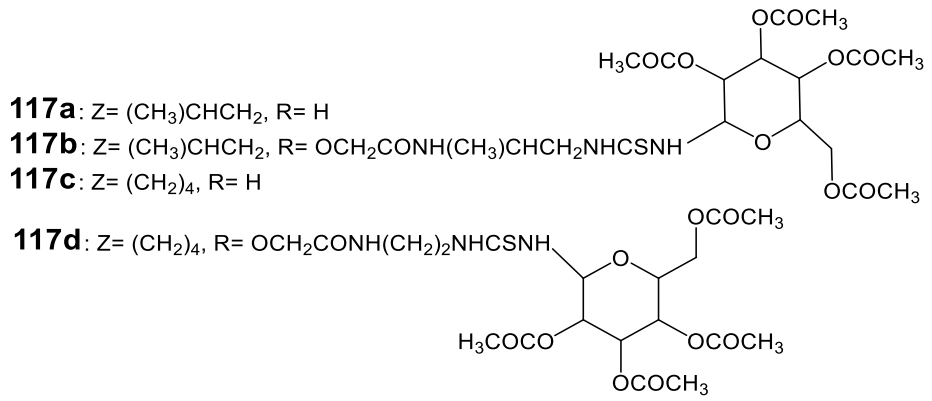

117a: Z= $(CH_3)CHCH_2$, R= H
117b: Z= $(CH_3)CHCH_2$, R= $OCH_2CONH(CH_3)CHCH_2NHCSNH$
117c: Z= $(CH_2)_4$, R= H
117d: Z= $(CH_2)_4$, R= $OCH_2CONH(CH_2)_2NHCSNH$

Scheme 28: Synthesis of calix[4]resorcinarene with glycoside residues and thiourea bridge (Ge *et al*., 2005)

Sakhaii and co-workers reported the stepwise synthesis of divalent glucocalix[4]resorcinarene through condensation of glucosyl aldehydes in the open form with 1,3-dimethoxybenzene. This reaction firstly yielded only diphenyl substituted glucitols (dimer) and any other attempts to obtain a calix[4]resorcinarene with four carbohydrate residues linked at the methylene bridges failed (Sakhaii *et al*., 2002). However, calix[4]resorcinarene bearing mixed substituents at the methylene bridges had already been reported by Rumboldt *et al*. who developed a two-step strategy to obtain calix[4]resorcinarenes with alternating alkyl or aryl substituents (Rumboldt *et al*., 1998). Sakhaii *et al*. used this strategy for the condensation of hexanal **119** with the gluco derivative **118** to give the corresponding calix[4]resorcinarene glucoside **120** (scheme 29). The reaction yielded only one conformational isomer which was the (*rctc*) diamond conformer, based on NMR analysis and *in silico* modelling (Sakhaii *et al*., 2002).

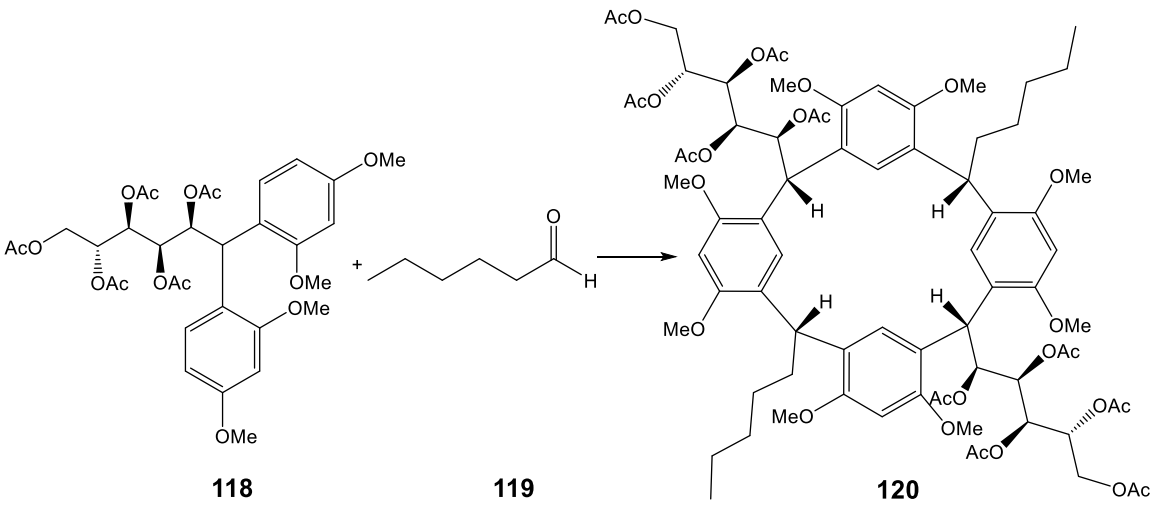

Reagents and conditions: $BF_3.Et_2O$, CH_2Cl_2, 1.5 h

Scheme 29: Calix[4]resorcinarene glucoside prepared by Lewis acid induced ring closure reaction (Titov *et al*., 2013)

Octafunctionalised calix[4]resorcinarenes with carbohydrate residues on the upper rim, have been synthesised by functionalising calix[4]resorcinarenes with 2-aminoethyl groups **110** on the upper rim which, when reacted with a series of unprotected oligosaccharide lactones such as D-lactonolactone, maltopentaose- lactone, D-cellobiosolactone, D-maltolactone and heptaose-lactone **121**, directly produced a series of calix[4]resorcinarene glycoclusters **81-83** and **122** with eight saccharide residues which terminate in either glucose or galactose (Scheme 30). Usually the spacer between the scaffold and the saccharide units is important to determine the efficiency of the interaction between the multivalent ligand and the targeted biomolecules. This is especially important when the orientation the binding sites of the receptor protein enables the formation of a multivalent complex, and the spacers should be long enough to permit the interaction of all the ligating groups simultaneously bearing in mind any entropic considerations (Aoyama 2005; Aoyama 2009).

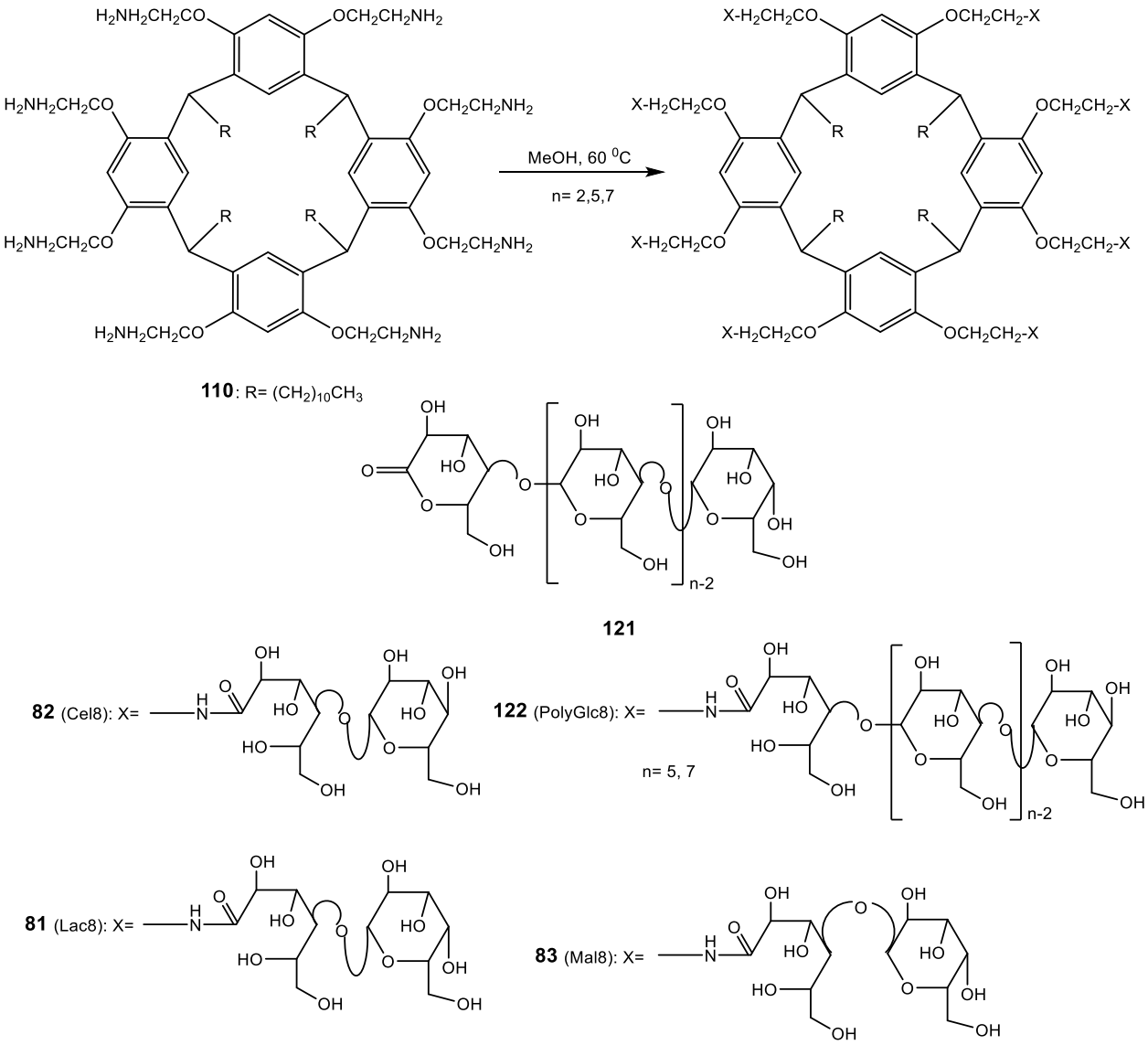

Scheme 30: Synthesis of hydroxylated octavalent glycocalix[4]resorcinarenes (Sansone *et al*., 2011)

Two glyco-calix[4]resorcinarenes bearing 14 terminating residues of galactose and linked each to the other by different linkers **123** (Figure 25), were synthesised and tested for their ability to bind to rat hepatocarcinoma cells. It was found that the two linked glycocalix[4]sorcinarenes could adhere selectively to pathological cells instead of the healthy cells, then surround the solid tumour by creating a network which should delay tumour growth or inhibit metastasis (Menger *et al*., 2004).

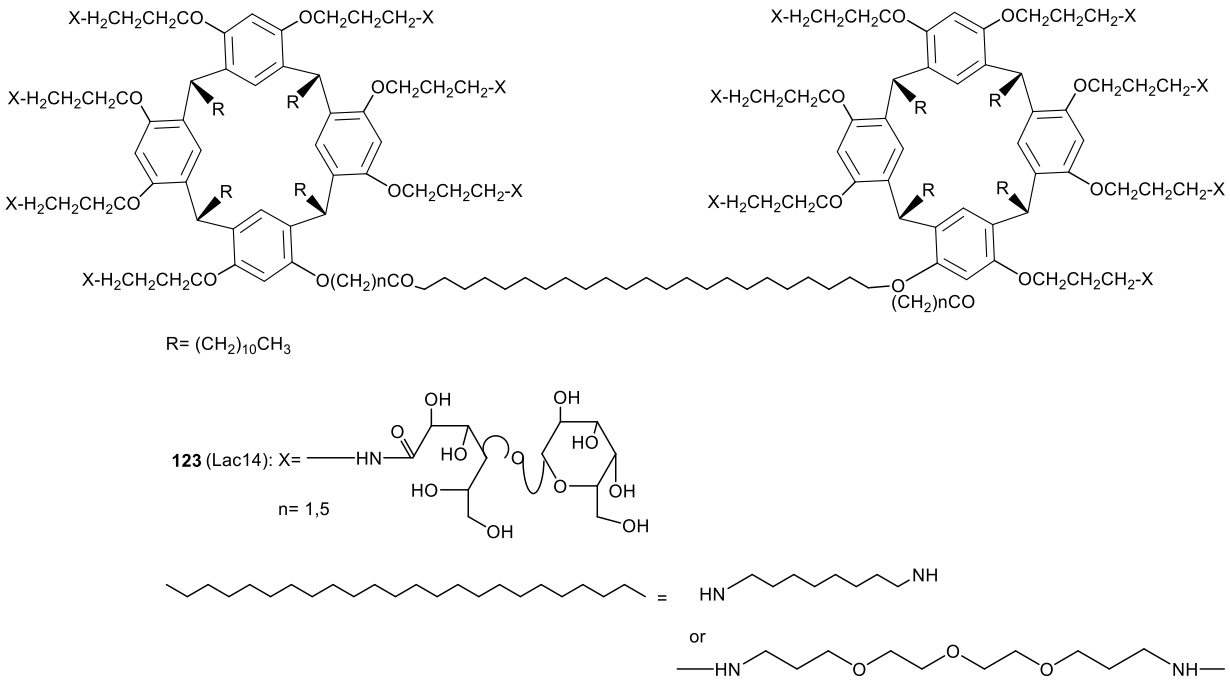

Figure 25: Glycocalix[4]resorcinarene for potential site-directed anticancer agents (Sansone *et al*., 2011)

Another method to conjugate disaccharide residues at the upper rim of a calix[4]resorcinarene scaffold was described by Hayashida *et al*. *via* alkylation the tetrathiolated cavitand **124** with a bromoethyl glycoside **125** in the presence of Cs_2CO_3. After hydrolysis the corresponding glycosylated calix[4]resorcinarene **126** presenting four maltose residues linked to the macrocyclic backbone through bridges of sulphide was produced (Scheme 31) (Hayashida *et al*., 1999).

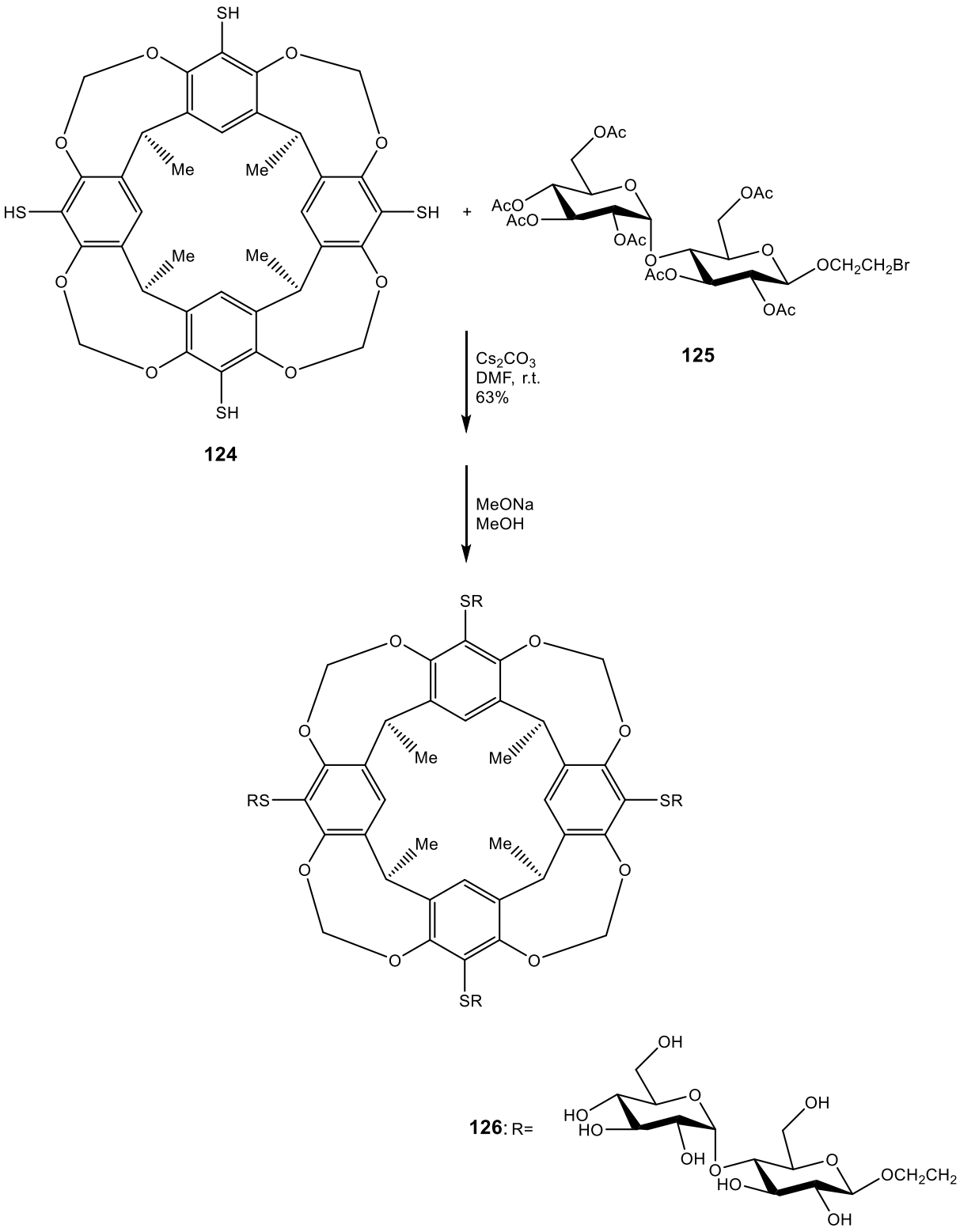

Scheme 31: Calix[4]resorcinarene glycocluster prepared by alkylation of the bowl shaped tetrathiol (Dondoni and Marra 2010)

Oshovsky *et al*. reported the synthesis of thiourea cavitand glycoclusters **133-136**: Reaction of tetrakis(aminomethyl) cavitand **127** with the thiocyanate derivatives of peracetylated glucose, galactose and cellobiose in pyridine at room temperature yielded the protected saccharide-thiourea functionalised cavitands **129**, **130** and **132**. Cavitand **131** was prepared from the reaction of pentyl derivative **128** with protected glucosyl isothiocyanate. Subsequent deacetylation of compounds **129-132** afforded saccharide-thiourea functionalised cavitands **133-136**. The solubilities of thiourea cavitand glycoclusters **133-136** in water was 0.5, 0.6, 0.8 and >300 mM L^{-1} respectively, the higher solubility of cavitand **136** in water reflecting the influence of four disaccharide residues. The solubility of **136** in water was even higher than the solubility of cavitands bearing dendritic surface with 45 tetraethylene glycol chains (221 mM L^{-1}) (Scheme 32) (Oshovsky *et al*., 2004).

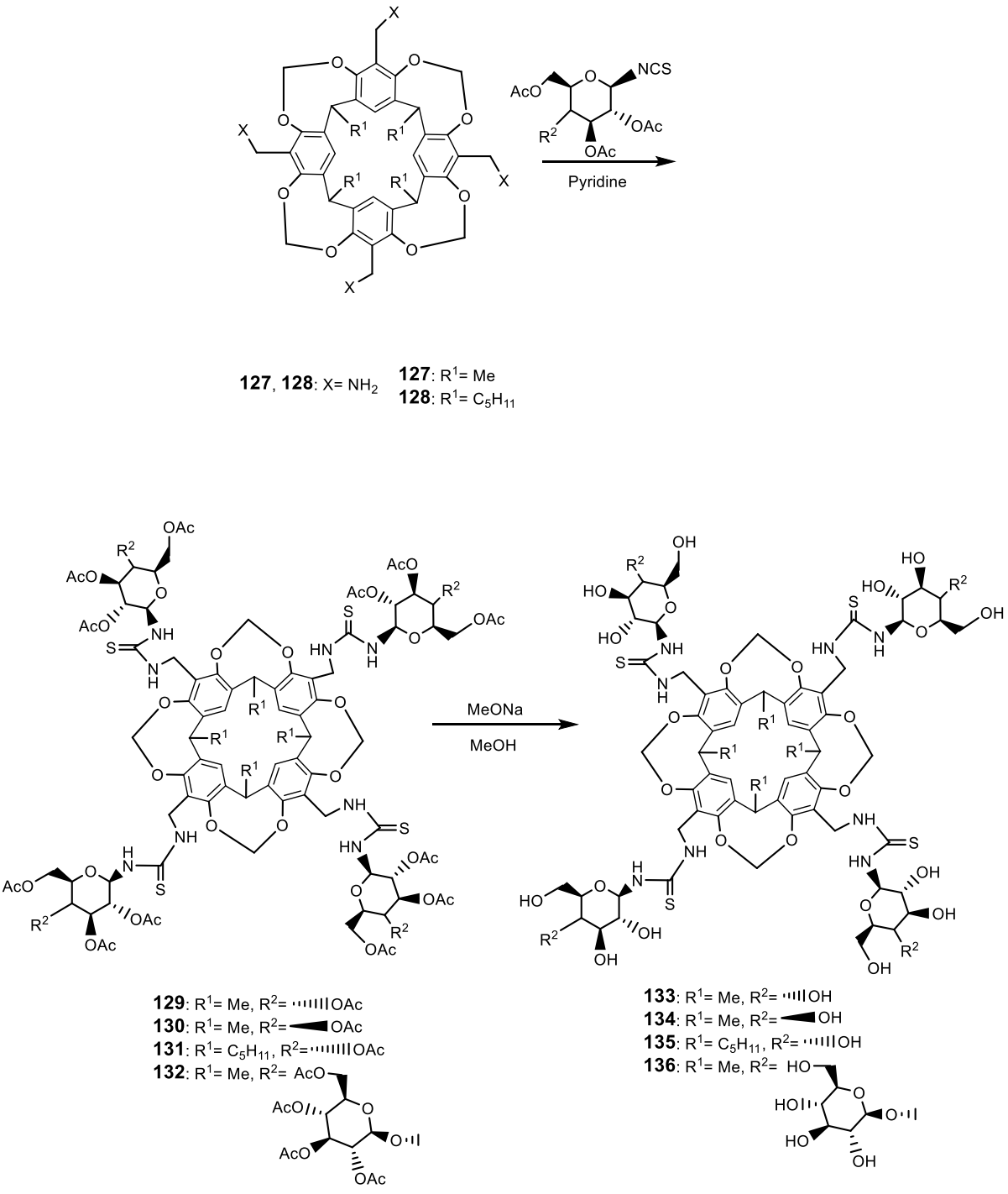

127, **128**: X= NH_2

127: R^1= Me
128: R^1= C_5H_{11}

129: R^1= Me, R^2= OAc
130: R^1= Me, R^2= OAc
131: R^1= C_5H_{11}, R^2= OAc
132: R^1= Me, R^2= AcO

133: R^1= Me, R^2= OH
134: R^1= Me, R^2= OH
135: R^1= C_5H_{11}, R^2= OH
136: R^1= Me, R^2= HO

Scheme 32: Synthesis of thioureamethyl cavitand glycoclusters (Oshovsky *et al*., 2004)

Calix[4]resorcinarenes provide the opportunity to attain different conformations of macrocycles bearing carbohydrates at the lower rim in two specific diastereoisomers, the *rccc* boat and *rctt* chair.

Tetravalent glucocalix[4]resorcinarenes bearing protected glucose residues have been prepared successfully using Lewis acid catalysis (Curtis 1997). The reaction of the tetraacetoxyglucoside of 4-hydroxybenzaldehyde with resorcinol in the presence of aluminium(III) chloride gave two isomeric products which were isolated as their octabutyrates, major isomer **137a** and minor isomer **137b**. The absolute configuration of the major isomer **137a** was determined using Xray crystallography. However, the absolute configuration of the minor isomer **137b** remains undetermined. In fact, the accurate isomer distributions and configurations of the other compounds reported have not been confirmed definitively. Efforts to recognise and identify any conformational isomers of other published compounds of calix[4]resorcinarenes derived from the tetraacetoxyglucoside of 3-, or 2-hydroxybenzaldehyde have, however, been unsuccessful with the exception of calix[4]resorcinarenes derived from the tetraacetoxyglucoside of 4-hydroxybenzaldehyde.

The aim of the research presented in this chapter was to repeat the synthesis of **137a** and **137b** reported in the original article (Curtis 1997). This included synthesis of calix[4]resorcinarenes derived from the tetraacetoxyglucoside of 4-, 3-, or 2-hydroxybenzaldehyde and the novel calix[4]resorcinarene derived from the tetraacetoxygalactoside of 4-hydroxybenzaldehyde. Isolation and identification of the conformational isomers contained within the crude reaction mixtures of calix[4]resorcinarene glucosides which was not previously achieved from the crude reaction mixtures of calix[4]resorcinarene glucosides before

acylation and isolate the pure conformational isomers as the octabutyrate in each case.

2.2 Synthesis of calix[4]resorcinarene glucosides

As part of synthetic approaches concentrated on selective functionalisation of the methine bridge units of calix[4]resorcinarenes with carbohydrate residues, the strategy employed which allows introduction of glucose-containing units at the lower rim began with the synthesis of glucosylated benzaldehydes suitable for condensation with resorcinol under Lewis acid catalysis.

The method used for the synthesis of calix[4]resorcinarene glucosides was adapted from that described by Curtis, which used an equimolar ratio of resorcinol and glycosidic aldehyde reactants followed by butyration in a two-step procedure (Scheme 33) (Curtis 1997).

The rationale behind butyration of the free hydroxyl units was to confer increased solubility of the calix[4]resorcinarene products in organic solvents and consequently aid separation of the expected conformational isomers from the crude reaction mixture.

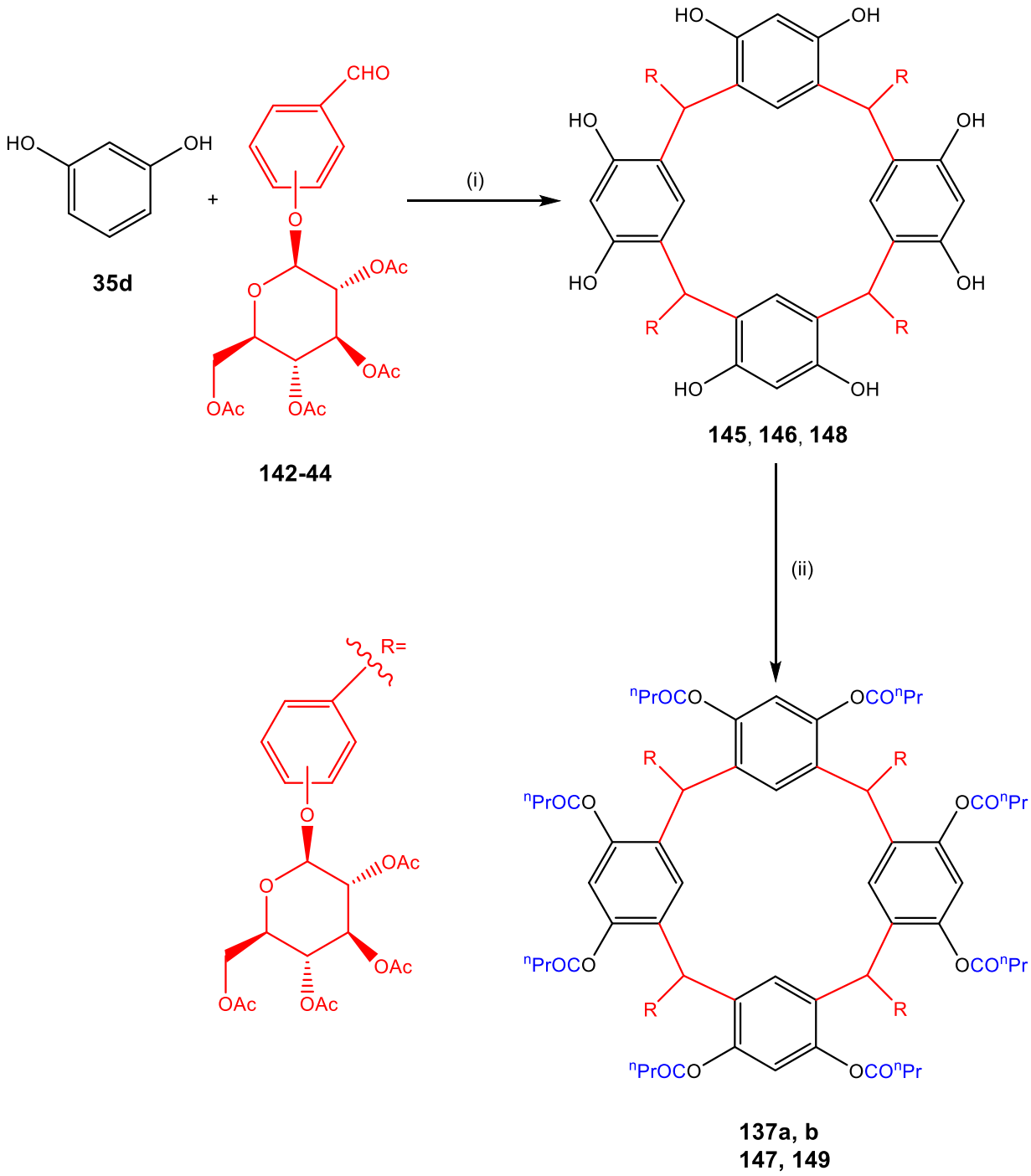

Reagents and conditions: (i) aluminium(III) chloride in nitrobenzene, 48-72 h, Et_2O: THF, (ii) butyric anhydride, pyridine, heating at 80 ^{0}C overnight

Scheme 33: Synthesis of calix[4]resorcinarene glucosides (Curtis 1997)

In order to prepare such simple calix[4]resorcinarene-based glycoclusters, the monoglycosidic aldehydes must firstly be produced.

Most carbohydrates occurring naturally are in nature connected *via O*-glycosyl bond at positions 1 or 6 on the carbohydrates, for this reason, it was decided to prepare aldehydes bearing carbohydrates groups linked through the same bonds on the 1 position, led to the formation *O*-linked glycosides.

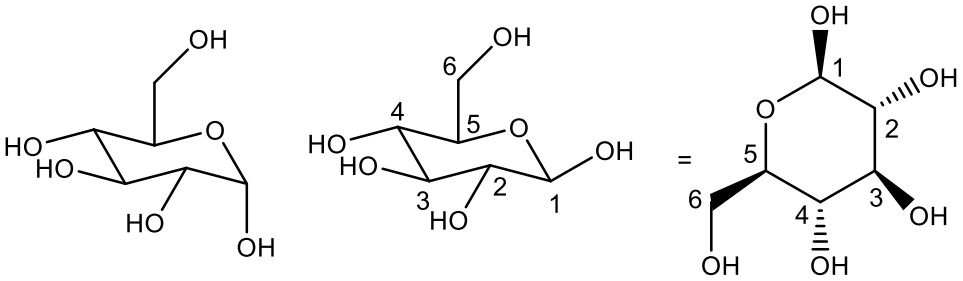

α-Glucose *β*-Glucose (Carbon numbered) *β*-Glucose (Carbon numbered)

In addition, protected carbohydrates were used rather than sugars with free hydroxyl groups in order to get glycosidic aldehydes with enhanced solubility in different organic solvents and can be readily purified utilising column chromatography.

2.2.1 Glycosylation of aromatic aldehydes (General method)

The commercially available 2,3,4,6-tetra-*O*-acetyl-*α*-D-glucopyranosyl bromide **138** as a donor of glucose moiety was separately coupled with aromatic aldehydes (4-, 3- and 2-hydroxybenzaldehyde) **139-141** in 1:1 molar ratio in the presence of silver oxide as a catalyst in MeCN using the Koenigs-Knorr method (Scheme 34) (Stavila *et al*., 2008). The reaction proceeded to give **142**, **143**, in 69% and 65% yield, respectively, after purification using standard silica gel column chromatography. In all cases the reaction yields were acceptable but not higher as a result of incomplete conversion of the aromatic aldehydes to the glycosidic aldehydes as showed on TLC, even after subjecting the reaction for longer periods of time.

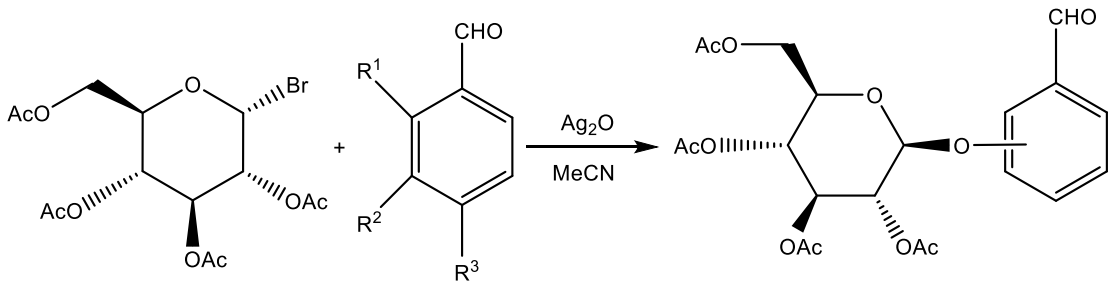

138

139: R^1=R^2= H, R^3= OH
140: R^1=R^3= H, R^2= OH
141: R^2=R^3= H, R^1= OH

142-144

Scheme 34: Synthesis of glucosylated benzaldehyde **142-144**

In case of compound **144**, the yield was lower at 27% as a result of formation of an isomeric glucoside in addition to the starting material 2-hydroxybenzaldehyde. This method was confirmed to be suitable for glycosylation of all aldehydes that was undertaken, since it gives the glycosides in a short reaction time 4 h, the reaction solvent is readily removed under reduced pressure, the work up was easy and the catalyst promotes the leaving

group departure and inversion of configuration of acetobromo-*α*-D-glucose with the formation of the thermodynamically more stable *β*-glycoside by nucleophilic substitution of alcohol.

The stereochemistry of the product observed is 1,2 *trans* as a result of participation of the acetyl group at 2-position during glycosidation by intramolecular nucleophilic addition, producing an orthoester with the *α*-orientation at the anomeric position. This intermediate is responsible for the introduction of the nucleophile on the *β*-position, the phenomenon being called neighbouring group participation (Scheme 35). The *β* anomeric configuration glycoside bond was proved by NMR (Wang *et al*., 2007; Laville *et al*., 2004; Chen *et al*., 2012).

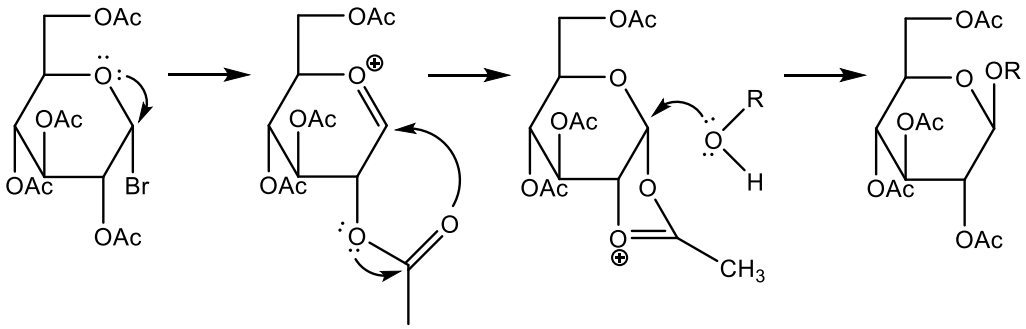

Scheme 35: Mechanism for Koenigs–Knorr glycosidic reaction showing participation of C-2 acetyl in glucose (Brito-Arias 2016)

2.2.2 Synthesis of calix[4]resorcinarene glucoside 145

Once the tetraacetoxyglucoside of 4-hydroxybenzaldehyde **142** (Figure 26) had been prepared the next step was to react it with resorcinol **35d**. The synthesis of the calix[4]resorcinarene was undertaken by Lewis acid catalysis using $AlCl_3$. This leads to the formation of an oxonium ion. The first step assumed the fast formation of intermediate 2, then by slow formation of the intermediate 6 either by the reaction of two molecules of the intermediate 4, or by the intermediate 5. Finally, the liner tetramer 6 undergoes fast cyclisation to give the calix[4]resorcinarene in the crown conformation (Scheme 36) (Boxhall *et al*., 2003).

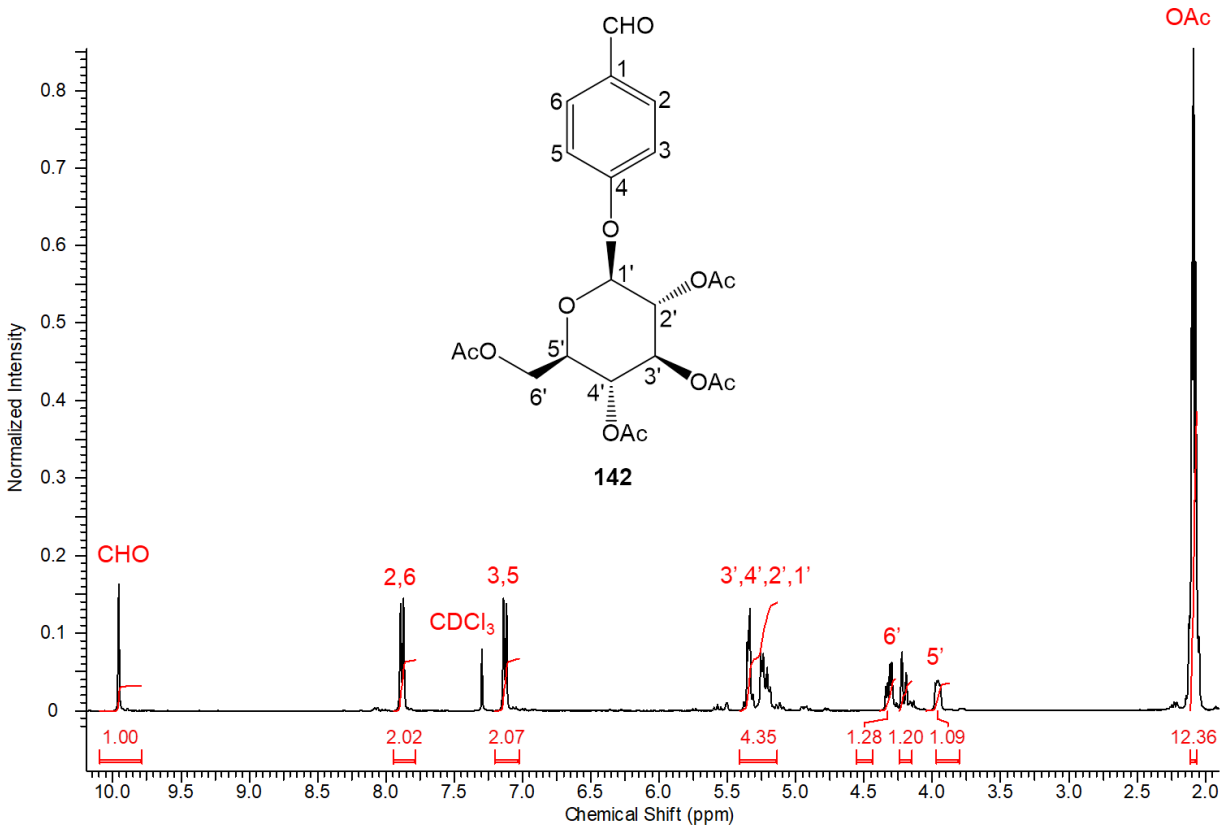

Figure 26: ^1H NMR spectrum of tetraacetoxyglucoside of 4-hydroxybenzaldehyde **142** in $CDCl_3$

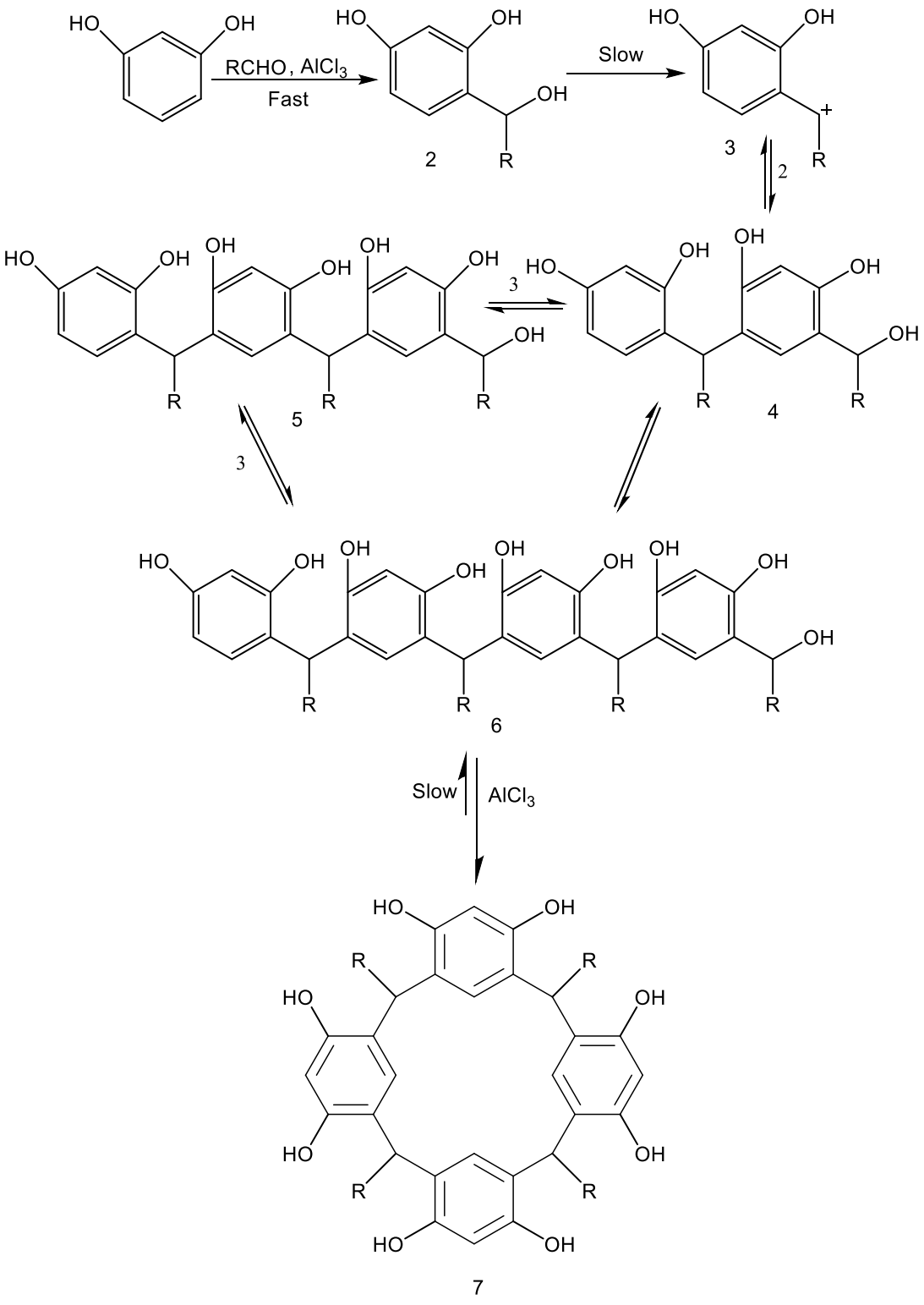

Scheme 36: Mechanism of Lewis acid catalysed formation of calix[4]resorcinarene (Boxhall *et al*., 2003)

The ^{1}H NMR spectrum of the crude mixture of product isolated showed the presence of residual nitrobenzene but also an indication that there may only be one major conformer produced from the reaction upon treatment at room temperature and for 2 days reaction time. It is noteworthy, that no further change was noticed on allowing the reaction to proceed for any further time.

Isolation and purification of this compound was conducted using preparative TLC using DCM: MeOH (4.5:0.5) as eluent, which led to isolation of a single band. The ^{1}H NMR spectrum obtained in d_6-acetone clearly shows the presence of one isomer as shown by two equivalent signals in the region in the spectrum 5.72-5.84 ppm for the methine bridge protons. A similar result was obtained when the mixture obtained from a separate, identical reaction was treated to column chromatography (Figure 27). The structure of this compound is also supported by mass spectrometry analysis. The spectrum gave molecular ion at *m*/*z* 1106.3512 that corresponds to $(M+2NH_4)^{2+}$. (Expected: *m*/*z* 1106.3506) (Appendix 1).

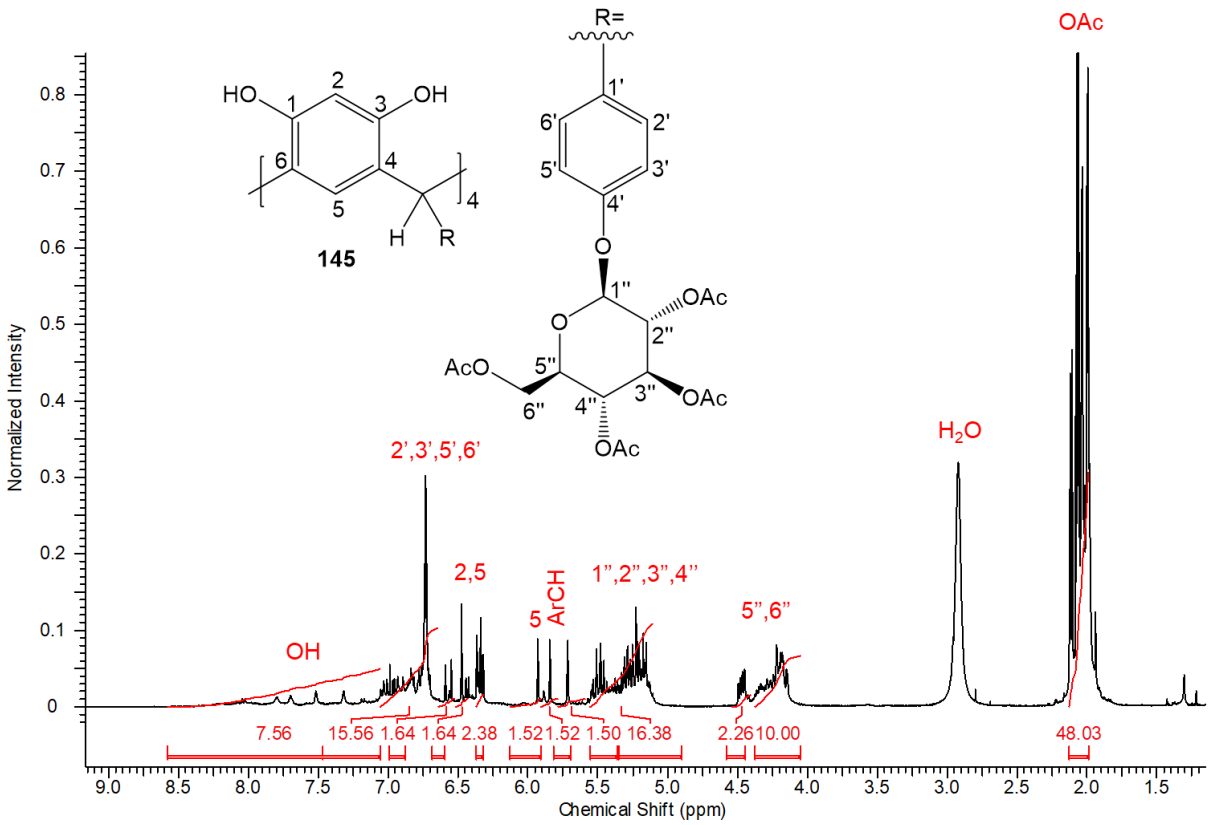
R=
OAc
HO
OH
145
2',3',5',6'
2,5
OH
5 ArCH
1",2",3",4"
5",6"
H2O
7.56
15.56
1.64
1.64
2.38
1.52
1.52
1.50
16.38
2.26
10.00
48.03
Normalized Intensity
Chemical Shift (ppm)

(a)

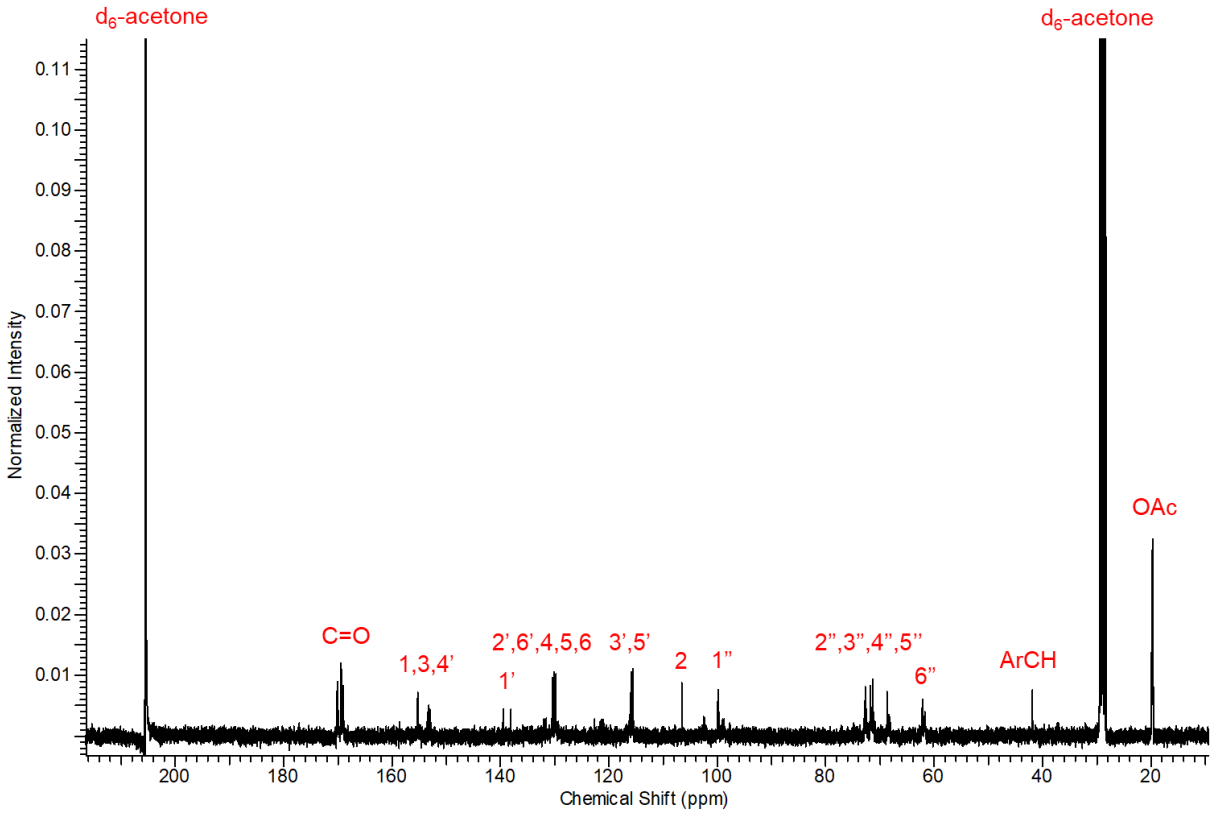

(b)

Figure 27: (a) ^{1}H NMR and (b) ^{13}C NMR spectra of calix[4]resorcinarene glucoside **145** recovered after preparative TLC in d_6-acetone

2.2.3 Synthesis of fully acylated glucocalix[4]resorcinarene 137

Due to the difficulties faced in isolation of the calix[4]resorcinarene glucosides and their limited solubility in a polar solvent, esterification of the crude mixture of calix[4]resorcinarene glucosides was undertaken by employing an excess of butyric anhydride and pyridine at an elevated temperature (80 ^{0}C). The mechanism involves the nucleophilic addition of a phenolic hydroxyl group to the electrophilic carbonyl of butyric anhydride, this addition produced an unstable intermediate which underwent elimination of a carboxylate anion to deliver an ester (Scheme 37). The acylated product is more amenable to isolation by chromatography and other techniques.

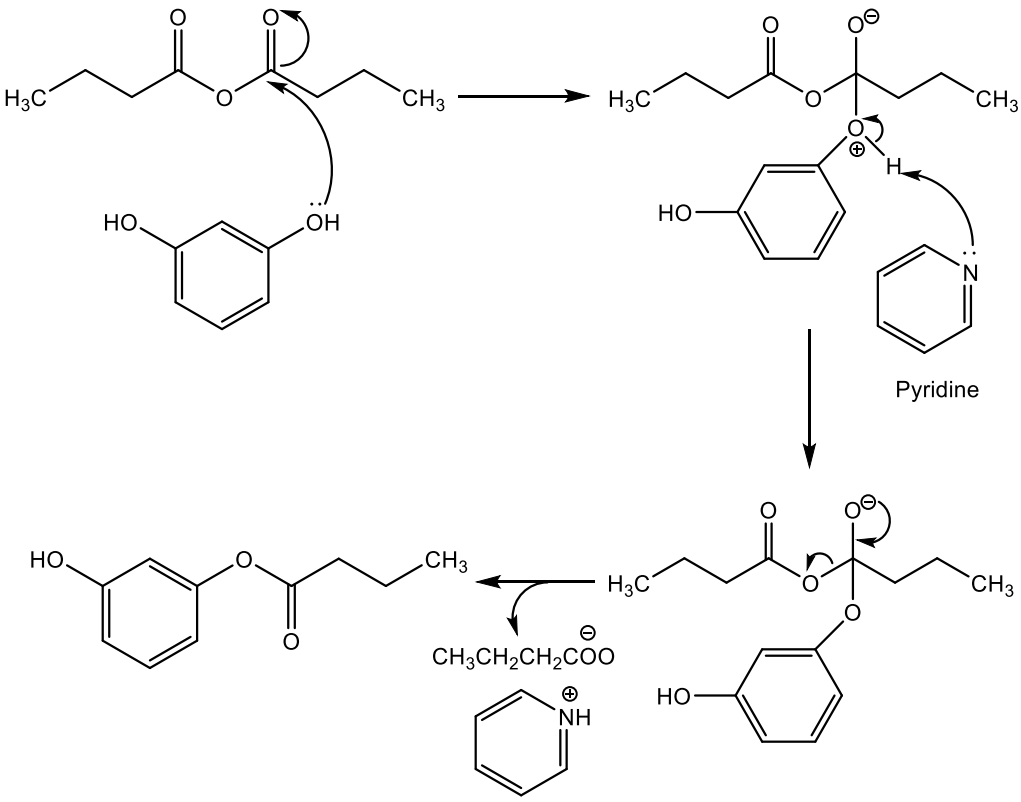

Scheme 37: Esterification mechanism

The ^{1}HNMR spectrum of the octabutyrated mixture showed the presence of three inequivalent signals in the region 5.83-6.07 ppm characteristics for the aromatic core protons, though it was difficult to assign the methine bridge protons because their signals overlapped with those characteristic for the carbohydrate residues. TLC showed two spots, one for a major isomer and the other for a minor isomer with other unidentifiable species, leading to the inference that, as anticipated, the mixture includes two isomers.

Isolation and purification these two isomers were undertaken by silica gel column chromatography using EtOAc: Pet. ether (2:1) as eluent. The ^{1}H NMR spectrum of the major isomer showed four resonances for the aromatic ring protons of the calix[4]resorcinarene highlighting the fact that the resorcinol residues are in two different environments. Two singlets were observed for the

methine bridge protons at 5.47 and 5.56 ppm (Figure 28), which was in agreement with spectrum of a previously described chair conformer of calix[4]resorcinarene by Hogberg (Hogberg 1980). The structure of **137a** is also supported by mass spectrometry analysis. The spectrum gave molecular ion at *m*/*z* 1386.5177 that corresponds to $(M+2NH_4)^{2+}$. (Expected: *m*/*z* 1386.5179) (Appendix 5). The crystal structure for the major conformational isomer has been obtained Curtis 1998, and shows clearly that the tetraglucosylated calix[4]resorcinarene has the *rctt* chair configuration displaying the substituents on the methine bridges. The consequence of this is that the carbohydrate residues are displayed outwards from the central hydrophobic core of the macrocycle (Figure 29).

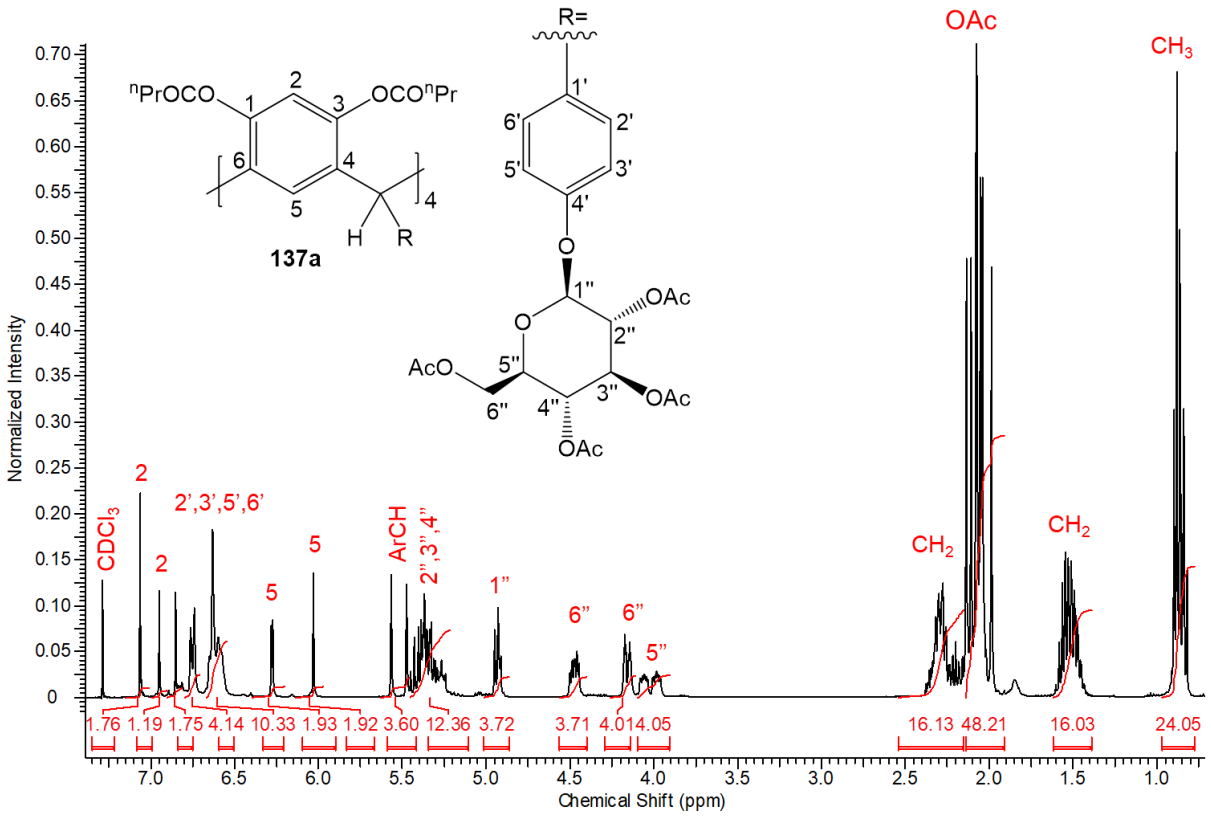

(a)

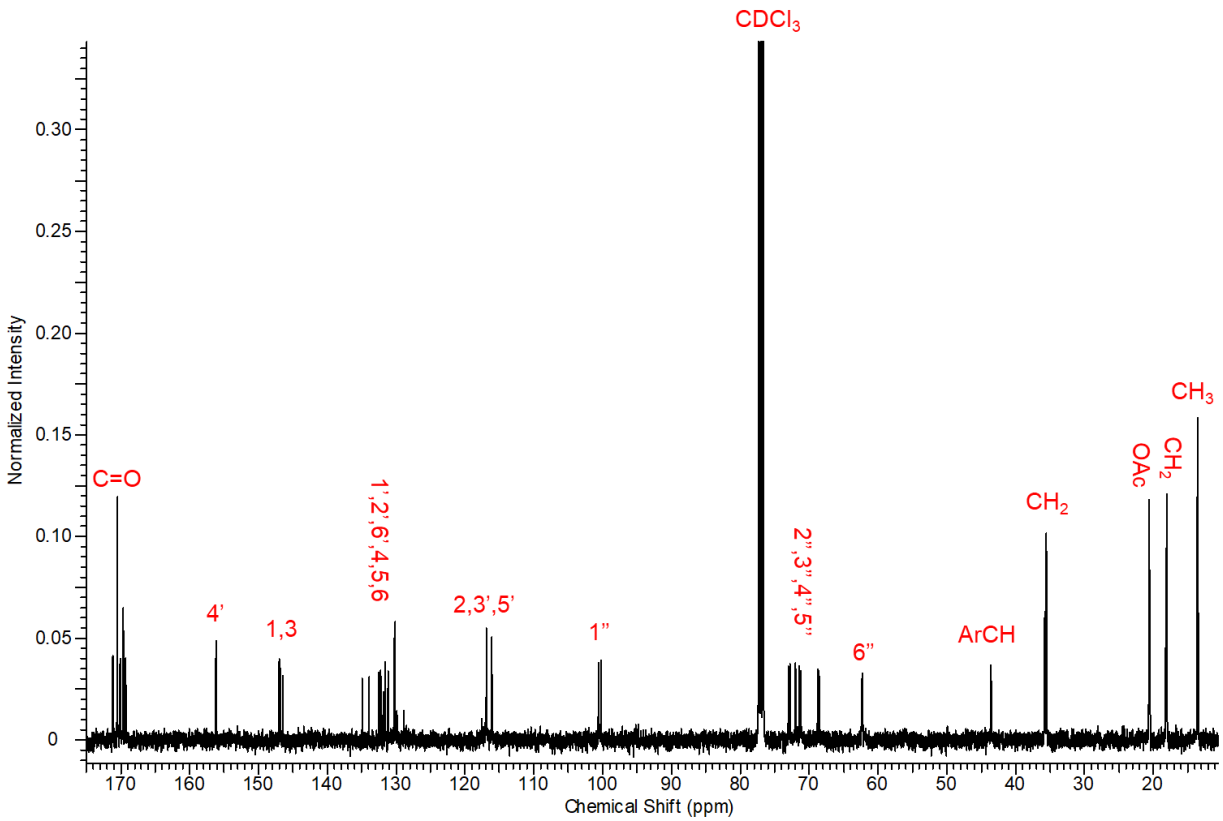
CDCl3
C=O
4'
1,3
1',2',6',4,5,6
2,3',5'
1''
2'',3'',4'',5''
6''
ArCH
CH2
OAc
CH2
CH3
Normalized Intensity
0.30
0.25
0.20
0.15
0.10
0.05
0
170
160
150
140
130
120
110
100
90
80
70
60
50
40
30
20
Chemical Shift (ppm)

(b)

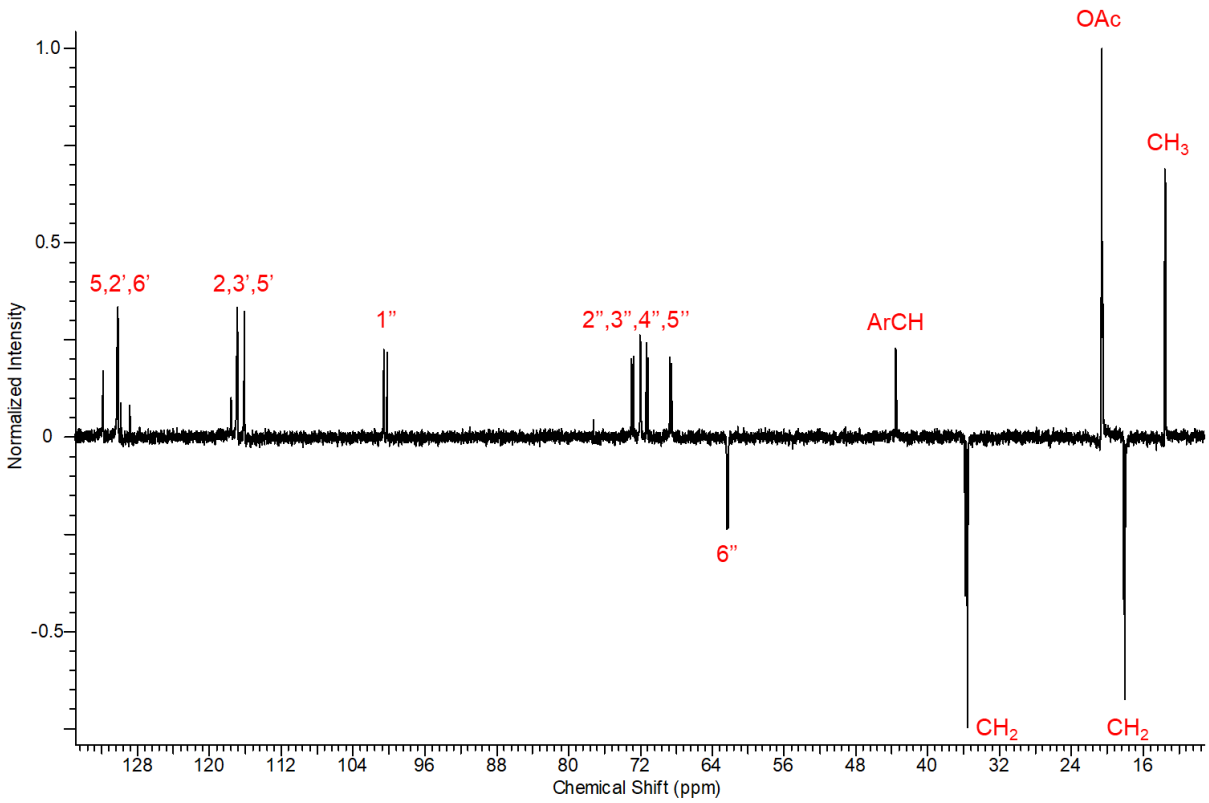

(c)

Figure 28: (a) ^{1}H NMR, (b) ^{13}C NMR and (c) DEPT135 spectra of calix[4]resorcinarene glucoside octabutyrate **137a** (major isomer) in $CDCl_3$

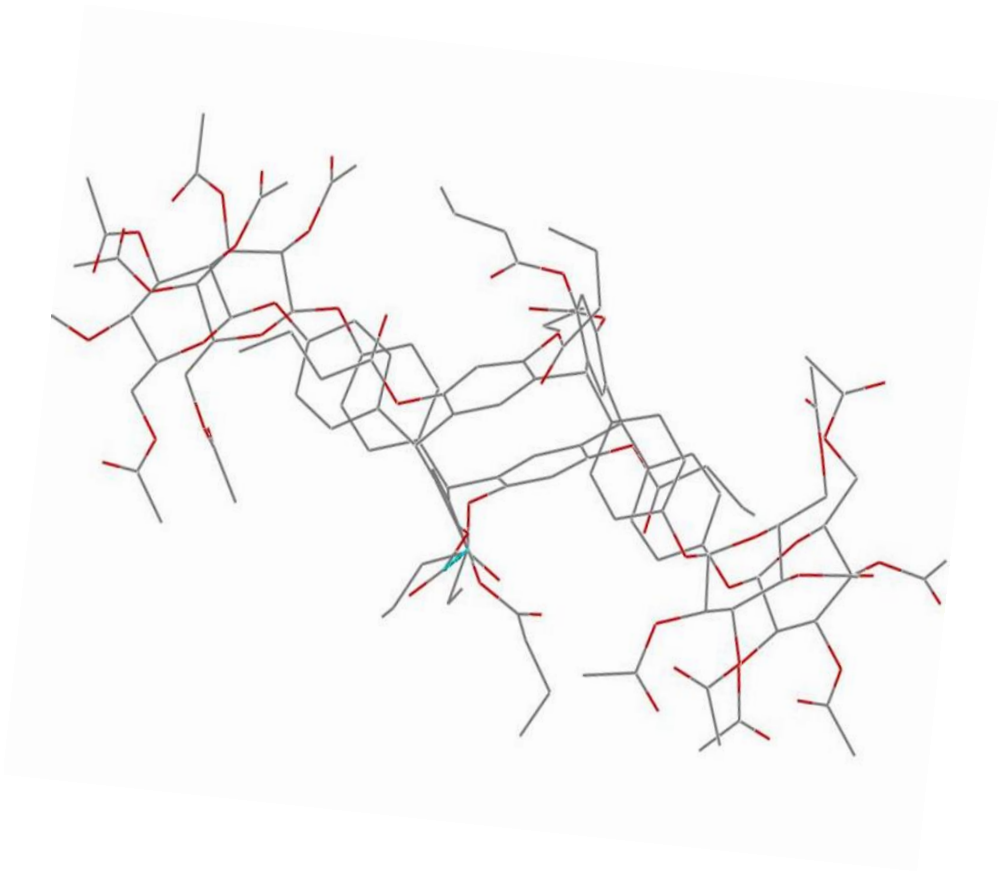

Figure 29: A view of the structure of the fully acylated major isomer of 4-glucosyl calix[4]resorcinarene derived from Xray crystallography (Curtis 1998)

The minor isomer was isolated in lower yield 4% following purification in comparison with the major isomer which was obtained in 40% yield after purification. The ^{1}H NMR analysis showed four singlets for the protons in the resorcinol units and a single doublet resonance for the methine bridge protons. This data exhibit that, as previously reported for compounds with aromatic rings substituted on the methine bridges, the minor product has the *rccc* isomer (Egberink *et al*., 1992).

The structure of **137b** is also supported by mass spectrometry analysis. The spectrum gave molecular ion at *m*/*z* 1386.5170 that corresponds to $(M+2NH_4)^{2+}$. (Expected: *m*/*z* 1386.5179) (Appendix 6). Notably, the crystal structure of this compound had not been obtained, but is expected to be a C_{2v} symmetric flattened boat, as noticed from the resonance of the aromatic rings of the calix[4]resorcinarene on the ^{1}H NMR time scale (Figure 30).

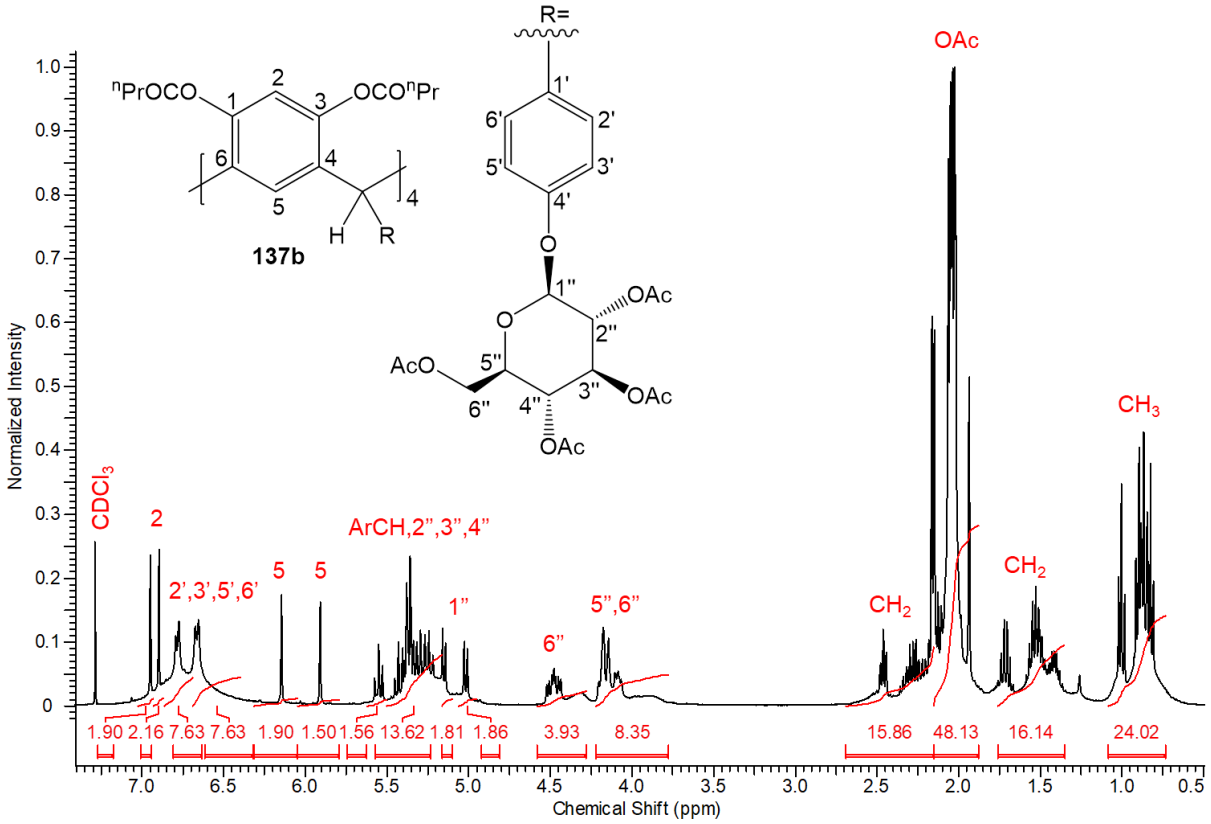

(a)

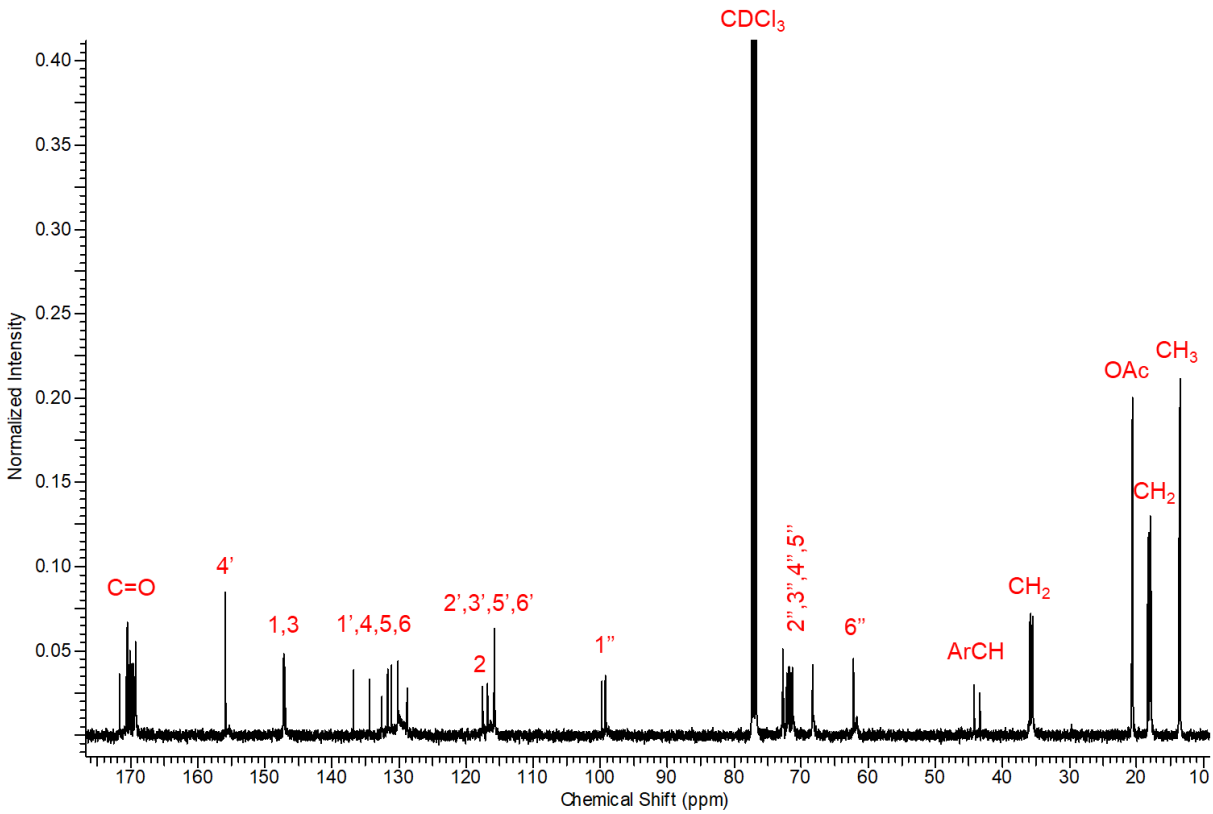
CDCl3
C=O
4'
1,3
1',4,5,6
2',3',5',6'
2
1"
2",3",4",5"
6"
ArCH
CH2
OAc
CH2
CH3
Normalized Intensity
Chemical Shift (ppm)

(b)

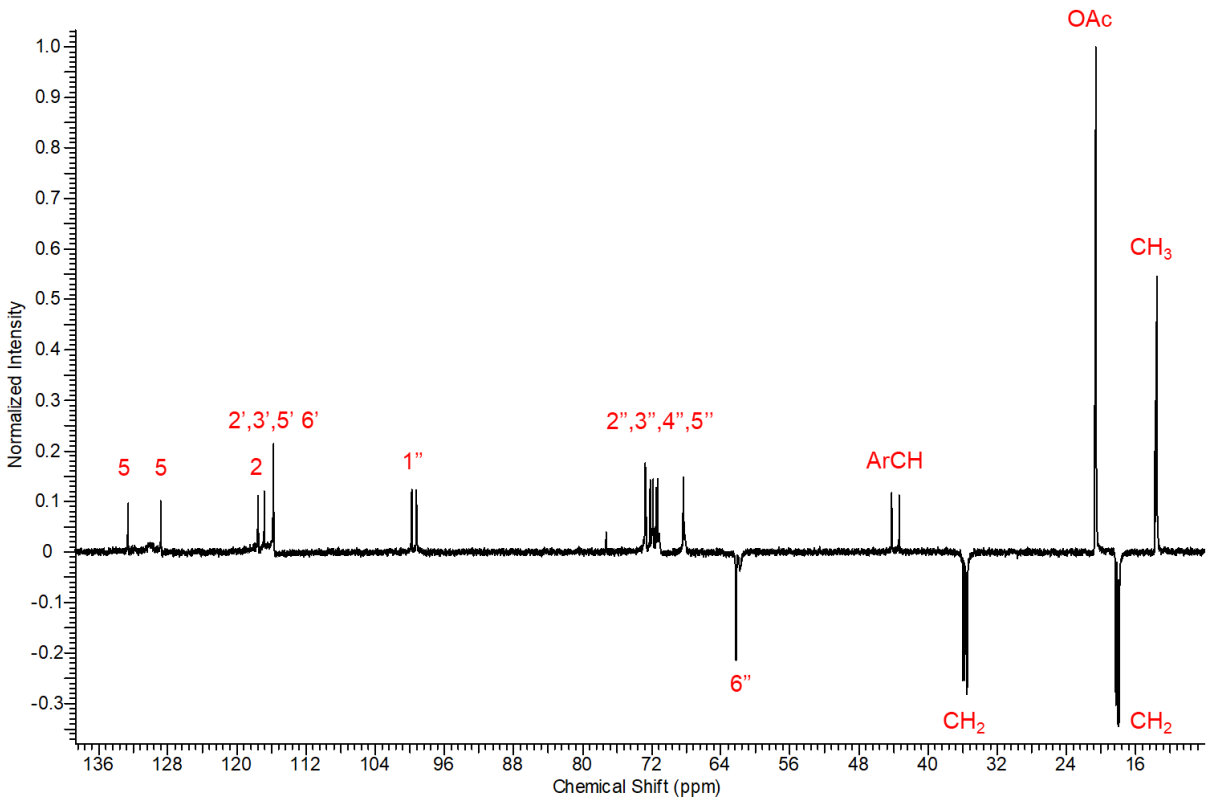

(c)

Figure 30: (a) ^{1}H NMR, (b) ^{13}C NMR and (c) DEPT135 spectra of calix[4]resorcinarene glucoside octabutyrate **137b** (minor isomer) in $CDCl_3$

2.2.4 Synthesis of calix[4]resorcinarene glucoside 146

The synthesis of the calix[4]resorcinarene glucoside **146** was carried out according to the general procedure from the tetraacetoxyglucoside of 3-hydroxybenzaldehyde (Figure 31) and resorcinol in a 1:1 molar ratio using $AlCl_3$ solution in nitrobenzene as a catalyst. The reaction time needed for the formation this compound was longer than that for compound **145** and extended from 48 to 72 h. Isolation and purification of this tetravalent glycocluster was conducted in two stages, using column chromatography eluting with DCM: MeOH (4.5:0.5), then using chromatotron chromatography eluting with DCM: MeOH: EtOAc (4:0.4:0.6), which furnished pure material of the title compound.

A similar result was also obtained using preparative TLC. The ^{1}H NMR spectrum (d_6-acetone) presented three equivalent singlets in the region 5.50-5.63 ppm for methine bridge protons referring to the presence of only one isomer (Figure 32). The structure of **146** is also supported by mass spectrometry analysis. The spectrum gave molecular ion at *m*/*z* 1106.3500 that corresponds to $(M+2NH_4)^{2+}$. (Expected: *m*/*z* 1106.3506) (Appendix 2).

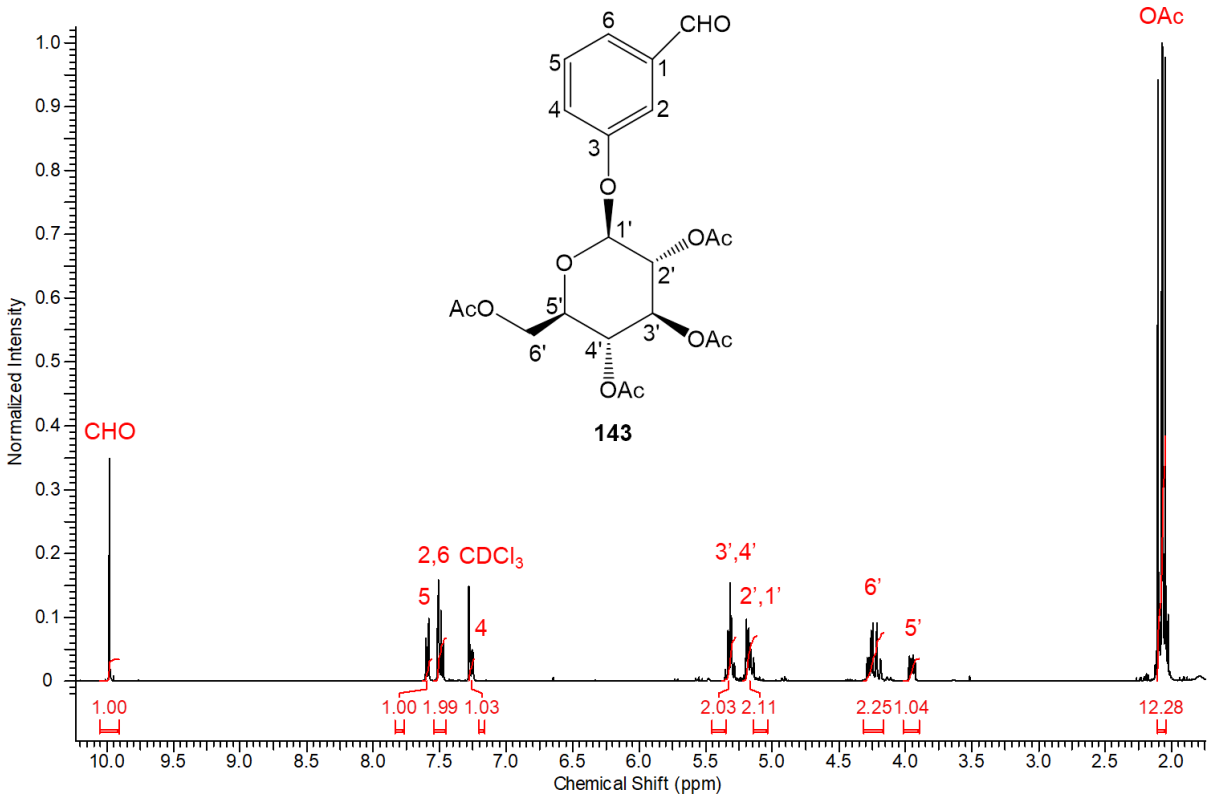

Figure 31: ^{1}H NMR spectrum of tetraacetoxyglucoside of 3-hydroxybenzaldehyde **143** in $CDCl_3$

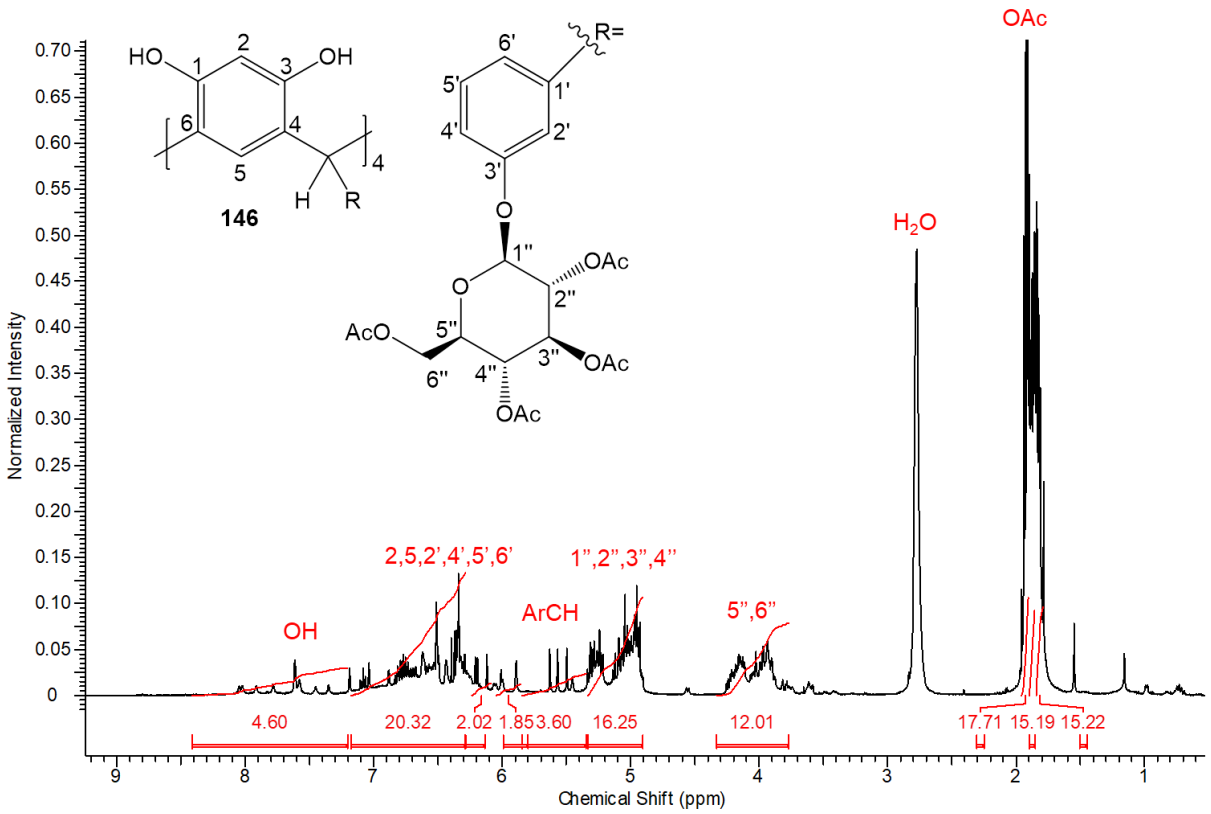

Figure 32: ^{1}H NMR spectrum of calix[4]resorcinarene glucoside **146** recovered after chromatotron chromatography in d_6-acetone

The direct acylation of the crude calix[4]resorcinarene glucoside **146** was performed according to the general procedure used for butyration of compound **145**. TLC of the crude octabutyrated mixture showed one major spot with other spots for the starting material and unknown compounds, on separation by silica gel column chromatography using EtOAc: Pet. ether (2:1) as eluent. The ^{1}H NMR spectrum of the major fraction showed a single doublet resonance for the protons at the methine bridges at 5.48 ppm (Figure 33). The structure of **147** is also supported by mass spectrometry analysis. The spectrum gave molecular ion at *m/z* 1386.5181 that corresponds to $(M+2NH_4)^{2+}$. (Expected: *m/z* 1386.5179) (Appendix 7).

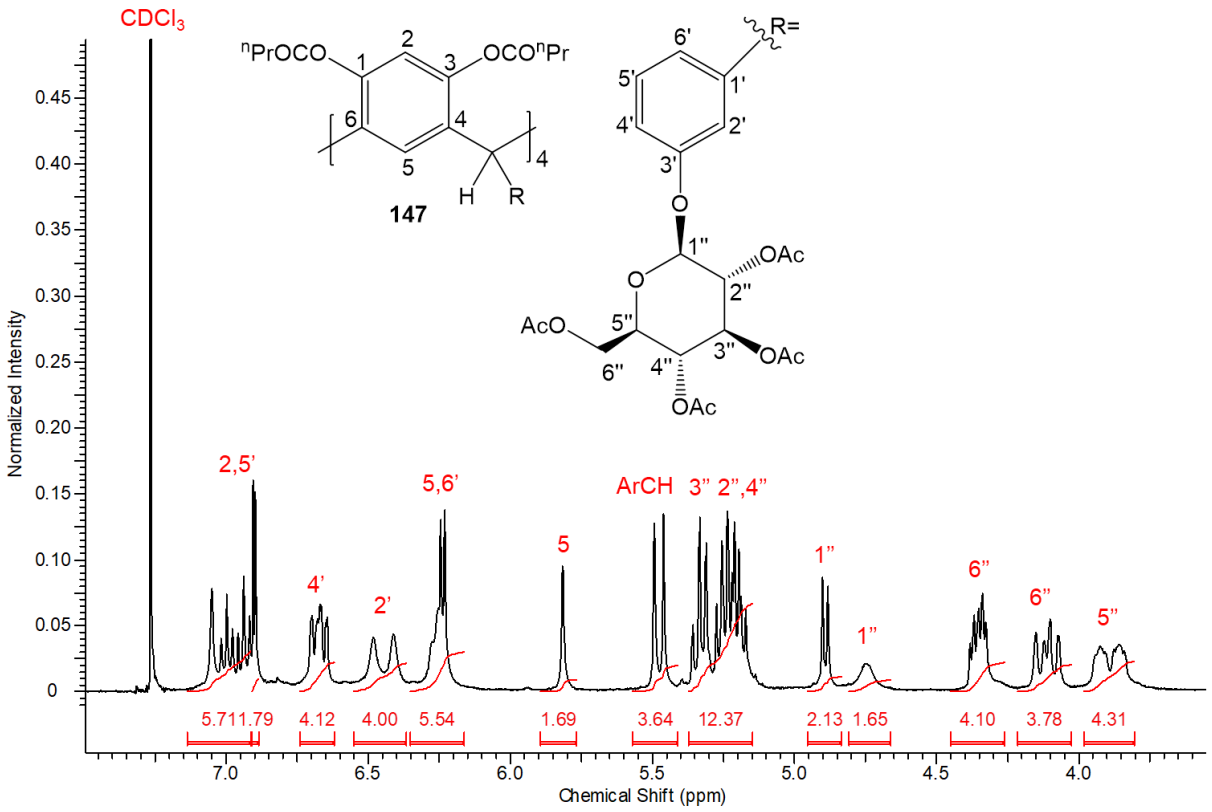
CDCl3
nPrOCO
OCOnPr
147
R=
AcO
OAc
2,5'
4'
2'
5,6'
5
ArCH 3" 2",4"
1"
1"
6"
6"
5"
5.71 1.79
4.12
4.00
5.54
1.69
3.64
12.37
2.13
1.65
4.10
3.78
4.31
Normalized Intensity
Chemical Shift (ppm)

(a)

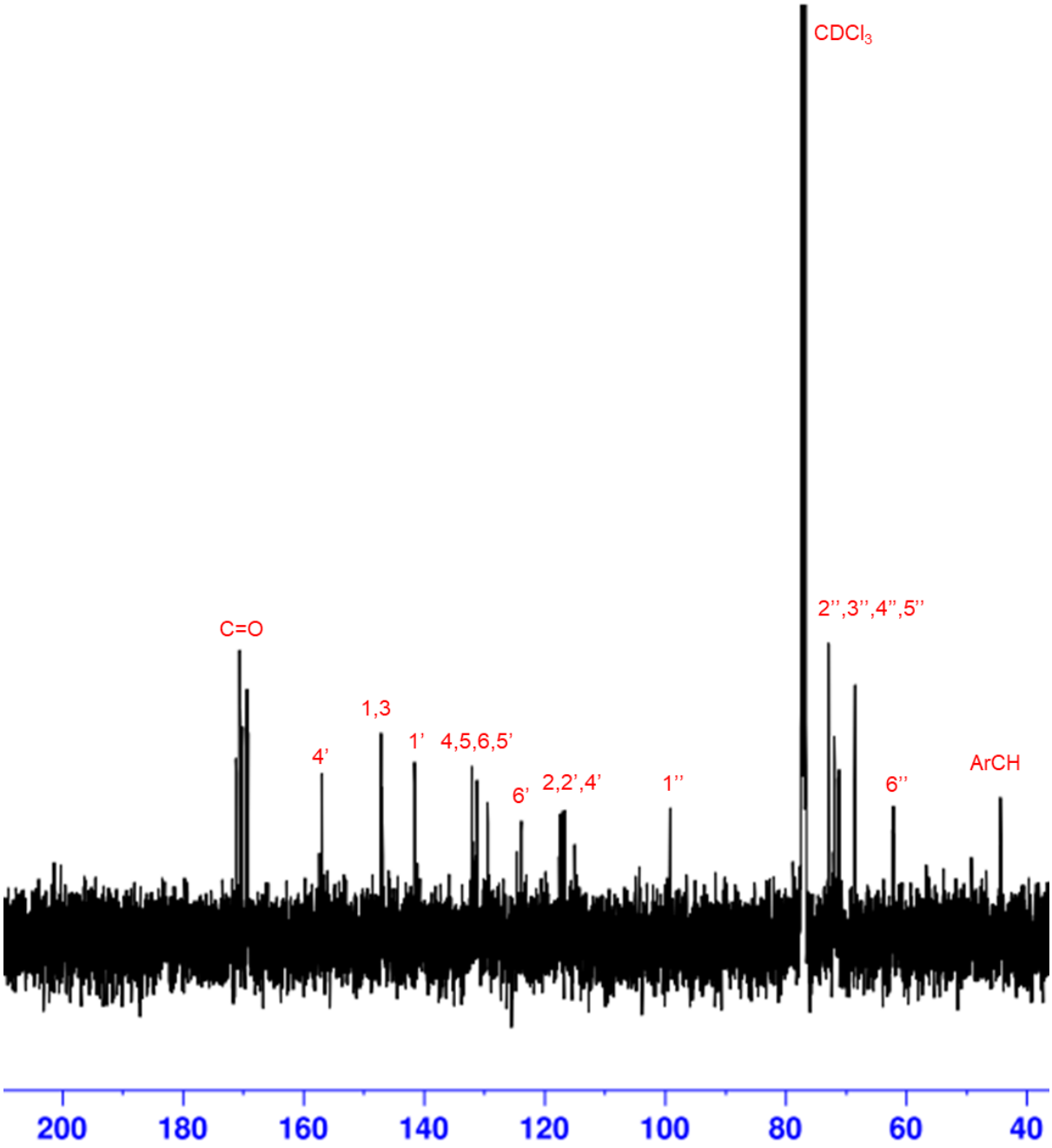

(b)

Figure 33: (a) ^{1}H NMR and (b) ^{13}C NMR spectra of calix[4]resorcinarene glucoside octabutyrate **147** in $CDCl_3$

2.2.5 Synthesis of calix[4]resorcinarene glucoside 148

The synthesis of the calix[4]resorcinarene glucoside **148** proceeded similarly to compounds **145** and **146** but starting from the tetraacetoxyglucoside of 2-

hydroxybenzaldehyde (Figure 34) and resorcinol in 1:1 molar ratio using $AlCl_3$ solution in nitrobenzene as a catalyst. The reaction time extended for 72 h to give this compound in a low yield 22%. The ^{1}H NMR spectrum of the crude mixture was complicated and it was difficult to characterise the resonance of the methine bridge protons or the number of isomers obtained for this compound. Many attempts had been employed to separate the pure calix[4]resorcinarene glucoside but eventually column chromatography eluting DCM: EtOAc: 2-propanol (4:0.5:0.35) followed by preparative TLC using DCM: MeOH (4.5:0.5) as eluent furnished one isomer of this compound as identified by ^{1}H NMR spectrum (Figure 35). The structure of **148** is also supported by mass spectrometry analysis. The spectrum gave molecular ion at *m*/*z* 1106.3497 that corresponds to $(M+2NH_4)^{2+}$. (Expected: *m*/*z* 1106.3506) (Appendix 3).

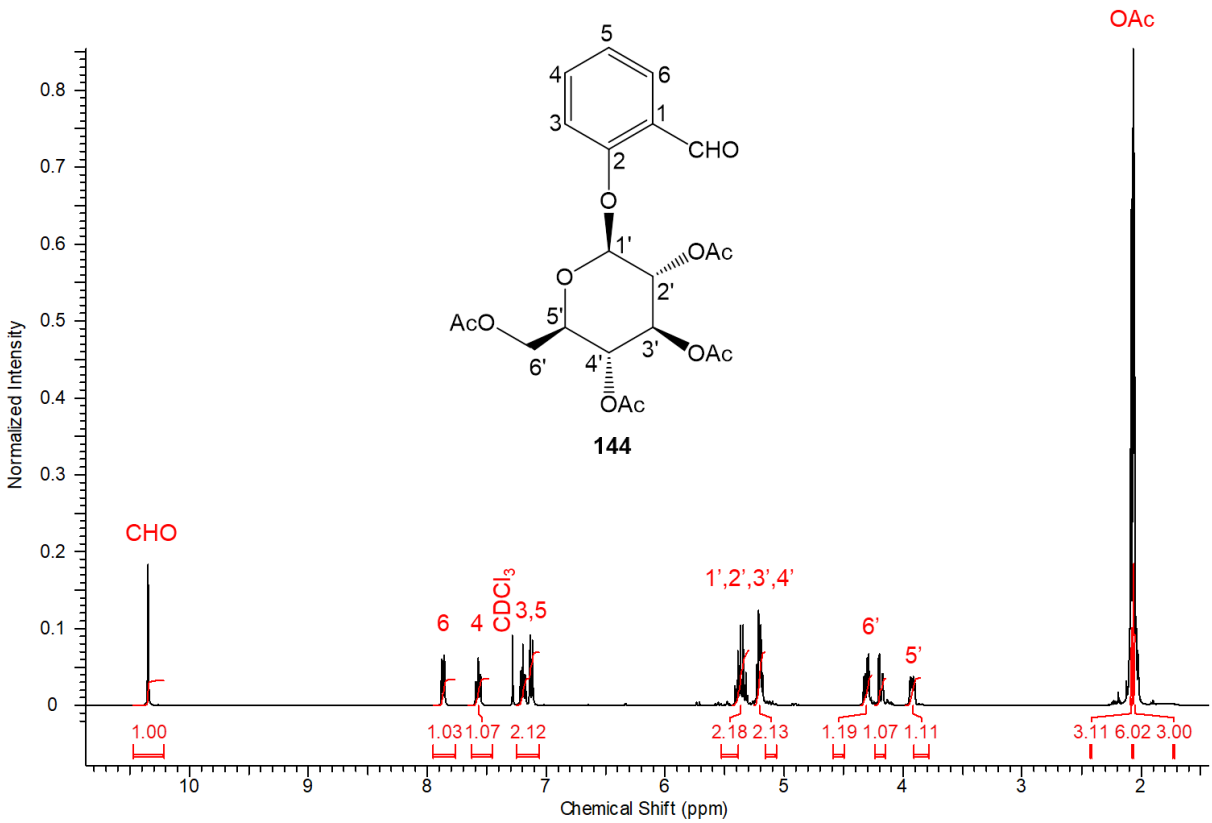

Figure 34: ^{1}H NMR spectrum of tetraacetoxyglucoside of 2-hydroxybenzaldehyde **144** in $CDCl_3$

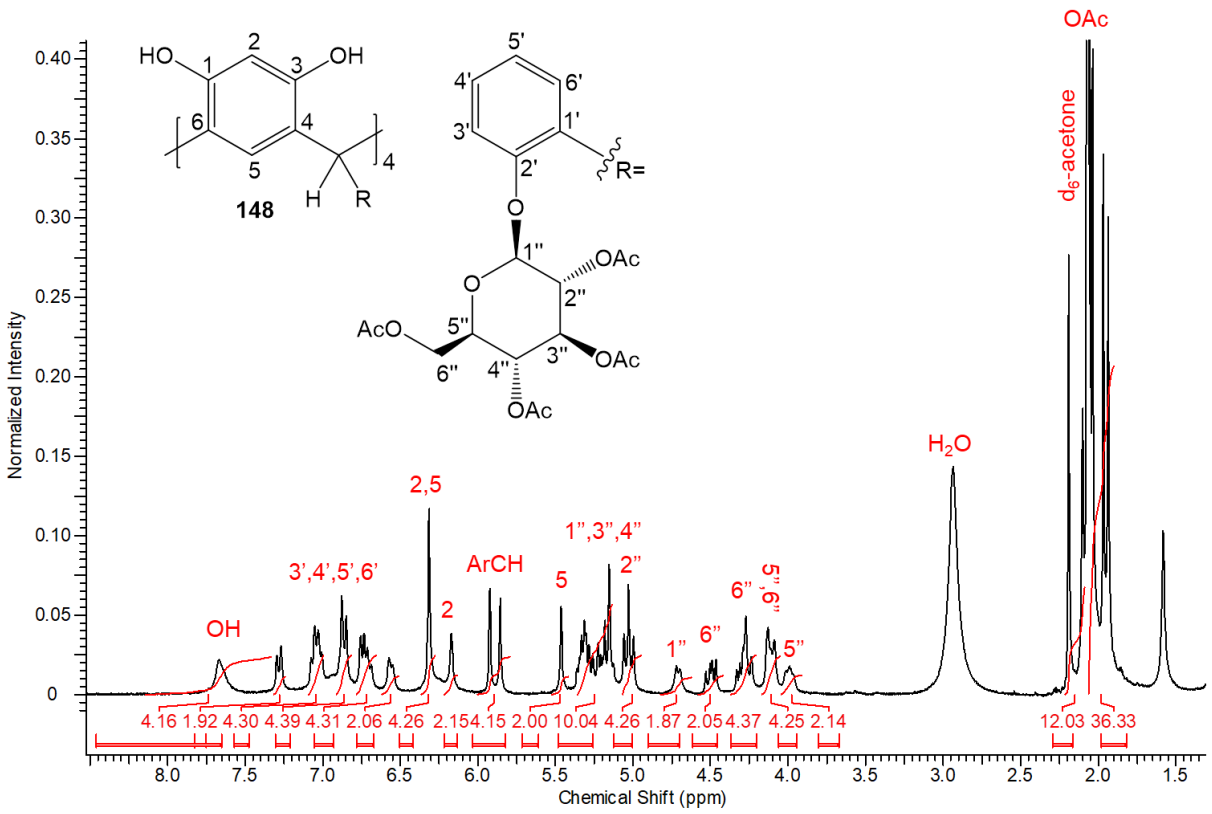

Figure 35: ^{1}H NMR spectrum of calix[4]resorcinarene glucoside **148** recovered after preparative TLC in d_6-acetone

Acylation of the crude precipitate **148** prepared directly without preceding purification was carried out depending upon the procedure had already been described for acylation of compounds **145** and **146**. The TLC showed one major spot and other light spots for unknown compounds, column chromatography was performed using EtOAc: Pet. ether (2:1) as eluent. The ^{1}H NMR spectrum of the major isolated fraction showed doublet peak for the bridging hydrogens resonating at 5.80 ppm. Four singlets in the region 5.92-7.35 ppm characteristics for the aromatic protons in the macrocycle, therefore, similarly to previously obtained data is expected that this octaester has also the r*ctt* chair diastereoisomer with C_{2h} symmetry (Figure 36). The structure of **149** is also supported by mass spectrometry analysis. The spectrum gave molecular ion at

m/z 1386.5182 that corresponds to $(M+2NH_4)^{2+}$. (Expected: *m/z* 1386.5179) (Appendix 8).

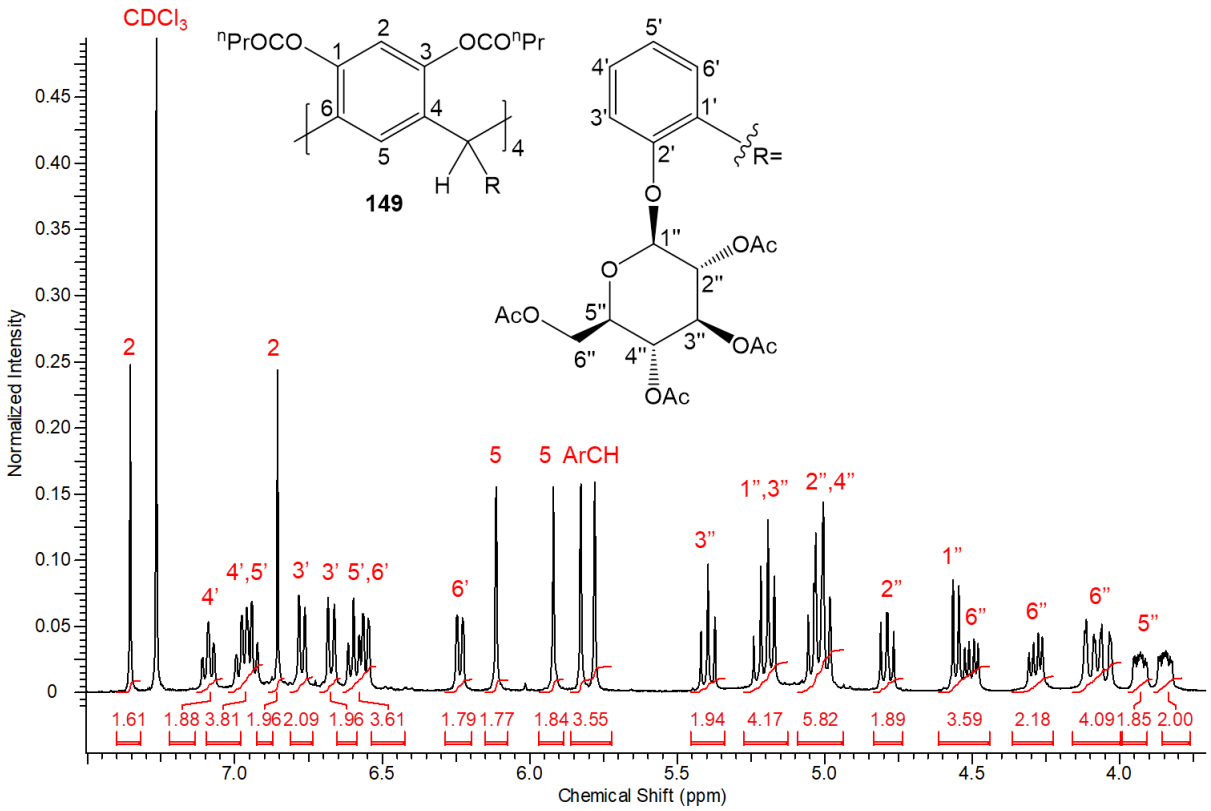

(a)

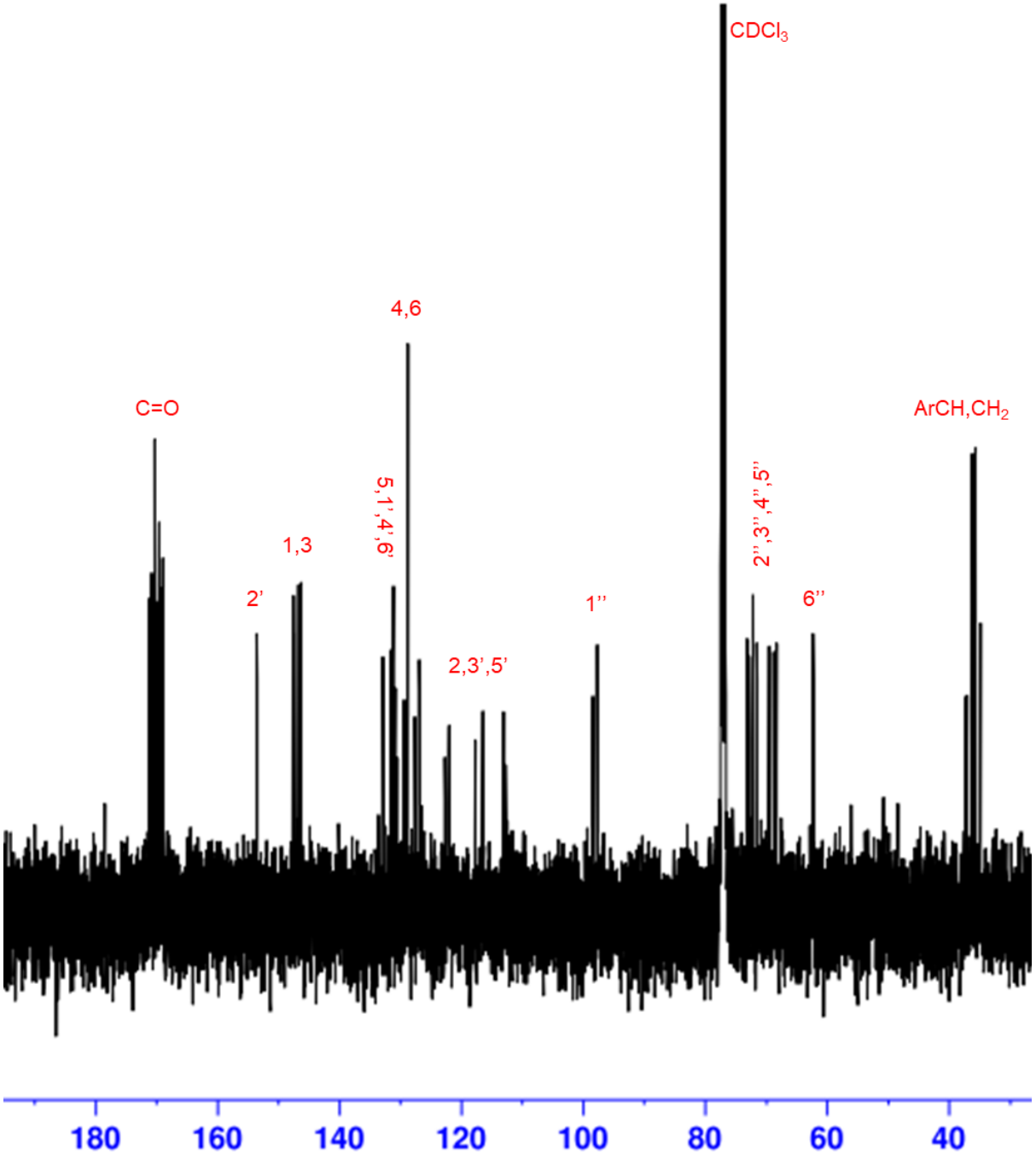
CDCl3
4,6
C=O
ArCH,CH2
5',1',4',6'
1,3
2''
,3'',4'',5''
2'
1''
6''
2,3',5'
180
160
140
120
100
80
60
40

(b)

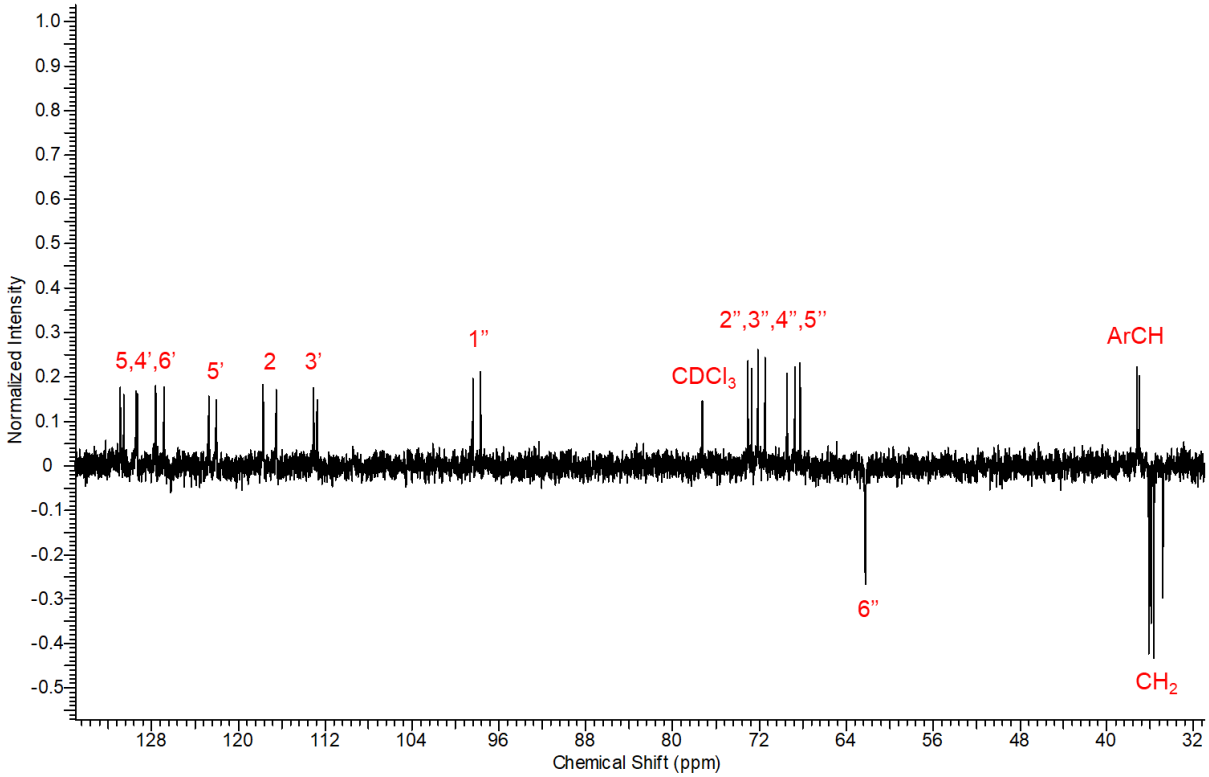

(c)

Figure 36: (a) ^{1}H NMR, (b) ^{13}C NMR and (c) DEPT135 spectra of calix[4]resorcinarene glucoside octabutyrate **149** in $CDCl_3$

2.3 Synthesis of novel calix[4]resorcinarene galactoside

A three step procedure was formulated for the synthesis of galactose bearing calix[4]resorcinarene required bromination of the commercial 1,2,3,4,6-penta-*O*-acetyl-*β*-D-galactose **150** by the protocol described in the literature (Mitchell *et al*., 2001). Then, 2,3,4,6-tetra-*O*-acetyl-*α*-bromo-D-galactopyranose **151** was reacted with 4-hydroxybenzaldehyde under similar conditions to that described for glucosylation of compounds **139-141**, to furnish the corresponding acetylated glycosidic aldehyde **152** in 74% after purification using column chromatography (Figure 37).

The beta galactoside was obtained as a major product under these conditions (Scheme 38).

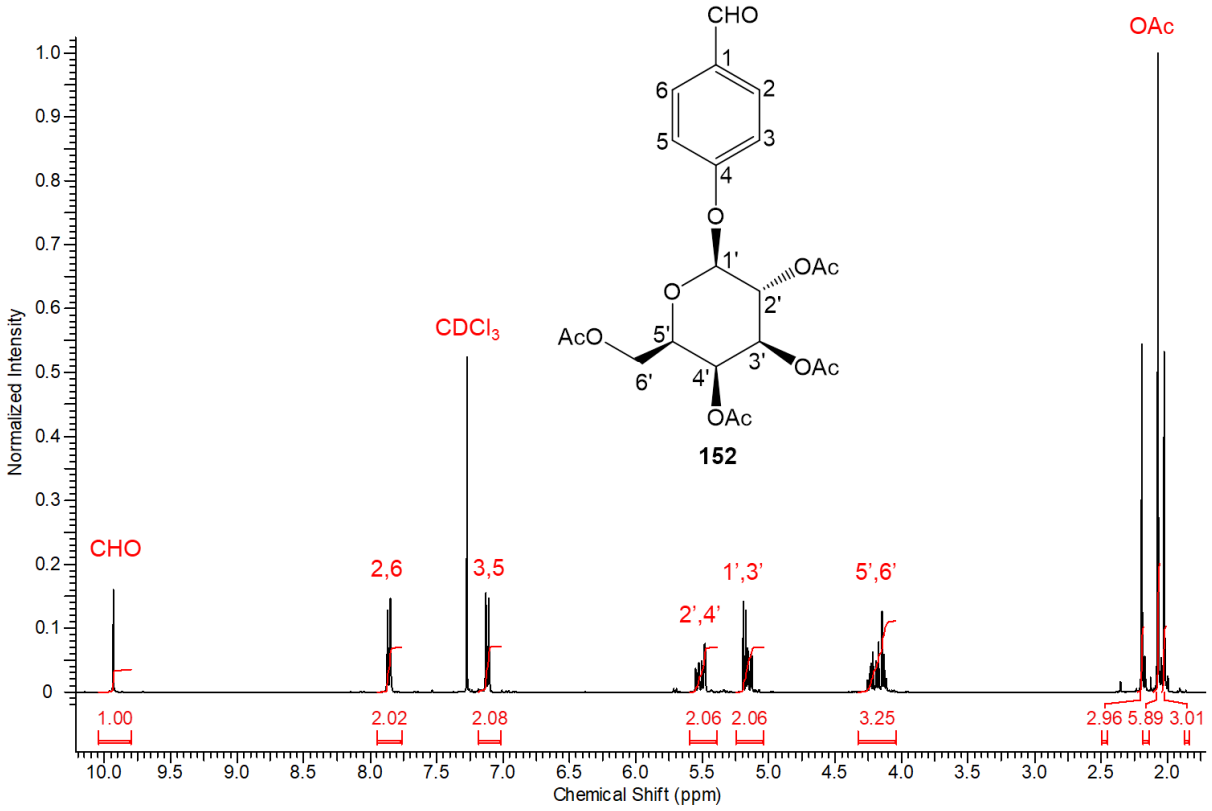

Figure 37: ^{1}H NMR spectrum of tetraacetoxygalactoside of 4-hydroxybenzaldehyde **152** in $CDCl_3$

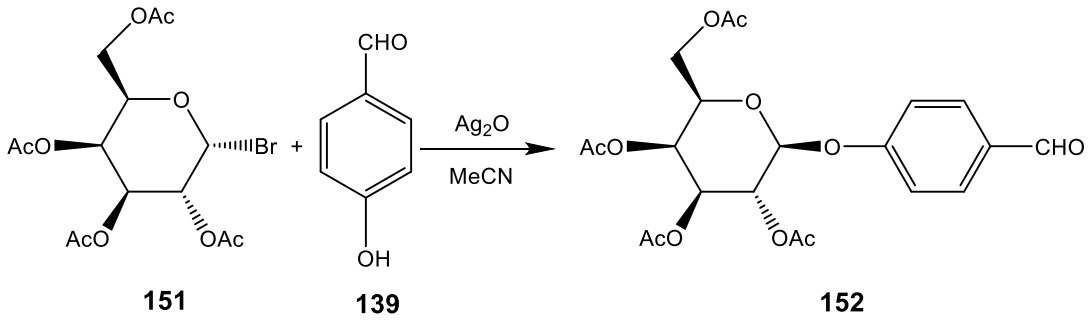

Scheme 38: Synthesis of beta phenyl galactoside

It has been reported that calix[4]resorcinarene bearing methoxy substituents can be prepared by $BF_3.Et_2O$ catalysis condensation of 3-alkoxy phenol or 1,3-dimethoxybenzene with different aldehydes to form calix[4]resorcinarene tetraalkyl or octaalkyl ethers (McIldowie *et al*., 2000; Boxhall *et al*., 2003; Ogoshi *et al*., 2009).

Therefore, in our study, we wished to synthesise the novel tetrameric calix[4]resorcinarene bearing galactose motifs using boron trifluoride $BF_3.Et_2O$ as Lewis acid catalysis. By coupling resorcinol to compound **152** in Et_2O as solvent, yielded the desired compound as yellow crystals after 24 h of reaction at r.t (Scheme 39).

This reaction proceeded smoothly and faster than using $AlCl_3$ as a catalyst for glucosylated calix[4]resorcinarene precursors. Additionally, the ^{1}H NMR and ^{13}C-NMR of the crude product, were clearer and less complex than that usually seen for those compounds due to trap the nitrobenzene and the solvent used in the extraction step which is normally occurs by the cavity of calix[4]resorcinarene (Puttreddy *et al*., 2018).

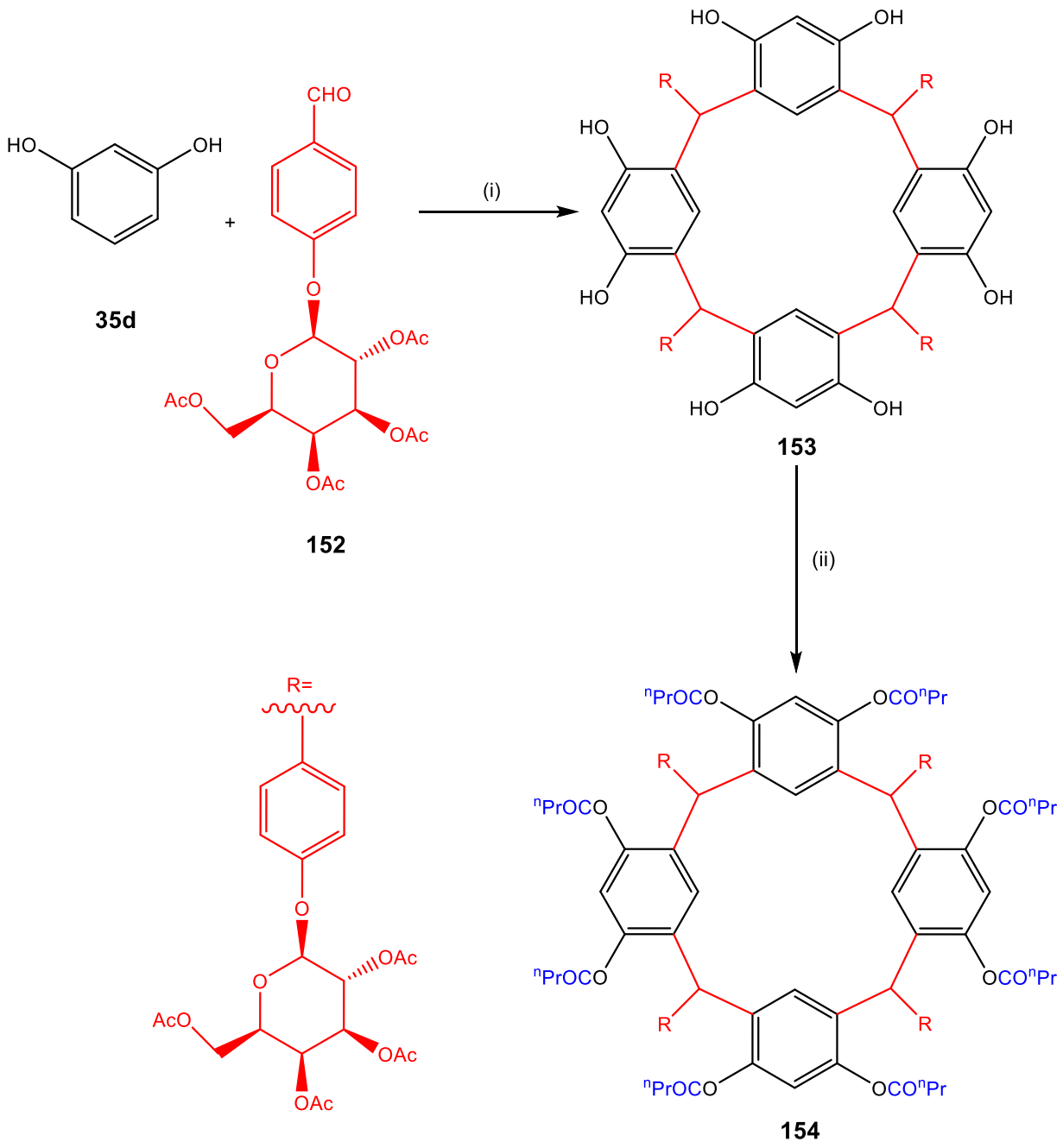

Reagents and conditions: (i) $BF_3.Et_2O$, 24 h, Et_2O (ii) butyric anhydride, pyridine, heating at 80 ^{0}C overnight

Scheme 39: Synthesis of calix[4]resorcinarene galactoside

The ^{1}HNMR spectrum in (d_6-acetone) showed characteristic signals of acetyl groups 1.94-2.24 ppm, characteristic signals for the glucose hydrogens 4.19-4.55, 5.18-5.66 ppm, methine bridge units between the aromatic rings at 5.71, 5.80 and 5.86 ppm, the fragments of the resorcinol units were confirmed in the spectrum with a chemical shift among 6.08-6.65; 7.28-7.81 ppm, and the aromatic protons of substituted glucose 6.72-7.13 ppm. These results led to the conclusion that, as expected, compound **153** presents two isomers (Figure 38).

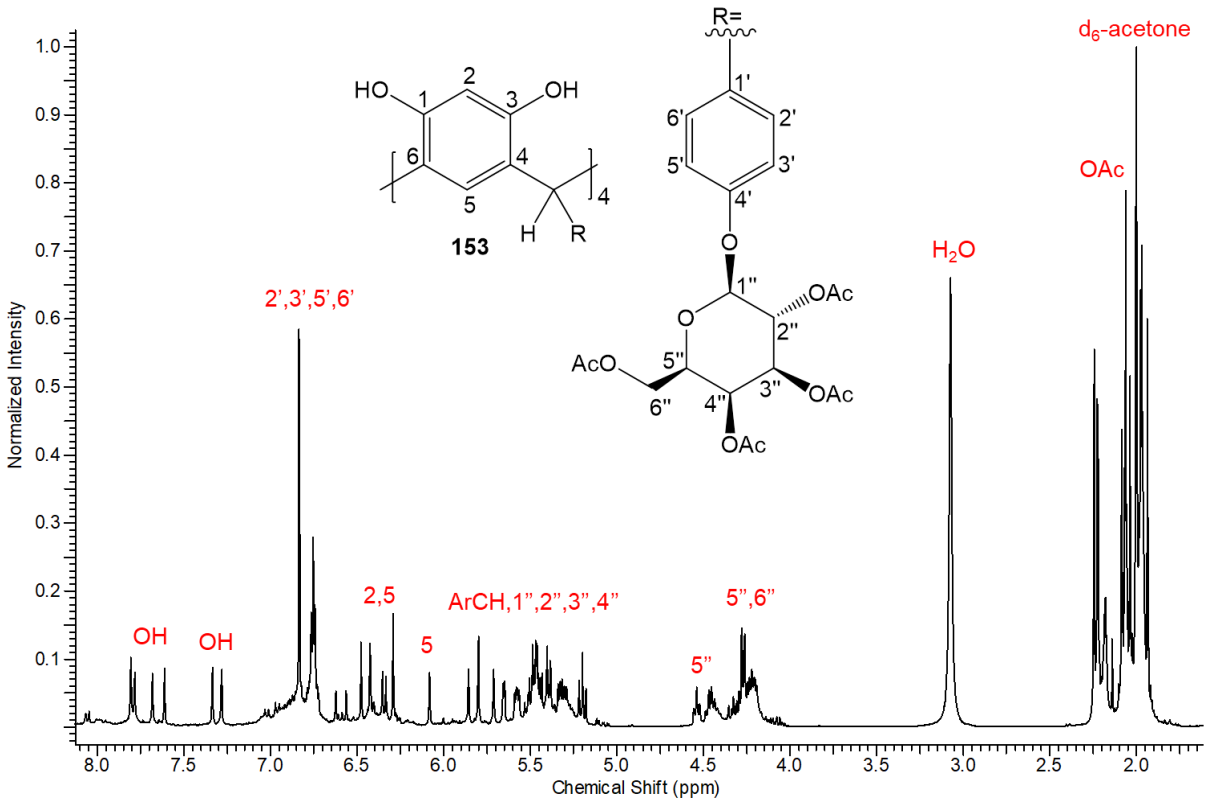

(a)

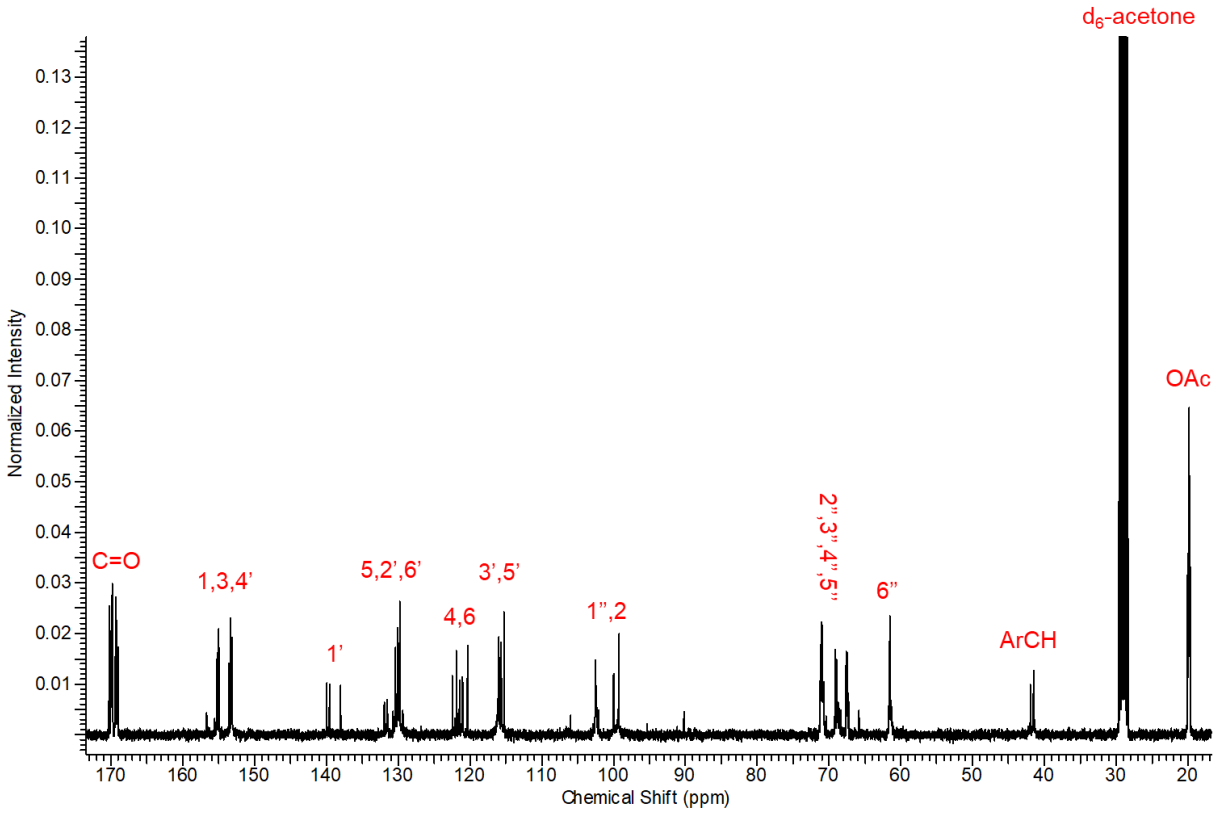
d6-acetone
OAc
C=O
1,3,4'
1'
5,2',6'
4,6
3',5'
1",2
2",3",4",5"
6"
ArCH
Normalized Intensity
Chemical Shift (ppm)

(b)

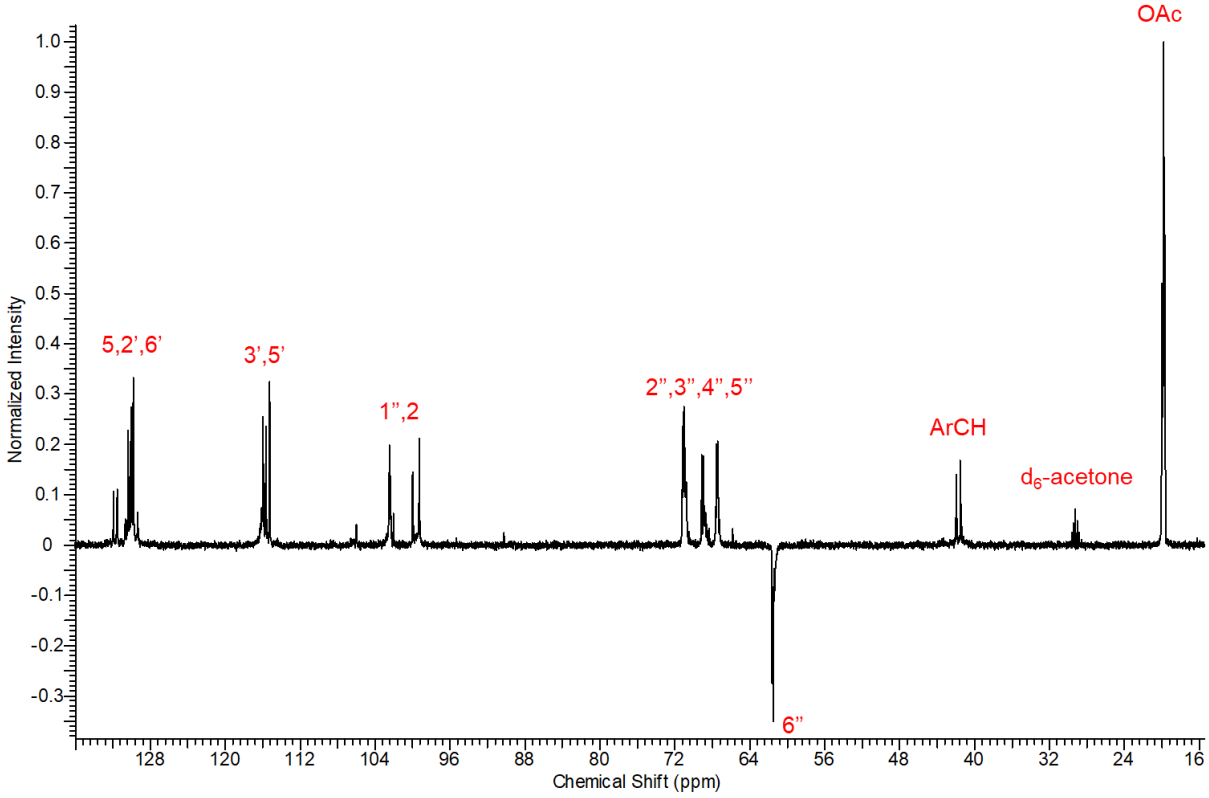

(c)

Figure 38: (a) ^{1}H NMR, (b) ^{13}C NMR and (c) DEPT135 spectra of calix[4]resorcinarene galactoside **153** (mixture of two isomers) in d_6-acetone

The calix[4]resorcinarene **153** was exposed to acylation conditions identical to those applied for compounds **145**, **146** and **148**. Generating mixture of two octaester-tetra(galactophenyl)calix[4]resorcinarenes **154a** and **154b** as identified by the ^{1}HNMR analysis of this mixture in $CDCl_3$, and appearance of three non-equivalent signals 5.96-6.21 ppm for the aromatic core protons of the macrocyclic. However, signals for the hydrogens at the methine bridges were in the characteristic range of the galactose protons, and was difficult to assign their chemical shifts precisely.

The TLC of the crude mixture was done prior to separation by column chromatography using EtOAc: Pet. ether (1.5:1) as eluent, and showed clearly the presence of two spots in close proximity to each other for a major and for a minor isomer, in addition to other light spots for unknown compounds.

The major diastereoisomer product was isolated in 14% yield, the ^{1}H NMR in $CDCl_3$ showed the presence of four signals for the aromatic hydrogens of resorcinol units (6.10, 6.29, 6.94, 7.04 ppm) and two singlets for the hydrogen atoms at the methine bridges at 5.46 and 5.58 ppm (Figure 39). The structure of **154a** is also supported by mass spectrometry analysis. The spectrum gave molecular ion at *m*/*z* 1386.5188 that corresponds to $(M+2NH_4)^{2+}$. (Expected: *m*/*z* 1386.5179) (Appendix 9).

The minor isomer was obtained in 5% yield after column chromatography, the ^{1}H NMR showed single doublet resonance for the bridging hydrogens at 5.37 ppm and single peaks for each pair of the aromatic hydrogens of resorcinol units (5.97, 6.29, 6.89, 6.92 ppm) and a pair of doubles for pendant aromatic substituents (Figure 40). The structure of **154b** is also supported by mass spectrometry analysis. The spectrum gave molecular ion at *m*/*z* 1386.5188 that corresponds to $(M+2NH_4)^{2+}$. (Expected: *m*/*z* 1386.5179) (Appendix 10).

As expected the ^{1}H and the ^{13}C NMR spectra of both calix[4]resorcinarenes functionalised with glucoside or galactoside residues were similar in case the protons and carbon signals for the resorcinol and the aromatic groups for both isomers, except the appearance of resonances for the carbohydrate residues were different. Each pair of octabutyrates showed almost corresponding infrared and mass spectra, but their R_f values on TLC, melting points and the ^{1}H NMR analysis were different also.

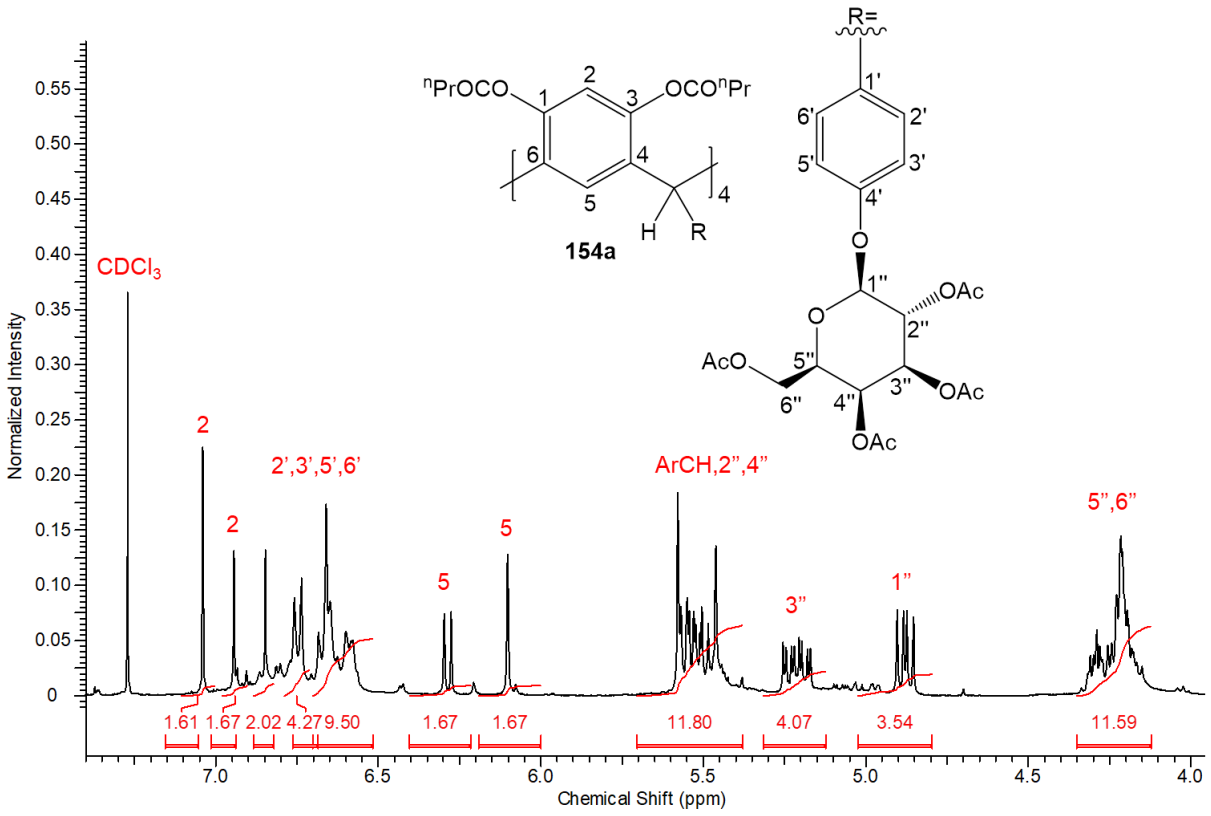
154a
CDCl3
2
2
2',3',5',6'
5
5
ArCH,2",4"
3"
1"
5",6"
1.61 1.67 2.02 4.27 9.50
1.67
1.67
11.80
4.07
3.54
11.59
Normalized Intensity
Chemical Shift (ppm)

(a)

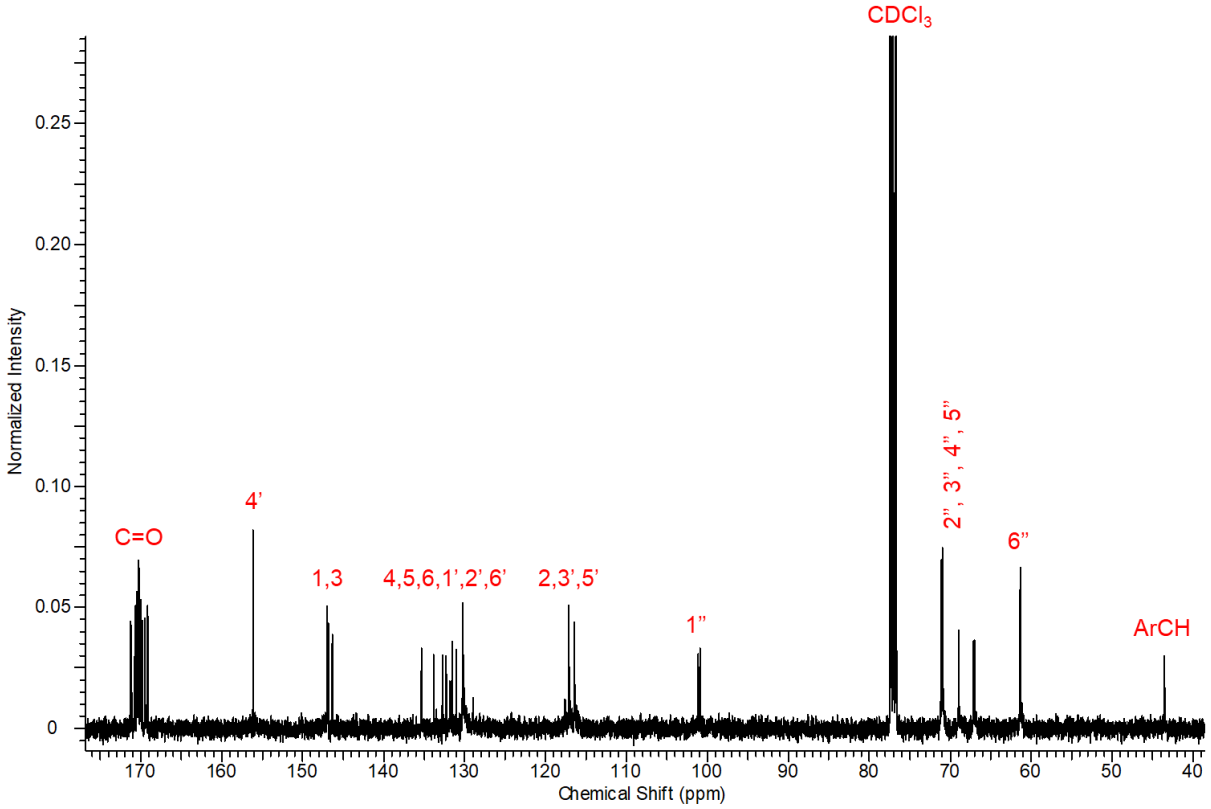
CDCl3
C=O
4'
1,3
4,5,6,1',2',6'
2,3',5'
1"
2", 3", 4", 5"
6"
ArCH
Normalized Intensity
Chemical Shift (ppm)

(b)

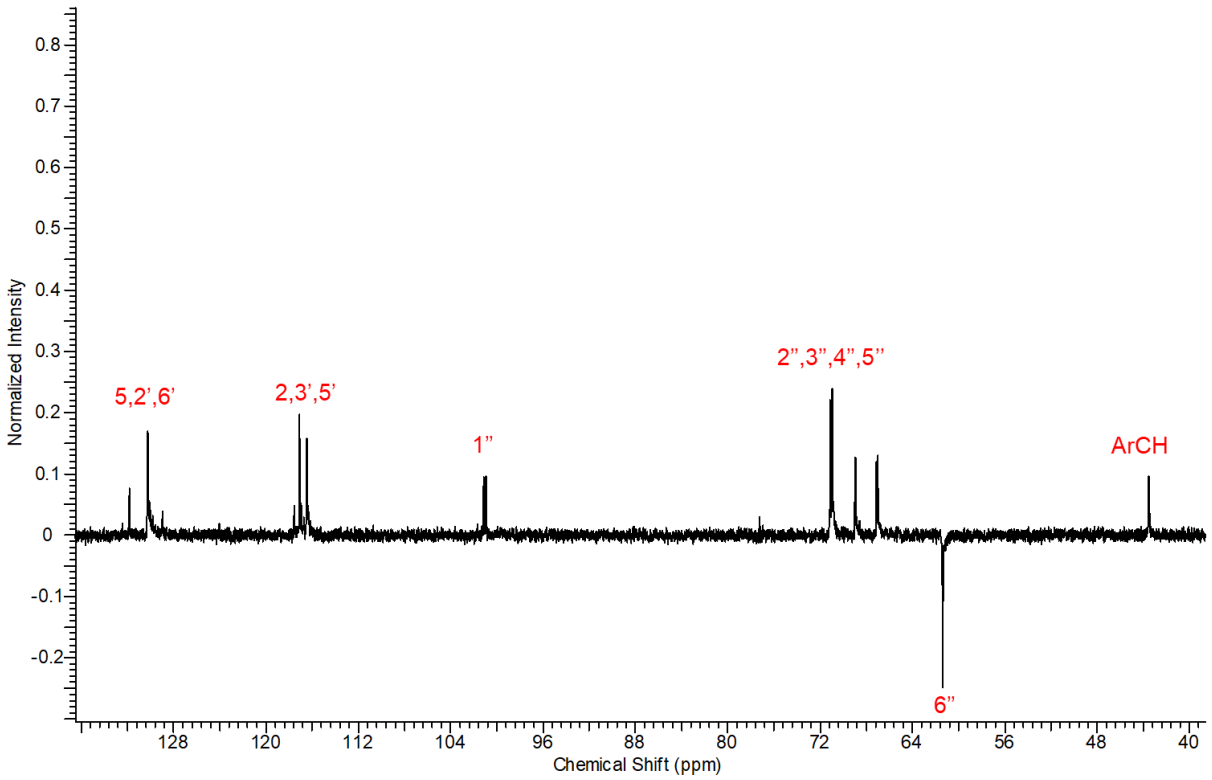

(c)

Figure 39: (a) ^{1}H NMR, (b) ^{13}C NMR and (c) DEPT135 spectra of calix[4]resorcinarene galactoside octabutyrate **154a** (major isomer) in $CDCl_3$

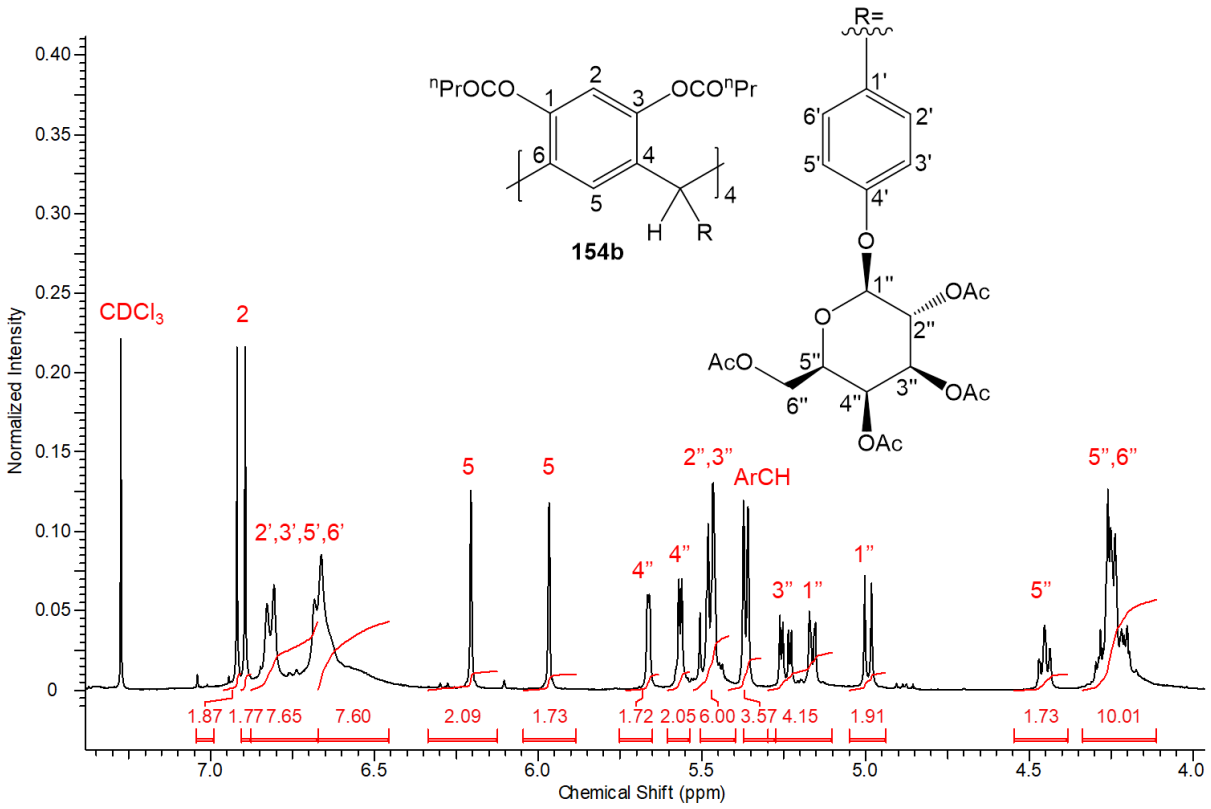
154b
CDCl3
2
2',3',5',6'
5
5
4"
4"
2",3"
ArCH
3"
1"
1"
5"
5",6"
1.87
1.77
7.65
7.60
2.09
1.73
1.72
2.05
6.00
3.57
4.15
1.91
1.73
10.01
Normalized Intensity
Chemical Shift (ppm)

(a)

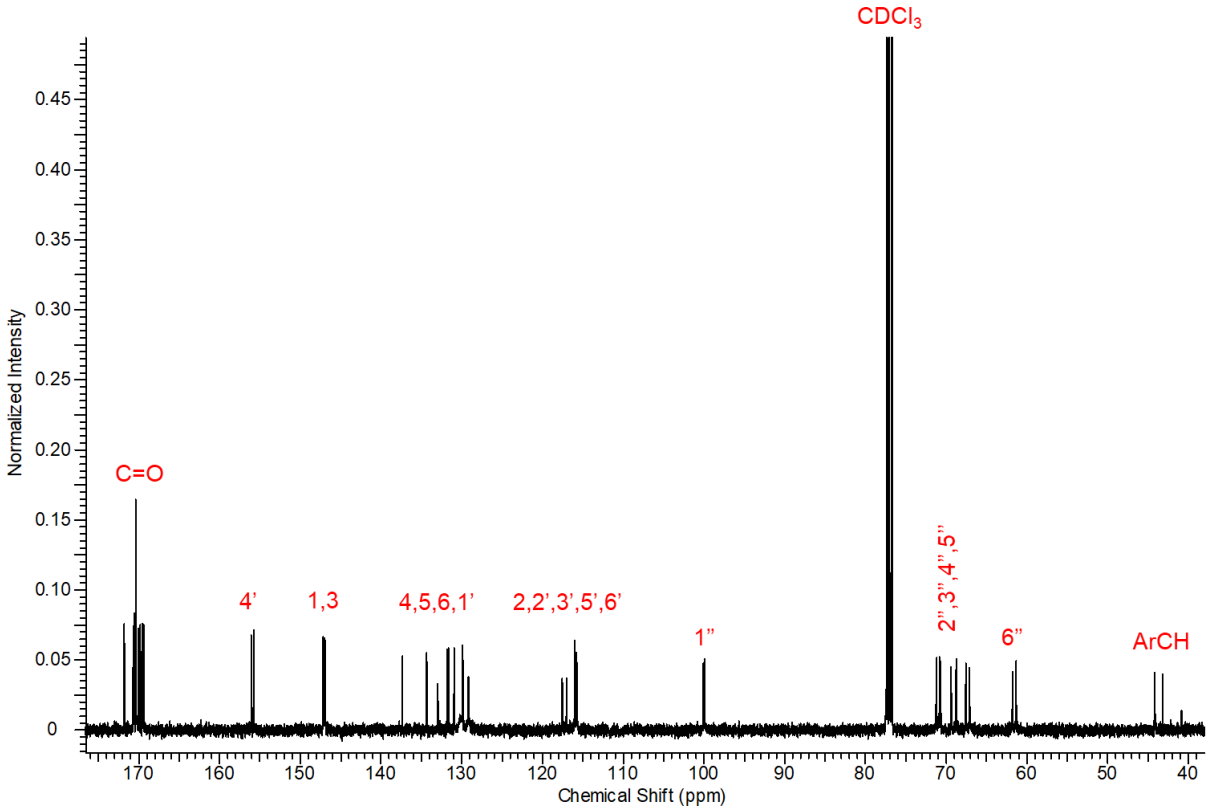
CDCl3
C=O
4'
1,3
4,5,6,1'
2,2',3',5',6'
1"
2",3",4",5"
6"
ArCH
Normalized Intensity
Chemical Shift (ppm)

(b)

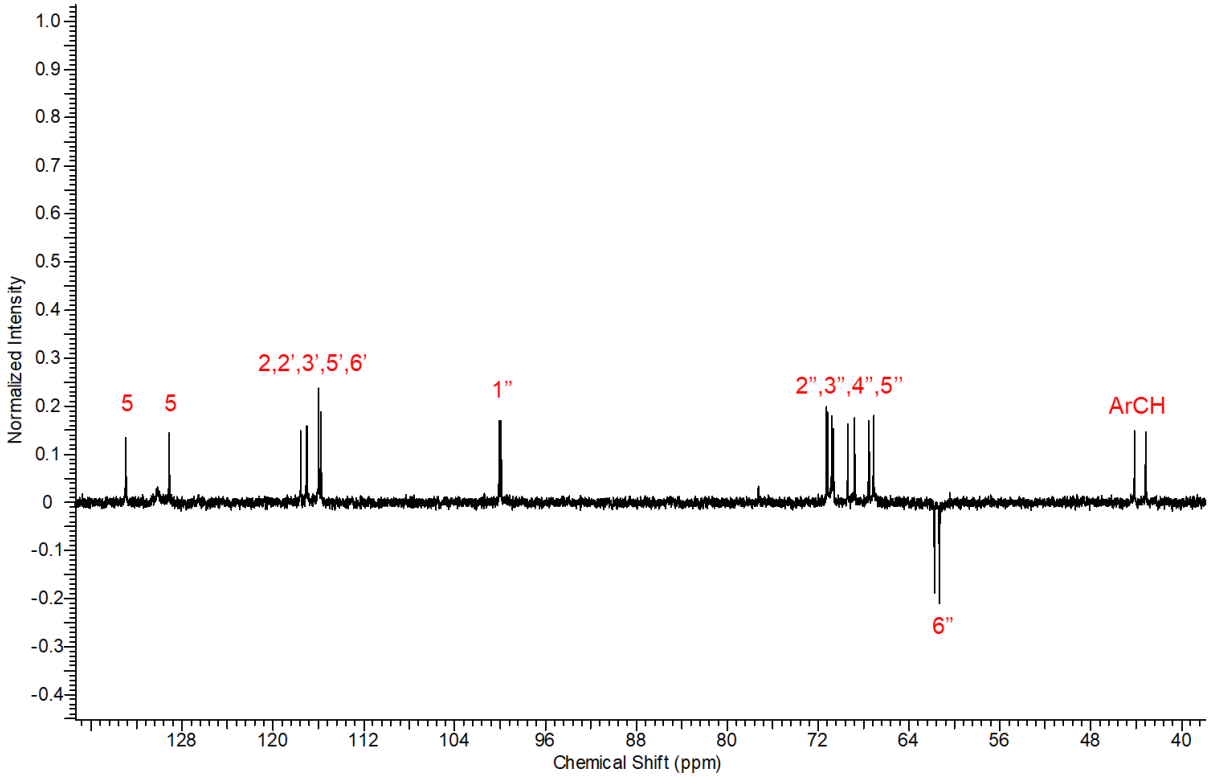

(c)

Figure 40: (a) ^{1}H NMR, (b) ^{13}C NMR and (c) DEPT135 spectra of calix[4]resorcinarene galactoside octabutyrate **154b** (minor isomer) in $CDCl_3$

After success in preparing a series of calix[4]resorcinarenes bearing monosaccharide- containing fragments in the lower rim, we transferred our attention to the synthesis of corresponding glycocalix[4]resorcinarenes in which disaccharide units are linked to the lower rim of the macrocycle.

The synthesis of these glycoclusters was based on our previous experience of the condensation of resorcinol with glycosylated benzaldehydes in the presence of a Lewis acid, in which the hydroxyl units of the carbohydrates are protected by the acetyl groups.

Amongst the methods described in the literature for the synthesis of glycosylated benzaldehydes include reaction of the corresponding acetobromodisaccharide with hydroxyl-benzaldehydes in the presence of NaOH in acetone. A low yield was obtained using this procedure, even when using prolonged reaction times (Driaf *et al*., 1996).

Other methods to prepare these compounds are also commonly used in which 4-(2',3',6',2'',3'',4'',6''-heptaacetyl-*β*-D-lactosyloxy)benzaldehyde was prepared by reaction of peracetylated lactosyl bromide with hydroxy benzaldehydes using phase transfer catalysis. This reaction proceeded either by using a two phase system of (1:1) water-chloroform in the presence of aqueous Na_2CO_3 or NaOH and using tetrabutyl- or tetraoctylammonium bromide as catalyst, or by using DCM as solvent instead partitioned with a saturated aqueous solution of K_2CO_3. These methods required heating in some cases or stirring from 3 h to overnight to give the required compound (Wen *et al*., 2008).

4-(2',3',6',2'',3'',4'',6''-Heptaacetyl-*β*-D-cellobiosyloxy)benzaldehyde has been reported as being prepared by treatment of 4-hydroxybenzaldehyde with 2,3,6,2',3',4',6'-hepta-*O*-acetyl-*α*-D-cellobiosyl bromide in DCM using 5% aqueous solution of NaOH and tetrabutylammonium bromide as catalyst. The required compound was obtained after 3 days of stirring at room temperature (Griesbeck *et al*., 2011).

In our study we wanted to prepare per-acetylated disaccharides conjugated with benzaldehydes at the anomeric position using the Koenigs-Knorr method. The linker preparation began with the bromination of per-acetylated carbohydrates according to a procedure described in the literature (Mitchell *et al*., 2001). In the presence of silver(I) oxide and MeCN as solvent,

2,3,6,2',3',4',6'-hepta-*O*-acetyl-*α*-D-lactosyl bromide **156** reacted with 4-hydroxybenzaldehyde in 1:1 molar ratio. The reaction was complete as shown by TLC monitoring and the mixture was subsequently subjected to purification using flash chromatography to give the corresponding glycoside **157** as white crystals in a reasonable yield of 60% (Figure 41).

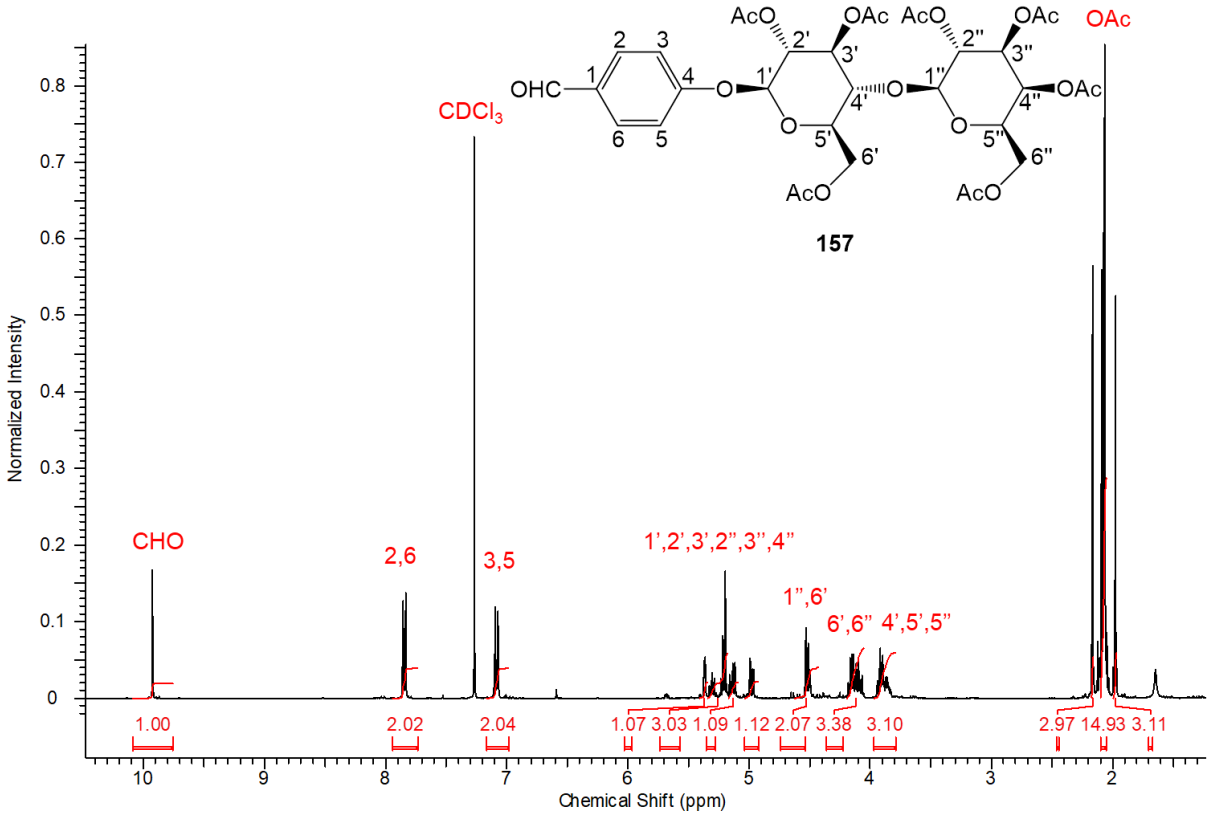

Figure 41: ^{1}H NMR spectrum of heptaacetoxylactoside of 4-hydroxybenzaldehyde **157** in $CDCl_3$

2.4 Synthesis of calix[4]resorcinarene lactoside 158

Preparation of tetra(4-lactophenyl)calix[4]resorcinarene through Lewis acid catalysed condensation using an equimolar ratio of resorcinol to 4-(2',3',6',2'',3'',4'',6''-heptaacetyl-*β*-D-lactosyl)benzaldehyde was carried out in a 15:10 mixture of Et_2O and THF at r.t. in a similar manner to that described for

compound **153** (Scheme 40). The product was characterised using usual methods, including ^{1}H NMR, ^{13}C NMR, DEPT135 and HSQCDEPT.

The ^{1}H NMR spectrum in d_6-acetone shows, as previously noticed for large pendant fragments, characteristic multiplet signals for aromatic groups between 6.51-7.20 ppm, characteristic signals for protons in the resorcinol units between 5.88-6.43; 7.28-7.70 ppm, doublet peaks for the methine bridge hydrogens 5.74 ppm, characteristic signals for lactose residues between 3.97-5.45 ppm and the acetyl groups between 1.88-2.22 ppm (Figure 42).

The ^{13}C NMR spectrum in d_6-acetone showed a significant signal at 41.9 ppm which confirmed the existence of methine bridge residues between the aromatic rings, and the aromatic carbons of resorcinol units appeared at 153.3, 153.1, 132.0, 102.4 and 102.2 ppm. Signals at 130.0, 129.7, 115.6 and 115.3 ppm were assigned to the pendant aromatic carbons (Figure 42).

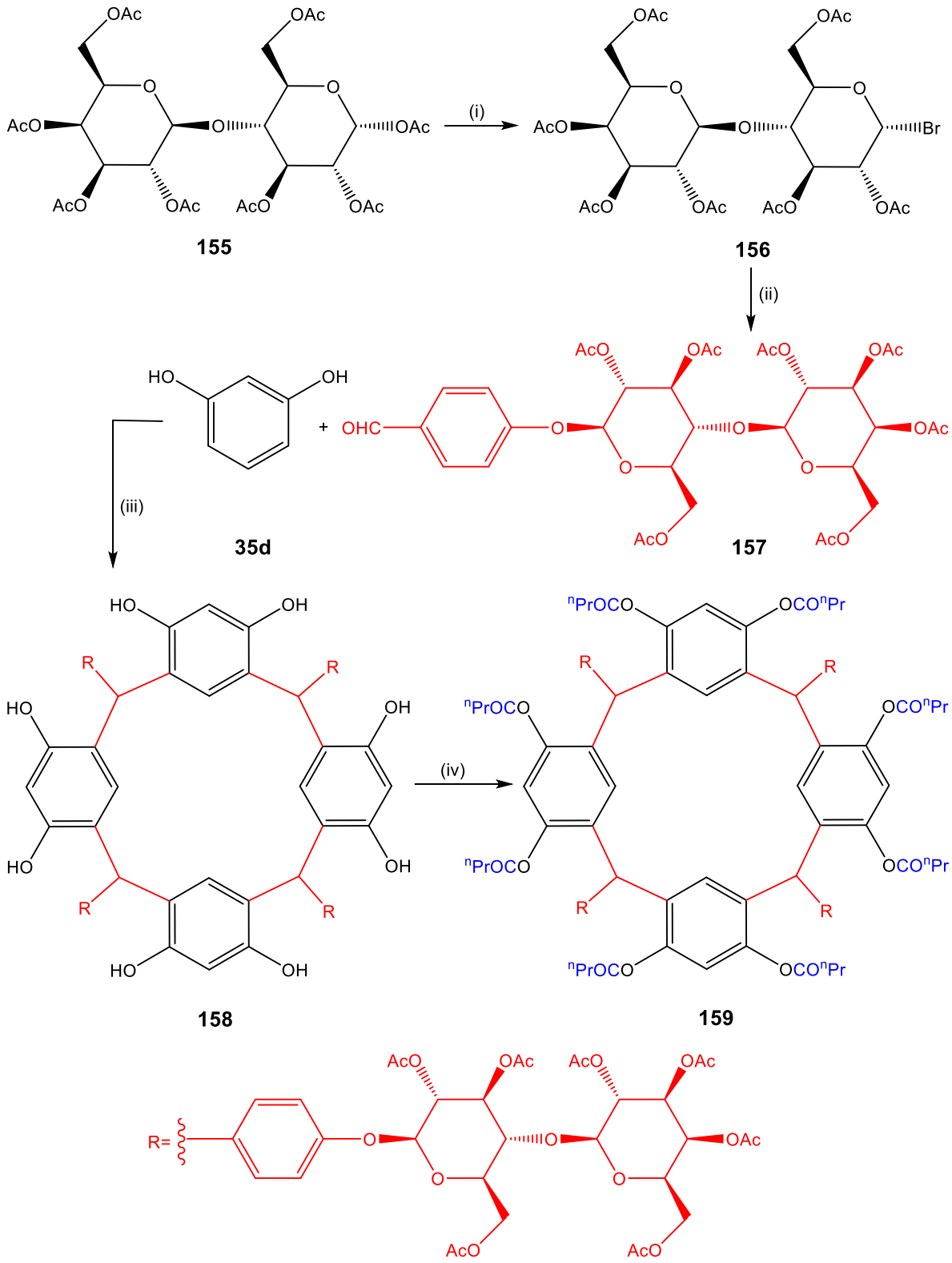

Scheme 40: Synthesis of calix[4]resorcinarene lactoside

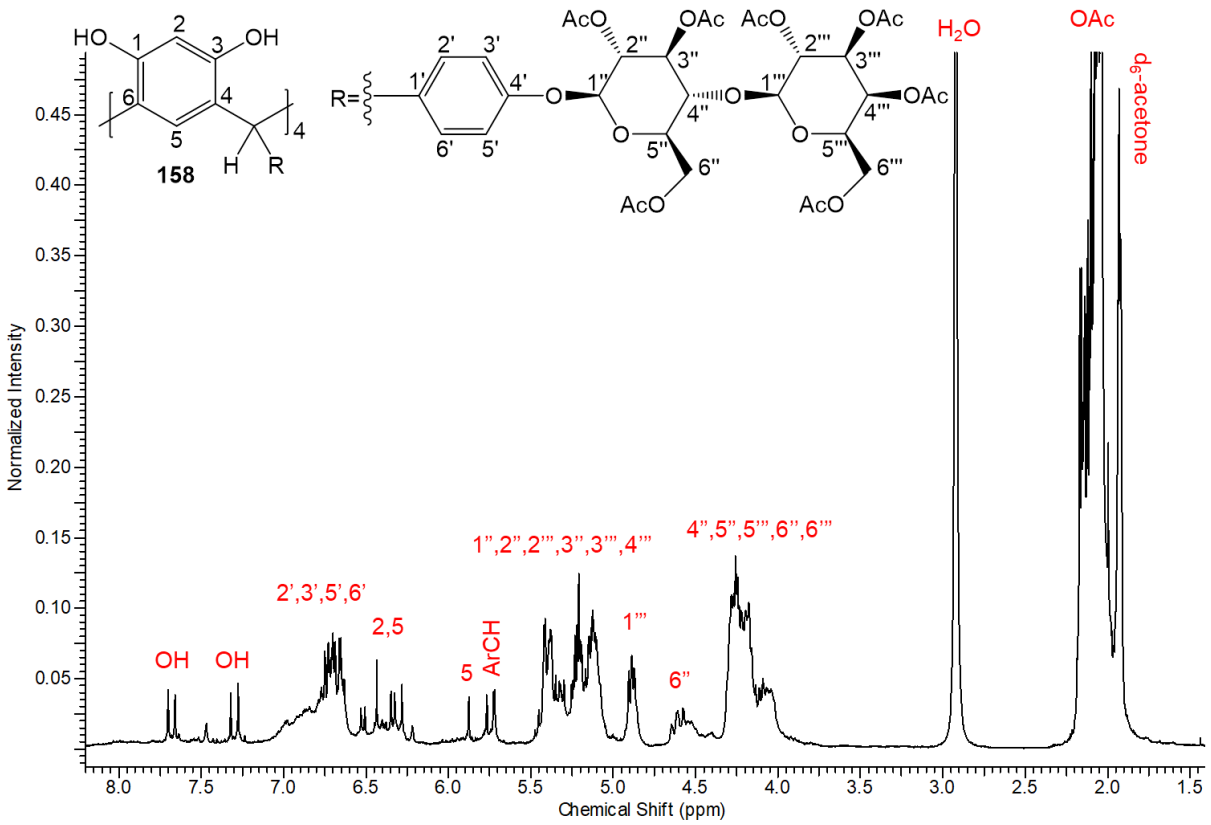
158
R=
AcO
OAc
H2O
d6-acetone
Normalized Intensity
Chemical Shift (ppm)
OH
OH
2',3',5',6'
2,5
5
ArCH
1'',2'',2''',3'',3''',4'''
1'''
6''
4'',5'',5''',6'',6'''

(a)

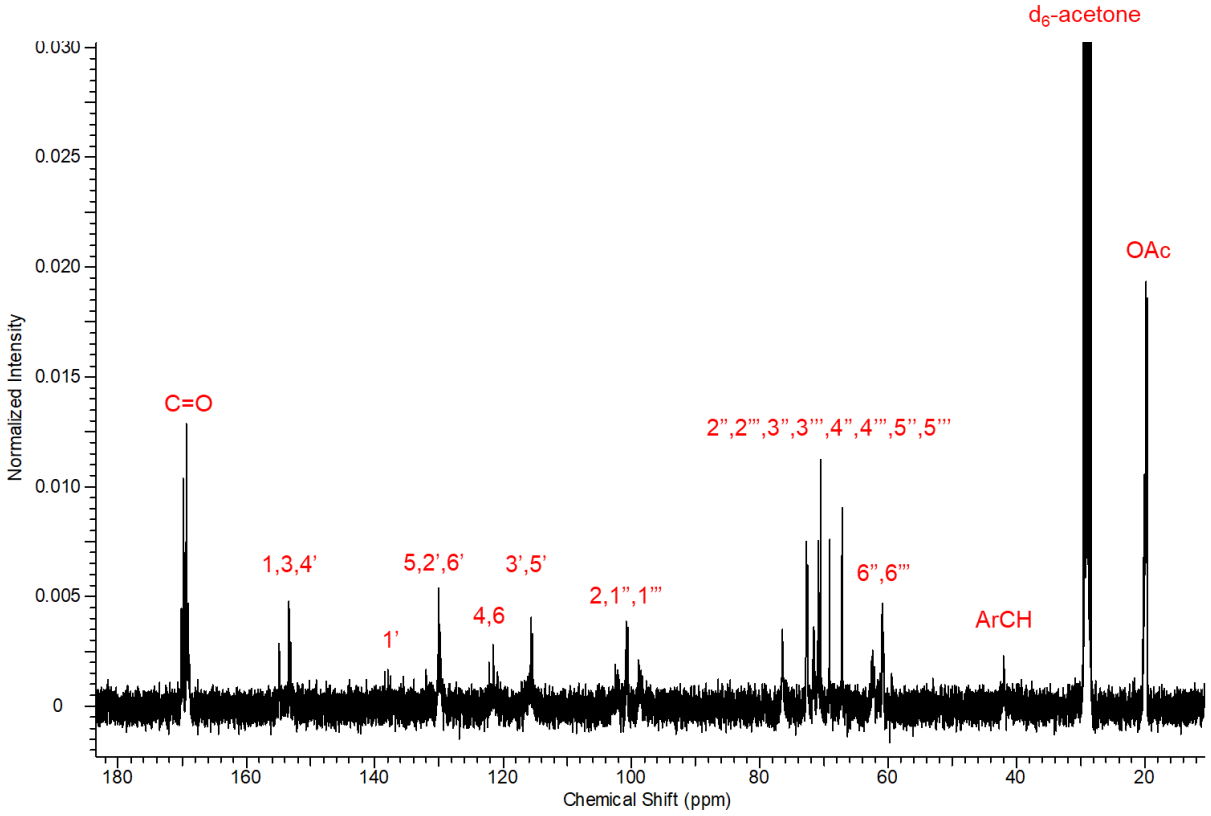
d6-acetone
OAc
Normalized Intensity
Chemical Shift (ppm)
C=O
1,3,4'
5,2',6'
3',5'
4,6
1'
2,1'',1'''
2'',2''',3'',3''',4'',4''',5'',5'''
6'',6'''
ArCH

(b)

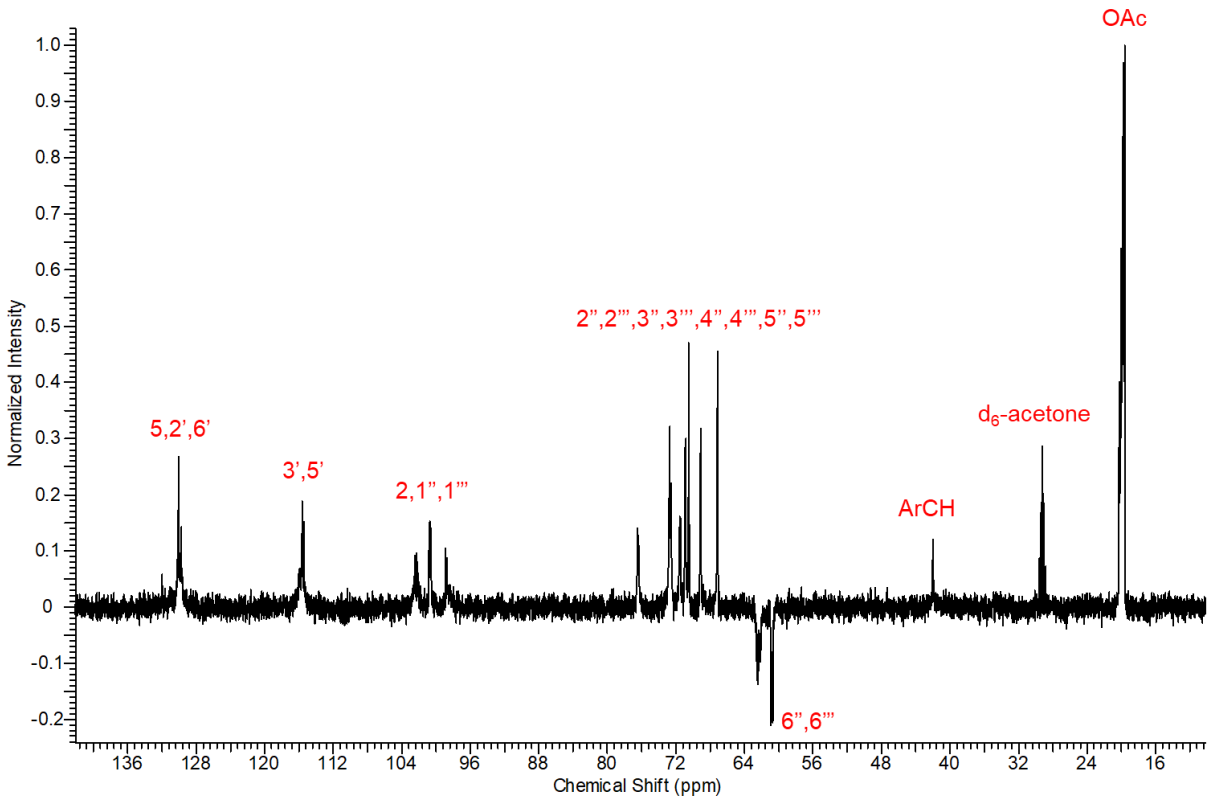

(c)

Figure 42: (a) ^{1}H NMR, (b) ^{13}C NMR and (c) DEPT135 spectra of calix[4]resorcinarene lactoside **158** in d_6-acetone

The lactose-functionalised glycocluster **158** was subjected to an acylation reaction utilising a mixture of butyric anhydride and pyridine, producing the octabutyrate- of tetra(4-lactophenyl)calix[4]resorcinarene **159**. TLC analysis of the crude mixture suggested the presence of two isomers by the presence of two spots (major and minor), the same result was estimated from the ^{1}H NMR spectrum which showed three non-equivalent signals in the region in the spectrum 5.83-6.02 ppm that contains resonances for the aromatic core protons as usually observed from the crude mixture of calix[4]resorcinarene precursors with 4-substituent aromatic rings at the methine bridges. However, upon purification by column chromatography using EtOAc: Pet. ether (3:1) as eluent and identification of the recovered compounds after column, the result was

expected: one major isomer was obtained as indicated by the presence of two resonances for protons at methine bridges 5.38 and 5.49 ppm, four signals with chemical shift 5.82, 5.90, 6.01 and 6.22 ppm with three singlet resonances between 6.88-6.91 ppm for the aromatic hydrogens of resorcinol units, together with the expected multiplet and doublet for the pendant aromatic units 6.41-6.75 and 6.98 ppm (Figure 43). The structure of **159** is also supported by mass spectrometry analysis. The spectrum gave molecular ion at *m*/*z* 1962.6890 that corresponds to $(M+2NH_4)^{2+}$. (Expected: *m*/*z* 1962.6870) (Appendix 11).

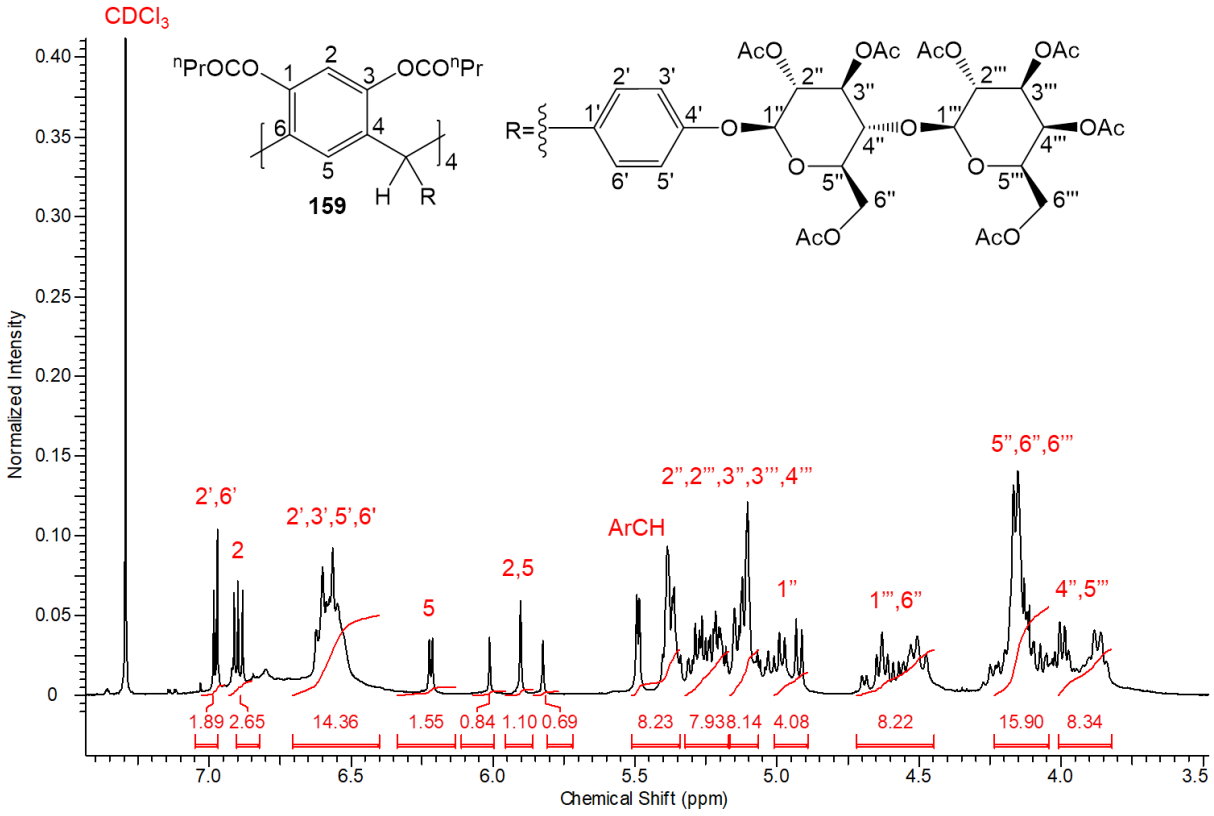

(a)

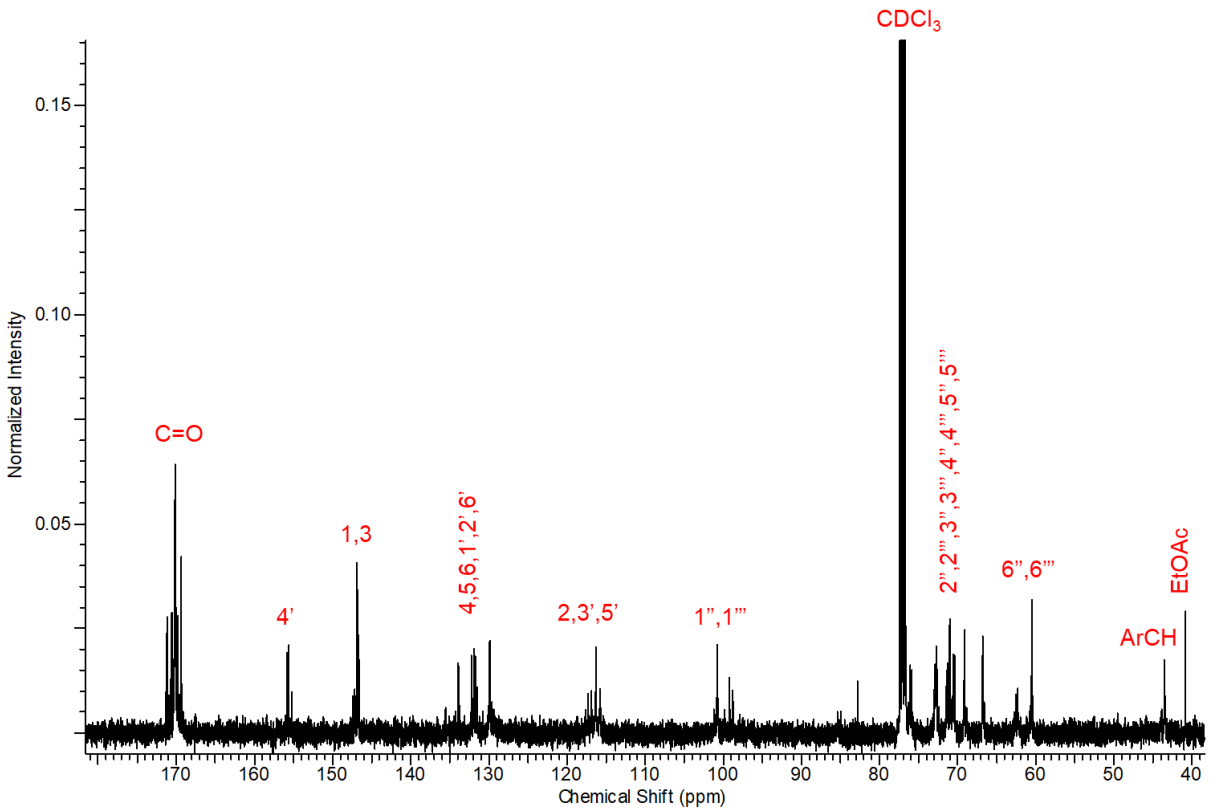
CDCl3
C=O
4'
1,3
4,5,6,1',2',6'
2,3',5'
1'',1'''
2'',2''',3'',3''',4'',4''',5'',5'''
6'',6'''
ArCH
EtOAc
Normalized Intensity
Chemical Shift (ppm)

(b)

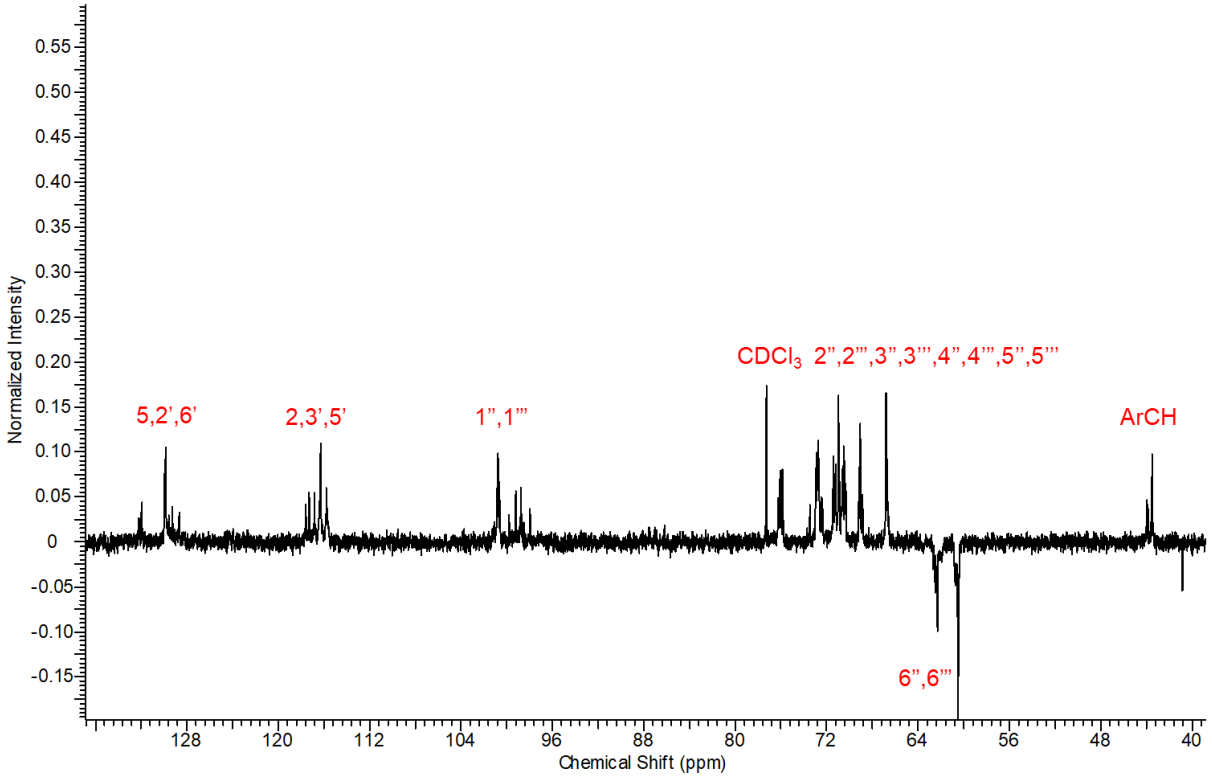
5,2',6'
2,3',5'
1'',1'''
CDCl3
2'',2''',3'',3''',4'',4''',5'',5'''
ArCH
6'',6'''
Normalized Intensity
Chemical Shift (ppm)

(c)

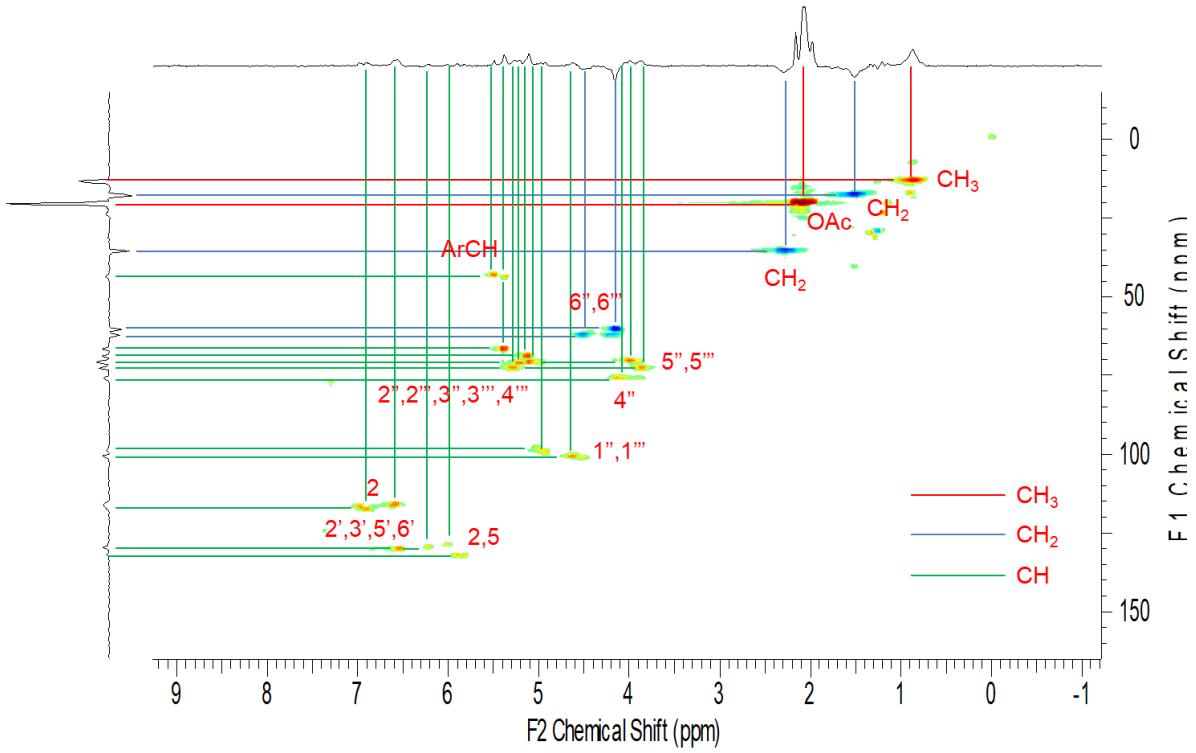

(d)

Figure 43: (a) ^{1}H NMR, (b) ^{13}C NMR, (c) DEPT135 and (d) HSQCDEPT spectra of calix[4]resorcinarene lactoside octabutyrate **159** in $CDCl_3$

2.5 Synthesis of calix[4]resorcinarene cellobioside 163

The synthesis of a macrocyclic carbohydrate cluster which displays four cellobiose residues on the lower rim was conducted by applying our previous synthetic methods, which have already been described.

The synthetic route consists of three steps (Scheme 41) beginning with bromination of peracetylated 1,2,3,6,2',3',4',6'-octa-*O*-acetyl-cellobiose **160**, which produced 2,3,6,2',3',4',6'-hepta-*O*-acetyl-*α*-D-cellobiosyl bromide **161**.

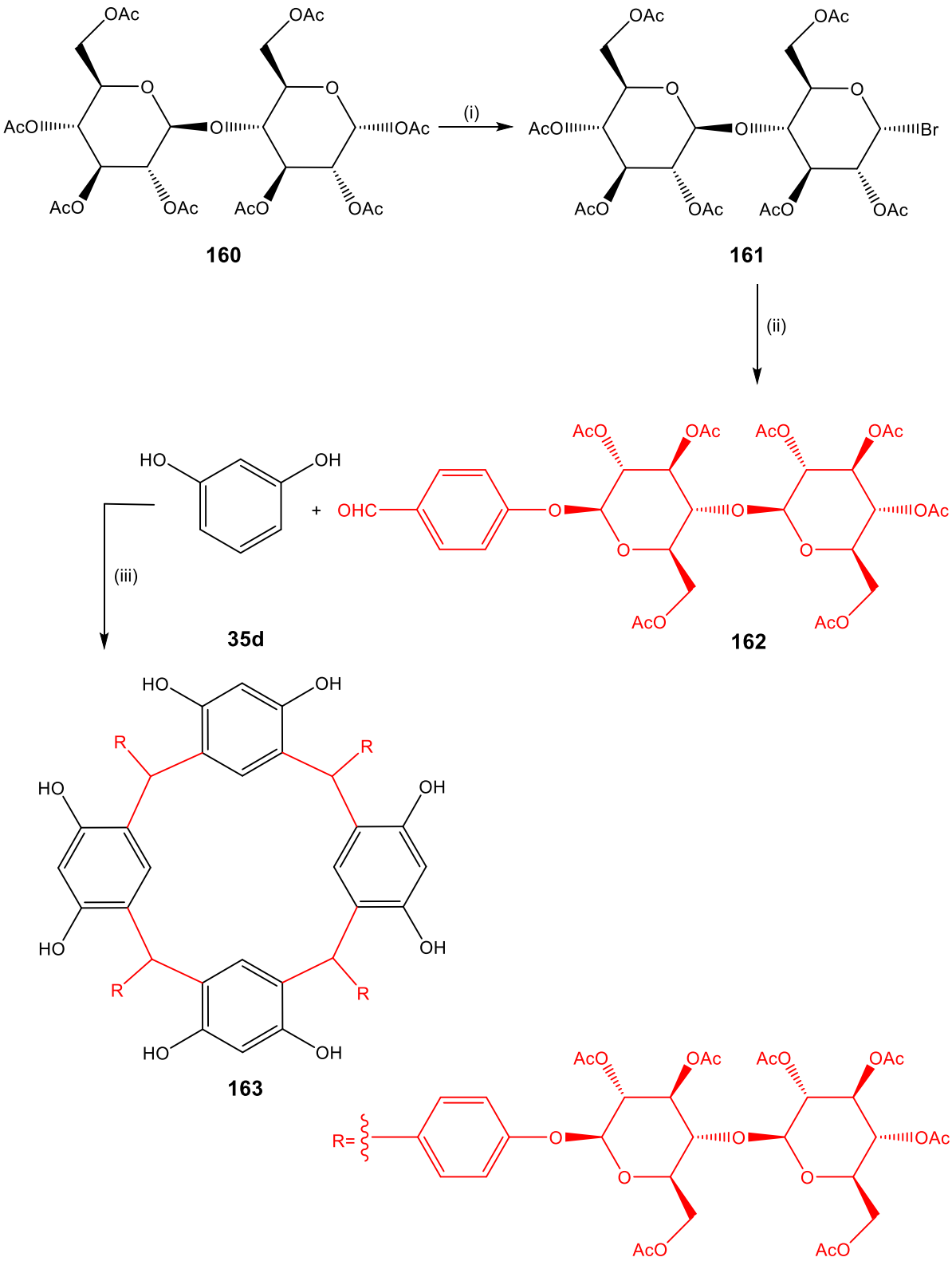

Reagents and conditions: (i) HBr/AcOH, DCM, (ii) Ag_2O, MeCN, 5h (iii) $BF_3.Et_2O$, 24 h, DCM

Scheme 41: Synthesis of calix[4]resorcinarene cellobioside

The glycosidation was conducted under Koenigs-Knorr conditions by condensation of an equimolar ratio of acetylated cellobiosyl bromide with 4-hydroxybenzaldehyde in MeCN and Ag_2O as a catalyst to produce glycoside **162**. The reaction was monitored by TLC and was completed in 5 h. The required compound was obtained in 62% yield after purification by column chromatography using EtOAc: Pet. ether (1.5:1) as eluent (Figure 44).

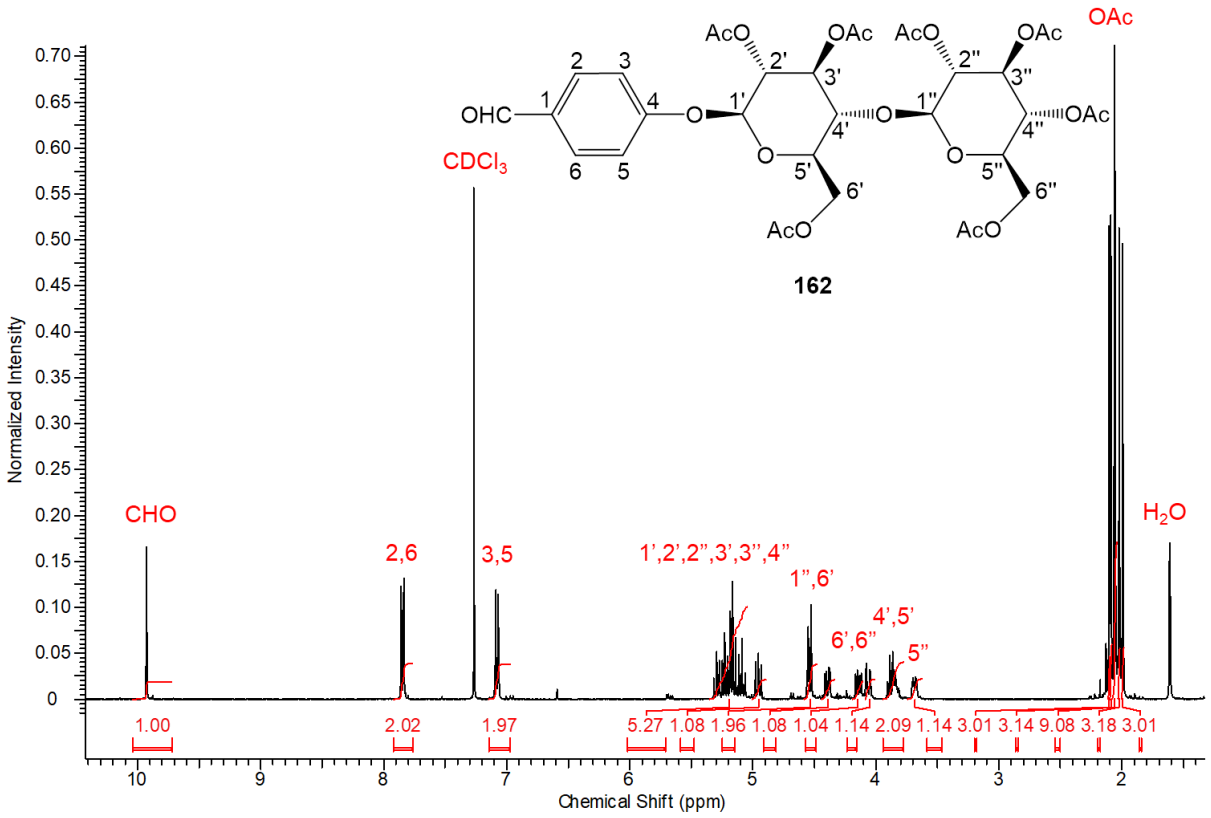

Figure 44: ^{1}H NMR spectrum of heptaacetoxycellobioside of 4-hydroxy benzaldehyde **162** in $CDCl_3$

Finally, the protected tetracellobiosyl calix[4]resorcinarene was synthesised according to the method reported in the literature (Kumar and Venkatakrishnan 2018). By condensation of 4-(2',3',6',2'',3'',4'',6''-heptaacetyl-*β*-D-cellobiosyl)benzaldehyde with resorcinol in 1:1 molar ratio and (2 eq.) of the Lewis acid boron trifluoride as catalyst. The reaction was worked up after 24 h

of stirring at r.t, affording a low yield of the corresponding compound. However, upon changing the solvent system to (Et_2O: THF) and using the same reaction conditions, no macrocyclisation was observed even after stirring for 4 days. TLC showed the presence of the aldehyde starting material before and after work-up, and this was also confirmed by ^{1}H NMR spectroscopy.

The structure of calix[4]resorcinarene cellobioside **163** was confirmed by ^{1}H NMR, ^{13}C NMR, DEPT135 and HSQCDEPT spectroscopy experiments and mass spectrometry. The protons of phenyl substituents gave a pair of doublets at 6.61 and 6.53 ppm, protons for resorcinol units appeared as singlet at 6.13 ppm and as a broad signal at 6.00 ppm, one singlet at 5.56 ppm, assigned to the methine hydrogens at the calix[4]resorcinarene bridges, while that related to cellobiose unit protons appeared with a chemical shift between 4.71-5.29 ppm and 3.84-4.49 ppm. The acetyl protons were observed as a multiplet between 1.79-1.97 ppm. The appearance of a single resonance for the bridging hydrogens and for each of the aromatic resorcinol protons (H *endo* and H *exo*) confirms that this compound has the *rccc* crown conformation (Moore *et al*., 2008) (Figure 45).

^{13}C NMR spectrum in d_6-acetone displayed three signals for the aromatic carbon atoms at 138.9, 129.7 and 115.0 ppm, a weak signal at 130.9 ppm as well as sharp signals at 153.3, 121.7, 120.8 and 102.5 ppm confirmed the presence of resorcinol units, and the presence of methine bridge carbons between the aromatic rings was confirmed at 42.2 ppm (Figure 45). The structure of **163** is also supported by mass spectrometry analysis. The spectrum gave molecular ion at *m*/*z* 1682.5200 that corresponds to $(M+2NH_4)^{2+}$. (Expected: *m*/*z* 1682.5195) (Appendix 4).

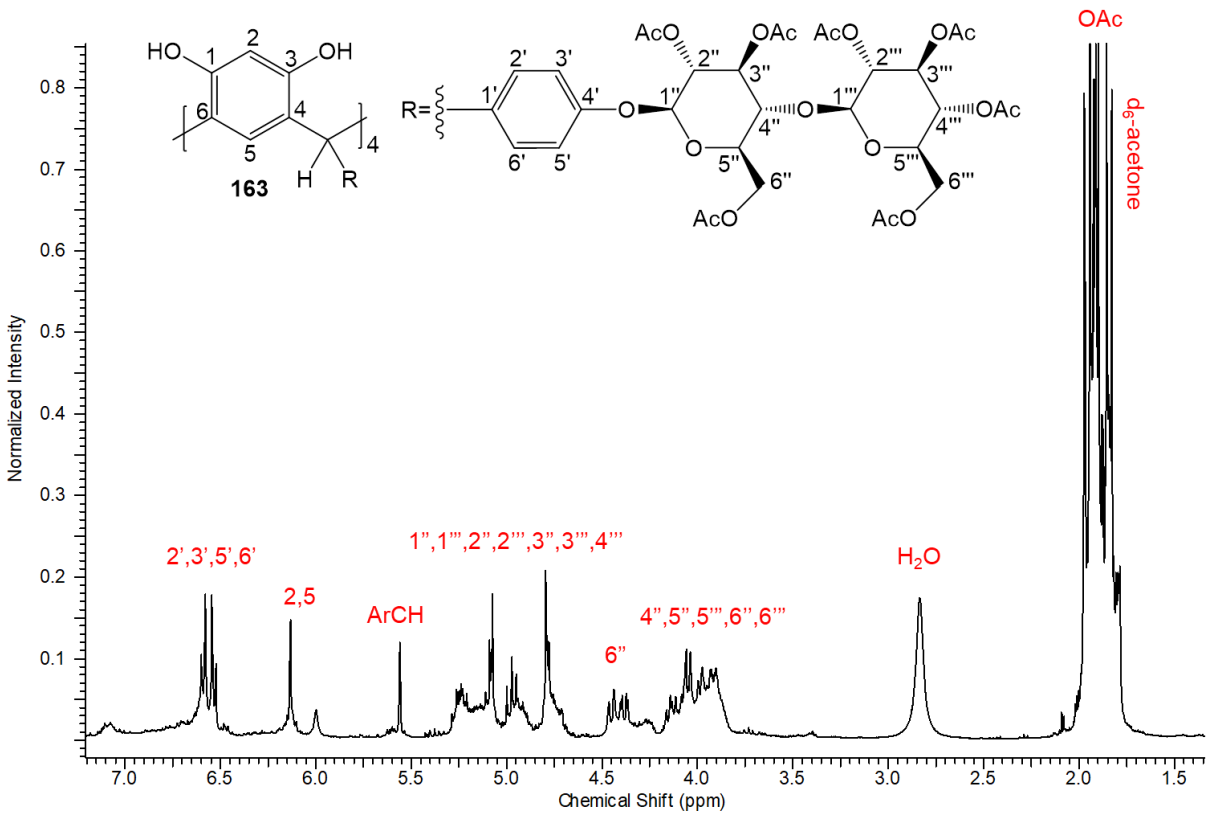
HO
OH
163
R=
AcO
OAc
OAc
d6-acetone
2',3',5',6'
2,5
ArCH
1'',1''',2'',2''',3'',3''',4'''
6''
4'',5'',5''',6'',6'''
H2O
Normalized Intensity
Chemical Shift (ppm)

(a)

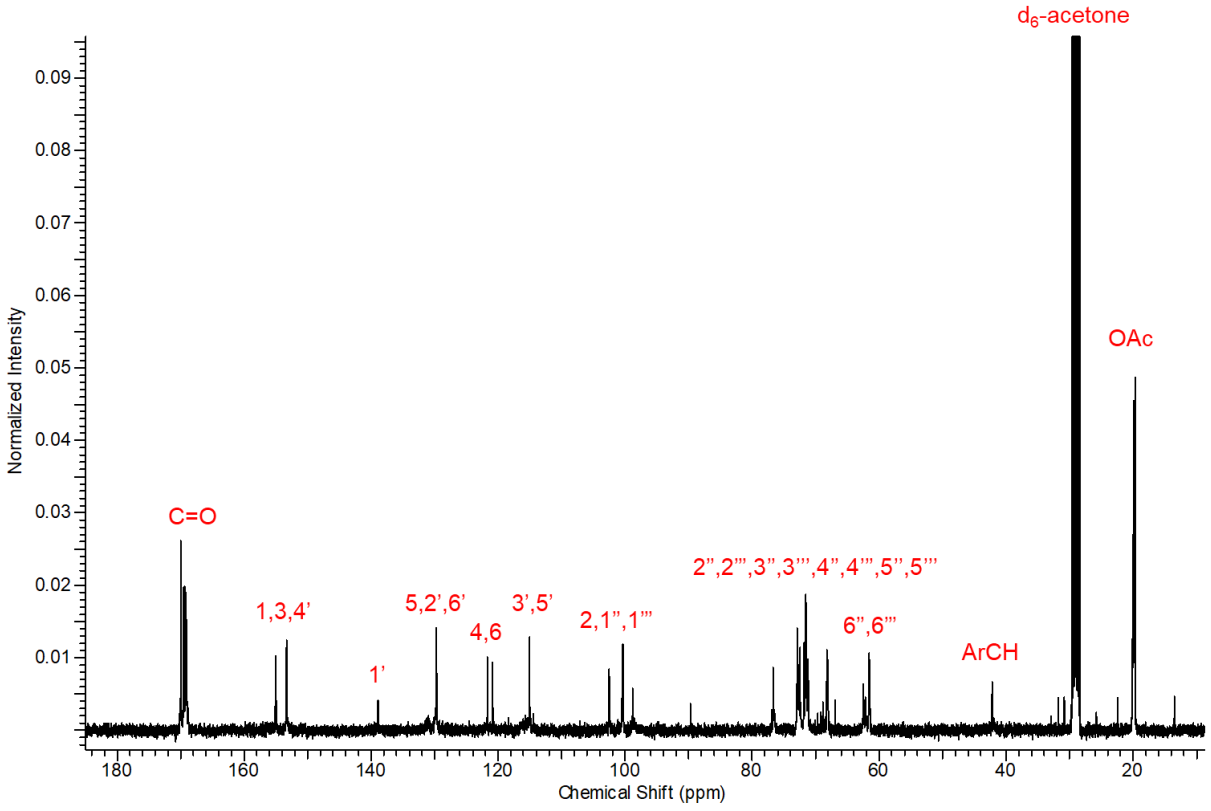
d6-acetone
OAc
C=O
1,3,4'
1'
5,2',6'
4,6
3',5'
2,1'',1'''
2'',2''',3'',3''',4'',4''',5'',5'''
6'',6'''
ArCH
Normalized Intensity
Chemical Shift (ppm)

(b)

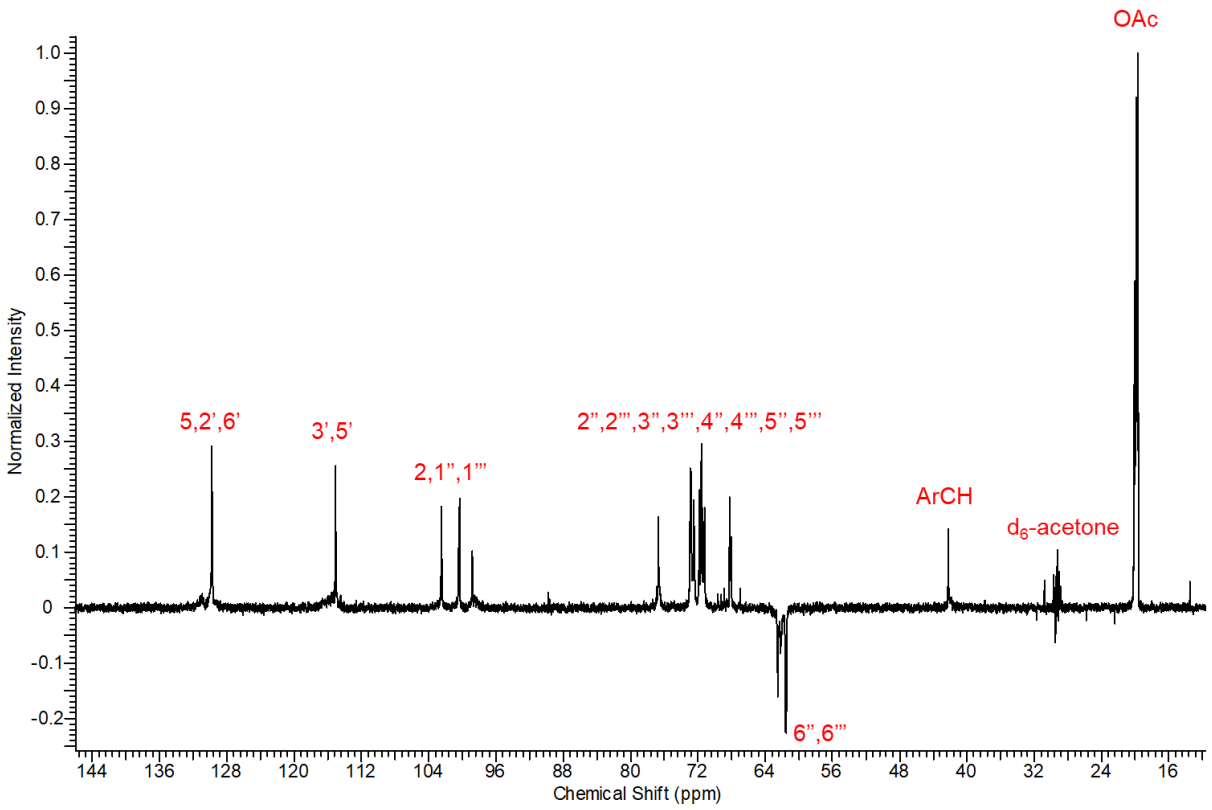
OAc
5,2',6'
3',5'
2,1'',1'''
2'',2''',3'',3''',4'',4''',5'',5'''
ArCH
d6-acetone
6'',6'''
Normalized Intensity
Chemical Shift (ppm)

(c)

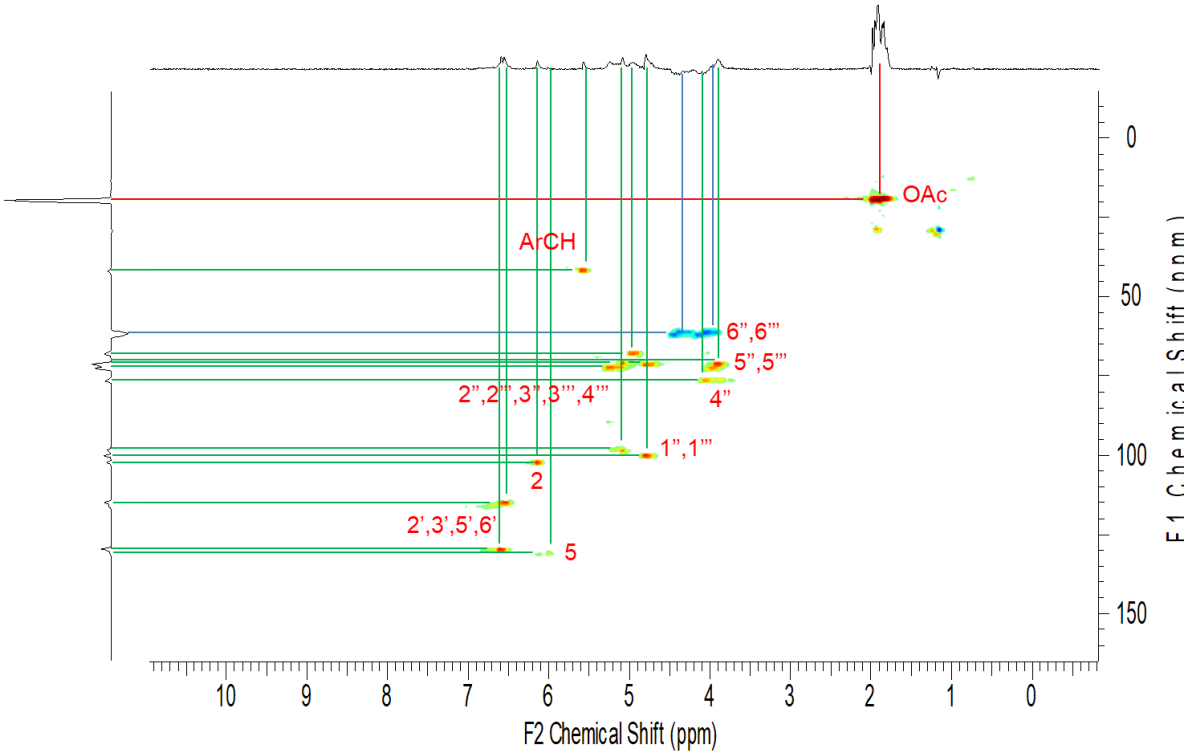

(d)

Figure 45: (a) ^{1}H NMR, (b) ^{13}C NMR, (c) DEPT135 and (d) HSQCDEPT spectra of calix[4]resorcinarene cellobioside **163** in d_6-acetone

2.6 Conclusion

Functionalisation of calix[4]resorcinarenes can be investigated from the starting substrates. By altering the position of the substituent residue on the aldehyde, the arrangement of the substituents on the lower rim of the scaffold can be influenced. A suitable select of reaction conditions *via* either prolonged treatment or the catalyst conferred condensation of resorcinol with a varied series of aldehydes bearing carbohydrate residue to form tetravalent calix[4]resorcinarene glucosides according to previously reported protocol. These cyclic tetramers display general scaffold for the design of conformational isomer and offer the binding of groups in a specific spatial orientation.

Despite the drawbacks associated with using Lewis acid for the synthesis of these calix[4]resorcinarenes, of low outcome yield, long reaction time and fatigued isolation of the calix[4]resorcinarene glucoside products, successful attempts had been made using flash column chromatography, preparative thin layer chromatography and the chromatotron chromatography to separate the conformational isomers resulted during these syntheses from the crude mixture before acylation.

All of the calix[4]resorcinarene glucosides was derivatised in the upper rim as their octabutyrates, two previously known isomeric compounds (major and minor isomers) **137a** and **137b** of calix[4]resorcinarenes based tetraacetoxyglucoside of 4-position of pendant aromatic unit were isolated. One isomer of each calix[4]resorcinarene based tetraacetoxyglucoside of 3- or 2-position on the aromatic group, were also isolated as their octabutyrates **147** and **149**.

Another analogue compound of calix[4]resorcinarene bearing galactoside glycocluster was introduced to this family of macrocycles and synthesised using different Lewis acid ($BF_3.Et_2O$). It was found that this Lewis acid which catalysed such reactions was facile and valuable procedure of gaining macrocycles in a shorter reaction time. This reaction generated two isomers which were separated as their octaester into major **154a** and minor **154b** isomers.

Two new tetravalent lactose and cellobiose functionalised calix[4]resorcinarenes were synthesised using the reaction of substituted benzaldehyde glycosides in a stepwise synthetic route. Using a mixture of Et_2O and THF as reaction solvent and a Lewis acid catalyst ($BF_3.Et_2O$), conditions

previously used for the synthesis of the calix[4]resorcinarene galactoside, the lactose calix[4]resorcinarene was accessed, but this was not effective for the synthesis of the corresponding tetracellobiosyloxy compound. Alternative conditions, previously reported by Kumar and Venkatakrishnan for the synthesis of tetramethoxy calix[4]resorcinarenes, allowed us to synthesise the tetracellobiosyl glycocluster **163** in a low yield.

Interestingly, characterisation of calix[4]resorcinarene lactoside using spectroscopic methods showed the presence of one conformation, isolated as the octabutyrate which was also delivered as one configuration as confirmed by NMR analysis. The synthesis of tetracellobiosyl calix[4]resorcinarene produced one configuration also which can be tentatively assigned to be in the *rccc* crown configuration.

The formation of one isomer of both compounds **158** and **163** with 4-substituted phenyl glycosides could be due to the size of the 4-glycosylated benzaldehydes which cannot adopt alternative configurations upon condensation with resorcinol.

CHAPTER 3: SYNTHESIS AND CHARACTERISATION OF NOVEL TETRA(4-HYDROXYPHENYLETHYL)CALIX[4]RESORCINARENES AND 4-HYDROXYPHENYL ACETALDEHYDE

The aim of this present work was to synthesise of new calix[4]resorcinarenes based on a 4-glucosylated derivatives of 4-hydroxyphenyl propanal **164** and 4-hydroxyphenyl acetaldehyde **165** (Figure 46).

In order to synthesise glucosylated calix[4]resorcinarenes **164** and **165**, a seven step synthesis was designed for both strategies. Starting from 3-(4'-hydroxyphenyl)propionic acid **166** (Scheme 42), the aldehyde **167** was envisaged to be readily prepared in six steps. The second sequence started from 2-(4'-hydroxyphenyl)acetic acid **168** (Scheme 47) to prepare the aldehyde **169** (Figure 46).

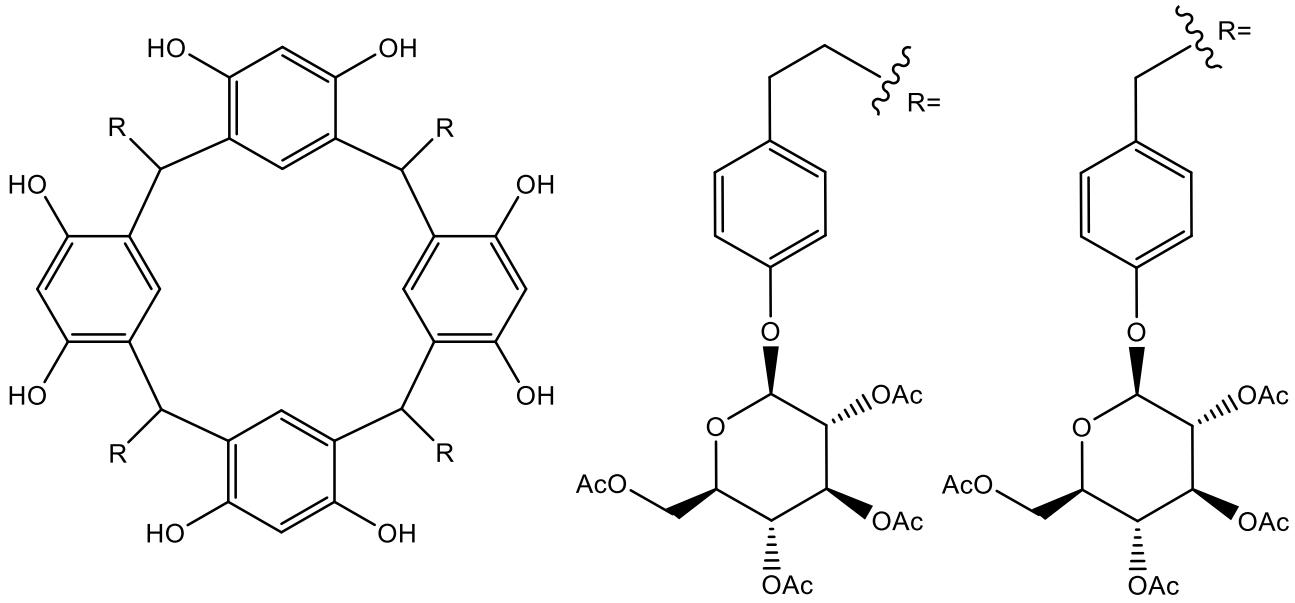

164, **165** **167** **169**

Figure 46: Proposed glucosylated aldehyde and calix[4]resorcinarene structures

The strategy was to prepare aldehydes **170** (Scheme 42) and **171** (Scheme 47) and conjugate each one of them with various carbohydrates to prepare a series of homologated glycosyloxybenzaldehydes for use in the synthesis of glycosylated calix[4]resorcinarenes, with the glycosylated aryl residues being separated from the calix[4]resorcinarene core by an alkyl spacers. The synthesis of tetravalent calix[4]resorcinarene glycosides would be possible by a condensation reaction between the glycosylated aldehydes with resorcinol and its derivatives (2-methylresorcinol and pyrogallol), using the same methodologies used previously to prepare glycosylated calix[4]resorcinarenes by Lewis acid catalysis.

The novel homologous glycosylated calix[4]resorcinarenes would be butyrated before purification of any conformational isomers yielded was attempted.

Unfortunately, the aldehyde fragments in **170** and **171** were unable to withstand reaction conditions commonly required for the synthesis of the corresponding glycosides. Therefore, it was decided to prepare aryl substituted calix[4]resorcinarenes as a replacement of the glycosidic one.

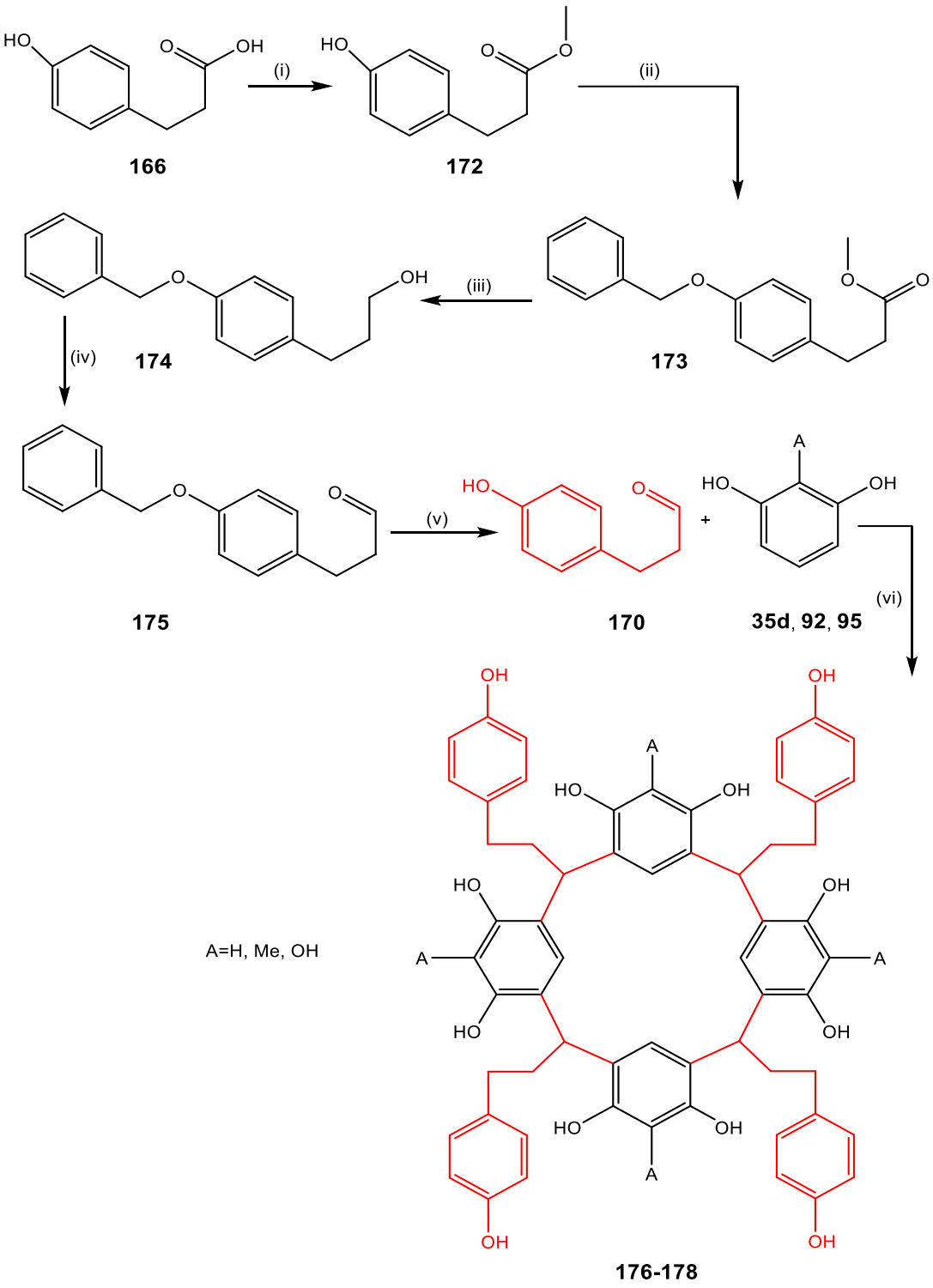

Reagents and conditions: (i) conc. H_2SO_4, MeOH, reflux 24 h (ii) KI, K_2CO_3, $PhCH_2Cl$, acetone, reflux 24 h (iii) $LiAlH_4$, THF, 0 ^{0}C to r.t, 2 h (iv) PCC, DCM, 0 ^{0}C to r.t, 3 h (v) H_2, Pd/C, MeOH, r.t (vi) conc. HCl, EtOH, reflux 4 h

Scheme 42: Synthesis of tetra(4-hydroxyphenylethyl)calix[4]resorcinarenes

3.1 Esterification of 4-hydroxyphenylpropionic acid towards ester 172

Starting from the commercially available 4-hydroxyphenylpropionic acid **166** (Scheme 42), the corresponding ester was prepared by a Fisher esterification, a nucleophilic acyl substitution reaction between the acid **166** and MeOH as reactant and solvent. Addition of a few drops of concentrated sulfuric acid catalyst were required to protonate the carboxylic acid and convert it into a stronger electrophile to be attacked by the nucleophilic alcohol at the C=O bond. The mechanism is shown in (Scheme 43). Work up of this reaction gave the corresponding methyl ester as white crystals in a quantitative yield (Tung *et al*., 2016). The structure of the product **172** was confirmed by ^{1}H NMR spectroscopy and showed appearance of methyl ester group at 3.72 ppm and the data was in a good agreement with the reference data.

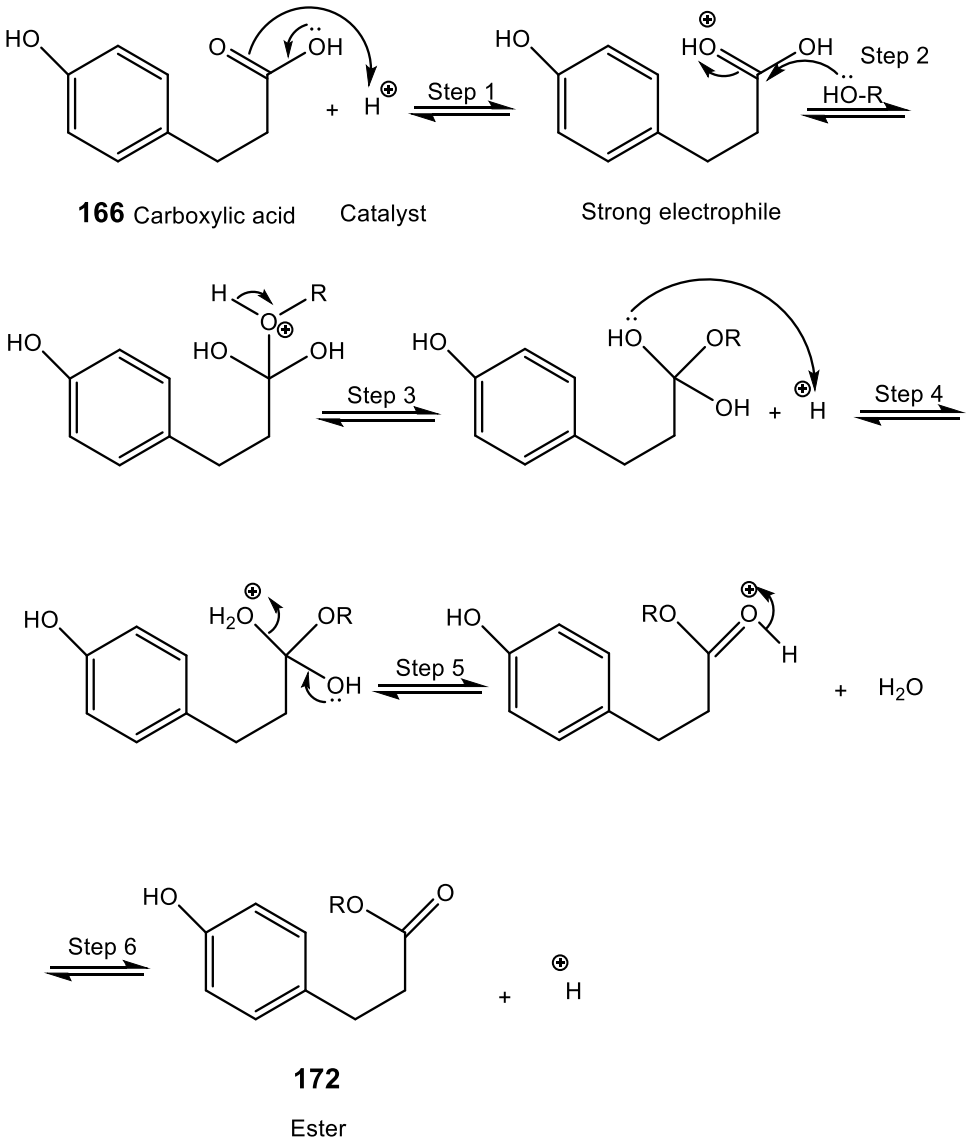

Scheme 43: Ester production *via* nucleophilic acyl substitution reaction between the acid and an alcohol

3.2 Protection of methyl 3-(4'-hydroxyphenyl)propanoate 172

Protecting the hydroxyl group on the aromatic ring is required for preparing compound **172** for the next step, since the subsequent nucleophilic substitution reactions of the phenol require basic conditions (Scheme 44). Compound **172** was benzylated by direct reaction with benzyl chloride in the presence of potassium carbonate and potassium iodide, using acetone as a solvent at 56 ^{0}C overnight, in a similar manner to that described in the literature (Herbert and Kattah 1990). The reaction was monitored by TLC which showed disappearance of the starting material and appearance of one spot for the product with a higher R_f value than the starting ester. After filtration and evaporation the filtrate, the solid product was purified by recrystallisation from n-hexane to afford monobenzyl ether **173** as yellow crystals in 83% yield.

The ^{1}H NMR spectrum showed peaks for the benzyl methylene protons at 5.08 ppm and for the benzyl aromatic protons at 7.35-7.49 ppm, which agreed with the reference data (Herbert and Kattah 1990).

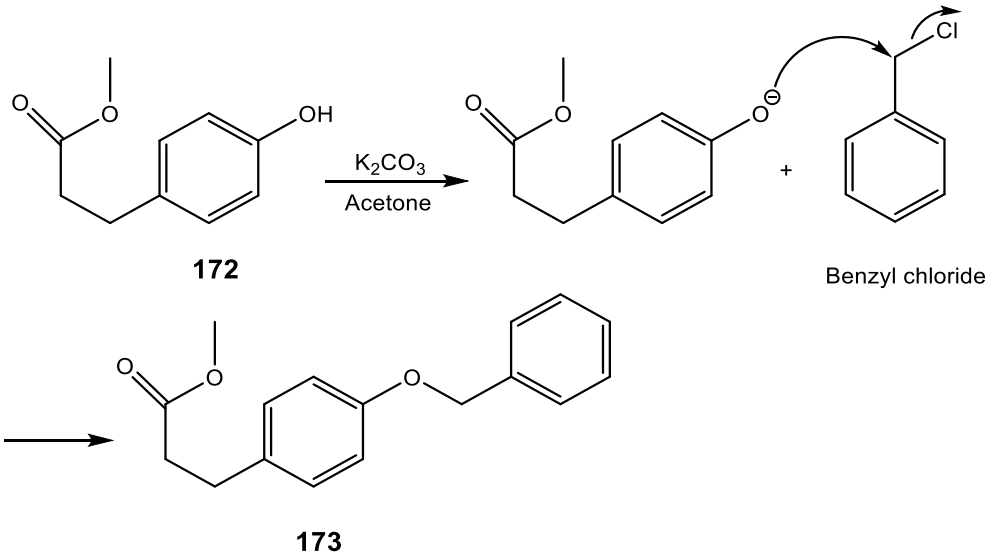

Scheme 44: Nucleophilic attack on benzyl chloride

3.3 Reduction of methyl 3-(4'-benzyloxyphenyl)propionate 173

Following benzylation, the ester **173** underwent reduction using $LiAlH_4$ as reducing agent to furnish the protected alcohol **174** in a quantitative yield. Reaction completion was indicated by TLC analysis after 2 h stirring at room temperature, which gave one spot for the product with lower R_f value than the protected ester. The mechanism of such a reaction involves formation of an aldehyde. The aldehyde formed is a strong electrophile and cannot be isolated therefore it reacts with another equivalent of $LiAlH_4$ (Scheme 45). ^1H NMR spectrum displayed three signals at 3.65, 2.64 and 1.85 ppm for the methylene protons which were matched with those previously characterised (Kantee *et al*., 2016).

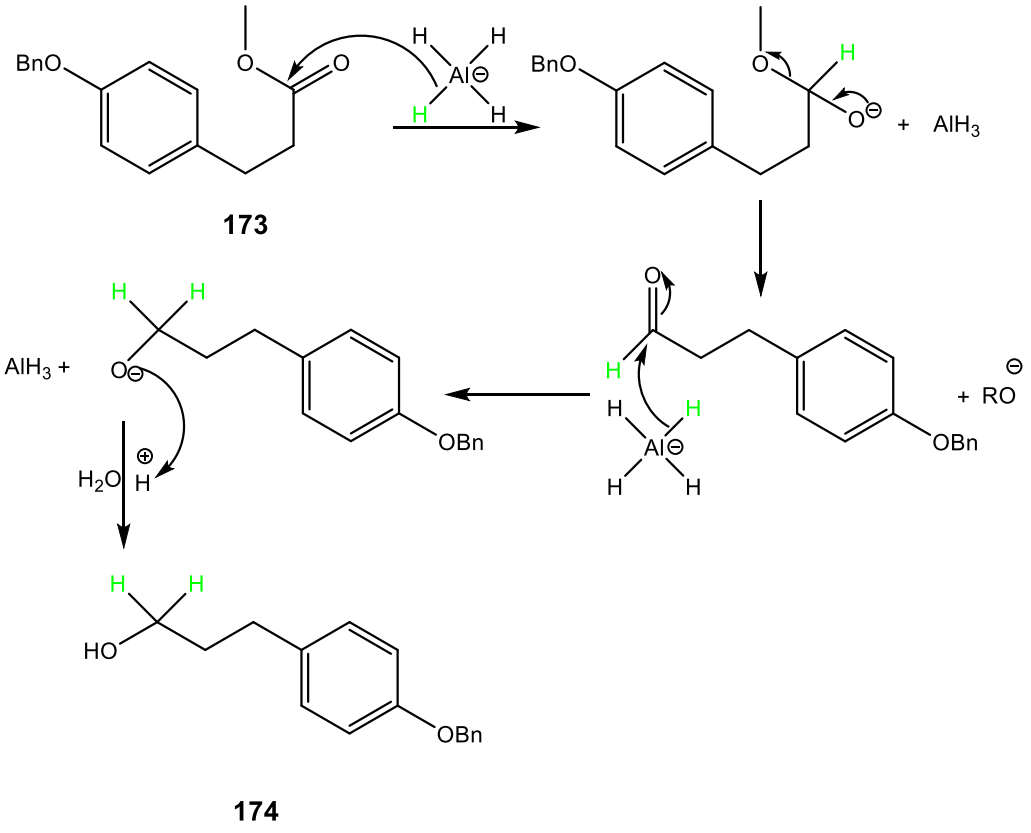

Scheme 45: Ester reduction by $LiAlH_4$ towards primary alcohol

3.4 Oxidation of 3-(4'-benzyloxyphenyl)propan-1-ol to carbonyl

Treatment of alcohol **174** with 1.5 eq. of pyridinium chlorochromate (PCC) in dry dichloromethane was conducted at 0 ^{0}C (Kashanna *et al*., 2012). After stirring for 3 h at room temperature, the TLC showed disappearance of the starting alcohol and appearance the product spot with higher R_f value than the starting alcohol. After evaporation of the solvent and extraction of the black gum with diethyl ether, the crude aldehyde was purified by chromatography on silica gel using EtOAc: Pet. ether (1:4) as eluent, affording the corresponding aldehyde **175** as a colourless oil in a moderate yield of 58%.

The structure of **175** was determined by spectroscopic analysis, especially the ^{1}H NMR spectrum which contained signals at 2.79 and 2.95 ppm for the two methylene groups and at 9.85 ppm for the aldehyde moiety, identical to that previously reported (Tadiparthi *et al*., 2017).

Among various oxidizing agents, PCC was preferred because it is mild, commercially available and soluble in organic solvent (DCM). It is used to convert primary alcohols exclusively to the corresponding aldehyde with high efficacy and on a large scale. The only drawback associated with this reagent is the formation of Cr(III) complexes and pyridinium chloride as by-products which are often difficult to remove (Scheme 46).

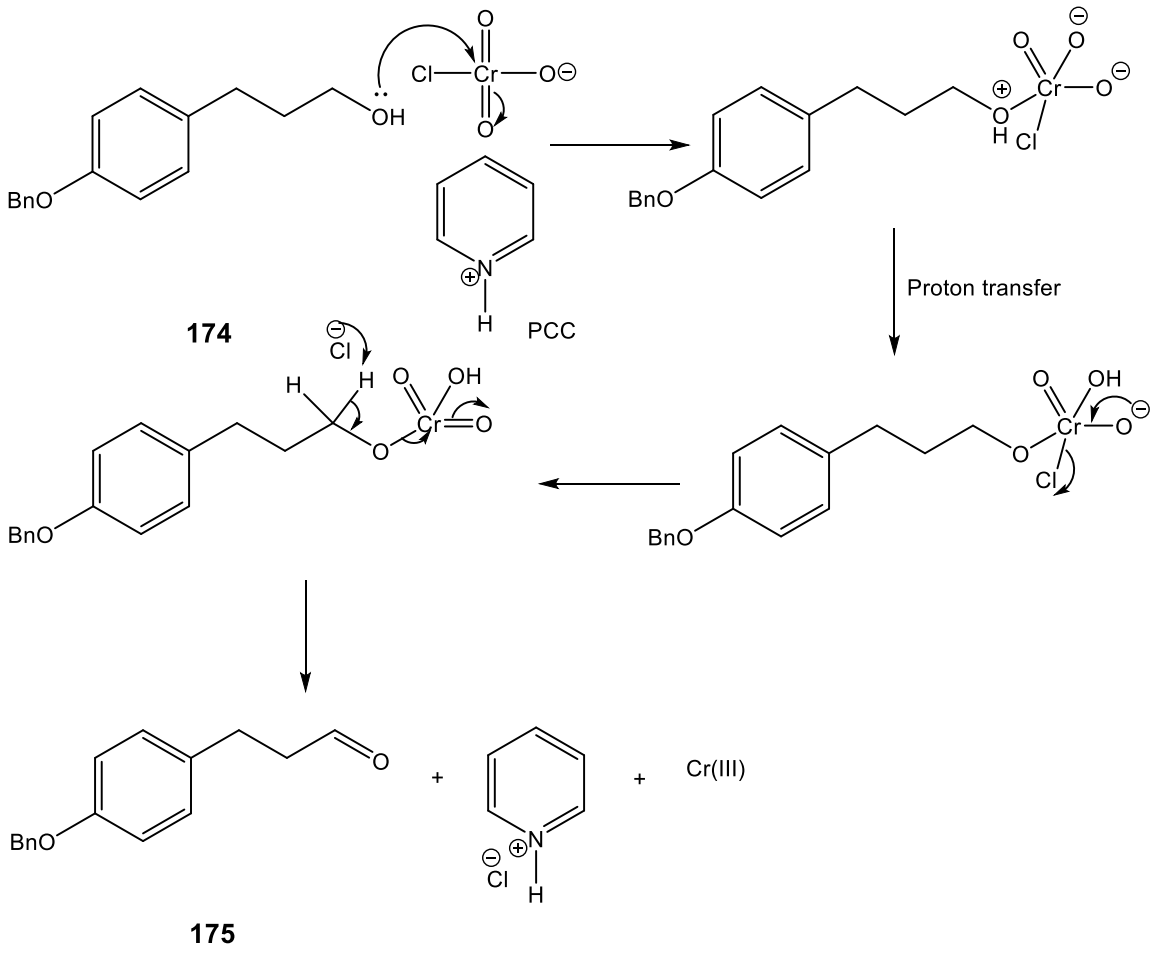

Scheme 46: Alcohol oxidation mechanism by PCC

3.5 Hydrogenolysis of 3-(4'-benzyloxyphenyl)propanal

The protecting benzyl ether of 3-(4'-benzyloxyphenyl)propanal **175** was removed under catalytic hydrogenation conditions using 5% palladium on charcoal as a catalyst in methanol, as shown in (Scheme 42). Reaction progress was monitored by TLC, which showed the protected aldehyde disappearing completely to give just the target compound with lower R_f value after stirring for 2 h at room temperature. The unprotected aldehyde **170** was obtained as a colourless oil in a yield of 72% after purification by column chromatography. The ^{1}H NMR spectrum of **170** was identical to reference data (Herbert and Kattah 1990) (Figure 47).

Notably, the first attempt to synthesise the unprotected aldehyde using catalytic hydrogenation failed since it appeared that the aldehyde group had also been reduced along with removal of the benzyl ether moiety. This indicated that timing of the reaction was critical.

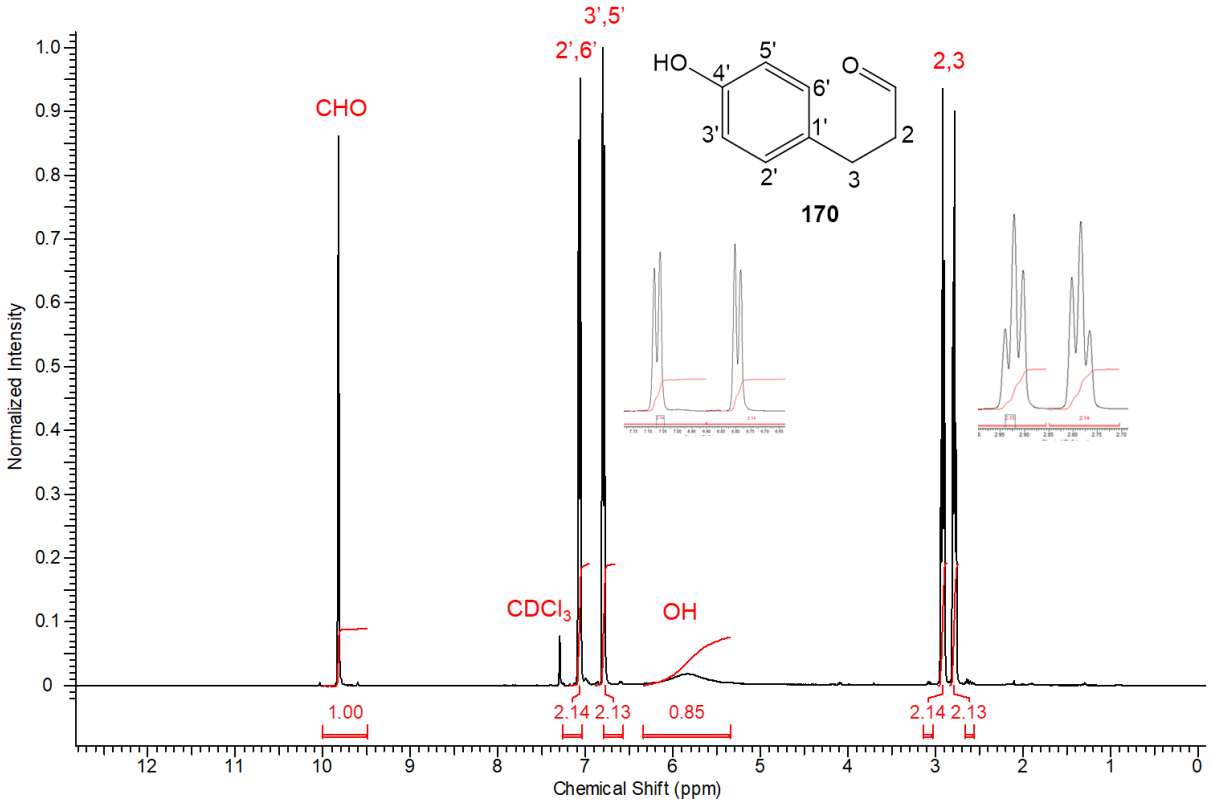

(a)

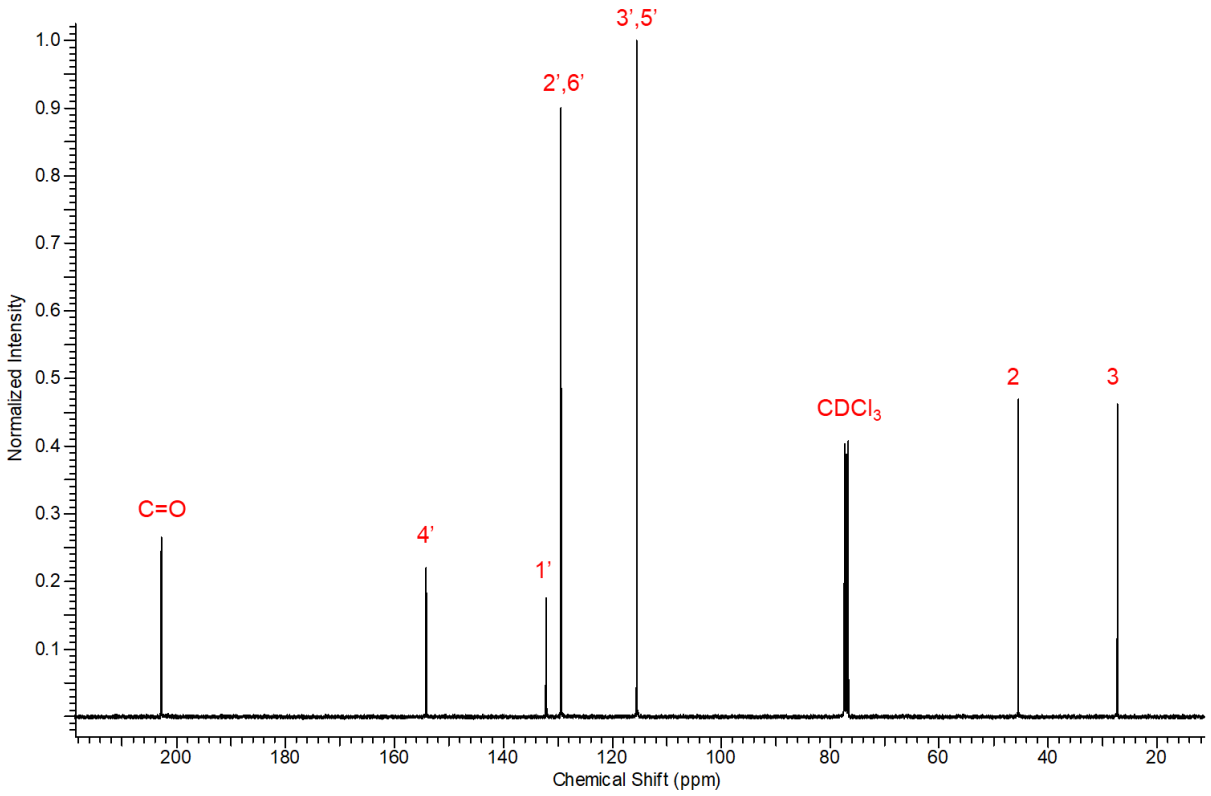

(b)

Figure 47: (a) ^{1}H NMR and (b) ^{13}C NMR spectra of 3-(4'-hydroxyphenyl)propanal **170** in $CDCl_3$

Once the pure 4-hydroxyphenyl propanal had been prepared, it was then envisaged that it could be reacted with a variety of suitably protected carbohydrate moieties to give the corresponding glycosylated aldehydes.

In an attempt to synthesise the novel tetraacetoxyglucoside of 4-hydroxyphenyl propanal **167,** compound **170** was initially reacted with acetobromoglucose **138** in the presence of silver(I) oxide in dry MeCN, using similar conditions to those employed for the glycosylation of hydroxybenzaldehydes **139-141** (Stavila *et al*., 2008). However, after stirring for 6 h at r.t, TLC analysis of the crude mixture suggested the presence of several new compounds. After column chromatography using EtOAc: Pet. ether (1:1) as eluent, the ^{1}H NMR spectra

obtained of combined fractions displayed the presence of unreacted acetobromoglucose and a mixture of unidentifiable species. The reaction was repeated with the starting aldehyde in excess and a prolonged reaction time of 24 h. Unfortunately, a similar result was obtained after column chromatography and analysing each component by ^{1}H NMR spectroscopy. The reaction was repeated many times using different combinations of conditions but with the same results.

In all cases, it is believed that the aldehyde **170** was oxidised under the reaction conditions to yield the corresponding acid (Tu *et al*., 1995).

The literature suggests that conversion of hydroxyaryl aldehydes to their corresponding *β*-glucosides can be achieved in a short reaction time under Koenigs-Knorr conditions using quinoline as a solvent. Therefore, it was decided to attempt this protocol in which compound **170** was reacted with acetobromoglucose in the presence of Ag_2O in quinoline for 25 min at r.t (Belyanin *et al*., 2012). The reaction mixture was then suspended in a mixture of EtOAc and 1 M HCl. Work up this experiment afforded a mixture of many compounds as suggested by TLC analysis. After flash chromatographic separation using EtOAc: Pet. ether (1.5:1) as eluent and analysing the fractions by ^{1}H NMR spectroscopy, one fraction was suggested to contain the desired product but mixed with another compound, potentially being the glycosylated alcohol. However, we were unable to separate this mixture further, even by preparative TLC. This experiment was repeated twice with substrate **170** in excess and for 2 h reaction time but similar results was obtained after separation by column chromatography as evidenced by ^{1}H NMR spectroscopy.

Another attempt at the Koenigs-Knorr reaction using a different substrate was attempted. Bromoacetylated lactose **156** and 4-hydroxyphenyl propanal **170** were subjected to the reaction conditions using MeCN as a solvent, but again the desired aldehyde was not obtained using this protocol.

As a result of the obvious problems associated with employing the Koenigs-Knorr method in our hands, various other processes were considered to prepare compound **167**. It was decided to attempt synthesis of this glycoside using Hunig's base (Sultana *et al*., 2006). Compound **170** was treated with an equimolar amount of acetobromoglucose and 10 eq. of diisopropylethylamine (Hunig's base) in dry MeCN. After 48 h stirring at r.t, the excess solvent was removed azetropically with toluene. No reaction was observed, again as indicated by ^{1}H NMR spectroscopy of the crude material.

It was then decided to attempt the synthesis of the aromatic glycoside **167** using phase transfer catalysis. In this way, compound **170** was reacted with acetobromoglucose **138** in the presence of a vigorously stirred aqueous solution of NaOH and tetrabutylammonium bromide (TBAB) in $CHCl_3$ (Mohri *et al*., 2003). After being stirred for 5 h at r.t., TLC analysis showed the presence of three different new spots with lower R_f value than the starting aldehyde, It was believed that the reaction has proceeded to yield the desired compound, but after column chromatography and ^{1}H NMR analysis of each group of fractions separated, a complex mixture of glycosides and aromatic compounds was obtained, with several different aldehydes being isolated in small amounts from the group of fractions obtained. Similar results were afforded upon repeating the reaction several times using DCM as a solvent with stirring for 3

days at r.t. (Chen *et al*., 2012) or using K_2CO_3 instead of NaOH in DCM (Wang *et al*., 2007).

Further attempts at the glycosylation of **170** with acetobromoglucose using different reported procedures were unsuccessful, including using a 4% aqueous solution of KOH and 4-dimethylaminopyridine (DMAP) in DCM (Xiang *et al*., 2006) or reaction in the presence of K_2CO_3 in dry acetone and dry DMF (Olsufyeva *et al*., 2003).

3.6 Synthesis of tetra(4-hydroxyphenylethyl)calix[4]resorcinarenes

In order to explore the reactivity and stability of 4-hydroxyphenyl propanal **170** under cyclooligomerisation reaction conditions, we decided to subject compound **170** to cyclisation with resorcinol utilising two different experimental methods:

Firstly, a mixture of equimolar amounts of the initial substrates was heated under reflux in the presence of concentrated HCl in EtOH, in a manner similar to that reported by Pfeiffer *et al*. (Pfeiffer *et al*., 2016). The product was precipitated from the reaction mixture using ice cold water to give the calix[4]resorcinarene **176** in 21% yield.

Analysis of the product by ^{1}H NMR spectroscopy showed two broad peaks at 8.57 and 8.19 ppm, corresponding to two kinds of phenolic hydroxyl groups in the upper and the lower rim. The characteristic signals of the ethyl link protons at 2.51-2.60 ppm and a one triplet at 4.38 ppm attributed to the hydrogen atoms at the methine bridges were also observed (Figure 48). This spectral pattern confirmed the structure was in the *rccc* (crown conformation), similarly to that previously synthesised and reported by other authors from different aldehydes

(Tunstad *et al*., 1989; Victorovna-Lijanova *et al*., 2008; Serkova *et al*., 2018). The structure of **176** is also supported by mass spectrometry analysis. The spectrum gave molecular ion at *m*/*z* 967.3693 that corresponds to $(M-H)^-$. (Expected: *m*/*z* 967.3693) (Appendix 12).

The second method used $AlCl_3$ solution in nitrobenzene as Lewis acid catalyst in dry Et_2O, conditions identical to those used for the synthesis of compound **145** under our standard conditions. Similarly to the above mentioned data, the ^1H NMR spectrum indicated one triplet at 4.38 ppm assigned to the methine proton at the carbon bridges.

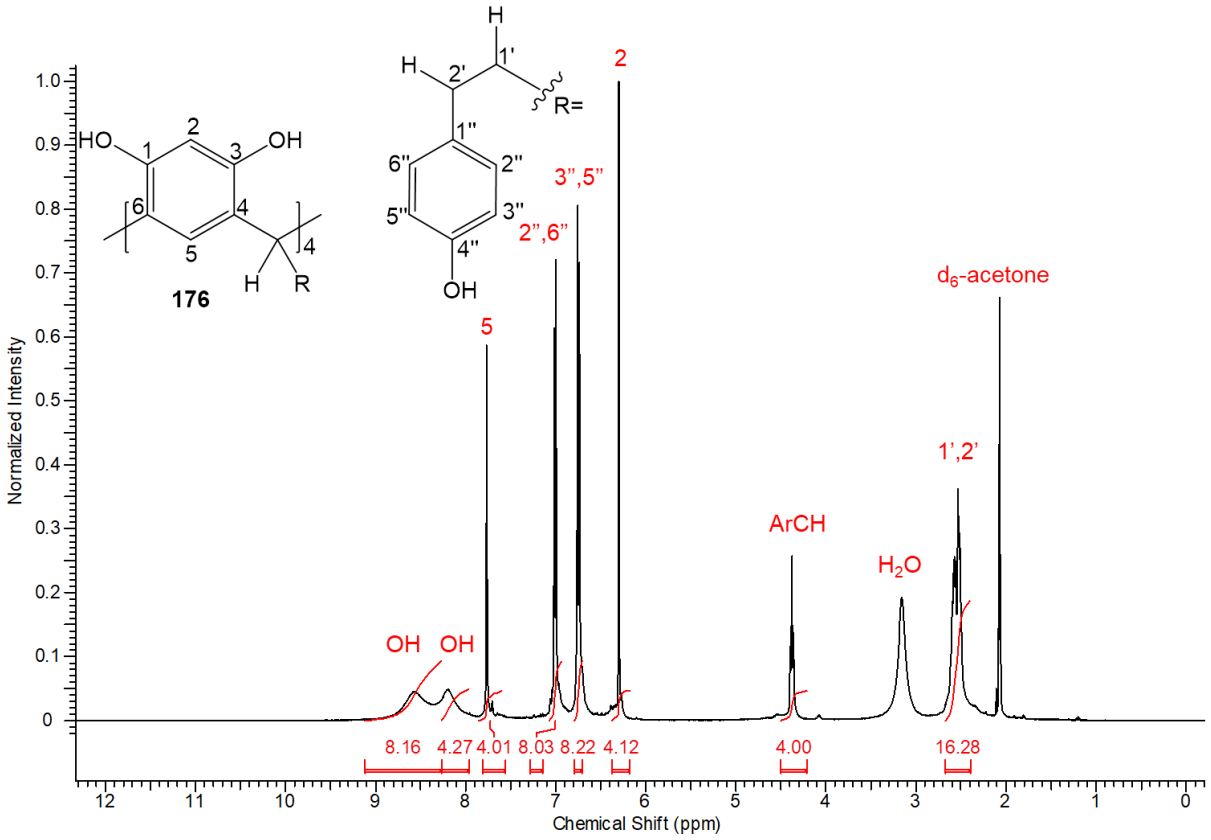

(a)

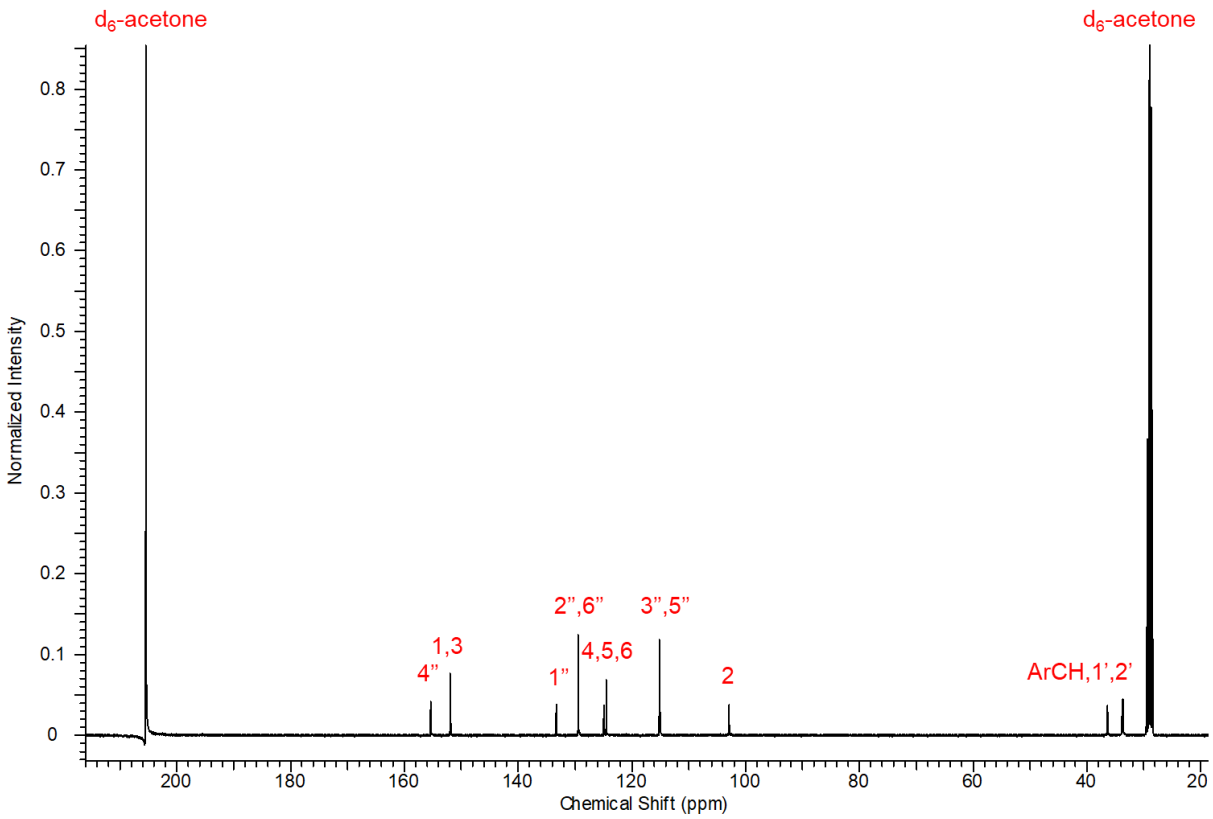

(b)

Figure 48: (a) ^{1}H NMR and (b) ^{13}C NMR spectra of tetra(4-hydroxyphenylethyl)calix[4]resorcinarene **176** in d_6-acetone

Reaction of compound **170** with 2-methylresorcinol and pyrogallol under protic acid-catalysed conditions also gave only the *rccc* isomer in the crown conformer, as indicated by ^{1}H and ^{13}C NMR spectroscopy. Each group of signals for compounds **177** and **178** in their NMR spectra appear as a single resonance, this is an indicative of highly symmetric structures in the cone conformation (Figure 49 and 50). The structure of **177** is also supported by mass spectrometry analysis. The spectrum gave molecular ion at *m*/*z* 1023.4313 that corresponds to $(M\text{-}H)^{-}$. (Expected: *m*/*z* 1023.4319) (Appendix 13). A satisfactory mass spectrum could not be obtained for **178** due to presence of some impurities in the crude product.

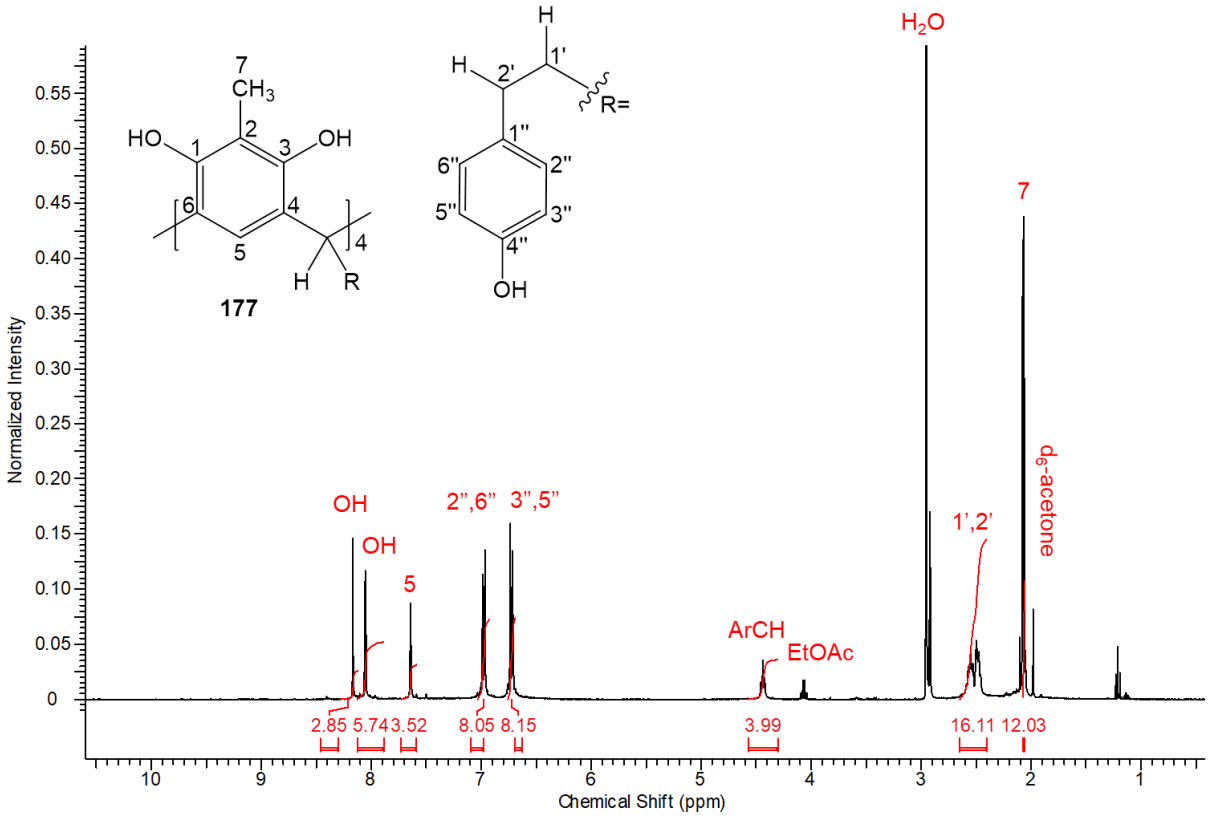
177
R=
H2O
7
d6-acetone
OH
OH
5
2",6"
3",5"
1',2'
ArCH
EtOAc
2.85
5.74
3.52
8.05
8.15
3.99
16.11
12.03
Normalized Intensity
Chemical Shift (ppm)

(a)

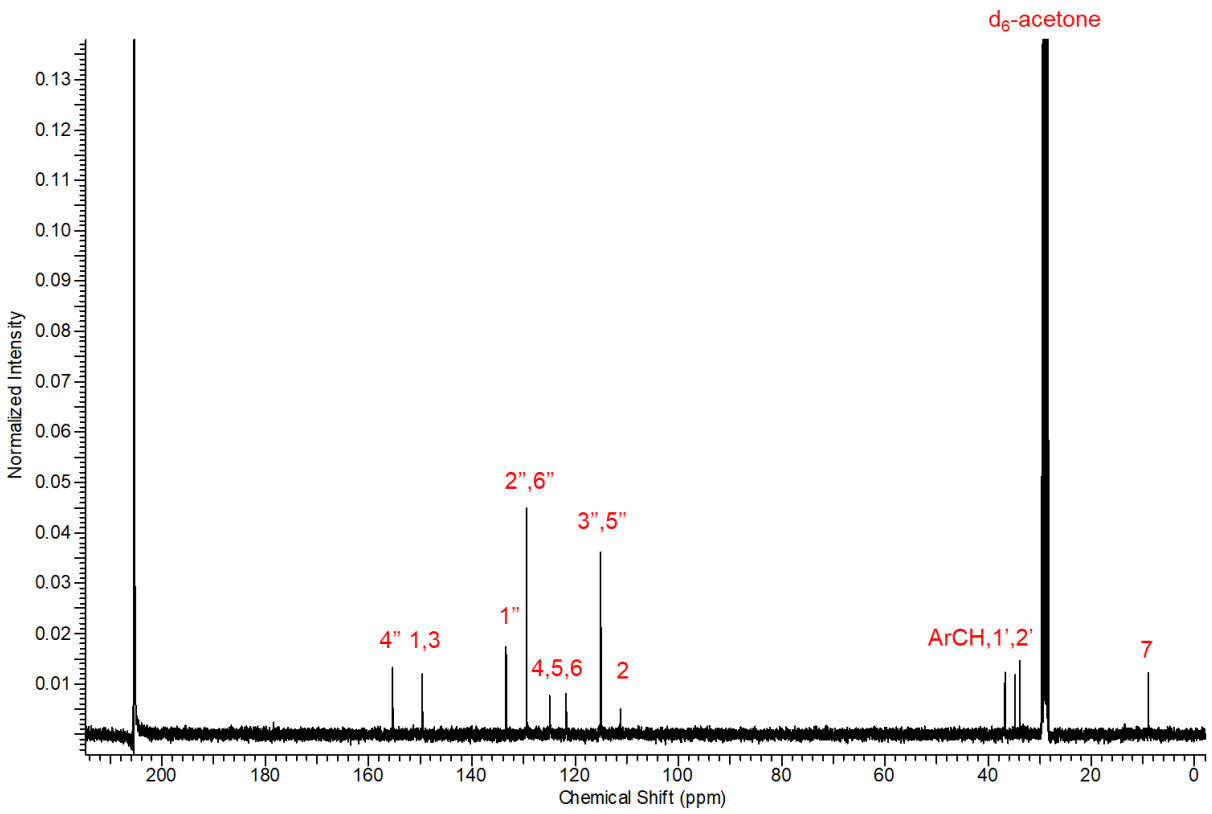

(b)

Figure 49: (a) ^{1}H NMR and (b) ^{13}C NMR spectra of tetra(4-hydroxyphenylethyl)calix[4]methylresorcinarene **177** in d_6-acetone

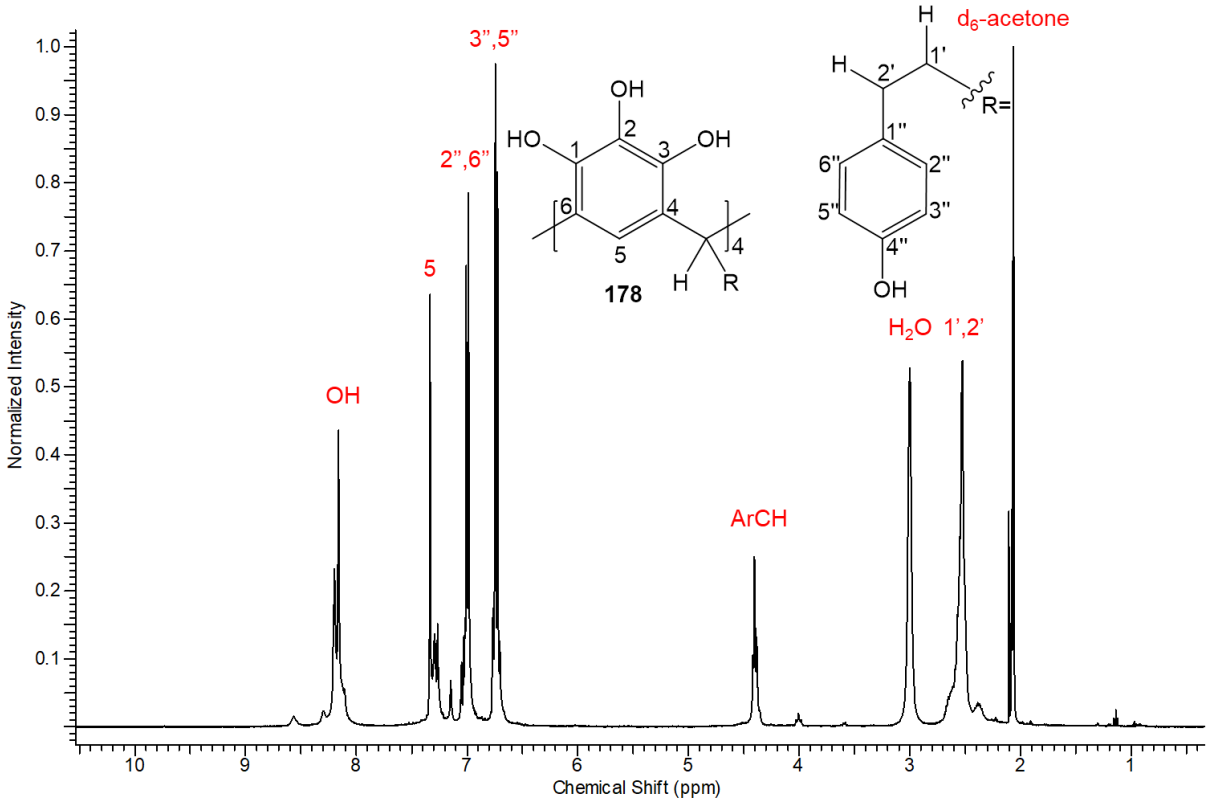
3",5"
2",6"
5
OH
ArCH
H2O 1',2'
d6-acetone
R=
178
Normalized Intensity
Chemical Shift (ppm)

(a)

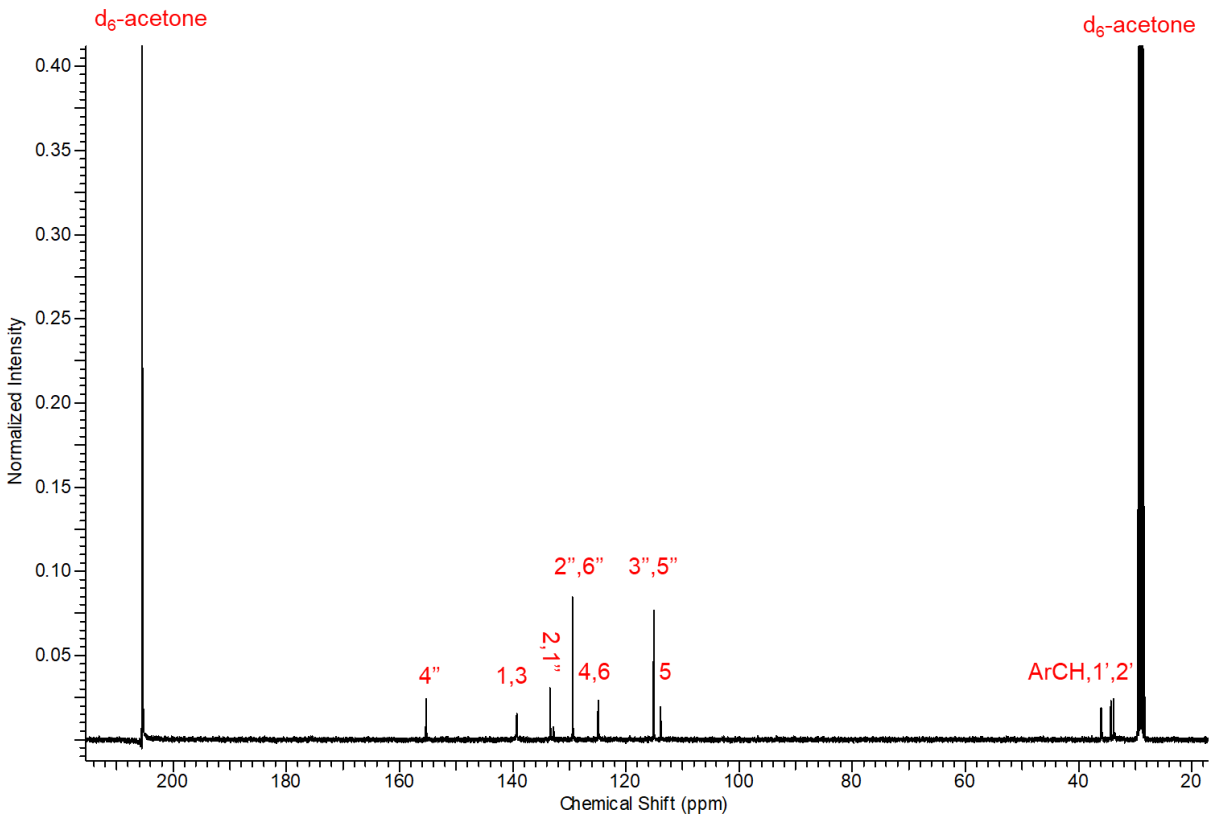

(b)

Figure 50: (a) ^{1}H NMR and (b) ^{13}C NMR spectra of tetra(4-hydroxyphenylethyl)calix[4]pyrogallolarene **178** in d_6-acetone

3.7 Preparation of 4-hydroxyphenyl acetaldehyde

4-Hydroxyphenyl acetaldehyde was prepared as described in (Scheme 47). The synthetic sequence started from the commercially available 4-hydroxyphenylacetic acid **168**, by adopting analogous experimental conditions described for the esterification of **166**. Thus, compound **168** was treated with MeOH and sulfuric acid at 70 ^{0}C to give the known methyl ester **179** as a colourless oil in 95% yield without purification.

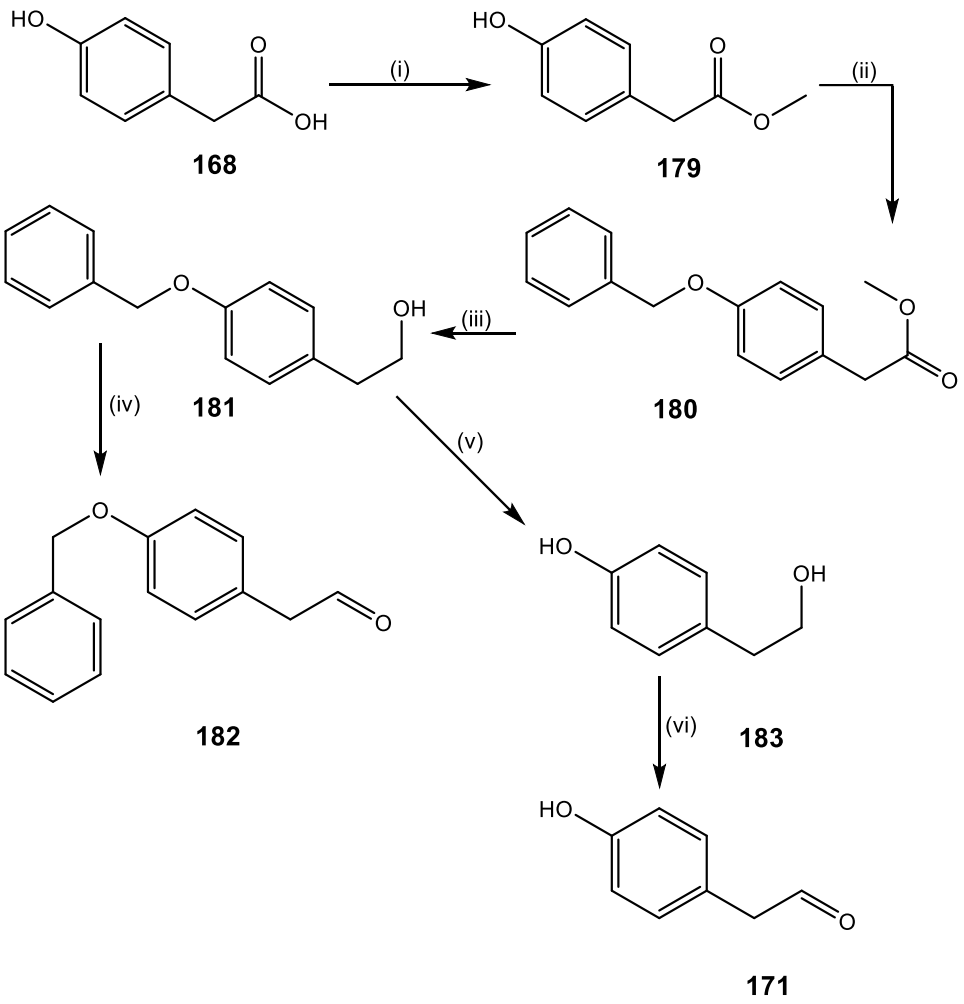

Reagents and conditions: (i) H_2SO_4, MeOH, reflux 24 h (ii) KI, K_2CO_3, $PhCH_2Cl$, acetone, reflux 24 h (iii) $LiAlH_4$, THF, 0 ^{0}C to r.t, 2 h (iv) Dess-Martin periodinane, DCM, 0 ^{0}C to r.t, 24 h (v) H_2, Pd/C, MeOH, r.t, 24 h (vi) SO_3-Pyridine, DMSO, TEA, r.t, 1 h

Scheme 47: Synthesis of 4-hydroxyphenyl acetaldehyde

The phenolic hydroxyl group of methyl 2-(4'-hydroxyphenyl)acetate **179** was subsequently protected by benzylation. Such protecting group has been previously used in the context of methyl 3-(4'-benzyloxyphenyl)propionate synthesis. Treatment of **179** with benzyl chloride and anhydrous potassium carbonate in acetone under reflux conditions gave the protected 2-(4'-benzyloxyphenyl)acetate **180**. Compound **180** was obtained as yellow crystals in 64% yield after recrystallisation from n-hexane.

Reduction of **180** was accomplished in the same manner as for compound **173**, with $LiAlH_4$ in THF to obtain 2-(4'-benzyloxyphenyl)ethanol **181** as an off-white solid in 93% yield.

In our previous synthetic strategy, we demonstrated that oxidation of alcohol **174** to aldehyde **175** by a PCC oxidation proceeded smoothly. Here, we expected that reaction of 2-(4'-benzyloxyphenyl)ethanol with 1.5 eq. of PCC would produce the expected aldehyde **182**. Surprisingly, the Corey-Suggs oxidation did not convert the alcohol **181** completely to the aldehyde **182** even after stirring for 24 h at r.t. as shown by TLC analysis. We were unable to separate the components of the reaction mixture by recrystallisation or by column chromatography. It appeared that the cleavage of a C-C bond had occurred (Scheme 48), as reported possible in the literature (Fernandes and Kumar 2003). The product mixture was proved by ^{1}H NMR analysis where two aldehydes appeared at 9.78 and 9.61 ppm.

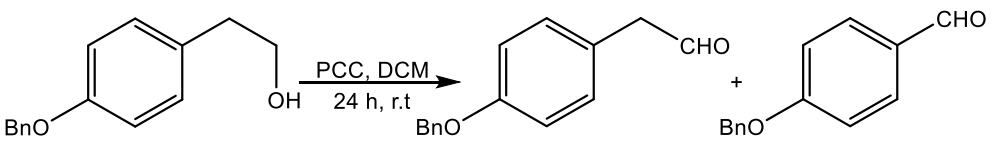

181 **182** **184**

Scheme 48: Synthetic endeavour by PCC oxidation (Fernandes and Kumar 2003)

Previously reported synthetic methods have shown that alcohols with a similar structure to the alcohol **181** could be oxidised selectivity to the aldehyde **182** using the Dess-Martin periodinane (DMP) as mild oxidant (Tilley *et al*., 2012). Compound **181** treated with DMP in DCM from 0 ^{0}C to r.t. for 24 h. The reaction mixture was quenched by washing with saturated aqueous solutions of $NaHCO_3$ and $Na_2S_2O_3$ to yield the corresponding aldehyde **182** as a pale yellow oil in 71% yield (Scheme 49).

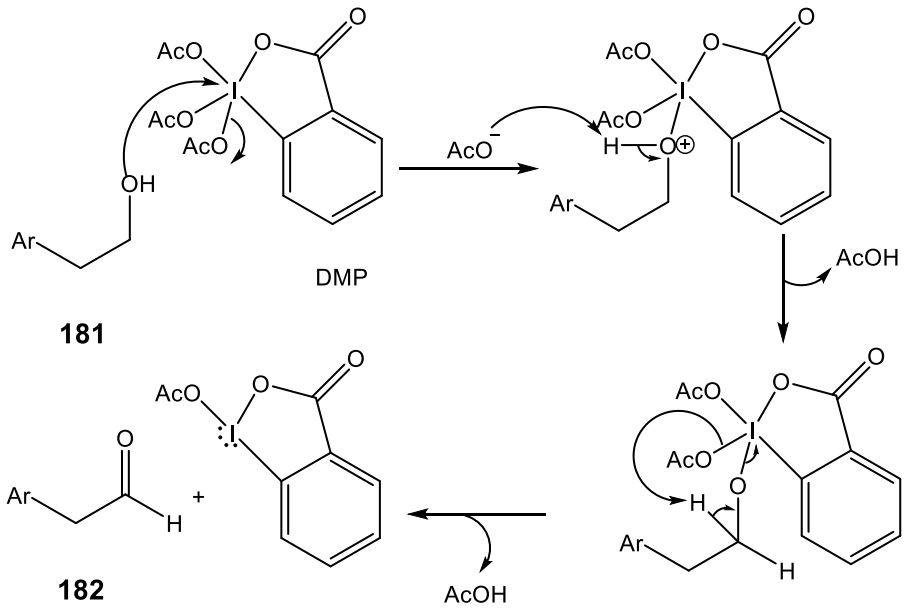

Scheme 49: Alcohol oxidation mechanism by Dess-Martin Periodinane (DMP)

The structure of the product was confirmed by ^{1}H NMR spectroscopy where the benzylic methylene protons were characteristic at 5.11 ppm and the aldehyde proton appeared as triplet at 9.76 ppm (Nadkarni *et al*., 2013).

An initial attempt to synthesise the target compound **171** by debenzylation of **182** using 5% Pd/C and H_2 gas in MeOH, failed to cleave the C-O bond after 48 h stirring at r.t. It was noticed that the majority of literature syntheses of the target compound **171** and analogues was by oxidising 4-hydroxyphenyl ethanol **183**. Therefore, it was decided to reattempt deprotection of 4-benzyloxyphenyl ethanol **181** using conditions previously reported by Fernandez-Pastor *et al.* (Fernandez-Pastor *et al*., 2016) Under these conditions, debenzylation of **181** was performed under catalytic hydrogenation again using 5% Pd/C in MeOH, with the derivative 4-hydroxyphenyl ethanol **183** being produced with a very good yield of 97%.

As a result of being this alcohol **183** being insoluble or slightly soluble in DCM, PCC or Dess-Martin oxidation were excluded in this state. The previously reported Parikh-Doering oxidation of 4-hydroxyphenyl ethanol **183** (Pyridine.SO_3, DMSO, Et_3N) (Vece and Vuocolo 2015) (Scheme 50) eventually afforded, after flash chromatography, the target aldehyde **171** as a colourless oil in low yield 33% (Figure 51).

The attractive feature of this reaction is that it proceeds rapidly and reaches completion after 30 min at r.t. The corresponding 4-hydroxyphenyl acetaldehyde **171** and 4-hydroxybenzaldehyde **139** were obtained after the reaction was left stirring for more than an hour. It is important to note that aldehyde **171** is also highly unstable and cannot be stored; therefore, it should

be used directly after synthesis. A similar finding was observed by Zhao *et al.* (Zhao *et al*., 2016).

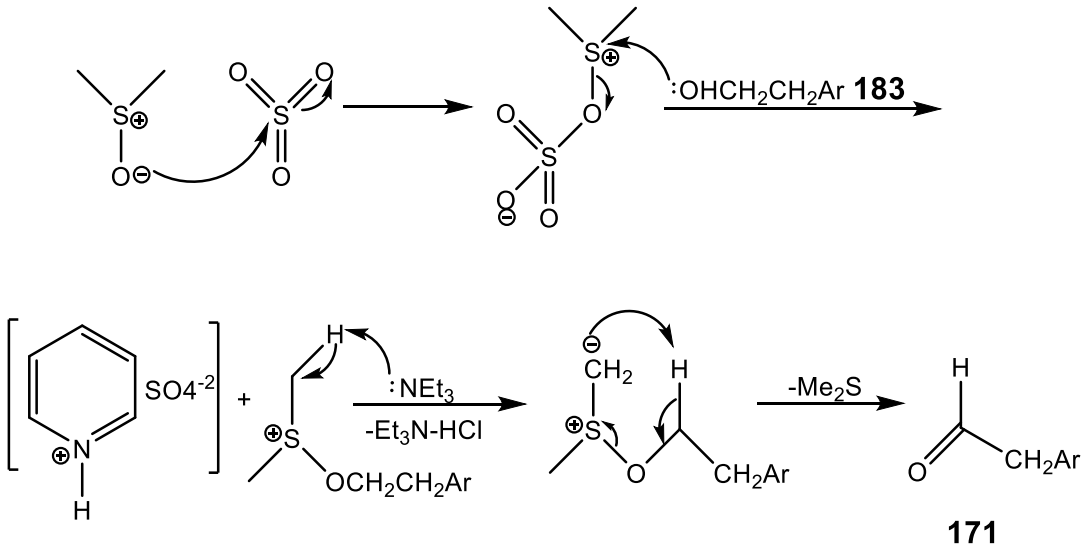

Scheme 50: Parikh-Doering oxidation mechanism

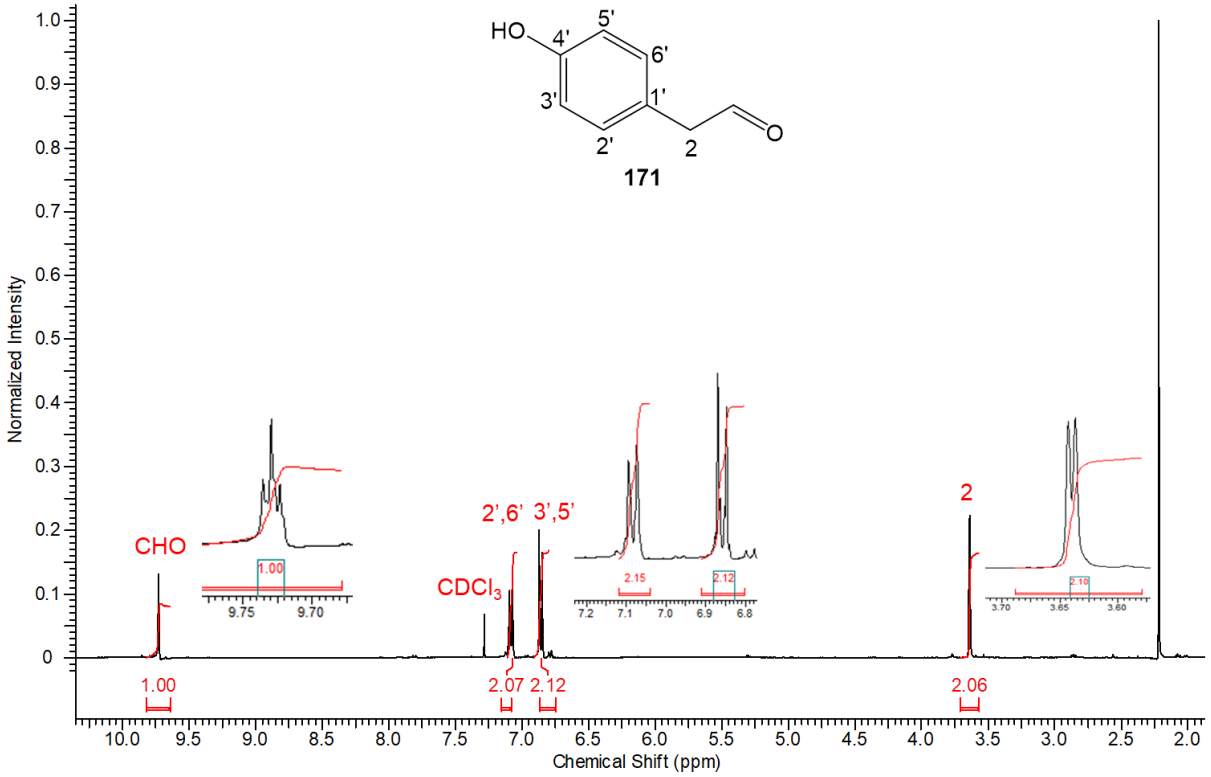

(a)

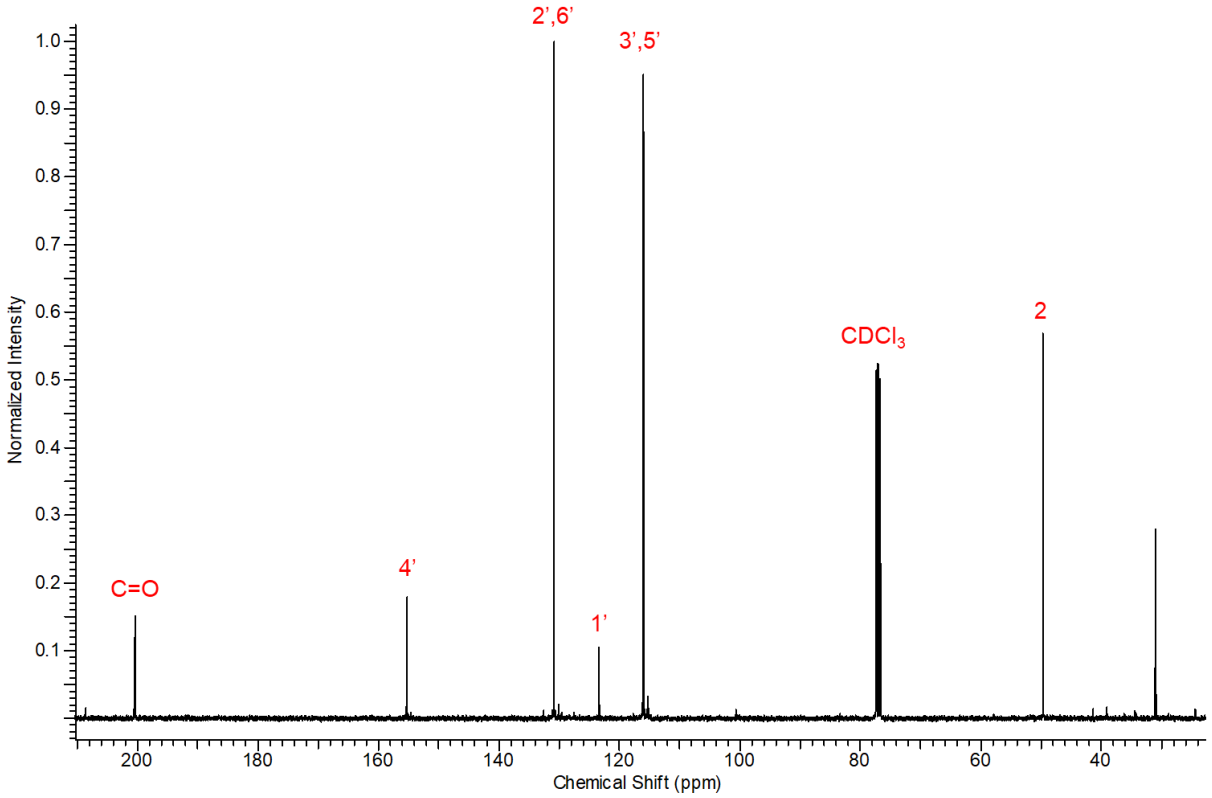

(b)

Figure 51: (a) ^{1}H NMR and (b) ^{13}C NMR spectra of 4-hydroxyphenyl acetaldehyde **171** in $CDCl_3$

An endeavour to prepare the glycoside of aldehyde **169** was unsuccessful and has not been reported here.

3.8 Conclusion

The two different synthetic approaches chosen to prepare glycosylated calix[4]resorcinarenes containing alkyl chains separating the aromatic residues from the lower rim of the molecule (Figure 46), failed to achieve this goal and several problems were encountered.

Despite various protocols at the synthesis of glucosylated aldehyde **167** derived from 4-hydroxyphenyl propanal had to be applied to synthesise the novel

aldehyde, but these were unsuccessful as ^{1}H NMR spectroscopy of different attempts of this synthesis suggesting the existence of either starting materials or producing different species.

Nevertheless, the synthesis of new substituted calix[4]resorcinarenes **176-178** from 4-hydroxyphenyl propanal was largely successful and leads to the formation of intentionally desired *rccc* isomer.

The second synthetic sequence (Scheme 47) followed to prepare the novel aldehyde **169** faced lots of problems which arose during the transformation between compounds and consequently, led to an aldehyde **171** was found to be unstable.

CHAPTER 4: SYNTHESIS AND CHARACTERISATION OF A NOVEL TETRA(4-GLUCOPHENYLETHYL)CALIX[4]RESORCINARENE

4.1 Background

In 1989 Cram and co-workers reported the cyclisation of aliphatic aldehydes functionalised with a benzene ring: this was conducted using equimolar quantities of resorcinol and the aldehyde catalysed by concentrated aqueous HCl in an ethanolic aqueous solution at 25 ^{0}C with for 24 h or longer. Only the C_4 symmetric isomer was isolated from reaction with dihydrocinnamaldehyde, phenylethanal, 4-nitrodihydrocinnamaldehyde and 4-bromodihydrocinnamaldehyde (Figure 52) (Tunstad *et al*., 1989).

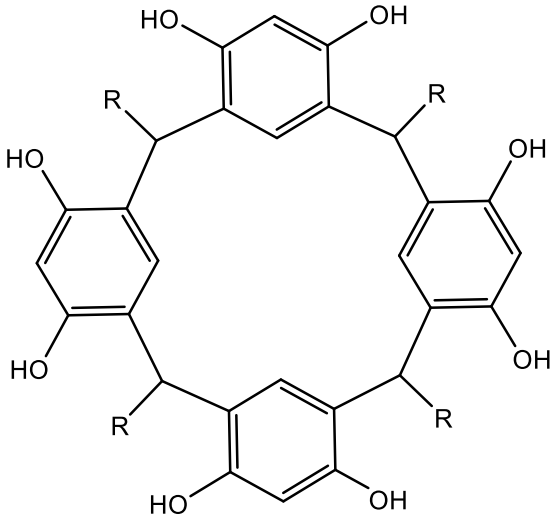

185: R= $CH_2C_6H_5$
186: R= $CH_2CH_2C_6H_5$
187: R= 4-$NO_2C_6H_4$-CH_2CH_2
188: R= 4-BrC_6H_4-CH_2CH_2

Figure 52: Calix[4]resorcinarenes functionalised with alkyl bridges containing aromatic group on the lower rim

Calix[4]resorcinarenes bearing bromine substituents at the 2-position **191** have been synthesised by bromination of calix[4]resorcinarenes and have been used extensively as building blocks for the construction of molecules with an enforced closed shell such as cavitands and carcerands (Bryant *et al*., 1991; Ugono *et al*., 2008). Morikawa *et al*. reported the direct synthesis of these compounds by cyclocondensation of an equimolar ratio of 2-bromoresorcinol **189** and phenylpropionaldehyde **190** in MeCN catalysed by trifluoromethane sulfonic acid (CF_3SO_3H) (9:1 v/v) (Scheme 51). The product that precipitated under standard conditions was the *rccc* isomer exclusively. The stereochemistry of the alkyl substituents was confirmed by comparison of its ^1H NMR spectra with that of an authentic sample. The cyclic tetramer showed one signal for the methine bridges and one signal for the intraannular aromatic proton, thus confirming that it existed in the *rccc* cone conformation (Morikawa *et al*., 2002).

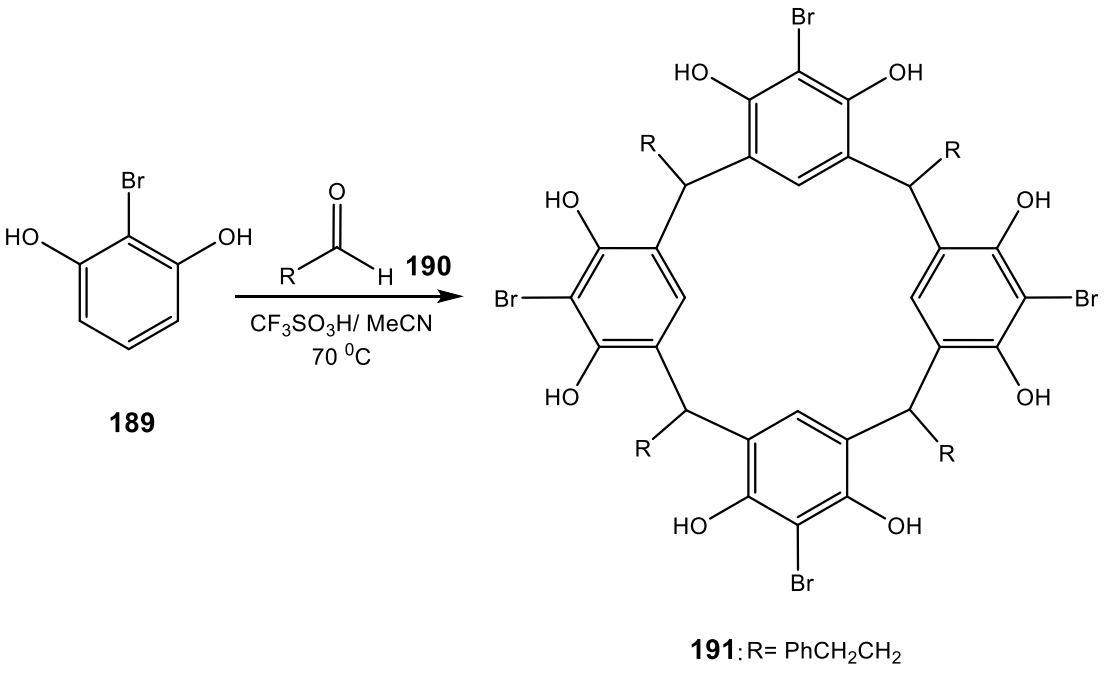

Scheme 51: Synthesis of brominated calix[4]resorcinarene (Morikawa *et al*., 2002)

Thankar *et al*. reported the synthesis of tetramethoxy calix[4]resorcinarene by the interaction of 3-alkoxyphenol **45** with dihydrocinnamaldehyde **190** using $BF_3.Et_2O$ as a Lewis acid catalyst (Scheme 52). In this case, the asymmetry is derived from the stereogenic axis and not from the stereogenic center. By using the process as previously reported by McIldowie *et al*. they obtained a racemic mixture in a good yield, and the predominate isomer possessed the C_4 symmetry or *rccc* configuration (Thakar *et al*., 2014).

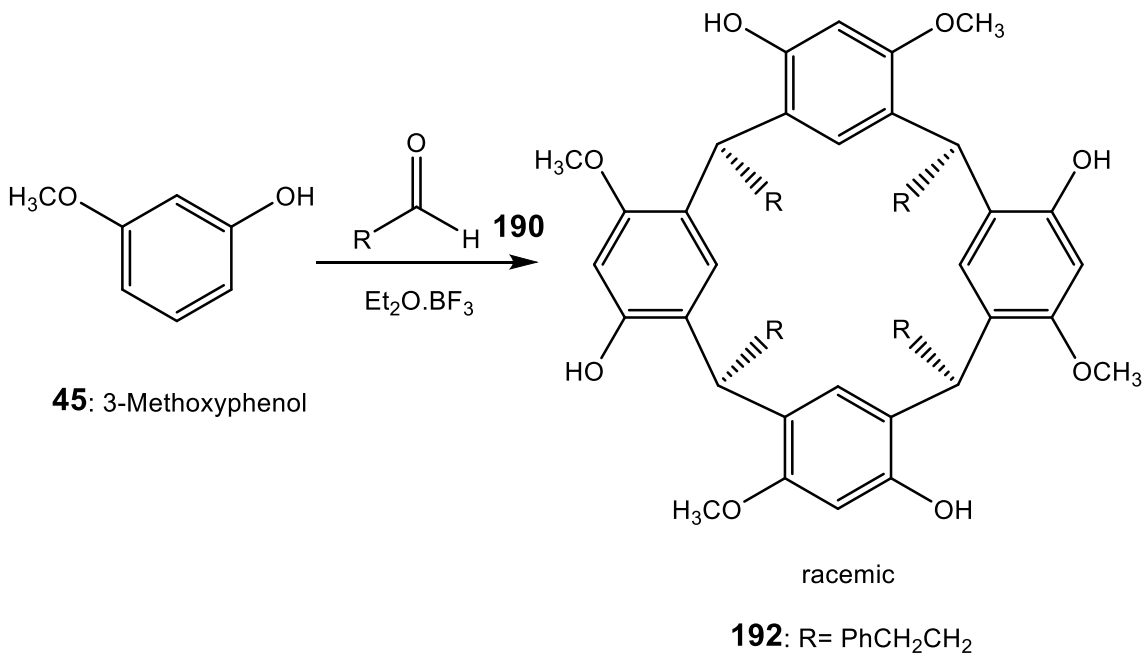

45: 3-Methoxyphenol

192: R= $PhCH_2CH_2$

Scheme 52: Synthesis of tetramethoxy calix[4]resorcinarene as a racemic mixture (Thakar *et al*., 2014)

The development of vehicles to aid in the solubilisation of hydrophobic drugs in aqueous media depends not only on the interaction between the water-hating cavity of calix[4]resorcinarenes (host) and the drug molecules (guest), but also on the groups attached at the rims of the host and the size of the drug molecules. In some cases the starting aldehyde used or the addition of particular groups to the calix[4]resorcinarene can cause the host molecules to aggregate in solution and form large capsule-like structures. In this case, the drug molecule can become encapsulated inside the capsule or associate in some other, unexpected way.

The aim of the work described in this chapter is to determine the effect of using an glycosidic aliphatic aldehyde on the isomer ratios and conformation of the product calix[4]resorcinarene. In particular, by using substituted phenylpropanal, products which are similar to those exploited by Cram *et al*. may be obtained. The five-step strategy for the synthesis of tetra(glucosyloxyphenylethyl)calix[4]resorcinarene octabutyrate **196** is shown in (Scheme 53): 2,3,4,6-tetra-*O*-acetyl-*β*-D-glucosylated 4-hydroxybenzaldehyde **142** was prepared from 2,3,4,6-tetra-*O*-acetyl-*β*-D-glucopyranosyl bromide **138** and 4-hydroxybenzaldehyde **139** according to procedure stated beforehand (page 100, Scheme 34) (Stavila *et al*., 2008).

Compound **142** was used as the starting material in the synthesis of 3-[4'-(2'',3'',4'',6''-tetra-*O*-acetyl-*β*-D-glucopyranosyloxy)phenyl]propanal **167** for the synthesis of compound **164**. The process for the synthesis of glycosidic aldehyde with alkyl chain **167** was carried out according to the general procedure for hydrogenation. Subsequent reaction with resorcinol delivered the novel calix[4]resorcinarene glycocluster **164**.

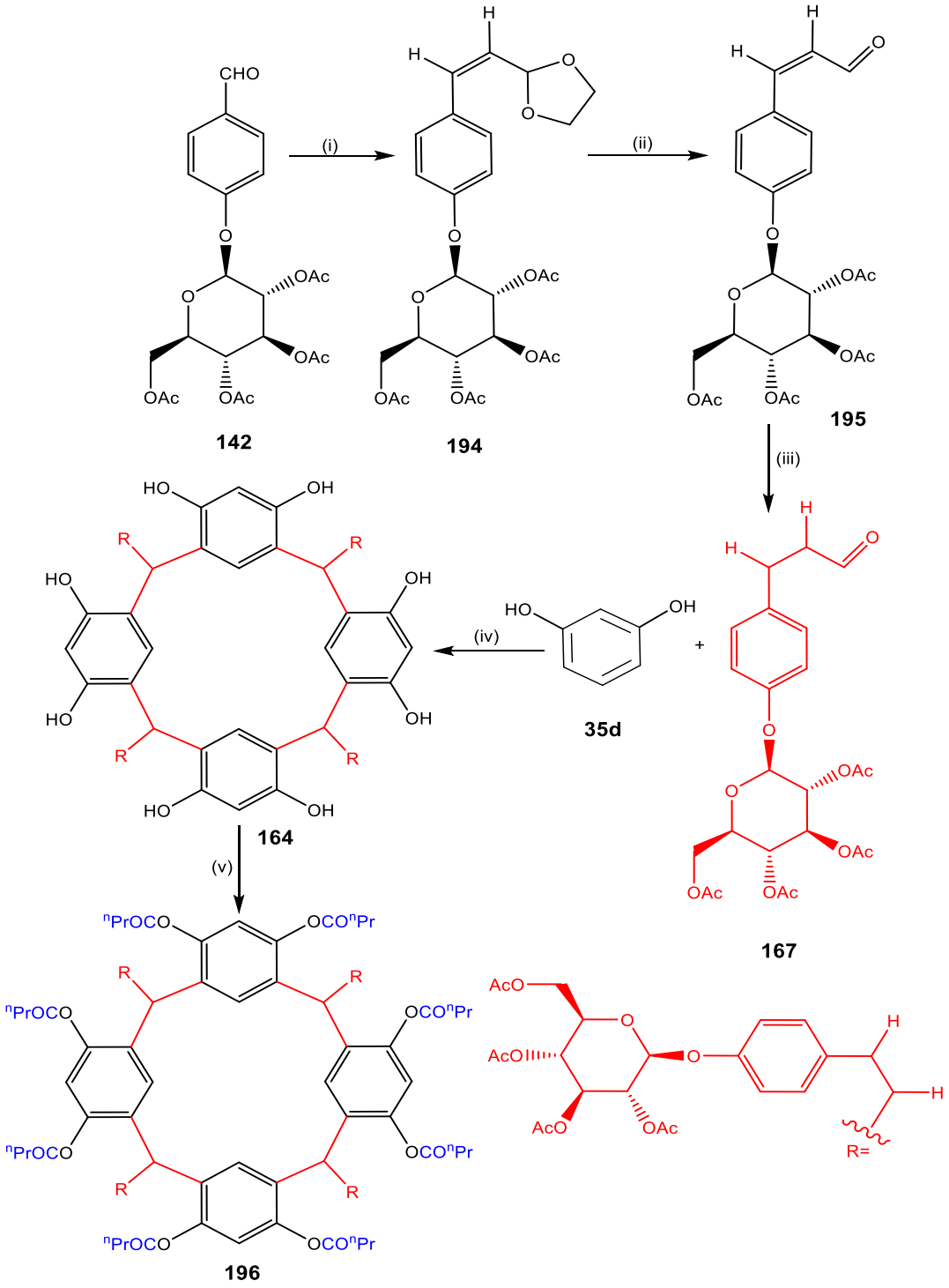

Reagents and conditions: (i) phosphonium salt **193**, KO^{t}Bu, THF, reflux, 24 h (ii) Br_2, CCl_4, HOAc, H_2O, 0 ^{0}C to r.t (iii) H_2, Pd/C 5%, MeOH (iv) anhyd $AlCl_3$, Et_2O, THF, 48 h, r.t (v) butyric anhydride, pyridine, 80 ^{0}C, 24 h

Scheme 53: Synthesis of tetra(4-glucophenylethyl)calix[4]resorcinarene octabutyrate **196**

4.2 Synthesis of 2-{2'-[4''-(2''',3''',4''',6'''-tetra-*O*-acetyl-*β*-D-glucopyranosyloxy)-phenyl]ethenyl}-1,3-dioxolane 194

Vinylogation of tetra-*O*-acetyl glucoside of 4-hydroxybenzaldehyde **142** using 1,3-dioxolane-2-ylmethyltriphenylphosphonium salt **193** was conducted using two different methods. The first method employed followed the literature method described by Daubresse (Daubresse *et al*., 1998) under phase transfer conditions by mixing the aldehyde (1 eq) with TDA-1 {tris[2-(2-methoxyethoxy)ethyl]amine} (1 eq) and the phosphonium salt (1.22 eq) **193** in a refluxing emulsion of saturated aqueous K_2CO_3 solution and DCM. This reaction was worked up by quenching with water and extraction with DCM, the organic layer was then washed with aqueous hydrochloric acid led to deliver *α*,*β*-unsaturated 1,3-dioxolane **194** in 5% yield.

The Wittig reaction following the method of Daubresse *et al*. led to the formation of compound **194** in a low yield which was not sufficient to complete the planned strategy for the synthesis of calix[4]resorcinarene glycocluster.

Therefore, following other literature precedent, it was decided to select different conditions for the Wittig reaction. Compound **194** was produced by treatment of 4-glucosylated benzaldehyde **142** with phosphonium salt **193** and potassium *tert*-butoxide in THF (Ka *et al*., 2016). After refluxing the mixture at 70 ^{0}C for 24 h, styryl-1,3-dioxolane glucoside **194** was obtained with a slightly improved yield of 25%.

Unfortunately, the yield obtained from a single reaction under these conditions was also inadequate to complete four more steps. Therefore, the reaction was repeated 26 times in order to obtain a sufficient amount.

The structure of the crude dioxolane **194** was confirmed by ^{1}H NMR spectra which indicated a *Z*/*E* ratio of approximately 66:34 (first method) and 55:45 (second method). In all cases the TLC of the crude reaction mixture showed two spots in close proximity to each other indicating two isomers with nearly the same R_f as for the starting glucosylated aldehyde. The purification was conducted on flash column chromatography using EtOAc: Pet. ether (1.5:1) as eluent. The ^{1}H NMR after purification contained signals at 3.93-4.00 and 4.07-4.12 ppm assigned to the methylene protons O-CH_2-CH_2-O. Two signals at 5.43, 5.51 ppm appeared as two doublets due to dioxolane methine proton. The vinylic protons were seen as double doublets each at 5.71, 6.09 and 6.77 ppm for $E-Z$ isomers (*cis* and *trans*). The triplet and double doublet for the aromatic protons were observed at 6.96-7.00, 6.34-7.39 ppm (Figure 53).

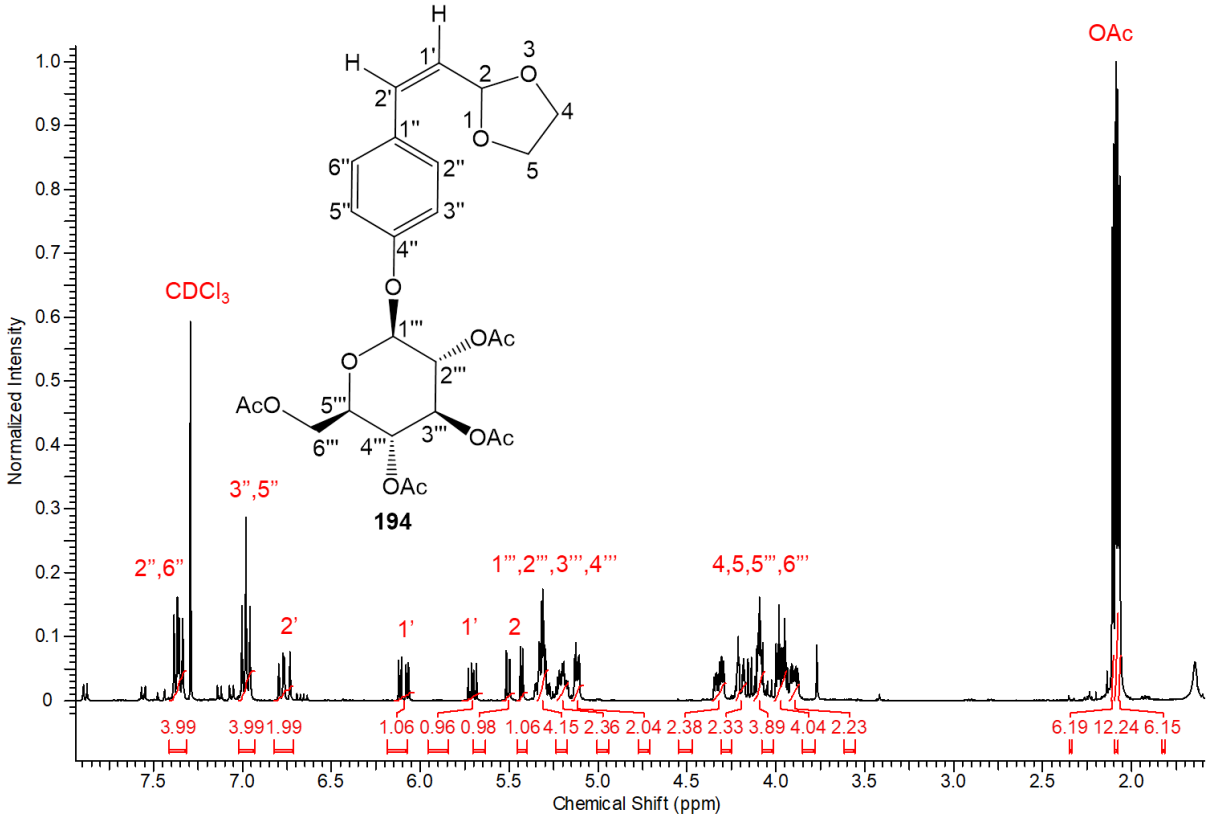

Figure 53: ^{1}H NMR spectrum of dioxolane *Z/E* mixture after column **194** in $CDCl_3$

One of the most important methods for the synthesis of alkenes is the Wittig reaction, which is the reaction of an aldehyde or ketone with phosphonium ylides. An ylide is a species with a positive charge on the phosphorus atom and negative charge on the adjacent carbon atom. Phosphonium ylides are prepared from phosphonium salts by treatment with a strong base (Scheme 54).

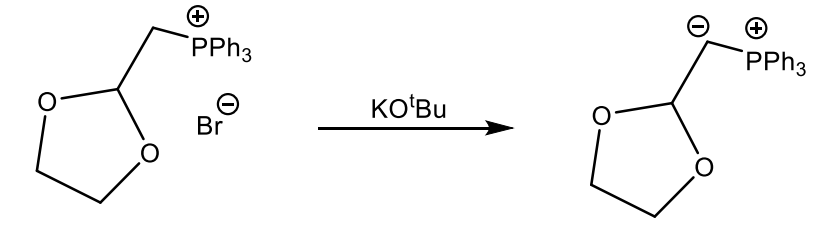

phosphonium salt **193** phosphonium ylide

Scheme 54: Phosphonium ylide formation

The mechanism of the Witting reaction involves the nucleophilic attack of the carbanion of the phosphonium ylide on the carbonyl group of the aldehyde to form a betaine as a zwitterionic intermediate. The betaine then closes by reaction of the negatively charged oxygen with the positively charged phosphorous to give an unstable four-membered cyclic intermediate called an oxaphosphetane. Finally, the oxaphosphetane ring cleaves to form an alkene along with triphenylphosphine oxide as a by-product. The phosphorous-oxygen double bond is very strong and it is the driving force for the forward reaction (Scheme 55).

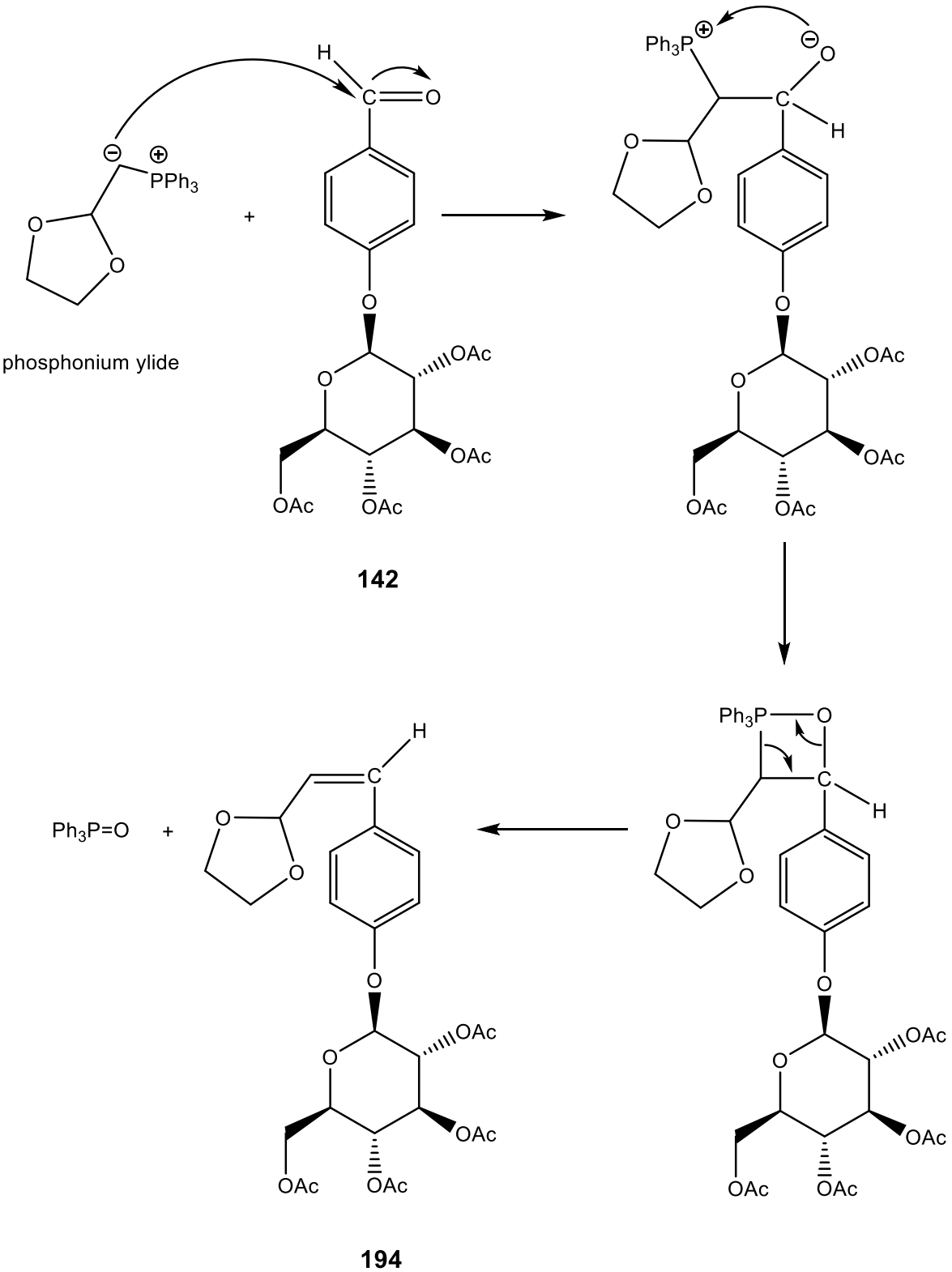

Scheme 55: Mechanism of dioxolane formation

Some Wittig reactions are *Z*-selective and some show *E*-selectivity on the products. The stereoselectivity is due to the nature of the substituent group in the ylide. Generally, there are two types of ylides, stabilised and unstabilised: Stabilised ylides refer to stabilising of the negative charge not only by the positively charged phosphorus atom but also by conjugation with substituents on the anionic carbon atom. Unstabilised ylides have no such interaction with substituents on the anionic carbon atom. The Wittig reaction is *E*-selective with stabilised ylides whereas it is *Z*-selective with non-stabilised ylides (Figure 54).

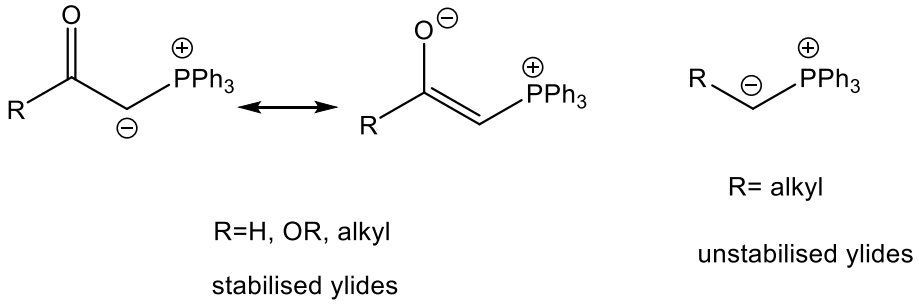

Figure 54: Stabilised and unstabilised ylides

To explain how the Z/*E*-selectivity in the Wittig reaction arises, consideration must be made to the fact that there may be two separate steps: formation of the oxaphosphetane and subsequent decomposition and elimination to give an alkene; the decomposition step can be used to explain the stereospecificity. In principle, addition of the ylide to the aldehyde can produce two diastereomers of the intermediate oxaphosphetane and then the stereospecific elimination step means that the geometrical isomer of the final alkene will reflect the stereoselectivity of this addition step.

With unstabilised ylides the *syn* oxaphosphetane is the favoured product, this is reflected by the formation of the corresponding *Z* alkene predominately. The

mechanism by which the *syn* oxaphosphetane produced has not been clearly established, one possible explanation depends on rules of orbital symmetry. By approaching the carbonyl compound and the ylide at right angles, they will react to form an oxaphosphetane ring in the transition state in one step. Keeping the large substituents away from each other leads to the formation of transition state which leads to the *syn* stereochemistry of oxaphosphetane (Scheme 56).

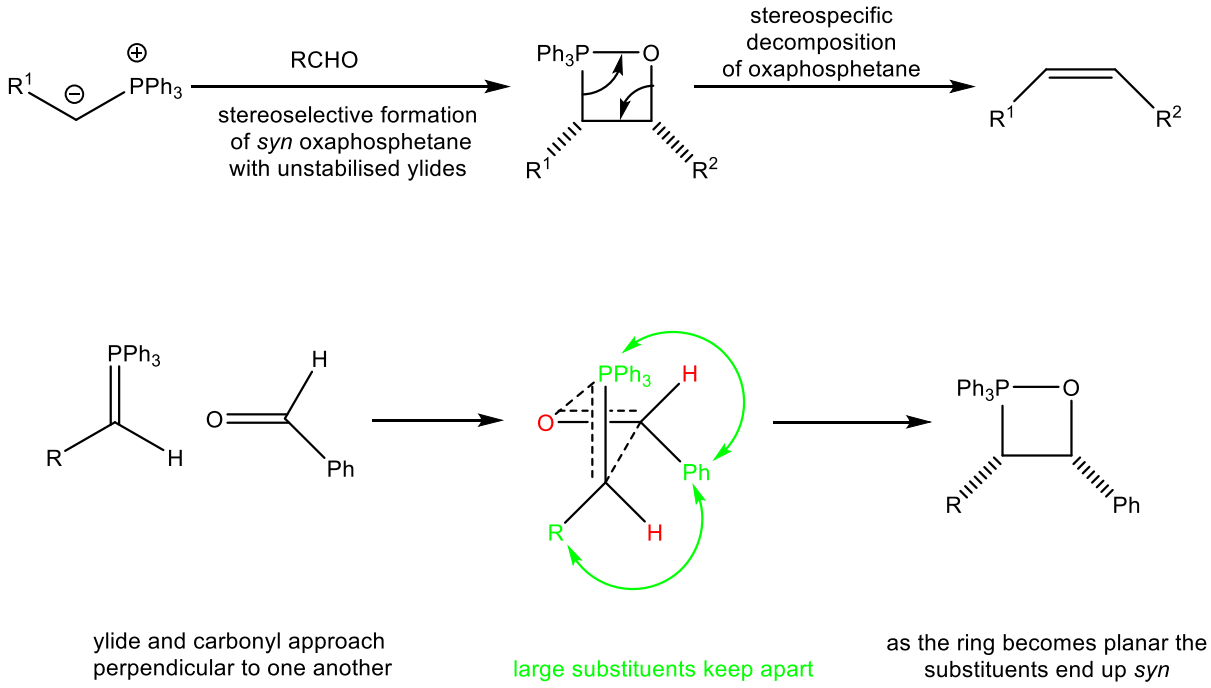

Scheme 56: Mechanism of *syn* oxaphosphetane formation and *Z* alkene (*cis*)

With stabilised ylides the stereoselectivity is opposite and gives the *E* isomer. Again, the mechanism is not entirely clear and there are different potential explanations. One which has been evidenced is that the stereoselectivity of the alkene product again relies upon the stereochemistry of the oxaphosphetane, which gives the *anti* diastereoisomer with stabilised ylides (Scheme 57).

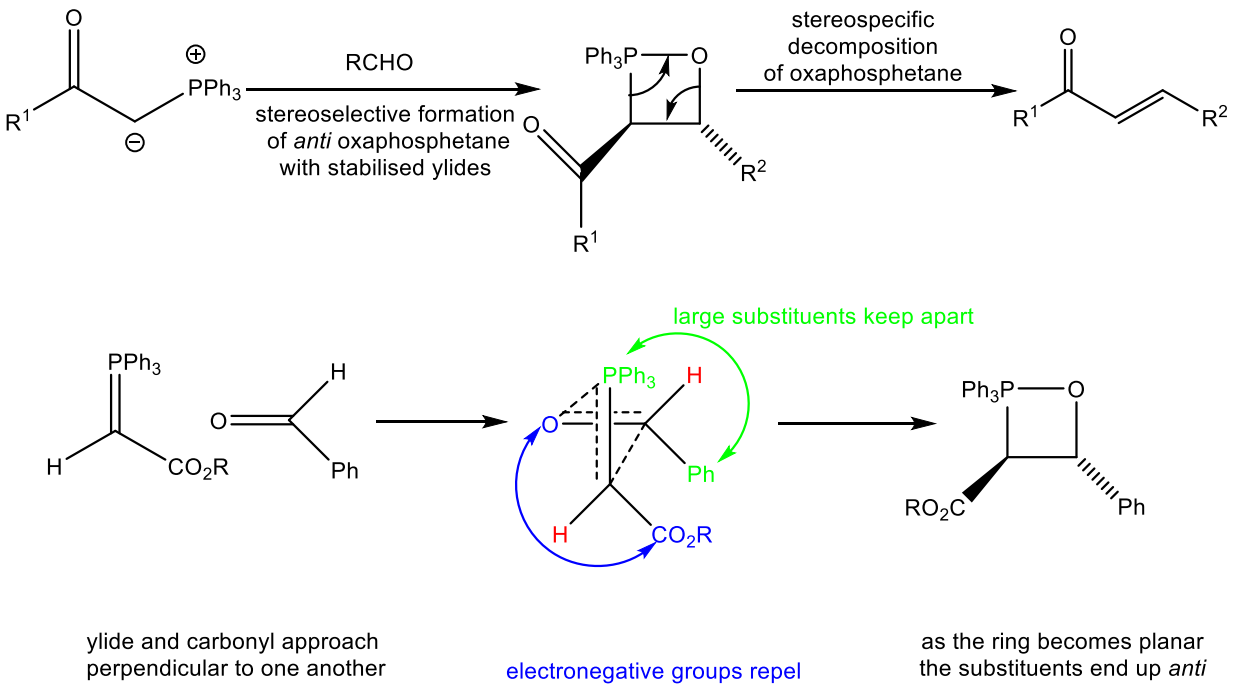

Scheme 57: Mechanism of *anti* oxaphosphetane formation and *E* alkene (*trans*)

It was believed that the *anti* oxaphosphetane is formed under thermodynamic control, but research suggests that it is likely that is produced under kinetic control. The difference with unstabilised ylides is that the electronegative stabilising group of the ylide and the polarised C=O bond of the aldehyde repel each another. As the ring become flattens out, the anion stabilising substituents of the ylide and the phenyl group of the aldehyde end up on opposite faces of the ring.

4.3 Acetal hydrolysis for preparing trans 4-glucophenylpropionaldehyde 195

Acetals are important protecting groups for aldehydes because acetals are stable to bases, basic nucleophiles and redox reagents. In addition, their formation is reversible because acetals can be hydrolysed in dilute acid and the original functional group is revealed following this hydrolysis. In our study, the cyclic acetal was formed by reaction of an aldehyde **142** with a phosphonium ylide in the Wittig reaction. To convert the dioxolane acetal back into an aldehyde required hydrolysis by aqueous acid to produce (*E*)-*α*,*β*-unsaturated aldehyde **195**.

The process involved treatment of both *Z*/*E* isomers with catalytic amounts of bromine in carbon tetrachloride at 0 ^{0}C for 1 h, followed by addition of dilute AcOH at r.t. After leaving the reaction for 24 h, followed by work-up, which included washings using KOH, $Na_2S_2O_3$ and $NaHCO_3$, syrup was obtained. Crystallisation from Et_2O led to the formation of a white powder. The glycosidic cinnamaldehyde **195** was purified using column chromatography using EtOAc: Pet. ether (1:1) as eluent to give the desired product in a yield of 74%.

The structure of compound **195** was confirmed by ^{1}H NMR, ^{13}C NMR and DEPT135 spectroscopy experiments. The ^{1}H NMR displayed signal resonances were consistent with the values supplied by the author (Daubresse *et al*., 1998), in which, the vinylic protons give two resonances at 6.66 ppm appeared as double doublets and at 7.46 ppm as a doublet, and the peaks of aromatic protons were observed at 7.06 ppm and 7.55 ppm as two doublets. The doublet signal at 9.70 ppm assigned to the aldehyde group with a couplet constant *J*=

7.7 Hz (Figure 55). The (*E*)-configuration was proved by the high value of the coupling constant (ca. 15.9 Hz) for the vinylic protons.

The mechanism involves, in the first step, the *Z* dioxolane substituted alkene is isomerised to the thermodynamically more stable *E* isomer using bromine *via* a radical mechanism. In the next step, the hydrolysis of dioxolane acetal proceed by protonation one of the oxygens, then the other oxygen attacks to liberate the activated one to form the oxonium ion. Thus, water will attack the carbonyl carbon to give the hemiacetal intermediate after deprotonating the attacking group and regeneration of the acid catalyst. Repeating these steps produces the aldehyde and the corresponding diol (Scheme 58).

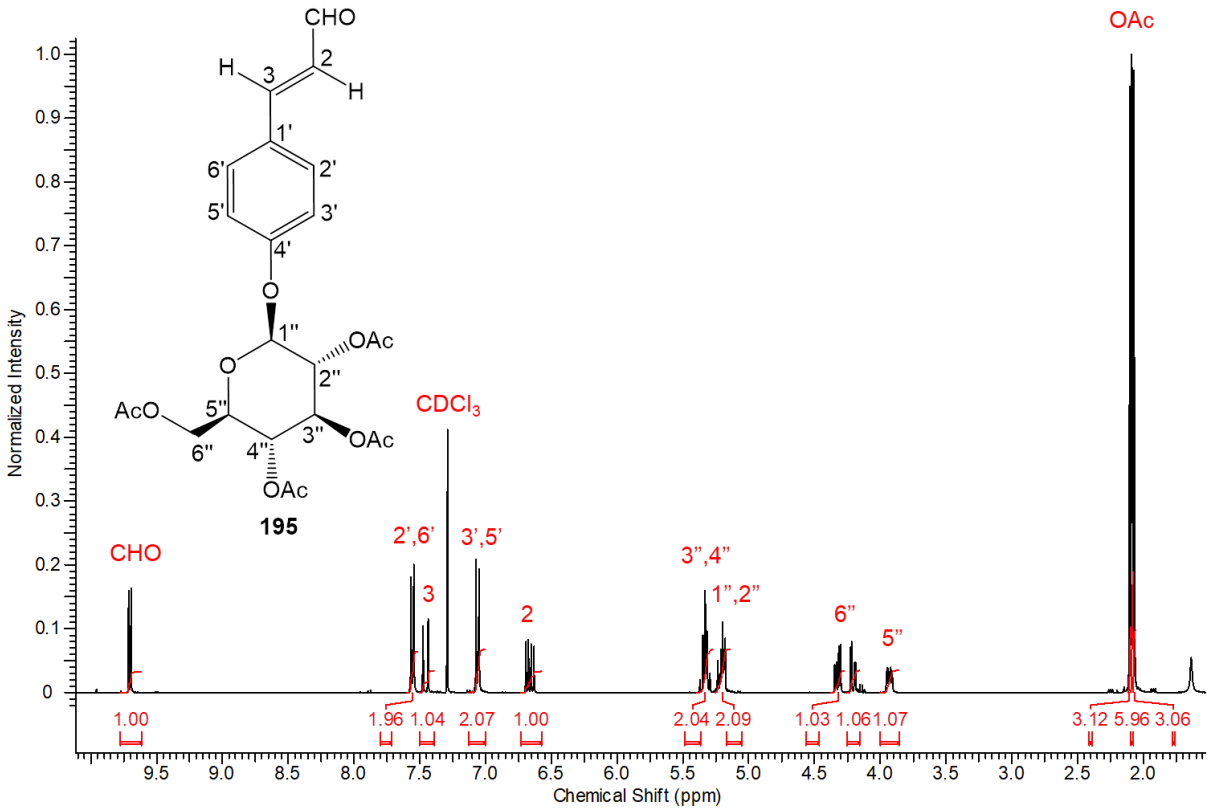

(a)

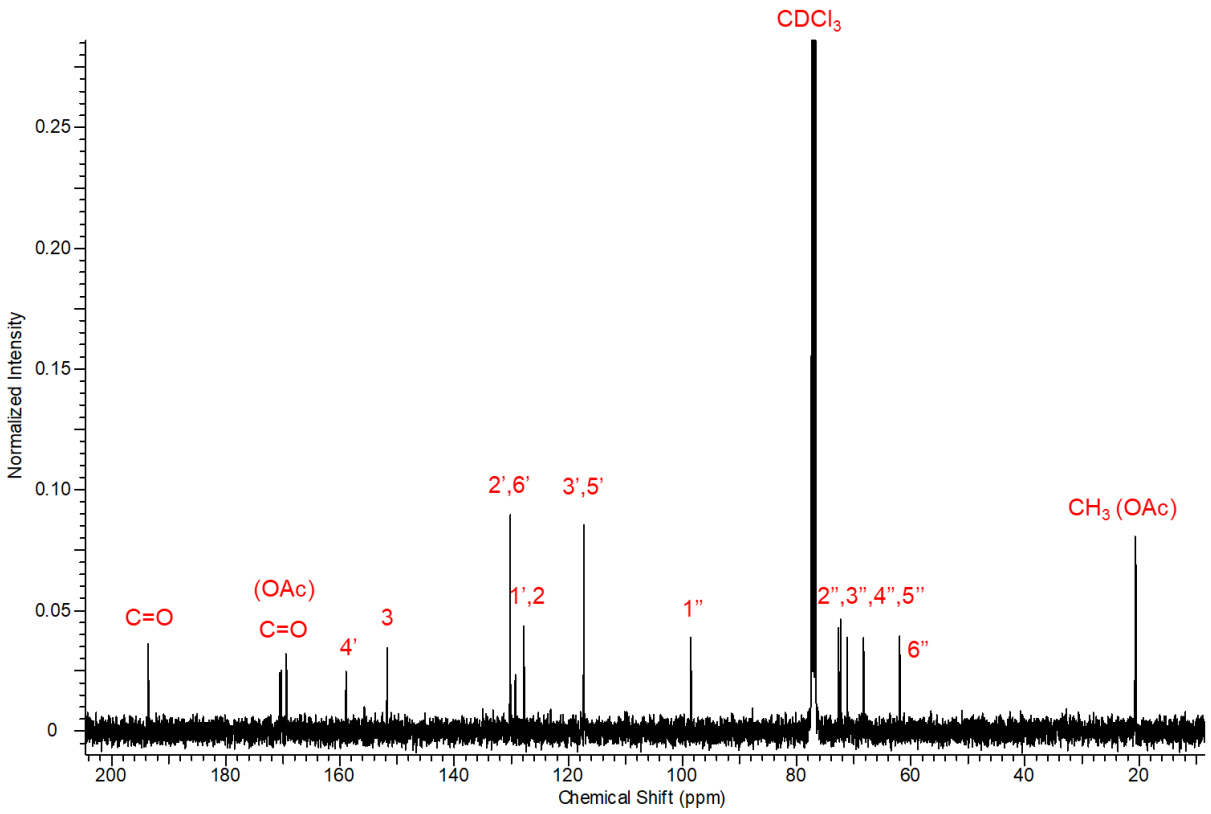

(b)

Figure 55: (a) ^{1}H NMR and (b) ^{13}C NMR spectra of (*E*)-*α*,*β*-unsaturated aldehyde **195** in $CDCl_3$

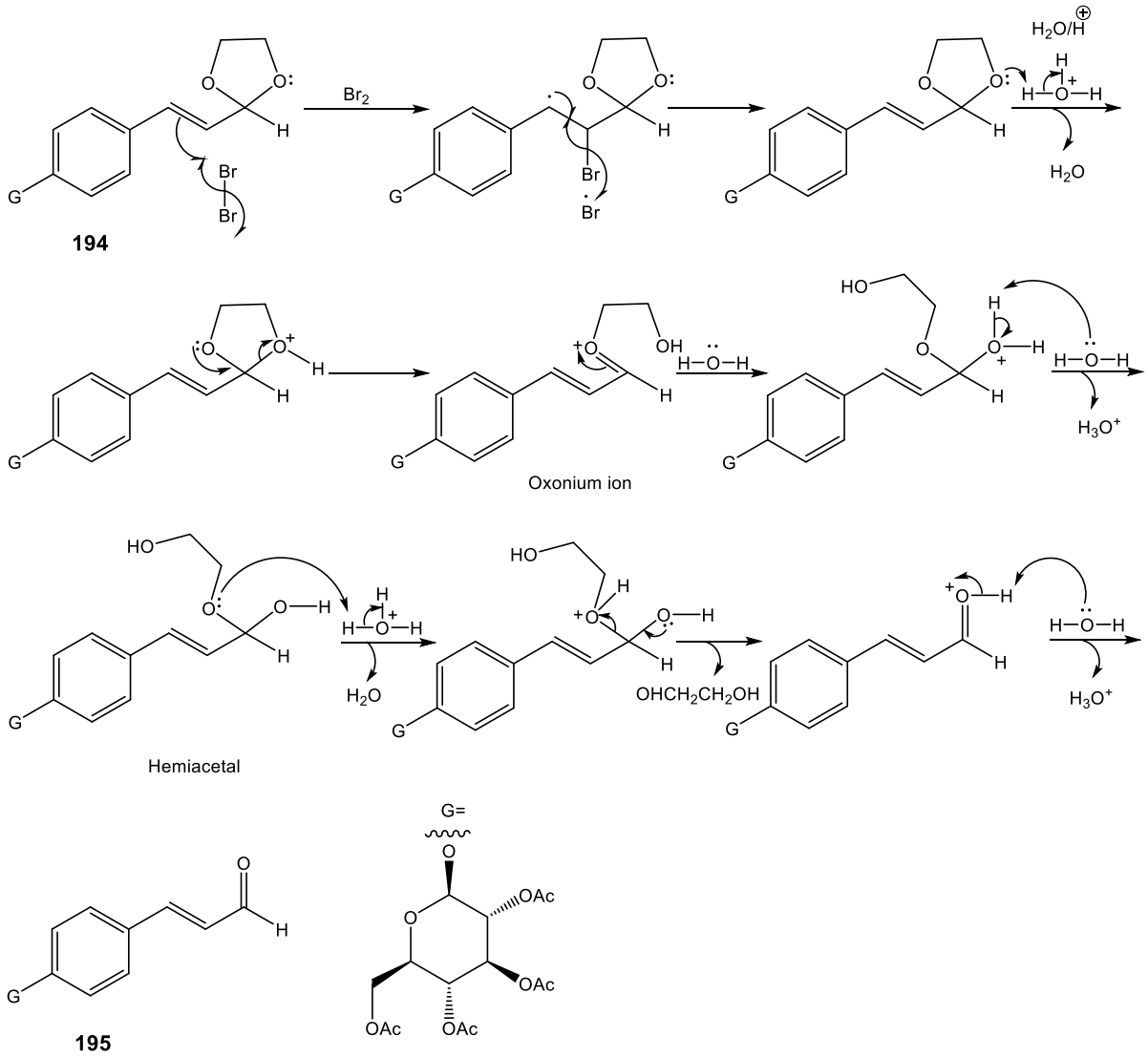

Scheme 58: Dioxolane hydrolysis mechanism

4.4 Hydrogenation of *trans*-cinnamaldehyde derivative 195 to give hydrocinnamaldehyde derivative 167

Trans-cinnamaldehyde is extensively used as an important substrate because its hydrogenation products are widely used in organic chemistry, biochemistry and pharmaceutical chemistry (Pritchard *et al*., 2015; Chen *et al*., 2017). The selective hydrogenation differs due to the potential of reduction of either the alkene unit, to form hydrocinnamaldehyde, or the carbonyl unit to give cinnamyl alcohol. The selectivity to give cinnamyl alcohol is commonly poor due to

thermodynamically preferable reduction of the C=C bond over the C=O bond (Szumelda *et al*., 2014).

In *α*,*β*-unsaturated carbonyl compounds the selective reduction of the alkene C=C bond can be achieved easily by reduction using hydrogen gas in the presence of a Pd/C catalyst (Choi *et al*., 2017). However, the situation with *α*,*β*-unsaturated aldehydes is challenging and mixtures of products often result (Li *et al*., 2018).

Hydrogenation selectivity is affected by the organic ligand, metal center, texture, structure and catalyst composition (shape, particle size, support and molar ratio of components), reaction conditions (solvent, temperature and pressure) and functional groups on the substrates (Shi *et al*., 2016; Li *et al*., 2016; Zhang *et al*., 2018).

In the field of metal transfer hydrogenation, metal hydride species produced from iridium (Chen *et al*., 2015), ruthenium (Azua *et al*., 2017), palladium (Ding *et al*., 2013) and nickel (Castellanos-Blanco *et al*., 2012) preferentially lead to hydrogenation of the C=C bond. By comparison, metal-ligand bifunctional H-M-NH catalysis selectivity leads to hydrogenation of the C=O bond in *α*,*β*-unsaturated carbonyl compounds (Baldino *et al*., 2016).

The commercially available palladium catalyst supported on carbon is well known as a selective catalyst for alkene C=C hydrogenation. However, its effective catalytic activity probably causes poor selectivity between alkene reduction and total reduction of all double bonds.

The catalyst makes the hydrogen react with double bonds with catalytic hydrogenation taking place on the metal surface. Therefore, the metal must be

finely divided and scattered on an inert support surface. This is the case for commercially available Pd/C catalyst, finely divided palladium on a carbon support.

In this study the hydrogenation of (*E*)-3-[4'-(2'',3'',4'',6''-tetra-*O*-acetyl-*β*-D-glucopyranosyloxy)phenyl]prop-2-enal **195** in methanol was achieved using Pd/C as catalyst.

Compound **167** was prepared using a modified method reported by Lee *et al*. (Lee *et al*., 2017). Treatment of *trans*-*α*,*β*-unsaturated aldehyde **195** with hydrogen gas in the presence of a catalytic amount of 5% Pd/C in MeOH as solvent at room temperature led to the selective hydrogenation of the olefinic C=C unit and formation of the saturated carbonyl compound **167** in 19% yield after 2 h.

The suggested mechanism involves the chemisorption of hydrogen onto the catalyst surface, a process that leads to cleavage of the H-H bonds and disperses hydrogen atoms on the surface to make them able to react with the organic substrate. The alkene can also coordinate to the metal, thereby hydrogen atoms can be moved from the catalyst to the alkene (Scheme 59).

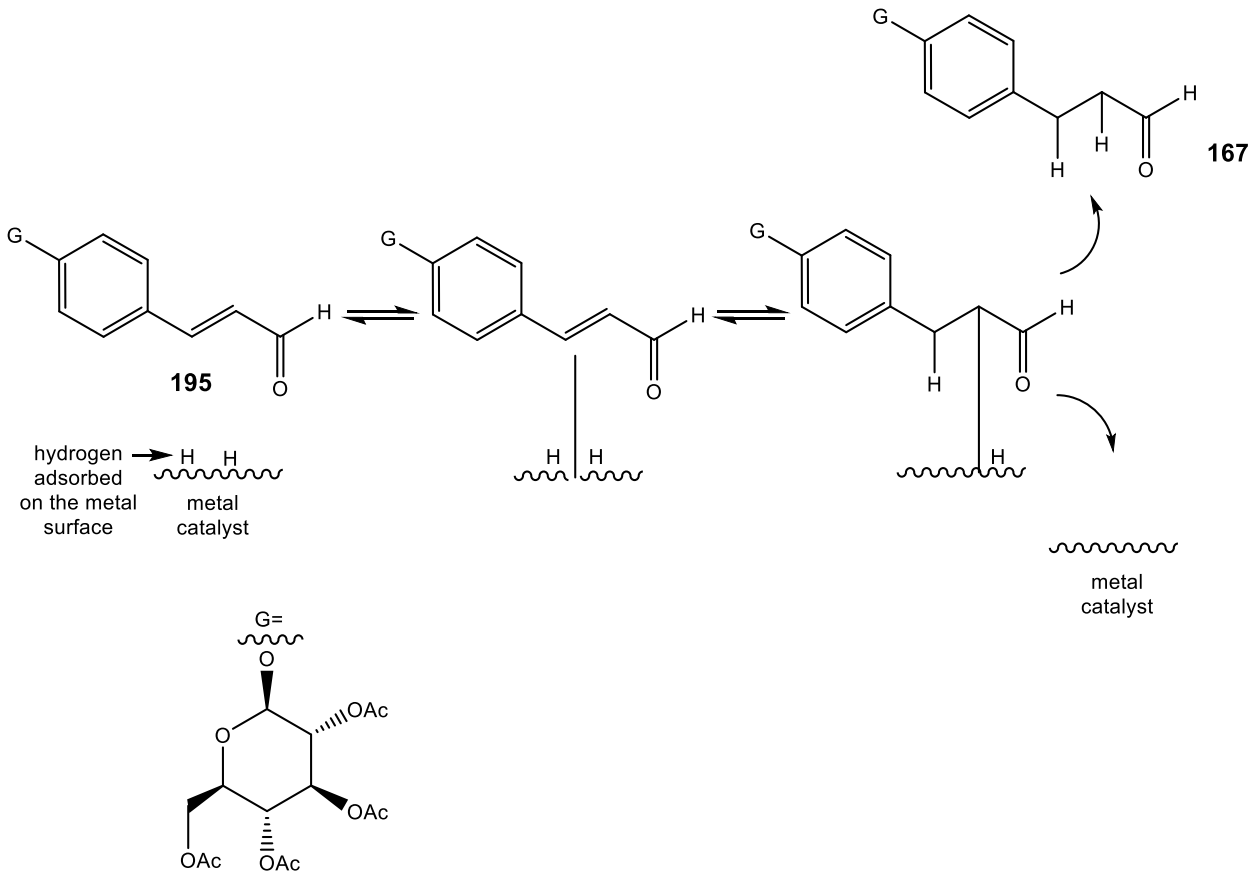

Scheme 59: Suggested hydrogenation mechanism

However, in some cases and under varied conditions it is difficult to control the selectivity of this reaction and a product mixture was obtained, consisting mainly of the saturated aldehyde together with the undesired saturated alcohol (Scheme 60) (Jahjah *et al*., 2011). The *α*,*β*-unsaturated alcohol was not observed on the ^{1}H NMR data as indicated by disappearing of the olefin moiety. Careful monitoring of the reaction until TLC indicated complete conversion of the starting material **195** led to the hydrocinnamaldehyde **167** being obtained as white crystals (Figure 56) following purification using column chromatography EtOAc: Pet. ether (2:1) as eluent. The ^{1}H NMR displayed two triplets at 2.76 and 2.92 ppm, indicating formation the saturated carbonyl compound.

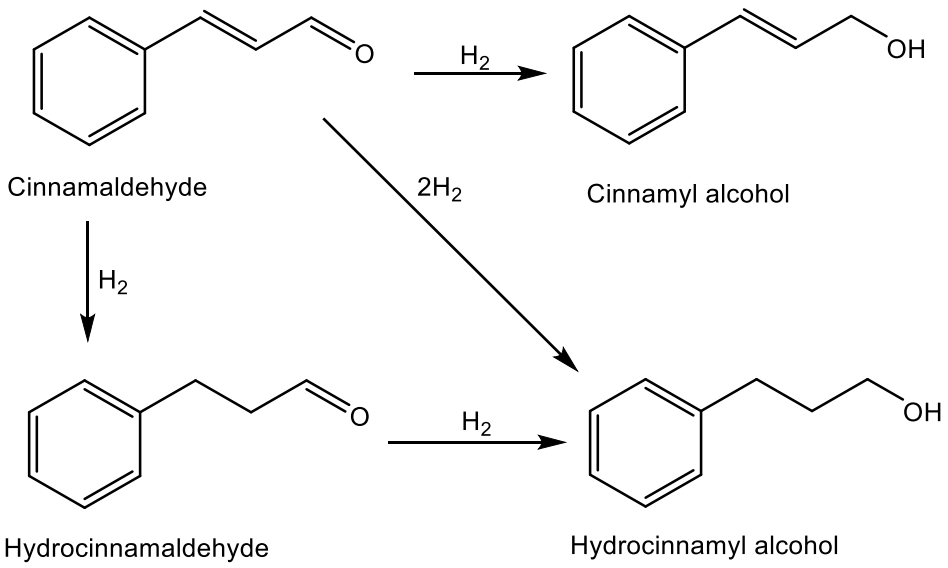

Scheme 60: Potential reaction pathways for cinnamaldehyde hydrogenation

(Jahjah *et al*., 2011)

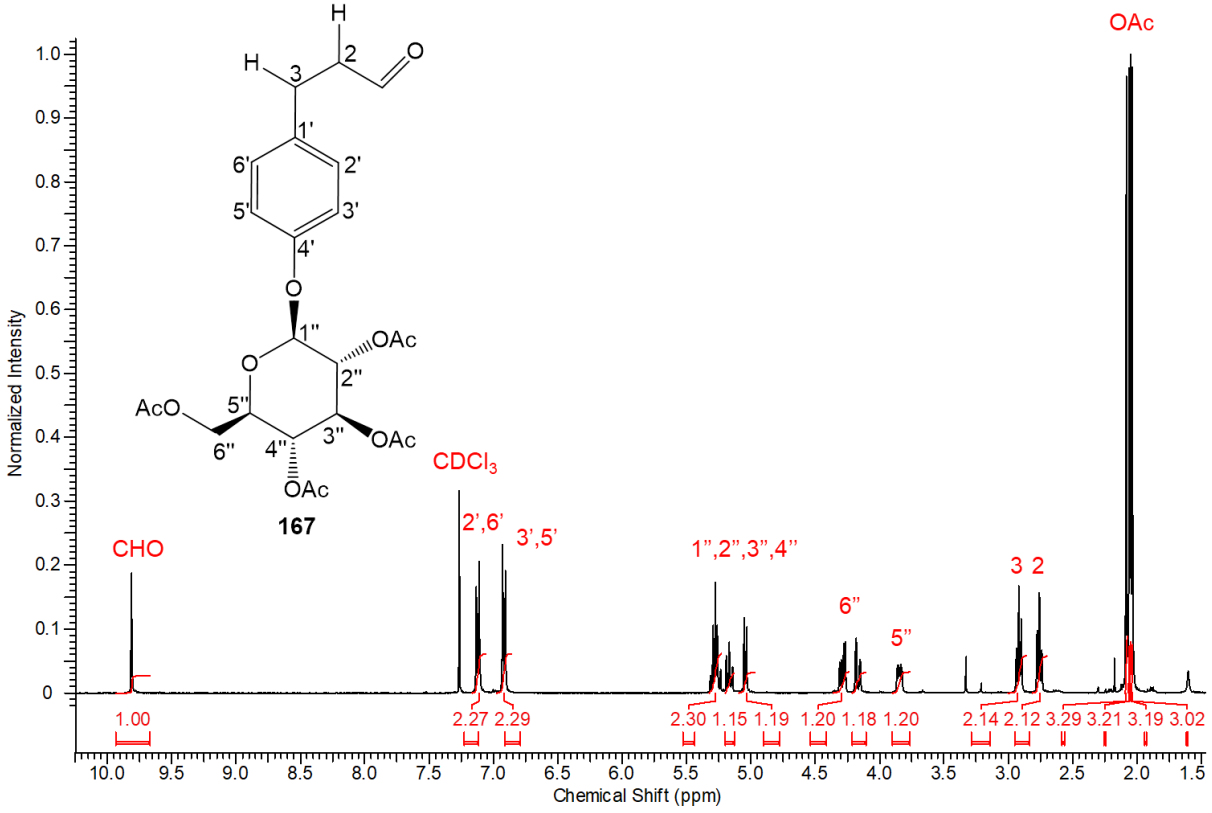

(a)

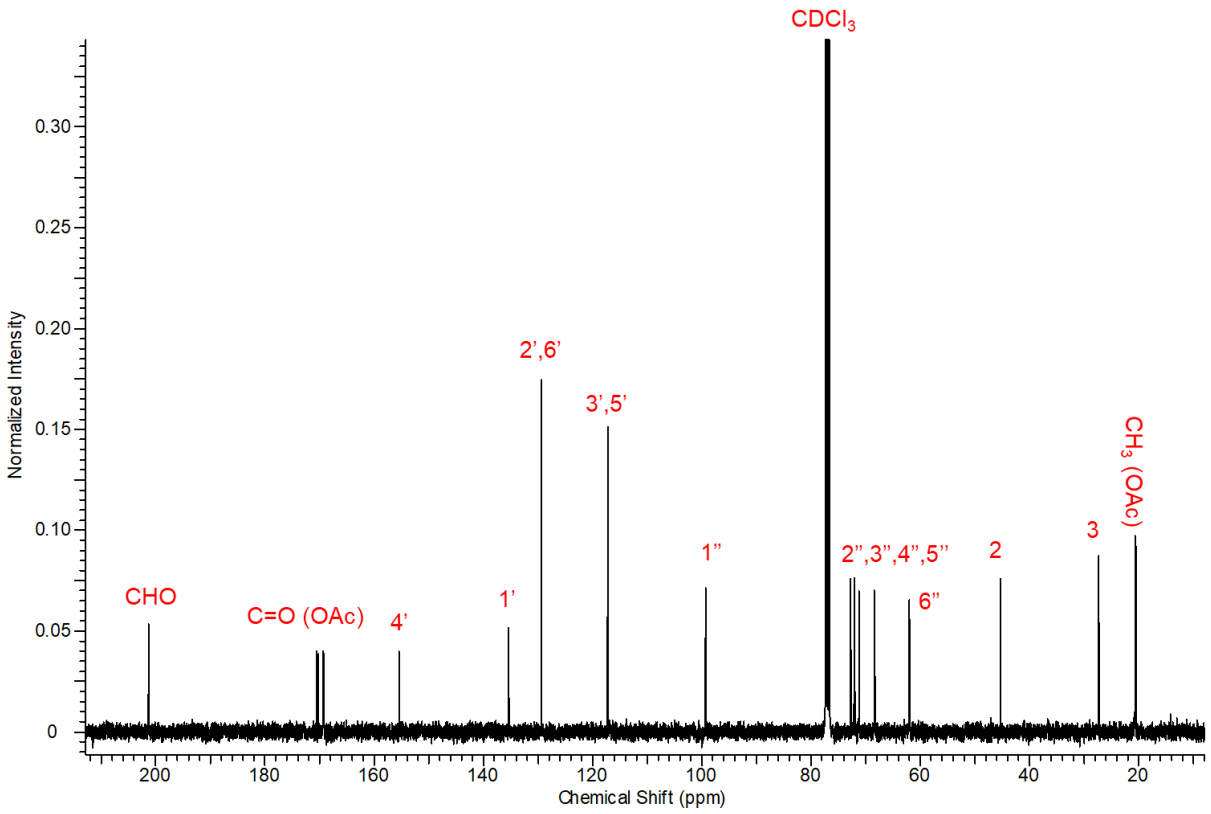

(b)

Figure 56: (a) ^{1}H NMR and (b) ^{13}C NMR spectra of tetraacetoxyglucoside of 4-phenylpropionaldehyde **167** in $CDCl_3$

4.5 Synthesis of tetra(4-glucophenylethyl)calix[4]resorcinarene

The preparation of lower-rim glucosylated calix[4]resorcinarene with ethyl bridges between the hydrophobic core and the aromatic residues was based upon a one-step cyclooligomerisation reaction according to scheme 53. We investigated the catalytic properties of a number of Lewis acids in the reaction of different aromatic aldehydes and resorcinol in dry Et_2O. Among them, anhydrous $AlCl_3$ shown high catalytic efficiency and promoted the cyclisation in a short reaction time. This result prompted us to apply these reaction conditions to the condensation reaction of 3-[4'-(2'',3'',4'',6''-tetra-*O*-acetyl-*β*-D-glucopyranosyloxy)phenyl]propanal **167** with resorcinol.

When we used an equimolar quantity of resorcinol and **167** with 1.5 equivalent of aluminium(III) chloride in an anhydrous solvent mixture of Et_2O and THF, the reaction was complete after 48 h stirring under N_2 at r.t. After work up of this experiment in the usual way we obtained 20% of a crude mixture of the desired compound. However, some signals expected to be present in the ^{1}H NMR and ^{13}C NMR spectra were absent, though the spectra were very clean. The structure of compound **164** was confirmed utilising a diversity of analytical techniques.

The important ^{1}H NMR, ^{13}C NMR and DEPT135 spectrum could be accurately assigned by heteronuclear single quantum correlation (HSQC). In the ^{1}H NMR spectrum of the crude mixture in (d_6-acetone), signal of the methine bridges was absent, while ethyl chain residues appeared as multiplet with chemical shifts of 2.37-2.76 ppm. Signals for glucose units were completely exhibited in the spectrum with a chemical shift between 4.00-4.46, 5.06-5.48 ppm and the acetyl protons were observed at 1.91-2.14 ppm. The δ values for the broad signals that referred to the resorcinol fragments were between 6.19-6.55 ppm. Multiplet signals are also observed at 6.68-7.42 ppm attributed to the aromatic protons. In DEPT135 four important signals associated with ethyl phenyl chains, resorcinol units and the aromatic groups were observed at 33.5, 102.9, 116.7 and 129.5 ppm. In the HSQCDEPT spectrum, the signal of the methine bridges showed a correlation with glucose protons.

The presence of multiplet for the ethyl chains, together with disappearance of signals for the methine groups that link the aromatic rings in the ^{1}H NMR or may be hidden since they overlap with signals assigned to the glucosyl residues, while the chemical shifts of those diagnostic protons which could be observed were to a large extent consistent with ^{1}H NMR data published by Cram,

(Tunstad *et al*., 1989) and correspond to the C_{4v} symmetry or *rccc* conformation (Figure 57).

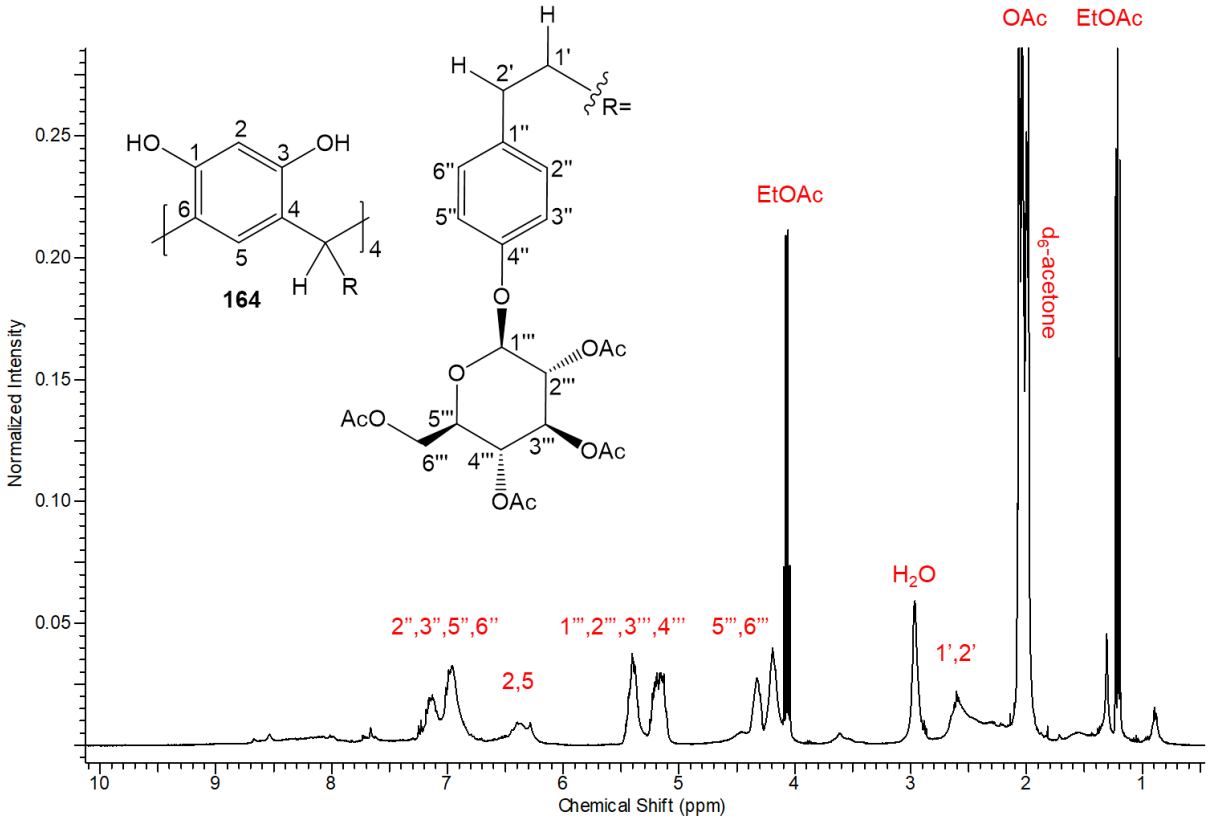

(a)

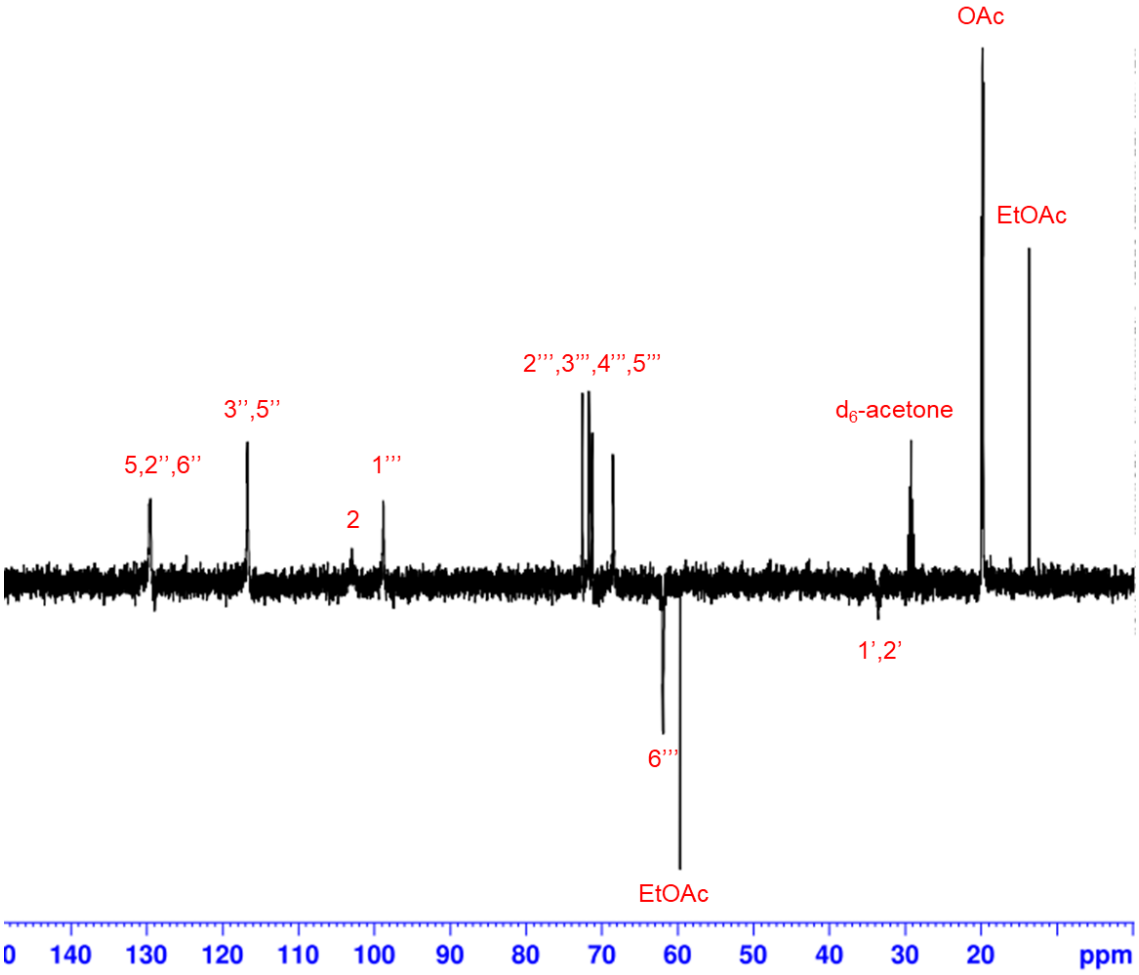

(b)

Figure 57: (a) ^{1}H NMR and (b) DEPT135 spectra of calix[4]resorcinarene glucoside **164** in d_6-acetone

In order to fully characterise the calix[4]resorcinarene obtained from the reaction of glucosylated aldehyde **167** with resorcinol **35d**, the crude mixture of protected tetra(4-glucophenylethyl)calix[4]resorcinarene was reacted with butyric anhydride in pyridine in a similar manner to that described for butyration of **145**. The crude reaction mixture was separated by means of silica column chromatography employing EtOAc: Pet. ether (2:1) as eluent which afforded the principal product as an off-white powder in a low yield of 12%.

The molecular structure of this derivative was confirmed by ^{1}H, ^{13}C NMR, DEPT135, 2D-NMR spectroscopy experiments and mass spectrometry. The ^{1}H NMR spectrum of **196** showed multiplet signals at 2.37-2.67 ppm for ethyl chain protons though these overlapped with signals characteristic of the acyl protecting groups. The signal at 4.23 ppm was attributed to the methine protons at the calix[4]resorcinarene bridges. In the aromatic region, the 2- and 5-protons of the tetrasubstituted resorcinol units appeared at 6.46-7.20 ppm and were overlapped with the aromatic ring hydrogens of the glucosylated phenyl residues. In order to emphasise the above assignments, the carbon signals in ^{13}C NMR spectrum were assigned using 1D- and 2D-NMR techniques, including DEPT135 and HSQCDEPT. The ^{13}C NMR spectrum showed a weak signal at 32.6 ppm, this signal showed correlation with the ethyl chain attached to the lower rim in the ^{13}C DEPT-^{1}H HSQC. While signals could be clearly assigned to the methine groups or the 2- and 5- protons of the tetrasubstituted resorcinol units in ^{13}C NMR, two weak signals were assigned in DEPT135 at 117.7 and 127.8 ppm as being due to calix[4]resorcinarene protons, and the protons at the methine bridges were observed in the ^{13}C DEPT-^{1}H HSQC correlation spectrum (Figure 58). The structure of the final compound is also supported by mass spectrometry analysis. The spectrum gave molecular ion at *m*/*z* 2872.0863 that corresponds to the mass of the desired calix[4]resorcinarene bound to one sodium ion $(M+Na)^{+}$. (Expected: *m*/*z* 2872.0822) (Appendix 14).

It is worth noting, that the signal for the methine hydrogens at the calix[4]resorcinarene bridges appeared as multiplet in the ^{1}H NMR amongst the characteristic resonances related to the protons attached to the glucose moieties, which hence affected on their resolution. However, overall, these

results gave us an indication that the calix[4]resorcinarene glycocluster obtained had an *rccc* conformation. These results also showed the important role played by the butyl group.

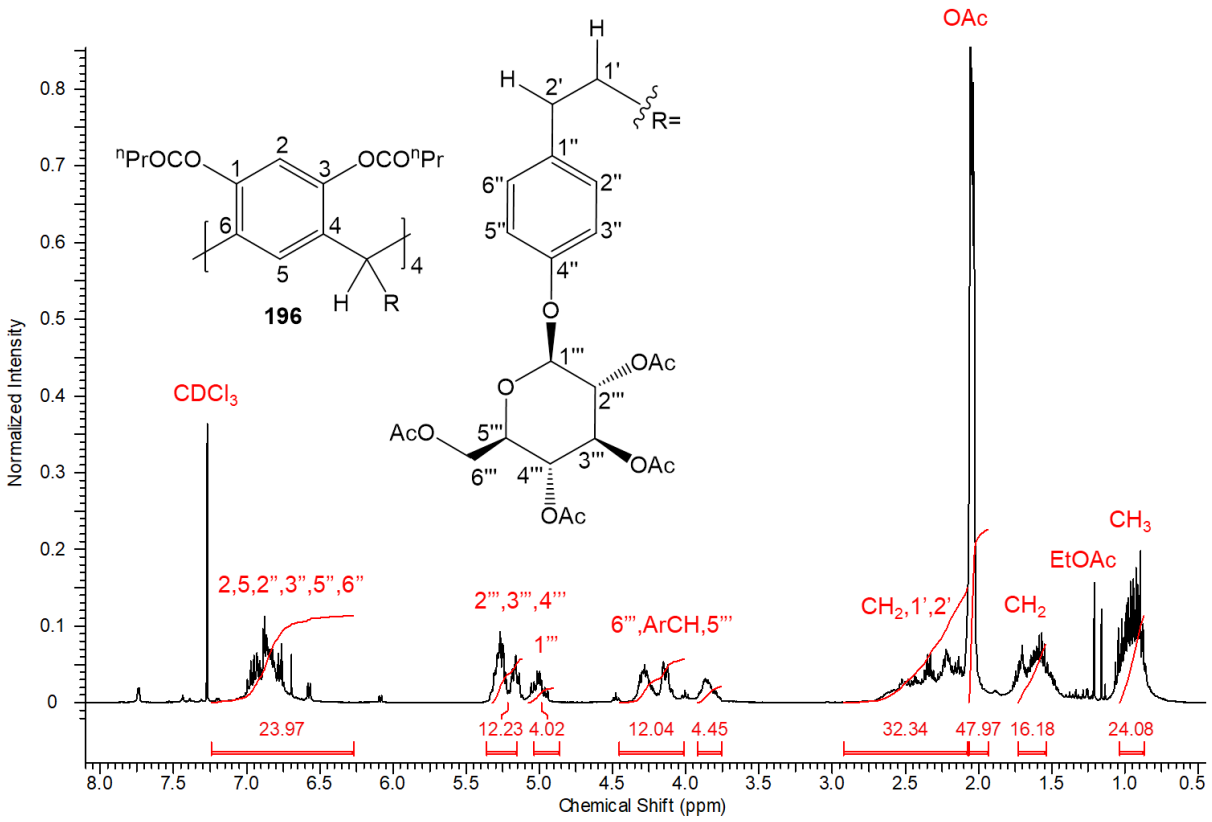

(a)

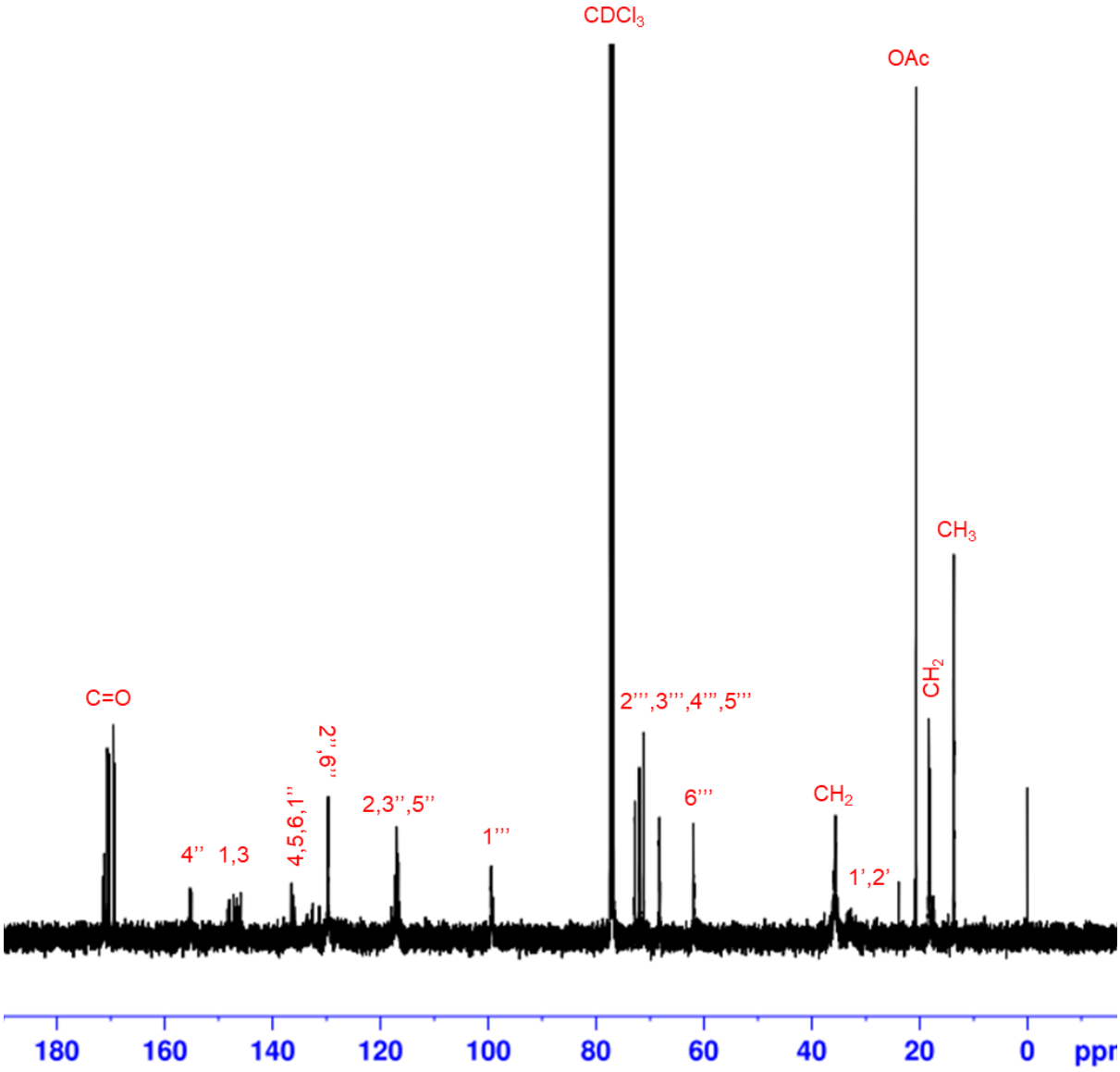
CDCl3
OAc
CH3
CH2
C=O
2''',3''',4''',5'''
2'',6''
4,5,6,1''
2,3'',5''
1'''
6'''
CH2
4'' 1,3
1',2'
180
160
140
120
100
80
60
40
20
0
ppr

(b)

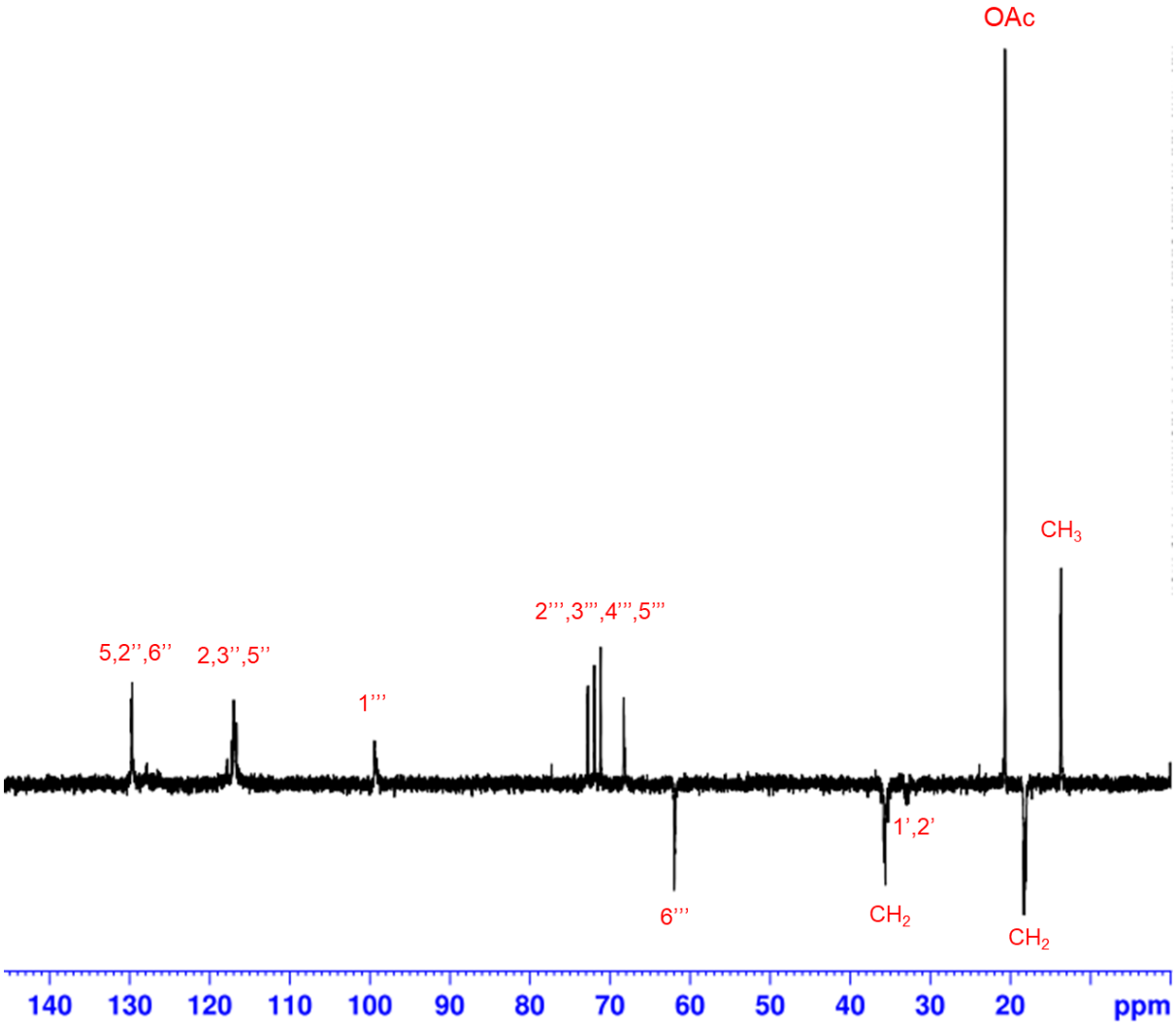
OAc
CH3
2''',3''',4''',5'''
5,2'',6''
2,3'',5''
1'''
1',2'
6'''
CH2
CH2
140
130
120
110
100
90
80
70
60
50
40
30
20
ppm

(c)

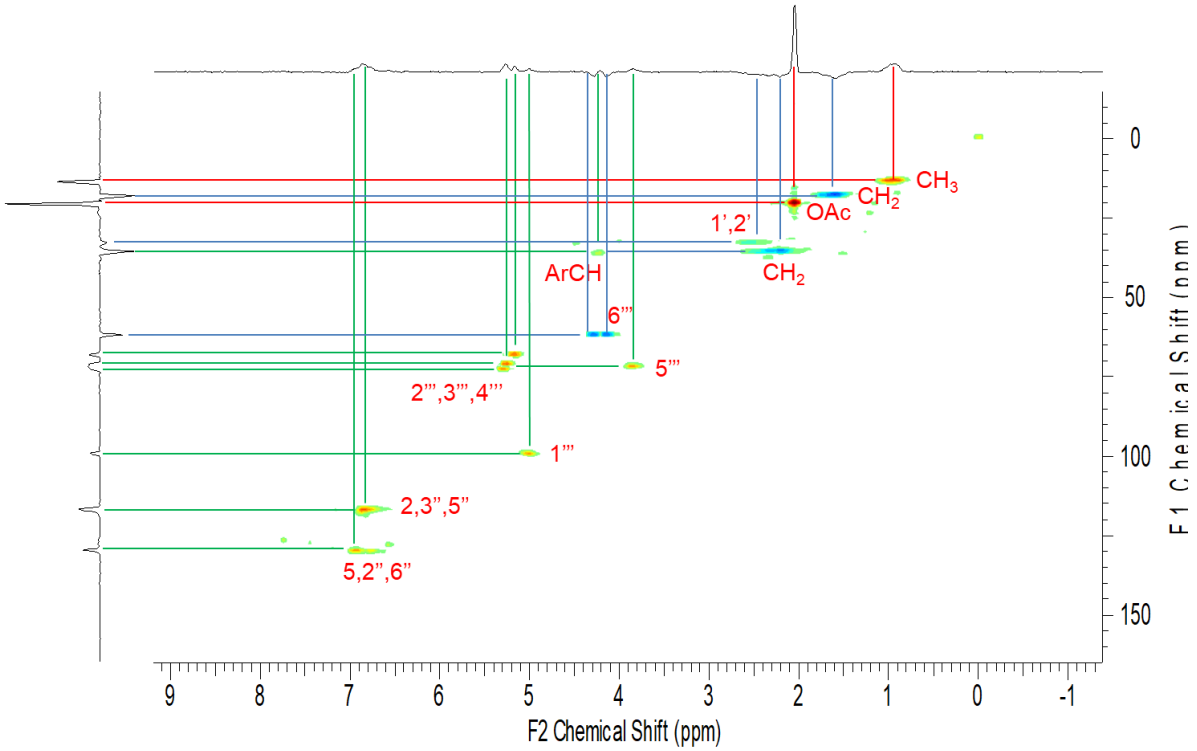

(d)

Figure 58: (a) ^{1}H NMR, (b) ^{13}C NMR, (c) DEPT135 and (d) HSQCDEPT spectra of tetra(4-glucophenylethyl)calix[4]resorcinarene octabutyrate **196** in $CDCl_3$

4.6 Conclusion

The results reported here highlight a route to prepare calix[4]resorcinarene glucoside with an alkyl chain at the lower rim, and derivative with eight functional groups on the upper rim, key for delivery of highly functionalised calix[4]resorcinarene. We demonstrated that anhydrous $AlCl_3$ is an efficient catalyst for the reaction of resorcinol with glucose-4-phenylpropionaldehyde and the convenient reaction procedure led to formation of calix[4]resorcinarene glucoside **164**. The condensation reaction under these conditions selectivity produced the *rccc* configuration and the macrocyclic ring is expected to adopt the crown conformer as observed by ^{1}H NMR, ^{13}C NMR and 2D-NMR analysis. We also noticed that aluminium(III) chloride powder is a more efficient catalyst

for the preparation of calix[4]resorcinarene glucoside than a solution of $AlCl_3$ in nitrobenzene, simply because it gave us the desired products without complexation or retention of the nitrobenzene as was noted previously.

CHAPTER 5: SYNTHESIS AND CHARACTERISATION OF NOVEL GLUCO-ARYL SUBSTITUTED CALIX[4]METHYLRESORCINARENES AND CALIX[4]PYROGALLOLARENE

5.1 Background

With the aim to synthesise aryl-substituted calix[4]resorcinarenes, the condensation of resorcinol, 2-methylresorcinol and pyrogallol with 4-(1-benzyl-1H-[1,2,3]-triazole-4-ylmethoxy)-benzaldehyde **197** was carried out in chloroform in the presence of trifluoroacetic acid (Scheme 61). It was noticed that the synthetic outcome of this reaction depended on the structure of the substrate resorcinol, for example the reaction of compound **197** with resorcinol afforded calix[4]resorcinarene as the *rccc* isomer **198a** in 53% yield. The condensation of aldehyde **197** with 2-methylresorcinol under the same reaction conditions gave a mixture of *rccc* (cone) **199a** and *rctt* (chair) **199b** isomers, in a 1:2.3 ratio, respectively, with a total yield of 66%. Only the *rccc* isomer in the crown conformer **200a** was isolated from the reaction of aldehyde **197** with pyrogallol (Knyazeva *et al*., 2018).

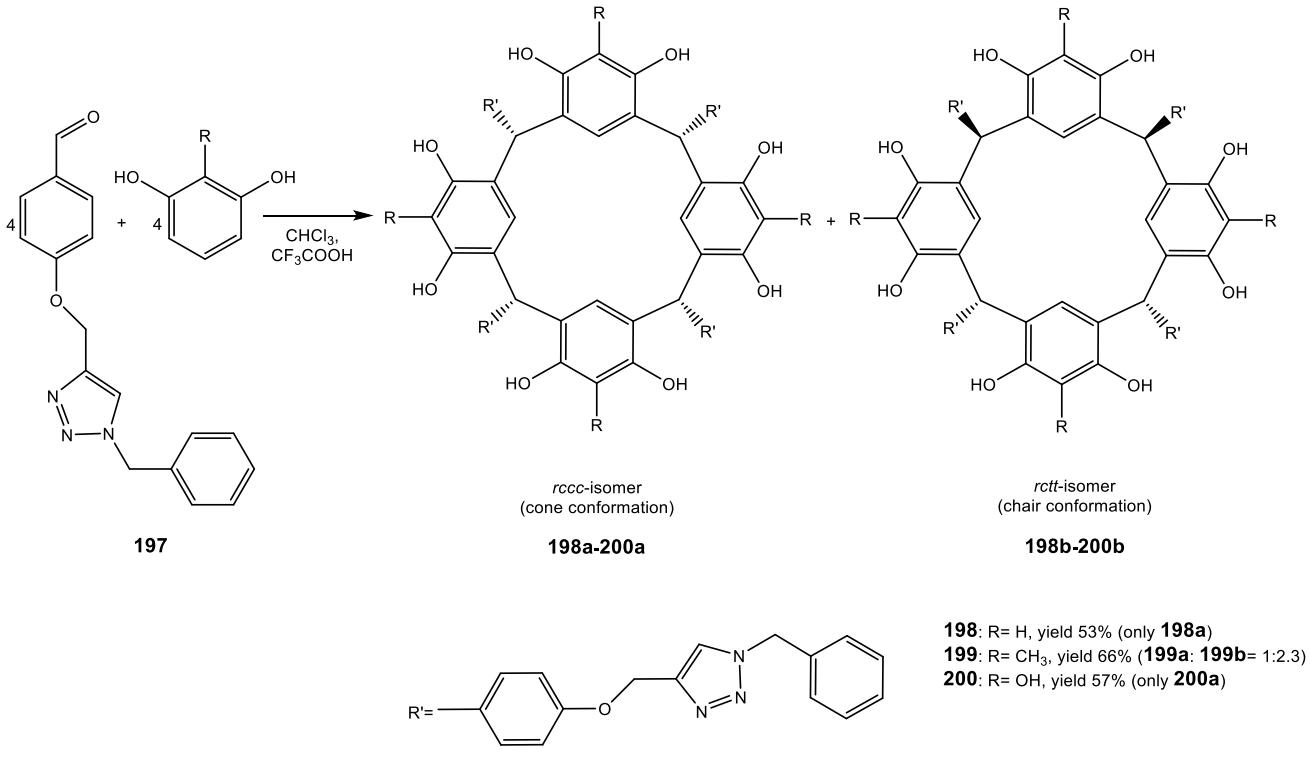

Scheme 61: Synthesis of calix[4]resorcinarenes containing triazole fragments

(Knyazeva *et al*., 2018)

Parulekar and co-workers reported the synthesis of calix[4]methylresorcinarenes by condensation of 2-methylresorcinol **95** with benzaldehyde or 4-bromobenzaldehyde **201** in 1:1 refluxed mixture of ethanol and concentrated aqueous hydrochloric acid. The corresponding calix[4]methylresorcinarenes **202** and **203** as the *rctt* (chair) isomers after characterisation using ^{1}H NMR and mass spectroscopy (Scheme 62) (Parulekar *et al*., 2015).

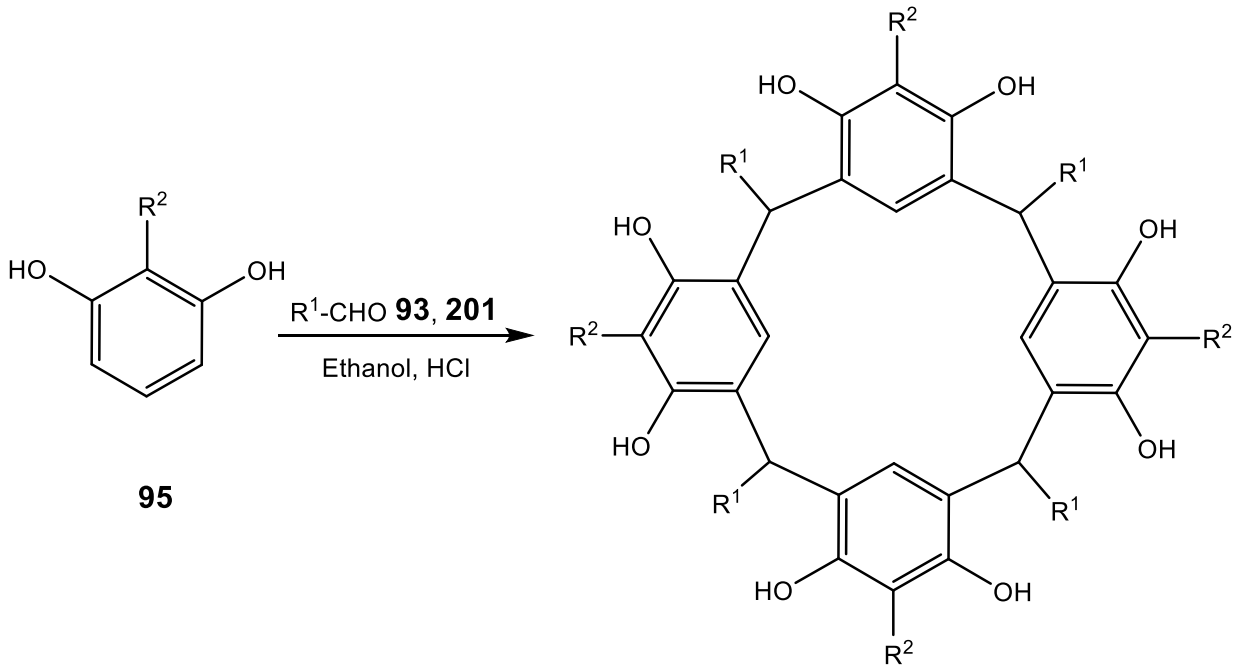

Scheme 62: Synthesis of calix[4]methylresorcinarenes (Parulekar *et al*., 2015)

The first representative of calix[4]resorcinarenes with four thiophosphoryl-containing residues on the lower rim were synthesised by the reaction of thiophosphorylated aldehydes **204** or **205** (thiophosphoryl unit located in 3 or 4 position on the aromatic ring relative to the aldehyde group) with resorcinol, 2-methylresorcinol and pyrogallol in alcoholic acidic media (Scheme 63). The ^{1}H

and ^{13}C NMR spectral data of compounds **206a-c** and **207a-c** were in agreement with the results obtained from single-crystal X-ray diffraction analysis and display double signals of protons and carbon atoms of resorcinol units. This attests to the opposite orientation of two resorcinol rings from other resorcinol groups (vertical and horizontal arrangements). This refers to that the molecules exist in *rctt* isomer (chair conformation) (Knyazeva *et al*., 2011).

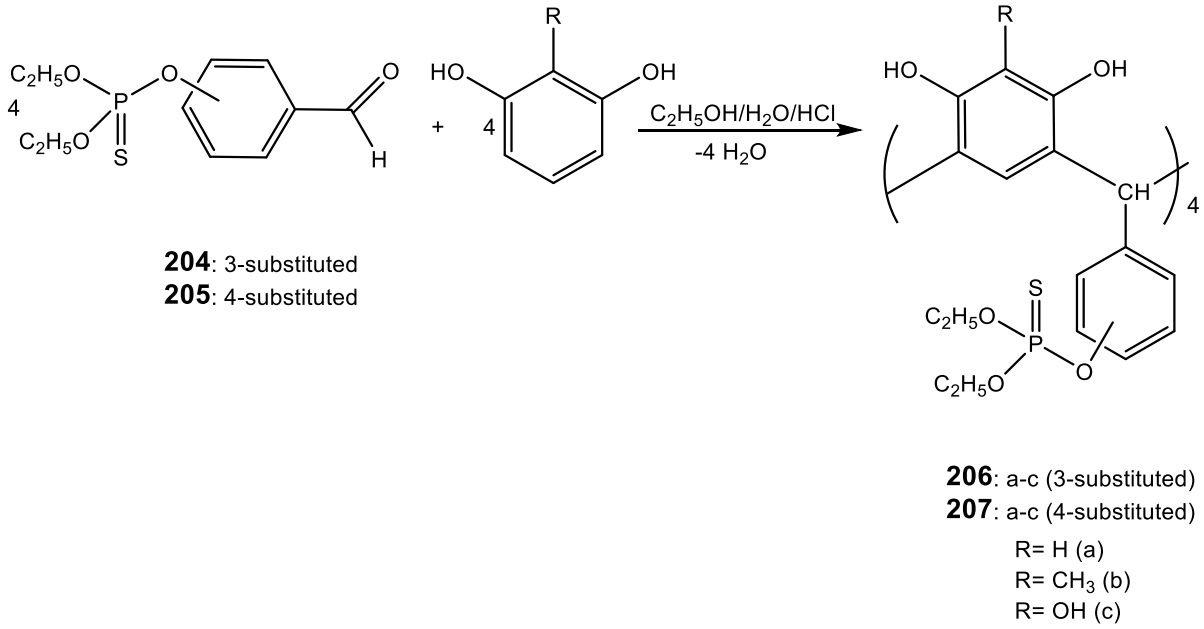

Scheme 63: Synthesis of calix[4]resorcinarenes bearing thiophosphorylated fragments on the lower rim (Knyazeva *et al*., 2011)

Different findings have been observed by Knyazeva *et al*.: condensation of equimolar quantities of the aldehyde 2-(4-formylphenoxy)-2-thioxa-5,5-dimethyl-1,3,2-dioxaphosphorinane **208** with resorcinol in chloroform and in the presence of trifluoroacetic acid, led to the formation calix[4]resorcinarene **209a** as the *rccc* isomer exclusively in 96% yield (Scheme 64). Reaction of 2-methylresorcinol with aldehyde **208** under the same conditions resulted in the formation of a mixture of *rccc*- and *rctt*-isomers **210a** and **210b** in a 5:1 ratio in a total yield of 89%. Finally, an analogous reaction of pyrogallol with compound

208, gave also a mixture of *rccc*- and *rctt*-isomers **211a** and **211b**, respectively, in 1:2 ratio and a combined yield of 93%. The effect of the nature of catalysts and solvents utilised on the isomeric ratios of the calix[4]resorcinarenes was also noted. Substitution of the mixture of trifluroacetic acid and chloroform with a mixture of ethanol, water and concentrated HCl gave only the *rctt* isomers of **210b** and **211b** stereoselectivly in moderate yield of 56% (Knyazeva *et al*., 2013).

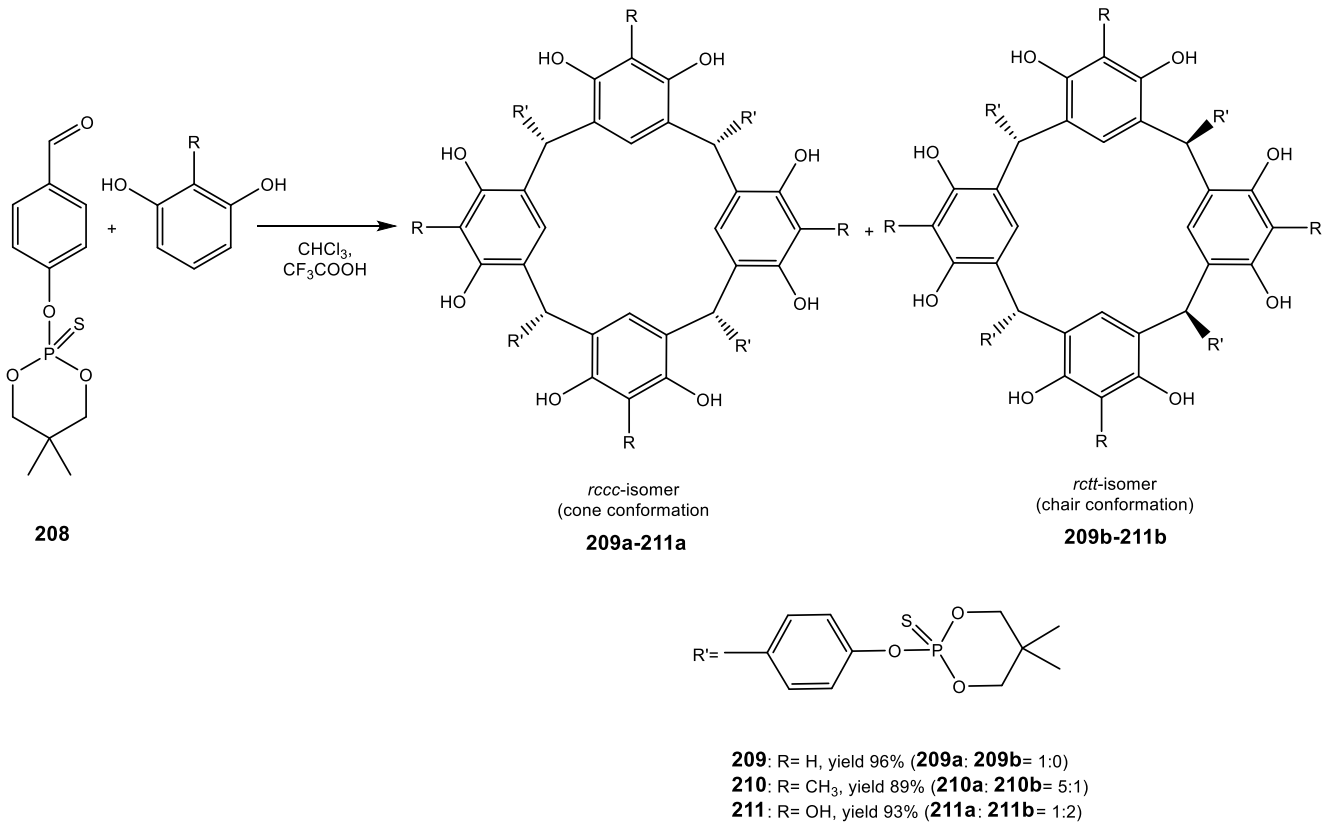

Scheme 64: Synthesis of thiophosphorylated calix[4]resorcinarenes (Knyazeva *et al*., 2013)

C-4-acetamidophenylcalix[4]methylresorcinarene **213** has been synthesised by using one-pot cyclocondensation reaction of 2-methylresorcinol and 4-acetamidobenzaldehyde **212** in refluxing ethanolic concentrated hydrochloric acid afforded calix[4]methylresorcinarene product in 83% yield after refluxing the reaction mixture for 24 h (Scheme 65). It was noted that the X-ray structure was in agreement with the ^{1}H NMR data and the calix[4]methylresorcinarene molecule adopted the chair conformation. It was also noted that the stability of this molecule in the crystalline state was influenced by the C-H…O and O-H…O intermolecular hydrogen-bonding between the hydroxyl groups and also the intermolecular hydrogen-bonding involving DMSO and water molecules with the phenolic moieties of the calix[4]methylresorcinarene molecules (Abosadiya *et al*., 2015).

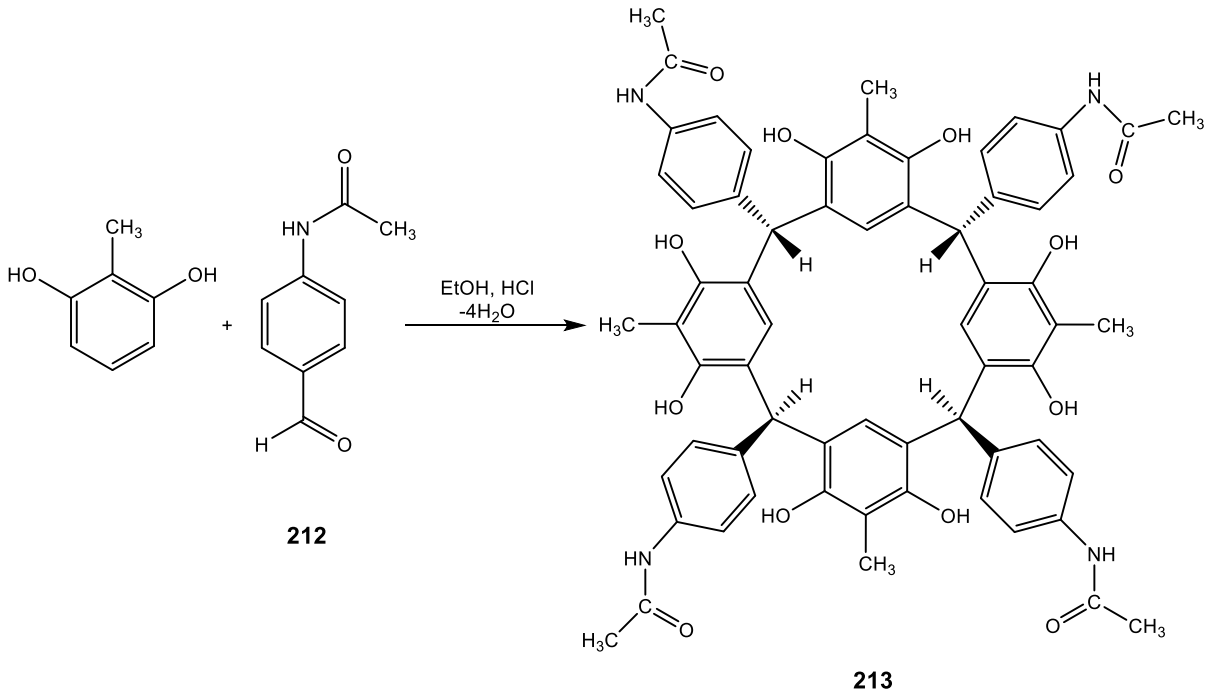

Scheme 65: Synthesis of *C*-4-acetamidophenylcalix[4]methylresorcinarene (Abosadiya *et al*., 2015)

Although various crystalline forms, cocrystals and solvates of calix[4]resorcinarenes and calix[4]pyrogallolarenes are reported, hydrates are uncommon due to low water solubility. Applications of these macrocycles in pharmaceutical and biological systems is also restricted as a consequence of their low water solubility and, hence, poor bioavailability.

Patil *et al*. reported the ethanolic protic-acid-catalysed synthesis of calix[4]pyrogallolarenes with 4-hydroxyphenyl groups attached at the methine bridge groups to improve the solubility of the calix[4]pyrogallolarenes in aqueous media. The crude product was found to contain a mixture of the chair and boat/cone conformers. The purification of the boat/cone conformer was carried out by solvent extraction, and the crystalline hydrate of the boat conformer of 4-hydroxyphenyl calix[4]pyrogallolarene **214** (Figure 59) was obtained by heating this compound in deionized water at 80 ^{0}C, subsequent gradual cooling to r.t. produced single crystals suitable for characterisation by single-crystal X-ray diffraction analysis. It was noted that the hydrate formed 3D arrangements supported by O-H…O hydrogen bonding between water molecules and the phenyl hydroxyl groups of the macrocycle (Patil *et al*., 2018).

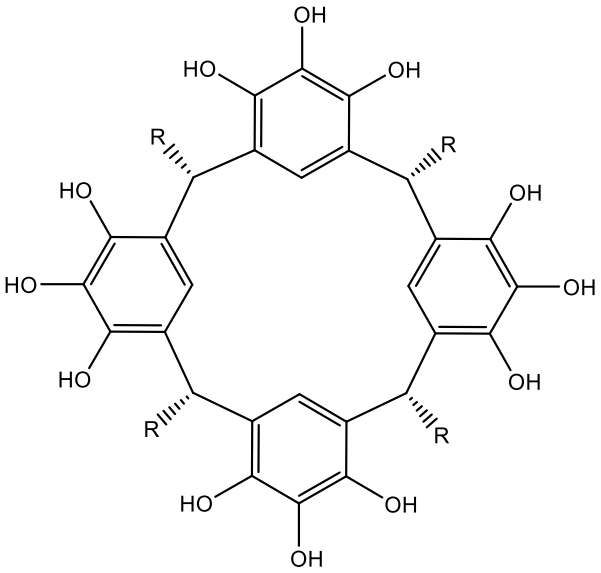

214: R= C_6H_4OH

Figure 59: 4-Hydroxyphenyl calix[4]pyrogallolarene **214**

This chapter describes the formation of calix[4]resorcinarenes with varied groups on the upper and the lower rim of the macrocyclic system as part of our investigation into the formation of calix[4]methylresorcinarenes and calix[4]pyrogallolarenes with different conformations. The predominating conformation and configuration of calix[4]resorcinarenes is determined by many factors, including: the nature of the substituents on the calix[4]resorcinarene framework, functional groups present on the calix[4]resorcinarene and reaction conditions. The conformation of the product calix[4]resorcinarene is one of the essential factors in determining the role of these macrocycles in supramolecular chemistry.

Reinhoudt *et al*. reported the synthesis of substituted calix[4]methylresorcinarenes by condensation of 2-methylresorcinol with various aromatic aldehydes under protic acid-catalysed conditions and found that the chair conformer was formed exclusively in these reactions (Middel *et al*., 1998). Similarly, Cram *et al*. also found that the condensation of benzaldehyde with substituted resorcinol gave calix[4]methylresorcinarene in the chair conformer (>97%), referring to the potential influence of the methyl group on the calix[4]methylresorcinarene conformation (Tunstad *et al*., 1989).

We aimed to explore the synthesis of calix[4]resorcinarenes having an increased number of possible hydrogen-bonding functionalities in order to investigate expanded self-assembled structures and for more understanding the structural conformations of symmetry substituted calix[4]resorcinarenes.

Herein, we present the synthesis and characterisation of novel substituted calix[4]methylresorcinarenes and calix[4]pyrogallolarene containing four glycoside fragments on the lower rim of the macrocycles *via* condensation

resorcinol derivatives like 2-methylresorcinol and pyrogallol with carbohydrates functionalised benzaldehydes (Scheme 66), different conformations of these compounds are also expected, it is therefore expected to increase the study of supramolecular chemistry of the substituted calix[4]methylresorcinarenes and calix[4]pyrogallolarene.

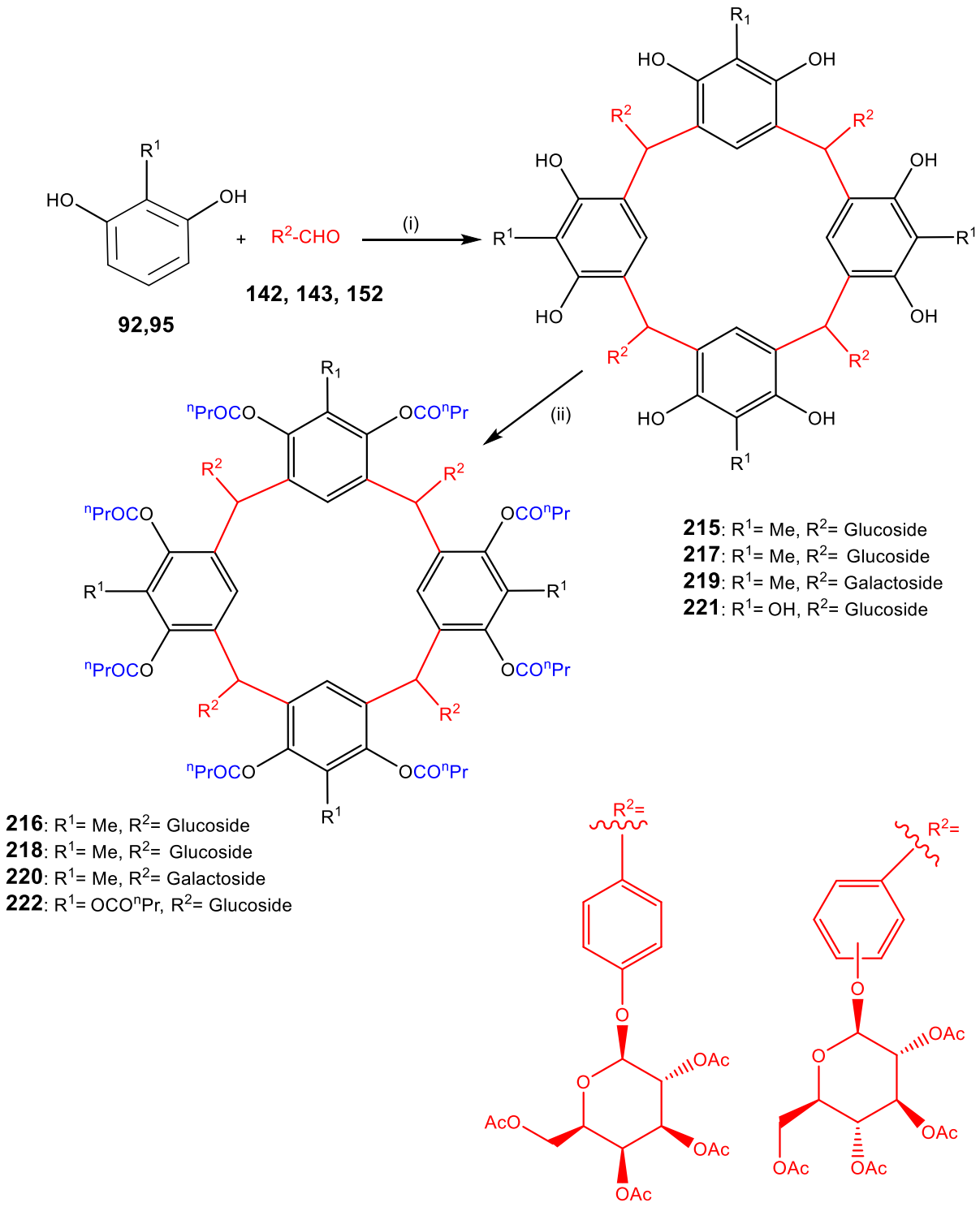

Reagents and conditions: (i) $AlCl_3$ in nitrobenzene, $AlCl_3$ anhyd. or $BF_3.Et_2O$, Et_2O: THF, 48-92 h, r.t (ii) butyric anhydride, pyridine, 80 ^{0}C, 24 h

Scheme 66: Synthesis of glycosylated calix[4]methylresorcinarenes and calix[4]pyrogallolarene

5.2 Synthesis of glycosylated ligand based on the calix[4]methylresorcinarene matrix

In order to design glucosylated calix[4]methylresorcinarene **215** as functionalised partner calix[4]resorcinarene glucoside, we used tetracetoxyglucoside of 4-hydroxybenzaldehyde **142** (page 100, Scheme 34), which was prepared according to a known method (Stavila *et al*., 2008).

The first attempt to synthesise calix[4]methylresorcinarene **215** using $AlCl_3$ in nitrobenzene as catalyst failed to yield the desired product. However, reaction of 2-methylresorcinol and aldehyde **142** in a 1:1 mixture of Et_2O and THF containing 2 eq. of anhydrous aluminium chloride ($AlCl_3$) as Lewis acid catalyst afforded 22% yield of the calix[4]methylresorcinarene **215**.

The conformation of the macrocycle **215** was confirmed according to ^{1}H- and DEPT135 and HSQC NMR, the ^{1}H NMR spectra of the compound in d_6-acetone solution showed mutiplet signals for the lower rim aryl substituents at 6.50-7.13 ppm, the aromatic resorcinol protons appeared in the spectrum as three singlets with chemical shift between 5.70-6.44 ppm, protons assigned to the glucose residues appeared between 5.01-5.53 and 4.13-4.65 ppm, the acetyl protecting groups appeared between 1.86-2.17 ppm. The signals for protons attached to the methyl groups of the resorcinol units were observed at 2.04-2.30 ppm and methine protons appeared as two singlets 5.68 and 5.76 ppm. The DEPT135 spectrum showed significant signals for the methylresorcinol units at 8.6, 8.7 and 8.8 ppm, and the signal for the methine bridges at 43.3 ppm.

In order to make the calix[4]methylresorcinarene product sufficiently soluble in a wide range of polar and a polar organic solvents the eight phenolic hydroxyl

groups were acylated. Butyration of the crude product was performed by treatment of **215** with butyric anhydride in the presence of pyridine for 24 h at 80 ^{0}C. TLC analysis of the resulting reaction mixture contained many spots which could correspond to the desired compound, though this could also have indicated decomposition of the product at this temperature or due to uncompleted cyclisation. Purification by silica gel column chromatography using EtOAc: Pet. ether (1.5:1) as eluent afforded the crystalline product **216** in 24 yield %.

The major acylation product **216**, was identified by ^{1}H NMR and ^{13}C NMR spectroscopy experiments, the protons of the aromatic substituent are represented by two sets of signals, two doublets are not well resolved at 6.62 ppm with integrated intensity 16 H. The signals for methyl group protons and the aromatic protons at 5- position of resorcinol residues. They give three sets of signals each, the signals of methyl groups at 1.72 (3H), 1.81 (3H) and 1.85 (6H) ppm and the expected three signals for resorcinol units protons at 5.80 (1H), 6.1 (2H) and 6.76 (1H) ppm. While, featuring signals for the methine protons, we were unable to determine them precisely, as a result of their chemical shifts in the range of glucose fragments. In the ^{13}C NMR spectrum methine bridge carbons showed a weak signal at 44.3 ppm (Figure 60). The structure of **216** is also supported by mass spectrometry analysis. The spectrum gave molecular ion at *m*/*z* 1414.5493 that corresponds to $(M+2NH_4)^{2+}$. (Expected: *m*/*z* 1414.5493) (Appendix 15).

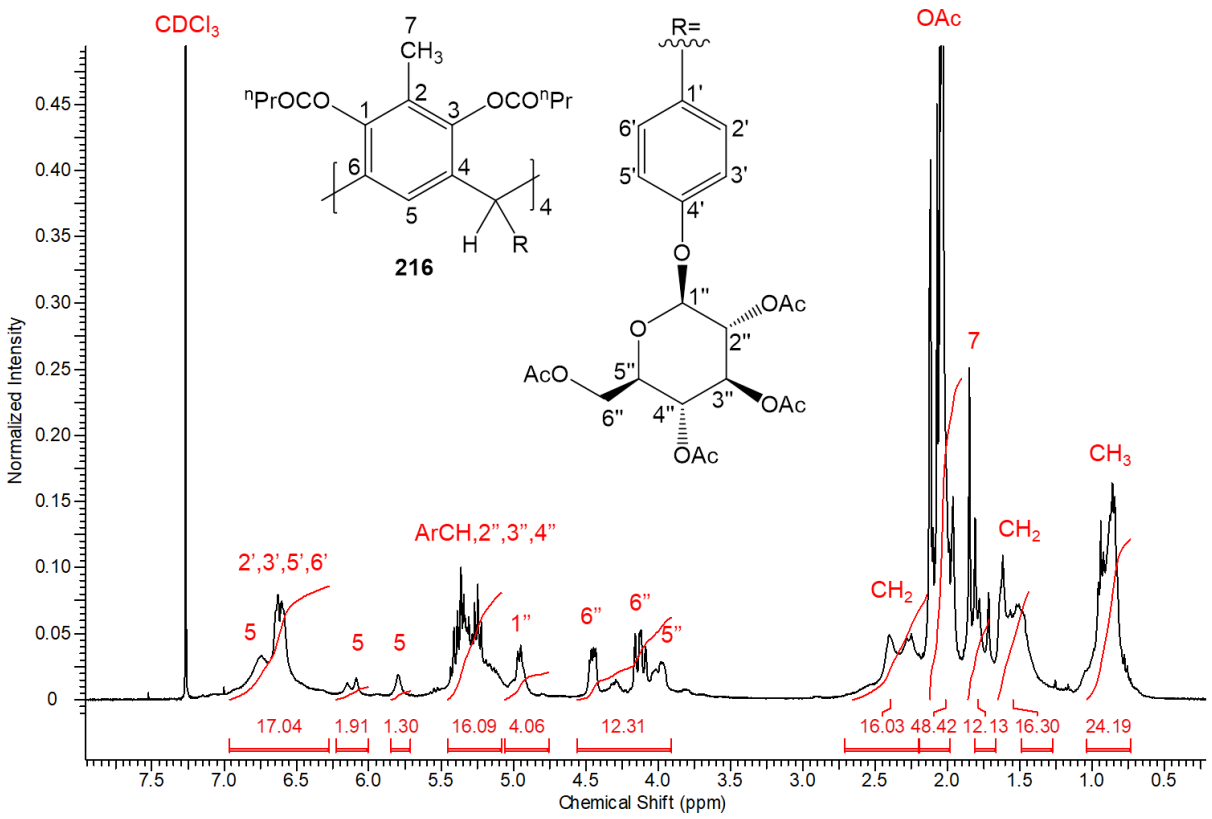
CDCl3
7
CH3
nPrOCO
OCOnPr
R=
OAc
216
AcO
OAc
2',3',5',6'
ArCH,2",3",4"
CH2
CH2
CH3
7
Normalized Intensity
Chemical Shift (ppm)
17.04
1.91
1.30
16.09
4.06
12.31
16.03
48.42
12.13
16.30
24.19

(a)

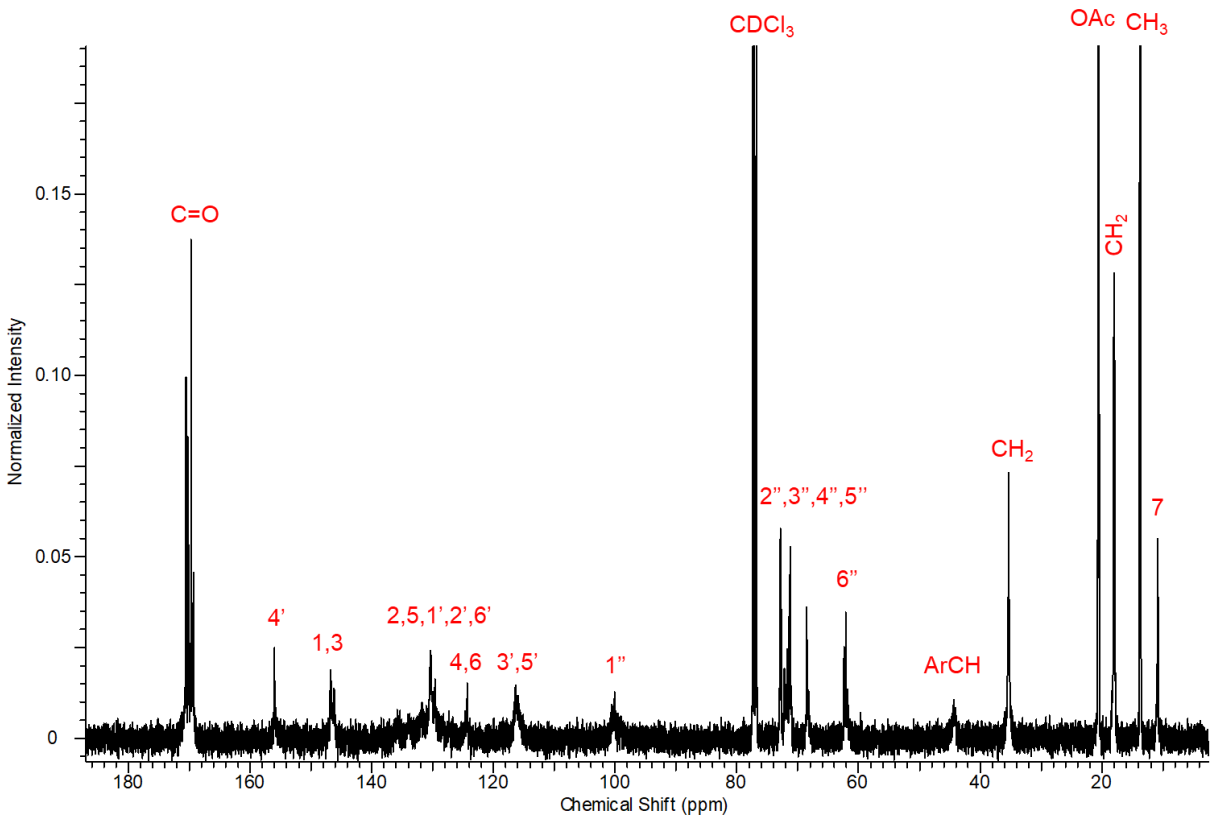

(b)

Figure 60: (a) ^{1}H NMR and (b) ^{13}C NMR spectra of tetra(4-glucophenyl)calix[4]methylresorcinarene octabutyrate **216** in $CDCl_3$

Similarly, condensation of equimolar amounts of 3-glucosylated benzaldehyde **143** (page 100, Scheme 34) with 2-methylresorcinol under similar conditions to those used for the 4-substituted counterpart resulted in the formation of novel glucosylated calix[4]methylresorcinarene **217** in 19% yield after stirring for 92 h under nitrogen and subsequent purification.

Characterisation of compound **217** was predominantly achieved by means of ^{1}H, ^{13}C and HSQC NMR spectroscopy experiments. In d_6-acetone solution the ^{1}H NMR spectrum of compound **217**, contained multiplet signals for the protons of the aromatic and resorcinol fragments at chemical shift 6.14-7.26 ppm, three signals appeared at 5.63-5.75 ppm related to the protons at the methine

bridges. The signals between 4.93-5.50 ppm and 4.02-4.41 ppm were assigned to the protons at glucose units; in addition, to the acetyl protecting groups were observed at 1.83-2.10 ppm. Finally, the assignment of signals for the methyl groups of resorcinol rings in the macrocycle system was done with the HSQC spectrum. In the HSQC spectrum, the signals at 8.3, 8.7 and 8.8 ppm showed a correlation with the methyl protons 2.03-2.28 ppm and confirm that these signals match with the methyl groups of resorcinol units.

To aid further understanding of the nature of the calix[4]methylresorcinarene product and to determine the expected conformers of compound **217**, butyration of the crude mixture **217** was undertaken using similar conditions to those descried previously for the butyration of analogous calix[4]resorcinarenes. The acylated product **218** possessed an enhanced solubility in non-polar organic solvents and analysis of the product by TLC revealed a complex mixture. The mixture was purified using silica gel column chromatographed using EtOAc: Pet. ether (1.5:1) as eluent to give calix[4]methylresorcinarene **218**.

The analytical data from ^{1}H, ^{13}C, and HSQC NMR spectroscopy experiments confirmed the proposed structure. Unexpected broad peaks were noticed in the ^{1}H NMR spectra in $CDCl_3$. The ^{13}C NMR spectrum in $CDCl_3$ showed signals for the ester groups, methyl groups of resorcinol units and for the aromatic system, which agree with structure of compound **218**, and assignments were unambiguously established through 2D-NMR (HSQC). However, a weak signal was observed for the bridging methine with no correlation in the HSQC spectrum, and also a weak signal at 124.6 ppm showed correlation with aromatic protons is expected it is for resorcinol protons at 5-position (Figure

61). The structure of **218** is also supported by mass spectrometry analysis. The spectrum gave molecular ion at *m*/*z* 1414.5499 that corresponds to $(M+2NH_4)^{2+}$. (Expected: *m*/*z* 1414.5493) (Appendix 16).

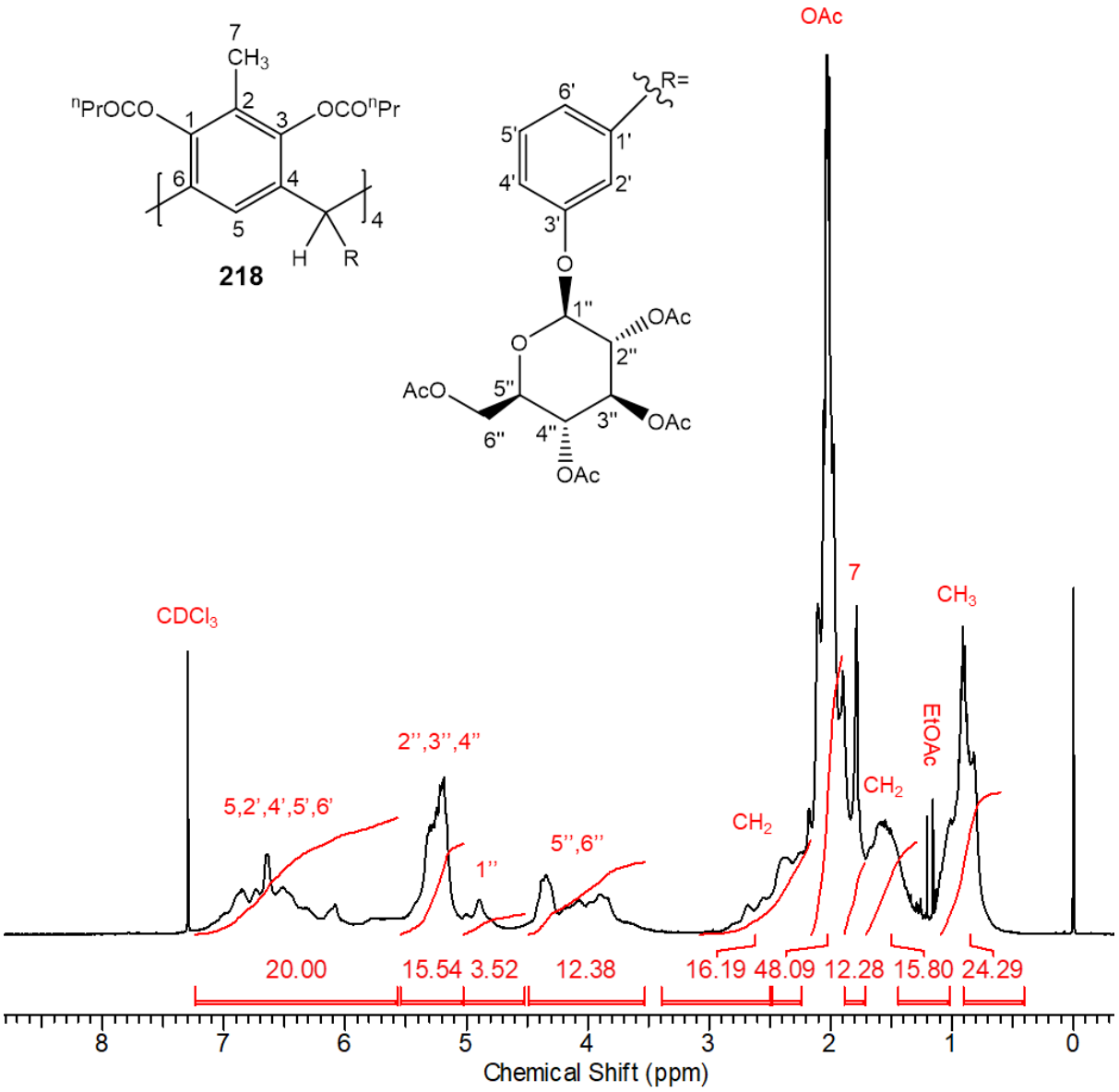

(a)

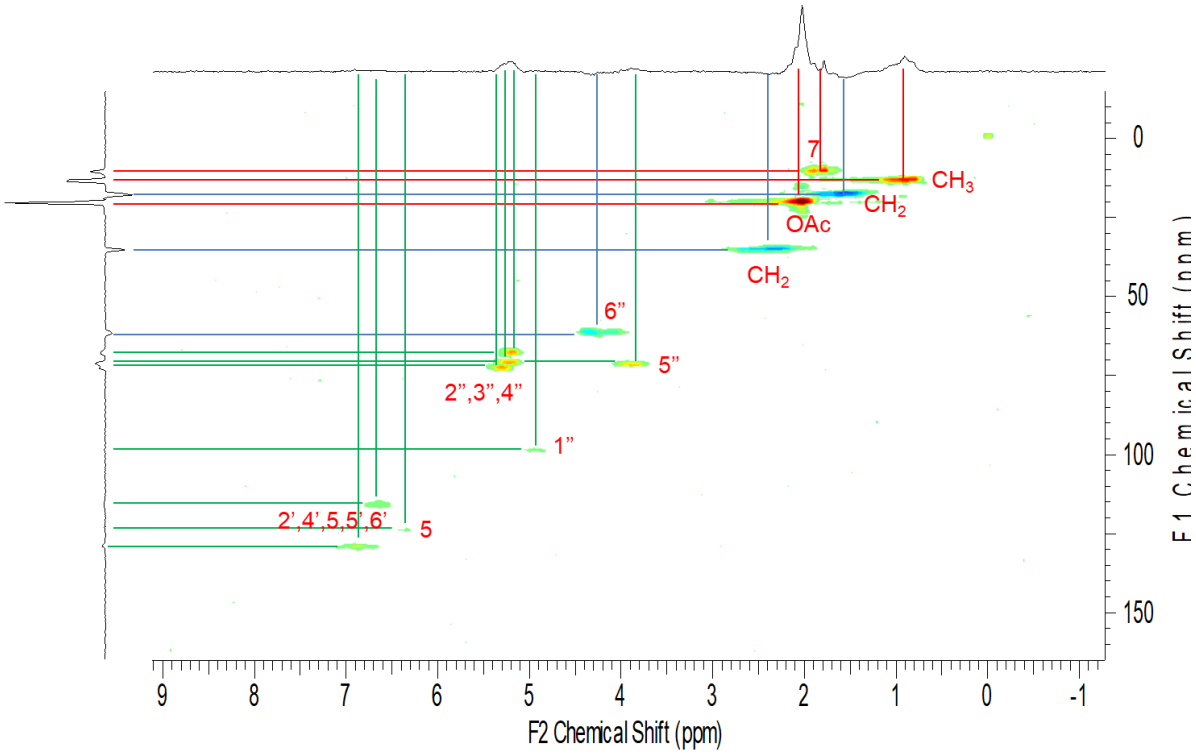

(b)

Figure 61: (a) ^{1}H NMR and (b) HSQCDEPT spectra of tetra(3-glucophenyl)calix[4]methylresorcinarene octabutyrate **218** in $CDCl_3$

The aldehyde **152** (page 125, Scheme 38) which possesses a galactose residue was also included in this study in order to demonstrate that other monosaccharides can be attached to the lower rim using this present strategy. Condensation of aldehyde **152** with 2-methylresorcinol was undertaken in dry Et_2O containing 2 eq. of $BF_3.Et_2O$ as Lewis acid catalyst at r.t for 48 h.

Formation of the corresponding calix[4]methylresorcinarene **219** was confirmed by acquiring the ^{1}H NMR spectrum in d_6-acetone: the spectrum showed similar features to data obtained for the analogous calix[4]methylresorcinarene **215** obtained from 4-glucosylated benzaldehyde, with some variations obviously due to the presence of the galactosyl residues. The ^{1}H NMR spectra displayed two resonances for the methine protons at 5.70 and 5.79 ppm and the methine carbon appeared as strong signal at 43.1 ppm in the ^{13}C NMR spectrum. The methyl groups of the tetrasubstitued resorcinol units appeared at 8.8, 8.7 and 8.6 ppm in the ^{13}C NMR.

The octabutyrate of macrocycle **220** was isolated after chromatographic separation using EtOAc: Pet. ether (1.5:1) as eluent. The structure of the product was established by ^{1}H NMR spectroscopy: a single resonance for the aromatic protons appeared as a doublet at 6.65 ppm. Three signals for the methyl substituted resorcinol were present at 1.76, 1.82 and 1.86 ppm. The three broad signals with different integrated intensity at 5.88, 6.13 and 6.76 ppm are expected for the internal aromatic ring protons. The signals for the methine links were present as a weak signal at 44.2 ppm in the ^{13}C NMR (Figure 62). The structure of **220** is also supported by mass spectrometry analysis. The spectrum gave molecular ion at *m*/*z* 1414.5494 that corresponds to $(M+2NH_4)^{2+}$. (Expected: *m*/*z* 1414.5493) (Appendix 17).

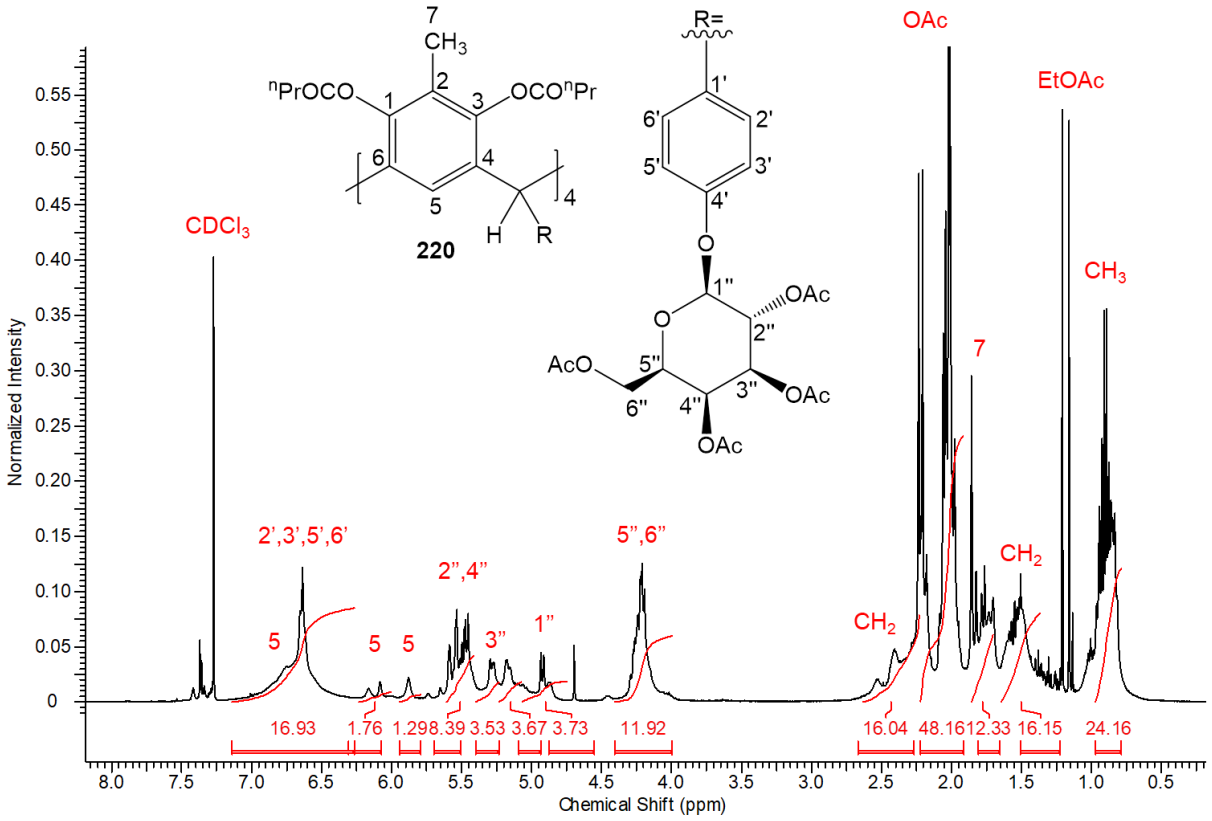
Normalized Intensity
Chemical Shift (ppm)
CDCl3
2',3',5',6'
2",4"
5",6"
1"
3"
CH2
CH3
OAc
EtOAc
7
16.93
1.76
1.29
8.39
3.53
3.67
3.73
11.92
16.04
48.16
12.33
16.15
24.16
220
R=

(a)

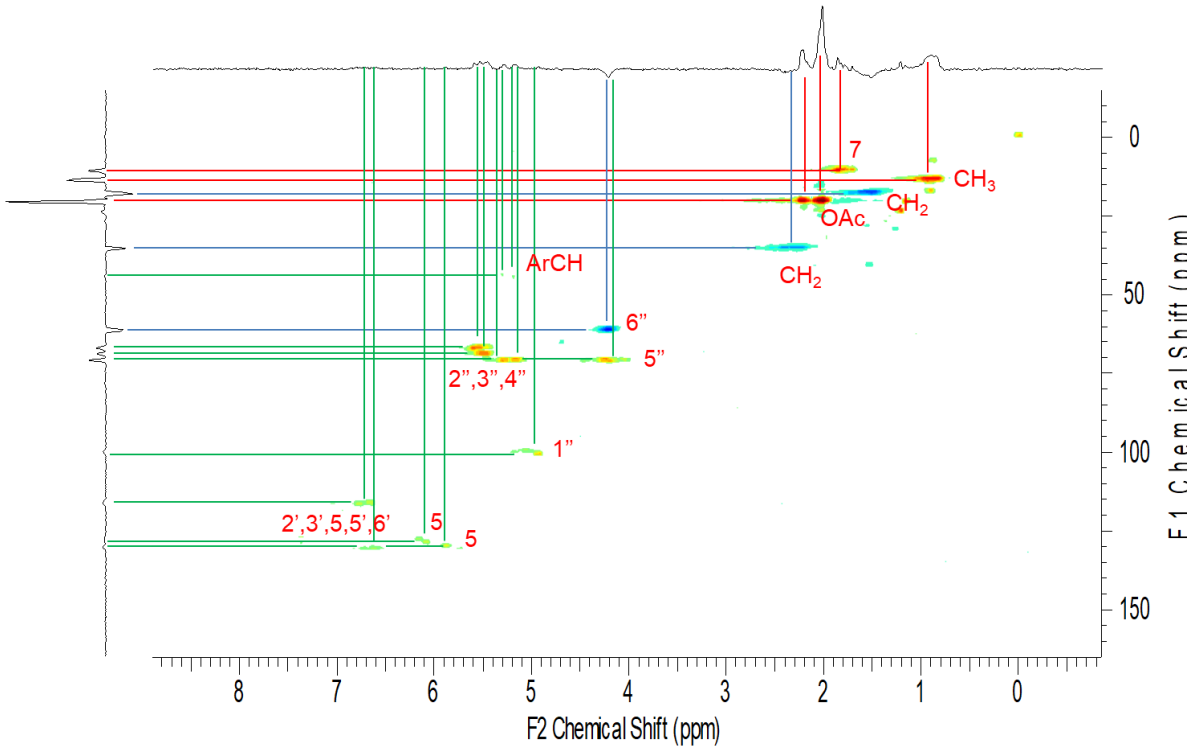

(b)

Figure 62: (a) ^{1}H NMR and (b) HSQCDEPT spectra of tetra(4-galactophenyl)calix[4]methylresorcinarene octabutyrate **220** in $CDCl_3$

5.3 Synthesis of calix[4]pyrogallolarene glucoside 221

In order to further develop the synthesis of calix[4]resorcinarenes that can act as templates for glycocluster formation, the glucosylated calix[4]pyrogallolarene **221** was prepared from the reaction of pyrogallol with tetraacetoxyglucoside of 4-hydroxybenzaldehyde in the presence of a solution of $AlCl_3$ in nitrobenzene under N_2 for 72 h. The general procedure of the reaction is outlined in scheme 63.

The reaction mixture took on a black colour directly after the addition of pyrogallol to the aldehyde-Lewis acid mixture in dry Et_2O/THF. Work-up of the reaction mixture gave compound **221** as a black solid of 16% yield. TLC

analysis of the reaction mixture showed that the starting material was no longer present in the mixture and just an intense spot was observed on the base line. Perhaps because of the 12 hydroxyl groups on the upper rim this aryl calix[4]pyrogallolarene **221** had limited solubility in organic solvents. Hence, it was very difficult to obtain reasonable characterisation data for this compound, despite $CDCl_3$, d_6-acetone and d_6-DMSO as solvents for NMR spectroscopy. The ^1H NMR showed broadened signals for each group of protons. Therefore, it was decided to butyrate the material to facilitate confirmation of the structure.

TLC of the corresponding butyrated calix[4]pyrogallolarene **222** showed an intense black spot on the base line, a very light spot with R_f value 0.41 and lots of contaminants. After subjecting that mixture to column chromatography eluting EtOAc: Pet. ether (2:1) a yellow powder was obtained in a very low yield of 7%. In the ^1H NMR spectrum of **222** a pair of doublets for the methine protons was observed at 5.46 and 5.61 ppm. Protons at the 5 position of the pyrogallol residues resonated as two signals integrating 1:1 at 6.08 and 6.30 ppm, which indicates the presence two matched pairs of pyrogallol residues in the matrix in concordance with C_{2h} symmetry (Figure 63). The structure of **222** is also supported by mass spectrometry analysis. The spectrum gave molecular ion at *m*/*z* 1558.5918 that corresponds to $(M+2NH_4)^{2+}$. (Expected: *m*/*z* 1558.5916) (Appendix 18).

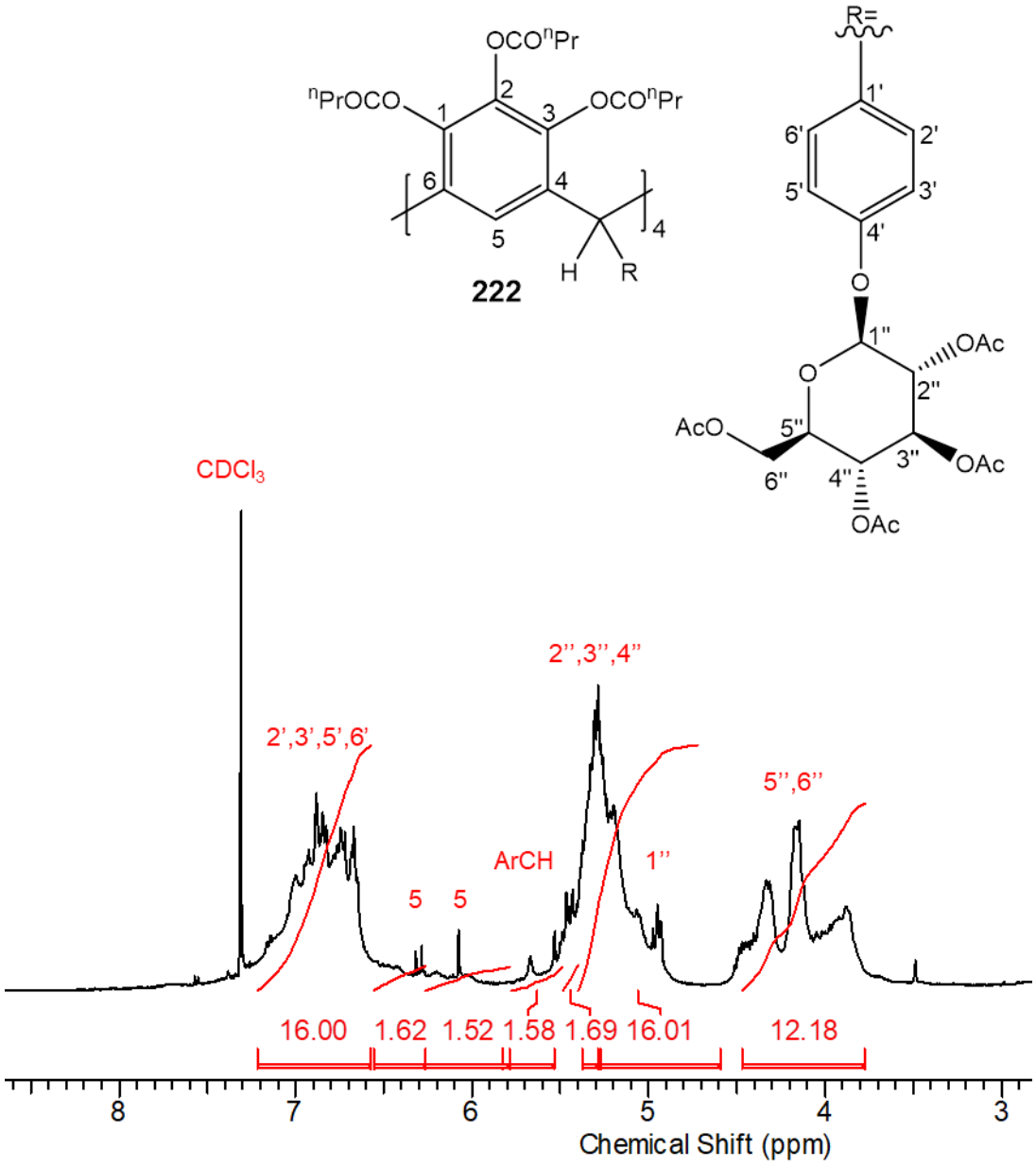
OCO^{n}Pr
^{n}PrOCO
OCO^{n}Pr
1
2
3
4
5
6
H
R
4
222
R=
1'
2'
3'
4'
5'
6'
O
1''
2''
3''
4''
5''
6''
OAc
OAc
OAc
AcO
O
CDCl$_3$
2',3',5',6'
5
5
ArCH
2'',3'',4''
1''
5'',6''
16.00
1.62
1.52
1.58
1.69
16.01
12.18
8
7
6
5
4
3
Chemical Shift (ppm)

(a)

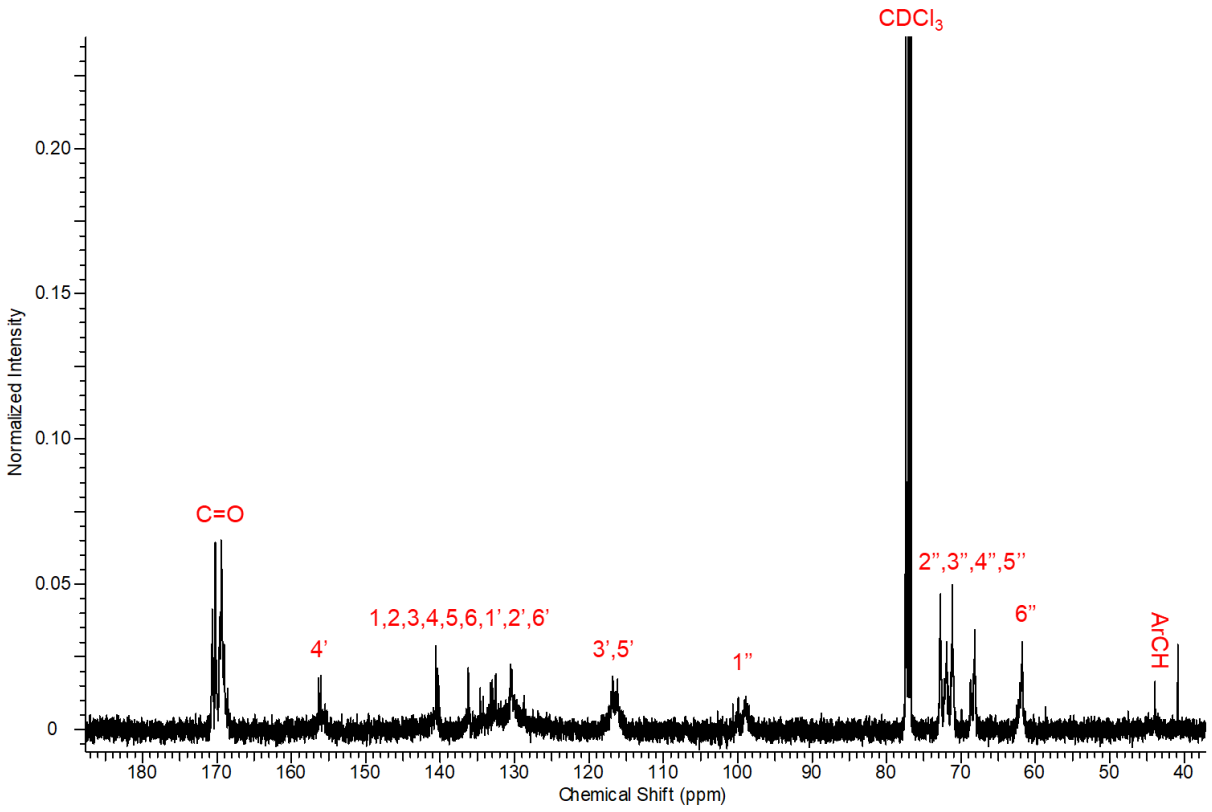

(b)

Figure 63: (a) ^{1}H NMR and (b) ^{13}C NMR spectra of tetra(4-glucophenyl)calix[4]pyrogallolarene octabutyrate **222** in $CDCl_3$

The glucosides derivatived from 3- and 2-hydroxybenzaldehydes **143** and **144** were also reacted with pyrogallol under Lewis acid-catalysed conditions in attempts to make the corresponding cyclic oligomers. Condensation of 3-glucosylated aldehyde **143** (page 100, Scheme 34) with pyrogallol under the same conditions employed for it is 4-substituted counterpart **142** (page 100, Scheme 34) did not yield the corresponding cyclic tetramer. TLC analysis showed starting material and few new products, this was further confirmed by the ^{1}H NMR spectrum. A similar result was obtained on changing the catalyst to anhydrous $AlCl_3$.

Also, no macrocyclisation occurred in the attempted condensation of 2-glucosylated benzaldehyde **144** (page 100, Scheme 34) with pyrogallol using $AlCl_3$ solution in nitrobenzene as catalyst, even after prolonged reaction times. The poor reactivity of both aldehydes **143** and **144** in reaction with pyrogallol may be influenced by the more prevalent steric hindrance associated with these aldehydes, though interaction of the Lewis acid with the additional hydroxyl group on pyrogallol cannot be ruled out since this may have given a stable complex which was also poorly reactive.

In previous experiments we attempted to prepare calix[4]resorcinarenes which possessed disaccharide residues on the lower rim.

In this present study, lactoside and cellobioside derived from 4-hydroxybenzaldehyde **157** (page 139, Scheme 40) and **162** (page 145, Scheme 41) were reacted with 2-methylresorcinol and pyrogallol under Lewis acid catalysis, using similar protocols as had been employed for the reaction of these aldehydes with resorcinol and subsequent butyration of macrocycles **223-226** (Scheme 67).

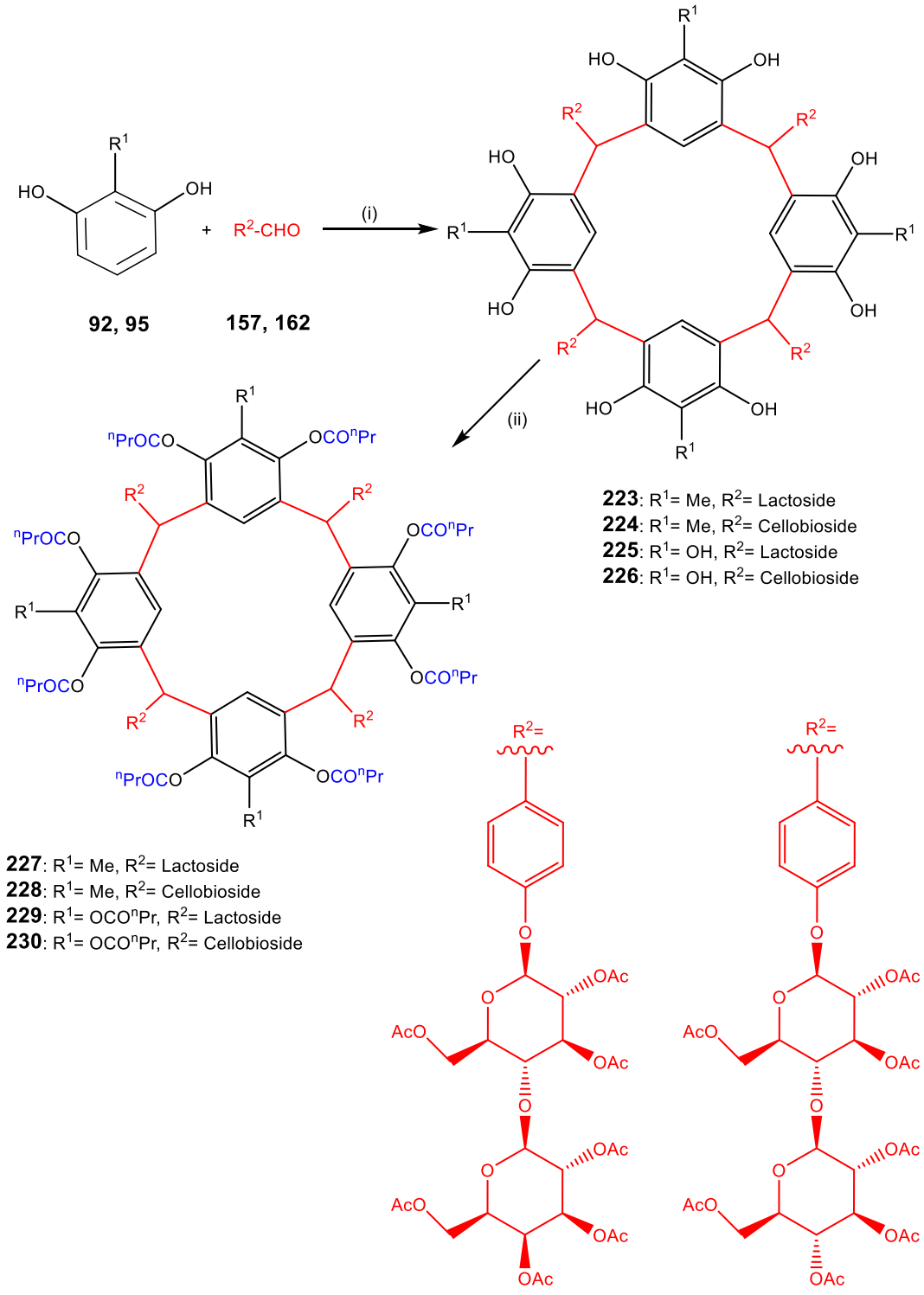

Reagents and conditions: (i) $BF_3.Et_2O$, DCM, 24 h, r.t (ii) butyric anhydride, pyridine, 80 ^{0}C, 24 h

Scheme 67: Synthesis of glycosylated calix[4]methylresorcinarenes and calix[4]pyrogallolarenes

The pattern observed in the ^{1}H NMR data of the acylated calix[4]methylresorcinarene lactoside **227** and calix[4]methylresorcinarene cellobioside **228**, isolated after column chromatography using EtOAc: Pet. ether (gradient ratio) was analogous, both calix structures showed the appearance of single set of signals for the four methyl groups of the resorcinol fragments at chemical shifts of 1.80-1.95 ppm, Weak signals for the protons in the macrocyclic core were observed and were not matched with expected number of protons, as well as, the proton and carbon signals of the methine linkage were absent from ^{1}H NMR and ^{13}C NMR. While two doublet signals of equal integrated intensity belonging to the 4-glycosylated benzene rings appeared at about 6.84-7.00 ppm.

In the ^{1}H NMR spectra of the octabutyrated calix[4]pyrogallolarene lactoside **229**, the aromatic protons of pyrogallol rings were observed at 5.89 and 6.15 ppm, but, the ^{13}C NMR was not well resolved, therefore, we could not use it to assign the signals related to the CH-bridges, these resonances were only assigned using 2D-NMR. Similarly, the ^{1}H NMR spectra of the calix[4]pyrogallolarene-based cellobiosyl benzaldehyde **230**, revealed unclean signals of the protons at 5-position of pyrogallol units and for the methine protons, In the ^{13}C NMR spectrum, also these resonances were not observed. A satisfactory mass spectrum could not be obtained for compounds **227**, **228**, **229** and **230** due to the low yields that led to unsuccessful purification.

5.4 Conclusion

The first representative of calix[4]methylresorcinarene and calix[4]pyrogallolarene with four glucose fragments on the aromatic substituents located on the methine bridges of the macrocycles was realised by the condensation of 2-methylresorcinol or pyrogallol with 4-glucosylated benzaldehyde in the presence of Lewis acids.

The suggested synthetic methods are single-step process led to the target compounds and provided single isomer relying on the experimental conditions used.

Modification of calix[4]methylresorcinarene on the lower rim was done by changing either the position of the glucose group or the kind of the carbohydrate included in the aromatic substituents. In this case, the reactivity of 3-glucosylated benzaldehyde or 4-galactosylated benzaldehyde for condensation with 2-methylresorcinol was experienced using two different Lewis acids. While, attempted to vary the nature of glucosylated derivatives of the hydroxybenzaldehydes on the calix[4]pyrogallolarene scaffold did not investigate, despite using different Lewis acids.

Finally, we demonstrated the spectral similarities of the conformational isomer of the acquired **216** and **220**. With 4-substituted benzaldehyde and 2-methylresorcinol, the expected conformational products are either in *ccc*-boat with C_{2v} symmetry or more likely in *rctt*-chair with C_{2h} symmetry, the *ccc*-crown with C_{4v} symmetry is excluded in this case. It is clear to elucidate that methyl or hydroxyl moieties of substituted calix[4]resorcinarenes may lead to structural stereoselectivities.

CHAPTER 6: SYNTHESIS AND CHARACTERISATION OF NOVEL TETRA(GLUCOMETHYL) & TETRA(GLUCOETHYL) CALIX[4]RESORCINARENES

Saccharide derivatives bearing ‘spacers’ able to form neoglycoconjugates have been observed to be beneficial in biological studies, and in the last few years a large number of neoglycoproteins have been synthesised for immunological research (Abronina *et al*., 2018). Several calix[4]resorcinarenes-spacer-carbohydrate conjugates with carbohydrates on the upper rim have been prepared by various approaches, for example by glycosylation of calix[4]resorcinarene-cavitand tetrathiol **124** with glycosyl bromides (page 93, Scheme 31) (Hayashida *et al*., 1999), or by reacting octa-2-hydroxyethoxytetraalkyl calix[4]resorcinarene **60d-f** and **84a-c** (page 68, Scheme 21) with a perbenzoylated glycosyl bromide (Hussain *et al*., 2017).

Following our research into the conformer-selective synthesis of calix[4]resorcinarenes bearing carbohydrate pendants on the lower-rim, we investigated a new strategy for the formation of calix[4]resorcinarene-based glycoclusters. In this strategy, the monosaccharide residues are conjugated with the calix[4]resorcinarene core through different spacer linkages (Scheme 68).

In order to generate the glycosidic spacer linkages, the spacers must contain two functional end groups. The carbohydrate residue can be facilely connected to the spacer molecule using a glucoside donor and the other terminal group can be converted to the necessary carbonyl group for calix[4]resorcinarene synthesis.

In this study, we aimed to expand our tetramerisation strategy to include calix[4]resorcinarene glucosides using aromatic free glucosylated aldehydes. This strategy was expected to deliver single conformational isomers with

selectivity towards the *rccc* cone and which may possess different self-assembling behaviours in water.

Furthermore, it may be possible to introduce other functional groups into the spacer on the bottom rim, a polar polyether for example, which could be expected to influence the aqueous solubility of the supramolecular product.

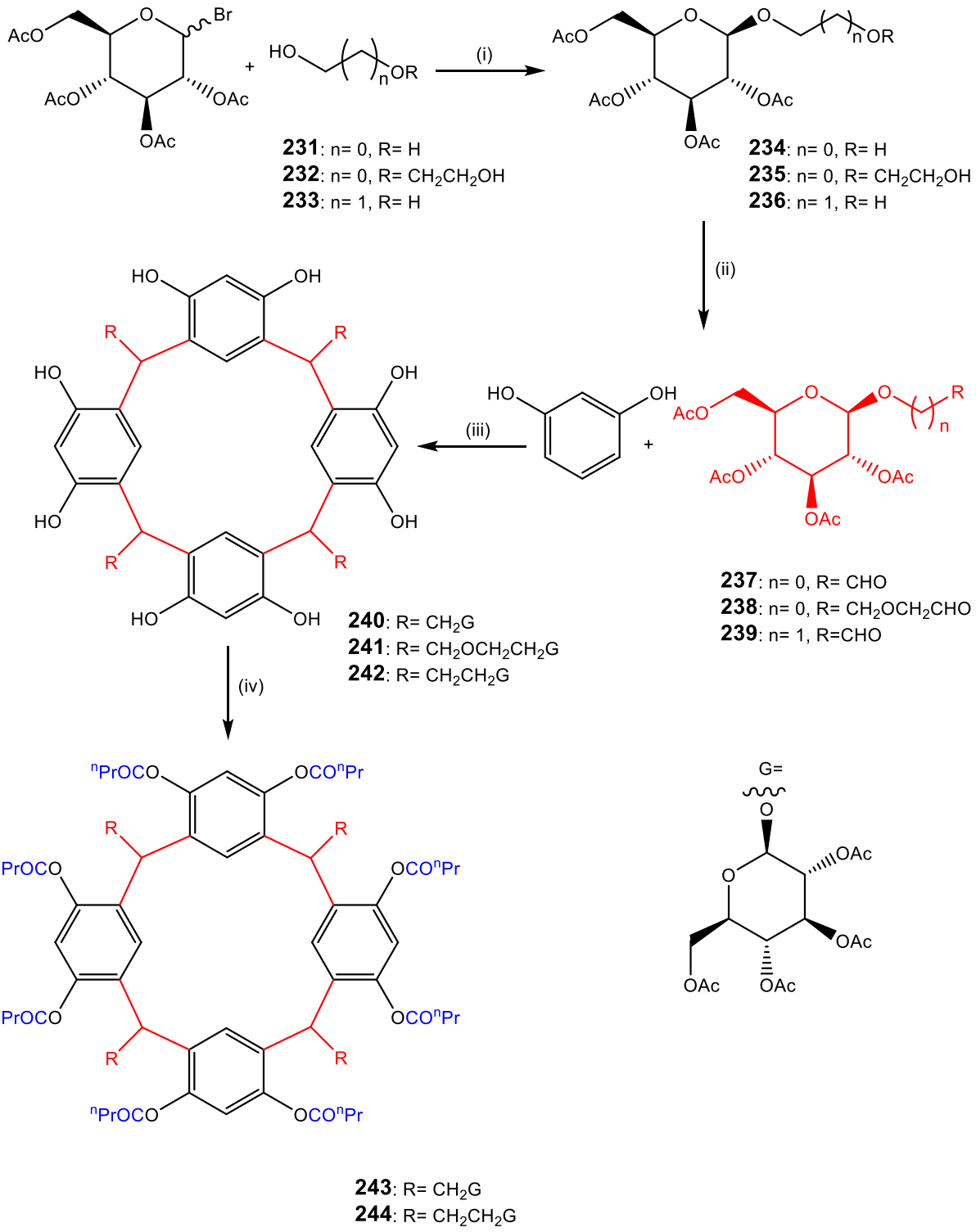

Reagents and conditions: (i) $HgBr_2$, DCM, 24 h (ii) Dess-Martin periodinane, DCM, 3 h r.t. (iii) Et_2O: THF, $BF_3.Et_2O$, 48 h (iv) butyric anhydride, pyridine, 24 h, 80 ^0C

Scheme 68: Synthesis of tetra(glucomethyl) & tetra(glucoethyl)calix[4]resorcinarene octabutyrates

6.1 Synthesis of calix[4]resorcinarene based on glucoside bearing alkyl bridges

The glucosylated calix[4]resorcinarene derivatives **243** and **244** were prepared as described in (Scheme 68). The first step included the synthesis of glucosides **234**, **235** and **236**, obtained by the method of Wang *et al.* from the reaction of the glycosyl donor **138** with ethylene glycol **231**, diethylene glycol **232** and 1, 3-propanediol **233**, respectively, in the presence of mercuric bromide as catalyst in dry dichloromethane under Helferich conditions. The expected glucoside derivatives **234-236**, were isolated in an analytically pure form after chromatography.

Then, each separated anomer was oxidised into an aldehyde using Dess-Martin periodinane oxidation in dry DCM at r.t. The glucosides **237** and **238**, were recovered as white solids following flash column chromatography in acceptable yields 45-63% (Figure 64 and 65). The glucoside **239** was obtained in a high yield of 93% and used without further purification (Figure 66) since the compound decomposed readily upon chromatographic separation.

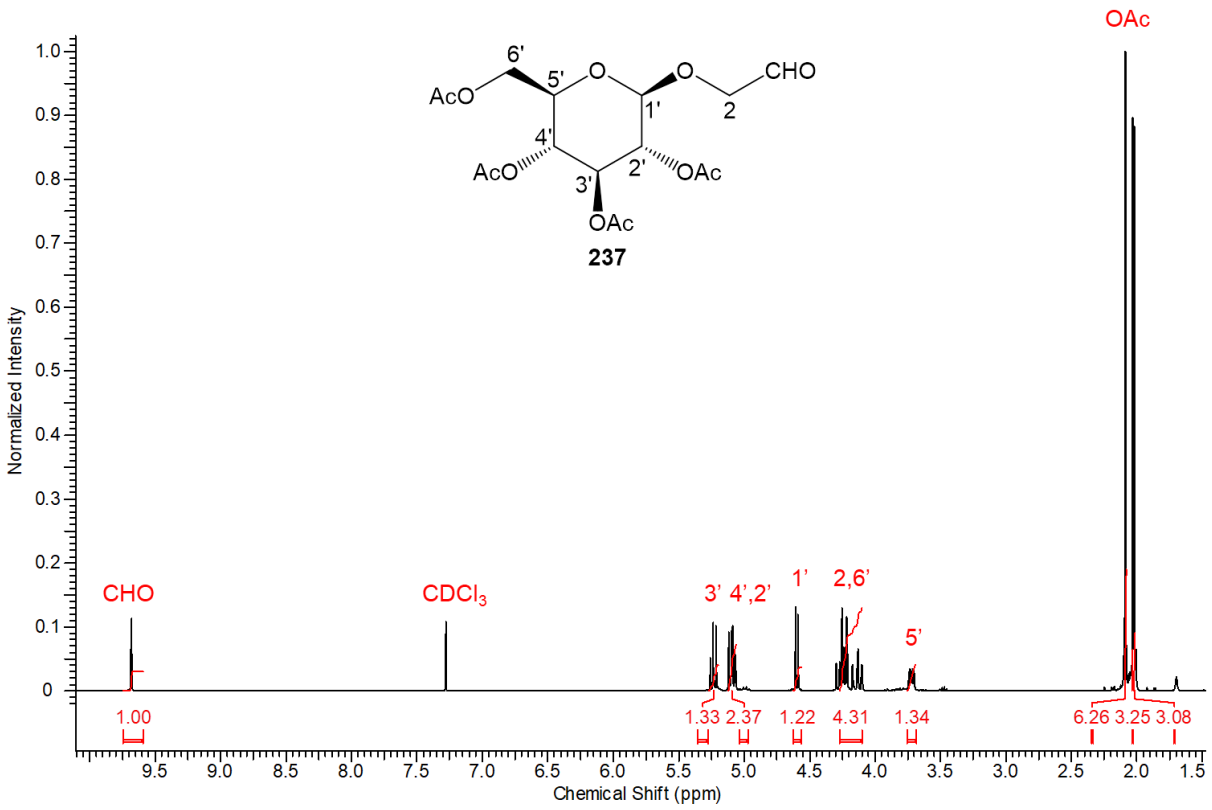

Figure 64: ^{1}H NMR spectrum of 2-oxoethyl(2',3',4',6'-tetra-*O*-acetyl-*β*-D-glucopyranoside) **237** in $CDCl_3$

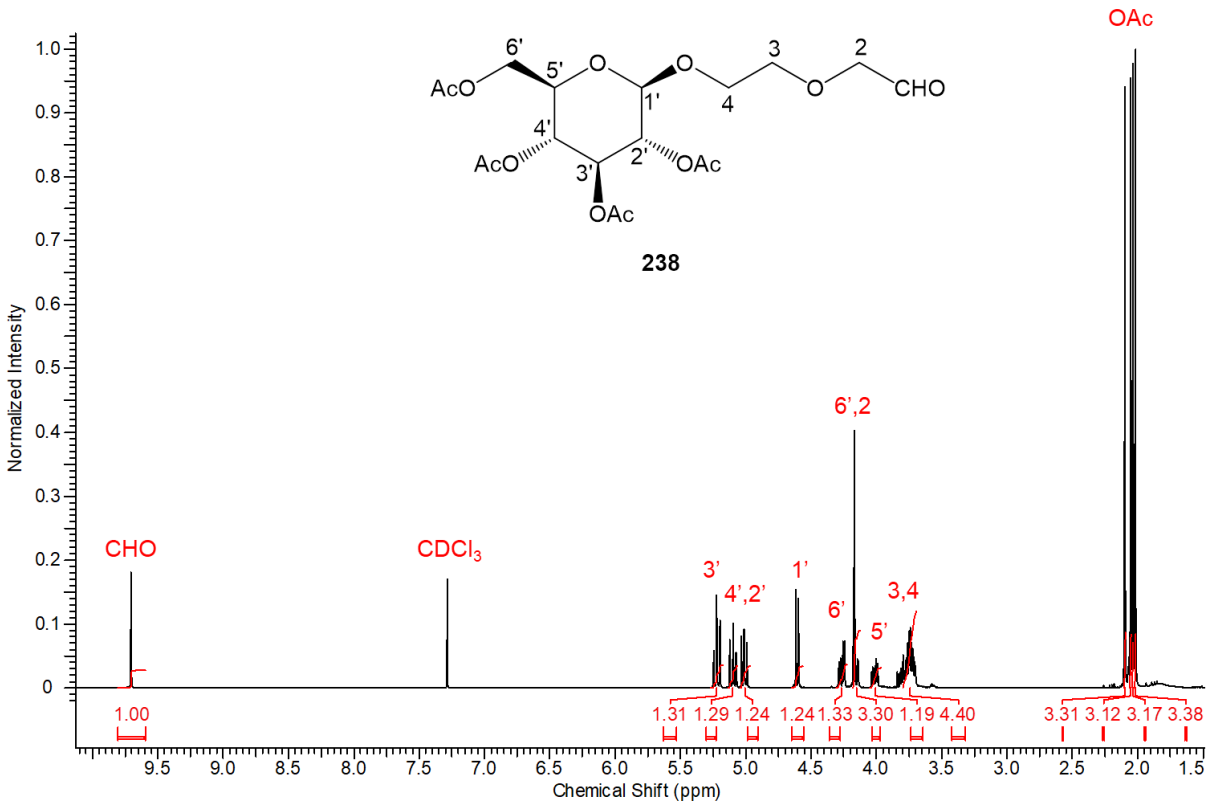

Figure 65: ^{1}H NMR spectrum of 2-((2',3',4',6'-tetra-*O*-acetyl-*β*-D-glucopyranoside)ethoxy)acetaldehyde **238** in $CDCl_3$

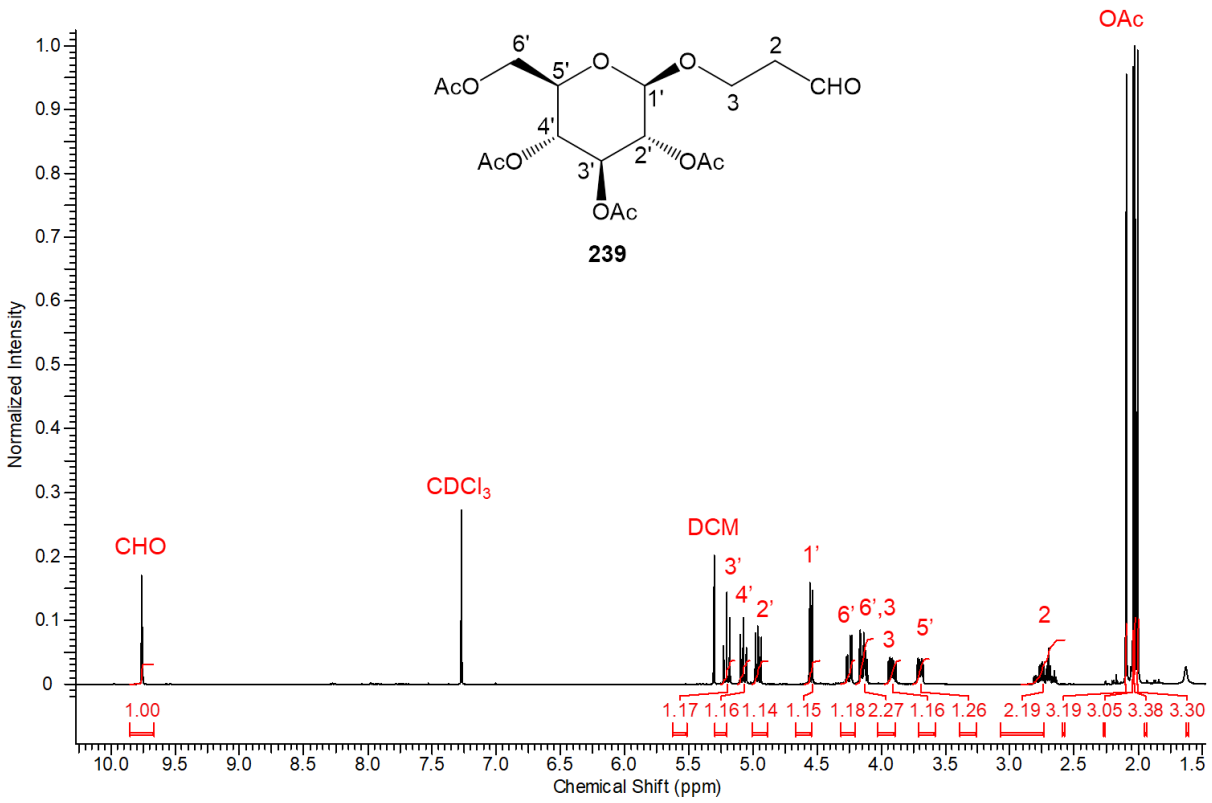

Figure 66: ^{1}H NMR spectrum of 3-oxopropyl(2',3',4',6'-tetra-*O*-acetyl-*β*-D-glucopyranoside) **239** in $CDCl_3$

The synthesis of tetrasubstituted calix[4]resorcinarenes **240-242** was achieved by stirring of the appropriate aldehyde and resorcinol in a mixture of Et_2O: THF under catalysis by $BF_3.Et_2O$ under nitrogen at r.t. for 48 h. Corresponding glycoconjugated calix[4]resorcinarenes **240-242** were obtained in poor yields.

The conformations of the glycoconjugates **240-242** afforded under these conditions could not be determined or estimated by NMR spectroscopy, the ^{1}H NMR spectrum just contained broadened signals for the glucose epitopes but the resorcinol unit protons were characteristic. The glycocluster mixtures were acylated according to the previously used method with butyric anhydride and pyridine, and after evaporation of the excess reagents under high vacuum,

unexpected results were noticed on TLC: dark spots were observed on the baseline with lighter spots having higher R_f values.

Purification of the crude butyrated mixture obtained from the reaction of resorcinol with the glucosylated acetaldehyde **237**, using column chromatography afforded one isomer of this derivative in a low yield. To prove the structure of **243**, several NMR experiments were undertaken, including a HSQC experiment.

In the ^{1}H NMR spectra, the most interesting aspect is the position of the signals of the methine bridges, the alkyl chains attached to the methine linkages and the aromatic resonances. As mentioned above the assignment of these signals was aided by the HSQC analysis. In the HSQC spectrum, a signal at 37.1 ppm showed correlation with the signals at 4.37-4.42 ppm. Hence the signal should be related to the protons at the bridged methine. The signal at 68.7 ppm has a correlation with the signal at 3.79 ppm; this signal is expected due to the methylene chain fragments. The signal at 117.0 ppm displayed correlation with the signals at 5.87-7.14 ppm. Hence the signal must be for the calix[4]resorcinarene cage protons (Figure 67). The structure of **243** is also supported by mass spectrometry analysis. The spectrum gave molecular ion at *m*/*z* 1262.4869 that corresponds to $(M+2NH_4)^{2+}$. (Expected: *m*/*z* 1262.4867) (Appendix 19).

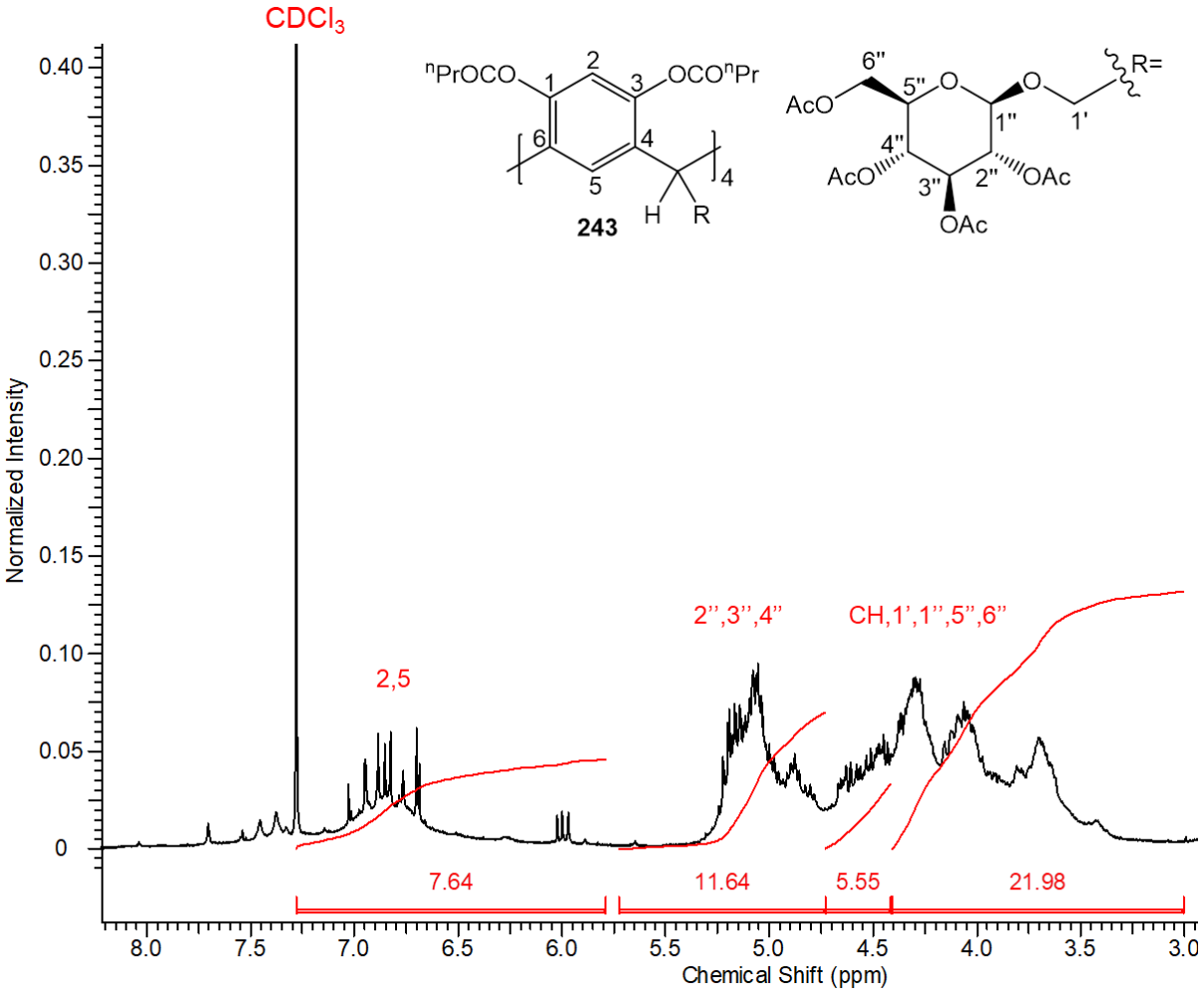
CDCl3
nPrOCO
OCOnPr
243
AcO
OAc
R=
2,5
2'',3'',4"
CH,1',1'',5",6"
7.64
11.64
5.55
21.98
Normalized Intensity
Chemical Shift (ppm)

(a)

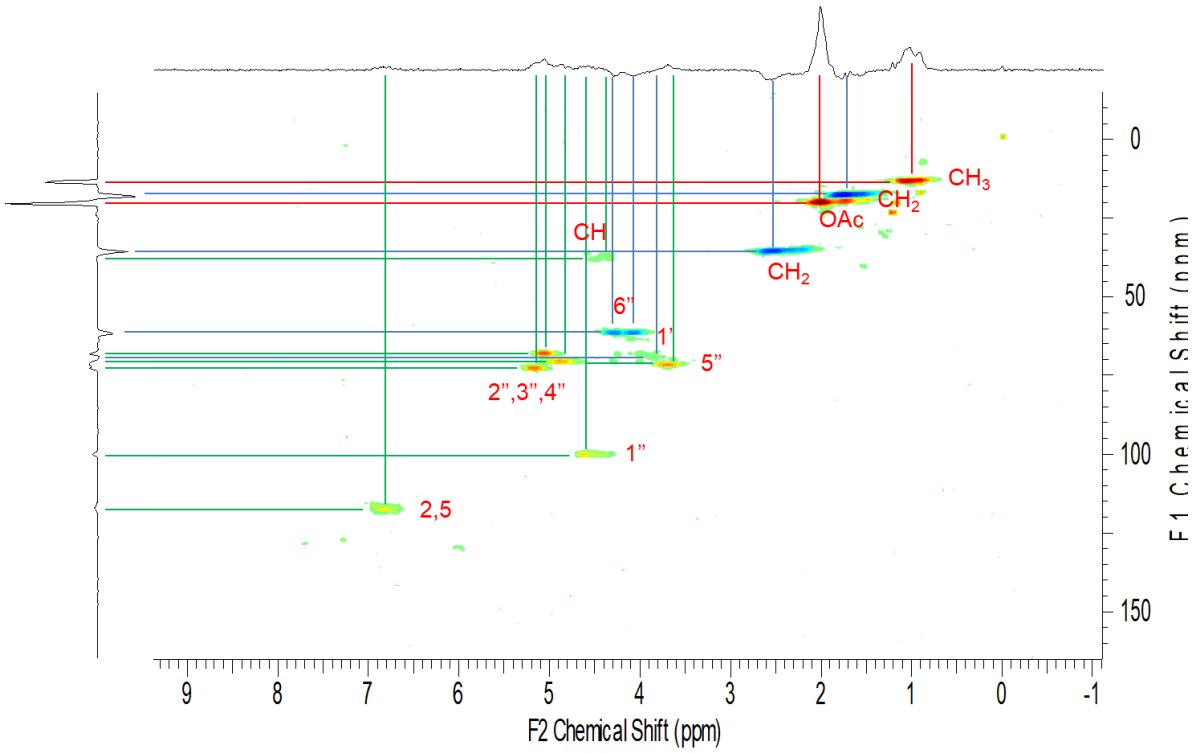

(b)

Figure 67: (a) ^{1}H NMR and (b) HSQCDEPT spectra of tetra(glucomethyl)calix[4]resorcinarene octabutyrate **243** in $CDCl_3$

Fractions obtained from column chromatography of the crude butyration product obtained from 3-oxopropyl glucose **239**, gave ^{1}H NMR data was broad, although all the resonances for the protons and carbons of the glucose, aliphatic chain and resorcinol moieties were assigned with the assistance of 2D-^{1}H NMR, but the signals that correspond to the bridging carbons were absent (Figure 68). However, the mass spectrometry indicated the presence of the compound **244**. The spectrum gave molecular ion at *m*/*z* 1290.5192 that corresponds to $(M+2NH_4)^{2+}$. (Expected: *m*/*z* 1290.5179) (Appendix 20).

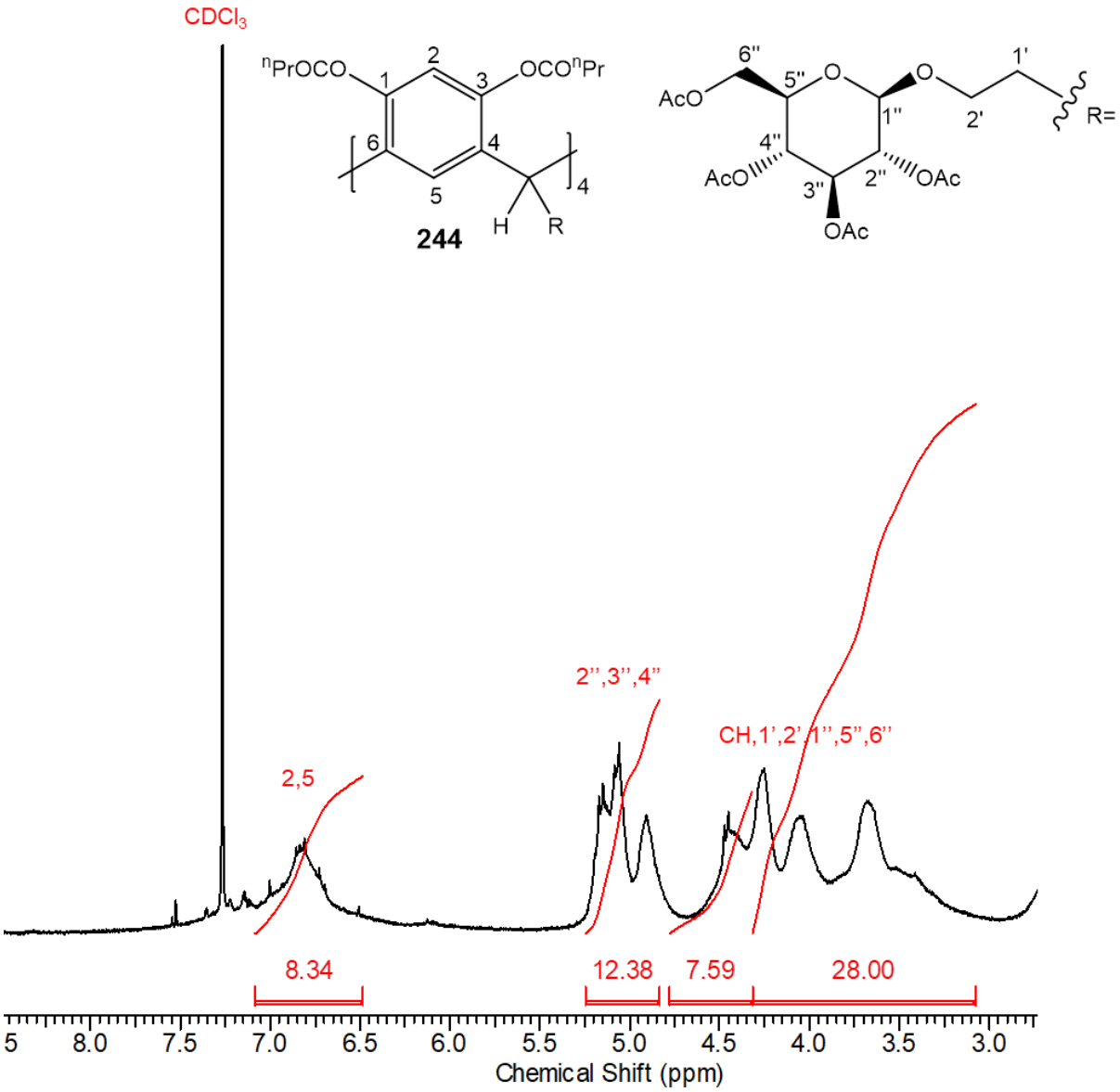
CDCl3
nPrOCO
OCOnPr
1
2
3
4
5
6
H
R
244
AcO
6''
5''
O
1''
1'
2'
R=
4''
AcO
3''
2''
OAc
OAc
2,5
2'',3'',4''
CH,1',2',1'',5'',6''
8.34
12.38
7.59
28.00
5
8.0
7.5
7.0
6.5
6.0
5.5
5.0
4.5
4.0
3.5
3.0
Chemical Shift (ppm)

(a)

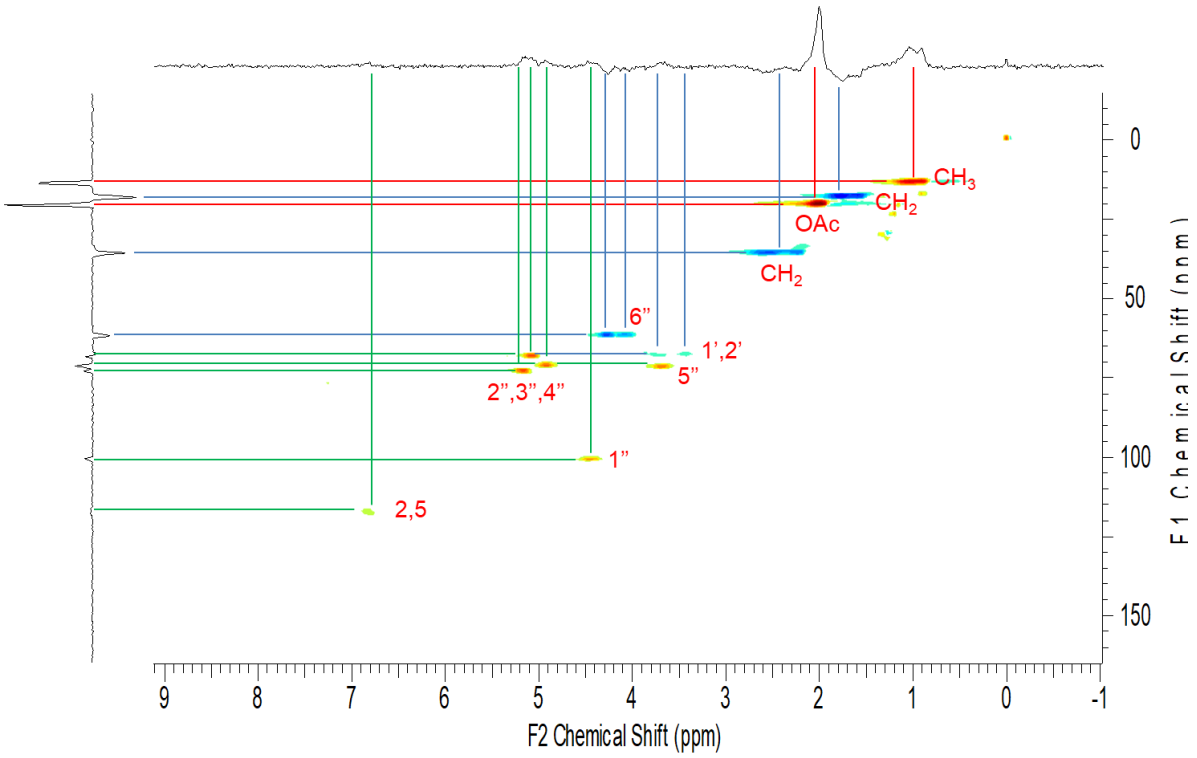

(b)

Figure 68: (a) ^{1}H NMR and (b) HSQCDEPT spectra of tetra(glucoethyl)calix[4]resorcinarene octabutyrate **244** in $CDCl_3$

6.2 Conclusion

The preparation of calix[4]resorcinarene glucoconjugates bearing an aliphatic spacer linking the carbohydrate residue to the calix[4]resorcinarene lower rim has been investigated. Aldehydes functionalised bridge molecules showed lower reactivity in condensation reaction with resorcinol than those functionalised aromatic spacer. In spite of this, the three aldehydes with different aliphatic spacers **237-239** were reacted with resorcinol but only the calix[4]resorcinarenes derived from the glucosylated acetaldehyde **243** and the glucosylated propanal **244** were produced in low yields and confirmed from spectroscopic analysis.

The reactivity of these aldehydes was dependent on the features of the aliphatic arms that linked the glucose fragment to the aldehyde group. Never the less, this work paves the route for using various types of bridge aldehyde bearing glycan terminal group in calix[4]resorcinarene synthesis.

CHAPTER 7: METHANOLYSIS of *rctt* CALIX[4]RESORCINARENE GLYCOCLUSTER

7.1 Hydrolysis of *rctt* calix[4]resorcinarene glucoside 137a

Amongst the goals for our research in this area of calix[4]resorcinarene chemistry is the use of glycosylated calix[4]resorcinarenes as targeted agents in nanopharmaceutics and nanomedicine. To that end, the carbohydrate residues and phenolic hydroxyl groups must be deprotected to make the calix[4]resorcinarenes soluble in water. Various methods have been reported for deacylation of carbohydrates but our choice is limited by the requirement to leave any sensitive carbohydrate residues intact.

Acylated calix[4]resorcinarene glucoside **137a** was chosen as a model compound because we had a significant quantity of this compound in hand. Firstly, acylated substrate **137a** was reacted in the presence of a mixture of methanol, triethylamine and water (8:1:1) to afford the deprotected glycocluster **245** (Dondoni *et al*., 1997). However, this proved to be unsuccessful as manifested in the ^{1}H NMR spectrum, most likely because the amount of water used in the reaction mixture was insufficient to break all the butyrate groups.

The mixture was subsequently subjected to similar reaction conditions, but this time using an excess of water and for an elongated reaction time (48 h). This reaction delivered a more complex mixture of products as evidenced again by ^{1}H NMR analysis.

Upon applying another commonly used method, compound **137a** was reacted with a catalytic amount of sodium methoxide in a mixture of MeOH and DCM (4:1, v/v). The novel polyhydroxylated glycocluster based on a calix[4]resorcinarene core **245** was produced as a red solid in 83% yield (Scheme 69) (Oshovsky *et al*., 2004).

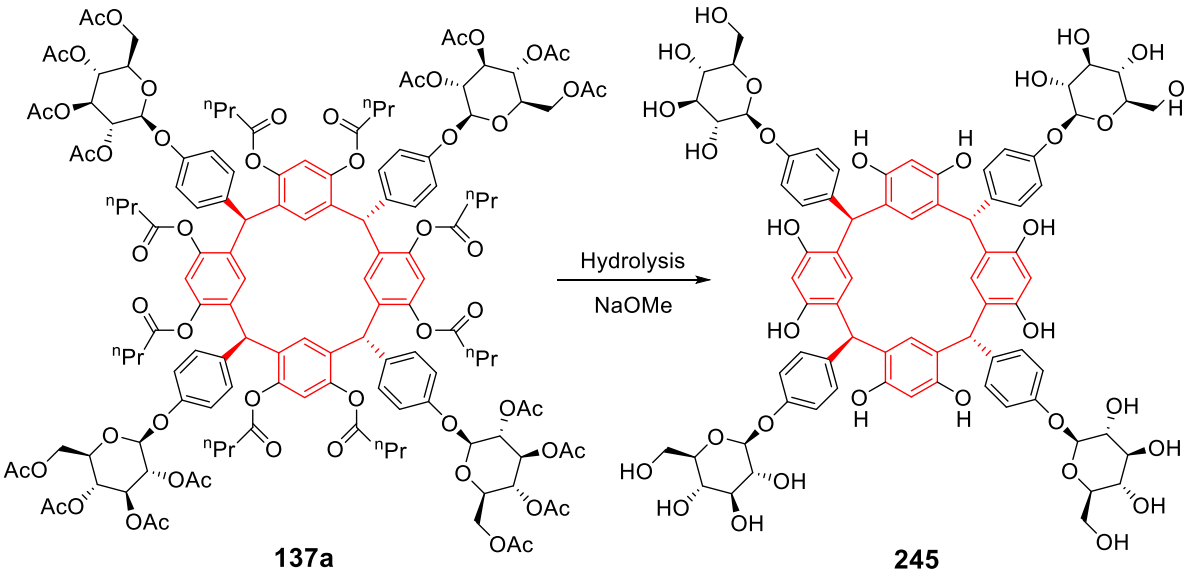

Scheme 69: Ester hydrolysis

Compound **245** was characterised using standard methods, especially ^{1}H NMR spectroscopy and mass spectrometry. The compound is stable in aqueous media and in polar solvents but is insoluble in $CDCl_3$ and other organic solvents.

In deuterated water, calix[4]resorcinarene glycocluster **245** showed broad signals, suggesting persistent intermolecular aggregates as a consequence of hydrogen bonds in solution. In spite of broadening of signals, the broad resonances accounting for the glucose and aromatic hydrogen atoms disclosed the nature of structure **245** (Figure 69b).

In an endeavour to further characterise the nature of configuration, we tested the ^{1}H NMR in deuterated DMSO, analogous trend was noticed for the (chemical shift values δ) of the glucose proton signals 3.01-3.80; 4.71-4.89 ppm, doublet signals for all the protons of the bridging methine residues 5.44-5.61 ppm and muliplet signals for the pendant aromatic units 6.58-7.25 ppm.

The remaining hydrogen signals for resorcinol fragments were almost corresponded (Figure 69a).

The structure of **245** is also supported by mass spectrometry analysis. The spectrum gave molecular ion at *m*/*z* 751.2244 that corresponds to $(M\text{-}2H)^{2-}$. (Expected: *m*/*z* 751.2238) (Appendix 21).

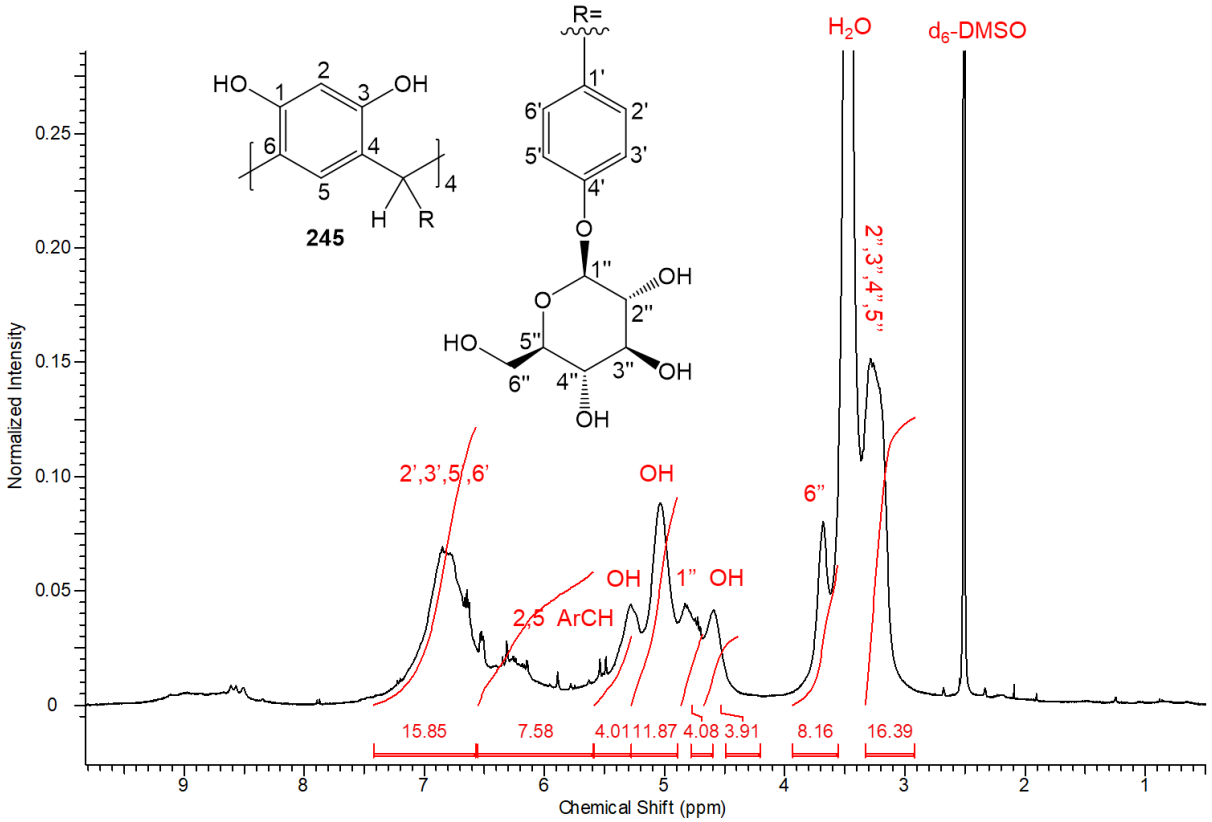

(a)

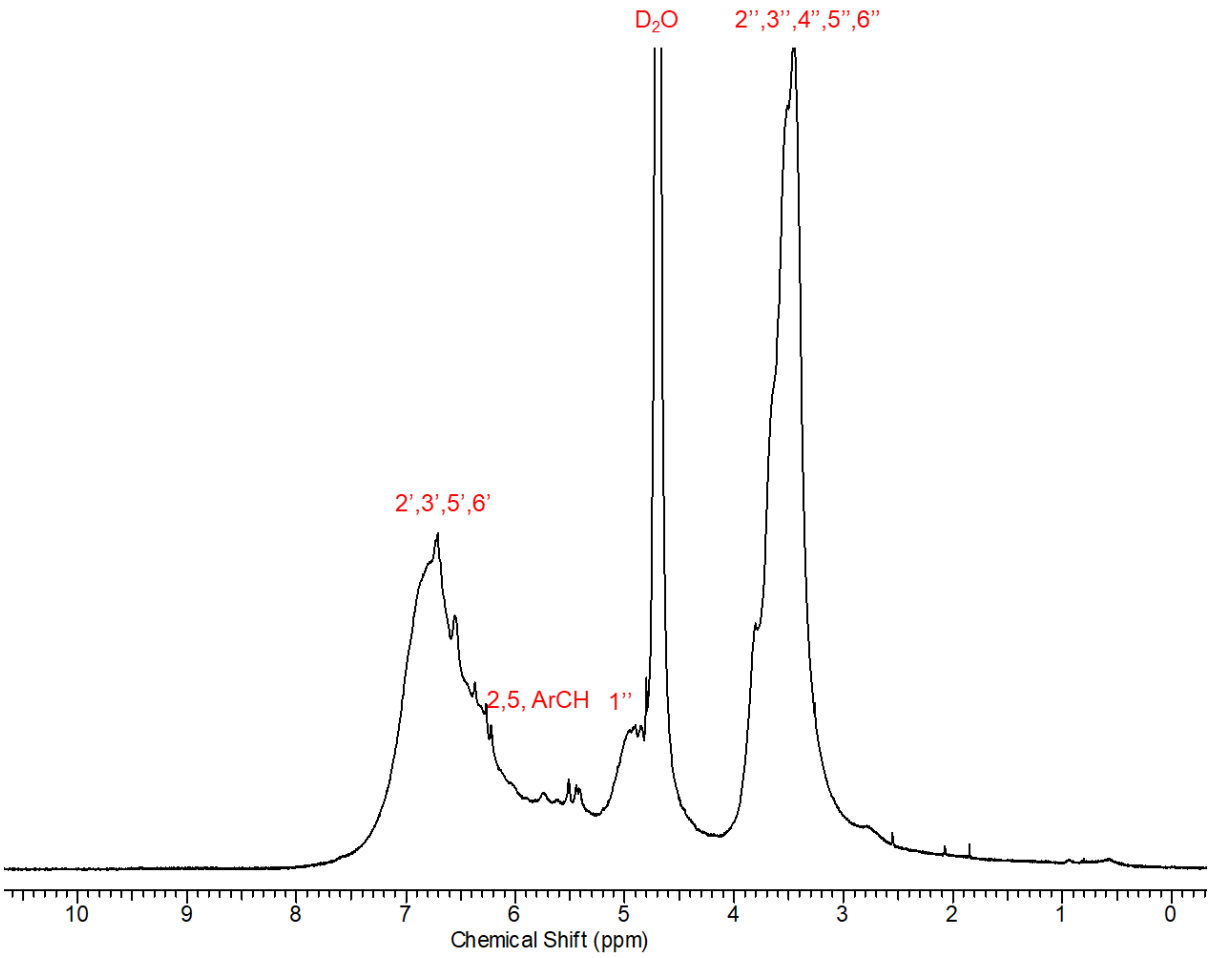

(b)

Figure 69: ^{1}H NMR spectra of hydroxylated glycocluster **245** in (a) d_6-DMSO and (b) D_2O

7.2 Dynamic light scattering measurements (DLS)

Dynamic light scattering (DLS) or also known as photon correlation spectroscopy (PCS) has emerged as one of the most important techniques to investigate the particle size and surface charge of nanoparticles created for drug delivery purposes, such as (macromolecules and peptides). Thus, these parameters play a great role for a range of biological affects of nanodrug delivery systems including cellular uptake, safety, toxicity, stability and dissolution performance. The principle of DLS is based on light scattering

intensity by particles in the solution which follow the principle of Brownian motion and produced from the random movement of particles present in the suspension depending on their size. Polydispersity index (PDI) is an option exists on the DLS software use to express the sorts of particles population or particle size distribution of nanosuspensions. A PDI value ranges between 0.1 to 0.25 indicates small size distribution in contrast with a PDI value of more than 0.5 shows a very wide size distribution. These values give the stability and the aggregation rate of nanosuspention (Bhattacharjee 2016).

Zeta potential measurement (ZP) is one of the important features that indicate to the stability of nanoparticle dispersions by measuring the properties of surface charge or voltage of nanoparticles and compared with the charge of the surrounded solution. The zeta potential value is affected by the size of nanoparticles, especially; particles of very small size that promote noticeable electrostatic repulsion and very stable zeta potential of ±30 mV. With zeta potential value a minimum of ±20 mV, the aggregation will not be resisted with poorly dispersed particles (Patel and Agrawal 2011; Bhattacharjee 2016).

One of the crucial factors that effect on DLS measurements is sample preparation, which should be done in water. Hydroxylated calix[4]resorcinarene glucoside **245** was highly soluble in aqueous media (~15 mg/mL) and DLS measurements were carried out in distilled water by using Zetasizer nano ZS (Malvern Instruments, UK). The particle size, zeta potential and size distribution were measured at four concentrations (1 mg/mL, 3 mg/mL, 6 mg/mL and 10 mg/mL). The measurements were performed in triplicate at room temperature.

As shown in figure 70, particle size values at each of the concentrations used (1 mg/mL, 3 mg/mL, 6 mg/mL and 10 mg/mL) were 150.3 nm ±1.02 nm, 160.16

nm ±15.43 nm, 189.66 nm ±5.25 nm and 168.13 nm ±37.25 nm, respectively. There was no significant increase in particle size noticed with increasing concentration. This indicated that particle or cluster formation within the aqueous environment was independent of concentration.

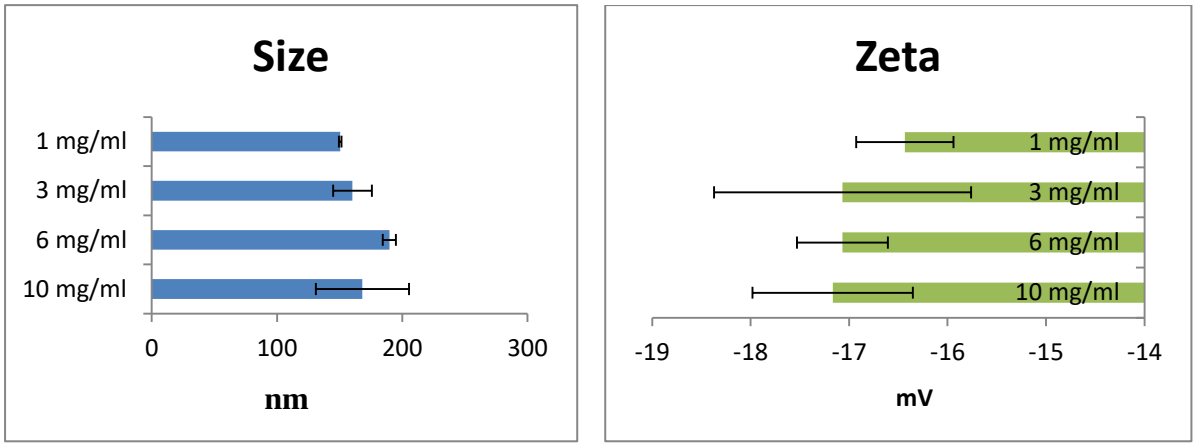

(A) (B)

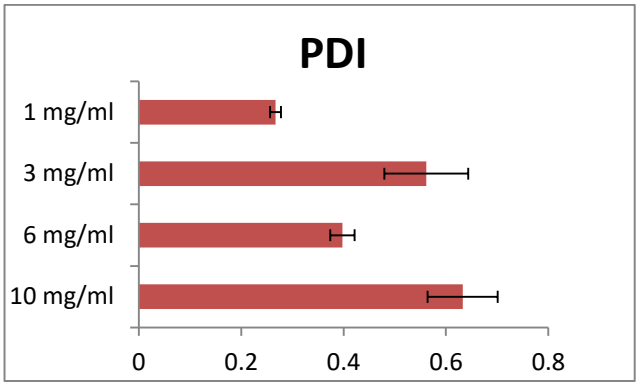

(C)

Figure 70: Representation (A) size, (B) zeta potential and (C) PDI of optimal formulation nanoaggregate of hydroxylated calix[4]resorcinarene glucoside with four different concentrations

Zeta potential values of the fully hydroxylated calix[4]resorcinarene glucoside with all concentrations were high and negatively charged which indicates the presence of polar hydroxyl groups that ionize in water (Scheme 70). The values were found to be -16.43 mV ±0.49 mV, -17.06 mV ±1.30 mV, -17.06 mV ±0.46 mV and -17.16 mV ±0.81 mV, respectively. As before, there was not any significant change of charge with an increase in concentration.

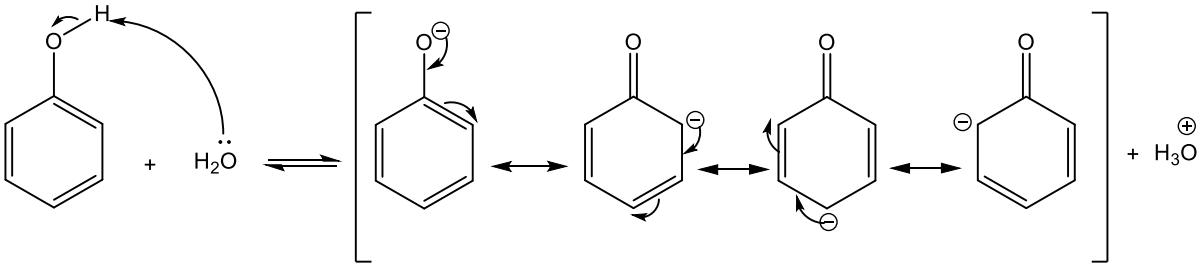

Scheme 70: Deprotonation and stabilisation of phenoxide ion by resonance

The polydispersity index (PDI) was measured at each of the increasing concentrations. The size of self-assembled species may vary in water at different concentrations, thus affecting particle size distribution dependent on concentration. The highest PDI were noticed of 3 mg/mL and 10 mg/mL concentration with a value of 0.56±0.08 and 0.63±0.06, respectively. However, the value for the 6 mg/mL solution was 0.39±0.02, lower than that of 3 mg/mL concentration, but higher than the value of 0.26±0.01 for the 1 mg/mL solution. The high polydispersity index values may be associated with the aggregation of molecules of unprotected calix[4]resorcinarene glucoside into different particle sizes in water.

7.3 Conclusion

We have further characterised the first model of a calix[4]resorcinarene glucoside bearing four monosaccharide substituents at the lower rim that is soluble in aqueous media. The properties of a hydroxylated calix[4]resorcinarene glucoside were studied, which showed good water solubility and stability. This opens the scope for using such molecules in molecular recognition approaches. The preliminary data obtained from particle size, zeta potential and size distribution measurements, evidence the promising use of glycocalix[4]resorcinarenes to interact with biologically relevant molecules, specifically hydrophobic drugs. This compound and the successful solvolysis conditions used in here could result in focusing investigations into the synthesis of further water soluble calix[4]resorcinarene glycosides, especially that derived from the corresponding *rccc* conformational isomer in order to increase their potential use as drug delivery systems or in other biological events such as, anti-adhesion or inhibition pathogens attack (virus and bacteria) to the cell, antifungal activity, targeted drug delivery systems for cancer treatments, immune response and cell trafficking. All occour as a result of interaction of glycocalix[4]resorcinarene with carbohydrates untis existent on the cell surface.

CHAPTER 8: LEWIS ACID INDUCED SYNTHESIS OF CALIX[4]RESORCINARENES

In continuation of our efforts to investigate other methods for the synthesis of complex calix[4]resorcinarenes, we wished to further demonstrate the utility of a range of Lewis acids as catalysts for the reaction of structurally complex aldehydes with resorcinols.

Many of the calix[4]resorcinarenes we investigated were already reported in the literature as being prepared by conventional mineral acid catalysed condensation reaction, with some other reports highlighting protocols which used Lewis acids for the synthesis of calix[4]resorcinarenes.

The principal reason for preparing these octols during our studies was not to isolate each compound or isomer in a pure form. Rather, it was to assess the reactivity and selectivity of each Lewis acid on the reaction and diastereoisomer distribution.

8.1 Synthesis of alkyl- and aryl-substituted calix[4]resorcinarenes

The general procedure employed involved reacting equal molar quantities of aliphatic or aromatic aldehydes with resorcinol, 2-methylresorcinol and pyrogallol in the presence of a Lewis acid. The reactions were conducted at room temperature in dry Et_2O and the reaction was monitored over various time periods (Scheme 71). Generally, products precipitated from solution and the reaction mixtures were worked up by diluting the mixture with a further 50 mL portion of Et_2O, suspending the precipitated calix[4]resorcinarenes in water and the solid products were collected by filtration.

With aliphatic aldehydes only the *rccc* configuration was isolated when R= H and R'= $CH_3(CH_2)_3$ using anhydrous $AlCl_3$. Other attempts at condensation of

resorcinol or analogues substituted at the 2-position with valeraldehyde or octanal using different Lewis acids were conducted but failed to give solid precipitate from the reaction mixture. The ^{1}H NMR spectrum of macrocycle **246** (Table 1) was analogous to that reported for the same calix[4]resorcinarene obtained by hydrochloric acid catalysed condensation (Tunstad *et al*., 1989).

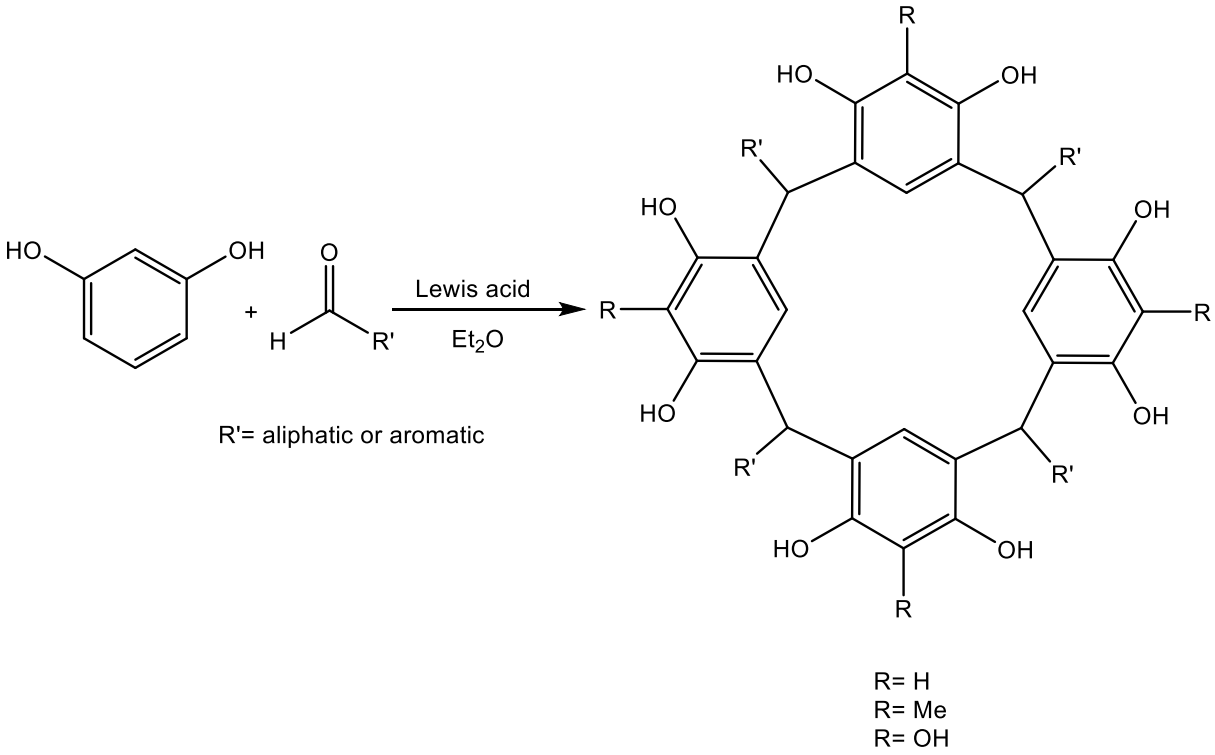

Scheme 71: Synthesis of alkyl and aryl substituted calix[4]resorcinarenes

The reaction of resorcinol with aromatic aldehydes was also studied and the structures are reported in table **1**. With benzaldehyde, a mixture of two diastereoisomers was obtained upon running three separate reactions with three different catalysts, the all-*cis* (*rccc*, C_{4v}) isomer and the *cis-trans-trans* (*rctt*, C_{2h}) isomer. The exact isomer ratio was not investigated, but based on ^{1}H NMR data of benzaldehyde-derived calix[4]resorcinarene displayed three singlets at δ 5.74, 5.78 and 5.88 ppm, in addition, six single resonances in the range 6.33-6.64 ppm for benzylic hydrogens and for each set of aromatic

protons at 2- and at 5-position of resorcinol rings. This was well correlated with the data observed for the same compound produced by Lewis acid catalysts (Barrett *et al*., 1999; Deleersnyder *et al*., 2007; Darvish and Khazraee 2014) but was not consistent with acid-catalysis (Senthan and Alexander 2015).

Table 1: Octols produced from the reaction of resorcinol, 2-methylresorcinol and pyrogallol with aliphatic and aromatic aldehydes

Run No.	Lewis acid	Macrocycles	R	R'	Isomer distribution
1	$AlCl_3$	**246**	H	$CH_3(CH_2)_3$	*rccc* (*C_{4v}*)
2	$AlCl_3.NO_2$	**37**	H	C_6H_5	*rccc: rctt*
3	$AlCl_3$	**37**	H	C_6H_5	*rccc: rctt*
4	$ZnCl_2$	**37**	H	C_6H_5	*rccc: rctt*
5	$AlCl_3.NO_2$	**247**	H	2-anisal	*rctt*
6	$AlCl_3$	**247**	H	2-anisal	*rctt*
7	$BF_3.Et_2O$	**247**	H	2-anisal	*rctt*
8	$TiCl_4$	**247**	H	2-anisal	*rctt*
9	$ZnCl_2$	**247**	H	2-anisal	*rctt*
10	$AlCl_3.NO_2$	**52d**	H	4-anisal	*rccc: rctt*
11	$AlCl_3$	**52d**	H	4-anisal	*rccc: rctt*
12	$BF_3.Et_2O$	**52d**	H	4-anisal	*rccc: rctt*
13	$TiCl_4$	**52d**	H	4-anisal	*rccc: rctt*
14	$ZnCl_2$	**52d**	H	4-anisal	*rccc: rctt*
15	$AlCl_3.NO_2$	**248**	H	4-$OCOCH_3$	*rccc* (*C_{2v}*)
16	$AlCl_3.NO_2$	**52h**	H	4-tolyl	*rccc* (*C_{2v}*)
17	$AlCl_3$	**52h**	H	4-tolyl	*rccc* (*C_{2v}*)

18	$TiCl_4$	**52h**	H	4-tolyl	*rccc* (*C_{2v}*)
19	$ZnCl_2$	**52h**	H	4-tolyl	*rccc* (*C_{2v}*)
20	$BF_3.Et_2O$	**52h**	H	4-tolyl	*rccc* (*C_{2v}*)
21	$AlCl_3.NO_2$	**202**	CH_3	C_6H_5	*rctt*
22	$AlCl_3$	**202**	CH_3	C_6H_5	*rccc: rctt*
23	$ZnCl_2$	**202**	CH_3	C_6H_5	*rctt*
24	$AlCl_3.NO_2$	-	CH_3	2-anisal	-
25	$AlCl_3$	**249**	CH_3	2-anisal	*rctt*
26	$TiCl_4$	-	CH_3	2-anisal	-
27	$BF_3.Et_2O$	**249**	CH_3	2-anisal	*rctt*
28	$ZnCl_2$	no ppt	CH_3	2-anisal	-
29	$BF_3.Et_2O$	**250**	CH_3	4-anisal	*rccc: rctt*
30	$ZnCl_2$	no ppt	CH_3	4-anisal	-
31	$TiCl_4$	-	CH_3	4-anisal	-
32	$AlCl_3.NO_2$	**250**	CH_3	4-anisal	*rccc: rctt*
33	$AlCl_3$	**250**	CH_3	4-anisal	*rccc: rctt*
34	$AlCl_3.NO_2$	**251**	CH_3	4-tolyl	*rctt*
35	$AlCl_3$	**251**	CH_3	4-tolyl	*rccc: rctt*
36	$TiCl_4$	**251**	CH_3	4-tolyl	*rccc: rctt*
37	$ZnCl_2$	**251**	CH_3	4-tolyl	*rctt*
38	$AlCl_3.NO_2$	**94**	OH	C_6H_5	*rccc: rctt*
39	$ZnCl_2$	**94**	OH	C_6H_5	*rccc: rctt*
40	$AlCl_3.NO_2$	-	OH	2-anisal	-
41	$AlCl_3$	-	OH	2-anisal	-
42	$TiCl_4$	-	OH	2-anisal	-
43	$ZnCl_2$	-	OH	2-anisal	-

44	$AlCl_3.NO_2$	**252**	OH	4-anisal	*rccc: rctt*
45	$AlCl_3$	-	OH	4-anisal	-
46	$TiCl_4$	-	OH	4-anisal	-
47	$ZnCl_2$	-	OH	4-anisal	-
48	$AlCl_3.NO_2$	-	OH	4-tolyl	-
49	$AlCl_3$	-	OH	4-tolyl	-
50	$TiCl_4$	-	OH	4-tolyl	-
51	$ZnCl_2$	-	OH	4-tolyl	-

In the condensation of resorcinol with 2-methoxybenzaldehyde, only one isomer was detected by the ^{1}H NMR of the crude that precipitated from the reactions, runs 5-9 (Table 1). The chair conformation product was expected to produce from these reactions, accordingly to previous reported finding from acid induce synthesis (Pfeiffer *et al*., 2016) or similar to our synthesised calix[4]resorcinarene from 2-glucosylated benzaldehyde by Lewis acid.

For the calix[4]resorcinarenes derived from 4-substituted benzaldehydes, the tetrameric nature of the macrocycles was diversified relying on the type of substituent on the benzaldehyde. When R'= 4-$CH_3OC_6H_4$, of the characterised products, runs 10-14 (Table 1), two isomers (*rccc* and *rctt*) were identified by the ^{1}H NMR data. It was important to note that each group of these compounds featured as a couple of signals with differences in the chemical shifts of the methine signals and resorcinol hydrogens for the two configurations. This fact is concordant with the detections of previous workers, used acid condition (Sarjono *et al*., 2007), and was not agreeable with Pfeiffer *et al*. suggestion, that was only of (*rctt*, C_{2h}) symmetry.

Other aromatic aldehydes such as 4-methylbenzaldehyde and 4-acetoxy benzaldehyde were also tested. In the synthesis of **248** and the products from runs 16-20, the corresponding calix[4]resorcinarenes were characterised as the *rccc* (boat conformation). The ^{1}H NMR spectra of these compounds in d_6-acetone display double resonances for the protons for the resorcinol constituents, as previously reported values (Funck *et al*., 2010). The possibility of presence traces of *rctt* isomer in the crude mixture of macrocycles **52h** is also existed.

In case of 4-methylbenzaldehyde, a big difference was noticed in the ^{1}H NMR spectra in d_6-DMSO, the observed ^{1}H NMR of macrocycles **52h** was characteristic of the *rccc* (cone conformation); where each group of protons match with a single resonance. One singlet at 5.63 ppm of the bridging methine and characteristic resonances for each of the four protons at 2- and of the four protons at 5-position of resorcinol fragments at δ 6.16 and 6.27 ppm indicated to the presence of *rccc* isomer.

Reaction of 2-substituted resorcinols with a series of substituted benzaldehydes was accomplished using a range of Lewis acids. Compared to the yields obtained from substituted resorcinol and analogous reactions with unsubstituted resorcinol, the yields of runs 21-51 are lower. Despite the existence of higher electron density in substituted resorcinol than that in resorcinol and consequently the electrophilic attack by the benzaldehyde lead to faster tetramerisation, but different findings were observed from the corresponding reactions. These are required longer reaction time than that of runs 1-20 and some catalysts did not give cyclisation or partial interaction occurred.

When R= CH_3 and R'= C_6H_5, compounds from runs 21 and 23 were isolated as the *rctt* isomers as indicated by the existence two signals at δ 2.10 and 2.27 ppm for the methyl groups of resorcinol fragments, beside two signals attributed to the intra annular resorcinol protons (Parulekar *et al*., 2015). Whereas, that from 22 of the same substrates but using different catalyst (anhydrous $AlCl_3$) came out as a mixture, probably *rccc* and the *rctt* isomers. Four sets of signals appeared for the methylresorcinol units and two resonances for the methine linkage referred to chair and boat conformation.

With R= CH_3 and R'= 2-$OCH_3C_6H_4$, the products from runs 24 and 26 showed the presence of starting material and the cyclisation was not completed within 48 h reaction time. Similar reactions, runs 25 and 27, used different catalysts and for longer reaction time (up to week), afforded the corresponding calix[4]resorcinarenes and were not precipitated in a pure status. However, they clearly show formation of a single isomer of *rctt* configuration by the ^1H NMR spectra. No solid product precipitated from run 28 on using $ZnCl_2$ as a catalyst.

The calix[4]methylresorcinarenes **250**, resulting upon reaction of 4-methoxybenzaldehyde with 2-methylresorcinol were observed in two isomers, probably (*rccc* and *rctt*) as indicated by the appearance two signals for the methine bridges and double resonances for the aromatic protons for each isomer were characteristics. This was not in agreement with the previous reported finding by Reinhoudt *et al*. (Middel *et al*., 1998). From run 31 ($TiCl_4$ catalyst), slightly condensed product was isolated. Again, no precipitate obtained from the run 30 catalysed by $ZnCl_2$.

Prosvirkin *et al*. have previously described the isomeric composition of calix[4]methylresorcinarene derived from 4-tolualdehyde and determined two

main products correspond to that tetramer (*rccc* and *rctt*) (Prosvirkin *et al*., 2005). Different investigation has been determined by Miao *et al*. that the corresponding compound produces in the chair conformation (Miao *et al*., 2003). The results obtained by our hand were differentiated based on the sort of catalyst used. Only single isomer as the *rctt* configuration was detected in synthesis of **251**, runs 34 and 37. In runs 35 and 36, two isomeric forms (*rccc* and *rctt*) were distinguished on the ^{1}H NMR spectra.

On applying a wide range of various Lewis acids in the condensation reaction of 2-hydroxyresorcinol with aromatic aldehydes, runs 38-51, the ^{1}H NMR chemical shifts in d_6-acetone for macrocycles **94**, showed well resolved mixture of conformations, potentially correspond to (*rccc* and *rctt*). Two single peaks at 5.30 and 5.78 ppm, additionally, two characteristic signals at 6.17 and 6.48 ppm for pyrogallol units were comparable with the literature estimation for the isolated isomers prepared by conventional method (Casas-Hinestroza and Maldonado 2018).

The reaction also worked well with R= OH and R'= 4-$CH_3OC_6H_4$, run 44, the ^{1}H NMR displayed two sets of signals for bridging methylene at 5.67 and 5.80 ppm, here also, possibly a mixture of diastereoisomers being presented. However, from runs 45-47, or when R'= 2-$CH_3OC_6H_4$, runs 40-43 or 4-$CH_3C_6H_4$, runs 48-51, partially condensed products were isolated.

In runs 40 and 48, pyrogallol condensed with 2-methoxybenzaldehyde and 4-toulaldehyde, respectively. Apparently, the products show single isomer as elucidated by the appearance of three resonances singlet for the methine bridges and pentasubstituted pyrogallol units in the ^{1}H NMR analysis.

8.2 Conclusion

We have provided alternative methods for the synthesis of aryl substituted calix[4]resorcinarenes in the presence of varied Lewis acids as catalysts. The benefits of these methods include the use of simple available catalysts, easy workup and in some cases rational reaction time periods in comparison with other Lewis acids synthesised and reported in the synthesis of calix[4]resorcinarenes.

Comparisons were made between the syntheses of macrocycles presented in table **1** and other reported methods. The results sometimes showed similarity and others were contradicted to the earlier reported procedures in terms of reactivity, stereoselectivity and yield products.

In this study we demonstrated that with aliphatic aldehydes and resorcinol or 2-substituted resorcinols, Lewis acids showed low reactivity and only one compound **246** of *rccc* isomer was produced. With benzaldehyde or substituted benzaldehydes and resorcinol or 2-substiuted resorcinols, the molecules possessed either all-*cis* (boat-like conformer) or *cis-trans-trans* (chair-like conformer) or mixtures of both were produced. Moreover, in the reaction of substituted benzaldehydes with pyrogallol, the amount of condensed products was very low for unknown reasons or could be associated with the low acidity or using low concentration of Lewis acids.

CHAPTER 9: GENERAL DISCUSSION AND CONCLUSION

It is known that carbohydrates play key roles in a number of essential biological phenomena, especially events triggered by receptor-mediated intermolecular interactions. For this reason, the initial milestones of this present study were to synthesise glycoconjugated compounds bearing monosaccharide epitopes at the lower rim of cyclic tetramer calix[4]resorcinarenes, in order to isolate different topologies of calix[4]resorcinarene glycosides with enhanced aqueous solubility. Each calix[4]resorcinarene conformation isolated may have different potential as a biomimetic structure. In this context, varying the nature of the aromatic aldehydes, which bear the carbohydrate residues, that take part in the Lewis acid catalysed condensation reaction with resorcinol provided glycosylated calix[4]resorcinarenes **145**, **146**, **148** and **153**. Conformers of these compounds were isolated as the octabutyrates after derivatisation the initial phenolic products from the condensation reaction: in general, the products of the condensation reactions starting from 4-substituted benzaldehyde glycosides were isolated as a mixture of conformers of each glycocluster. However, only one conformation of glycocluster was isolated from reactions starting with glucosylated derivatives of 2- and 3-hydroxybenzaldehydes.

Following the effective syntheses of glycoclusters bearing monosaccharide residues, the subsequent aim was to introduce disaccharide ligands at the lower rim of the calix[4]resorcinarene scaffold in an attempt to provide molecules with a significant increase in solubility in aqueous media. Here, compounds **158** and **163** were successfully synthesised by reacting lactosyl and cellobiosyl derivatives of 4-hydroxy benzaldehyde with resorcinol. Remarkably, the reactions delivered only one conformer in each case,

delivering the pure ester of compound **159** and the octaphenol of calix[4]resorcinarene **163**.

Carbohydrates confer important physico-chemical properties on the glycocluster compounds, particularly related to solubility in aqueous media and the potential ability to recognise lectins and cells. At the same time, however, the significant hydrophobicity of calix[4]resorcinarene matrices and the presence of a modest number of hydrophilic sugar motifs limits their aqueous solubility and potentially hinder their biological applications. To overcome these limitations and to explore isolation of different conformations of calix[4]resorcinarene glycosides, we aimed to prepare glycosidic aldehydes with various spacer units of various length and flexibility. It was anticipated that the spacers may influence the conditions required to prepare the corresponding calix[4]resorcinarenes and the increased hydrophobic region on the lower rim of these calix[4]resorcinarenes may have a significant effect upon the ability of these compounds to act as drug solubilising agents.

Unfortunately, attempts to prepare the glucosylated derivatives of 4-hydroxyphenyl propanal **167** and 4-hydroxyphenyl acetaldehyde **169**, required for the calix[4]resorcinarene synthesis, from their acid derivatives was unsuccessful. The principal issue was the instability of the aldehydes **170** and **171** under the numerous glycosylation conditions employed. As a consequence, the parent aryl substituted calix[4]resorcinarenes were prepared from the substrate 4-hydroxyphenyl propanal by acid catalysis and the three calix[4]resorcinarenes were isolated in the all-*cis* (*rccc*) configuration.

The successful synthesis of the novel glycosidic aldehyde **167** was accomplished *via* Wittig reaction and the synthesis of the corresponding

calix[4]resorcinarene glucoside **164** was investigated by using anhydrous $AlCl_3$ as a catalyst. The stereoselective formation of the glycocluster **164** in *rccc* configuration was one of the advantages of using the aldehyde **167** in the reaction with resorcinol. This strategy could provide an entry point for further development on the calix[4]resorcinarene framework.

Addition of functional groups to calix[4]resorcinarene glycosides on the upper rim was undertaken using resorcinol derivatives 2-methylresorcinol and pyrogallol in condensation with glycosylated aldehydes. All of these reactions produced only one conformer as shown by NMR spectroscopy: The appearance of the spectra of the products **216**, **218**, **220** and **222** varied but showed similar resonances to those of conformational isomers obtained from the condensation reactions starting with resorcinol. This indicated to the influential role played by these groups on the isomeric composition of the macrocycles produced.

An alternative strategy was used to obtain glucosylated aldehydes with an alkyl spacer between the carbonyl group and the carbohydrate residues. 2-Glucose acetaldehyde **237**, 2-glucoseethoxy acetaldehyde **238** and 3-oxopropyl glucose **239** were prepared according to established methodology. The successful synthesis of corresponding calix[4]resorcinarene glucosides was achieved from reaction of resorcinol with the glucosides **237** and **239**. There is obvious potential here for developing the synthesis of glycoclusters bearing carbohydrate moieties linked through different spacers since the spacer arms could be further extended to include different ratios of hydrophilic and hydrophobic properties.

Finally, in order to be suitable for use as drug solubilising agents an essential requirement of any calix[4]resorcinarene is that it must be soluble in aqueous media. This was readily achieved by cleaving all of the protecting groups from the carbohydrate residue and calix[4]resorcinarene upper rim of *rctt* glycocluster **137a**. Standard measurements of relative solubility, particle size, zeta potential and size distribution were made for the major conformational isomer. It would be highly desirable to make all the prepared compounds soluble in aqueous media, especially the minor conformational isomer of glycocluster **137b**, anticipated to be the *rccc* conformer, and then any conformers deemed suitable would then be investigated for their ability to solubilise a range of hydrophobic drugs. This would be the best foundation for future research in this area.

CHAPTER 10: MATERIAL AND METHODS

10.1 Synthesis and characterisation of compounds

All chemicals and reagents were purchased from Alfa Aesar, Sigma-Aldrich, Fisher and ACROS and unless otherwise stated were used without further treatment. Most reactions were carried out under a nitrogen atmosphere. Solvents were either used as received or stored over molecular sieves (4 Å).

Thin layer chromatography (TLC) was undertaken using aluminium plates pre-coated with 60 F_{254} silica gel (Merck). TLC plates were visualised using UV light, 5% solution H_2SO_4 in MeOH or potassium permanganate solution. R_f values were calculated as the distance travelled by the spotting material over the distance travelled by the eluent system. Preparative TLC plates used were with thickness (1000 µm) and size (20x20 cm) (Material Harvest Ltd, Cambridge); PLC Silica gel 60 F_{254}, (2 mm), (Merk). Chromatotron chromatography was undertaken using glass plates coated with silica gel 60 PF_{254} containing gypsum (Merck) prepared in-house. Column chromatography was performed on silica gel (40-63 µm) (VWR) and all mixtures were dissolved in DCM and pre-absorbed on a small amount of silica gel before placing on top of the column and elution.

Melting points of materials were measured using a Bibby Stuart Scientific Melting point apparatus and were uncorrected. Infrared spectra were obtained using a Thermo Nicolet Nexus FT-IR spectrophotometer.

^{1}H and ^{13}C NMR spectra were recorded on a Bruker Avance instruments with frequencies (^{1}H at 300 MHz, ^{13}C at 75 MHz) and (^{1}H at 400 MHz, ^{13}C at 100 MHz). NMR samples were prepared by dissolving the substance in deuterated solvents ($CDCl_3$, d_6-acetone, d_6-DMSO or D_2O). All chemical shifts (δ) are quoted in ppm using $SiMe_4$ as an internal reference and coupling constant (*J*

values) are given in Hertz (Hz). Multiplicities of the NMR peaks are described as singlet (s), doublet (d), triplet (t), quartet (q), double-doublet (dd), double double doublet (ddd), multiplet (m) and broard signals are denoted as br.

Mass spectrometry of the final compounds was carried out by the National Mass Spectrometry Facility at Swansea University on a Waters Xevo G2-S QT or a ThermoFisher LTQ Orbitrap XL ETD Hybrid Ion Trap-Orbitrap Mass Spectrometer using electrospray ionization in either positive or negative ion mode.

10.2 Synthesis of peracetylglycosyl bromides (General Procedure)

The acetylated carbohydrates (1 eq) with a solution of HBr (33% in AcOH, 13 eq) were mixed in a round flask containing DCM (50 mL) cooled to 0 ^{0}C for 1 hr. The reaction was left to stir overnight at r.t and the reaction progress was monitored by TLC. The mixture was subsequently diluted with DCM (100 mL) and the organic layer was washed with ice water (100 ml), saturated aq. solution $NaHCO_3$ (100 mL x 2), brine (100 mL x 2) and dried ($MgSO_4$). The mixture was filtered and solvent evaporated under reduced pressure to give the title compounds **151**, **156** and **161** (Mitchell *et al*., 2001).

10.2.1 2,3,4,6-Tetra-*O*-acetyl-*α*-D-galactopyranosyl bromide 151

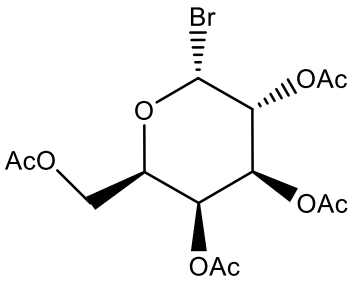

151

Compound **151** was synthesised according to the general procedure from 1,2,3,4,6-penta-*O*-acetyl-*β*-D-galactose **150** (5.85 g, 15 mmol). Sample was obtained as a colourless gum (5.46 g, 13.28 mmol, 89%), which was used without further purification.

R_f of compound **151** (EtOAc: Pet. ether, 1:1): 0.69

10.2.2 2,3,6,2’,3’,4’,6’-Hepta-*O*-acetyl-*α*-D-lactosyl bromide 156

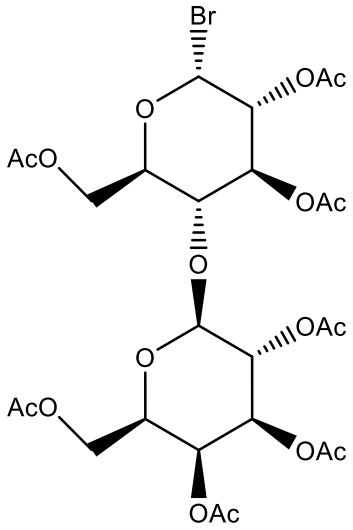

156

Compound **156** was synthesised according to the general procedure from 1,2,3,6,2’,3’,4’,6’-octa-*O*-acetyl-lactose **155** (6.00 g, 115 mmol). Sample was recrystallised from Et_2O to give the title compound as a white solid (3.25 g, 4.65 mmol).

Yield: 52%

R_f of compound **156** (EtOAc: Pet. ether, 2:1): 0.63

Vmax (cm^{-1}): 1741 (C=O ester), 1369 (C-H bending), 1212, 1040 (C-O stretching), 904 (C-H bending), 599 (C-Br).

^1H NMR (400 MHz $CDCl_3$): δ 6.53, (1H, d, *J* 4.2, H1-Lac), 5.56, (1H, t, *J* 9.7x(2), H3-Lac), 5.36, (1H, dd, *J* 3.4,0.9, H4’-Lac), 5.14, (1H, dd, *J* 10.4, 7.9, H2’-Lac), 4.96, (1H, dd, *J* 10.5, 3.5, H3’-Lac), 4.77, (1H, dd, *J* 10, 4, H2-Lac), 4.49-4.53, (2H, m, H1’-, H6-Lac), 4.06-4.23, (4H, m, H5-, H6, H6’-Lac), 3.84-3.91, (2H, m,

H5’-, H4-Lac), 2.17, (3H, s, OAc), 2.14, (3H, s, OAc), 2.10, (3H, s, OAc), 2.08, (3H, s, OAc), 2.07, (3H, s, OAc), 2.06, (3H, s, OAc), 1.97, (3H, s, OAc).

^{13}C NMR (100 MHz $CDCl_3$): δ 170.3, 170.2, 170.1, 170.1, 170.0, 169.2, 168.9 (C=O); 100.8, 86.3, 75.0, 72.9, 71.0, 70.8, 70.7, 69.5, 69.0, 66.5, 61.0, 60.8 (C-Lactose); 20.8, 20.8, 20.6, 20.5 (OAc-Lactose) (Bier *et al*., 2017).

10.2.3 2,3,6,2’,3’,4’,6’-Hepta-*O*-acetyl-α-D-cellobiosyl bromide 161

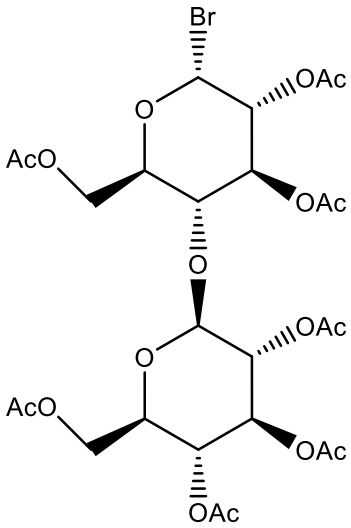

161

Compound **161** was synthesised according to the general procedure from 1,2,3,6,2’,3’,4’,6’-octa-*O*-acetyl-cellobiose **160** (6.00 g, 115 mmol). Sample was recrystallised from Et_2O to give the title compound as a white solid (4.55 g, 6.50 mmol).

Yield: 74%

R_f of compound **161** (EtOAc: Pet. ether, 1.5:1): 0.43

Vmax (cm^{-1}): 2957 (C-H stretching), 1737 (C=O ester), 1367 (C-H bending), 1215, 1040 (C-O stretching), 907 (C-H bending), 596 (C-Br).

^{1}H NMR (400 MHz $CDCl_3$): δ 6.53, (1H, d, *J* 4, H1-Cel), 5.54, (1H, t, *J* 9.7x(2), H3- Cel), 5.06-5.18, (2H, m, H4'-, H3'-Cel), 4.95, (1H, dd, *J* 9.2, 8.1, H2'-Cel), 4.77, (1H, dd, *J* 10, 4, H2-Cel), 4.52-4.56, (2H, m, H6b-, H1'-Cel), 4.38, (1H, dd, *J* 12.5, 4.4, H6a'-Cel), 4.15-4.22, (2H, m, H6a-, H4-Cel), 4.05, (1H, dd, *J* 12.5, 2.2, H6b'-Cel), 3.84, (1H, t, *J* 9.7x(2), H5-Cel), 3.66-3.70, (1H, m, H5'-Cel), 2.15, (3H, s, OAc), 2.10, (6H, s, OAc), 2.05, (6H, s, OAc), 2.02, (3H, s, OAc), 1.99, (3H, s, OAc) (Xu *et al*., 2008).

^{13}C NMR (100 MHz $CDCl_3$): δ 170.5, 170.2, 170.1, 170.0, 169.3, 169.3, 168.9 (C=O); 100.5, 86.4, 75.2, 72.9, 72.9, 72.0, 71.5, 70.7, 69.4, 67.7, 61.5, 60.9 (C-Cellobiose); 20.8, 20.7, 20.6, 20.5 (OAc-Cellobiose).

10.3 Glycosylation of Hydroxyarylaldehyde (General procedure)

2,3,4,6-Tetra-*O*-acetyl-*α*-D-glucopyranosyl bromide (1 eq) and hydroxybenzaldehyde (1 eq) were dissolved in anhydrous MeCN (100 mL). Silver(I) oxide (freshly prepared) (4.2 eq) was added and the reaction was stirred for 4 h at r.t. The solvent was subsequently evaporated under reduced pressure and the resulting residue was taken up in EtOAc, filtered and the solvent was removed. The crude mixture was purified by silica gel column chromatography to afford the corresponding glycosylated aldehydes (Stavila *et al*., 2008).

10.3.1 4-(2',3',4',6'-Tetra-*O*-acetyl-*β*-D-glucopyranosyloxy)benzaldehyde 142

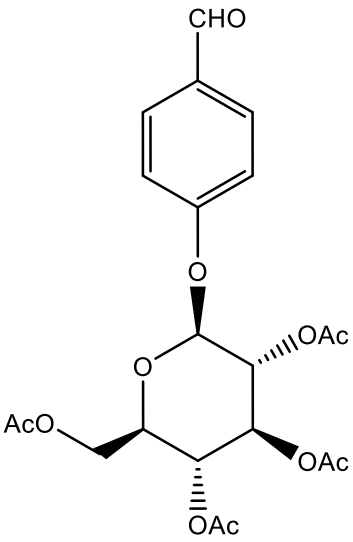

142

Compound **142** was synthesised according to the general procedure from 4-hydroxybenzaldehyde (2.44 g, 20 mmol), 2,3,4,6-tetra-*O*-acetyl-*α*-D-glucopyranosyl bromide (8.22 g, 20 mmol) and silver(I) oxide (freshly prepared) (20 g, 84 mmol) in anhydrous MeCN (200 mL). The reaction was stirred for 16 h at r.t. The crude mixture was purified by silica gel column chromatography using EtOAc: Pet. ether (1:1.5) as eluent to afford white crystals of compound **142** (6.23 g, 13.77 mmol).

Yield: 69%

R_f of compound **142** (EtOAc: Pet. ether, 1:1.5): 0.12

Mp: 134-136 ^{0}C

Vmax (cm^{-1}): 2962 (C-H stretching), 1733 (C=O ester), 1690 (C=O aldehyde), 1599, 1504 (C=C arene), 1365 (C-H bending), 1217, 1034 (C-O stretching).

^{1}H NMR (400 MHz $CDCl_3$): δ 9.95, (1H, s, CHO), 7.88, (2H, d, *J* 7.8, H2,6-Ar), 7.13, (2H, d, *J* 7.9, H3,5-Ar), 5.19-5.36, (4H, m, H3',4',2',1'-Glu), 4.32, (1H, dd, *J* 5.4, 5.5, H6b'-Glu), 4.21, (1H, dd, *J* 2.3, H6a'-Glu), 3.94-3.98, (1H, m, H5'-Glu), 2.07-2.10, (12H, OAc) (Wang *et al*., 2007).

^{13}C NMR (100 MHz $CDCl_3$): δ 190.6 (CHO); 170.4, 170.1, 169.3, 169.1 (C=O); 161.2, 131.9, 131.8, 116.8 (aromatic carbons); 98.1, 72.5, 72.3, 71.0, 68.1, 61.9 (C-Glucose); 20.6, 20.5 (OAc-Glucose).

10.3.2 3-(2',3',4',6'-Tetra-*O*-acetyl-*β*-D-glucopyranosyloxy)benzaldehyde 143

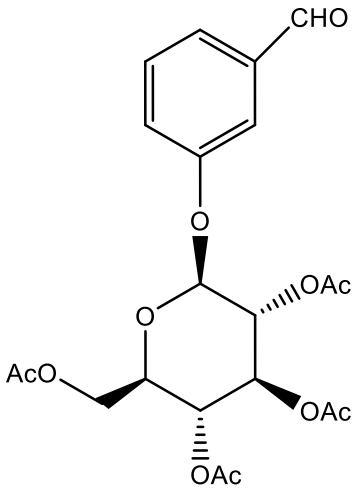

143

Compound **143** was synthesised similarly to compound **142** from 3-hydroxybenzaldehyde (1.22 g, 10 mmol), 2,3,4,6-tetra-*O*-acetyl-*α*-D-glucopyranosyl bromide (4.11 g, 10 mmol) and silver(I) oxide (freshly prepared) (10 g, 42 mmol) in anhydrous MeCN (100 mL). The crude mixture was purified by silica gel column chromatography using EtOAc: Pet. ether (1:1.5) as eluent to afford off-whit crystals of compound **143** (2.96 g, 6.54 mmol).

Yield: 65%

R_f of compound **143** (EtOAc: Pet. ether, 1:1.5): 0.10

Mp: 99-102 ^{0}C

Vmax (cm^{-1}): 2940, 2863 (C-H stretching), 1745, 1731 (C=O ester), 1696 (C=O aldehyde), 1592, 1482 (C=C arene), 1365 (C-H bending), 1205, 1031 (C-O stretching).

^{1}H NMR (400 MHz $CDCl_3$): δ 9.98, (1H, s, CHO), 7.59, (1H, m, H5-Ar), 7.50, (2H, m, H2,6-Ar), 7.27, (1H, m, H4-Ar), 5.31-5.33, (2H, m, H3',4'-Glu), 5.14-5.20 (2H, m, H2',1'-Glu), 4.18-4.29, (2H, m, H6'-Glu), 3.93-3.97 (1H, m, H5'-Glu), 2.10, (3H, s, OAc), 2.08, (3H, s, OAc), 2.07, (3H, s, OAc), 2.05, (3H, s, OAc) (Laville *et al*., 2004).

^{13}C NMR (100 MHz $CDCl_3$): δ 191.5 (CHO); 170.7, 170.2, 170.1, 169.6, 169.4, 169.3 (C=O); 157.2, 137.8, 130.3, 126.0, 123.7, 115.0 (aromatic carbons); 98.5, 72.6, 72.2, 71.0, 68.1, 61.9 (C-Glucose); 20.7, 20.7, 20.7, 20.6, 20.6 (OAc-Glucose).

10.3.3 2-(2',3',4',6'-Tetra-*O*-acetyl-*β*-D-glucopyranosyloxy)benzaldehyde 144

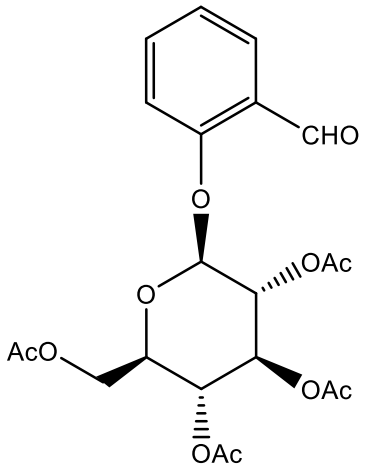

144

Compound **144** was synthesised similarly to compound **142** from 2-hydroxybenzaldehyde (2.44 g, 20 mmol), 2,3,4,6-tetra-*O*-acetyl-*α*-D-glucopyranosyl bromide (8.22 g, 20 mmol) and silver(I) oxide (freshly prepared) (20 g, 42 mmol) in anhydrous MeCN (200 mL). The crude mixture was purified by silica gel column chromatography using EtOAc: Pet. ether (1:1) as eluent to afford white crystals of compound **144** (2.40 g, 5.30 mmol).

Yield: 27%

R_f of compound **144** (EtOAc: Pet. ether, 1:1): 0.65

Mp: 126-128 ^{0}C

Vmax (cm^{-1}): 2961 (C-H stretching), 1745 (C=O ester), 1682 (C=O aldehyde), 1600, 1483 (C=C arene), 1364 (C-H bending), 1203, 1036 (C-O stretching).

^{1}H NMR (300 MHz $CDCl_3$): δ 10.36, (1H, d, *J* 0.8, CHO), 7.88, (1H, dd, *J* 7.7, H6-Ar), 7.56-7.61, (1H, m, H4-Ar), 7.12-7.24 (2H, m, H3,5-Ar), 5.32-5.43, (2H,

m, H3',4'-Glu), 5.19-5.25, (2H, m, H1',2'-Glu), 4.32, (1H, dd, *J* 5.1, 5.3, H6'-Glu), 4.2, (1H, dd, *J* 2.4, 2.6, H6'-Glu), 3.90-3.95, (1H, m, H5'-Glu), 2.10, (3H, s, OAc), 2.08, (6H, d, OAc), 2.07, (3H, s, OAc) (Chen *et al*., 2012).

^{13}C NMR (100 MHz $CDCl_3$): δ 189.1 (CHO); 170.5, 170.1, 169.3, 169.2 (C=O); 158.7, 135.7, 128.3, 126.1, 123.6, 115.9 (aromatic carbons); 99.0, 72.4, 72.2, 70.8, 68.1, 61.7 (C-Glucose); 20.8, 20.8, 20.7, 20.6, 20.5 (OAc-Glucose).

10.3.4 4-(2',3',4',6'-Tetra-*O*-acetyl-*β*-D-galactopyranosyloxy)benzaldehyde 152

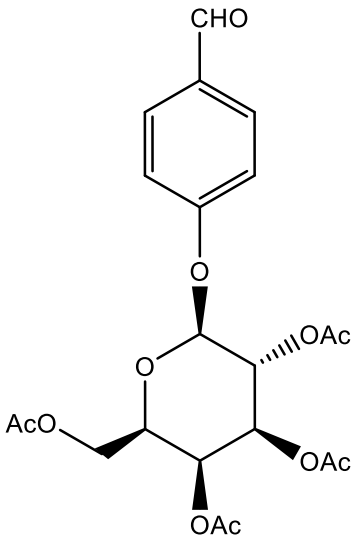

152

Compound **152** was synthesised similarly to compound **143** from 4-hydroxybenzaldehyde (1.22 g, 10 mmol), 2,3,4,6-tetra-*O*-acetyl-*α*-bromo-D-galactopyranose (4.11 g, 10 mmol) and silver(I) oxide (freshly prepared) (10 g, 42 mmol) in anhydrous MeCN (100 mL). The crude mixture was purified by silica gel column chromatography using EtOAc: Pet. ether (1:1) as eluent to afford a white solid of compound **152** (3.39 g, 7.49 mmol).

Yield: 74%

R_f of compound **152** (EtOAc: Pet. ether, 1:1): 0.32

Vmax (cm^{-1}): 1744 (C=O ester), 1692 (C=O aldehyde), 1600, 1583, 1507 (C=C arene), 1367 (C-H bending), 1209, 1042 (C-O stretching), 752 (C-H bending).

^{1}H NMR (400 MHz $CDCl_3$): δ 9.93, (1H, s, CHO), 7.86, (2H, d, *J* 8.2, H2,6-Ar), 7.12, (2H, d, *J* 8.7, H3,5-Ar), 5.53, (1H, dd, *J* 10.5, 7.9, H4'-Gal), 5.48, (1H, d, *J* 3.4, H2'-Gal), 5.18, (1H, d, *J* 7.9, H1'-Gal), 5.14, (1H, dd, *J* 10.4, 3.4, H3'-Gal), 4.11-4.26, (3H, m, H5', H6'-Gal), 2.19, (3H, s, OAc), 2.07, (6H, s, OAc), 2.03, (3H, s, OAc) (Wen *et al*., 2008).

^{13}C NMR (100 MHz $CDCl_3$): 190.7 (CHO); 170.3, 170.1, 170.0, 169.3 (C=O); 161.3, 131.8, 116.7 (aromatic carbons); 98.6, 71.3, 70.6, 68.4, 66.7, 61.3 (C-Galactose); 20.7, 20.6, 20.6, 20.5 (OAc-Galactose).

10.3.5 4-(2’,3’,6’,2’’,3’’,4’’,6’’-Heptaacetyl-*β*-D-lactosyl)benzaldehyde **157**

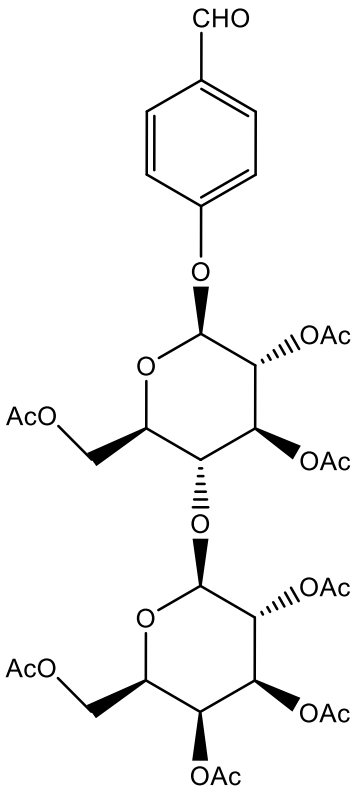

157

Compound **157** was synthesised similarly to compound **142** from 4-hydroxybenzaldehyde (0.73 g, 6 mmol), 2,3,6,2’,3’,4’,6’-hepta-*O*-acetyl-*α*-D-lactosyl bromide (4.19 g, 6 mmol) and silver(I) oxide (freshly prepared) (5.83 g, 25.20 mmol) in anhydrous MeCN (60 mL). The reaction was stirred for 5 h at r.t. The crude mixture was purified by silica gel column chromatography using EtOAc: Pet. ether (1:1) as eluent to afford white crystals of compound **157** (2.74 g, 3.70 mmol).

Yield: 60%

R_f of compound **157** (EtOAc: Pet. ether, 1:1): 0.26

Mp: 75-76 ^{0}C

Vmax (cm^{-1}): 3024 (C-H stretching), 1742 (C=O ester), 1693 (C=O aldehyde), 1601, 1583, 1508 (C=C arene), 1367 (C-H bending), 1211, 1165, 1043 (C-O stretching), 750 (C-H bending).

^{1}H NMR (400 MHz $CDCl_3$): δ 9.93, (1H, s, CHO), 7.85, (2H, d, *J* 4.8, H2,6-Ar), 7.08, (2H, d, *J* 5, H3,5-Ar), 5.37, (1H, d, *J* 2.6, H3'-Lac), 5.18-5.33, (3H, m, H1',3'',4''-Lac), 5.14, (1H, dd, *J* 10.5, 7.9, H2''-Lac), 4.98, (1H, dd, *J* 10.4, 3.4, H2'-Lac), 4.50-4.53, (2H, m, H1'',6'-Lac), 4.07-4.18, (3H, m, H6',6''-Lac), 3.83-3.94, (3H, m, H4',5',5''-Lac), 2.16, (3H, s, OAc), 2.09, (3H, s, OAc), 2.08, (3H, s, OAc), 2.07, (9H, s, OAc), 1.98, (3H, s, OAc) (Wen *et al*., 2008).

^{13}C NMR (100 MHz $CDCl_3$): δ 190.6 (CHO); 170.4, 170.3, 170.2, 170.1, 170.0, 169.6, 169.5, 169.1 (C=O); 161.2, 131.8, 116.7 (aromatic carbons); 101.1, 97.7, 76.0, 73.0, 72.6, 71.2, 70.9, 70.7, 69.0, 66.5, 61.9, 60.8 (C-Lactose); 20.7, 20.7, 20.6, 20.5 (OAc-Lactose).

10.3.6 4-(2',3',6',2'',3'',4'',6''-Heptaacetyl-*β*-D-cellobiosyl)benzaldehyde 162

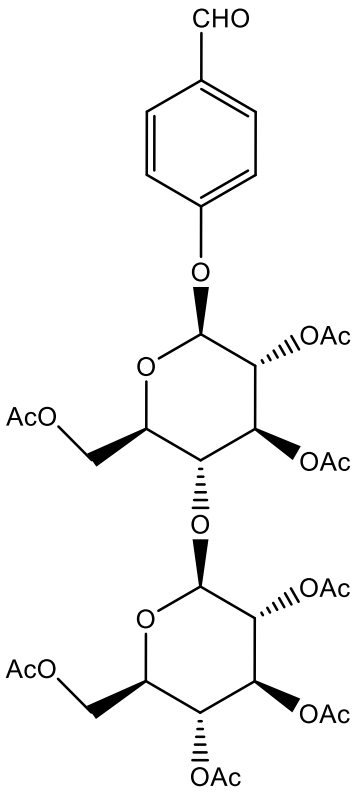

162

Compound **162** was synthesised similarly to compound **157** from 4-hydroxybenzaldehyde (0.73 g, 6 mmol), 2,3,6,2',3',4',6'-hepta-*O*-acetyl-*α*-D-cellobiosyl bromide (4.19 g, 6 mmol) and silver(I) oxide (freshly prepared) (5.83 g, 25.20 mmol) in anhydrous MeCN (60 mL). The reaction was stirred for 5 h at r.t. The crude mixture was purified by silica gel column chromatography using EtOAc: Pet. ether (1.5:1) as eluent to afford white crystals of compound **162** (2.77 g, 3.74 mmol).

Yield: 62%

R_f of compound **162** (EtOAc: Pet. ether, 1.5:1): 0.44

Mp: 192-194 ^{0}C

Vmax (cm^{-1}): 2962 (C-H stretching), 1743 (C=O ester), 1699 (C=O aldehyde), 1602, 1508 (C=C arene), 1366 (C-H bending), 1216, 1165, 1034 (C-O stretching).

^{1}H NMR (400 MHz $CDCl_3$): δ 9.93, (1H, s, CHO), 7.85, (2H, d, *J* 5, H2,6-Ar), 7.08, (2H, d, *J* 8.7, H3,5-Ar), 5.06-5.32, (5H, m, H1',3',2'',3'',4''-Cel), 4.96, (1H, dd, *J* 9.2, 8, H2'-Cel), 4.53-4.56, (2H, m, H1'',6'-Cel), 4.39, (1H, dd, *J* 12.5, 4.3, H6''-Cel), 4.14, (1H, dd, *J* 11.9, 5.6, H6'-Cel), 4.06, (1H, dd, *J* 12.5, 2.1, H6''-Cel), 3.80-3.91, (2H, m, H4',5'-Cel), 3.66-3.71, (1H, m, H5''-Cel), 2.11, (3H, s, OAc), 2.09, (3H, s, OAc), 2.06, (9H, m, OAc), 2.02, (3H, s, OAc), 2, (3H, s, OAc) (Griesbeck *et al*., 2011).

^{13}C NMR (100 MHz $CDCl_3$): δ 190.7 (CHO); 170.5, 170.2, 170.1, 169.7, 169.5, 169.3, 169.0 (C=O); 161.2, 131.8, 131.7, 116.7 (aromatic carbons); 100.8, 97.8, 76.2, 73.0, 72.8, 72.3, 72.0, 71.5, 71.1, 67.6, 61.8, 61.5 (C-Cellobiose); 20.7, 20.6, 20.6, 20.5, 20.5 (OAc-Cellobiose).

10.4 Synthesis of calix[4]resorcinarene glycosides (General procedure)

To a stirred solution of aldehyde (1 eq) in a mixture of Et_2O and THF (1:1 ratio, 40 mL) was added a solution of $AlCl_3.PhNO_2$ (4 eq) and the mixture was stirred under nitrogen for 15 min. Subsequently, resorcinol (1 eq) was added and the mixture was stirred at r.t for a further 48 h. A precipitate was obtained by adding the reaction mixture to Et_2O (200 mL). The precipitate was filtered and washed many times with Et_2O. The solid was then dissolved in EtOAc and the organic

layer was washed with water (100 mL x 2) then dried ($MgSO_4$). The solvent was evaporated under reduced pressure to give the desired compounds as crude solid (Curtis 1997).

10.4.1 Calix[4]resorcinarene glucoside 145

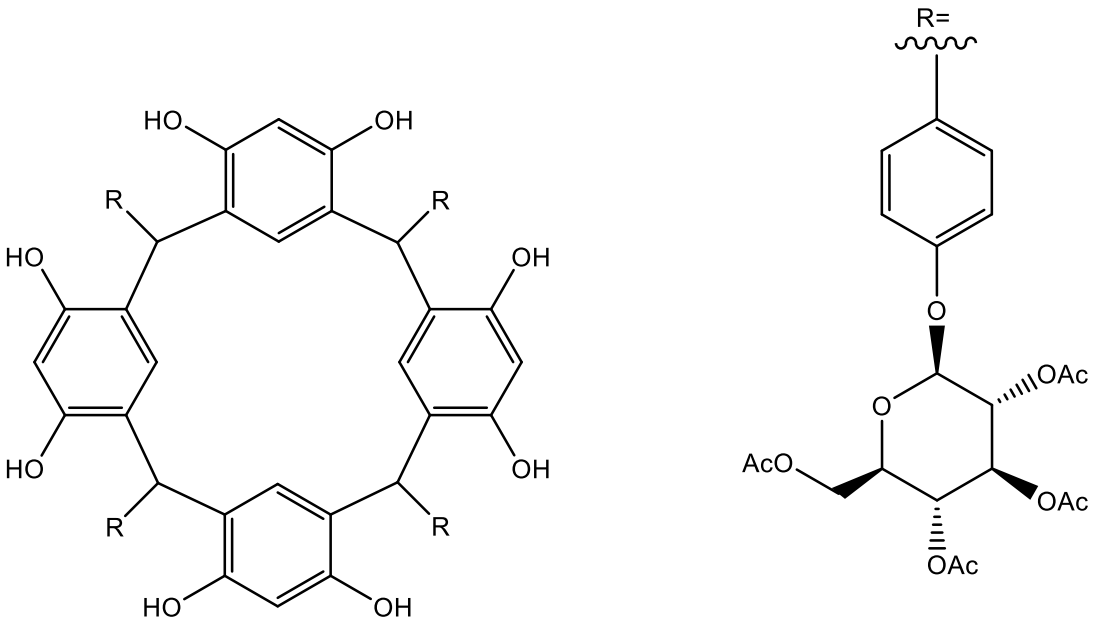

145

Compound **145** was synthesised according to the general procedure from 4-(2',3',4',6'-tetra-*O*-acetyl-*β*-D-glucopyranosyloxy)benzaldehyde (4.88 g, 10.79 mmol), resorcinol (1.18 g, 10.79 mmol) and $AlCl_3.PhNO_2$ (4.60 mL, 43.14 mmol) in a mixture of Et_2O and THF (1:1 ratio, 50 mL) gave a red precipitate of the desired compound (4.46 g, 2.04 mmol, 19%). A portion of the crude mixture was purified by preparative TLC using DCM: MeOH (4.5:0.5) as eluent to afford a red precipitate of compound **145**.

R_f of compound **145** (DCM: MeOH, 4.5:0.5): 0.31

Vmax (cm^{-1}): 3445 (O-H stretching), 1742 (C=O ester), 1604, 1505 (C=C arene), 1431, 1367 (C-H bending), 1212, 1033 (C-O stretching).

^{1}H NMR (400 MHz d_6-acetone): δ 7.19-8.22, (8H, m, ArOH), 6.67-7.19, (16H, m, H2',3',5',6'-Ar), 6.57, (2H, d, H2-Ar), 6.48, (2H, s, H2-Ar), 6.24-6.45, (2H, m, H5-Ar), 5.93, (2H, s, H5-Ar), 5.84, (2H, s, ArCH), 5.72, (2H, s, ArCH), 5.03-5.63, (16H, m, H1'',2'',3'',4''-Glu), 4.47, (2H, dd, *J* 11.5; 6.4, H6''-Glu), 4.08-4.38, (10H, m, H5'',6''-Glu), 1.94-2.12, (48H, m, OAc).

^{13}C NMR (100 MHz d_6-acetone): δ 170.1, 170.0, 169.9, 169.4, 169.4, 169.4, 169.3, 169.1, 169.1, 169.0, 169.0 (C=O); 155.3, 155.2, 153.5, 153.2, 153.0, 139.5, 138.1, 131.9, 131.5, 130.3, 130.0, 129.7, 115.9, 115.5, 106.5 (aromatic carbons); 99.7, 72.7, 71.7, 71.4, 68.7, 62.1 (C-Glucose); 41.9 (ArCH); 20.0, 19.9, 19.9, 19.8, 19.8, 19.7, 19.7 (OAc-Glucose).

Mass Spectrum: Expected: *m*/*z* 1106.3506 $(M+2NH_4)^{2+}$. Observed: *m*/*z* 1106.3512

10.4.2 Calix[4]resorcinarene glucoside 146

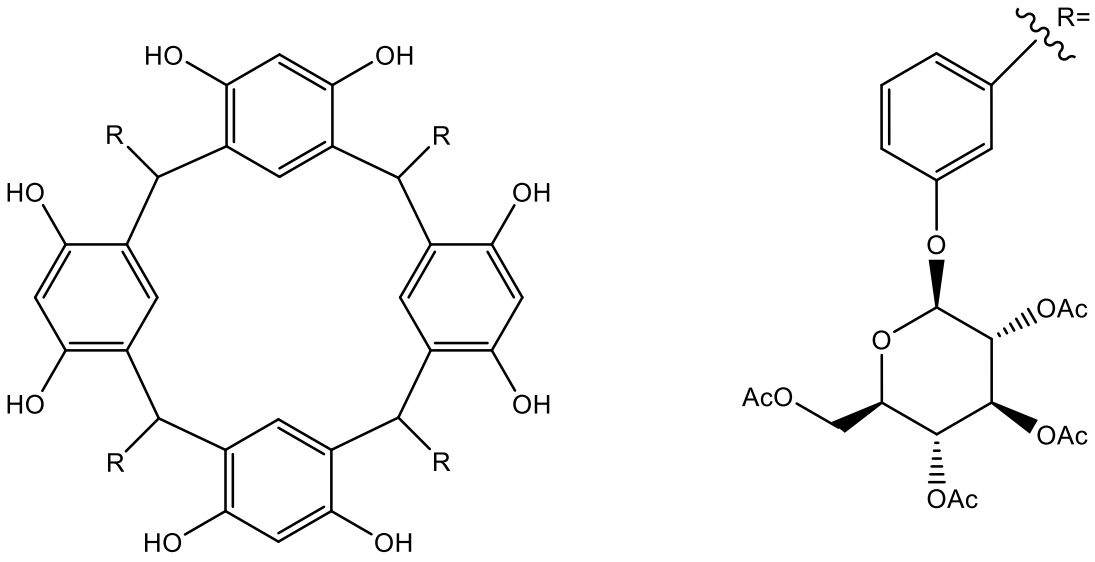

146

Compound **146** was synthesised according to the general procedure from 3-(2',3',4',6'-tetra-*O*-acetyl-*β*-D-glucopyranosyloxy)benzaldehyde (2.26 g, 5 mmol), resorcinol (0.55 g, 5 mmol) and $AlCl_3.PhNO_2$ (2.13 mL, 20 mmol) in a mixture of Et_2O and THF (1:1 ratio, 40 mL) gave a red precipitate of the desired compound (1.94 g, 0.89 mmol, 18%). A portion of the crude mixture was purified by chromatotron chromatography using DCM: MeOH: EtOAc (4:0.4:0.6) as eluent to afford a red precipitate of compound **146**.

R_f of compound **146** (DCM: MeOH: EtOAc, 4:0.4:0.6): 0.37

Mp: 190-194 ^{0}C

Vmax (cm^{-1}): 3463 (O-H stretching), 1739 (C=O ester), 1606, 1486 (C=C arene), 1433, 1367 (C-H bending), 1212, 1033 (C-O stretching), 907, 840, 786 (C-H bending).

^{1}H NMR (400 MHz d_6-acetone): δ 7.23-8.17, (8H, m, ArOH), 6.28-7.19, (20H, m, H2,2',4',5',6'-Ar), 5.86-6.21, (4H, m, H5-Ar), 5.50-5.63, (4H, s, ArCH), 4.84-5.38, (16H, m, H1'',2'',3'',4''-Glu), 3.82-4.39, (12H, m, H5'',6''-Glu), 1.79-1.96, (48H, m, OAc).

Mass Spectrum: Expected: *m*/*z* 1106.3506 $(M+2NH_4)^{2+}$. Observed: *m*/*z* 1106.3500

10.4.3 Calix[4]resorcinarene glucoside 148

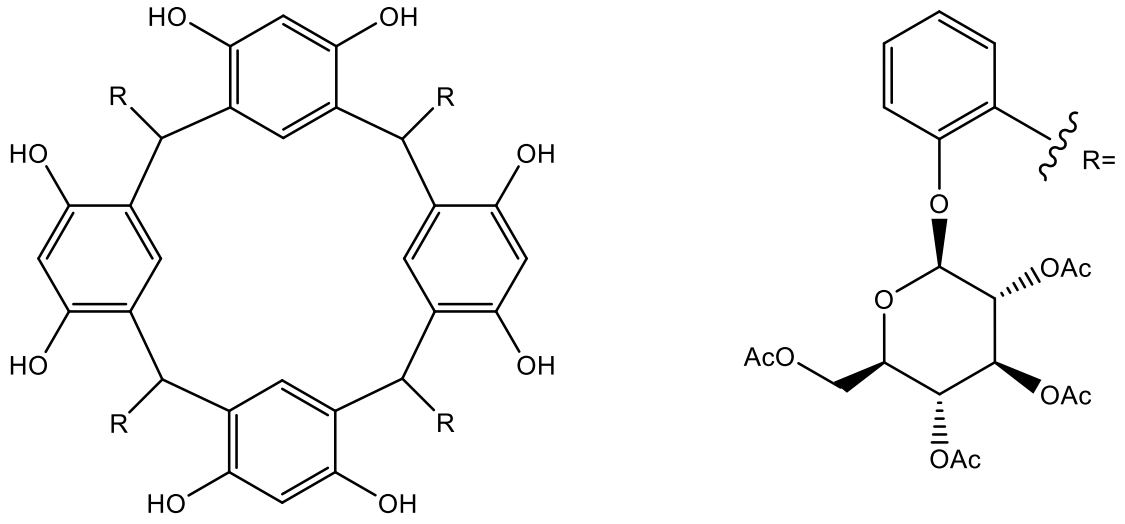

148

Compound **148** was synthesised according to the general procedure from 2-(2',3',4',6'-tetra-*O*-acetyl-*β*-D-glucopyranosyloxy)benzaldehyde (2.26 g, 5 mmol), resorcinol (0.55 g, 5 mmol) and $AlCl_3.PhNO_2$ (2.13 mL, 20 mmol) in a mixture of Et_2O and THF (1:1 ratio, 40 mL) gave a red precipitate of the desired compound (2.40 g, 1.10 mmol, 22%). A portion of the crude mixture was purified by preparative TLC using DCM: MeOH (4.5:0.5) as eluent to afford a red precipitate of compound **148**.

R_f of compound **148** (DCM: MeOH, 4.5:0.5): 0.27

^{1}H NMR (300 MHz d_6-acetone): δ 7.55-7.82, (8H, brs, ArOH), 7.28, (2H, d, *J* 7.7, ArH), 6.95-7.12, (4H, q, ArH), 6.86, (4H, d, *J* 8.1, ArH), 6.66-6.79, (4H, m, ArH), 6.48-6.61, (2H, d, ArH), 6.3, (4H, s, H2,5-Ar), 6.17, (2H, s, H2-Ar), 5.89, (4H, d, *J* 20, ArCH), 5.46, (2H, s, H5-Ar), 5.10-5.39, (10H, m, H1'',3'',4''-Glu), 5.03, (4H, t, *J* 9.2$_x$(2), H2''-Glu), 4.72, (2H, d, H1''-Glu), 4.41-4.57, (2H, dd, H6''-Glu), 4.19-4.38, (4H, m, H6''-Glu), 4.06-4.17, (4H, m, H5'',6''-Glu), 3.39-4.04, (2H, m, H5''-Glu), 1.84-2.27, (48H, m, OAc).

Mass Spectrum: Expected: *m*/*z* 1106.3506 $(M+2NH_4)^{2+}$. Observed: *m*/*z* 1106.3497

10.4.4 Calix[4]resorcinarene galactoside 153

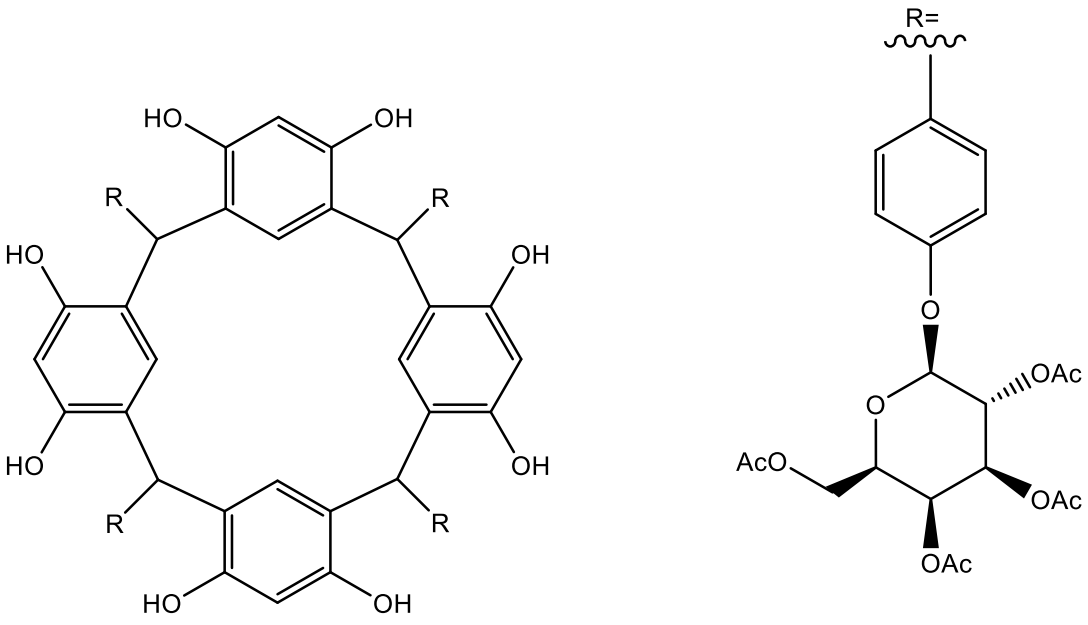

153

To a stirred solution of 4-(2',3',4',6'-tetra-*O*-acetyl-*β*-D-galactopyranosyloxy)benzaldehyde (1.50 g, 3.31 mmol) in Et_2O (20 mL) was

added $BF_3.Et_2O$ (0.40 mL, 3.31 mmol) and the mixture was stirred under nitrogen for 15 min. Subsequently, resorcinol (0.36 g, 3.31 mmol) was added and the mixture was stirred at r.t for a further 24 h. A precipitate was obtained by adding the reaction mixture to Et_2O (200 mL). The precipitate was filtered and washed many times with Et_2O. The solid was then dissolved in EtOAc and the organic layer was washed with water (100 mL x 2) then dried ($MgSO_4$). The solvent was evaporated under reduced pressure to give the desired compound as yellow crystals.

10.4.5 Calix[4]resorcinarene lactoside 158

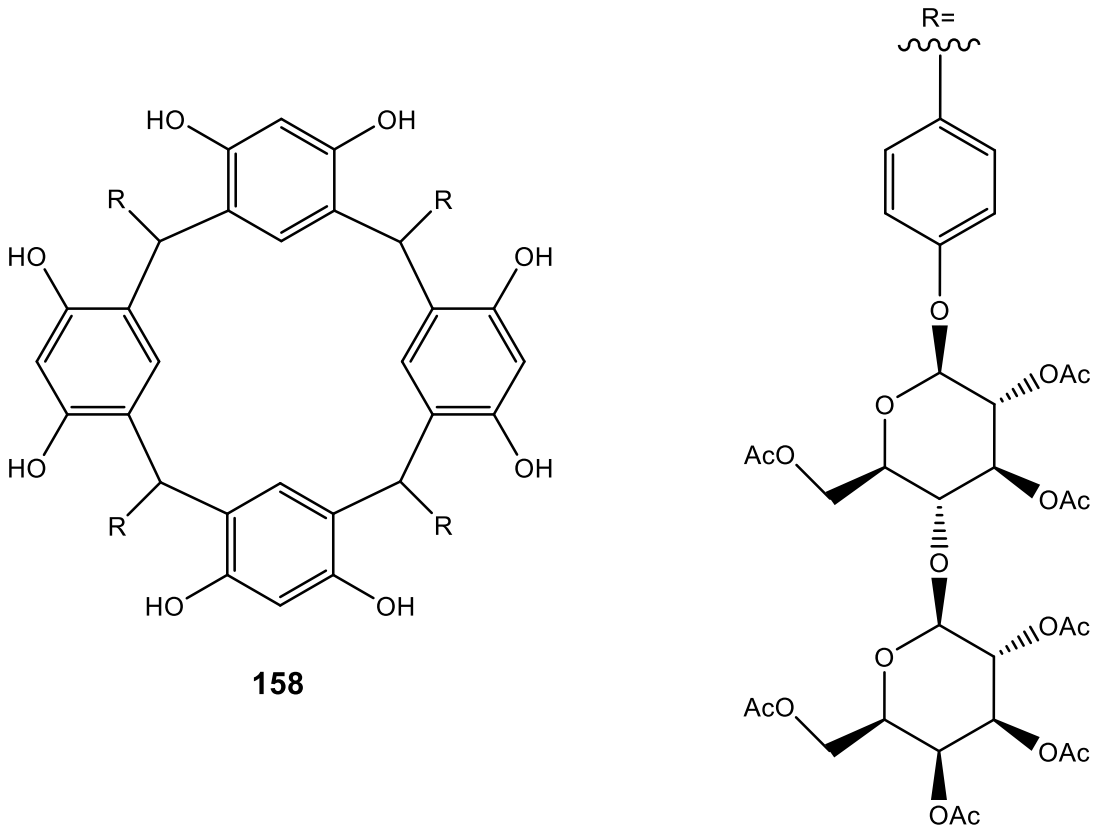

158

Compound **158** was synthesised similarly to compound **153** from 4-(2',3',6',2'',3'',4'',6''-heptaacetyl-*β*-D-lactosyl)benzaldehyde (2.00 g, 2.70 mmol), resorcinol (0.29 g, 2.70 mmol) and $BF_3.Et_2O$ (0.66 mL, 5.40 mmol) in a mixture

of Et_2O: THF (1.5:1 ratio, 25 mL). The reaction was stirred for 48 h at r.t. The crude mixture was obtained as a red powder (1.97 g, 0.59 mmol, 22%).

10.4.6 Calix[4]resorcinarene cellobioside 163

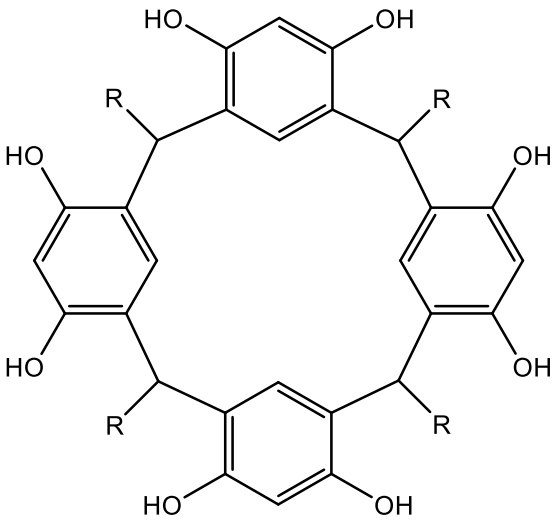

163

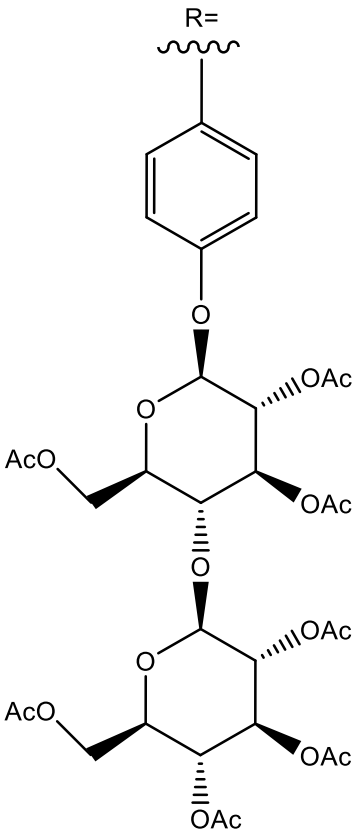

To a stirred solution of 4-(2',3',6',2'',3'',4'',6''-heptaacetyl-*β*-D-cellobiosyl)benzaldehyde (0.53 g, 0.71 mmol) and resorcinol (0.07 g, 0.71 mmol) in anhydrous DCM (15 mL) was added $BF_3.Et_2O$ (0.17 mL, 1.43 mmol) and stirring was continued overnight under N_2 atmosphere. The reaction mixture was then diluted with water (20 mL) and DCM (40 mL); the organic layer was washed with brine (50 mL), dried ($MgSO_4$) and evaporated under reduced pressure to give the title compound as a yellow solid (0.23 g, 0.07 mmol, 10%) (Kumar and Venkatakrishnan 2018).

Mass Spectrum: Expected: *m*/*z* 1682.5195 $(M+2NH_4)^{2+}$. Observed: *m*/*z* 1682.5200

10.5 Esterfication of calix[4]resorcinarene glycosides and analogues (General procedure)

To a suspension of the crude calix[4]resorcinarene glycoside in pyridine (5 mL), butyric anhydride (30 mL) was added and the mixture was stirred overnight at 80 ^{0}C. The solvents were removed using vacuum distillation giving a brown oily mixture, that was separated by silica gel column chromatography to yield the butyrated calix[4]resorcinare glycosides (Curtis 1997).

10.5.1 Acylated calix[4]resorcinarene glucoside 137

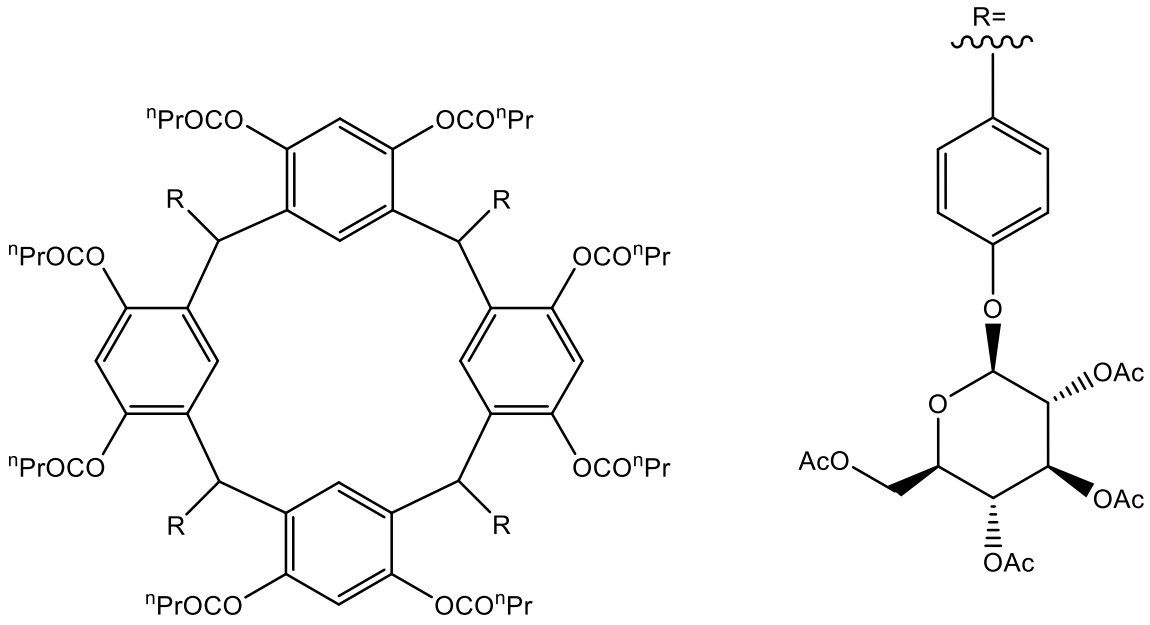

137

Compound **137** was synthesised according to the general procedure. The crude mixture of calix[4]resorcinarene glucoside **145** (4.46 g, 2.04 mmol) was reacted with butyric anhydride (60 mL) and pyridine (10 mL), the crude product was

separated by silica gel column chromatography using EtOAc: Pet. ether (2:1) as eluent to yield the major (2.24 g, 0.82 mmol) and the minor (0.28 g, 0.10 mmol) isomers of the butyrated calix[4]resorcinarene glucosides.

Major isomer 137a

Yield: 40%

R_f of compound **137a** (EtOAc: Pet. ether, 2:1): 0.26

Mp: 230-233 ^{0}C

Vmax (cm^{-1}): 2968 (C-H stretching), 1746 (C=O ester), 1608, 1507, 1490 (C=C arene), 1366 (C-H bending), 1216, 1130, 1033 (C-O stretching), 907 (C-H bending).

^{1}H NMR (400 MHz $CDCl_3$): δ 7.06, (2H, s, H2-Ar), 6.95, (2H, s, H2-Ar), 6.85, (2H, s, ArH), 6.75, (4H, d, *J* 8.8, ArH), 6.54-6.67, (10H, m, ArH), 6.28, (2H, d, *J* 3.2, H5-Ar), 6.03, (2H, s, H5-Ar), 5.56, (2H, s, ArCH), 5.47, (2H, s, ArCH), 5.22-5.45, (12H, m, H2'',3'',4''-Glu), 4.87-5.00, (4H, m, H1''-Glu), 4.41-4.55, (4H, m, H6''-Glu), 4.13-4.22, (4H, m, H6''-Glu), 4.06, (2H, ddd, *J* 6.2x(2); 3.5, H5''-Glu), 3.98, (2H, ddd, *J* 6.5x(2); 3.1, H5''-Glu), 2.16-2.42, (16H, m, $COCH_2$), 1.99-2.14, (48H, m, OAc-Glu), 1.42-1.60, (16H, m, CH_2), 0.79-0.94, (24H, m, CH_3).

^{13}C NMR (100 MHz $CDCl_3$): δ 171.2, 171.1, 170.4, 170.1, 170.0, 169.6, 169.4, 169.2 (C=O); 156.2, 156.1, 147.0, 146.9, 146.8, 146.4, 134.9, 133.9, 132.5, 132.2, 131.8, 131.6, 131.1, 130.2, 130.1, 129.8, 128.8, 117.5, 116.8, 116.1 (aromatic carbons); 100.5, 100.2, 72.9, 72.7, 72.0, 71.9, 71.3, 71.2, 68.7, 68.5, 62.3, 62.2 (C-Glucose); 43.5 (ArCH); 35.8, 35.7, 35.5 ($COCH_2$); 20.6, 20.6, 20.6, 20.5, 20.5, 20.4 (OAc-Glucose); 18.1, 18.0, 18.0 (CH_2); 13.6, 13.5 (CH_3).

Mass Spectrum: Expected: *m*/*z* 1386.5179 $(M+2NH_4)^{2+}$. Observed: *m*/*z* 1386.5177

Minor isomer 137b

Yield: 4%

R_f of compound **137b** (EtOAc: Pet. ether, 2:1): 0.11

Mp: 139-142 ^{0}C

Vmax (cm^{-1}): 2967 (C-H stretching), 1747 (C=O ester), 1608, 1507 (C=C arene), 1366 (C-H bending), 1216, 1131, 1033 (C-O stretching), 907 (C-H bending).

^{1}H NMR (400 MHz $CDCl_3$): δ 6.95, (2H, s, H2-Ar), 6.90, (2H, s, H2-Ar), 6.78, (8H, d, *J* 8.2, ArH), 6.66, (8H, d, *J* 7.8, ArH), 6.15, (2H, s, H5-Ar), 5.91, (2H, s, H5-Ar), 5.53-5.57, (2H, t, H3''-Glu), 5.20-5.47, (10H, m, H2'',3'',4''-Glu), 5.37, (4H, d, *J* 8.7, ArCH), 5.15, (2H, d, *J* 7.9, H1''-Glu), 5.02, (2H, d, *J* 7.9, H1''-Glu), 4.38-4.65, (4H, m, H6''-Glu), 4.02-4.28, (8H, m, H5'',6''-Glu), 2.11-2.48, (16H, m, $COCH_2$), 1.93-2.16, (48H, m, OAc-Glu), 1.36-1.76, (16H, m, CH_2), 0.76-1.09, (24H, m, CH_3).

^{13}C NMR (100 MHz $CDCl_3$): δ 171.6, 170.6, 170.6, 170.5, 170.5, 170.1, 169.9, 169.7, 169.6, 169.3, 169.2 (C=O); 155.9, 147.2, 147.2, 147.1, 147.0, 136.7, 134.3, 132.5, 131.7, 131.7, 131.1, 130.1, 128.7, 117.5, 116.8, 115.7 (aromatic carbons); 99.7, 99.2, 72.7, 72.7, 72.2, 71.8, 71.5, 71.3, 68.3, 68.3, 62.2 (C-Glucose); 44.2, 43.3 (ArCH); 35.9, 35.7, 35.5, 35.4 ($COCH_2$); 20.7, 20.6, 20.6, 20.6, 20.5 (OAc-Glucose); 18.3, 18.1, 17.9, 17.8 (CH_2); 13.7, 13.6, 13.5 (CH_3).

Mass Spectrum: Expected: *m*/*z* 1386.5179 $(M+2NH_4)^{2+}$. Observed: *m*/*z* 1386.5170

10.5.2 Acylated calix[4]resorcinarene glucoside 147

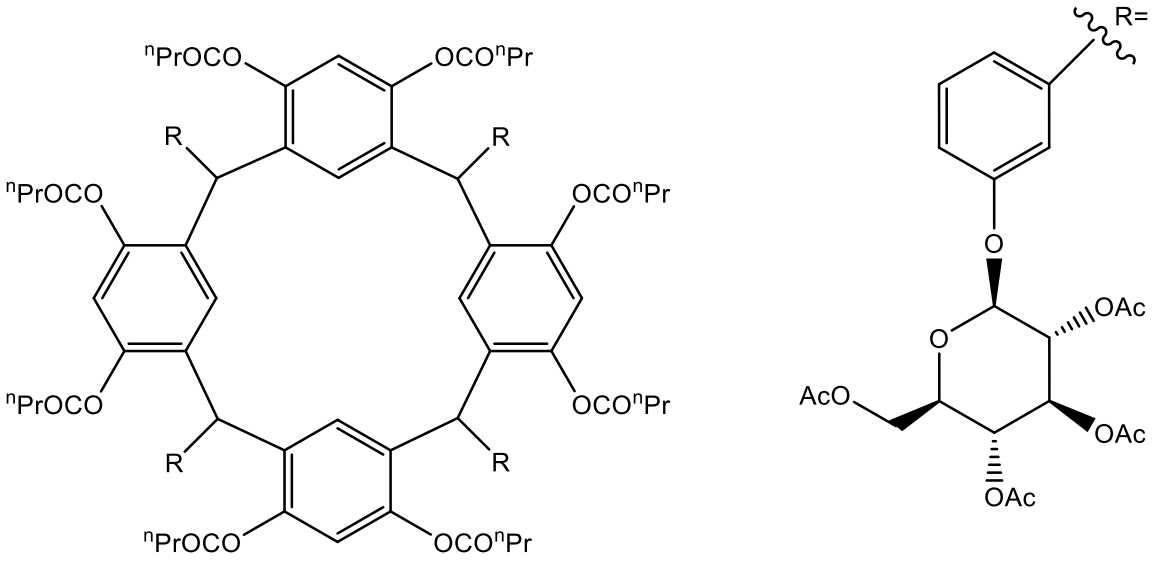

147

Compound **147** was synthesised according to the general procedure. The crude mixture of calix[4]resorcinarene glucoside **146** (1.61 g, 0.74 mmol) was reacted with butyric anhydride (30 mL) and pyridine (5 mL), the crude product was separated by silica gel column chromatography using EtOAc: Pet. ether (2:1) as eluent to yield one product of the butyrated calix[4]resorcinarene glucoside (0.32 g, 0.12 mmol).

Yield: 16%

R_f of compound **147** (EtOAc: Pet. ether, 2:1): 0.41

Mp: 130-133 ^{0}C

Vmax (cm^{-1}): 2967 (C-H stretching), 1746 (C=O ester), 1588, 1487 (C=C arene), 1365 (C-H bending), 1214, 1129, 1034 (C-O stretching), 906 (C-H bending).

^{1}H NMR (400 MHz $CDCl_3$): δ 6.92-7.14, (6H, m, H2,5'-Ar), 6.9, (2H, d, *J* 3.5, H5'-Ar), 6.60-6.76, (4H, m, H4'-Ar), 6.36-6.66, (4H, m, H2'-Ar), 6.25-6.33, (4H, m, H6'-Ar), 6.24, (2H, d, *J* 5.6, H5-Ar), 5.82, (2H, s, H5-Ar), 5.48, (4H, d, *J* 13, ArCH), 5.15-5.38, (12H, m, H2'',3'',4''-Glu), 4.89, (2H, d, *J* 7.7, H1''-Glu), 4.67-4.81, (2H, brs, H1''-Glu), 4.27-4.47, (4H, m, H6''-Glu), 4.03-4.22, (4H, m, H6''-Glu), 3.81-3.98, (4H, m, H5''-Glu), 2.18-2.50, (16H, m, $COCH_2$), 1.94-2.13, (48H, m, OAc-Glu), 1.40-1.58, (16H, m, CH_2), 0.78-0.97, (24H, m, CH_3)

^{13}C NMR (100 MHz $CDCl_3$): δ171.1, 171.1, 170.5, 170.4, 170.4, 170.1, 170.1, 169.5, 169.4, 169.3, 169.2 (C=O); 156.9, 147.1, 141.5, 132.0, 129.4, 123.8, 117.4, 116.9, 116.5 (aromatic carbons); 99.1, 72.8, 71.9, 71.2, 68.4, 62.1 (C-Glucose); 44.3 (ArCH); 35.8, 35.7, 35.5 ($COCH_2$); 20.6, 20.6, 20.5, 20.4 (OAc-Glucose); 18.1, 18.0, 17.9 (CH_2); 13.5, 13.5, 13.4 (CH_3).

Mass Spectrum: Expected: *m/z* 1386.5179 $(M+2NH_4)^{2+}$. Observed: *m/z* 1386.5181

10.5.3 Acylated calix[4]resorcinarene glucoside 149

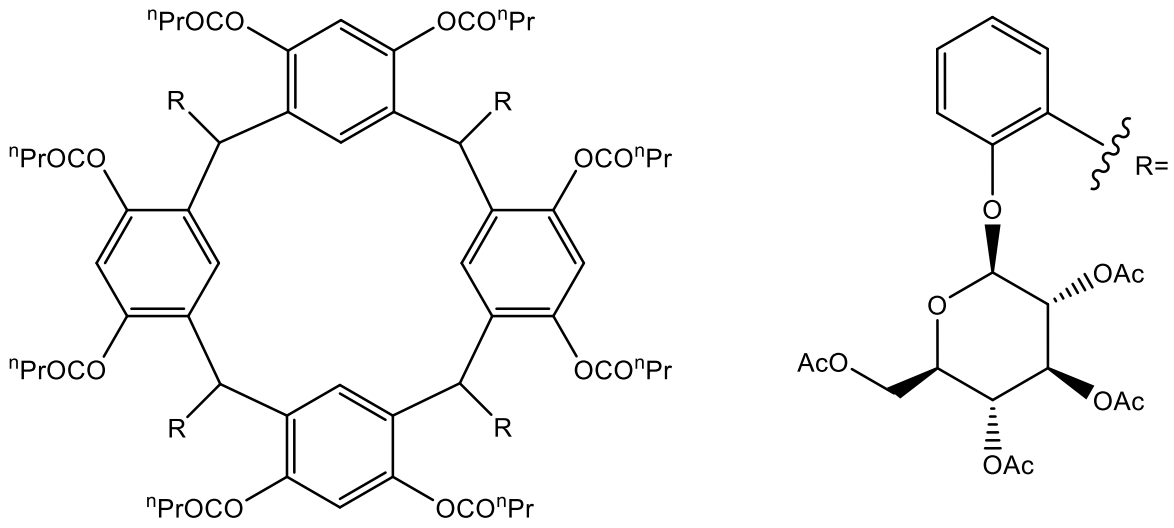

149

Compound **149** was synthesised according to the general procedure. The crude mixture of calix[4]resorcinarene glucoside **148** (2.40 g, 1.10 mmol) was reacted with butyric anhydride (30 mL) and pyridine (5 mL), the crude product was separated by silica gel column chromatography using EtOAc: Pet. ether (2:1) as eluent to yield one product of the butyrated calix[4]resorcinarene glucoside (0.6 g, 0.23 mmol).

Yield: 20%

R_f of compound **149** (EtOAc: Pet. ether, 2:1): 0.36

Mp: 244-247 ^{0}C

Vmax (cm^{-1}): 2966 (C-H stretching), 1747 (C=O ester), 1588, 1489 (C=C arene), 1455, 1366 (C-H bending), 1216, 1131, 1034 (C-O stretching), 906, 750 (C-H bending).

^{1}H NMR (400 MHz $CDCl_3$): δ 7.35, (2H, s, H2-Ar), 7.05-7.15, (2H, m, H4'-Ar), 6.91-7.02, (4H, m, H4',5'-Ar), 6.85, (2H, s, H2-Ar), 6.77, (2H, d, *J* 8.1, H3'-Ar), 6.67, (2H, d, *J* 8.2, H3'-Ar), 6.52-6.62, (4H, m, H5',6'-Ar), 6.24, (2H, dd, *J* 7.6; 1.3, H6'-Ar), 6.11, (2H, s, H5-Ar), 5.92, (2H, s, H5-Ar), 5.80, (4H, d, *J* 18.7, ArCH), 5.4, (2H, t, *J* 9.5x(2), H3''-Glu), 5.14-5.28, (4H, m, H1'',3''-Glu), 4.94-5.10, (6H, m, H2'',4''-Glu), 4.79, (2H, dd, *J* 9.5; 8.1, H2''-Glu), 4.56, (2H, d, *J* 7.9, H1''-Glu), 4.5, (2H, dd, *J* 12.3; 5.7, H6''-Glu), 4.28, (2H, dd, *J* 12.2; 5.7, H6''-Glu), 4.01-4.15, (4H, m, H6''-Glu), 3.93, (2H, ddd, *J* 9.9; 5.7; 2.3, H5''-Glu), 3.85, (2H, ddd, *J* 10; 5.7; 2.2, H5''-Glu), 2.12-2.68, (16H, m, $COCH_2$), 1.91-2.10, 1.24 (48H, m, OAc-Glu), 1.39-1.70, (16H, m, CH_2), 0.70-1.03, (24H, m, CH_3).

^{13}C NMR (100 MHz $CDCl_3$): δ 171.2, 170.8, 170.4, 170.4, 170.2, 169.9, 169.6, 169.6, 169.5, 169.2, 168.9 (C=O); 153.5, 153.4, 147.6, 147.5, 146.7, 146.3, 132.8, 131.5, 131.1, 130.8, 129.4, 129.2, 128.7, 127.6, 126.9, 126.8, 122.0, 117.7, 116.4, 113.0 (aromatic carbons); 98.4, 97.6, 73.0, 72.7, 72.1, 71.4, 69.4, 68.7, 68.2, 62.2 (C-Glucose); 37.2, 37.0 (ArCH); 36.1, 35.9, 35.6, 34.8 ($COCH_2$); 20.8, 20.8, 20.6, 20.6, 20.4 (OAc-Glucose); 18.1, 18.0, 17.8, 17.6 (CH_2); 13.7, 13.6, 13.6, 13.5 (CH_3).

Mass Spectrum: Expected: *m*/*z* 1386.5179 $(M+2NH_4)^{2+}$. Observed: *m*/*z* 1386.5182

10.5.4 Acylated calix[4]resorcinarene galactoside 154

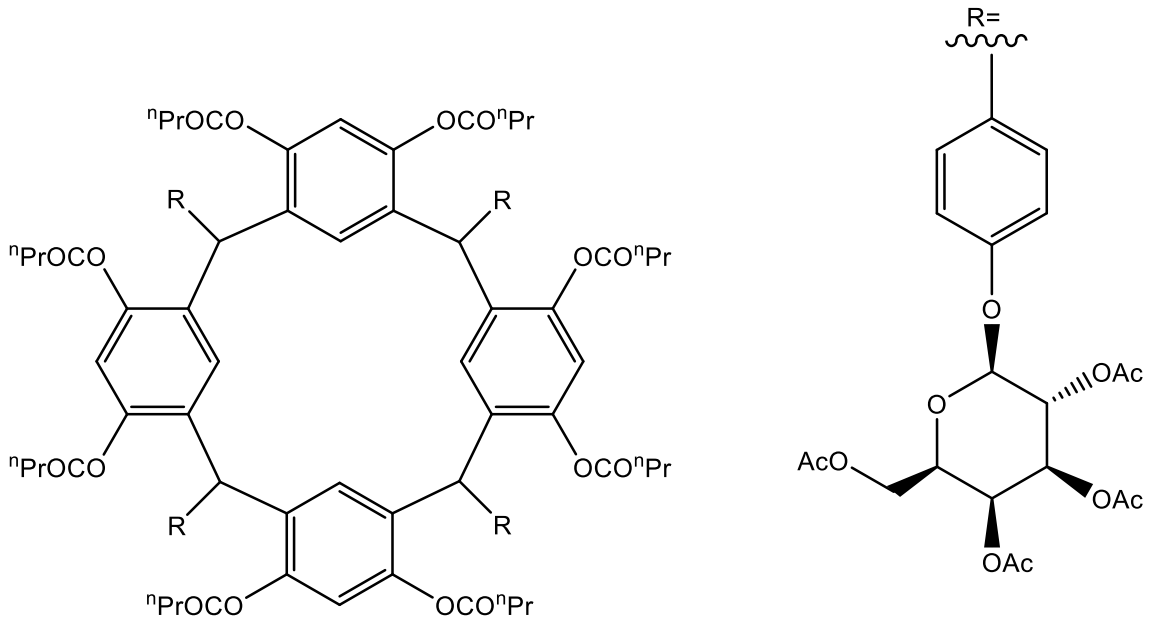

154

Compound **154** was synthesised according to the general procedure. The crude mixture of calix[4]resorcinarene galactoside **153** (1.10 g, 0.50 mmol) was reacted with butyric anhydride (30 mL) and pyridine (5 mL), the crude product was separated by silica gel column chromatography using EtOAc: Pet. ether (1.5:1) as eluent to yield the major (0.19 g, 0.07 mmol) and the minor (0.07 g, 0.02 mmol) isomers of the butyrated calix[4]resorcinarene galactosides.

Major isomer 154a

Yield: 14%

R_f of compound **154a** (EtOAc: Pet. ether, 1.5:1): 0.33

Mp: 121-125 ^{0}C

Vmax (cm^{-1}): 2968 (C-H stretching), 1745 (C=O ester), 1607, 1507 (C=C arene), 1367 (C-H bending), 1216, 1129, 1072 (C-O stretching), 916 (C-H bending).

^{1}H NMR (400 MHz $CDCl_3$): δ 7.04, (2H, s, H2-Ar), 6.94, (2H, s, H2-Ar), 6.85, (2H, s, ArH), 6.75, (4H, d, *J* 8.8, ArH) 6.58-6.68, (10H, m, ArH), 6.29, (2H, d, *J* 8.7, H5-Ar), 6.10, (2H, s, H5-Ar), 5.58, (2H, s, ArCH), 5.48-5.57, (8H, m, H2'',4''-Gal), 5.46, (2H, s, ArCH), 5.21, (4H, ddd, *J* 19.6; 10.4; 3.5, H3''-Gal), 4.88, (4H, dd, *J* 12.2; 8, H1''-Gal), 4.15-4.34, (12H, m, H5'',6''-Gal), 2.11-2.37, (16H, m, $COCH_2$), 2.00-2.08, 2.22-2.23, (48H, m, OAc-Gal), 1.44-1.59, (16H, m, CH_2), 0.82-0.93, (24H, m, CH_3).

^{13}C NMR (100 MHz $CDCl_3$): δ 171.2, 171.1, 170.7, 170.6, 170.5, 170.5, 170.3, 170.2, 170.0, 169.8, 169.5, 169.1 (C=O); 156.1, 147.0, 147.0, 146.8, 146.3, 135.3, 133.8, 132.7, 132.2, 131.8, 131.5, 131.0, 130.2, 130.2, 130.0, 117.1, 116.4 (aromatic carbons); 101.1, 100.9, 71.1, 70.9, 68.9, 68.9, 67.1, 67.0, 61.3, 61.1 (C-Galactose); 43.5 (ArCH); 35.8, 35.6, 35.5, 35.5 ($COCH_2$); 20.6, 20.6, 20.6, 20.6 (OAc-Galactose); 18.1, 18.0, 18.0, 18.0, 17.8 (CH_2); 13.6, 13.5, 13.5 (CH_3).

Mass Spectrum: Expected: *m/z* 1386.5179 $(M+2NH_4)^{2+}$. Observed: *m/z* 1386.5188

Minor isomer 154b

Yield: 5%

R_f of compound **154b** (EtOAc: Pet. ether, 1.5:1): 0.24

Mp: 116-120 ^{0}C

Vmax (cm^{-1}): 2968 (C-H stretching), 1754 (C=O ester), 1609, 1508, 1492 (C=C arene), 1367 (C-H bending), 1216, 1131, 1073 (C-O stretching), 917 (C-H bending).

^{1}H NMR (400 MHz $CDCl_3$): δ 6.92, (2H, s, H2-Ar), 6.89, (2H, s, H2-Ar), 6.82, (8H, d, *J* 8.4, ArH), 6.67, (8H, d, *J* 8.2, ArH), 6.29, (2H, s, H5-Ar), 5.97, (2H, s, H5-Ar), 5.66, (2H, d, *J* 2, H4''-Gal), 5.57, (2H, d, *J* 3.4, H4''-Gal), 5.45-5.51, (6H, m, H2'',3''-Gal), 5.37, (4H, d, *J* 5.1, ArCH), 5.24, (2H, dd, *J* 10.4; 3.4, H3''-Gal), 5.16, (2H, d, *J* 7.6, H1''-Gal), 4.99, (2H, d, *J* 8.1, H1''-Gal), 4.44-4.47, (2H, t, H5''-Gal), 4.17-4.31, (10H, m, H5'',6''-Gal), 2.08-2.51, (16H, m, $COCH_2$), 1.94-2.06, 2.23, (48H, m, OAc-Gal), 1.23-1.76, (16H, m, CH_2), 0.78-1.03, (24H, m, CH_3).

^{13}C NMR (100 MHz $CDCl_3$): δ 171.8, 170.6, 170.6, 170.5, 170.5, 170.4, 170.3, 170.0, 169.8, 169.5, 169.4 (C=O); 156.0, 155.7, 147.1, 147.1, 147.0, 146.9, 137.3, 134.3, 131.8, 131.6, 130.9, 129.9, 129.1, 117.5, 117.0, 115.9, 115.7 (aromatic carbons); 100.0, 99.9, 71.2, 71.2, 70.8, 70.6, 69.4, 68.7, 67.5, 67.1, 61.7, 61.3 (C-Galactose); 44.1, 43.1 (ArCH); 35.9, 35.8, 35.4, 35.3 ($COCH_2$); 20.8, 20.8, 20.7, 20.6, 20.6, 20.6, 20.5 (OAc-Galactose); 18.3, 18.1, 17.8, 17.8, 17.4 (CH_2); 13.7, 13.6, 13.5, 13.5 (CH_3).

Mass Spectrum: Expected: *m/z* 1386.5179 $(M+2NH_4)^{2+}$. Observed: *m/z* 1386.5188

10.5.5 Acylated calix[4]resorcinarene lactoside 159

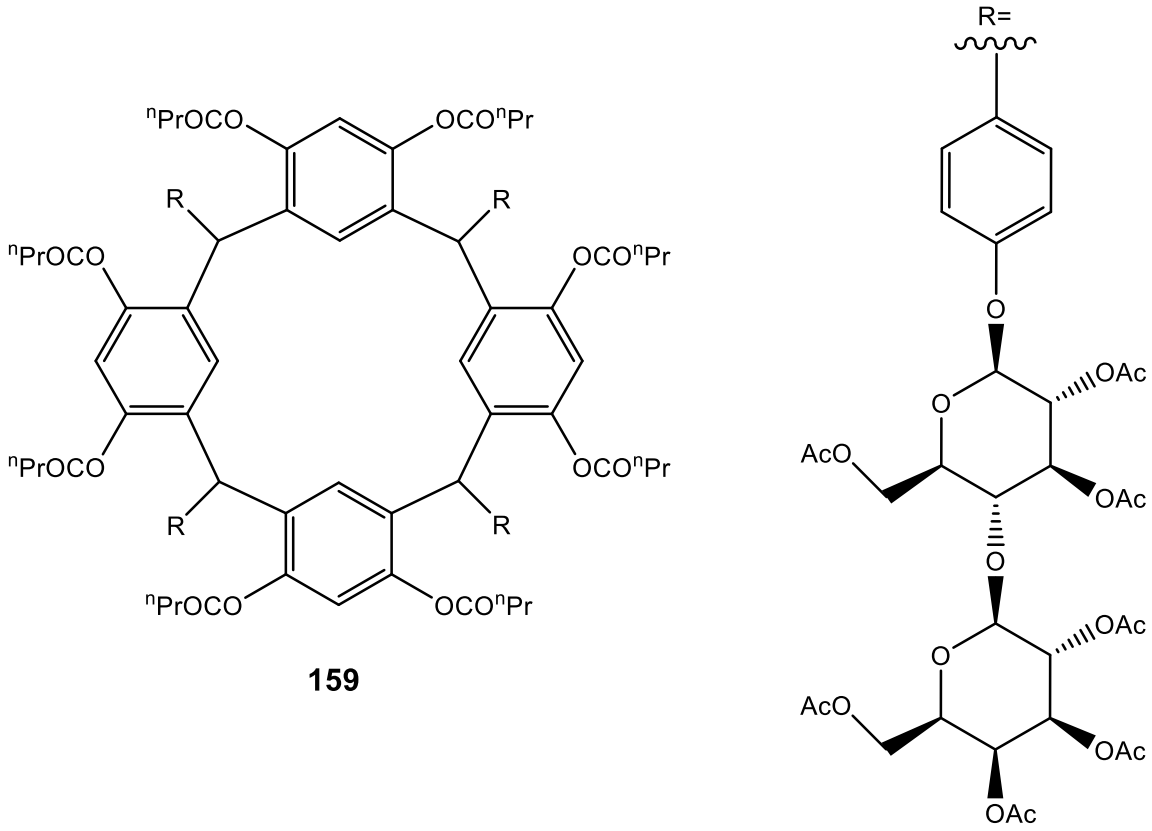

159

Compound **159** was synthesised according to the general procedure. The crude mixture of calix[4]resorcinarene lactoside **158** (1.50 g, 0.45 mmol) was reacted with butyric anhydride (30 mL) and pyridine (5 mL), the crude product was separated by silica gel column chromatography using EtOAc: Pet. ether (3:1) as eluent to yield one product of the butyrated calix[4]resorcinarene lactoside (0.16 g, 0.04 mmol).

Yield: 9%

R_f of compound **159** (EtOAc: Pet. ether, 3:1): 0.46

Mp: 149-153 ^{0}C

Vmax (cm^{-1}): 2968 (C-H stretching), 1745 (C=O ester), 1507 (C=C arene), 1366 (C-H bending), 1214, 1132, 1042 (C-O stretching), 901 (C-H bending).

^{1}H NMR (400 MHz $CDCl_3$): δ 6.98, (2H, d, ArH), 6.88-6.91, (3H, m, ArH), 6.41-6.75, (14H, m, ArH), 6.22, (2H, d, *J* 4.3, ArH), 6.01, (1H, s, ArH), 5.90, (1H, s, ArH), 5.82, (1H, s, ArH), 5.49, (2H, d, *J* 3.7, ArCH), 5.34-5.43, (6H, m, ArCH+ H3''-Lac), 5.17-5.31, (8H, m, H3''',4'''-Lac), 5.01-5.15, (8H, m, H2'',2'''-Lac), 4.85-4.99, (4H, m, H1''-Lac), 4.39-4.78, (8H, m, H1''',6''-Lac), 4.07-4.33, (16H, m, H5'',6'',6'''-Lac), 3.79-4.04, (8H, m, H4'',5'''-Lac), 2.18-2.51, (16H, m, $OCOCH_2$), 1.86-2.17, (84H, m, OAc-Lac), 1.35-1.73, (16H, m, CH_2), 0.69-1.03, (24H, m, CH_3).

^{13}C NMR (100 MHz $CDCl_3$): 171.2, 171.1, 170.6, 170.5, 170.2, 170.2, 170.1, 170.1, 170.1, 170.0, 169.9, 169.9, 169.8, 169.8, 169.3 (C=O); 155.7, 155.5, 146.8, 146.7, 146.6, 131.8, 129.9, 129.8, 116.3 (aromatic carbons); 100.8, 70.9, 69.1, 69.0, 66.8, 60.5 (C-Lactose); 43.96, 43.50 (ArCH); 35.7, 35.7, 35.5, 35.4 ($COCH_2$); 20.9, 20.8, 20.7, 20.7, 20.6, 20.6, 20.5, 18.2, 18.1 (OAc-Lactose); 18.0, 18.0, 17.9, 17.9, 17.9, 17.4, 17.2 (CH_2); 13.6, 13.6, 13.6, 13.5, 13.5, 13.4 (CH_3).

Mass Spectrum: Expected: *m*/*z* 1962.6870 $(M+2NH_4)^{2+}$. Observed: *m*/*z* 1962.6890

10.6 Methyl 3-(4'-hydroxyphenyl)propanoate 172

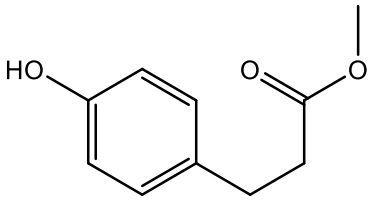

172

3-(4'-hydroxyphenyl)propanoic acid (16.60 g, 100 mmol) was dissolved in MeOH (100 mL), concentrated H_2SO_4 (2 drops) were added. The reaction mixture was refluxed for 24 h at 70 ^{0}C, the solvent was evaporated under reduced pressure and the residue was taken up in EtOAc (100 mL) then washed with saturated aqueous solution of $NaHCO_3$ (100 mL x 2), brine (100 mL x 2) and dried ($MgSO_4$). The filtrate was concentrated under reduced pressure to yield the pure ester as white crystals (17.57 g, 97.50 mmol) (Tung *et al*., 2016).

Yield: 97%

R_f of compound **172** (EtOAc: Pet. ether, 1:1): 0.66

Mp: 40-41 ^{0}C

Vmax (cm^{-1}): 3419 (O-H stretching), 3006, 2952 (C-H stretching), 1717 (C=O ester), 1614, 1593, 1515 (C=C arene), 1445, 1432, 1378 (C-H bending), 1266 (O-H bending), 1193, 1172, 825.

^{1}H NMR (400 MHz $CDCl_3$): δ 7.06, (2H, d, *J* 6.8, ArH), 6.83, (2H, d, *J* 6.6, ArH), 3.72, (3H, s, $COOCH_3$), 2.92, (2H, t, *J* 6.1, CH_2), 2.66, (2H, t, *J* 5.6x (2), CH_2).

^{13}C NMR (75 MHz $CDCl_3$): δ 174.2 (C=O); 154.2, 132.1, 129.3, 115.4, 114.9 (aromatic carbons); 51.8, 36.1, 30.0 (aliphatic carbons).

10.7 Methyl 3-(4'-benzyloxyphenyl)propionate 173

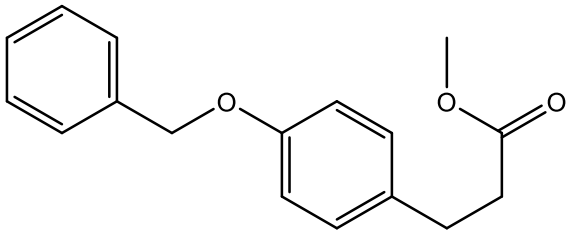

173

To a solution of methyl 3-(4'-hydroxyphenyl)propanoate (16.2 g, 89.90 mmol) in acetone (250 mL) was added potassium iodide (20.83 g, 125.50 mmol), anhydrous potassium carbonate (73.56 g, 532.29 mmol) and benzyl chloride (16.04 mL, 139.34 mmol). The reaction mixture was refluxed overnight at 56 ^{0}C. The cooled mixture filtered and evaporated under reduced pressure. The residue was recrystallised from n-hexane to yield the title compound as yellow crystals (20.17 g, 74.61 mmol) (Herbert and Kattah 1990).

Yield: 83%

R_f of compound **173** (EtOAc: Pet. ether, 1:1): 0.84

Mp: 77-78 ^{0}C

Vmax (cm^{-1}): 3029, 2954, 2911, 2864 (C-H stretching), 1723 (C=O ester), 1610, 1581, 1510 (C=C arene), 1463, 1453, 1382 (C-H bending).

^{1}H NMR (300 MHz $CDCl_3$): δ 7.35-7.49, (5H, m, Ph), 7.17, (2H, d, *J* 8.7, ArH), 6.96, (2H, d, *J* 8.7, ArH), 5.08, (2H, s, OCH_2), 3.71, (3H, s, $COOCH_3$), 2.95, (2H, t, *J* 7.7x(2), CH_2), 2.65, (2H, t, CH_2).

^{13}C NMR (75 MHz $CDCl_3$): δ 173.4 (C=O); 157.3, 137.1, 132.9, 129.3, 128.6, 128.4, 127.9, 127.5, 115.3, 114.9 (aromatic carbons); 70.0, 51.6, 36.0, 30.1 (aliphatic carbons).

10.8 3-(4'-Benzyloxyphenyl)propan-1-ol 174

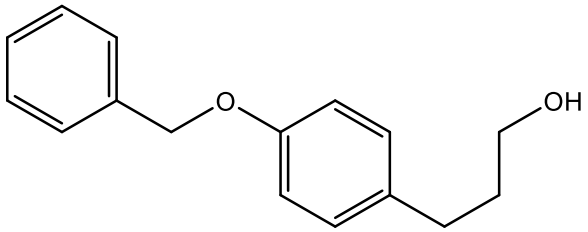

174

To a stirred suspension of lithium aluminium hydride (4.17 g, 110 mmol) in anhydrous THF (50 mL) was added a solution of methyl 3-(4-benzyloxyphenyl)propionate (19.82 g, 73.31 mmol) in THF (150 mL) dropwise at 0 ^{0}C. The reaction mixture was stirred at r.t. under N_2 for 2 h, then water was added dropwise to remove the excess reagent and acidified with concentrated HCl. The mixture was extracted with EtOAc (100 mL), washed with brine (100 mL x 2) and dried ($MgSO_4$). The solvent was removed under reduced pressure to give the pure alcohol as white crystals (17.62 g, 72.71 mmol) (Kantee *et al*., 2016).

Yield: 99%

R_f of compound **174** (EtOAc: Pet. ether, 1:1): 0.22

Mp: 63-64 ^{0}C

Vmax (cm^{-1}): 3298 (O-H stretching), 3058, 3033, 2938, 2864 (C-H stretching), 1608, 1581, 1509 (C=C arene), 1453, 1380 (C-H bending), 1239 (=C-O-C stretching).

^{1}H NMR (400 MHz $CDCl_3$): δ 7.29-7.43, (5H, m, Ph), 7.11, (2H, d, *J* 7.7, ArH), 6.9, (2H, d, *J* 7.7, ArH), 5.03, (2H, s, OCH_2), 3.65, (2H, t, CH_2OH), 2.64, (2H, t, *J* 7.5x(2), CH_2), 1.85, (2H, p, *J* 6.8x(4), CH_2), 1.44, (1H, brs, OH).

^{13}C NMR (100 MHz $CDCl_3$): δ 157.1, 137.2, 134.2, 129.3, 128.5, 128.3, 128.0, 127.9, 127.6, 127.4, 114.8 (aromatic carbons); 70.1, 62.2, 34.4, 31.2 (aliphatic carbons).

10.9 3-(4'-Benzyloxyphenyl)propanal 175

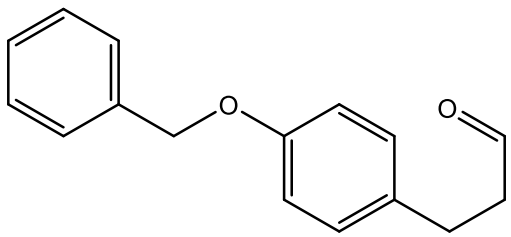

175

PCC (18.60 g, 86.66 mmol) was suspended in dry DCM (50 mL), a solution of 3-(4'-benzyloxyphenyl)propan-1-ol (14.00 g, 57.77 mmol) in DCM (100 mL) was added at 0 ^{0}C. The reaction mixture was allowed to stir at r.t for 3 h, when TLC analyses showed that the reaction was complete. The reaction mixture was reduced under reduced pressure and was extracted with Et_2O (100 mL x 3). The solvent was isolated by filtering the black solid and concentrated under reduced pressure.

The residue was purified by silica gel column chromatography using EtOAc: Pet. ether (1:4) as eluent to yield the aldehyde as a colourless oil (8.00 g, 33.29 mmol) (Kashanna *et al*., 2012; Tadiparthi *et al*., 2017).

Yield: 58%

R_f of compound **175** (EtOAc: Pet. ether, 1:4): 0.35

Mp: 36-38 ^{0}C

Vmax (cm^{-1}): 3033, 2928, 2733 (C-H stretching), 1716 (C=O aldehyde), 1609, 1580, 1511 (C=C arene), 1452, 1381 (C-H bending), 1236 (=C-O-C stretching).

^{1}H NMR (400 MHz $CDCl_3$): δ 9.85, (1H, s, CHO), 7.35-7.49, (5H, m, Ph), 7.16, (2H, d, *J* 7.8, ArH), 6.96, (2H, d, *J* 7.7, ArH), 5.09, (2H, s, OCH_2), 2.95, (2H, t, CH_2), 2.79, (2H, t, CH_2CHO).

^{13}C NMR (100 MHz $CDCl_3$): δ 201.7 (C=O); 157.3, 137.1, 132.6, 130.1, 129.2, 128.6, 128.4, 127.9, 127.4, 115.0, 114.9, 114.8 (aromatic carbons); 70.1, 45.5, 27.3 (aliphatic carbons).

10.10 3-(4'-Hydroxyphenyl)propanal 170

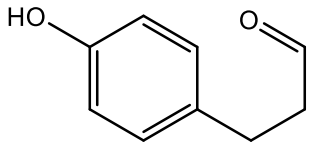

170

A solution of 3-(4'-benzyloxyphenyl)propanal (9.79 g, 40.74 mmol) in dry MeOH (100 mL) and Pd/C (5%, 1.20 g) was degassed with N_2 for 5 min then stirred under an atmosphere of H_2 at r.t. until TLC analyses showed the completion of the reaction. The reaction mixture was filtered off through celite and the filtrate was evaporated under reduced pressure. The residue was subjected to silica gel column chromatography using EtOAc: Pet. ether (1:2) as eluent to yield the title compound as a colourless oil (4.39 g, 29.23 mmol) (Herbert and Kattah 1990).

Yield: 72%

R_f of compound **170** (EtOAc: Pet. ether, 1:2): 0.20

Mp: 46-48 ^{0}C

Vmax (cm^{-1}): 3347 (O-H stretching), 3013, 2943, 2928, 2866 (C-H stretching), 1691 (C=O aldehyde), 1608, 1591, 1512 (C=C arene), 1433 (C-H bending), 1192.

^{1}H NMR (400 MHz $CDCl_3$): δ 9.82, (1H, s, CHO), 7.07, (2H, d, *J* 7.8, H2',6'-Ar), 6.79, (2H, d, *J* 7.7, H3',5'-Ar), 5.88, (1H, broad s, OH), 2.92, (2H, t, CH_2), 2.78, (2H, t, CH_2CHO).

^{13}C NMR (100 MHz $CDCl_3$): δ 202.8 (C=O); 154.2, 132.1, 129.6, 129.4, 115.5, 115.1 (aromatic carbons); 45.4, 27.3 (aliphatic carbons).

10.11 Synthesis of aryl substituted calix[4]resorcinarenes

10.11.1 Tetra(4-hydroxyphenylethyl)calix[4]resorcinarene 176 (General procedure)

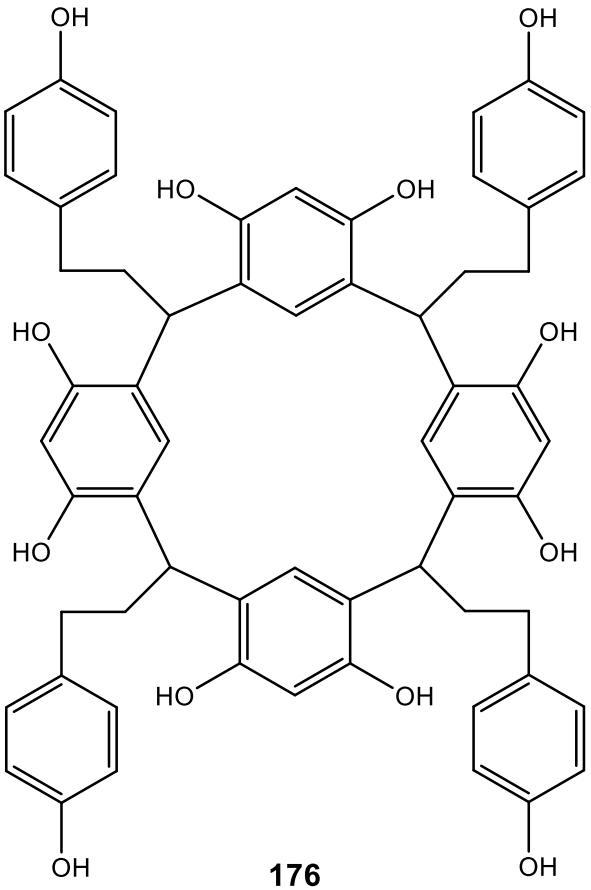

176

Resorcinol (0.54 g, 4.99 mmol) and 4-hydroxyphenyl propanal (0.75 g, 4.99 mmol) were dissolved in EtOH (40 mL), then concentrated HCl (0.74 mL) was added dropwise with stirring. The reaction mixture was heated to reflux for 4 h at 105 ^{0}C, the mixture was allowed to cool down to r.t. A precipitate was formed by adding the reaction mixture to cold water. The precipitate was filtered and

dried in an oven to yield the title compound as a yellow precipitate (1.00 g, 1.03 mmol).

Yield: 21%

Vmax (cm^{-1}): 3251 (O-H stretching), 2933 (C-H stretching), 1611, 1511 (C=C arene), 1436 (C-H bending), 1217, 1167, 1085, 824.

^{1}H NMR (400 MHz d_6-Acetone): δ 8.57, (8H, broad s, ArOH), 8.19, (4H, broad s, ArOH), 7.77, (4H, s, H5-Ar), 7.01, (8H, d, *J* 8.4, H2'',6''-Ar), 6.75, (8H, d, *J* 8.4, H3'',5''-Ar), 6.30, (4H, s, H2-Ar), 4.38, (4H, t, *J* 7.3x(2), ArCH), 2.51-2.60, (16H, m, CH_2-CH_2).

^{13}C NMR (100 MHz d_6-Acetone): δ 155.3, 151.9, 133.2, 129.4, 124.9, 124.4, 115.1, 102.9 (aromatic carbons); 36.3, 33.8 (CH_2-CH_2); 33.6 (ArCH).

Mass Spectrum: Expected: *m*/*z* 967.3693 $(M-H)^-$. Observed: *m*/*z* 967.3693

10.11.2 Tetra(4-hydroxyphenylethyl)calix[4]methylresorcinarene 177

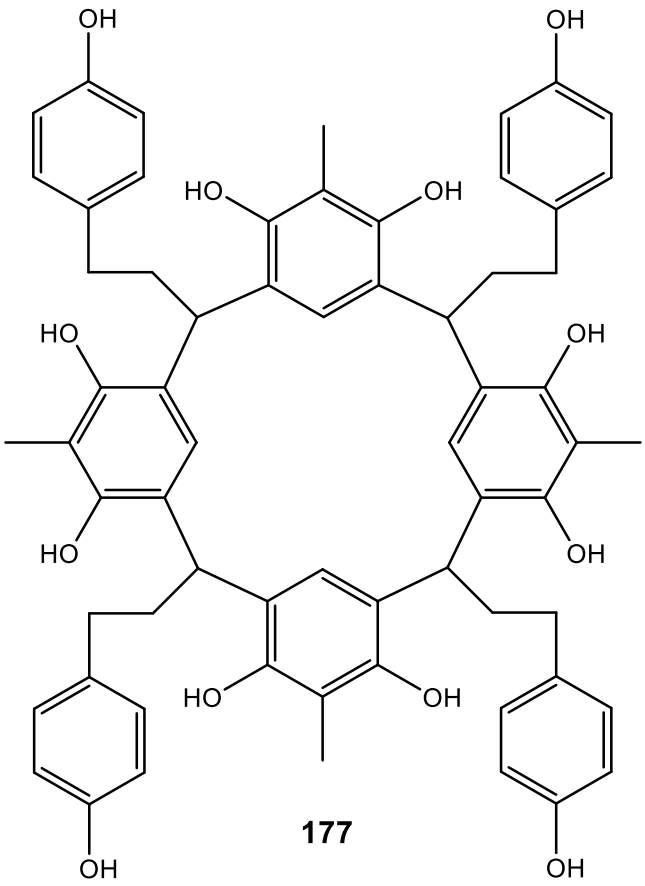

177

Compound **177** was synthesised similarly to compound **176** from 4-hydroxyphenyl propanal (0.70 g, 4.66 mmol), 2-methylresorcinol (0.58 g, 4.66 mmol) gave the title compound as a red precipitate (1.19 g, 1.16 mmol).

Yield: 25%

Vmax (cm^{-1}): 3334 (O-H stretching), 2939, 2864 (C-H stretching), 1613, 1513 (C=C arene), 1476, 1444 (C-H bending), 1294 (O-H bending), 1233, 1169, 1093, 824.

^{1}H NMR (400 MHz d_6-Acetone): δ 8.17, (4H, s, ArOH), 8.05, (8H, s, ArOH), 7.64, (4H, s, H5-Ar), 6.97, (8H, d, H2'',6''-Ar), 6.73, (8H, d, *J* 4.5, H3'',5''-Ar), 4.44, (4H, t, ArCH), 2.46-2.59, (16H, m, CH_2-CH_2), 2.06, (12H, m, CH_3).

^{13}C NMR (100 MHz d_6-Acetone): δ 155.3, 155.2, 149.6, 133.3, 129.4, 124.9, 121.7, 115.0, 114.9, 111.2, 111.1 (aromatic carbons); 36.7 (CH_2); 34.7 (ArCH); 33.9 (CH_2); 9.0 (CH_3).

Mass Spectrum: Expected: *m*/z 1023.4319 $(M-H)^-$. Observed: *m*/*z* 1023.4313

10.11.3 Tetra(4-hydroxyphenylethyl)calix[4]pyrogallolarene 178

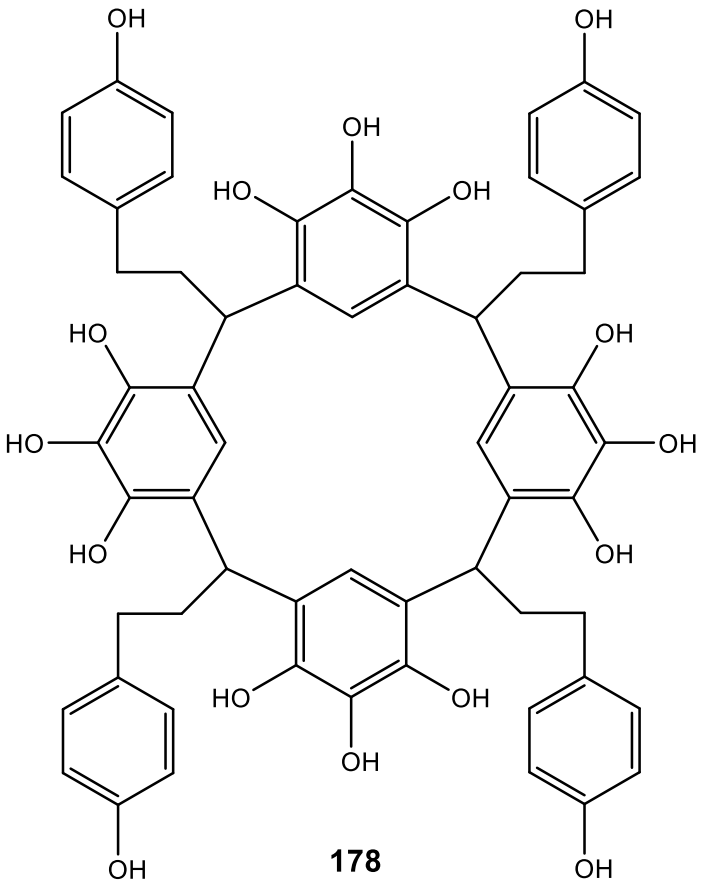

178

Compound **178** was synthesised similarly to compound **176** from 4-hydroxyphenyl propanal (0.70 g, 4.66 mmol), pyrogallol (0.59 g, 4.66 mmol) gave the title compound as brown precipitate.

10.12 Methyl 2-(4'-hydroxyphenyl)acetate 179

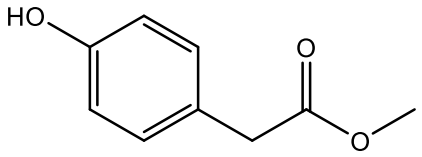

179

Compound **179** was synthesised similarly to compound **172** from 4-hydroxyphenylacetic acid (15.20 g, 100 mmol) to give the pure ester as a colourless oil (15.71 g, 94.54 mmol) (Hajji *et al*., 2006).

Yield: 95%

R_f of compound **179** (EtOAc: Pet. ether, 1:1): 0.75

Vmax (cm^{-1}): 3379 (O-H stretching), 3023, 2953 (C-H stretching), 1711 (C=O ester), 1614, 1596, 1514 (C=C arene), 1437 (C-H bending), 1219, 1159, 1009.

^{1}H NMR (400 MHz $CDCl_3$): δ 7.13, (2H, d, *J* 8.4, ArH), 6.78, (2H, d, *J* 8.4, ArH), 3.74, (3H, s, OCH_3), 3.60, (2H, s, CH_2CO).

^{13}C NMR (100 MHz $CDCl_3$): δ 173.6 (C=O); 155.2, 130.4, 130.1, 125.4, 115.9, 115.6 (aromatic carbons); 52.3, 40.3 (aliphatic carbons).

10.13 (4-Benzyloxyphenyl)-acetic acid methyl ester 180

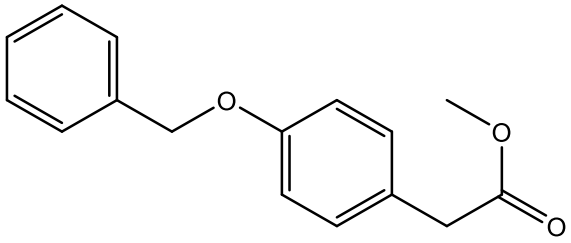

180

To a solution of methyl 2-(4'-Hydroxyphenyl)acetate (15.50 g, 93.27 mmol) in acetone (250 mL) was added potassium iodide (21.61 g, 130.21 mmol), anhydrous potassium carbonate (76.32 g, 552.26 mmol) and benzyl chloride (16.63 mL, 144.57 mmol). The reaction mixture was refluxed overnight at 56 ^{0}C. The cooled mixture filtered and evaporated under reduced pressure. The residue was recrystallised from n-hexane to yield the title compound as yellow crystals (15.32 g, 59.77 mmol) (Desage-El Murr *et al*., 2006).

Yield: 64%

R_f of compound **180** (EtOAc: Pet. ether, 1:1): 0.79

Mp: 58-60 ^{0}C

Vmax (cm^{-1}): 3034, 2959, 2930, 2871 (C-H stretching), 1723 (C=O ester), 1607, 1582, 1508 (C=C arene), 1263, 1234, 1166 (=C-O-C), 1010 (C-H bending).

^{1}H NMR (300 MHz $CDCl_3$): δ 7.36-7.49, (5H, m, Ph), 7.24, (2H, d, *J* 8.5, ArH), 6.99, (2H, d, ArH), 5.09, (2H, s, OCH_2), 3.72, (3H, s, $COOCH_3$), 3.61, (2H, s, CH_2CO).

^{13}C NMR (75 MHz $CDCl_3$): δ 172.3 (C=O); 157.9, 137.0, 130.7, 130.3, 128.8, 128.6, 128.4, 128.1, 128.0, 126.3, 115.3, 114.9 (aromatic carbons); 70.0, 52.0, 40.3 (aliphatic carbons).

10.14 2-(4'-Benzyloxyphenyl)ethanol 181

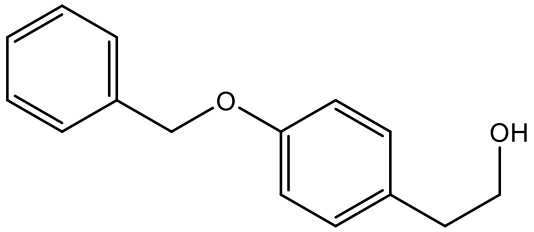

181

Compound **181** was synthesised similarly to compound **174** from (4-benzyloxy-phenyl)acetic acid methyl ester (15.00 g, 58.52 mmol), $LiALH_4$ (1.5 eq) to give the pure alcohol as an off-white solid (12.47 g, 54.62 mmol) (Lingamurthy *et al*., 2016).

Yield: 93%

R_f of compound **181** (EtOAc: Pet. ether, 1:1): 0.32

Mp: 83-85 ^{0}C

Vmax (cm^{-1}): 3287 (O-H stretching), 3060, 3032, 2933, 2858 (C-H stretching), 1608, 1579, 1510 (C=C arene), 1452, 1384 (C-H bending), 1234 (=C-O-C).

^{1}H NMR (400 MHz $CDCl_3$): δ 7.25-7.37, (5H, m, Ph), 7.07, (2H, d, *J* 7.6, ArH), 6.86, (2H, d, *J* 7.8, ArH), 4.98, (2H, s, OCH_2), 3.75, (2H, t, *J* 6.1x(2), CH_2OH), 2.74, (2H, t, *J* 6.1x(2), CH_2), 1.4, (1H, broad s, OH).

^{13}C NMR (100 MHz $CDCl_3$): δ 157.5, 137.1, 130.7, 130.0, 128.5, 127.9, 127.4, 115.0 (aromatic carbons); 70.1, 63.8, 38.3 (aliphatic carbons).

10.15 2-(4'-Benzyloxyphenyl)acetaldehyde 182

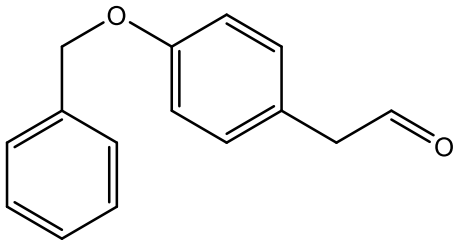

182

DMP (2.22 g, 5.25 mmol) was added to a solution of 2-(4'-benzyloxyphenyl)ethanol (1.00 g, 4.38 mmol) in DCM (15 mL) at 0 ^{0}C. The reaction mixture was allowed to stir overnight at r.t., diluted with DCM and washed with saturated aqueous solution of $NaHCO_3$ (25 mL x 3) then with saturated aqueous solution of $Na_2S_2O_3$ (25 mL x 2). The organic layer was washed with brine (25 mL x 2), dried ($MgSO_4$) and concentrated under reduced pressure. The residue was purified by silica gel column chromatography using EtOAc: Pet. ether (1:2) as eluent to give the aldehyde as a pale yellow oil (0.71 g, 3.14 mmol) (Tilley *et al*., 2012; Nadkarni *et al*., 2013).

Yield: 71%

R_f of compound **182** (EtOAc: Pet. ether, 1:2): 0.45

Vmax (cm^{-1}): 3031, 2873 (C-H stretching), 1718 (C=O aldehyde), 1610, 1582, 1509 (C=C arene), 1453, 1382 (C-H bending), 1238, 1175 (=C-O-C), 1011.

^{1}H NMR (400 MHz $CDCl_3$): δ 9.76, (1H, t, *J* 2.4x(2), CHO), 7.35-7.49, (5H, m, Ph), 7.17, (2H, d, ArH), 7.02, (2H, d, ArH), 5.11, (2H, s, OCH_2), 3.67, (2H, d, *J* 2.3, CH_2CHO).

^{13}C NMR (100 MHz $CDCl_3$): δ 199.6 (C=O); 158.2, 136.9, 130.4, 128.7, 128.0, 127.4, 124.0, 115.4 (aromatic carbons); 70.1, 49.7 (aliphatic carbons).

10.16 2-(4'-Hydroxyphenyl)ethanol 183

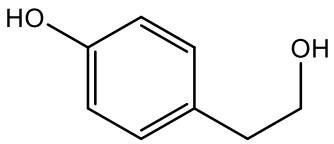

183

4-Benzyloxyphenyl ethanol (5.12 g, 22.42 mmol) was dissolved in dry MeOH (100 mL) and Pd/C 5% (0.93 g) was added as a catalyst. The mixture was degassed with N_2 for 10 min then stirred overnight under H_2 atmosphere. The catalyst was removed by filtration on a pad of silica gel and the solution was evaporated under reduced pressure to yield the title compound as white crystals (3.00 g, 21.71 mmol) (Fernandez-Pastor *et al*., 2016).

Yield: 97%

R_f of compound **183** (EtOAc: Pet. ether, 1:1): 0.26

Mp: 90-91 ^{0}C

Vmax (cm^{-1}): 3380, 3126 (O-H stretching), 3023, 2927, 2879 (C-H stretching), 1611, 1510 (C=C arene), 1450 (C-H bending), 1359, 1343, 1228, 1050, 1013, 815.

^{1}H NMR (400 MHz d_6-DMSO): δ 9.15, (1H, s, OH), 7.01, (2H, d, ArH), 6.68, (2H, d, ArH), 4.6, (1H, t, *J* 5.2x(2), OH), 3.54, (2H, q, *J* 7.2x(2): 5.1, CH_2OH), 2.62, (2H, t, *J* 7.3x(2), CH_2)

^{13}C NMR (100 MHz d_6-DMSO): δ 155.9, 155.5, 130.1, 130.0, 129.9, 115.4, 115.0 (aromatic carbons); 63.0, 38.7 (aliphatic carbons).

10.17 2-(4'-Hydroxyphenyl)acetaldehyde 171

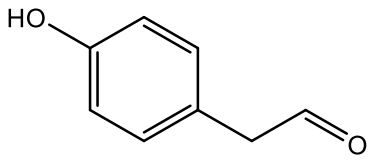

171

To a mixture of 4-hydroxyphenyl ethanol (1.00 g, 7.23 mmol) in DMSO (8 mL), and TEA (2.20 mL, 16 mmol), a solution of SO_3.Pyridine (2.50 g, 16 mmol) in DMSO (9 mL) was added dropwise under N_2 atmosphere. After 1 h of stirring at r.t., the reaction mixture was quenched with water, acidified with 2 M HCl (10 mL) and extracted with EtOAc. The organic layer was washed with brine, dried ($MgSO_4$) and concentrated under reduced pressure. Purification by silica gel column chromatography using EtOAc: Pet. ether (1:2) as eluent furnished the aldehyde as a colourless oil (0.32 g, 2.35 mmol) (Vece and Vuocolo 2015).

Yield: 33%

R_f of compound **171** (EtOAc: Pet. ether, 1:2): 0.37

Vmax (cm^{-1}): 3352 (O-H stretching), 1708 (C=O aldehyde), 1612, 1595, 1513 (C=C arene), 1443 (C-H bending), 1363, 1221, 827.

^{1}H NMR (400 MHz $CDCl_3$): δ 9.73, (1H, t, CHO), 7.08, (2H, d, *J* 8.6, H2',6'-Ar), 6.86, (2H, d, *J* 4.4, H3',5'-Ar), 3.64, (2H, d, *J* 2.3, CH_2).

^{13}C NMR (100 MHz $CDCl_3$): δ 200.4 (CHO); 155.3, 130.8, 123.4, 115.9 (aromatic carbons); 49.7 (CH_2).

10.18 2-{2'-[4''-(2''',3''',4''',6'''-Tetra-*O*-acetyl-*β*-D-glucopyranosyloxy)-phenyl]ethenyl}-1,3-dioxolane 194

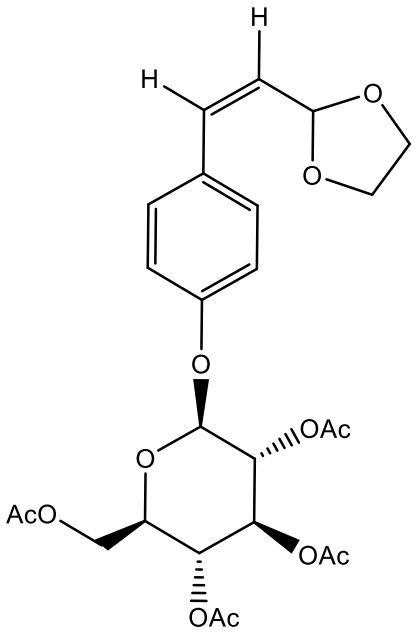

194

4-(2',3',4',6'-Tetra-*O*-acetyl-*β*-D-glucopyranosyloxy)benzaldehyde (3.40 g, 7.51 mmol) was dissolved in THF (75 mL) with KO^tBu (0.84 g, 7.50 mmol), 1,3-dioxolan-2-ylmethyltriphenylphosphonium bromide (3.95 g, 9.21 mmol) was

added portionwise and the reaction mixture heated under reflux with stirring overnight. The reaction mixture was diluted with water (100 mL) and extracted with EtOAc, the aqueous layer was extracted with DCM (50 mL x 2). The combined organic layers dried ($MgSO_4$) and concentrated under reduced pressure. The crude mixture was purified by silica gel column chromatography using EtOAc: Pet. ether (1.5:1) as eluent to yield the title compound as a mixture of *E*/*Z* isomers as a white powder (0.97 g, 0.93 mmol) (Ka *et al*., 2016).

Yield: 25%

R_f of compound **194** (EtOAc: Pet. ether, 1.5:1): 0.34 and 0.26 for *E*/*Z* isomers

Vmax (cm^{-1}): 2964 (C-H stretching), 1739 (C=O ester), 1603, 1509 (C=C arene), 1366 (C-H bending), 1213, 1031 (C-O stretching), 847 (C-H bending).

^{1}H NMR (400 MHz $CDCl_3$): δ 6.34-7.39, (4H, dd, H2'',6''-Ar), 6.96-7.00, (4H, t, H3'',5''-Ar), 6.77, (2H, dd, *J* 2.1, ArC<u>H</u>2'), 6.09, (1H, dd, *J* 16; 6.1, CH=C<u>H</u>1'), 5.71, (1H, dd, *J* 11.6; 7.5, CH=C<u>H</u>1'), 5.51, (1H, d, *J* 6.7, C<u>H</u>2), 5.43, (1H, d, *J* 6.1, C<u>H</u>2), 5.30-5.33, (4H, m, H3''',4'''-Glu), 5.17-5.24, (2H, m, H2'''-Glu), 5.11-5.13, (2H, m, H1'''-Glu), 4.29-4.35, (2H, m, H6'''-Glu), 4.18-4.22, (2H, m, H6'''-Glu), 4.07-4.12, (4H, m, CH_2-CH_2), 3.93-4.00, (4H, m, CH_2-CH_2), 3.87-3.92, (2H, m, H5'''-Glu), 2.06-2.11, (24H, m, OAc).

^{13}C NMR (100 MHz $CDCl_3$): δ 170.5, 170.2, 169.3, 169.2 (C=O); 156.8, 156.4 (aromatic carbon); 133.9 (Ar<u>C</u>H=); 131.8, 131.2, 131.0, 130.3, 130.1, 128.2 (aromatic carbons); 124.3 (=CH); 117.2, 117.0, 116.8, 116.6 (aromatic carbons); 103.8 (CH); 98.9, 72.7, 72.5, 72.3, 72.2, 72.1, 71.2, 71.0, 68.3, 61.9, 61.9 (C-Glucose); 65.1, 65.0 (CH_2-CH_2); 21.0, 20.6, 20.6, 20.5, 20.5 (OAc-Glucose).

10.19 (*E*)-3-[4'-(2'',3'',4'',6''-Tetra-*O*-acetyl-*β*-D-glucopyranosyloxy)phenyl]prop-2-enal 195

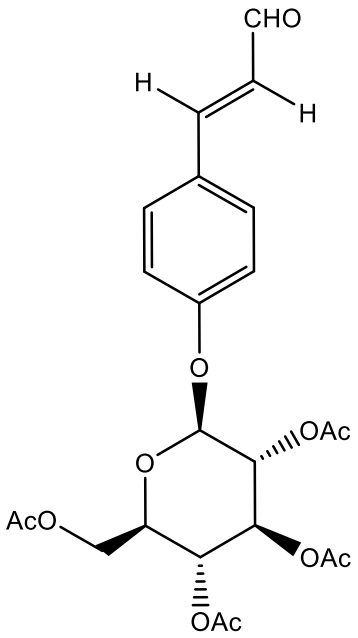

195

The *E*/*Z* mixture of 2-{2'-[4''-(2''',3''',4''',6'''-tetra-*O*-acetyl-*β*-D-glucopyranosyloxy)phenyl]ethenyl}-1,3-dioxolane (1.82 g, 3.48 mmol) was dissolved in CCl_4 (50 mL) and cooled to 0 ^{0}C then a solution of Br_2 (0.02 g, 0.13 mmol) in CCl_4 (5 mL) was added. After 5 min the mixture was stirred for 1 h at r.t. and water (5 mL) and AcOH (5 mL) were added and stirring was continued overnight. The reaction mixture was diluted with DCM (50 mL) and an aqueous solution of KOH was added. The aqueous layer was extracted with DCM (50 mL x 2), the combined organic layers were washed with a saturated aqueous solution of $Na_2S_2O_3$ (100 mL), saturated aqueous $NaHCO_3$ (100 mL), water (100 mL), dried ($MgSO_4$) and the solvent concentrated under reduced pressure. The crude mixture was refluxed with Et_2O (50 mL) for 3 h and allowed to cool to

r.t. After 24 h at r.t. a white powder was collected (1.24 g, 2.6 mmol) (Daubresse *et al*., 1998).

Yield: 74%

R_f of compound **195** (EtOAc: Pet. ether, 1:1): 0.32

Mp: 150-152 ^{0}C

Vmax (cm^{-1}): 2960 (C-H stretching), 1739 (C=O ester), 1664 (C=O aldehyde), 1626 (C=C), 1603, 1511 (C=C arene), 1365 (C-H bending), 1211, 1033 (C-O stretching), 914, 825, 742, 723 (C-H bending).

^{1}H NMR (400 MHz $CDCl_3$): δ 9.70, (1H, d, *J* 7.7, CHO), 7.55, (2H, d, H2',6'-Ar), 7.46, (1H, d, *J* 15.9, C<u>H</u>3), 7.06, (2H, d, H3',5'-Ar), 6.66, (1H, dd, *J* 15.9, 7.7, C<u>H</u>2), 5.30-5.37, (2H, m, H3'',4''-Glu), 5.18-5.24, (2H, m, H1'',2''-Glu), 4.32, (1H, dd, *J* 5.4, H6b''-Glu), 4.21, (1H, dd, J 2.4, H6a''-Glu), 3.91-3.95, (1H, m, H5''-Glu), 2.11, (3H, s, OAc), 2.09, (6H, s, OAc), 2.07, (3H, s, OAc).

^{13}C NMR (100 MHz $CDCl_3$): δ 193.5 (CHO); 170.5, 170.2, 169.4, 169.2 (C=O); 158.9 (aromatic carbon); 151.7 (Ar<u>C</u>H=); 130.2 (aromatic carbons); 129.3 (CHCHO); 127.8, 117.3 (aromatic carbons); 98.4, 72.6, 72.3, 71.1, 68.2, 61.9 (C-Glucose); 20.7, 20.6 (OAc-Glucose).

10.20 3-[4'-(2'',3'',4'',6''-Tetra-*O*-acetyl-*β*-D-glucopyranosyloxy)phenyl]propanal 167

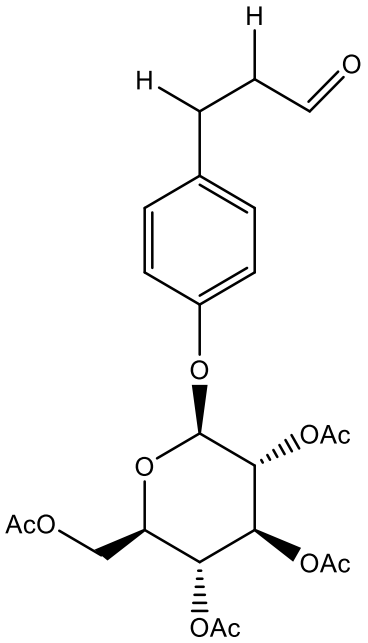

167

To a solution of (*E*)-3-[4'-(2'',3'',4'',6''-tetra-*O*-acetyl-*β*-D-glucopyranosyloxy)phenyl] prop-2-enal (3.85 g, 8.05 mmol) in MeOH (100 mL) was added 5% Pd/C (600 mg). The solution was degassed with N_2 for 10 min then stirred under H_2 atmosphere for 2 h. The reaction mixture was filtered and the filtrate concentrated under reduced pressure, the crude product was purified by silica gel column chromatography using EtOAc: Pet. ether (2:1) as eluent to produce white crystals of compound **167** (0.75 g, 1.56 mmol).

Yield: 19%

R_f of compound **167** (EtOAc: Pet. ether, 2:1): 0.61

Mp: 139-141 ^{0}C

Vmax (cm^{-1}): 2957 (C-H stretching), 1746 (C=O), 1612, 1513 (C=C arene), 1372 (C-H bending), 1209, 1038 (C-O stretching), 909 (C-H bending).

^{1}H NMR (400 MHz $CDCl_3$): δ 9.81, (1H, t, *J* 1.2x(2), CHO), 7.12, (2H, d, *J* 8.7, H2',6'-Ar), 6.92, (2H, d, H3',5'-Ar), 5.25, (3H, m, H2'',3'',4''-Glu), 5.04, (1H, d, *J* 7.6, H1''-Glu), 4.29, (1H, dd, *J* 5.3, H6b''-Glu), 4.17, (1H, dd, *J* 2.4, H6a''-Glu), 3.84, (1H, m, H5''-Glu), 2.92, (2H, t, CH_2), 2.76, (2H, t, CH_2), 2.08, (3H, s, OAc), 2.06, (3H, s, OAc), 2.05, (3H, s, OAc), 2.04, (3H, s, OAc).

^{13}C NMR (100 MHz $CDCl_3$): δ 201.3 (CHO); 170.5, 170.2, 169.3, 169.2 (C=O); 155.4, 135.3, 129.3, 117.2 (aromatic carbons); 99.3, 72.7, 72.0, 71.2, 68.3, 61.9 (C-Glucose); 45.3, 27.3 (aliphatic carbons); 20.6, 20.6, 20.6, 20.5 (OAc-Glucose).

10.21 Synthesis of tetra(4-glucophenylethyl)calix[4]resorcinarene 164

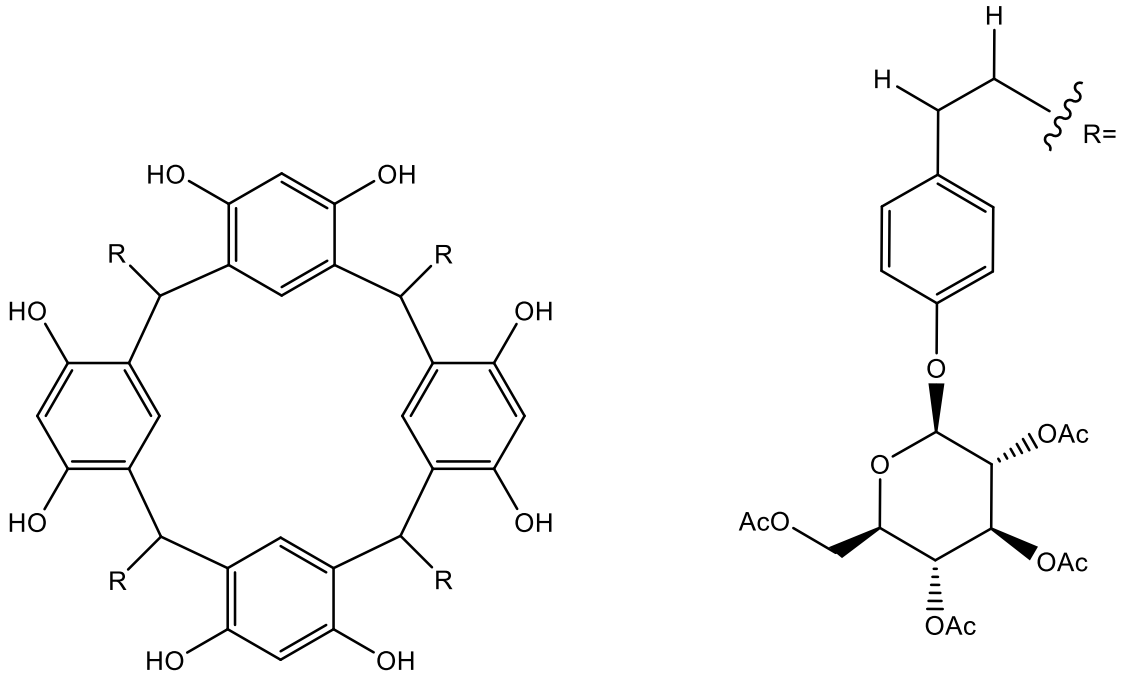

164

A solution of 3-[4'-(2'',3'',4'',6''-tetra-*O*-acetyl-*β*-D-glucopyranosyloxy)phenyl]propanal (1.24 g, 2.58 mmol) in a mixture of Et_2O and THF (1:1 ratio, 30 mL) was added anhydrous $AlCl_3$ (1.5 eq) and the mixture was stirred under N_2 for 15 min. Subsequently, resorcinol (0.28 g, 2.58 mmol) was added and the mixture was stirred at r.t. for a further 48 h. A precipitate was obtained by adding the reaction mixture to Et_2O (100 mL). The precipitate was filtered and washed many times with Et_2O. The solid was then dissolved in EtOAc and the organic layer was washed with water (100 mL x 3) then dried ($MgSO_4$). The solvent was concentrated under reduced pressure to give the desired compound as a red precipitate (1.20 g, 0.52 mmol, 20%), which was subjected to the acylation without further purification.

10.22 Acylation of tetra(4-glucophenylethyl)calix[4]resorcinarene

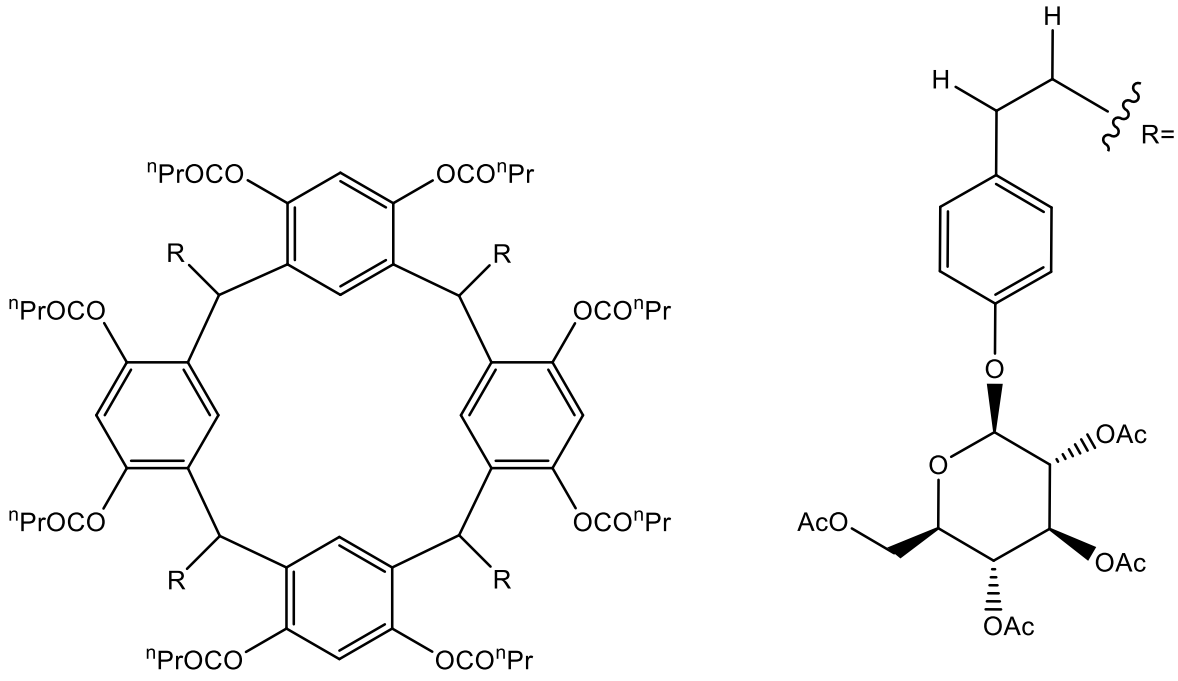

196

Compound **196** was synthesised according to the general procedure. The crude mixture of tetra(4-glucophenylethyl)calix[4]resorcinarene **164** (1.79 g, 0.78 mmol) was reacted with butyric anhydride (30 mL) and pyridine (5 mL), the crude product was separated by silica gel column chromatography using EtOAc: Pet. ether (2:1) as eluent to yield one product of the butyrated calix[4]resorcinarene glucoside as off-white powder (0.26 g, 0.09 mmol).

Yield: 12%

R_f of compound **196** (EtOAc: Pet. ether, 2:1): 0.35

Mp: 106-108 ^{0}C

Vmax (cm^{-1}): 2965 (C-H stretching), 1748 (C=O ester), 1609, 1509 (C=C arene), 1366 (C-H bending), 1216, 1132, 1034 (C-O stretching), 907 (C-H bending).

^{1}H NMR (400 MHz $CDCl_3$): δ 6.46-7.20, (24H, m, H2,5,2'',3'',5'',6''-Ar), 5.11-5.47, (12H, m, H2''',3''',4'''-Glu), 4.91-5.09, (4H, m, H1'''-Glu), 4.06-4.42, (12H, m, ArCH + H6'''-Glu), 3.74-3.95, (4H, m, H5'''-Glu), 2.11-2.83, (32H, m, CH_2CH_2, $COCH_2$), 1.96-2.05, (48H, m, OAc-Glu), 1.46-1.76, (16H, m, CH_2), 0.73-1.08, (24H, m, CH_3).

^{13}C NMR (100 MHz $CDCl_3$): δ 171.4, 171.1, 170.5, 170.2, 169.4, 169.2 (C=O); 155.3, 155.2, 154.9, 147.9, 147.8, 147.2, 147.0, 146.5, 146.2, 146.0, 145.8, 136.4, 136.2, 136.1, 135.9, 132.5, 131.2, 131.1, 129.7, 129.6, 117.9, 117.1, 116.9, 116.8, 116.6 (aromatic carbons); 99.4, 72.7, 71.9, 71.1, 68.2, 61.9 (C-Glucose); 35.6, 35.5 ($COCH_2$); 32.6 (CH_2-CH_2); 20.7, 20.6, 20.6 (OAc-Glucose); 18.2, 18.2, 18.2, 18.1, 18.0, 17.9, 17.4 (CH_2); 13.7, 13.6, 13.6, 13.5 (CH_3).

Mass Spectrum: Expected: *m/z* 2872.0822 $(M+Na)^+$. Observed: *m/z* 2872.0863

10.23 Synthesis of calix[4]methylresorcinarene glycosides (General procedure)

To a stirred solution of glycosyl benzaldehyde (1 eq) in a mixture of Et_2O and THF (1:1 ratio, 30 mL) was added anhydrous $AlCl_3$ (2 eq) and the mixture was stirred under N_2 for 15 min. Subsequently, 2-methylresorcinol (1 eq) was added and the mixture was stirred at r.t. for a further 48 h. A precipitate was obtained by adding the reaction mixture to Et_2O (100 mL). The precipitate was filtered and washed many times with Et_2O. The solid was then dissolved in EtOAc and the organic layer was washed with water (100 mL x 2) then dried ($MgSO_4$). The solvent was concentrated under reduced pressure to give the desired compounds as crude solids.

10.23.1 Calix[4]methylresorcinarene glucoside 215

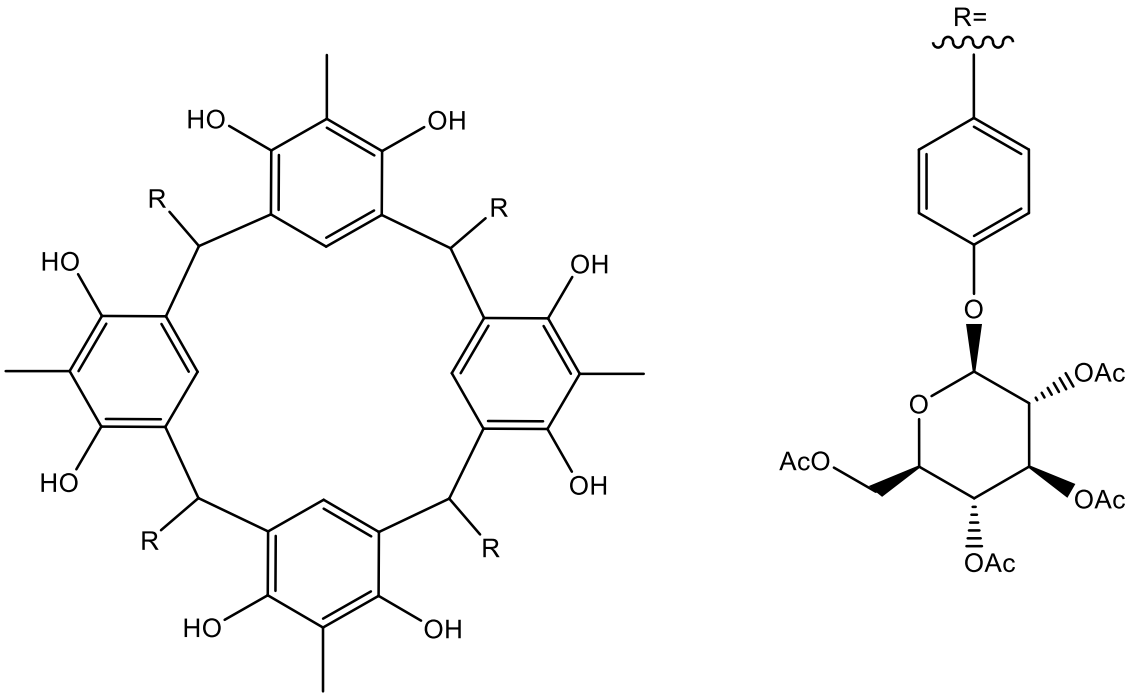

215

Compound **215** was synthesised according to the general procedure from 4-(2',3',4',6'-tetra-*O*-acetyl-*β*-D-glucopyranosyloxy)benzaldehyde (1.50 g, 3.31 mmol), 2-methylresorcinol (0.41 g, 3.31 mmol) and anhydrous $AlCl_3$ (0.88 g, 6.63 mmol) in a mixture of Et_2O and THF (1:1 ratio, 30 mL) gave a red precipitate of the desired compound (1.64 g, 0.73 mmol, 22%).

10.23.2 Calix[4]methylresorcinarene glucoside 217

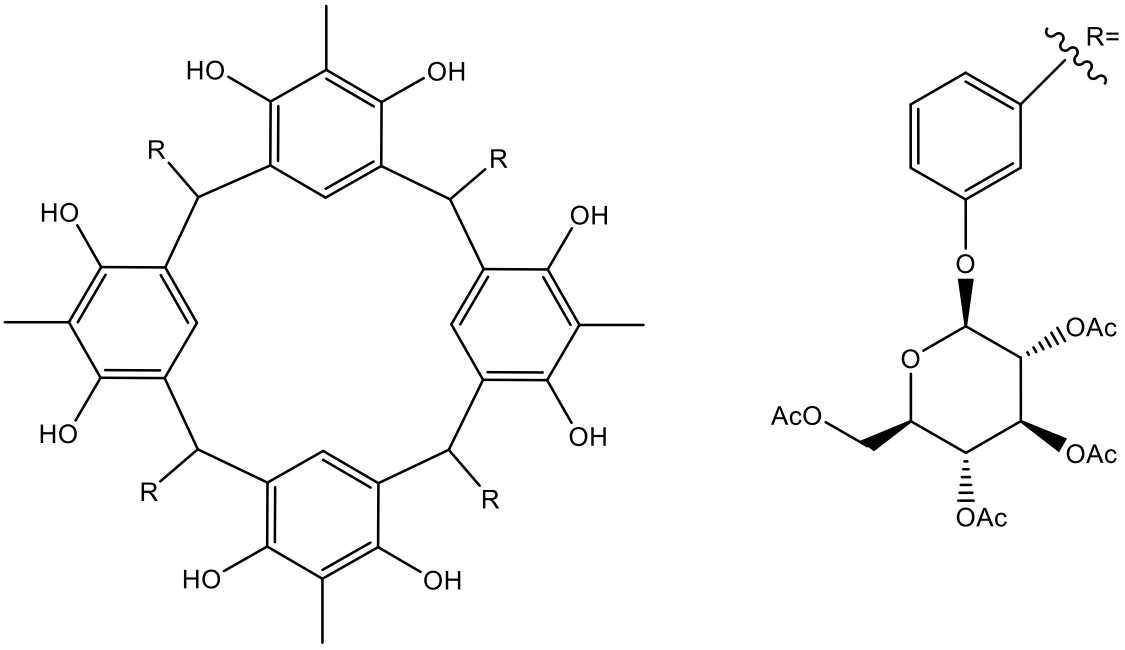

217

Compound **217** was synthesised according to the general procedure from 3-(2',3',4',6'-tetra-O-acetyl-*β*-D-glucopyranosyloxy)benzaldehyde (1.20 g, 2.65 mmol), 2-Methylresorcinol (0.32 g, 2.65 mmol) and anhydrous $AlCl_3$ (0.70 g, 5.30 mmol) in a mixture of Et_2O and THF (1:1 ratio, 20 mL) gave a red precipitate of the desired compound (1.14 g, 0.51 mmol, 19%).

10.23.3 Calix[4]methylresorcinarene galactoside 219

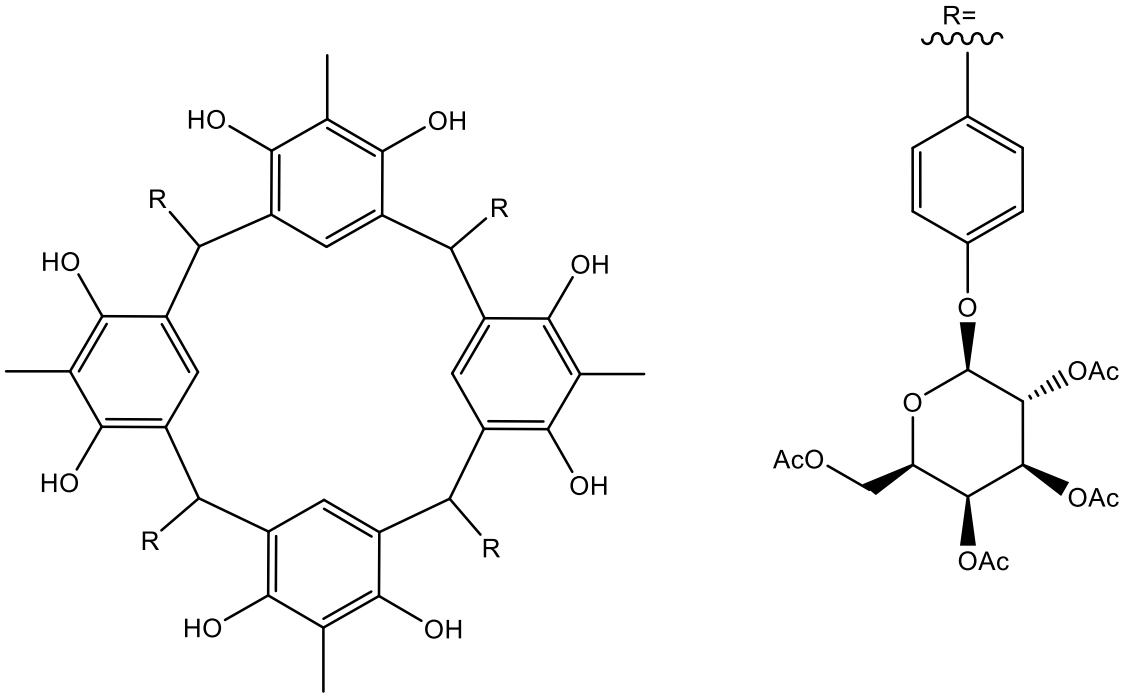

219

Compound **219** was synthesised according to the general procedure from 4-(2',3',4',6'-tetra-*O*-acetyl-*β*-D-galactopyranosyloxy)benzaldehyde (0.80 g, 1.77 mmol), 2-Methylresorcinol (0.21 g, 1.77 mmol) and $BF_3.Et_2O$ (0.43 mL, 3.53 mmol) in Et_2O (15 mL) gave a yellow precipitate of the desired compound (0.57 g, 0.25 mmol, 14%).

10.23.4 Calix[4]methylresorcinarene lactoside 223

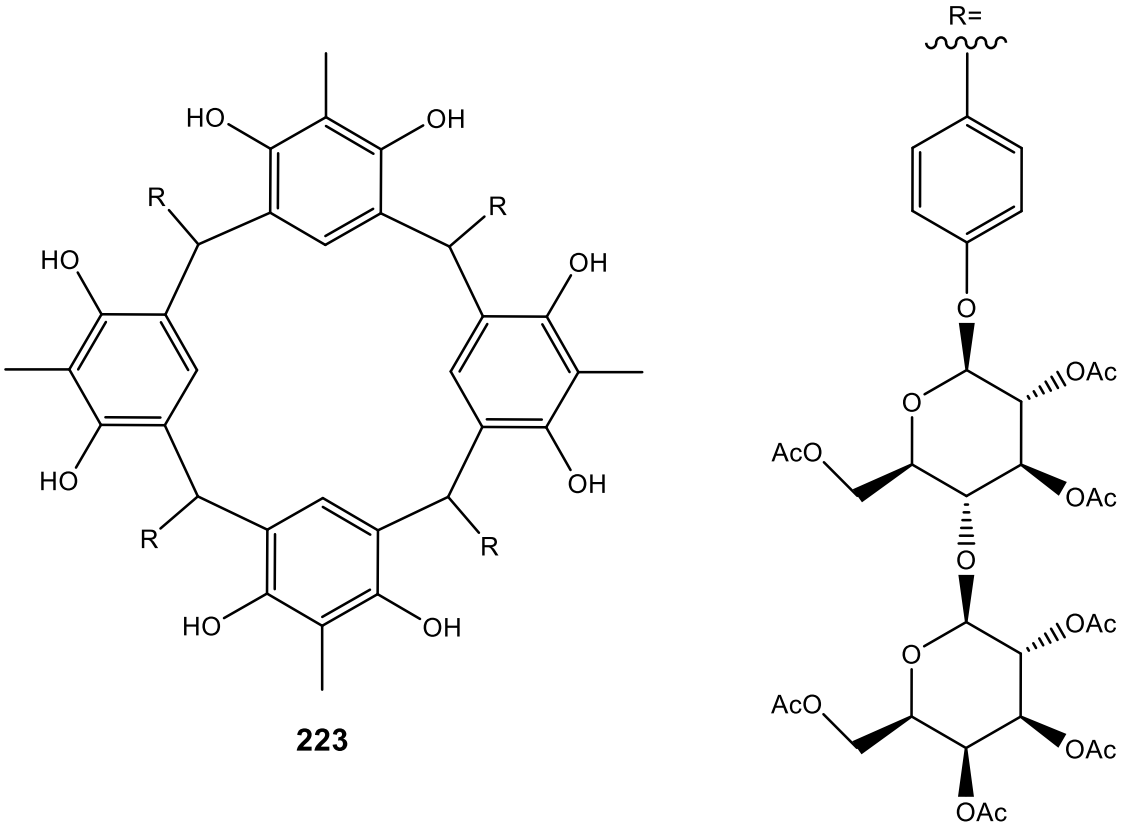

223

To a stirred solution of 4-(2',3',6',2'',3'',4'',6''-heptaacetyl-*β*-D-lactosyl)benzaldehyde (0.46 g, 0.62 mmol) and 2-methylresorcinol (0.07 g, 0.62 mmol) in anhydrous DCM (15 mL) was added $BF_3.Et_2O$ (0.15 mL, 1.24 mmol) and stirring was continued overnight under N_2 atmosphere. The reaction mixture was then diluted with water (20 mL) and DCM (40 mL), the organic layer was washed with brine (50 mL), dried ($MgSO_4$) and evaporated under reduced pressure to give the title compound (0.41 g, 0.12 mmol, 19%).

10.23.5 Calix[4]methylresorcinarene cellobioside 224

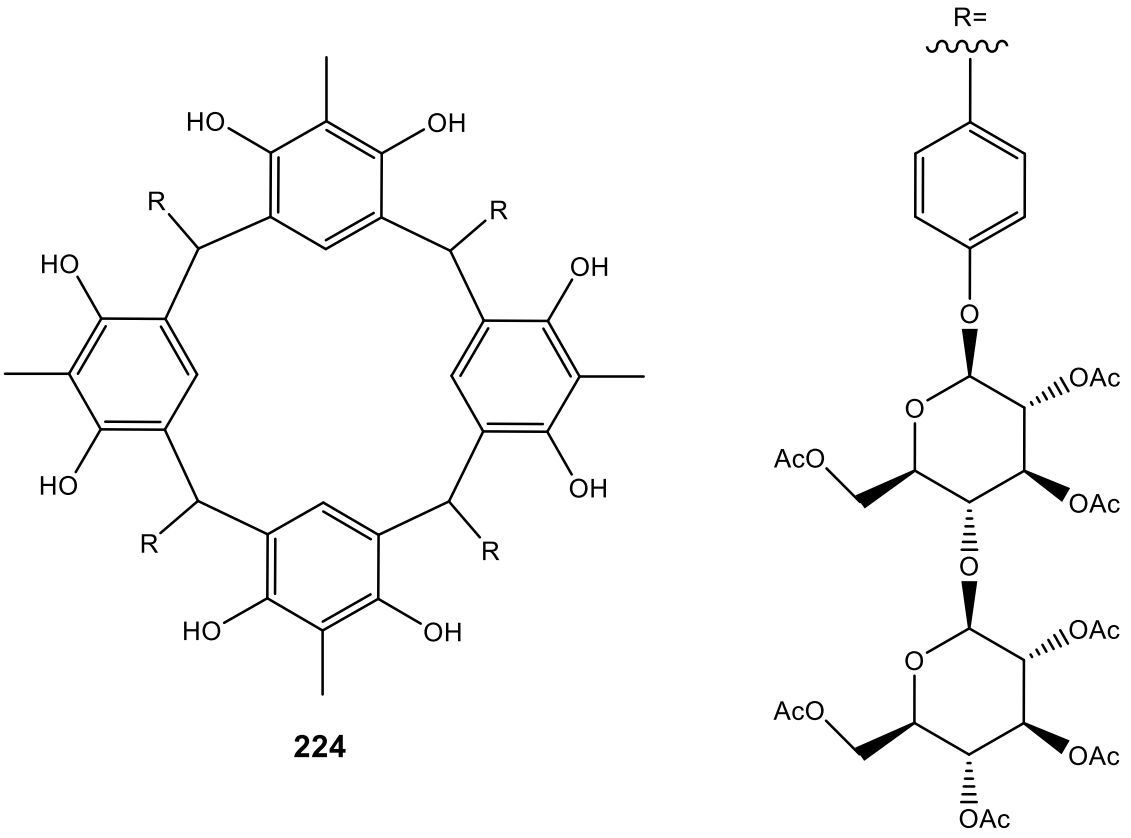

224

Compound **224** was synthesised similarly to compound **223** from 4-(2',3',6',2'',3'',4'',6''-heptaacetyl-*β*-D-cellobiosyl)benzaldehyde (0.50 g, 0.67 mmol), 2-methylresorcinol (0.08 g, 0.67 mmol) and $BF_3.Et_2O$ (0.16 mL, 1.35 mmol) gave the desired compound (0.49 g, 0.14 mmol, 21%).

10.24 Esterfication of calix[4]methylresorcinarene glycosides

10.24.1 Acylated calix[4]methylresorcinarene glucoside 216

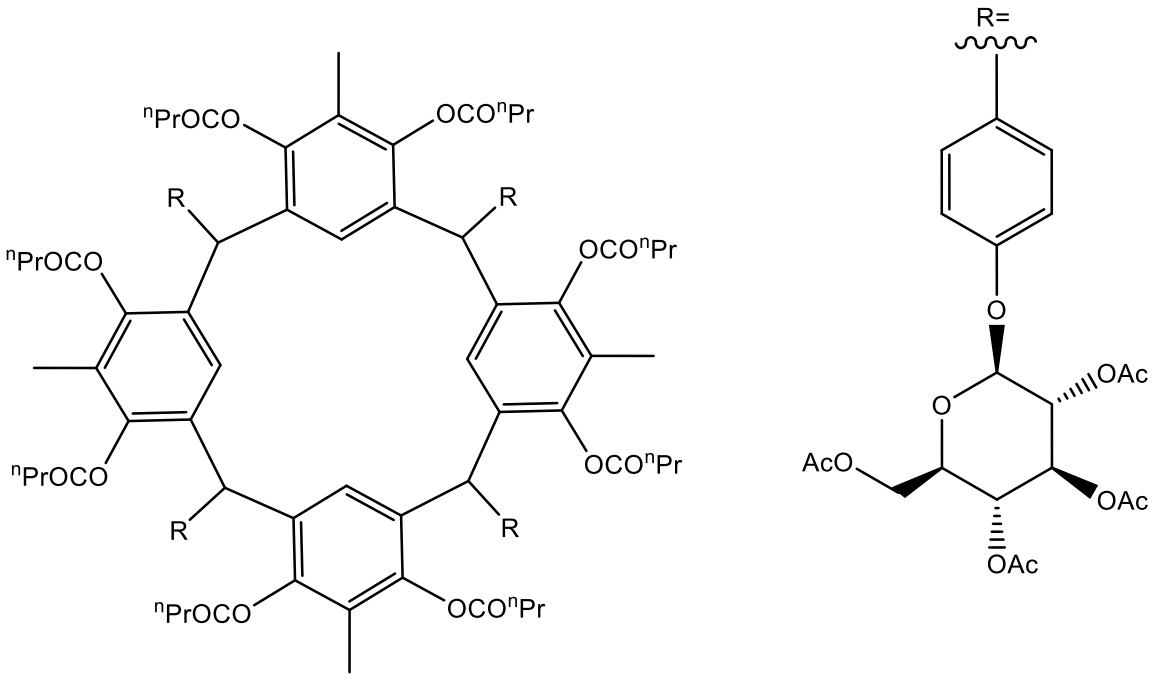

216

Compound **216** was synthesised according to the general procedure. The crude mixture of calix[4]methylresorcinarene glucoside **215** (3.05 g, 1.36 mmol) was reacted with butyric anhydride (30 ml) and pyridine (5 ml), the crude product was separated by silica gel column chromatography using EtOAc: Pet. ether (1.5:1) as eluent to yield one product of the butyrated calix[4]methylresorcinarene glucoside as yellow crystals (0.93 g, 0.33 mmol).

Yield: 24%

R_f of compound **216** (EtOAc: Pet. ether, 1.5:1): 0.16

Mp: 132-135 ^{0}C

Vmax (cm^{-1}): 2967 (C-H stretching), 1747 (C=O ester), 1608, 1507 (C=C arene), 1365 (C-H bending), 1216, 1132, 1071, 1033 (C-O stretching), 907 (C-H bending).

^{1}H NMR (400 MHz $CDCl_3$): δ 6.76, (1H, brs, H5-Ar), 6.62, (16H, dd, *J* 15.1; 6.8, H2',3',5',6'-Ar), 6.1, (2H, d, H5-Ar), 5.80, (1H, brs, H5-Ar), 5.11-5.64, (16H, m, ArCH+ H2'',3'',4''-Glu), 4.96, (4H, d, *J* 7.9, H1''-Glu), 3.86-4.61, (12H, m, H5'',6''-Glu), 2.20-2.65, (16H, m, $COCH_2$), 1.96-2.17, (48H, m, OAc-Glu), 1.85, (6H, s, CH_3-resorcinol), 1.81, (3H, s, CH_3-resorcinol), 1.72, (3H, s, CH_3-resorcinol), 1.42-1.63, (16H, m, CH_2), 0.65-1.13, (24H, m, CH_3).

^{13}C NMR (100 MHz $CDCl_3$): δ 170.6, 170.5, 170.2, 170.0, 169.7, 169.6, 169.5, 169.3 (C=O); 156.0, 146.8, 146.6, 146.2, 131.8, 131.6, 130.3, 129.6, 124.3, 116.2 (aromatic carbons); 100.1, 72.9, 72.7, 72.1, 71.9, 71.7, 71.4, 71.2, 68.5, 62.3, 62.0 (C-Glucose); 44.3 (ArCH); 35.3, 35.3 ($COCH_2$); 20.7, 20.6, 20.6, 20.6, 20.5, 20.5, 20.4 (OAc-Glucose); 18.1, 18.0, 17.9 (CH_2); 13.8, 13.7, 13.6 (CH_3); 10.8 (CH_3-resorcinol).

Mass Spectrum: Expected: *m*/*z* 1414.5493 $(M+2NH_4)^{2+}$. Observed: *m*/*z* 1414.5493

10.24.2 Acylated calix[4]methylresorcinarene glucoside 218

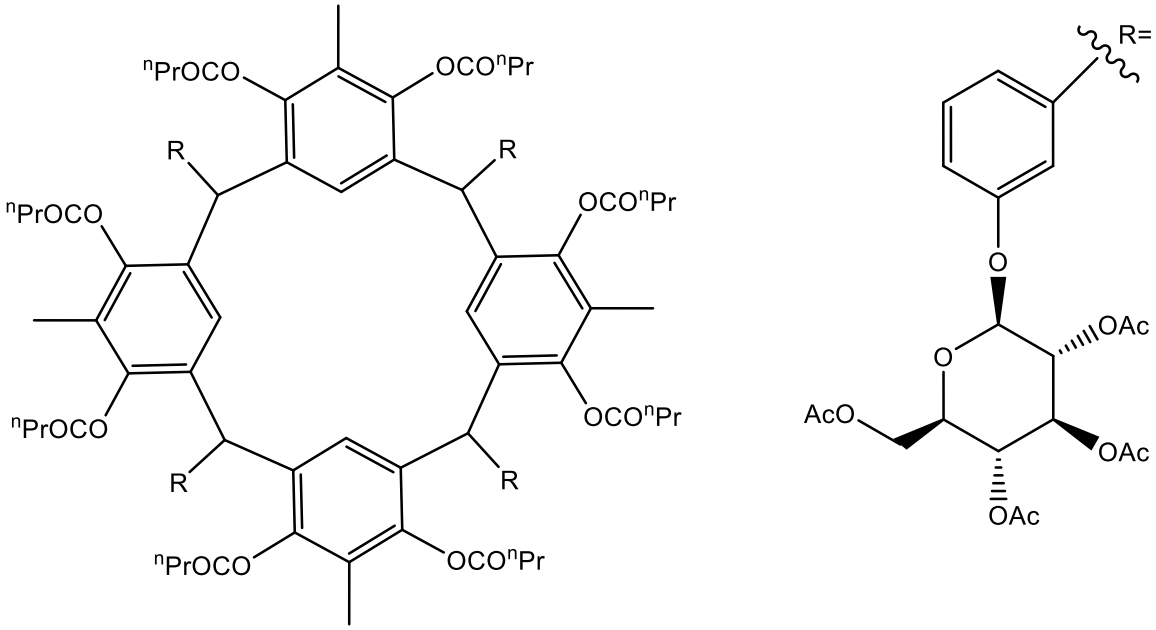

218

Compound **218** was synthesised according to the general procedure. The crude mixture of calix[4]methylresorcinarene glucoside **217** (3.00 g, 1.34 mmol) was reacted with butyric anhydride (30 mL) and pyridine (5 mL), the crude product was separated by silica gel column chromatography using EtOAc: Pet. ether (1.5:1) as eluent to yield one product of the butyrated calix[4]methylresorcinarene glucoside as a yellow powder (0.61 g, 0.22 mmol).

Yield: 16%

R_f of compound **218** (EtOAc: Pet. ether, 1.5:1): 0.28

Mp: 127-130

Vmax (cm^{-1}): 2967 (C-H stretching), 1747 (C=O ester), 1588 (C=C arene), 1428, 1365 (C-H bending), 1214, 1133, 1034 (C-O stretching), 905 (C-H bending).

^{1}H NMR (400 MHz $CDCl_3$): δ 5.71-7.22 (20H, m, H5,2',4',5',6'-Ar), 5.08-5.65 (16H, m, H2'',3'',4''-Glu+ ArCH), 4.74-5.03 (4H, m, H1''-Glu), 3.65-4.57 (12H, m, H5'',6''-Glu), 2.22-3.04 (16H, m, $COCH_2$), 1.89-2.17 (48H, m, OAc-Glu), 1.70-1.82 (12H, m, CH_3-resorcinol), 1.26-1.67 (16H, m, CH_2), 0.67-1.19 (24H, m, CH_3).

^{13}C NMR (100 MHz $CDCl_3$): δ 170.5, 170.1, 169.7, 169.3 (C=O); 146.4, 128.9, 124.6, 115.6 (aromatic carbons); 72.9, 72.8, 71.8, 71.2, 68.3, 62.0, 61.4 (C-Glucose); 35.5, 35.4 ($COCH_2$); 20.5, 20.5 (OAc-Glucose); 18.4, 18.2, 18.0, 17.9 (CH_2); 13.7, 13.6, 13.4 (CH_3); 10.8, 10.7 (CH_3-resorcinol).

Mass Spectrum: Expected: *m*/*z* 1414.5493 $(M+2NH_4)^{2+}$. Observed: *m*/*z* 1414.5499

10.24.3 Acylated calix[4]methylresorcinarene galactoside 220

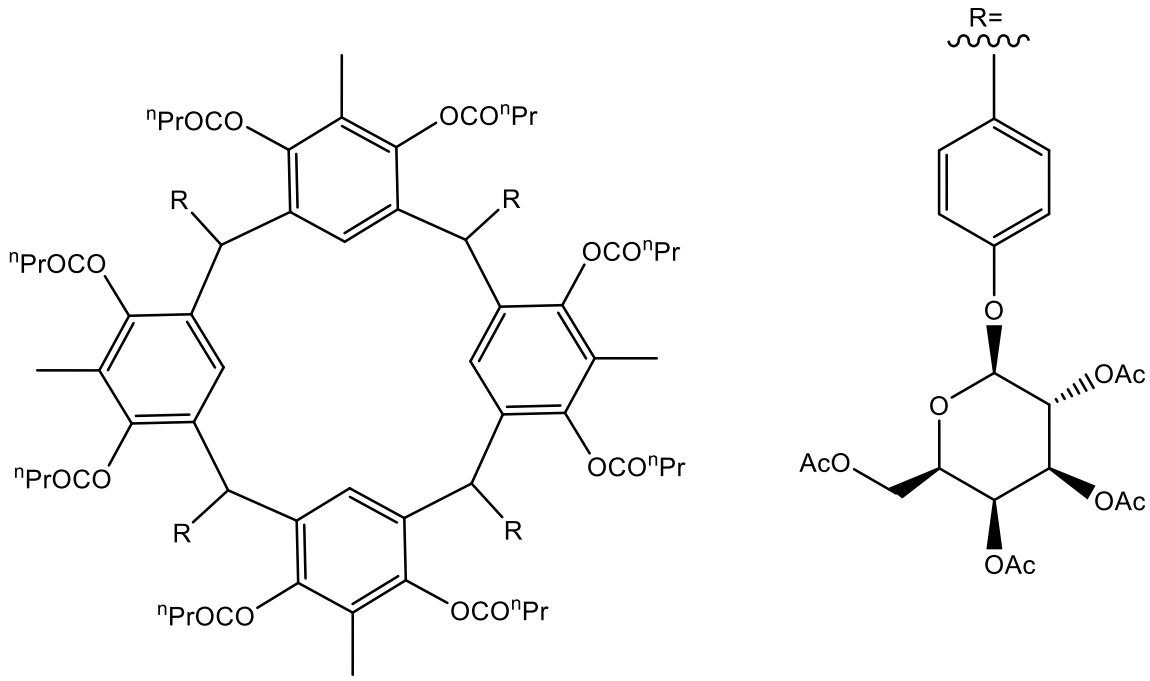

220

Compound **220** was synthesised according to the general procedure. The crude mixture of calix[4]methylresorcinarene galactoside **219** (0.50 g, 0.22 mmol) was reacted with butyric anhydride (30 mL) and pyridine (5 mL), the crude product was separated by silica gel column chromatography using EtOAc: Pet. ether (1.5:1) as eluent to yield one product of the butyrated calix[4]methylresorcinarene galactoside as yellow crystals (0.04 g, 0.01 mmol).

Yield: 6%

R_f of compound **220** (EtOAc: Pet. ether, 1.5:1): 0.22

Mp: 131-134

Vmax (cm^{-1}): 2966 (C-H stretching), 1745 (C=O ester), 1608, 1507 (C=C arene), 1367 (C-H bending), 1217, 1132, 1072 (C-O stretching), 916 (C-H bending).

^{1}H NMR (400 MHz $CDCl_3$): δ 6.76, (1H, brs, H5-Ar), 6.65, (16H, d, *J* 7.7, H2',3',5',6'-Ar), 6.13, (2H, d, H5-Ar), 5.88, (1H, brs, H5-Ar), 5.40-5.74, (8H, m, H2'',4''-Gal), 5.28, (4H, d, *J* 7.7, H3''-Gal+ ArCH), 5.17, (4H, d, *J* 7.9, H3''-Gal+ ArCH), 4.92, (2H, d, *J* 8.1, H1''-Gal), 4.77-4.88, (2H, brs, H1''-Gal), 3.90-4.51, (12H, m, H5'',6''-Gal), 2.30-2.77, (16H, m, $COCH_2$), 1.94-2.26, (48H, m, OAc-Gal), 1.86, 1.82, 1.76 (12H, m, CH_3-resorcinol), 1.27-1.65, (16H, m, CH_2), 0.74-1.08, (24H, m, CH_3).

^{13}C NMR (100 MHz $CDCl_3$): δ 170.7, 170.6, 170.3, 170.2, 170.1, 169.7, 169.5, 169.1 (C=O); 156.0, 146.6, 130.3, 128.5, 127.6, 126.9, 116.4 (aromatic carbons); 71.2, 71.0, 70.9, 69.1, 68.9, 67.1, 67.0, 65.3, 61.4 (C-Galatose); 44.2* (ArCH); 35.4, 35.2 ($COCH_2$); 20.8, 20.6, 20.6, 20.6, 20.5 (OAc-Galactose); 18.1, 18.0, 17.9, 17.4, 17.2 (CH_2); 13.8, 13.7, 13.6, 13.6 (CH_3); 10.8* (CH_3-resorcinol).

Mass Spectrum: Expected: *m*/*z* 1414.5493 $(M+2NH_4)^{2+}$. Observed: *m*/*z* 1414.5494

* Peaks are not assigned in ^{13}C NMR spectrum but clearly observed from DEPT and HSQC analysis

10.24.4 Acylated calix[4]methylresorcinarene lactoside 227

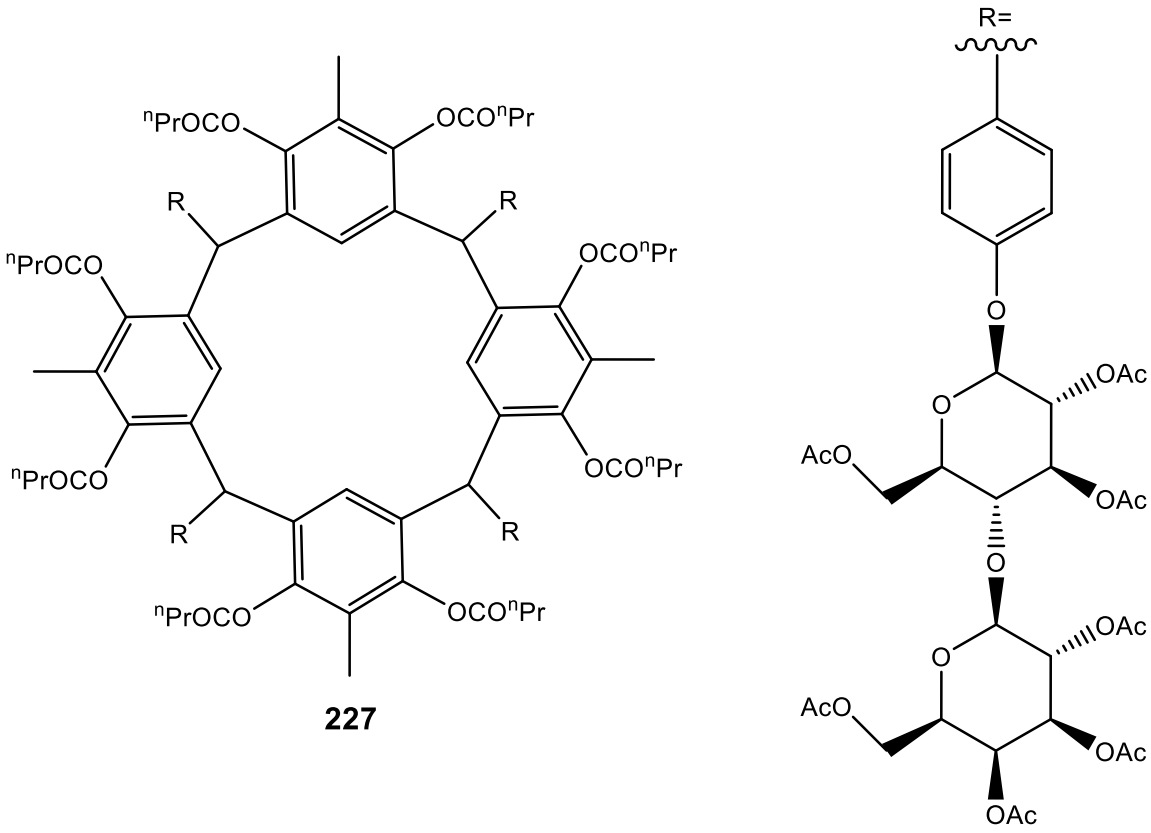

227

Compound **227** was synthesised according to the general procedure. The crude mixture of calix[4]methylresorcinarene lactoside **223** (0.40 g, 0.12 mmol) was reacted with butyric anhydride (30 mL) and pyridine (5 mL), the crude product was separated by silica gel column chromatography using EtOAc: Pet. ether (gradient ratio) as eluent to yield one product of the butyrated calix[4]methylresorcinarene lactoside.

10.24.5 Acylated calix[4]methylresorcinarene cellobioside 228

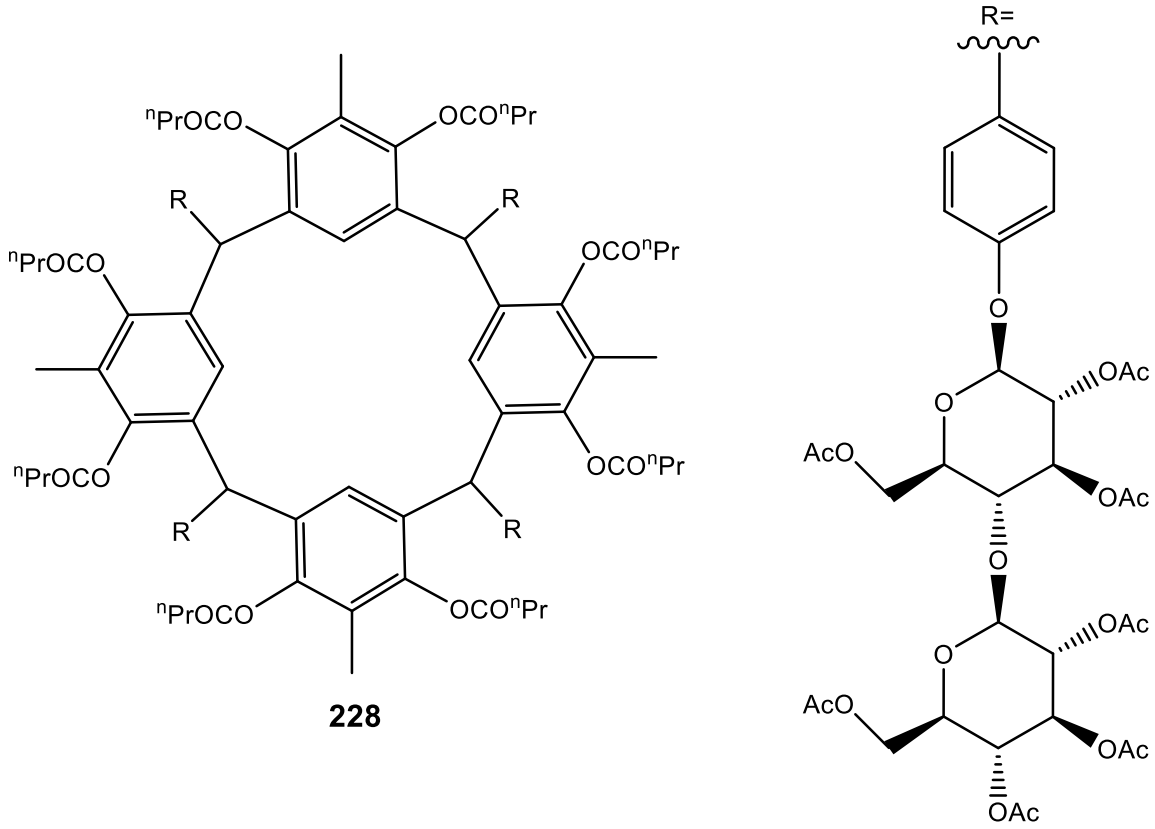

228

Compound **228** was synthesised according to the general procedure. The crude mixture of calix[4]methylresorcinarene cellobioside **224** (0.47 g, 0.14 mmol) was reacted with butyric anhydride (30 ml) and pyridine (5 ml), the crude product was separated by silica gel column chromatography using EtOAc: Pet. ether (gradient ratio) as eluent to yield one product of the butyrated calix[4]methylresorcinarene cellobioside.

10.25 Synthesis of calix[4]pyrogallolarene glycosides

10.25.1 Calix[4]pyrogallolarene glucoside 221

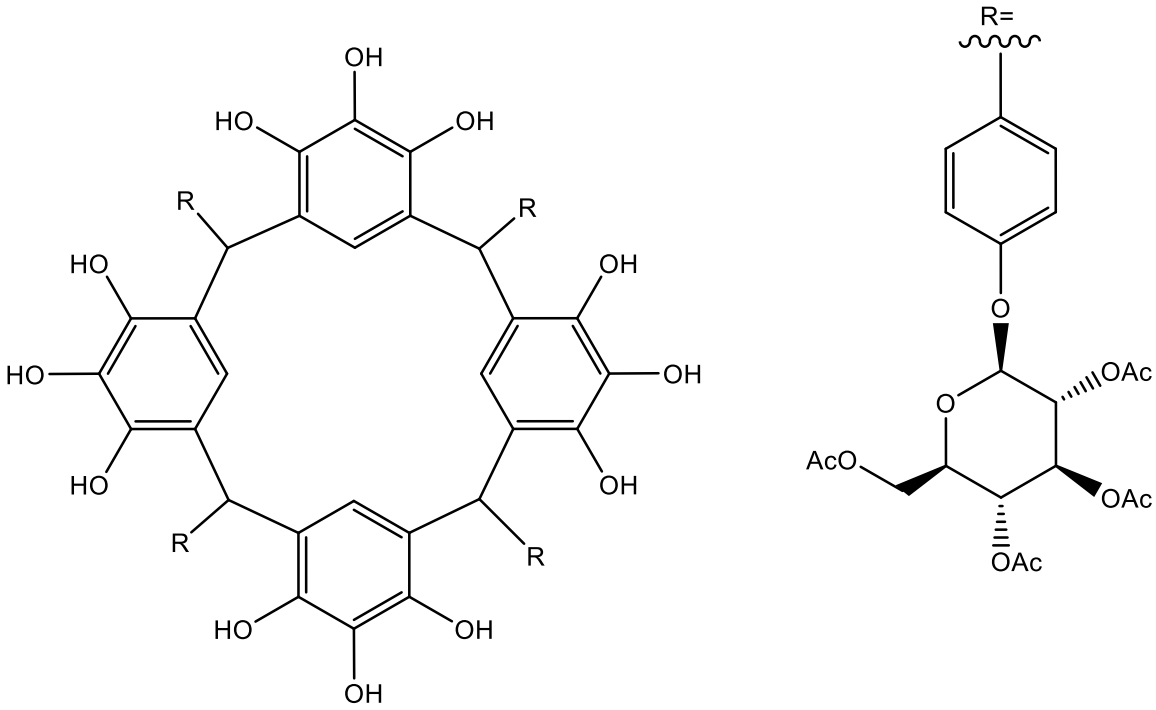

221

To a stirred solution of 4-(2',3',4',6'-tetra-*O*-acetyl-*β*-D-glucopyranosyloxy)benzaldehyde (2.87 g, 6.34 mmol) in a mixture of Et_2O and THF (1:1 ratio, 50 mL) was added a solution of $AlCl_3.PhNO_2$ (2.70 mL, 25.37 mmol) and the mixture was stirred under N_2 for 15 min. Subsequently, pyrogallol (0.80 g, 6.34 mmol) was added and the mixture was stirred at r.t for a further 72 h. A precipitate was obtained by adding the reaction mixture to Et_2O (200 mL). The precipitate was filtered and washed many times with Et_2O. The solid was then dissolved in EtOAc and the organic layer was washed with water (100 mL x 4) then dried ($MgSO_4$). The solvent was evaporated under reduced pressure to give the desired compound as a black solid (2.31 g, 1.03 mmol, 16%).

10.25.2 Calix[4]pyrogallolarene lactoside 225

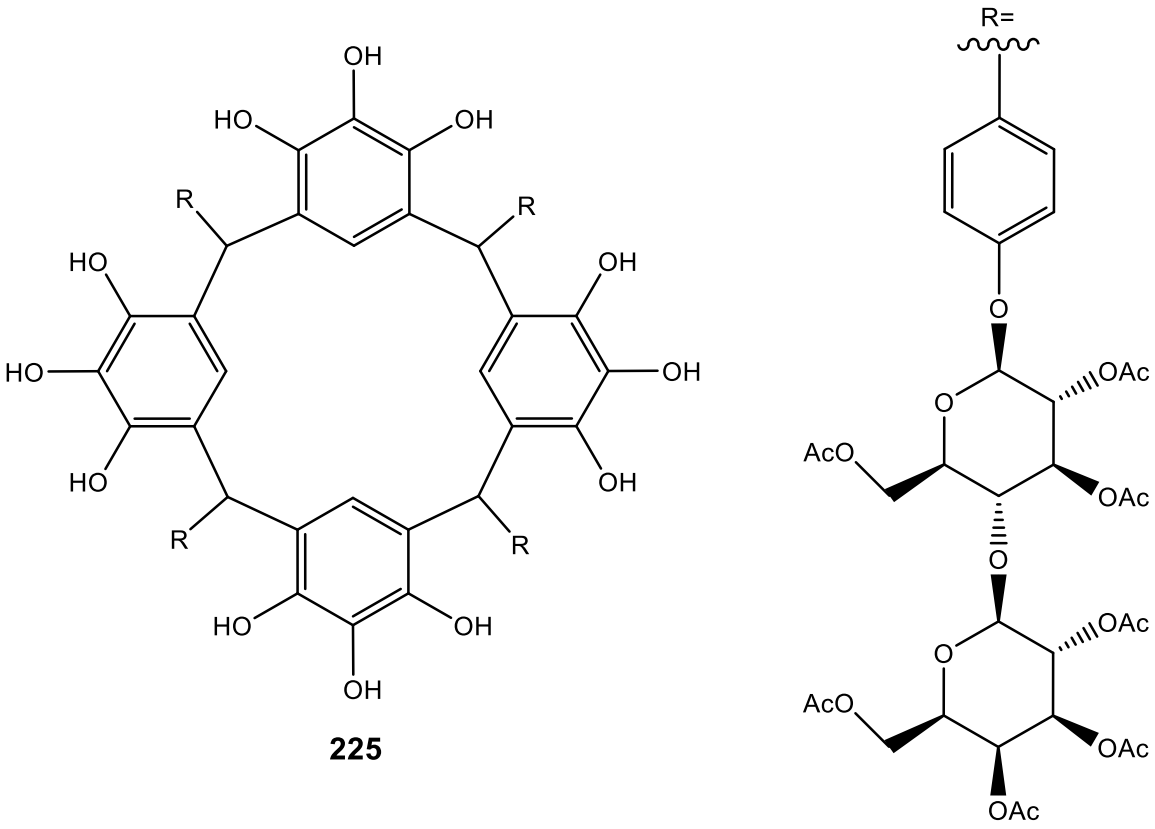

225

To a stirred solution of 4-(2',3',6',2'',3'',4'',6''-heptaacetyl-*β*-D-lactosyl)benzaldehyde (0.70 g, 0.94 mmol) and pyrogallol (0.11 g, 0.94 mmol) in anhydrous DCM (20 mL) was added $BF_3.Et_2O$ (0.23 mL, 1.89 mmol) and stirring was continued overnight under N_2 atmosphere. The reaction mixture was then diluted with water (30 mL) and DCM (50 mL), the organic layer was washed with brine (50 mL), dried ($MgSO_4$) and evaporated under reduced pressure to give the title compound as a brown solid (0.52 g, 0.15 mmol, 16%).

10.25.3 Calix[4]pyrogallolarene cellobioside 226

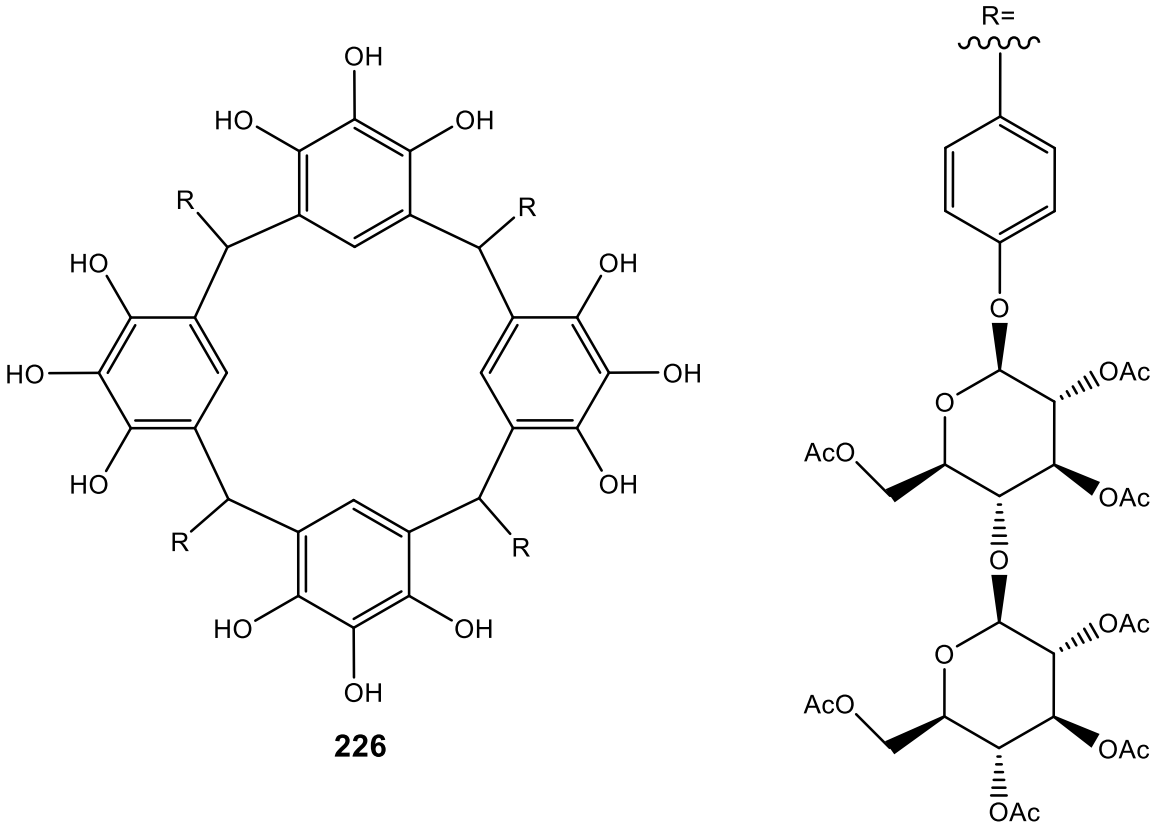

226

Compound **226** was synthesised similarly to compound **225** from 4-(2',3',6',2'',3'',4'',6''-heptaacetyl-*β*-D-cellobiosyl)benzaldehyde (0.50 g, 0.67 mmol), pyrogallol (0.08 g, 0.67 mmol) and $BF_3.Et_2O$ (0.16 ml, 1.35 mmol) in anhydrous DCM (15 mL) gave the desired compound as a brown solid (0.40 g, 0.12 mmol, 17%).

10.26 Esterfication of calix[4]pyrogallolarene glycosides

10.26.1 Acylated calix[4]pyrogallolarene glucoside 222

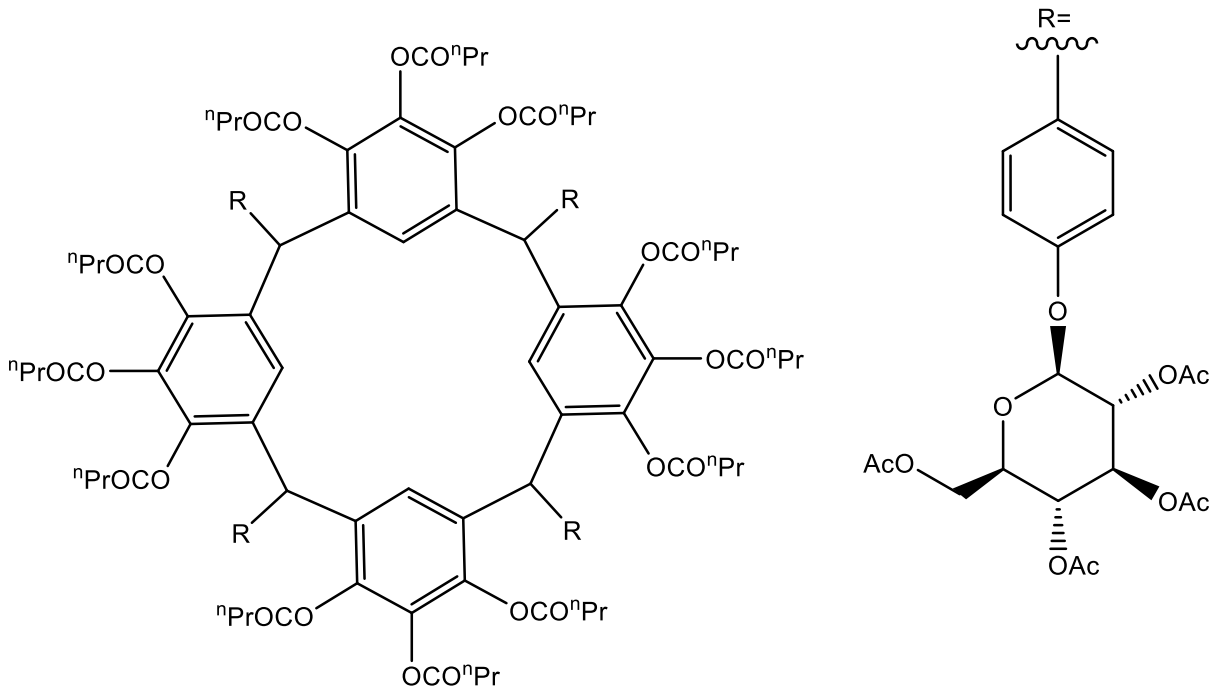

222

Compound **222** was synthesised according to the general procedure. The crude mixture of calix[4]pyrogallolarene glucoside **221** (2.31 g, 1.03 mmol) was reacted with butyric anhydride (30 mL) and pyridine (5 mL), the crude product was purified by silica gel column chromatography using EtOAc: Pet. ether (2:1) as eluent to yield one product of the butyrated calix[4]pyrogallolarene glucoside as a yellow powder (0.23 g, 0.07 mmol).

Yield: 7%

R_f of compound **222** (EtOAc: Pet. ether, 2:1): 0.41

Mp: 130-134 ^{0}C

Vmax (cm^{-1}): 2967 (C-H stretching), 1746 (C=O ester), 1607, 1508 (C=C arene), 1436, 1365 (C-H bending), 1217, 1177, 1126, 1070, 1033 (C-O stretching), 907 (C-H bending).

^{1}H NMR (400 MHz $CDCl_3$): δ 6.54-7.12, (16H, m, H2',3',5',6'-Ar), 6.30, (2H, d, H5-Ar), 6.08, (2H, s, H5-Ar), 5.61, (2H, d, ArCH), 5.46, (2H, d, *J* 4.5, ArCH), 4.89-5.14, (16H, m, H1'',2'',3'',4''-Glu), 3.75-4.40, (12H, m, H5'',6''-Glu), 2.21-2.79, (24H, m, $COCH_2$), 1.97-2.20, (48H, m, OAc-Glu), 1.39-1.87, (24H, m, CH_2), 0.68-1.18, (36H, m, CH_3).

^{13}C NMR (100 MHz $CDCl_3$): δ 170.6, 170.6, 170.2, 170.1, 170.0, 169.7, 169.6, 169.5, 169.4, 169.3, 169.1, 169.0, 168.9 (C=O); 156.2, 156.0, 140.5, 140.3, 140.2, 136.2, 132.9, 132.6, 132.4, 130.5, 130.4, 116.8, 116.1 (aromatic carbons); 72.7, 71.9, 71.3, 71.1, 68.7, 68.2, 61.8 (C-Glucose); 43.9* (ArCH); 35.5, 35.4, 35.1, 35.0, 34.9 ($COCH_2$); 20.8, 20.7, 20.7, 20.6 (OAc-Glucose); 18.3, 18.2, 18.1, 18.1, 18.0, 17.9, 17.5, 17.2 (CH_2); 13.7, 13.6, 13.6, 13.5, 13.5 (CH_3).

Mass Spectrum: Expected: *m*/*z* 1558.5916 $(M+2NH_4)^{2+}$. Observed: *m*/*z* 1558.5918

* Peaks are not assigned in ^{13}C NMR spectrum but clearly observed from DEPT and HSQC analysis

10.26.2 Acylated calix[4]pyrogallolarene lactoside 229

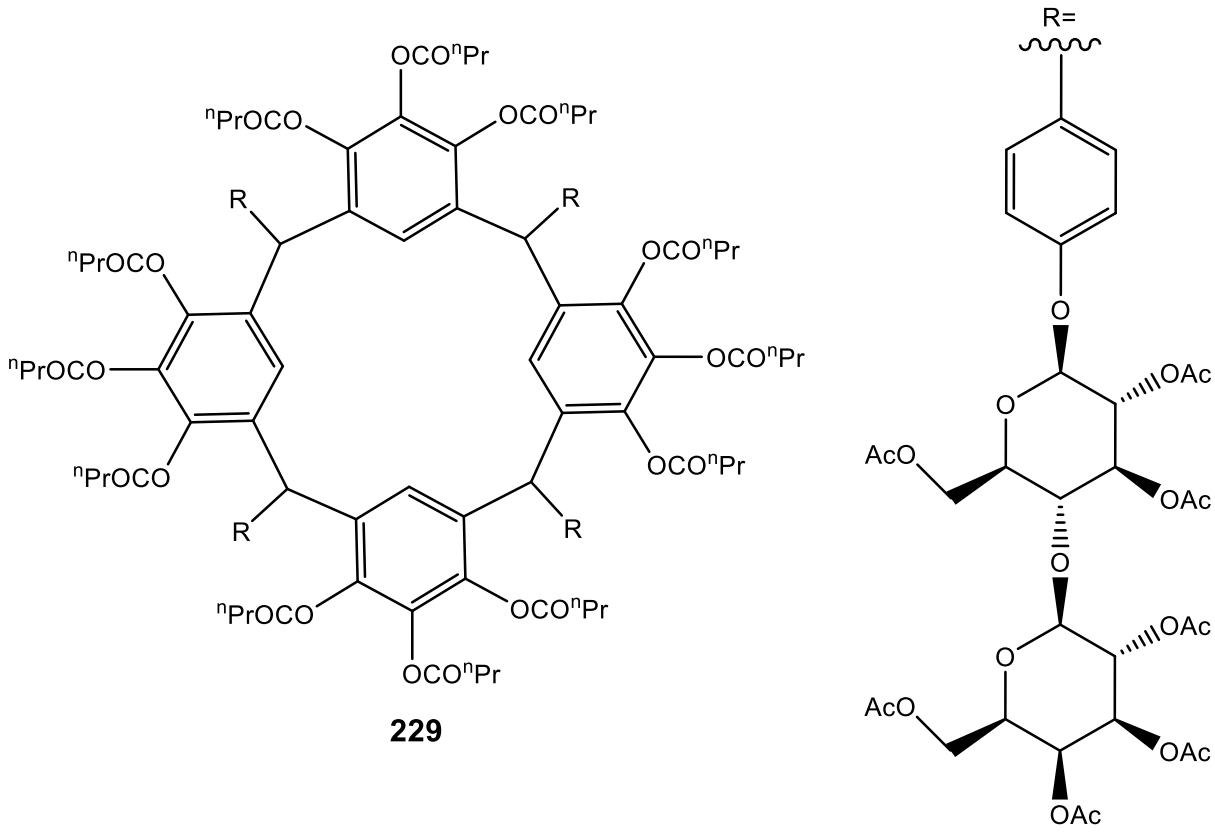

229

Compound **229** was synthesised according to the general procedure. The crude mixture of calix[4]pyrogallolarene lactoside **225** (0.50 g, 0.15 mmol) was reacted with butyric anhydride (30 mL) and pyridine (5 mL), the crude product was separated by silica gel column chromatography using EtOAc: Pet. ether (gradient ratio) as eluent to yield one product of the butyrated calix[4]pyrogallolarene lactoside.

10.26.3 Acylated calix[4]pyrogallolarene cellobioside 230

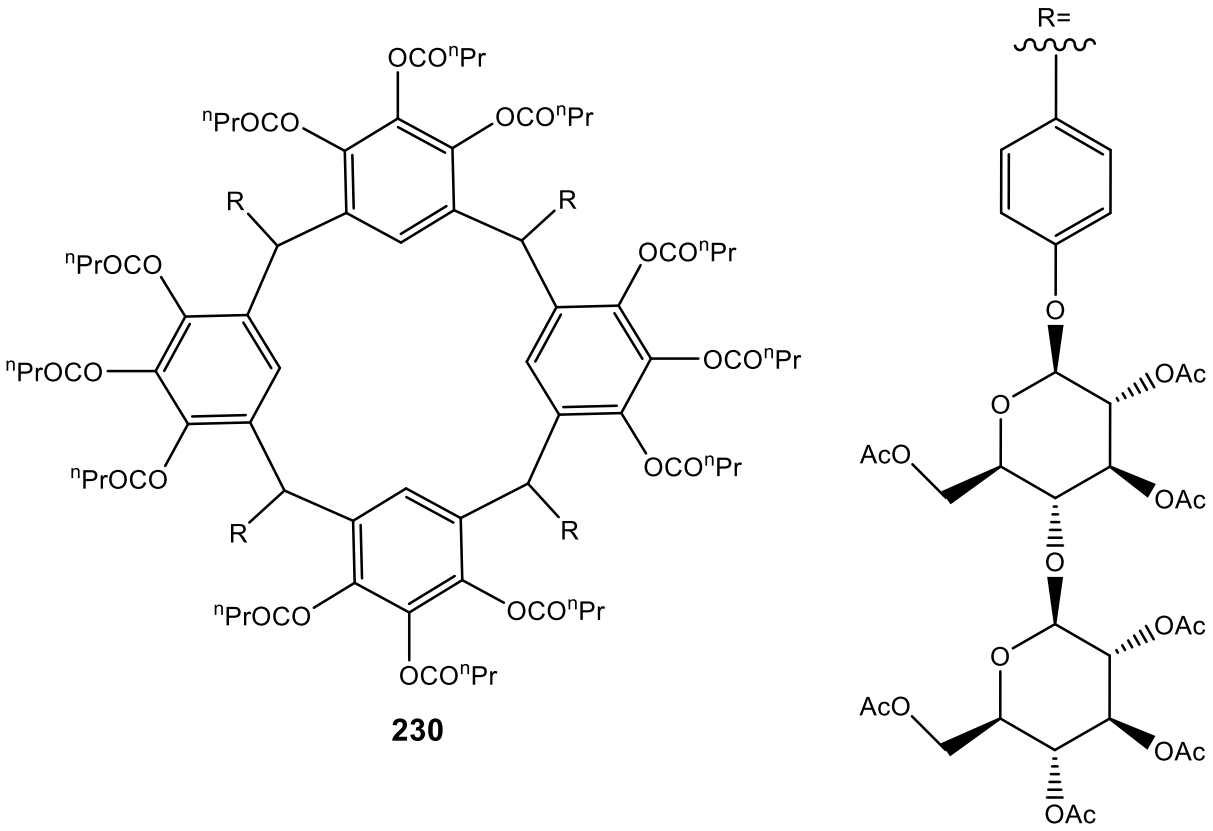

230

Compound **230** was synthesised according to the general procedure. The crude mixture of calix[4]pyrogallolarene cellobioside **226** (0.75 g, 0.22 mmol) was reacted with butyric anhydride (30 mL) and pyridine (5 mL), the crude product was separated by silica gel column chromatography using EtOAc: Pet. ether (gradient ratio) as eluent to yield one product of the butyrated calix[4]pyrogallolarene cellobioside.

10.27 Synthesis of glycol-*β*-D-monoglucosides tetraacetate (General procedure)

To a solution of 2,3,4,6-tetra-*O*-acetyl-*α*-D-glucopyranosyl bromide (4.11 g, 10 mmol) in dry DCM (50 mL), a corresponding diol (10 mL) was added under N_2 atmosphere. After stirring for 15 min at r.t. $HgBr_2$ (3.80 g, 10 mmol) was added to the mixture and stirring was continued overnight. The reaction mixture was diluted with DCM (50 mL) and washed with aqueous solution of KI 5% (50 mL x 3) and water (100 mL), dried ($MgSO_4$) and evaporated under reduced pressure. Colourless oil was obtained followed by silica gel column chromatography to yield the corresponding glycols (Wang *et al*., 2007).

10.27.1 2-Hydroxy ethyl 2',3',4',6'-tetra-*O*-acetyl-*β*-D-glucopyranoside 234

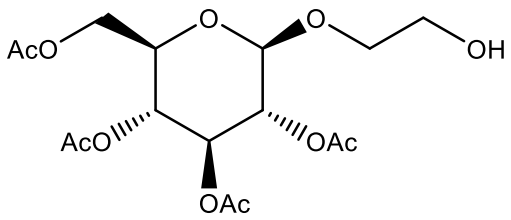

234

Compound **234** was synthesised according to the general procedure from ethylene glycol (10 mL, 179.30 mmol), the crude mixture was purified by silica gel column chromatography using EtOAc: Pet. ether (3:1) as eluent to give the title compound as a white solid (1.46 g, 3.72 mmol).

Yield: 37%

R_f of compound **234** (EtOAc: Pet. ether, 3:1): 0.31

Mp: 103-104 ^{0}C

Vmax (cm^{-1}): 3467 (O-H stretching), 2963 (C-H stretching), 1750, 1716 (C=O ester), 1380, 1363 (C-H bending), 1237, 1206, 1057, 1034 (C-O stretching), 907.

^{1}H NMR (400 MHz $CDCl_3$): δ 5.24, (1H, t, H3'-Glu), 4.99-5.09, (2H, m, H2',4'-Glu), 4.56, (1H, d, *J* 7.9, H1'-Glu), 4.2, (2H, d, *J* 4.2, CH_2), 3.85, (2H, t, CH_2), 3.66-3.78, (3H, m, H5',6a',6b'-Glu), 2.46, (1H, t, OH), 2.10, (3H, s, OAc), 2.06, (3H, s, OAc), 2.04, (3H, s, OAc), 2.01, (3H, s, OAc).

^{13}C NMR (100 MHz $CDCl_3$): δ 170.6, 170.2, 169.4, 169.4 (C=O); 101.4, 73.1, 72.6, 71.9, 71.3, 68.4 (C-Glucose+ CH_2); 62.0, 62.0 (CH_2OH, C-Glucose); 20.6, 20.6, 20.6 (OAc-Glucose).

10.27.2 5-Hydroxy-3-oxapentyl 2',3',4',6'-tetra-*O*-acetyl-*β*-D-glucopyranoside 235

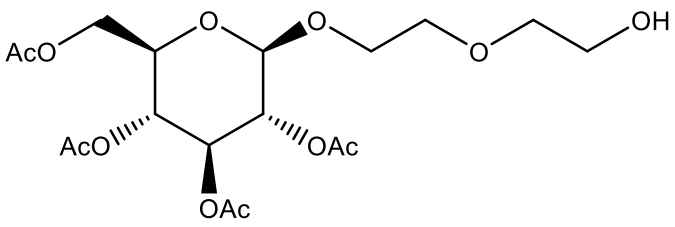

235

Compound **235** was synthesised according to the general procedure from diethyleneglycol (10 mL, 105.35 mmol), the crude mixture was purified by silica gel column chromatography using EtOAc: Pet ether (4:1) as eluent to give the title compound as a white solid (1.46 g, 3.34 mmol).

Yield: 33%

R_f of compound **235** (EtOAc: Pet. ether, 4:1): 0.22

Mp: 85-86 ^{0}C

Vmax (cm^{-1}): 3528 (O-H stretching), 2970 (C-H stretching), 1752, 1721 (C=O ester), 1375 (C-H bending), 1209, 1028 (C-O stretching).

^{1}H NMR (400 MHz $CDCl_3$): δ 5.22, (1H, t, H3'-Glu), 5.1, (1H, t, H4'-Glu), 5.01, (1H, dd, *J* 9.4, 8.1, H2'-Glu), 4.62, (1H, d, *J* 7.8, H1'-Glu), 4.27, (1H, dd, H6b'-Glu), 4.15, (1H, dd, H6a'-Glu), 3.95-3.99, (1H, m, CH), 3.57-3.77, (8H, m, $CH_2CH_2OCH_2CH$+ H5'-Glu), 2.29, (1H, t, OH), 2.10, (3H, s, OAc), 2.06, (3H, s, OAc), 2.03, (3H, s, OAc), 2.01, (3H, s, OAc).

^{13}C NMR (100 MHz $CDCl_3$): δ 170.7, 170.2, 169.5, 169.4 (C=O); 100.7, 72.7, 72.4, 71.8, 71.3, 70.0, 68.9, 68.3, 61.9, 61.6 (C-Glucose+ $CH_2CH_2OCH_2CH_2$); 20.7, 20.7, 20.6, 20.6 (OAc-Glu).

10.27.3 3-Hydroxy propyl 2',3',4',6'-tetra-*O*-acetyl-*β*-D-glucopyranoside 236

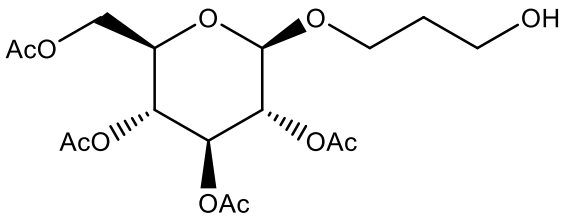

236

Compound **236** was synthesised according to the general procedure from 1,3-propanediol (10 mL, 138.37 mmol), the crude mixture was purified by silica gel column chromatography using EtOAc: Pet. ether (3:1) as eluent to give the title compound as a white solid (1.08 g, 2.65 mmol).

Yield: 26%

R_f of compound **236** (EtOAc: Pet. ether, 3:1): 0.28

Mp: 93-94 ^{0}C

Vmax (cm^{-1}): 3527 (O-H stretching), 2966 (C-H stretching), 1737 (C=O ester), 1382 (C-H bending), 1211, 1162, 1096, 1035 (C-O stretching), 906.

^{1}H NMR (400 MHz $CDCl_3$): δ 5.21, (1H, t, H3'-Glu), 5.08, (1H, t, H4'-Glu), 4.99, (1H, dd, *J* 9.5, 7.9, H2'-Glu), 4.53, (1H, d, *J* 7.9, H1'-Glu), 4.25, (1H, dd, *J* 4.9, H6b'-Glu), 4.17, (1H, dd, *J* 2.6, H6a'-Glu), 3.98-4.04, (1H, m, CH), 3.67-3.75, (4H, m, CH_2CH+ H5'-Glu), 2.10, (3H, s, OAc), 2.06, (3H, s, OAc), 2.03, (3H, s, OAc), 2.01, (3H, s, OAc), 1.89, (1H, t, *J* 5.7x(2), OH), 1.78-1.87, (2H, m, CH_2).

^{13}C NMR (100 MHz $CDCl_3$): δ 170.7, 170.2, 169.5, 169.4 (C=O); 100.7, 72.7, 71.8, 71.2, 68.4 (C-Glucose); 67.7 (CH_2); 61.9 (C-Glucose); 60.0 (CH_2OH); 32.0 ($CH_2\underline{C}H_2CH_2OH$); 20.7, 20.6, 20.6, 20.6 (OAc-Glucose).

10.28 Synthesis of bridge aldehydes functionalised *β*-D-monoglucosides tetraacetate (General procedure)

To a stirred solution of hydroxyl alkyl glucosides (1 eq) in dry DCM (30 mL) under N_2, DMP (1 eq) was added as a solid to the reaction mixture. After stirring for 3 h at r.t., saturated aqueous solution of $NaHCO_3$ with $Na_2S_2O_3$ (40 mL) was added to the reaction mixture with stirring for 5 min, the mixture was diluted with DCM and separated. The organic layer dried ($MgSO_4$) and the solvent was evaporated under reduced pressure, colourless oil was obtained followed by silica gel column chromatography to yield the corresponding aldehyde glucosides (Wang *et al*., 2007).

10.28.1 2-(2',3',4',6'-Tetra-*O*-acetyl-*β*-D-glucopyranosyloxy)acetaldehyde 237

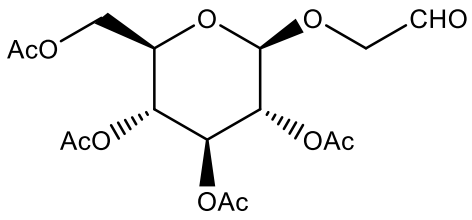

237

Compound **237** was synthesised according to the general procedure from 2-hydroxy ethyl 2',3',4',6'-tetra-*O*-acetyl-*β*-D-glucopyranoside (1.40 g, 3.56 mmol), the crude mixture was purified by silica gel column chromatography using

EtOAc: Pet. ether (2:1) as eluent to give the title compound as a white solid (0.89 g, 2.28 mmol).

Yield: 63%

R_f of compound **237** (EtOAc: Pet. ether, 2:1): 0.30

Mp: 98-99 ^{0}C

Vmax (cm^{-1}): 2954 (C-H stretching), 1734 (C=O), 1367 (C-H bending), 1205, 1032 (C-O stretching), 906.

^{1}H NMR (400 MHz $CDCl_3$): δ 9.68, (1H, d, *J* 0.6, CHO), 5.25, (1H, t, H3'-Glu), 5.07-5.12, (2H, m, H2',4'-Glu), 4.6, (1H, d, *J* 7.9, H1'-Glu), 4.10-4.30, (4H, m, H6a',6b'-Glu, CH_2), 3.70-3.74, (1H, m, H5'-Glu), 2.09, (6H, d, OAc), 2.03, (3H, s, OAc), 2.02, (3H, s, OAc).

^{13}C NMR (100 MHz $CDCl_3$): δ 199.8 (CHO); 170.5, 170.1, 169.4, 169.3 (C=O); 100.9 (C-Glucose); 74.1 (CH_2CHO); 72.5, 72.1, 70.9, 68.2, 61.7 (C-Glucose); 20.6, 20.5, 20.5 (OAc-Glucose).

10.28.2 2-((2',3',4',6'-Tetra-*O*-acetyl-*β*-D-glucopyranosyloxy)ethoxy)acetaldehyde 238

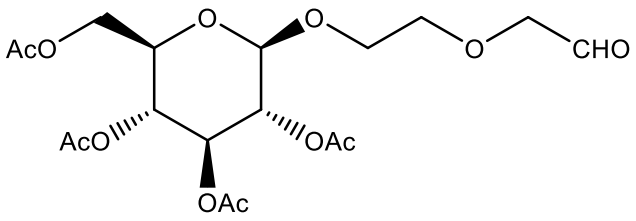

238

Compound **238** was synthesised according to the general procedure from 5-hydroxy-3-oxapentyl 2',3',4',6'-tetra-*O*-acetyl-*β*-D-glucopyranoside (1.46 g, 3.32 mmol), the crude mixture was purified by silica gel column chromatography using EtOAc: Pet. ether (3:1) as eluent to give the title compound as a white solid (0.66 g, 1.52 mmol).

Yield: 45%

R_f of compound **238** (EtOAc: Pet. ether, 3:1): 0.31

Mp: 102-103 ^{0}C

Vmax (cm^{-1}): 2964 (C-H stretching), 1744 (C=O), 1367 (C-H bending), 1211, 1033 (C-O stretching), 908, 897.

^{1}H NMR (400 MHz $CDCl_3$): δ 9.70, (1H, s, CHO), 5.21, (1H, t, H3'-Glu), 5.1, (1H, t, H4'-Glu), 5.01, (1H, dd, *J* 9.6, 8, H2'-Glu), 4.61, (1H, d, *J* 7.9, H1'-Glu), 4.27, (1H, dd, *J* 4.8, H6b'-Glu), 4.16, (3H, m, H6a'-Glu, CH_2CHO), 4.01, (1H, ddd, *J* 10.8, 4.7, 3.1, H5'-Glu), 3.70-3.82, (4H, m, CH_2CH_2), 2.10, (3H, s, OAc), 2.05, (3H, s, OAc), 2.04, (3H, s, OAc), 2.02, (3H, s, OAc).

^{13}C NMR (100 MHz $CDCl_3$): δ 200.2 (CHO); 170.6, 170.2, 169.4, 169.4 (C=O), 100.8 (C-Glucose); 76.8 (CH_2CHO); 72.7, 71.8, 71.2, 70.7, 69.1, 68.3 (C-Glucose+ OCH_2CH_2O); 61.8 (C-Glucose); 20.7, 20.6, 20.5 (OAc-Glucose).

10.28.3 3-oxopropyl 2',3',4',6'-tetra-*O*-acetyl-*β*-D-glucopyranoside 239

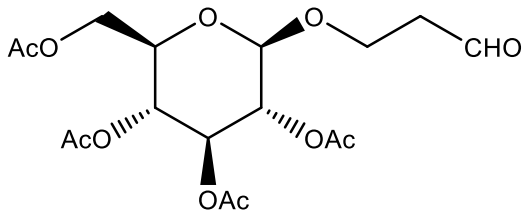

239

Compound **239** was synthesised according to the general procedure from 3-hydroxy propyl 2',3',4',6'-tetra-*O*-acetyl-*β*-D-glucopyranoside (1.20 g, 2.95 mmol) to give the title compound as a white solid (1.11 g, 2.74 mmol).

Yield: 93%

R_f of compound **239** (EtOAc: Pet. ether, 2:1): 0.44

^{1}H NMR (400 MHz $CDCl_3$): δ 9.76, (1H, t, *J* 1.3x(2), CHO), 5.21, (1H, t, H3'-Glu), 5.09, (1H, t, H4'-Glu), 4.96, (1H, dd, *J* 9.6, 8, H2'-Glu), 4.55, (1H, d, *J* 7.9, H1'-Glu), 4.25, (1H, dd, *J* 4.6, H6b'-Glu), 4.11-4.17, (2H, m, H6a'-Glu, CH), 3.89-3.94, (1H, m, CH), 3.68-3.72, (1H, m, H5'-Glu), 2.64-2.81, (2H, m, CH_2CHO), 2.09, (3H, s, OAc), 2.04, (3H, s, OAc), 2.03, (3H, s, OAc), 2.00, (3H, s, OAc).

^{13}C NMR (100 MHz $CDCl_3$): δ 199.9 (CHO); 170.6, 170.2, 169.4, 169.2 (C=O); 100.9, 72.6, 71.8, 71.0, 68.3, 63.5, 61.8 (C-Glucose); 43.5 (CH_2-CH_2); 20.7, 20.6, 20.6 (OAc-Glucose).

10.29 Synthesis of tetra(glucomethyl), tetra(glucoethoxymethyl) & tetra(glucoethyl)calix[4]resorcinarene (240, 241 and 242) (General procedure)

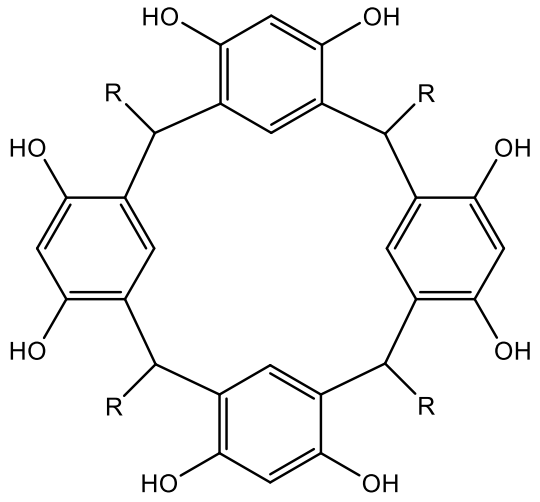

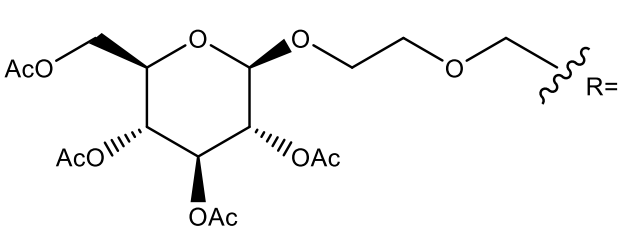

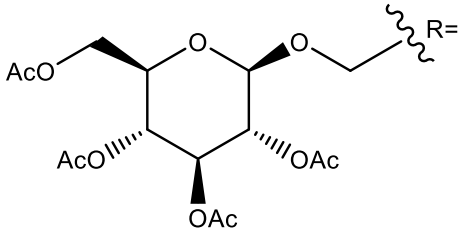

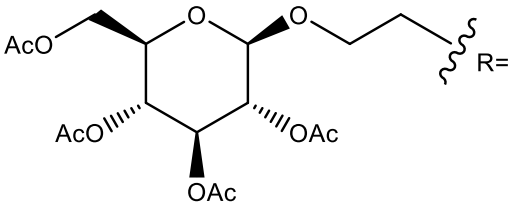

To a stirred solution of bridge aldehydes functionalised *β*-D-monoglucosides tetraacetate (1 eq) in a mixture of Et_2O and THF (1:1 ratio, 20 mL) was added $BF_3.Et_2O$ (2 eq) and the mixture was stirred under nitrogen for 15 min. Subsequently, resorcinol (1 eq) was added and the mixture was stirred at r.t for a further 48 h. A precipitate was obtained by adding the reaction mixture to Et_2O (200 mL). The precipitate was filtered and washed many times with Et_2O. The solid was then dissolved in EtOAc and the organic layer was washed with water (100 mL x 2) then dried ($MgSO_4$). The solvent was evaporated under reduced pressure to give the title compounds as crude solids.

10.29.1 Tetra(glucomethyl)calix[4]resorcinarene 240

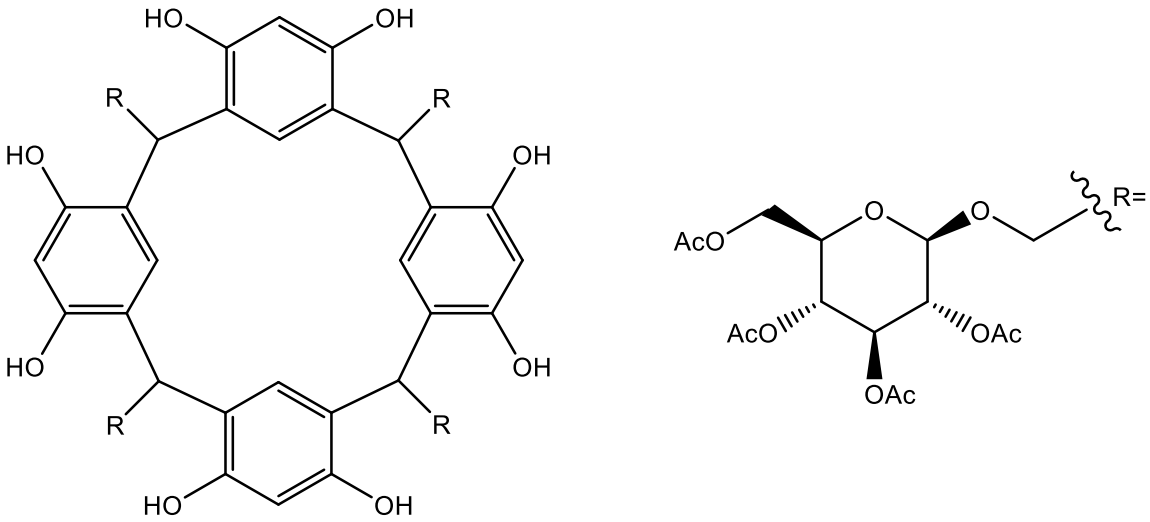

240

Compound **240** was synthesised according to the general procedure from 2-(2',3',4',6'-tetra-*O*-acetyl-*β*-D-glucopyranosyloxy)acetaldehyde (1.00 g, 2.56 mmol), resorcinol (0.28 g, 2.56 mmol) and $BF_3.Et_2O$ (0.63 mL, 5.12 mmol) in a mixture of Et_2O and THF (1: 1 ratio, 20 mL) gave the title compound as a red precipitate (0.83 g, 0.43 mmol, 17%).

10.29.2 Tetra(glucoethoxymethyl)calix[4]resorcinarene 241

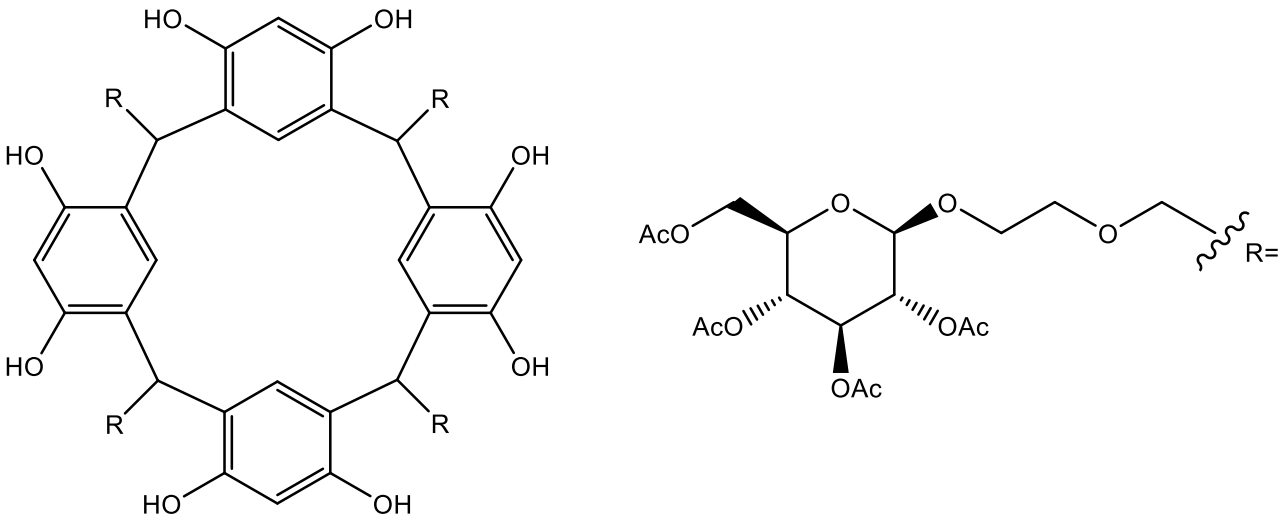

241

Compound **241** was synthesised according to the general procedure from 2-((2',3',4',6'-tetra-*O*-acetyl-*β*-D-glucopyranosyloxy)ethoxy)acetaldehyde (0.83 g, 1.91 mmol), resorcinol (0.21 g, 1.91 mmol) and $BF_3.Et_2O$ (0.47 mL, 3.82 mmol) in a mixture of Et_2O and THF (1: 1 ratio, 15 mL) gave the title compound as a red precipitate (0.78 g, 0.37 mmol, 19%).

10.29.3 Tetra(glucoethyl)calix[4]resorcinarene 242

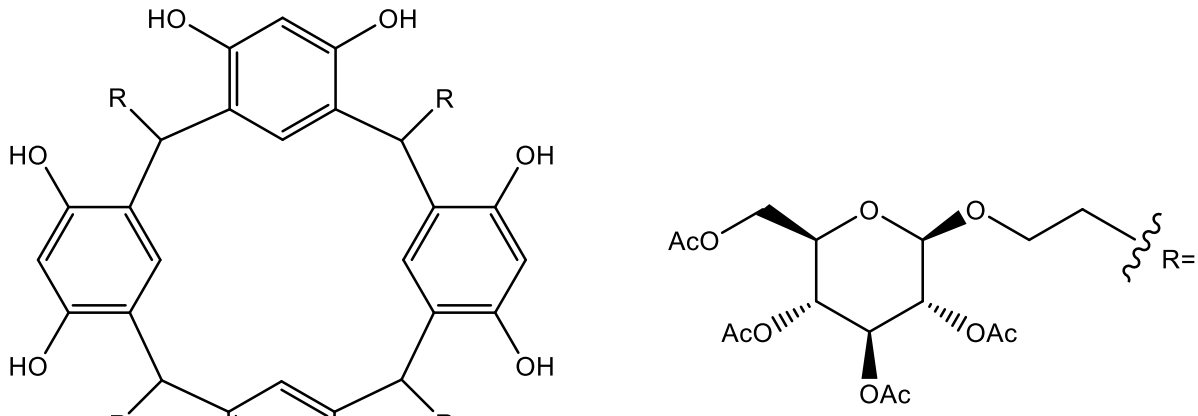

242

Compound **242** was synthesised according to the general procedure from 3-oxopropyl 2',3',4',6'-tetra-*O*-acetyl-*β*-D-glucopyranoside (1.00 g, 2.47 mmol), resorcinol (0.27 g, 2.47 mmol) and $BF_3.Et_2O$ (0.61 mL, 4.94 mmol) in a mixture of Et_2O and THF (1: 1 ratio, 20 mL) gave the title compound as a red precipitate (0.59 g, 0.29 mmol, 12%).

10.30 Esterfication of calix[4]resorcinarene glucosides

10.30.1 Acylated calix[4]resorcinarene glucoside 243

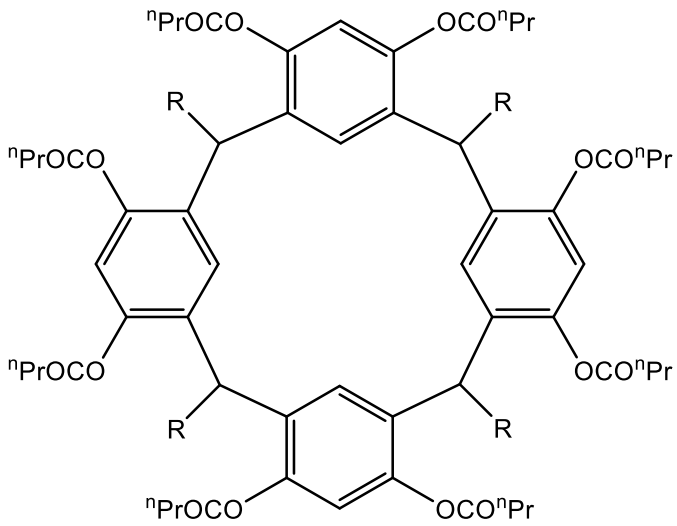

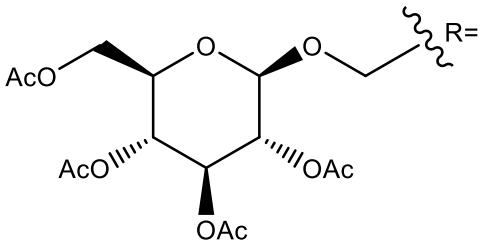

243

Compound **243** was synthesised according to the general procedure. The crude mixture of calix[4]resorcinarene glucoside **240** (0.68 g, 0.35 mmol) was reacted with butyric anhydride (30 mL) and pyridine (5 mL), the crude product was separated by silica gel column chromatography using EtOAc: Pet. ether (2:1) as eluent to yield one product of the butyrated calix[4]resorcinarene glucoside as an off-white powder.

Yield: 3%

R_f of compound **243** (EtOAc: Pet. ether, 2:1): 0.64

Mp: 96-100

Vmax (cm^{-1}): 2967, 2878 (C-H stretching), 1747 (C=O ester), 1497 (C=C arene), 1430, 1366 (C-H bending), 1214, 1131 (C-O stretching), 906 (C-H bending).

^{1}H NMR (400 MHz $CDCl_3$): δ 5.87-7.14, (8H, m, H2,5-Ar), 4.74-5.48, (12H, m, H2'',3'',4''-Glu), 4.42-4.71, (6H, m, H1''-Glu+ CH-methine), 3.48-4.40, (22H, m, H5'',6''-Glu+ CH_2+ CH-methine), 2.33-2.85, (16H, m, $COCH_2$), 1.89-2.28, (48H, m, OAc-Glu), 1.49-1.87, (16H, m, CH_2), 0.67-1.16, (24H, m, CH_3).

^{13}C NMR (100 MHz $CDCl_3$): δ 171.2, 170.7, 170.3, 170.1, 169.4, 169.3 (C=O); 147.4, 128.2 (aromatic carbons); 100.4, 72.7, 71.9, 70.9, 68.4, 68.2, 61.6 (C-Glucose); 35.9, 35.8, 35.1 ($COCH_2$); 20.7, 20.6, 20.3, 20.2, 20.0 (OAc-Glucose); 18.5, 18.4, 18.3, 18.3, 18.2, 18.1, 18.0, 17.8, 17.4, 17.2 (CH_2); 14.6 (CH_3).

Mass Spectrum: Expected: *m*/*z* 1262.4867 $(M+2NH_4)^{2+}$. Observed: *m*/*z* 1262.4869

10.30.2 Acylated calix[4]resorcinarene glucoside 244

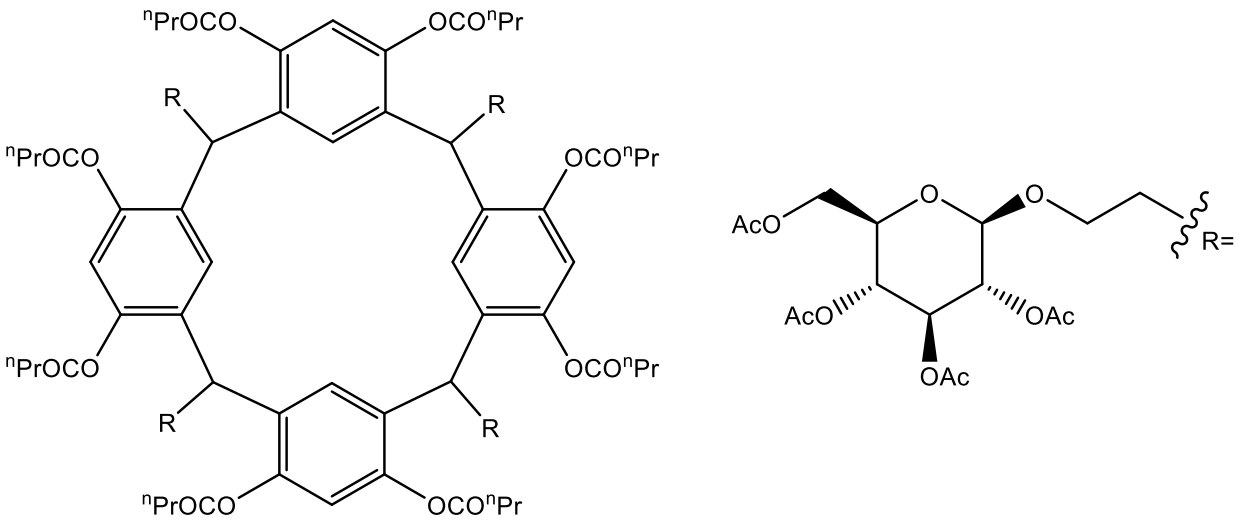

244

Compound **244** was synthesised according to the general procedure. The crude mixture of calix[4]resorcinarene glucoside **242** (0.59 g, 0.29 mmol) was reacted with butyric anhydride (30 mL) and pyridine (5 mL), the crude product was

separated by silica gel column chromatography using EtOAc: Pet. ether (2:1) as eluent to yield one product of the butyrated calix[4]resorcinarene glucoside as an off-white powder.

R_f of compound **244** (EtOAc: Pet. ether, 2:1): 0.32

Vmax (cm^{-1}): 2968, 2878 (C-H stretching), 1745 (C=O ester), 1494, 1458 (C=C arene), 1365 (C-H bending), 1217, 1131, 1096, 1033 (C-O stretching), 908, 749 (C-H bending).

^{1}H NMR (400 MHz $CDCl_3$): δ 6.39-7.18, (8H, m, H2,5-Ar), 4.75-5.44, (12, m, H2'',3'',4''-Glu), 4.37-4.67, (8H, m, H1''-Glu+ CH-methine), 3.91-4.34, (8H, m, H6''-Glu), 3.13-3.87, (20H, m, H5''-Glu+ CH_2-CH_2), 2.14-2.77, (16H, m, $COCH_2$), 1.88-2.13, (48H, m, OAc-Glu), 1.42-1.86, (16H, m, CH_2), 0.72-1.13, (24H, m, CH_3).

^{13}C NMR (100 MHz $CDCl_3$): δ 170.6, 170.1, 169.4 (C=O); 72.9, 71.2, 68.3, 61.8 (C-Glucose); 35.8 ($COCH_2$); 20.7, 20.6 (OAc-Glucose); 18.2, 17.4 (CH_2); 13.6, 13.5 (CH_3).

Mass Spectrum: Expected: *m*/*z* 1290.5179 $(M+2NH_4)^{2+}$. Observed: *m*/*z* 1290.5192

10.31 Deacylation of *rctt* calix[4]resorcinarene glucoside 137a

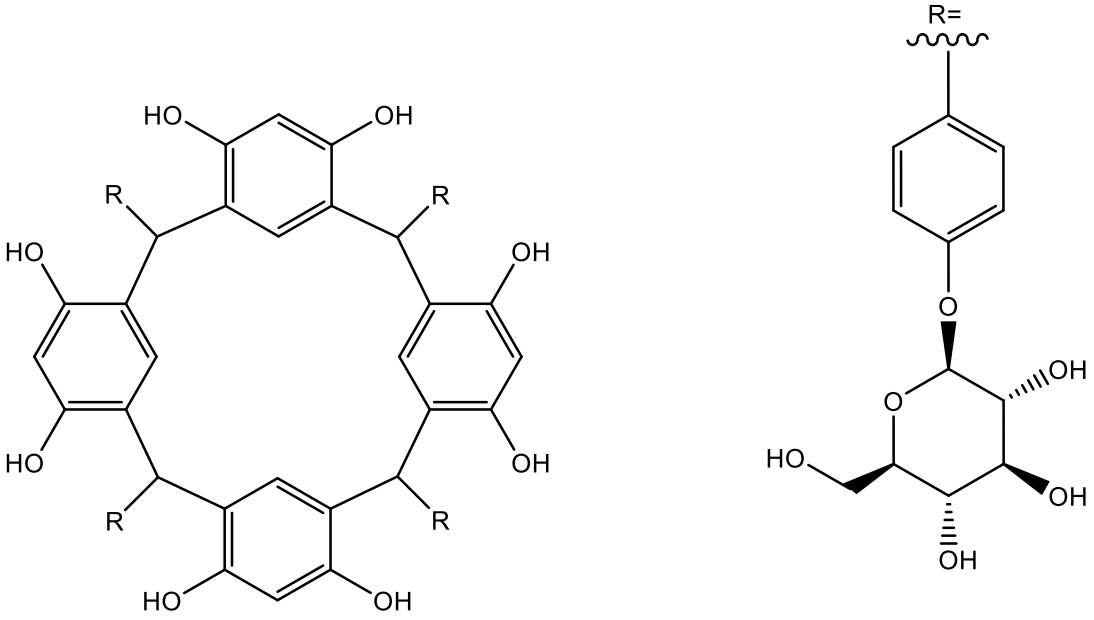

245

The pure acylated calix[4]resorcinarene glucoside **137a** (1.29 g, 0.47 mmol) was suspended in a mixture of MeOH and DCM (4:1 ratio, 20 mL), then a catalytic amount of sodium methoxide (0.10 g, 1.85 mmol) was added and stirred overnight at r.t. The reaction mixture was diluted with water (10 mL), then neutralised with (Amberlite IR-120 H^+), filtered and evaporated under reduced pressure. The residue was extracted from a mixture of DIPE and water (100 mL x 3) to afford the deprotected glycocluster **245** as a red precipitate (0.59 g, 0.39 mmol).

Yield: 83%

Mp: > 350

Vmax (cm^{-1}): 3317 (O-H stretching), 1606, 1504 (C=C arene), 1372 (O-H bending), 1224, 1067, 1036, 1013 (C-O stretching).

^{1}H NMR (400 MHz d_6-DMSO): δ 6.58-7.25, (16H, m, H2',3',5',6'-Ar), 5.89-6.53, (8H, m, H2,5-Ar), 5.44-5.61, (4H, d, ArCH), 4.91-5.42, (12H, m, OH), 4.71-4.89, (4H, m, H1''-Glu), 4.45-4.69, (4H, brs, OH), 3.01-3.80, (24H, m, H2'',3'',4'',5'',6''-Glu).

^{13}C NMR (100 MHz d_6-DMSO): δ 155.8, 153.2, 132.1, 129.9, 128.9, 115.8 (aromatic carbons); 100.8, 77.0, 73.7, 70.0, 61.0 (C-Glucose).

Mass Spectrum: Expected: *m*/*z* 751.2238 $(M-2H)^{2-}$. Observed: *m*/*z* 751.2244

CHAPTER 11: REFERENCES

Abosadiya, H.M., Hasbullah, S.A. and Yamin, B.M., 2015. Synthesis and Crystal Structure of a Ternary Lattice Inclusion System of C-4-acetamidophenylcalix[4]-2-methylresorcinarene dimethylsulfoxide tetrasolvate dihydrate. *Bull. Korean Chem. Soc.*, 36(12), pp.2895-2900.

Abronina, P.I., Zinin, A.I., Romashin, D.A., Tereshina, V.V., Chizhov, A.O. and Kononov, L.O., 2018. Application of a Janus aglycon with dual function in benzyl-free synthesis of spacer-armed oligosaccharide fragments of polysaccharides from rhizobacterium Azospirillum brasilense sp7. *Carbohydrate research*, 464, pp.28-43.

Aleandri, S., Casnati, A., Fantuzzi, L., Mancini, G., Rispoli, G. and Sansone, F., 2013. Incorporation of a calixarene-based glucose functionalised bolaamphiphile into lipid bilayers for multivalent lectin recognition. *Org. Biomol. Chem.*, *11*(29), pp.4811-4817.

Alex, J.M., Rennie, M.L., Volpi, S., Sansone, F., Casnati, A. and Crowley, P.B., 2018. Phosphonated calixarene as a “molecular glue” for protein crystallization. *Cryst. Growth Des.*, 18(4), pp.2467-2473.

Ali, M., Ahmed, I., Nasir, S., Duznovic, I., Niemeyer, C.M. and Ensinger, W., 2018. Potassium-induced ionic conduction through a single nanofluidic pore modified with acyclic polyether derivative. *Analytica chimica acta*., 1039, pp.132-139.

Aoyama, Y. (2004) Macrocyclic Glycoclusters: From Amphiphiles through Nanoparticles to Glycoviruses. *Chem. Eur. J*., 10, pp.588-593.

Aoyama, Y., 2005. Glycovirus. *Trends in Glycoscience and Glycotechnology*, 17(94), pp.39-47.

Aoyama, Y., 2009. Structure and Function of Molecular Assembly. A Personal Reminiscence. *Bull. Chem. Soc. Jpn.*, 82(4), pp.419-438.

Aoyama, Y., Kanamori, T., Nakai, T., Sasaki, T., Horiuchi, S., Sando, S. and Niidome, T., 2003. Artificial viruses and their application to gene delivery. Size-controlled gene coating with glycocluster nanoparticles. *J. Am. Chem. Soc.*, 125(12), pp.3455-3457.

Araki, K., Inada, K., Otsuka, H. and Shinkai, S., 1993. Conformational Isomerism in and Binding Properties to Alkali-Metals and an Ammonium Salt of *O*-alkylated Homooxacalix[3]arenes. *Tetrahedron*, 49(42), pp.9465-9478.

Arami, A., Karami, B. and Khodabakhshi, S., 2015. Yttrium(III) Nitrate: A Powerful Catalyst for Green and Rapid Synthesis of Some Supramolecules. *J. Chin. Chem. Soc.*, 62(1), pp.13-16.

Arimori, S., Nagasaki, T. and Shinkai, S., 1995. Self-assembly of tetracationic amphiphiles bearing a calix [4] arene core. Correlation between the core structure and the aggregation properties. *J. Chem. Soc., Perkin Trans. 2*, (4), pp.679-683.

Arnott, G.E., 2018. Inherently Chiral Calixarenes: Synthesis and Applications. *Chem. Eur. J.*, 24(8), pp.1744-1754.

Ashwin, B.C.M.A., Saravanan, C., Senthilkumaran, M., Sumathi, R., Suresh, P. and Muthu Mareeswaran, P., 2018. Spectral and electrochemical investigation

of *p*-sulfonatocalix[4]arene-stabilized vitamin E aggregation. *SUPRAMOLECULAR CHEMISTRY*, 30(1), pp.32-41.

Athar, M., Kongor, A., Panchal, M., Jha, P.C. and Jain, V., 2017. Entrapment of toxic anions using calixarenes framework. *MOJ Toxicol*, 3(6), pp.74-77.

Athar, M., Lone, M.Y. and Jha, P.C., 2017. Theoretical assessment of calix[n]arene as drug carriers for second generation tyrosine kinase inhibitors. *Journal of Molecular Liquids*, 247, pp.448-455.

Athar, M., Lone, M.Y. and Jha, P.C., 2018. Designing of calixarene based drug carrier for dasatinib, lapatinib and nilotinib using multilevel molecular docking and dynamics simulations. *Journal of Inclusion Phenomena and Macrocyclic Chemistry*, 90(1-2), pp.157-169.

Azua, A., Finn, M., Yi, H., Beatriz Dantas, A. and Voutchkova-Kostal, A., 2017. Transfer Hydrogenation from Glycerol: Activity and Recyclability of Iridium and Ruthenium Sulfonate-Functionalized N-Heterocyclic Carbene Catalysts. *ACS Sustainable Chem. Eng.*, 5(5), pp.3963-3972.

Baeyer, A.V., 1872. Ueber die verbindungen der aldehyde mit den phenolen. *Berichte der deutschen chemischen gesellschaft*, 5(1), pp.280-282.

Bagnacani, V., Sansone, F., Donofrio, G., Baldini, L., Casnati, A. and Ungaro, R., 2008. Macrocyclic Nonviral Vectors: High Cell Transfection Efficiency and Low Toxicity in a Lower Rim Guanidinium Calix[4]arene. *Org. Lett.,* 10, pp.6-21.

Baldini, L., Casnati, A., Sansone, F. and Ungaro, R., 2007. Calixarene-based multivalent ligands. *Chem. Soc. Rev.*, 36(2), pp.254-266.

Baldini, L., Sansone, F., Casnati, A. and Ungaro, R., 2012. *Supramolecular Chemistry: from Molecules to Nanomaterials*. *Calixarenes in molecular recognition*, 3, pp.863-894.

Baldino, S., Facchetti, S., Nedden, H.G., Zanotti-Gerosa, A. and Baratta, W., 2016. Chemoselective Transfer Hydrogenation of Aldehydes with $HCOONH_4$ Catalyzed by RuCl (CNNPh)(PP) Pincer Complexes. *ChemCatChem*, 8(20), pp.3195-3198. Available at: http://hdl.handle.net/2318/1693291

Banerjee, R., 2018. Nanotechnology in drug delivery: present status and a glimpse into the future. *Ther. Deliv*., 9(4), 231-232.

Barrett, A.G., Braddock, D.C., Henschke, J.P. and Walker, E.R., 1999. Ytterbium (III) triflate-catalysed preparation of calix[4]resorcinarenes: Lewis assisted Brønsted acidity. *J. Chem. Soc., Perkin Trans. 1*. pp.873-878.

Belyanin, M.L., Stepanova, E.V. and Ogorodnikov, V.D., 2012. First total chemical synthesis of natural acyl derivatives of some phenolglycosides of the family Salicaceae. *Carbohydrate research*, 363, pp.66-72.

Beyeh, N.K., Jo, H.H., Kolesnichenko, I., Pan, F., Kalenius, E., Anslyn, E.V., Ras, R.H. and Rissanen, K., 2017. Recognition of Viologen Derivatives in Water by N-Alkyl Ammonium Resorcinarene Chlorides. *J. Org. Chem.*, 82(10), pp.5198-5203.

Beyeh, N.K., Pan, F., Valkonen, A. and Rissanen, K., 2015. Encapsulation of secondary and tertiary ammonium salts by resorcinarenes and pyrogallarenes: the effect of size and charge concentration. *CrystEngComm*, 17(5), pp.1182-1188.

Bhattacharjee, S., 2016. DLS and zeta potential–What they are and what they are not?. *Journal of Controlled Release*, 235, pp.337-351.

Bibal, B., 2018. Acetylcholine receptors in water. *Supramolecular Chemistry*, 30(4), pp.243-254.

Bier, C., Binder, D., Drobietz, D., Loeschcke, A., Drepper, T., Jaeger, K.E. and Pietruszka, J., 2017. Photocaged carbohydrates: versatile tools for controlling gene expression by light. *Synthesis*, 49(01), pp.42-52.

Bojarová, P. and Křen, V., 2016. Sugared biomaterial binding lectins: achievements and perspectives. *Biomater. Sci.*, 4(8), pp.1142-1160.

Bonaccorso, C., Migliore, R., Volkova, M.A., Arena, G. and Sgarlata, C., 2017. Self-assembling of supramolecular adducts by sulfonato-calix[4]arene and pyridinium gemini guests in neutral aqueous solution. *Thermochimica Acta*, 656, pp.47-52.

Bourgeois, J.M. and Stoeckli-Evans, H., 2005. Synthesis of New Resorcinarenes Under Alkaline Conditions. *Helv. Chim. Acta*., 88(10), pp.2722-2730.

Bowley, N.D., Funck, M., Laventine, D.M., Dalgarno, S.J. and Cave, G.W., 2014. Pyridinium encapsulation within a novel cyano-footed pyrogallol[4]arene nanocapsule. *Supramolecular Chemistry*, 26(3-4), pp.229-232.

Boxhall, J.Y., Page, P.C.B., Elsegood, M.R., Chan, Y., Heaney, H., Holmes, K.E. and McGrath, M.J., 2003. The Synthesis of Axially Chiral Resorcinarenes from Resorcinol Monoalkyl Ethers and Aldehyde Dimethylacetals. *Synlett*, 07, pp.1002-1006.

Brito-Arias, M., 2016. *Synthesis and Characterization of Glycosides*, 2nd Edition. [e-book] Springer, Cham. pp.81-168.

Bryant, J.A., Blanda, M.T., Vincenti, M. and Cram, D.J., 1991. Host-guest complexation. 55. Guest capture during shell closure. *J. Am. Chem. Soc.*, 113(6), pp.2167-2172.

Buhleier, E., Wehner, W. and Vögtle, F., 1978. ′ Cascade′-and′ Nonskid-Chain-Like′ Synthesis of Molecular Cavity Topologies. *Synthesis*, 2, pp.155-158.

Cai, L., Gu, Z., Zhong, J., Wen, D., Chen, G., He, L., Wu, J. and Gu, Z., 2018. Advances in glycosylation-mediated cancer-targeted drug delivery. *Drug Discovery Today,* 23(5), pp.1126-1138.

Casas-Hinestroza, J.L. and Maldonado, M., 2018. Conformational Aspects of the O-acetylation of C-tetra(phenyl)calixpyrogallol[4]arene. *Molecules*, 23(5), pp.1225-1233.

Casnati, A., Sansone, F. and Ungaro, R., 2003. Peptido-and glycocalixarenes: playing with hydrogen bonds around hydrophobic cavities. *Acc. Chem. Res.*, 36(4), pp.246-254.

Castellanos-Blanco, N., Flores-Alamo, M. and García, J.J., 2012. Nickel-Catalyzed Alkylation and Transfer Hydrogenation of *α*,*β*-unsaturated Enones with Methanol. *Organometallics*, 31(2), pp.680-686.

Castillo-Aguirre, A., Rivera-Monroy, Z. and Maldonado, M., 2017. Selective *O*-Alkylation of the Crown Conformer of Tetra(4-hydroxyphenyl)calix[4]resorcinarene to the Corresponding Tetraalkyl Ether. *Molecules*, 22(10), pp.1660-1670.

Cave, G.W., Raston, C.L. and Scott, J.L., 2001. Recent advances in solventless organic reactions: towards benign synthesis with remarkable versatility. *Chem. Commun.,* 21, pp.2159-2169.

Cecioni, S., Faure, S., Darbost, U., Bonnamour, I., Parrot-Lopez, H., Roy, O., Taillefumier, C., Wimmerová, M., Praly, J.P., Imberty, A. and Vidal, S., 2011. Selectivity among two lectins: Probing the Effect of Topology, Multivalency and Flexibility of “Clicked” Multivalent Glycoclusters. *Chem. Eur. J.*, 17(7), pp.2146-2159.

Cecioni, S., Lalor, R., Blanchard, B., Praly, J.P., Imberty, A., Matthews, S.E. and Vidal, S., 2009. Achieving High Affinity towards a Bacterial Lectin through Multivalent Topological Isomers of Calix[4]arene Glycoconjugates. *Chem. Eur. J.*, 15(47), pp.13232-13240.

Cecioni, S., Praly, J.P., Matthews, S.E., Wimmerová, M., Imberty, A. and Vidal, S., 2012. Rational design and synthesis of optimized glycoclusters for multivalent lectin–carbohydrate interactions: influence of the linker arm. *Chem. Eur. J.*, 18(20), pp.6250-6263.

Chen, C.Y., Sun, J.G., Liu, F.Y., Fung, K.P., Wu, P. and Huang, Z.Z., 2012. Synthesis and biological evaluation of glycosylated psoralen derivatives. *Tetrahedron*, 68(12), pp.2598-2606.

Chen, M.X., Li, T., Peng, S. and Tao, D., 2016. Supramolecular nanocapsules from the self-assembly of amphiphilic calixarene as a carrier for paclitaxel. *New J. Chem.*, 40(12), pp.9923-9929.

Chen, S., Meng, L., Chen, B., Chen, W., Duan, X., Huang, X., Zhang, B., Fu, H. and Wan, Y., 2017. Poison Tolerance to the Selective Hydrogenation of Cinnamaldehyde in Water over an Ordered Mesoporous Carbonaceous Composite Supported Pd Catalyst. *ACS Catal.*, 7(3), pp.2074-2087.

Chen, S.J., Lu, G.P. and Cai, C., 2015. A base-controlled chemoselective transfer hydrogenation of *α*,*β*-unsaturated ketones catalyzed by $[IrCp^*Cl_2]_2$ with 2-propanol. *RSC Adv.*, 5(17), pp.13208-13211.

Chen, W., Li, L., Zhang, X., Liang, Y., Pu, Z., Wang, L. and Mo, J., 2017. Curcumin: a calixarene derivative micelle potentiates anti-breast cancer stem cells effects in xenografted, triple-negative breast cancer mouse models. *Drug delivery*, 24(1), pp.1470-1481.

Choi, H., Ham, S.Y., Cha, E., Shin, Y., Kim, H.S., Bang, J.K., Son, S.H., Park, H.D. and Byun, Y., 2017. Structure–Activity Relationships of 6- and 8-Gingerol Analogs as Anti-Biofilm Agents. *J. Med. Chem.*, 60(23), pp.9821-9837.

Chopra, N. and Sherman, J.C., 1997. A Bis (carceplex) from a Cyclic Tetramer of Cavitands. *Angew. Chem. Int. Ed. Engl.*, 36(16), pp.1727-1729.

Cometti, G., Dalcanale, E., Du, vosel A., Levelut, A.M., 1990. New Bowl-shaped Columnar Liquid Crystals. *J. Chem. Soc*., *Chem. Commun*., 2, pp.163–165.

Compostella, F., Pitirollo, O., Silvestri, A. and Polito, L., 2017. Glyco-gold nanoparticles: synthesis and applications. *Beilstein journal of organic chemistry*, 13(1), pp.1008-1021.

Consoli, G.M., Di Bari, I., Blanco, A.R., Nostro, A., D'Arrigo, M., Pistarà, V. and Sortino, S., 2017. Design, Synthesis, and Antibacterial Activity of a Multivalent

Polycationic Calix[4]arene–NO Photodonor Conjugate. *ACS Med. Chem. Lett.*, 8(8), pp.881-885.

Cousin, J.M. and Cloninger, M.J., 2016. The Role of Galectin-1 in Cancer Progression, and Synthetic Multivalent Systems for the Study of Galectin-1. *Int. J. Mol. Sci.*, 17(9), pp.1566-1587.

Cram, D.J., 1988. The Design of Molecular Hosts, Guests, and Their Complexes (Nobel Lecture). *Angew. Chem. Int. Ed. Engl*., 27, pp.1009-1020.

Cram, D.J., 1983. Cavitands: organic hosts with enforced cavities. *Science*, pp.1177-1183.

Cram, D.J., 1986. 'Preorganization—from solvents to spherands'. *Angew. Chem., Int. Ed. Engl.*, 25(12), pp.1039-1057.

Curtis, A.D., 1997. Novel calix[4]resorcinarene glycosides. *Tetrahedron letters*, 38(24), pp.4295-4296.

Curtis, A.D., 1998. Novel calix[4]resorcinarene glycosides. Unpublished data

Da Silva, E., Shahgaldian, P. and Coleman, A.W., 2004. Haemolytic properties of some water-soluble *para*-sulphonato-calix-[n]-arenes. *Int. J. Pharm.,* 273, pp.57-62.

Darvish, F. and Khazraee, S., 2014. Molecular iodine: An efficient and environment-friendly catalyst for the synthesis of calix[4]resorcinarenes. *C. R. Chimie*, 17(9), pp.890-893.

Daubresse, N., Francesch, C., Mhamdi, F. and Rolando, C., 1998. Coniferin and derivatives: a fast and easy synthesis via the aldehyde series using phase-transfer catalysis. *Synthesis*, 1998(2), pp.157-161.

Delbianco, M., Bharate, P., Varela-Aramburu, S. and Seeberger, P.H., 2015. Carbohydrates in Supramolecular Chemistry. *Chem. rev*., 116(4), pp.1693-1752.

Deleersnyder, K., Mehdi, H., Horváth, I.T., Binnemans, K. and Parac-Vogt, T.N., 2007. Lanthanide(III) nitrobenzenesulfonates and *p*-toluenesulfonate complexes of lanthanide(III), iron(III), and copper(II) as novel catalysts for the formation of calix[4]resorcinarene. *Tetrahedron*, 63(37), pp.9063-9070.

Denavit, V., Lainé, D., Tremblay, T., St-Gelais, J. and Giguère, D., 2018. Synthetic Inhibitors of Galectins: Structures and Syntheses. *Trends in Glycoscience and Glycotechnology*, 30(172), pp.SE21-SE40.

Desage-El Murr, M., Nowaczyk, S., Le Gall, T. and Mioskowski, C., 2006. Synthesis of Pulvinic Acid and Norbadione A Analogues by Suzuki–Miyaura Cross-Coupling of Benzylated Intermediates. *Eur. J. Org. Chem.*, 2006(6), pp.1489-1498.

Ding, B., Zhang, Z., Liu, Y., Sugiya, M., Imamoto, T. and Zhang, W., 2013. Chemoselective Transfer Hydrogenation of *α*,*β*-unsaturated Ketones Catalyzed by Pincer-Pd Complexes Using Alcohol as a Hydrogen Source. *Org. Lett.*, 15(14), pp.3690-3693.

Dondoni, A. and Marra, A., 2010. Calixarene and calixresorcarene glycosides: their synthesis and biological applications. *Chem. Rev.*, 110(9), pp.4949-4977.

Dondoni, A., Marra, A., Scherrmann, M.C., Casnati, A., Sansone, F. and Ungaro, R., 1997. Synthesis and Properties of *O*-Glycosyl Calix[4]arenes (Calixsugars). *Chem. Eur. J.*, 3(11), pp.1774-1782.

Driaf, K., Granet, R., Krausz, P., Kaouadji, M., Verneuil, B., Thomasson, F., Chulia, A.J., Spiro, M., Biais, J.C. and Bolbach, G., 1996. Synthesis of glycosylated cationic porphyrins as potential agents in photodynamic therapy. *Can. J. Chem.*, *74*(8), pp.1550-1563.

Egberink, R.J., Cobben, P.L., Vverboom, W., Harkema, S. and Reinhoudt, D.N., 1992. Högberg compounds with a functionalized box-like cavity. *Journal of inclusion phenomena and molecular recognition in chemistry*, 12(1-4), pp.151-158.

Erdtman, H., Högberg, S., Abrahamsson, S. and Nilsson, B., 1968. Cyclooligomeric phenol-aldehyde condensation products I. *Tetrahedron Letters*, 9(14), pp.1679-1682.

Ermakova, A.M., Morozova, J.E., Shalaeva, Y.V., Syakaev, V.V., Gubaidullin, A.T., Voloshina, A.D., Zobov, V.V., Nizameev, I.R., Bazanova, O.B., Antipin, I.S. and Konovalov, A.I., 2018. Nanoconjugates of a calixresorcinarene derivative with methoxy poly(ethylene glycol) fragments for drug encapsulation. *Beilstein J. Nanotechnol.*, 9(1), pp.2057-2070.

Fahmy, S.A., Ponte, F., El-Rahman, M.K.A., Russo, N., Sicilia, E. and Shoeib, T., 2018. Investigation of the host-guest complexation between 4-sulfocalix[4]arene and nedaplatin for potential use in drug delivery. *Spectrochimica Acta Part A: Molecular and Biomolecular Spectroscopy*, 193, pp.528-536.

Fernandes, R.A. and Kumar, P., 2003. PCC-mediated novel oxidation reactions of homobenzylic and homoallylic alcohols. *Tetrahedron letters*, 44(6), pp.1275-1278.

Fernandez-Pastor, I., Fernandez-Hernandez, A., Rivas, F., Martinez, A., Garcia-Granados, A. and Parra, A., 2016. Synthesis and antioxidant activity of hydroxytyrosol alkyl-carbonate derivatives. *Journal of natural products*, 79(7), pp.1737-1745.

Fowler, D.A., Tian, J., Barnes, C., Teat, S.J. and Atwood, J.L., 2011. Cocrystallization of C-butyl pyrogallol[4]arene and C-propan-3-ol pyrogallol[4]arene with gabapentin. *CrystEngComm*, 13(5), pp.1446-1449.

Fujimoto, K., Hayashida, O., Aoyama, Y., Guo, C.T., Hidari, K.I.P.J. and Suzuki, Y., 1999. A Macrocyclic Sialic Acid Cluster as a Host, as an Adsorbate, and as a Ligand for Lectin and Virus. *Chemistry Letters*, 28(12), pp.1259-1260.

Fujimoto, K., Miyata, T. and Aoyama, Y., 2000. Saccharide-Directed Cell Recognition and Molecular Delivery Using Macrocyclic Saccharide Clusters: Masking of Hydrophobicity to Enhance the Saccharide Specificity. *J. Am. Chem. Soc*., 122(14), pp.3558-3559.

Fujimoto, T., Shimizu, C., Hayashida, O. and Aoyama, Y., 1997. Solution-to-Surface Molecular-Delivery System Using a Macrocyclic Sugar Cluster. Sugar-Directed Adsorption of Guests in Water on Polar Solid Surfaces. *J. Am. Chem. Soc*., 119(28), pp.6676-6677.

Fujisawa, I., Kitamura, Y., Kato, R. and Aoki, K., 2018. Crystal structures of resorcin[4]arene and pyrogallol[4]arene complexes with proline: A model for

proline recognition through CH··· π interaction. *Journal of Molecular Structure*, 1163, pp.336-344.

Funck, M., Guest, D.P. and Cave, G.W., 2010. Microwave-assisted synthesis of resorcin[4]arene and pyrogallol[4]arene macrocycles. *Tetrahedron Letters*, 51(49), pp.6399-6402.

Gabius, H.J., André, S., Jiménez-Barbero, J., Romero, A. and Solís, D., 2011. From lectin structure to functional glycomics: principles of the sugar code. *Trends in biochemical sciences*, 36(6), pp.298-313.

Galan, A. and Ballester, P., 2016. Stabilization of reactive species by supramolecular encapsulation. *Chem. Soc. Rev.*, 45(6), pp.1720-1737.

Gasparello, J., Manicardi, A., Casnati, A., Corradini, R., Gambari, R., Finotti, A. and Sansone, F., 2019. Efficient cell penetration and delivery of peptide nucleic acids by an argininocalix[4]arene. *SCIENTIFIC REPORTS*, 9(1), pp.3036-3045.

Ge, Y., Cai, Y. and Yan, C., 2005. Synthesis of Thiourea-Bridged Cluster Glycoside Calixarenes. *Synthetic communications*, 35(18), pp.2355-2361.

Geissner, A., Seeberger, P.H., 2016. Glycan arrays: from basic biochemical research to bioanalytical and biomedical applications. *Annu. Rev*. *Anal*. *Chem*., 9, pp.223-247.

Geraci, C., Consoli, G.M., Galante, E., Bousquet, E., Pappalardo, M. and Spadaro, A., 2008. Calix[4]arene decorated with four Tn antigen glycomimetic units and P_3CS immunoadjuvant: Synthesis, Characterization, and Anticancer Immunological evaluation. *Bioconjugate Chem.*, 19(3), pp.751-758.

Giuliani, M., Morbioli, I., Sansone, F. and Casnati, A., 2015. Moulding calixarenes for biomacromolecule targeting. *Chem. Commun.*, 51(75), pp.14140-14159.

Glushko, V.V., Serkova, O.S., Smoyan, G.N., Vasyanina, L.K. and Maslennikova, V.I., 2017. Pre-organized oligofunctional ligands based on *rctt*-C-naphthyl-resorcinarene: Synthesis and complex formation. *Phosphorus, Sulfur, and Silicon and the Related Elements*, 192(9), pp.1054-1060.

Granata, G., Paterniti, I., Geraci, C., Cunsolo, F., Esposito, E., Cordaro, M., Blanco, A.R., Cuzzocrea, S. and Consoli, G.M., 2017. Potential eye drop based on a calix[4]arene nanoassembly for curcumin delivery: Enhanced drug solubility, stability, and anti-inflammatory effect. *Mol. Pharmaceutics*, 14(5), pp.1610-1622.

Griesbeck, A.G., Miranda, M.A. and Uhlig, J., 2011. Sweet chiral porphyrins as singlet oxygen sensitizers for asymmetric Type II photooxygenation. *Photochem & Photobiol Sci*, 10(9), pp.1431-1435.

Gui, X. and Sherman, J.C., 2001. Host-guest binding of simple cavitands in water. *Chem. Commun.*, 24, pp.2680-2681.

Gutsche, C.D. and Bauer, L.J., 1985. Calixarenes. 13. The conformational properties of calix[4]arenes, calix[6]arenes, calix[8]arenes, and oxacalixarenes. *J. Am. Chem. Soc.*, 107(21), pp.6052-6059.

Gutsche, C.D., Dhawan, B., No, K.H. and Muthukrishnan, R., 1981. Calixarenes. 4. The Synthesis, Characterization, and Properties of the

Calixarenes from *p-tert*-Butylphenol. *J. Am. Chem. Soc.*, 103(13), pp.3782-3792.

Hajji, C., Roller, S., Beigi, M., Liese, A. and Haag, R., 2006. Polyglycerol-Supported Chromium-Salen as a High-Loading Dendritic Catalyst for Stereoselective Diels–Alder Reactions. *Advanced Synthesis & Catalysis*, 348(12-13), pp.1760-1771.

Han, J., Song, X., Liu, L. and Yan, C., 2007. Synthesis, crystal structure and configuration of acetylated aryl Pyrogallol[4]arenes. *J. Incl. Phenom. Macrocycl Chem.*, 59(3-4), pp.257-263.

Hayashida, O., Nishiyama, K., Matsuda, Y. and Aoyama, Y., 1999. Preparation and host-guest interactions of novel macrocyclic sugar clusters having mono- and oligosaccharides. *Tetrahedron letters*, 40(17), pp.3407-3410.

Herbert, R.B. and Kattah, A.E., 1990. The biosynthesis of Sceletium alkaloids in Sceletium subvelutinum L. Bolus. *Tetrahedron*, 46(20), pp.7105-7118.

Hidayat, R., Sugihara, O., Tsuchimori, M., Kagami, M., Nishikubo, T. and Kaino, T., 2007. Binding of europium complex to polymerizable macrocyclic molecules and its optical properties. *Optical Materials*, 29(11), pp.1367-1374.

Hillyer, M.B., Gibb, C.L., Sokkalingam, P., Jordan, J.H., Ioup, S.E. and Gibb, B.C., 2016. Synthesis of water-soluble deep-cavity cavitands. *Org. lett.*, 18(16), pp.4048-4051.

Hoegberg, A.G.S., 1980. Two Stereoisomeric Macrocyclic Resorcinol-Acetaldehyde Condensation Products. *J. Org. Chem.*, 45(22), pp.4498-4500.

Hogberg, A.G.S., 1980. Stereoselective Synthesis and DNMR Study of Two 1, 8, 15-22-Tetraphenyl[1_4]metacyclophana-3, 5, 10, 12, 17, 19, 24, 26-octols. *J. Am. Chem. Soc.*, 102(19), pp.6046-6050.

Hoskins, C. and Curtis, A.D.M., 2015. Simple Calix[n]arenes and Calix[4]resorcinarenes as Drug Solubilizing Agents. *J. Nanomed. Res.,* 2(3), pp.1–8.

Hussain, H., Du, Y., Tikhonova, E., Mortensen, J.S., Ribeiro, O., Santillan, C., Das, M., Ehsan, M., Loland, C.J., Guan, L. and Kobilka, B.K., 2017. Resorcinarene-Based Facial Glycosides: Implication of Detergent Flexibility on Membrane-Protein Stability. *Chem. Eur. J.*, 23(28), pp.6724-6729.

Iwanek, W. and Syzdol, B., 1999. Lewis acid-induced synthesis of octamethoxyresorcarenes. *Synthetic communications*, 29(7), pp.1209-1216.

Iwanek, W., 1998. Chiral calixarenes derived from resorcinol. Part 3: Functionalization of octaester derivatives with chiral amines and amino alcohols. *Tetrahedron: Asymmetry*, 9(18), pp.3171-3174.

Jahjah, M., Caron, B., Menuel, S., Monflier, E., Djakovitcha, L. and Pinela, C., 2011. Hydrogenation of cinnamaldehyde with heterogeneous catalyst in the presence of cyclodextrins. *ARKIVOC*, 7, pp.406-415.

Jain, A., Jain, A., Parajuli, P., Mishra, V., Ghoshal, G., Singh, B., Shivhare, U.S., Katare, O.P. and Kesharwani, P., 2017. Recent advances in galactose-engineered nanocarriers for the site-specific delivery of siRNA and anticancer drugs. *Drug Discovery Today,* 23(5), pp.960-973.

Jain, V.K. and Kanaiya, P.H., 2011. Chemistry of calix[4]resorcinarenes. *Russian Chemical Reviews*, 80(1), pp.75-102.

Jebali, A., Nayeri, E.K., Roohana, S., Aghaei, S., Ghaffari, M., Daliri, K. and Fuente, G., 2017. Nano-carbohydrates: Synthesis and application in genetics, biotechnology, and medicine. *Advances in colloid and interface science*, 240, pp.1-14.

Jose, T., Cañellas, S., Pericàs, M.A. and Kleij, A.W., 2017. Polystyrene-supported bifunctional resorcinarenes as cheap, metal-free and recyclable catalysts for epoxide/CO_2 coupling reactions. *Green Chem.*, 19(22), pp.5488-5493.

Journey, S.N., Teppang, K.L., Garcia, C.A., Brim, S.A., Onofrei, D., Addison, J.B., Holland, G.P. and Purse, B.W., 2017. Mechanically induced pyrogallol[4]arene hexamer assembly in the solid state extends the scope of molecular encapsulation. *Chem. Sci.*, 8(11), pp.7737-7745.

Jumina, Siswanta, D., Nofiati, K., Imawan, A.C., Priastomo, Y. and Ohto, K., 2019. Synthesis of C-4-Hydroxy-3-methoxyphenylcalix[4]resorcinarene and Its Application as Adsorbent for Lead(II), Copper(II) and Chromium(III). *Bulletin of the Chemical Society of Japan*, 92(4), pp.825-831.

Ka, S.M., Chao, L.K., Lin, J.C., Chen, S.T., Li, W.T., Lin, C.N., Cheng, J.C., Jheng, H.L., Chen, A. and Hua, K.F., 2016. A low toxicity synthetic cinnamaldehyde derivative ameliorates renal inflammation in mice by inhibiting NLRP3 inflammasome and its related signaling pathways. *Free Radical Biology and Medicine*, 91, pp.10-24.

Kantee, K., Rukachaisirikul, V. and Tadpetch, K., 2016. Synthesis of tetrahydropyranyl diarylheptanoids from Dioscorea villosa. *Tetrahedron Letters*, 57(31), pp.3505-3509.

Kashanna, J., Jangili, P., Kumar, R.A. and Das, B., 2012. The First Stereoselective Total Synthesis of a Naturally Occurring Bioactive Diarylheptanoid,(3R, 6E)-1, 7-Bis (4-hydroxyphenyl) hept-6-en-3-ol, through Two Different Approaches. *Helvetica Chimica Acta*, 95(9), pp.1666-1671.

Kashapov, R.R., Rassadkina, R.I., Ziganshina, A.Y., Mukhitova, R.K., Mamedov, V.A., Zhukova, N.A., Kadirov, M.K., Nizameev, I.R., Zakharova, L.Y. and Sinyashin, O.G., 2016. Controlling the release of hydrophobic compounds by a supramolecular amphiphilic assembly. *RSC Adv.*, 6(45), pp.38548-38552.

Kazakova, E.K., Morozova, J.E., Prosvirkin, A.V., Pich, A.Z., Gubanov, E.P., Muslinkin, A.A., Habicher, W.D. and Konovalov, A.I., 2004. Self-Assembly of Octaaminoamido Derivatives of Resorcin[4]arene in Water− A “Cell-Like” Submicron-Scale Hydrogel Structure. *Eur. J. Org. Chem.*, 2004(15), pp.3323-3329.

Khan, K., Badshah, S., Ahmad, N., Rashid, H. and Mabkhot, Y., 2017. Inclusion Complexes of a New Family of Non-Ionic Amphiphilic Dendrocalix[4]arene and Poorly Water-Soluble Drugs Naproxen and Ibuprofen. *Molecules*, 22(5), pp.783-792.

Khokhar, T.S., Memon, S., Panhwar, Q.K., Memon, F.N., Memon, A.A., Samejo, M.Q., Muneer, S. and Tulu, M., 2017. Complexation of ibuprofen with water soluble *p*-sulfonatocalix[4]arene: A potential candidate for drug delivery application. *Pak. J. Pharm. Sci.*, 30(3), pp.783-788.

Kim, S.K., Kang, B.G., Koh, H.S., Yoon, Y.J., Jung, S.J., Jeong, B., Lee, K.D. and Yoon, J., 2004. A new imidazolium cavitand for the recognition of dicarboxylates. *Org. lett.*, 6(25), pp.4655-4658.

Knyazeva, I.R., Burilov, A.R., Fazleeva, G.M., Nuretdinov, I.D.A., Gryaznova, T.V., Budnikova, Y.G., Khrisanforova, V.V., Gubaidullin, A.T., Gabidullin, B.M., Syakaev, V.V. and Pudovik, M.A., 2011. New Calix[4]resorcinols with Thiophosphoryl-containing fragments. *Phosphorus, Sulfur, and Silicon and the Related Elements*, 186(9), pp.1972-1980.

Knyazeva, I.R., Mukhamedyanova, K.M., Syakaev, V.V., Gubaidullin, A.T., Habicher, W.D. and Burilov, A.R., 2018. Synthesis of *rccc*-and *rctt*-diastereoisomers of novel triazole-containing calix[4]resorcinols. *Tetrahedron Letters*, 59(17), pp.1683-1685.

Knyazeva, I.R., Sokolova, V.I., Gruner, M., Habicher, W.D., Syakaev, V.V., Khrizanforova, V.V., Gabidullin, B.M., Gubaidullin, A.T., Budnikova, Y.H., Burilov, A.R. and Pudovik, M.A., 2013. One-step synthesis of *rccc*-and *rctt*-diastereomers of novel calix[4]resorcinols based on a *para*-thiophosphorylated derivative of benzaldehyde. *Tetrahedron Letters*, 54(27), pp.3538-3542.

Kumar, P. and Venkatakrishnan, P., 2018. Coumarin[4]arene: A Fluorescent Macrocycle. *Org. Lett.*, 20(5), pp.1295-1299.

Kunsági-Máté, S., Nagy, L., Nagy, G., Bitter, I. and Kollár, L., 2003. Complex Formation of Fe(II) and Fe(III) Ions with Octafunctionalized C-Methyl-calix[4]resorcinarene Possessing− OCH_2COOH (K) Moieties. *J. Phys. Chem. B*, 107(20), pp.4727-4731.

Kunsági-Máté, S., Szabó, K., Lemli, B., Bitter, I., Nagy, G. and Kollár, L., 2004. Increased complexation ability of water-soluble calix[4]resorcinarene octacarboxylate toward phenol by the assistance of Fe(II) ions. *J. Phys. Chem. B*, 108(40), pp.15519-15522.

Laaf, D., Bojarová, P., Elling, L. and Křen, V., 2018. Galectin–Carbohydrate Interactions in Biomedicine and Biotechnology. *Trends in Biotechnology*, 37(4), pp.402-415.

Latxague, L., Gaubert, A. and Barthélémy, P., 2018. Recent Advances in the Chemistry of Glycoconjugate Amphiphiles. *Molecules*, 23(1), pp.89-113.

Laville, I., Pigaglio, S., Blais, J.C., Loock, B., Maillard, P., Grierson, D.S. and Blais, J., 2004. A study of the stability of tri (glucosyloxyphenyl) chlorin, a sensitizer for photodynamic therapy, in human colon tumoural cells: a liquid chromatography and MALDI-TOF mass spectrometry analysis. *Bioorg. Med. Chem.*, 12(13), pp.3673-3682.

Lazar, A., Da Silva, E., Navaza, A., Barbey, C. and Coleman, A.W., 2004. A new packing motif for *para*-sulfonatocalix[4]arene: the solid state structure of the *para*-sulfonatocalix[4]arene D-arginine complex. *Chem. Commun.*, (19), pp.2162-2163.

Lee, J.H., Shin, S.C., Seo, S.H., Seo, Y.H., Jeong, N., Kim, C.W., Kim, E.E. and Keum, G., 2017. Synthesis and in vitro antiproliferative activity of C5-benzyl substituted 2-amino-pyrrolo[2,3-d] pyrimidines as potent Hsp90 inhibitors. *Bioorganic & medicinal chemistry letters*, 27(2), pp.237-241.

Lee, Y.C. and Lee, R.T., 1995. Carbohydrate-protein interactions: basis of glycobiology. *Acc. Chem. Res.*, 28(8), pp.321-327.

Li, D. and Qi, L., 2018. Self-assembly of inorganic nanoparticles mediated by host-guest interactions. *Current Opinion in Colloid & Interface Science*, 35, pp.59-67.

Tiwari, A. and Uzun, L., 2015. Advanced Functional Materials. [e-book]: John Wiley & Sons, Inc. Hoboken, New Jersey, and Scrivener.

Li, H., Zhong, Y., Zhang, L., Wu, W., Lai, X., Chen, Z. and Zeng, X., 2017. Synthesis of sulphonic lanthanum complex based on C-methylcalix[4]resorcinarene and its thermo-oxidative aging resistance for natural rubber. *PLASTICS, RUBBER AND COMPOSITES*, 46(6), pp.251-257.

Li, W., Wang, Y., Chen, P., Zeng, M., Jiang, J. and Jin, Z., 2016. Thermoregulated phase-transfer iridium nanoparticle catalyst: highly selective hydrogenation of the C=O bond for *α*,*β*-unsaturated aldehydes and the C=C bond for *α*,*β*-unsaturated ketones. *Catal. Sci.Technol.*, 6(20), pp.7386-7390.

Li, Y., Cheng, H., Lin, W., Zhang, C., Wu, Q., Zhao, F. and Arai, M., 2018. Solvent effects on heterogeneous catalysis in selective hydrogenation of cinnamaldehyde over a conventional Pd/C catalyst. *Catal. Sci. Technol*., 8, pp.3580-3589.

Lingamurthy, M., Jagadeesh, Y., Ramakrishna, K. and Rao, B.V., 2016. DDQ-Promoted Benzylic/Allylic sp^3 C–H Activation for the Stereoselective Intramolecular C–N Bond Formation: Applications to the Total Synthesis of (−)-

Codonopsinine,(+)-5-epi-Codonopsinine,(+)-Radicamine B, and (−)-Codonopsinol. *The Journal of organic chemistry*, 81(4), pp.1367-1377.

Lis, H. and Sharon, N., 1998. Lectins: carbohydrate-specific proteins that mediate cellular recognition. *Chem. Rev.*, 98(2), pp.637-674.

Liu, Y., Shi, K. and Ma, D., 2019. Water-Soluble Pillar[n]arene Mediated Supramolecular Self-Assembly: Multi-Dimensional Morphology Controlled by Host Size. *Chem. Asian J.*, 14(2), pp.307-312.

Ma, J.C. and Dougherty, D.A., 1997. The cation− π interaction. *Chem. Rev.*, 97(5), pp.1303-1324.

Madasamy, K., Gopi, S., Kumaran, M.S., Radhakrishnan, S., Velayutham, D., Mareeswaran, P.M. and Kathiresan, M., 2017. A supramolecular investigation on the interactions between ethyl terminated bis–viologen derivatives with sulfonato calix[4]arenes. *ChemistrySelect*, 2(3), pp.1175-1182.

Maerz, A.K., Thomas, H.M., Power, N.P., Deakyne, C.A. and Atwood, J.L., 2010. Dimeric nanocapsule induces conformational change. *Chem. Commun.*, 46(8), pp.1235-1237.

Marra, A., Scherrmann, M.C., Dondoni, A., Ungaro, R., Casnati, A. and Minari, P., 1995. Sugar Calixarenes: Preparation of Calix[4]arenes Substituted at the Lower and Upper Rims with *O*-Glycosyl Groups. *Ange. Chem. Int. Ed. Engl.*, 33(23-24), pp.2479-2481.

Martin, A.D., Houlihan, E., Morellini, N., Eggers, P.K., James, E., Stubbs, K.A., Harvey, A.R., Fitzgerald, M., Raston, C.L. and Dunlop, S.A., 2012. Synthesis and Toxicology of *p*-Phosphonic Acid Calixarenes and *O*-Alkylated Analogues

as Potential Calixarene-Based Phospholipids. *ChemPlusChem*, 77(4), pp.308-313.

Matsuura, K., 2018. Synthetic Approaches to Construct Viral capsid-like Spherical Nanomaterials. *Chem. Commun*., 54, pp.8944-8959.

McIldowie, M.J., Mocerino, M., Skelton, B.W. and White, A.H., 2000. Facile Lewis acid catalyzed synthesis of C_4 symmetric resorcinarenes. *Org. Lett.,* 2(24), pp.3869-3871.

McKinlay, R.M., Thallapally, P.K., Cave, G.W. and Atwood, J.L., 2005. Hydrogen-Bonded Supramolecular Assemblies as Robust Templates in the Synthesis of Large Metal-Coordinated Capsules. *Angew. Chem. Int. Ed.*, 44(35), pp.5733-5736.

Mendoza-Cardozo, S., Pedro-Hernández, L.D., Organista-Mateos, U., Allende-Alarcón, L.I., Martínez-Klimova, E., Ramírez-Ápan, T. and Martínez-García, M., 2019. In vitro activity of resorcinarene-chlorambucil conjugates for therapy in human chronic myelogenous leukemia cells. *Drug development and industrial pharmacy*, pp.1-16.

Menger, F.M., Bian, J., Sizova, E., Martinson, D.E. and Seredyuk, V.A., 2004. Bolaforms with fourteen galactose units: a proposed site-directed cohesion of cancer cells. *Organic letters*, 6(2), pp.261-264.

Menon, S.K., Modi, N.R., Mistry, B. and Joshi, K., 2011. Improvement of some pharmaceutical properties of mycophenolate mofetil (MMF) by *para* sulphonatocalix [4]resorcinarene inclusion complex. *J. Incl. Phenom. Macrocycl. Chem.,* 70, pp.121-128.

Mezo, A.R. and Sherman, J.C., 1998. Water-soluble cavitands: Synthesis of methylene-bridged resorcin[4]arenes containing hydroxyls and phosphates at their feet and bromomethyls and thiomethyls at their rims. *J. Org. Chem.*, 63(20), pp.6824-6829.

Miao, S., Adams, R.D., Guo, D.S. and Zhang, Q.F., 2003. Structural conformers of symmetry substituted resorcin[4]arenes. *Journal of molecular structure*, 659(1-3), pp.119-128.

Michael, A., 1883. On the Action of Aldehydes on Phenols I. *Am. Chem. J.*, *5*, pp.338-349.

Middel, O., Verboom, W., Hulst, R., Kooijman, H., Spek, A.L. and Reinhoudt, D.N., 1998. Bridging of resorcin[4]arenes in the chair conformation to cavitands having two pairs of axial and equatorial substituents. *J. Org. Chem.*, 63(23), pp.8259-8265.

Mitchell, S.A., Pratt, M.R., Hruby, V.J. and Polt, R., 2001. Solid-Phase Synthesis of *O*-Linked Glycopeptide Analogues of Enkephalin. *J. Org. Chem*., 66(7), pp.2327-2342.

Mo, J., Eggers, P.K., Yuan, Z.X., Raston, C.L. and Lim, L.Y., 2016. Paclitaxel-loaded phosphonated calixarene nanovesicles as a modular drug delivery platform. *Scientific reports*, 6, pp.23489-23500.

Mohri, K., Watanabe, Y., Yoshida, Y., Satoh, M., Isobe, K., Sugimoto, N. and Tsuda, Y., 2003. Synthesis of glycosylcurcuminoids. *Chem. Pharm. Bull.*, *51*(11), pp.1268-1272.

Moore, D. and Matthews, S.E., 2009. *O*-alkyl resorcarenes: where are we now?.*J. Incl. Phenom. Macrocycl.Chem.*, 65(1-2), pp.137-155.

Moore, D., Watson, G.W., Gunnlaugsson, T. and Matthews, S.E., 2008. Selective formation of the *rctt* chair stereoisomers of octa-*O*-alkyl resorcin[4]arenes using Brønsted acid catalysis. *New J. Chem.*, 32(6), pp.994-1002.

Morbioli, I., Porkolab, V., Magini, A., Casnati, A., Fieschi, F. and Sansone, F., 2017. Mannosylcalix[n]arenes as multivalent ligands for DC-SIGN. *Carbohydrate research*, 453, pp.36-43.

Morikawa, O., Iyama, E., Oikawa, T., Kobayashi, K. and Konishi, H., 2006. Conformational properties of C_{2v}-symmetrical resorcin[4]arene tetraethers. *J. Phys. Org. Chem.*, 19(3), pp.214-218.

Morikawa, O., Ueno, R., Nakajima, K., Kobayashi, K. and Konishi, H., 2002. Trifluoromethanesulfonic acid-catalyzed synthesis of resorcinarenes: Cyclocondensation of 2-bromoresorcinol with aldehydes. *Synthesis*, 2002(6), pp.0761-0765.

Morozova, J.E., Syakaev, V.V., Kazakova, E.K., Shalaeva, Y.V., Nizameev, I.R., Kadirov, M.K., Voloshina, A.D., Zobov, V.V. and Konovalov, A.I., 2016. Amphiphilic calixresorcinarene associates as effective solubilizing agents for hydrophobic organic acids: construction of nano-aggregates. *Soft matter*, 12(25), pp.5590-5599.

Morozova, J.E., Syakaev, V.V., Shalaeva, Y.V., Ermakova, A.M., Nizameev, I.R., Kadirov, M.K. and Konovalov, A.I., 2018. Nanoassociates of amphiphilic

carboxy-calixresorcinarene and cetylpyridinuim chloride: The search of optimal macrocycle/surfactant molar ratio. *Colloids and Surfaces A: Physicochemical and Engineering Aspects*, 553, pp.569-577.

Moussa, Y.E., Ong, Y.Q.E., Perry, J.D., Cheng, Z., Kayser, V., Cruz, E., Kim, R.R., Sciortino, N. and Wheate, N.J., 2018. Demonstration of in vitro host-guest complex formation and safety of *para*-sulfonatocalix[8]arene as a delivery vehicle for two antibiotic drugs. *Journal of pharmaceutical sciences*, 107(12), pp.3105-3111.

Moussaoui, S.A., Damaj, Z., Wehbie, M., Rostaing, S.P. and Karamé, I., 2017. Alternative and Eco-Friendly Synthesis of Tetrakis(Aminomethyl)Calix-[4]-Resorcinarene. *International Journal of Organic Chemistry*, 7(04), pp.403-411.

Murayama, K. and Aoki, K., 1998. Resorcin[4]arene dimer linked by eight water molecules and incorporating a tetraethylammonium ion: guest-driven capsule formation via cation–π interactions. *Chem. Commun*., 5: pp.607-608.

Murray, J., Kim, K., Ogoshi, T., Yao, W. and Gibb, B.C., 2017. The aqueous supramolecular chemistry of cucurbit[n]urils, pillar[n]arenes and deep-cavity cavitands. *Chem. Soc. Rev.*, 46(9), pp.2479-2496.

Mutihac, L., Lee, J.H., Kim, J.S. and Vicens, J., 2011. Recognition of amino acids by functionalized calixarenes. *Chem. Soc. Rev.*, *40*(5), pp.2777-2796.

Nadkarni, D.H., Murugesan, S. and Velu, S.E., 2013. Total synthesis of zyzzyanones A–D. *Tetrahedron*, 69(20), pp.4105-4113.

Nakai, T., Kanamori, T., Sando, S. and Aoyama, Y., 2003. Remarkably size-regulated cell invasion by artificial viruses. Saccharide-dependent self-

aggregation of glycoviruses and its consequences in glycoviral gene delivery. *J. Am. Chem. Soc.*, 125(28), pp.8465-8475.

Negin, S., Li, R., Kulikov, O.V., Daschbach, M.M. and Gokel, G.W., 2014. Ion transport through bilayer membranes mediated by pyrogallol[4]arenes. *Inorganica Chimica Acta*, 417, pp.177-185.

Nguyen, Q.T., Sahoo, S.K. and Choi, H.J., 2018. Inclusion complexation of a deep cavitand with imidazoquinoxaline flaps forming stable vase-like conformation. *Tetrahedron*, 74(15), pp.1759-1766.

Niederl, J.B. and Vogel, H.J., 1940. Aldehyde—Resorcinol Condensations. *Journal of the American Chemical Society*, 62(9), pp.2512-2514.

Nikolelis, D.P., Raftopoulou, G., Psaroudakis, N. and Nikoleli, G.P., 2009. Development of an electrochemical chemosensor for the rapid detection of zinc based on air stable lipid films with incorporated calixarene phosphoryl receptor. *Intern. J. Environ. Anal. Chem.*, 89(3), pp.211-222.

Nuwaysir, L.M., Castoro, J.A., Yang, C.L.C. and Wilkins, C.L., 1992. Gas-phase host-guest chemistry of carcerands and hemicarcerands. *J. Am. Chem. Soc.*, 114(14), pp.5748-5751.

Ogoshi, T., Kitajima, K., Umeda, K., Hiramitsu, S., Kanai, S., Fujinami, S., Yamagishi, T.A. and Nakamoto, Y., 2009. Lewis acid-catalyzed synthesis of dodecamethoxycalix[4]arene from 1, 3, 5-trimethoxybenzene and its conformational behavior and host–guest property. *Tetrahedron*, 65(51), pp.10644-10649.

Olsufyeva, E.N., Tevyashova, A.N., Trestchalin, I.D., Preobrazhenskaya, M.N., Platt, D. and Klyosov, A., 2003. Synthesis and antitumor activity of new D-galactose-containing derivatives of doxorubicin. *Carbohydrate research*, 338(13), pp.1359-1367.

Ortiz Mellet, C., Benito, J.M. and García Fernández, J.M., 2010. Preorganized, Macromolecular, Gene-Delivery Systems. *Chem. Eur. J*., 16, pp.6728-6742.

Oshima, T., Goto, M. and Furusaki, S., 2002. Extraction behavior of amino acids by calix[6]arene carboxylic acid derivatives. *Journal of inclusion phenomena and macrocyclic chemistry*, 43(1-2), pp.77-86.

Oshovsky, G.V., Verboom, W., Fokkens, R.H. and Reinhoudt, D.N., 2004. Anion Complexation by Glycocluster Thioureamethyl Cavitands: Novel ESI-MS-Based Methods for the Determination of K_a Values. *Chem. Eur. J.,* 10, pp.2739-2748.

Ostos, F.J., Lebrón, J.A., Moyá, M.L., López-López, M., Sánchez, A., Clavero, A., García-Calderón, C.B., Rosado, I.V. and López-Cornejo, P., 2017. *P*-Sulfocalix[6]arene as Nanocarrier for Controlled Delivery of Doxorubicin. *Chemistry–An Asian Journal*, 12(6), pp.679-689.

Otsuka, H. and Shinkai, S., 1996. Stereochemical control of calixarenes useful as rigid and conformationally diversiform platforms for molecular design. *Supramol. Sci*., 3(4), pp.189-205.

Pan, F., Beyeh, N.K. and Rissanen, K., 2015. Concerted Halogen-Bonded Networks with N-Alkyl Ammonium Resorcinarene Bromides: From Dimeric

Dumbbell to Capsular Architectures. *Journal of the American Chemical Society*, 137(32), pp.10406-10413.

Parulekar, S., Muppalla, K., Husain, A. and Bisht, K.S., 2015. Multifold ring closing metathesis reactions in the formation of resorcin[4]arene cavitands. *RSC Adv.*, 5(32), pp.25477-25484.

Pashirova, T.N., Gibadullina, E.M., Burilov, A.R., Kashapov, R.R., Zhiltsova, E.P., Syakaev, V.V., Habicher, W.D., Rümmeli, M.H., Latypov, S.K., Konovalov, A.I. and Zakharova, L.Y., 2014. Amphiphilic *O*-functionalized calix[4]resocinarenes with tunable structural behavior. *RSC Adv.*, 4(20), pp.9912-9919.

Patel, M.B., Valand, N.N., Modi, N.R., Joshi, K.V., Harikrishnan, U., Kumar, S.P., Jasrai, Y.T. and Menon, S.K., 2013. Effect of *p*-sulfonatocalix[4]resorcinarene (PSC [4]R) on the solubility and bioavailability of a poorly water soluble drug lamotrigine (LMN) and computational investigation. *RSC. Adv.,* 3, pp.15971-15981.

Patel, V.R. and Agrawal, Y.K., 2011. Nanosuspension: An approach to enhance solubility of drugs. *J. Adv. Pharm. Tech. Res.*, 2(2), pp.81-87.

Patil, R.S., Zhang, C. and Atwood, J.L., 2016. Process development for separation of conformers from derivatives of resorcin[4]arenes and pyrogallol[4]arenes. *Chem. Eur. J.*, 22(43), pp.15202-15207.

Patil, R.S., Zhang, C., Sikligar, K., Baker, G.A. and Atwood, J.L., 2018. Formation of Water Channels in the Crystalline Hydrates of Macrocyclic Compounds. *Chem. Eur. J.*, 24(13), pp.3299-3304.

Payne, R.M. and Oliver, C.L., 2018. A propanol-seamed C-methylcalix[4]resorcinarene hexamer accessible via solution crystallization, liquid-assisted grinding and vapour sorption. *CrystEngComm*, 20(14), pp.1919-1922.

Perret, F. and Coleman, A.W., 2011. Biochemistry of anionic calix[n]arenes. *Chem. Commun.*, 47(26), pp.7303-7319.

Perret, F., Lazar, A.N. and Coleman, A.W., 2006. Biochemistry of the *para*-sulfonato-calix[n]arenes. *Chem. Commun.*, (23), pp.2425-2438.

Peterson, K.E., Smith, R.C. and Mohan, R.S., 2003. Bismuth compounds in organic synthesis. Synthesis of resorcinarenes using bismuth triflate. *Tetrahedron letters*, 44(42), pp.7723-7725.

Pfeiffer, C.R., Feaster, K.A., Dalgarno, S.J. and Atwood, J.L., 2016. Syntheses and characterization of aryl-substituted pyrogallol[4]arenes and resorcin[4]arenes. *CrystEngComm.*, 18(2), pp.222-229.

Pfeiffer, C.R., Fowler, D.A. and Atwood, J.L., 2014. Endo vs Exo Bowl: Complexation of Xanthone by Pyrogallol[4]arenes. *Cryst. Growth Des.*, 14(8), pp.4205-4213.

Pillai, G., 2014. Nanomedicines for Cancer Therapy: An Update of FDA Approved and Those under Various Stages of Development. *SOJ Pharm. Pharm. Sci.*, 1(2), pp.1-13.

Pisagatti, I., Barbera, L., Gattuso, G., Patanè, S., Parisi, M.F. and Notti, A., 2018. Novel PEGylated calix[5]arenes as carriers for Rose Bengal. *Supramolecular Chemistry*, 30(8), pp.658-663.

Pod, S.N., Mustafina, A.R., Koppehele, A.H., Grüner, M., Habicher, W.D., Buzykin, B.I. and Konovalov, A.I., 2004. Synthesis of per-*O*-(carboxymethyl) calix[4]pyrogallols and their complexation with some alkaline metal and lanthanide ions. *Russ. Chem. Bull.*, Int.Ed., 53(6), pp.1181-1188.

Podyachev, S.N., Syakaev, V.V., Sudakova, S.N., Shagidullin, R.R., Osyanina, D.V., Avvakumova, L.V., Buzykin, B.I., Latypov, S.K., Bauer, I., Habicher, W.D. and Konovalov, A.I., 2007. Synthesis of new calix[4]arenes functionalizated by acetylhydrazide groups. *Journal of Inclusion Phenomena and Macrocyclic Chemistry*, 58(1-2), pp.55-61.

Pollok, C.H., Zhang, Q., Tiefenbacher, K. and Merten, C., 2017. Chirality Induction from a Chiral Guest to the Hydrogen-Bonding Network of Its Hexameric Resorcinarene Host Capsule. *ChemPhysChem*, 18(15), pp.1987-1991.

Pritchard, J., Filonenko, G.A., van Putten, R., Hensen, E.J. and Pidko, E.A., 2015. Heterogeneous and homogeneous catalysis for the hydrogenation of carboxylic acid derivatives: history, advances and future directions. *Chem. Soc. Rev.*, 44(11), pp.3808-3833.

Prosvirkin, A.V., Kazakova, E.K., Gubaidullin, A.T., Litvinov, I.A., Gruner, M., Habicher, W.D. and Konovalov, A.I., 2005. Synthesis of *rctt*, *rccc*, and *rcct* diastereomers of calix[4]methylresorcinarenes based on *p*-tolualdehyde. X-ray diffraction study of the *rcct* isomer. Formation of *rctt* and *rccc* cavitands in a cone conformation. *Russ. Chem. Bull.*, 54(11), pp.2550-2557.

Puttreddy, R., Beyeh, N.K., Jurček, P., Turunen, L., Trant, J.F., Ras, R.H. and Rissanen, K., 2018. Host-guest complexes of C-propyl-2-bromoresorcinarene with aromatic N-oxides. *Supramolecular Chemistry*, 30(5-6), pp.445-454.

Puttreddy, R., Beyeh, N.K., Ras, R.H. and Rissanen, K., 2017. Host–Guest Complexes of C-Ethyl-2-methylresorcinarene and Aromatic N, N′-Dioxides. *ChemistryOpen*, 6(3), pp.417-423.

Raj, A.M., Talluri, S.G., Dubus, M., Gupta, S., Mondal, B. and Ramamurthy, V., 2018. Probing the pH dependent assembly-disassembly of water-soluble organic capsules with coumarins and anthracene. *Journal of Photochemistry and Photobiology A: Chemistry*, 355, pp.398-407.

Reina, J.J. and Rojo, J., 2015. *Carbohydrate Chemistry: State of the Art and Challenges for Drug Development:* An Overview on Structure, Biological Roles, Synthetic Methods and Application as Therapeutics. Carbohydrate Multivalent Systems: Synthesis and Therapeutic Opportunities. pp. 419-439.

Roberts, B.A., Cave, G.W., Raston, C.L. and Scott, J.L., 2001. Solvent-free synthesis of calix[4]resorcinarenes. *Green Chem*., 3, pp.280-284.

Rodik, R.V., Boyko, V.I. and Kalchenko, V.I., 2009. Calixarenes in bio-medical researches. *Current Medicinal Chemistry*, 16(13), pp.1630-1655.

Rose, K.N., Barbour, L.J., Orr, G.W., and Atwood, J.L., 1998. Self-assembly of carcerand-like dimers of calix[4]resorcinarene facilitated by hydrogen bonded solvent bridges. *Chem. Commun*., 3, pp.407-408.

Rumboldt, G., Böhmer, V., Botta, B. and Paulus, E.F., 1998. Rational Synthesis of Resorcarenes with Alternating Substituents at Their Bridging Methine Carbons. *J. Org. Chem*., 63(26), pp.9618-9619.

Ryzhkina, I.S., Pashirova, T.N., Kudryavtseva, L.A., Timosheva, A.P., Arkhipov, V.P., Idiyatullin, Z.S., Popova, E.V., Burilov, A.R. and Konovalov, A.I., 2004. Aggregation behavior and catalytic activity of systems based on calix[4]resorcinarene derivatives and surfactants. 1. Mixed micellization of aminomethylated calix[4]resorcinarenes with cetyltrimethylammonium bromide in aqueous dimethylformamide. *Russ. Chem. Bull.*, Int. Ed., 53(7), pp.1520-1527.

Sakhaii, P., Verdier, L., Ikegami, T. and Griesinger, C., 2002. Synthesis of a Novel Class of Carbohydrate-Containing Calix[4]resorcinarene Adopting an Asymmetrical Diamond Structure. *Helv. Chim. Acta*., 85, pp.3895-3908.

Samanta, K., Ranade, D.S., Upadhyay, A., Kulkarni, P.P. and Rao, C.P., 2017. A Bimodal, Cationic, and Water-Soluble Calix[4]arene Conjugate: Design, Synthesis, Characterization, and Transfection of Red Fluorescent Protein Encoded Plasmid in Cancer Cells. *ACS Appl. Mater. Interfaces*, 9(6), pp.5109-5117.

Sanabria, E., Esteso, M.Á., Vargas, E. and Maldonado, M., 2018. Experimental comparative study of solvent effects on the structure of two sulfonated resorcinarenes. *Journal of Molecular Liquids*, 254, pp.391-397.

Sansone, F. and Casnati, A., 2013. Multivalent glycocalixarenes for recognition of biological macromolecules: glycocalyx mimics capable of multitasking. *Chem. Soc. Rev.*, 42(11), pp.4623-4639.

Sansone, F., Dudic, M., Donofrio, G., Rivetti, C., Baldini, L., Casnati, A., Cellai, S. and Ungaro, R., 2006. DNA Condensation and Cell Transfection Properties of Guanidinium Calixarenes: Dependence on Macrocycle Lipophilicity, Size, and Conformation. *J. Am. Chem. Soc*., 128(45), pp.14528-14536.

Sansone, F., Rispoli, G., Casnati, A. and Ungaro, R., 2011. Multivalent glycocalixarenes. pp. 36-63. [e-book] Bentham Science.

Sardjono, R.E. and Rachmawati, R., 2017. Green Synthesis of Oligomer Calixarenes. In *Green Chemical Processing and Synthesis*. [e-book] Indonesia: Available through: Indonesia University, Bandung.

Sardjono, R.E., Musthapa, I., Rosliana, I., Khoerunnisa, F. and Yuliani, G., 2018. A Green Synthesis of a Novel Calix[4]Resorcinarene from 7-Hydroxycitronellal Using Microwave Irradiation. *Indone. J. Chem.*, 18(1), pp.53-59.

Sarjono, R.E., Paramitha, B., Hendaryani, I., Siswanta, D., Santosa, S.J., Anwar, C., Sastrohamidjojo, H., Ohto, K. and Oshima, T., 2007. Adsorption Characteristics of Pb(II) and Cr(III) onto C-4-Methoxyphenylcalix[4]resorcinarene in Batch and Fixed Bed Column Systems. *J. Chin. Chem. Soc.*, 54(5), pp.1167-1178.

Senthan, S.A. and Alexander, V., 2015. Synthesis, luminescence, and electrochemical studies of a new series of octanuclear ruthenium(II) complexes of tolylterpyridine appended calixresorcarenes. *Dalton Trans.*, 44(33), pp.14813-14822.

Serkova, O.S., Kamkina, A.V., Egorova, M.A. and Maslennikova, V.I., 2018. Octacarbamoylated and octathiocarbamoylated resorcinarenes: transformations and acceptor properties. *Russ. Chem. Bull.*, *Int.Ed.,* 67(2), pp.321-327.

Shahgaldian, P., Sciotti, M.A. and Pieles, U., 2008. Amino-substituted amphiphilic calixarenes: Self-assembly and interactions with DNA. *Langmuir*, 24(16), pp.8522-8526.

Shalaeva, Y.V., Morozova, J.E., Gubaidullin, A.T., Saifina, A.F., Syakaev, V.V., Ermakova, A.M., Nizameev, I.R., Kadirov, M.K., Ovsyannikov, A.S. and Konovalov, A.I., 2018. Gold nanoparticles, capped by carboxy-calix[4]resorcinarenes: effect of structure and concentration of macrocycles on the nanoparticles size and aggregation. *Journal of Inclusion Phenomena and Macrocyclic Chemistry*, 92(1-2), pp.211-221.

Shchelik, I.S., Magasumova, A.I. and Sebyakin, Y.L., 2015. Glycodendrimers and Their Derivatives as Potential Therapeutic Agents. *Macroheterocycles*, 8(2), pp.199-217.

Sherman, J., 2003. Molecules that can't resist templation. *Chem. Commun.*, (14), pp.1617-1623.

Shi, Y.S., Yuan, Z.F., Wei, Q., Sun, K.Q. and Xu, B.Q., 2016. Pt–FeO x/SiO 2 catalysts prepared by galvanic displacement show high selectivity for cinnamyl alcohol production in the chemoselective hydrogenation of cinnamaldehyde. *Catal. Sci.Technol.*, 6(19), pp.7033-7037.

Shiao, T.C. and Roy, R., 2012. Glycodendrimers as functional antigens and antitumor vaccines. *New J. Chem*., 36, pp.324-339.

Shinkai, S., Mori, S., Koreishi, H., Tsubaki, T. and Manabe, O., 1986. Hexasulfonated calix[6]arene derivatives: a new class of catalysts, surfactants, and host molecules. *J. Am. Chem. Soc.*, 108(9), pp.2409-2416.

Sinha, R., Kim, G.J., Nie, S. and Shin, D.M., 2006. Nanotechnology in cancer therapeutics: bioconjugated nanoparticles for drug delivery. *Mol. Cancer Ther.*, 5(8), pp.1909-1917.

Song, J., Li, H., Chao, J., Dong, C. and Shuang, S., 2012. Spectroscopic studies on the inclusion interaction of *p*-sulfonatocalix[6]arene with vitamin B6. *J. Incl. Phenom. Macrocycl. Chem*., 72, pp.389-395.

Soni, N., Tekade, M., Kesharwani, P., Bhattacharya, P., Maheshwari, R., Dua, K., M Hansbro, P. and Kumar Tekade, R., 2017. Recent advances in oncological submissions of dendrimer. *Curr. Pharm. Des.*, 23(21), pp.3084-3098.

Soomro, Z.H., Cecioni, S., Blanchard, H., Praly, J.P., Imberty, A., Vidal, S. and Matthews, S.E., 2011. CuAAC synthesis of resorcin[4]arene-based glycoclusters as multivalent ligands of lectins. *Org. Biomol. Chem.*, 9(19), pp.6587-6597.

Spiel, P.D., Sikligar, K., Baker, G.A., Kelley, S.P. and Atwood, J.L., 2018. Cocrystallization of C-Propyl Pyrogallol[4]arene and the Pharmaceutical Gabapentin. *Journal of Chemical Crystallography*, pp.1-6.

Stavila, V., Stortz, Y., Franc, C., Pitrat, D., Maurin, P. and Hasserodt, J., 2008. Effective Repression of the Fragmentation of a Hexadentate Ligand Bearing an

Auto-Immolable Pendant Arm by Iron Coordination. *Eur. J. Inorg. Chem.*, 2008(25), pp.3943-3947.

Strobel, M., Kita-Tokarczyk, K., Taubert, A., Vebert, C., Heiney, P.A., Chami, M. and Meier, W., 2006. Self-Assembly of Amphiphilic Calix[4]arenes in Aqueous Solution. *Adv. Funct. Mater.*, 16(2), pp.252-259.

Sultana, I., Shimamoto, M., Obata, R., Nishiyama, S. and Sugai, T., 2006. An expeditious chemo-enzymatic synthesis of dihydronorcapsaicin *β*-D-glucopyranoside. *Science and Technology of Advanced Materials*, 7(2), pp.197-201.

Sun, Y., Yan, C.G., Yao, Y., Han, Y. and Shen, M., 2008. Self-Assembly and Metallization of Resorcinarene Microtubes in Water. *Adv. Funct. Mater.*, 18(24), pp.3981-3990.

Svenson, S. and Tomalia, D.A., 2012. Dendrimers in biomedical applications-reflections on the field. *Adv. Drug Deliv. Rev*., 64, pp.102-115.

Syakaev, V.V., Kazakova, E.K., Morozova, J.E., Shalaeva, Y.V., Latypov, S.K. and Konovalov, A.I., 2012. Guest controlled aggregation of amphiphilic sulfonatomethylated calix[4]resorcinarenes in aqueous solutions. *J. Colloid Interface Sci*., 370, pp.19-26.

Syakaev, V.V., Morozova, J.E., Bogdanov, A.V., Shalaeva, Y.V., Ermakova, A.M., Voloshina, A.D., Zobov, V.V., Nizameev, I.R., Kadirov, M.K., Mironov, V.F. and Konovalov, A.I., 2018. Solubilization of azo-dye-modified isatin derivative by amphiphilic carboxyresorcinarenes: the effect of macrocycle

structure on the supramolecular association. *Colloids and Surfaces A,* 555, pp.368-377.

Syakaev, V.V., Mustafina, A.R., Elistratova, J.G., Latypov, S.K. and Konovalov, A.I., 2008. Head-to-tail aggregates of sulfonatomethylated calix[4]resorcinarene in aqueous solutions. *Supramolecular Chemistry*, 20(5), pp.453-460.

Szumelda, T., Drelinkiewicz, A., Kosydar, R. and Gurgul, J., 2014. Hydrogenation of cinnamaldehyde in the presence of PdAu/C catalysts prepared by the reverse “water-in-oil” microemulsion method. *Applied Catalysis A: General*, 487, pp.1-15.

Tadiparthi, K., Raghavendra, S. and Kamal, A., 2017. Lipase-Catalyzed Resolution of 1-[4-(Benzyloxy)phenyl]hex-5-en-3-ol: Synthesis of (-)-Centrolobine. *Asian J. Chem.*, 29(10), pp.2321-2326.

Thakar, A.S., Parekh, H.M., Pansuriya, P.B., Friedrich, H.B. and Maguire, G.E., 2014. Preparation of Enantiomerically Pure C_4-Symmetric Tetramethoxyresorcarenes by Using the (–)-(*S*)-1-Phenylethyl Isocyanate Chiral Auxiliary. *Eur. J. Org. Chem.*, 2014(21), pp.4600-4609.

Tilley, A.J., Zanatta, S.D., Qin, C.X., Kim, I.K., Seok, Y.M., Stewart, A., Woodman, O.L. and Williams, S.J., 2012. 2-Morpholinoisoflav-3-enes as flexible intermediates in the synthesis of phenoxodiol, isophenoxodiol, equol and analogues: Vasorelaxant properties, estrogen receptor binding and Rho/RhoA kinase pathway inhibition. *Bioorganic & medicinal chemistry*, 20(7), pp.2353-2361.

Timmerman, P., Verboom, W. and Reinhoudt, R., 1996. Tetrahedron report number 390. *Tetrahedron Lett.,* 52(8), pp.2263–2704.

Titov, D.V., Gening, M.L., Tsvetkov, Y.E. and Nifantiev, N.E., 2013. Oligodentate glycoconjugates based on calixarenes: methods for the synthesis and biological activity. *Russ. Chem. Bull.*, *Int.Ed*., 62(3), pp.577-604.

Tomalia, D.A. and Fréchet, J.M., 2002. Discovery of Dendrimers and Dendritic Polymers: a Brief Historical Perspective. *J. Polym. Sci. Part A: Polym. Chem*., 40, pp.2719-2728.

Tu, Y. Q., Byriel, K.A., Kennard, C.H.L., Kitching, W., 1995. Bromination–dehydrobromination route to some naturally occurring 1, 6-dioxaspiro [4.4]-nonenes and-nonadienes. *J. Chem. Soc., Perkin Trans. 1*, (10), pp.1309-1315.

Tung, C.L., Wong, C.T., Fung, E.Y.M. and Li, X., 2016. Traceless and chemoselective amine bioconjugation via phthalimidine formation in native protein modification. *Org. lett.*, 18(11), pp.2600-2603.

Tunstad, L.M., Tucker, J.A., Dalcanale, E., Weiser, J., Bryant, J.A., Sherman, J.C., Helgeson, R.C., Knobler, C.B. and Cram, D.J., 1989. Host-guest complexation. 48. Octol building blocks for cavitands and carcerands. *J. Org. Chem.*, 54(6), pp.1305-1312.

Ugono, O., Moran, J.P. and Holman, K.T., 2008. Closed-surface hexameric metal–organic nanocapsules derived from cavitand ligands. *Chem. Commun.,* (12), pp.1404-1406.

Ukhatskaya, E.V., Kurkov, S.V., Matthews, S.E., El Fagui, A., Amiel, C., Dalmas, F. and Loftsson, T., 2010. Evaluation of a cationic calix[4]arene:

Solubilization and self-aggregation ability. *International journal of pharmaceutics*, 402(1-2), pp.10-19.

Valand, N.N., Patel, M.B. and Menon, S.K., 2015. Curcumin-*p*-sulfonatocalix[4]resorcinarene (p-SC[4]R) interaction: thermo-physico chemistry, stability and biological evaluation. *RSC Adv.*, 5(12), pp.8739-8752.

Varki, A., 1993. Biological roles of oligosaccharides: all of the theories are correct. *Glycobiology*, 3(2), pp.97-130.

Vece, V. and Vuocolo, G., 2015. Multicomponent synthesis of novel coelenterazine derivatives substituted at the C-3 position. *Tetrahedron*, 71(46), pp.8781-8785.

Victorovna-Lijanova, I., Reyes-Valderrama, M.I., Maldonado, J.L., Ramos-Ortiz, G., Tatiana, K. and Martínez-García, M., 2008. Synthesis and cubic nonlinear optical behavior of phenyl and ferrocenyl-ended resorcinarene-based dendrimers. *Tetrahedron*, 64(19), pp.4460-4467.

Waidely, E., Pumilia, C., Malagon, A., Vargas, E.F., Li, S. and Leblanc, R.M., 2015. Host–Guest Complexation of a Pyrogallol[4]arene Derivative at the Air–Water Interface. *Langmuir*, 31(4), pp.1368-1375.

Wang, B., Jia, A.Q., Yang, H.M., Liu, J.L. and Zhang, Q.F., 2018. Encapsulation of ferrocenes by hydrogen-bonded pyrogallol [4] arene dimers. *Z. Naturforsch. B*, 73(8), pp.597-600.

Wang, G.S., Zhang, H.Y., Ding, F. and Liu, Y., 2011. Preparation and characterization of inclusion complexes of topotecan with sulfonatocalixarene. *J. Incl. Phenom. Macrocycl. Chem*., 69, pp.85-89.

Wang, G.S., Zhang, H.Y., Li, D., Wang, P.Y. and Liu, Y., 2011. Characterisation and antiproliferative activity of irinotecan and sulphonatocalixarene inclusion complex. *Supramolecular Chemistry*, 23(6), pp.441-446.

Wang, S., Liu, D., Zhang, X., Li, S., Sun, Y., Li, J., Zhou, Y. and Zhang, L., 2007. Study on glycosylated prodrugs of toxoflavins for antibody-directed enzyme tumor therapy. *Carbohydrate research*, 342(9), pp.1254-1260.

Warmuth, R., 2012. Supramolecular Chemistry: From Molecules to Nanomaterials. Carcerands and Hemicarcerands. John Wiley & Sons.

Weinelt, F. and Schneider, H.J., 1991. Mechanisms of macrocycle genesis. The Condensation of Resorcinol with Aldehydes. *J. Org. Chem.*, 56(19), pp.5527-5535.

Wen, H., Lin, C., Que, L., Ge, H., Ma, L., Cao, R., Wan, Y., Peng, W., Wang, Z. and Song, H., 2008. Synthesis and biological evaluation of helicid analogues as novel acetylcholinesterase inhibitors. *European journal of medicinal chemistry*, 43(1), pp.166-173.

Wenzel, T.J., 2014. Calixarenes and calix[4]resorcinarenes as chiral NMR solvating agents. *J. Incl. Phenom. Macrocycl. Chem.*, *78*, pp.1-14.

Wheate, N.J., Abbott, G.M., Tate, R.J., Clements, C.J., Edrada-Ebel, R. and Johnston, B.F., 2009. Side-on binding of *p*-sulphonatocalix[4]arene to the dinuclear platinum complex *trans*-[{PtCl(NH_3)$_2$}$_2$ μ-dpzm]$^{2+}$ and its implications for anticancer drug delivery. *J. Inorg. Biochem*., 103, pp.448-454.

Williams, D. and Westwell, M., 1998. Aspects of weak interactions. *Chem. Soc. Rev.*, 27(1), pp.57-64.

Xiang, J.N., Jiang, L.H., Chen, C.Y., Fu, Z.Y., Duan, J.F., He, X.X. and Wang, K.M., 2006. Studies on the Synthesis and Antiproliferative Activities of 13-*cis*-Retinoyl Sugar Derivatives. *Journal of carbohydrate chemistry*, 25(7), pp.595-614.

Xu, X., Tan, Q. and Hayashi, M., 2008. Versatile and mild synthesis of di-and trisaccharidic 2-enopyranosyl cyanides by cyanation of per-*O*-acetylglycals with trimethylsilyl cyanide catalyzed by palladium(II) acetate. *Synthesis*, 2008(5), pp.770-776.

Xue, Y., Guan, Y., Zheng, A. and Xiao, H., 2013. Amphoteric calix[8]arene-based complex for pH-triggered drug delivery. *Colloids and Surfaces B: Biointerfaces*, 101, pp.55-60.

Yan, C., Chen, W., Chen, J., Jiang, T. and Yao, Y., 2007. Microwave irradiation assisted synthesis, alkylation reaction, and configuration analysis of aryl pyrogallol[4]arenes. *Tetrahedron*, 63(39), pp.9614-9620.

Yang, W. and de Villiers, M.M., 2004. The solubilization of the poorly water soluble drug nifedipine by water soluble 4-sulphonic calix[n]arenes. *Eur. J. Pharm. Biopharm*., 58, pp.629-636.

Yang, Y.W., Sun, Y.L. and Song, N., 2014. Switchable Host–Guest Systems on Surfaces. *Acc. Chem. Res*., 47, pp.1950-1960.

Yu, G. and Chen, X., 2019. Host-Guest Chemistry in Supramolecular Theranostics. *Theranostics*, 9(11), pp.3041-3074.

Yu, X., Tu, C., He, L., Wang, R., Sun, G., Yan, D. and Zhu, X., 2009. Self-assembly of Supramolecular Amphiphile Constructed by Hydrophilic Calix[4]arene Derivative and Phenol Palmitate. *J. Macromol. Sci., Part A: Pure and Applied Chemistry*, 46, pp.360-367.

Zangabad, P.S., Karimi, M., Mehdizadeh, F., Malekzad, H., Ghasemi, A., Bahrami, S., Zare, H., Moghoofei, M., Hekmatmanesh, A. and Hamblin, M.R., 2017. Nanocaged platforms: modification, drug delivery and nanotoxicity. Opening synthetic cages to release the tiger. *Nanoscale*, 9(4), pp.1356-1392.

Zhang, C., Patil, R.S., Barnes, C.L. and Atwood, J.L., 2017. Preparation of Anionic Metal-Seamed Pyrogallol[4]arene Nanocapsules via Surface Functionalization. *Cryst. Growth Des.*, 17(9), pp.4541-4543.

Zhang, M.J., Tan, D.W., Li, H.X., Young, D.J., Wang, H.F., Li, H.Y. and Lang, J.P., 2018. Switchable Chemoselective Transfer Hydrogenations of Unsaturated Carbonyls Using Copper(I) N-Donor Thiolate Clusters. *J. Org. Chem.*, 83(3), pp.1204-1215.

Zhang, Y., Su, K., Zhou, H., Han, Z. and Yuan, D., 2017. Stabilization of Allylic Amine N-oxide through Cocrystallization with Pyrogallol[4]arene. *Cryst. Growth Des.*, 17(11), pp.5625-5628.

Zhao, T., Kurpiewska, K., Kalinowska-Tłuścik, J., Herdtweck, E. and Dömling, A., 2016. *α*-Amino Acid-Isosteric *α*-Amino Tetrazoles. *Chem. Eur. J.*, 22(9), pp.3009-3018.

Zhou, Y., Li, H. and Yang, Y.W., 2015. Controlled drug delivery systems based on calixarenes. *Chinese Chemical Letters*, *26*(7), pp.825-828.

Appendices

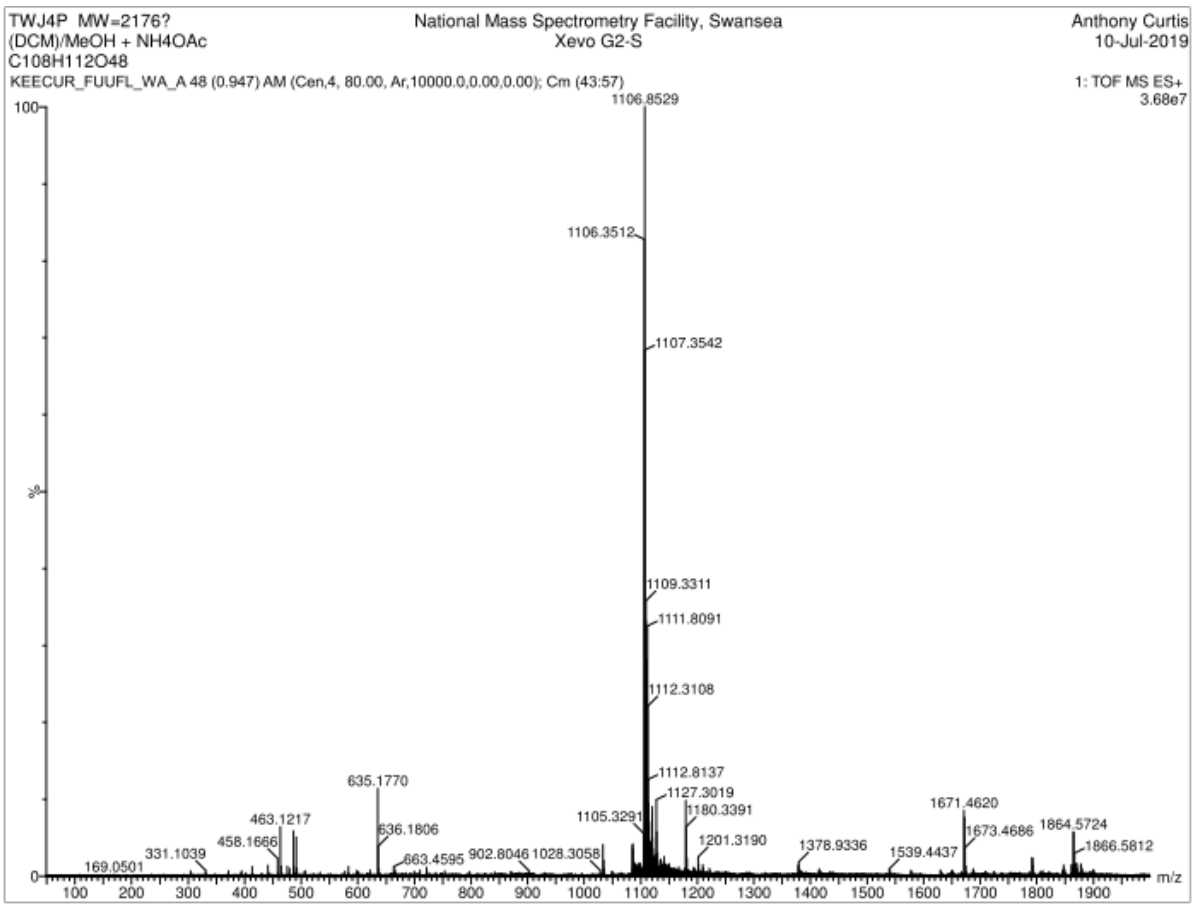
TWJ4P MW=2176?
(DCM)/MeOH + NH4OAc
C108H112O48
National Mass Spectrometry Facility, Swansea
Xevo G2-S
Anthony Curtis
10-Jul-2019
KEECUR_FUUFL_WA_A 48 (0.947) AM (Cen,4, 80.00, Ar,10000.0,0.00,0.00); Cm (43:57)
1: TOF MS ES+
3.68e7
1106.8529
1106.3512
1107.3542
1109.3311
1111.8091
1112.3108
1112.8137
1127.3019
1180.3391
1105.3291
635.1770
636.1806
463.1217
458.1666
331.1039
169.0501
663.4595
902.8046
1028.3058
1201.3190
1378.9336
1539.4437
1671.4620
1673.4686
1864.5724
1866.5812
%
m/z

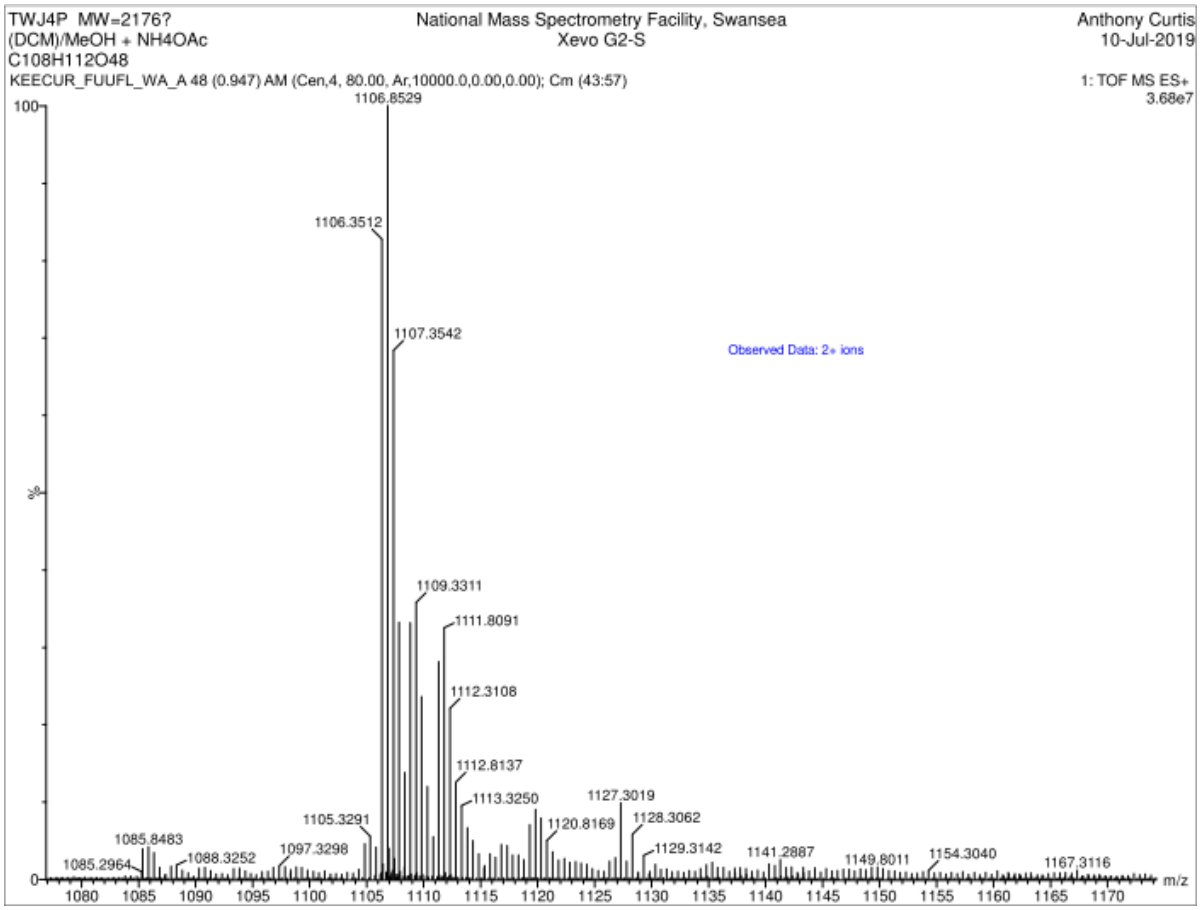
TWJ4P MW=2176?
(DCM)/MeOH + NH4OAc
C108H112O48
National Mass Spectrometry Facility, Swansea
Xevo G2-S
Anthony Curtis
10-Jul-2019
KEECUR_FUUFL_WA_A 48 (0.947) AM (Cen,4, 80.00, Ar,10000.0,0.00,0.00); Cm (43:57)
1: TOF MS ES+
3.68e7
Observed Data: 2+ ions
1106.8529
1106.3512
1107.3542
1109.3311
1111.8091
1112.3108
1112.8137
1113.3250
1127.3019
1128.3062
1120.8169
1105.3291
1085.8483
1088.3252
1085.2964
1097.3298
1129.3142
1141.2887
1149.8011
1154.3040
1167.3116
%
m/z

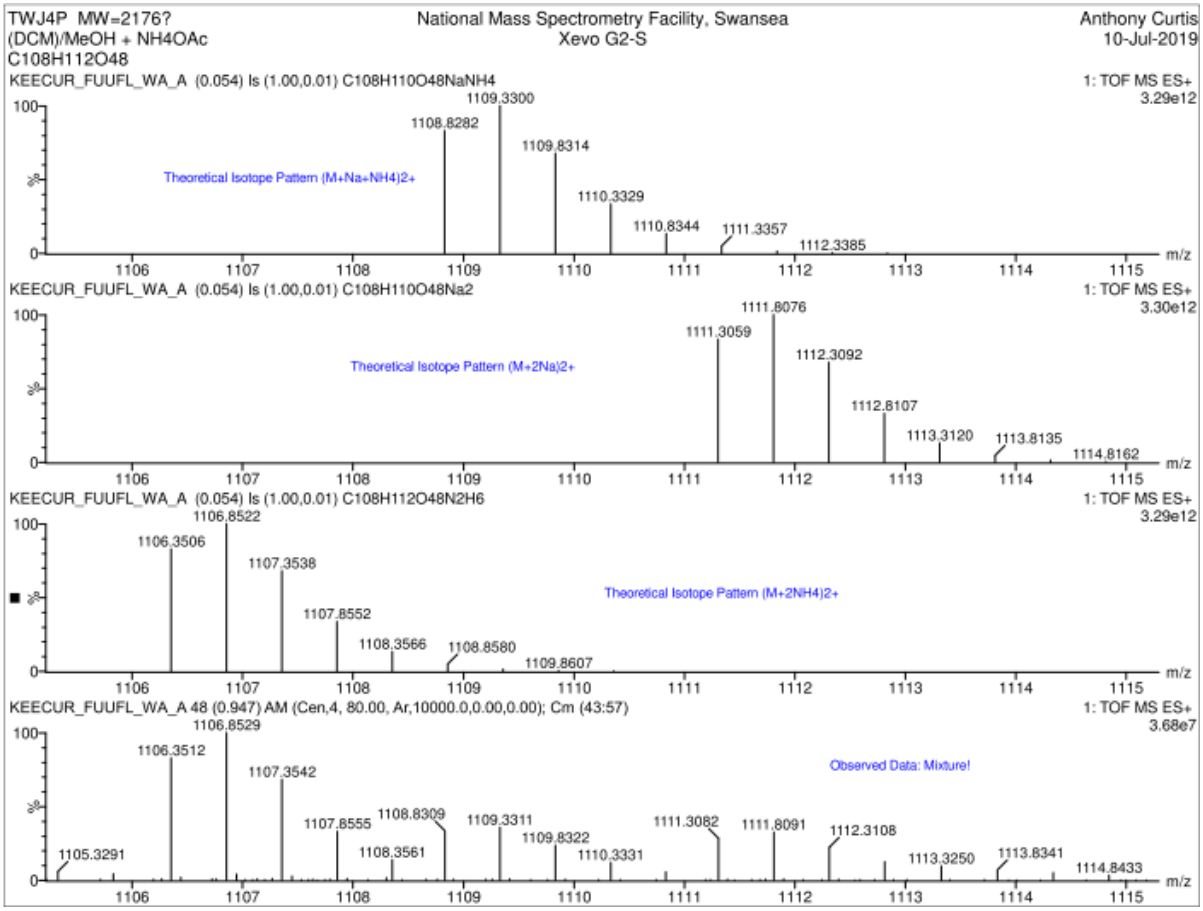

Appendix 1: Mass spectrum of **145**

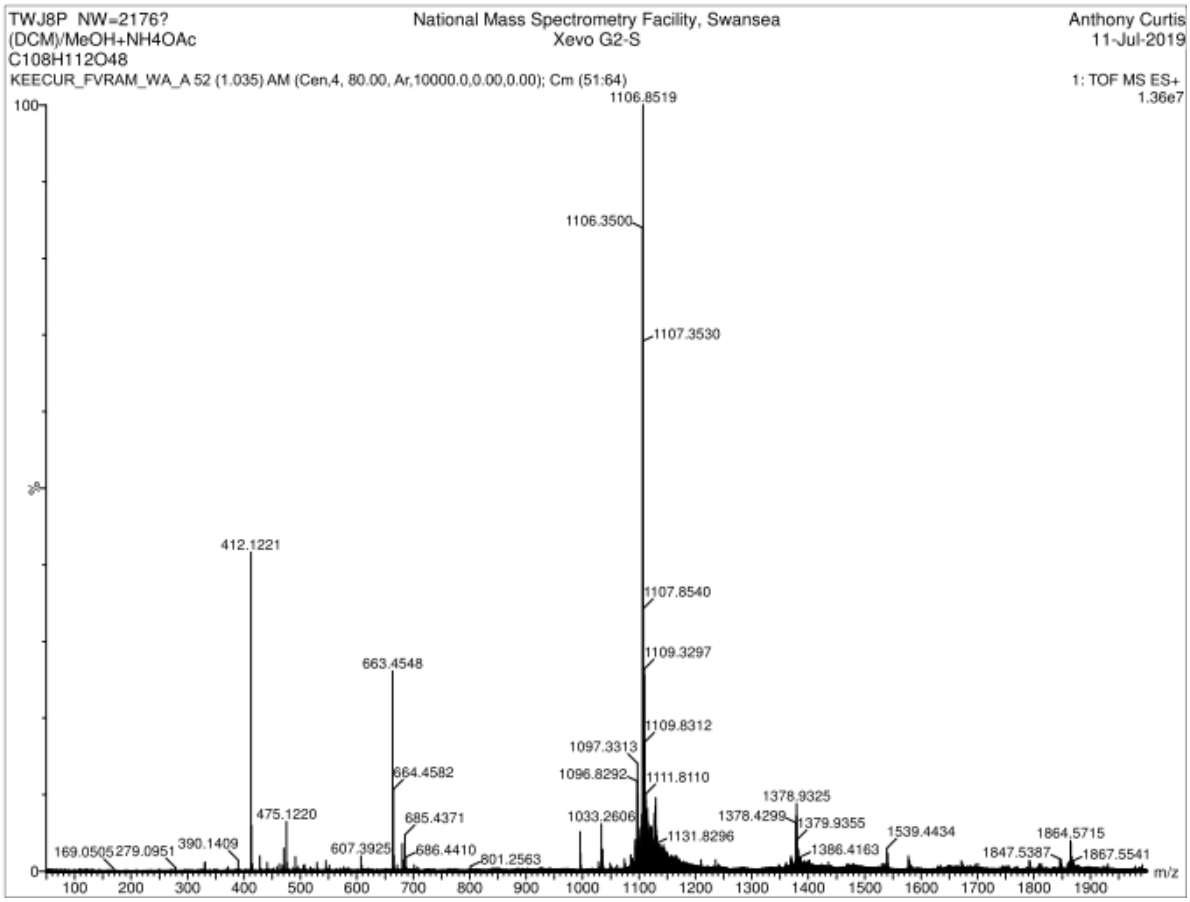
TWJ8P NW=2176?
(DCM)/MeOH+NH4OAc
C108H112O48
National Mass Spectrometry Facility, Swansea
Xevo G2-S
Anthony Curtis
11-Jul-2019
KEECUR_FVRAM_WA_A 52 (1.035) AM (Cen,4, 80.00, Ar,10000.0,0.00,0.00); Cm (51:64)
1: TOF MS ES+
1.36e7
1106.8519
1106.3500
1107.3530
412.1221
1107.8540
663.4548
1109.3297
1109.8312
1097.3313
664.4582
1096.8292
1111.8110
1378.9325
475.1220
685.4371
1033.2606
1378.4299
1379.9355
1539.4434
1131.8296
1386.4163
1864.5715
169.0505
279.0951
390.1409
607.3925
686.4410
801.2563
1847.5387
1867.5541
%
m/z

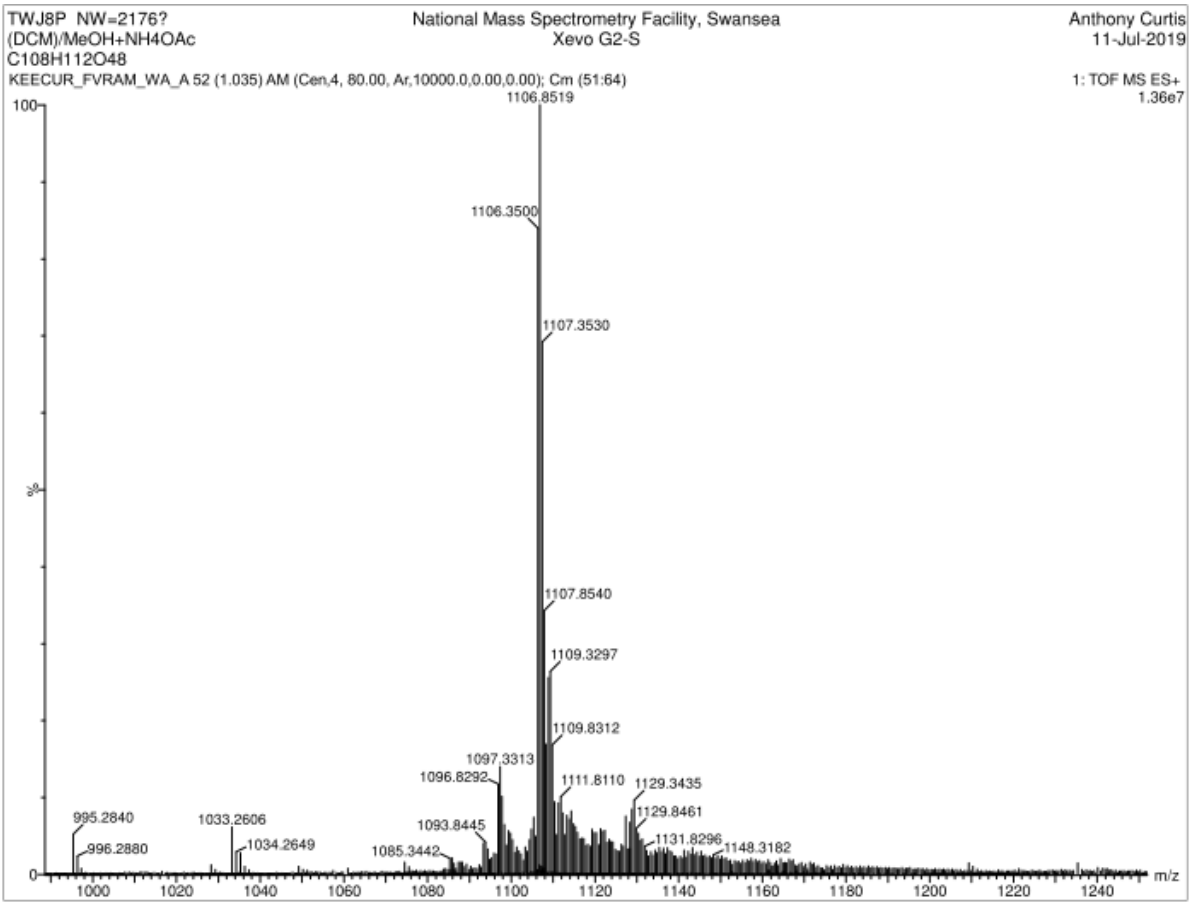
TWJ8P NW=2176?
(DCM)/MeOH+NH4OAc
C108H112O48
National Mass Spectrometry Facility, Swansea
Xevo G2-S
Anthony Curtis
11-Jul-2019
KEECUR_FVRAM_WA_A 52 (1.035) AM (Cen,4, 80.00, Ar,10000.0,0.00,0.00); Cm (51:64)
1: TOF MS ES+
1.36e7
1106.8519
1106.3500
1107.3530
1107.8540
1109.3297
1109.8312
1097.3313
1096.8292
1111.8110
1129.3435
1129.8461
995.2840
1033.2606
1093.8445
1131.8296
996.2880
1034.2649
1085.3442
1148.3182
%
m/z

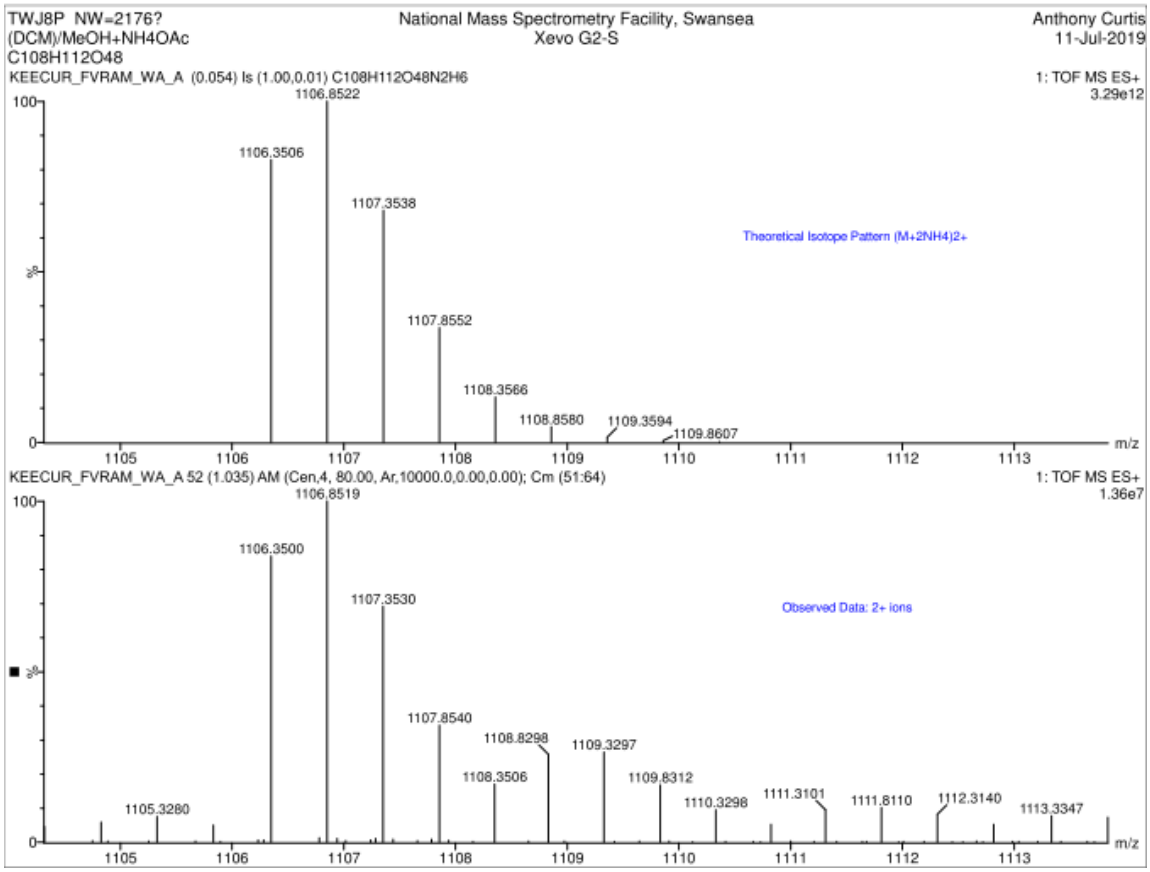

Appendix 2: Mass spectrum of **146**

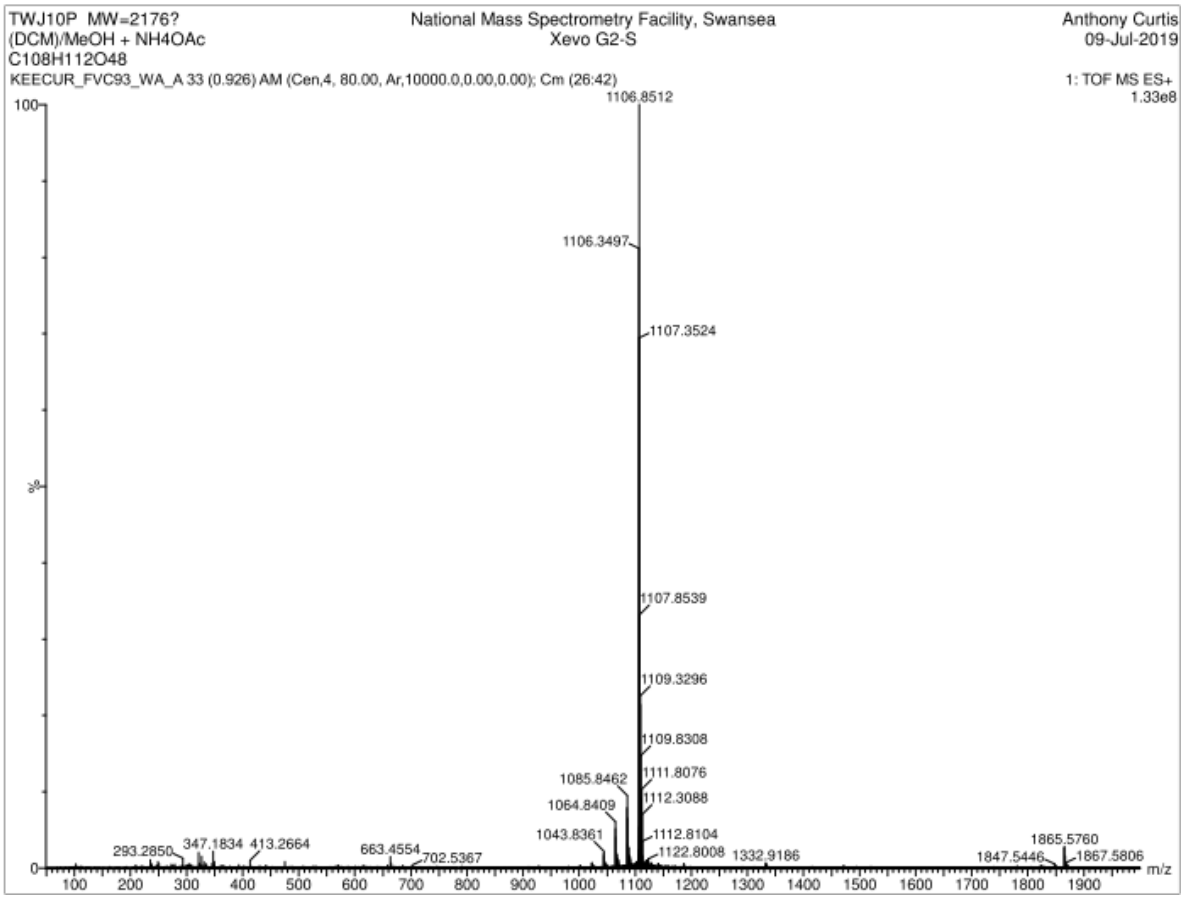
TWJ10P MW=2176?
(DCM)/MeOH + NH4OAc
C108H112O48
National Mass Spectrometry Facility, Swansea
Xevo G2-S
Anthony Curtis
09-Jul-2019
KEECUR_FVC93_WA_A 33 (0.926) AM (Cen,4, 80.00, Ar,10000.0,0.00,0.00); Cm (26:42)
1: TOF MS ES+
1.33e8
1106.8512
1106.3497
1107.3524
1107.8539
1109.3296
1109.8308
1111.8076
1085.8462
1112.3088
1064.8409
1112.8104
1043.8361
1122.8008
1332.9186
293.2850
347.1834
413.2664
663.4554
702.5367
1865.5760
1847.5446
1867.5806
%
m/z

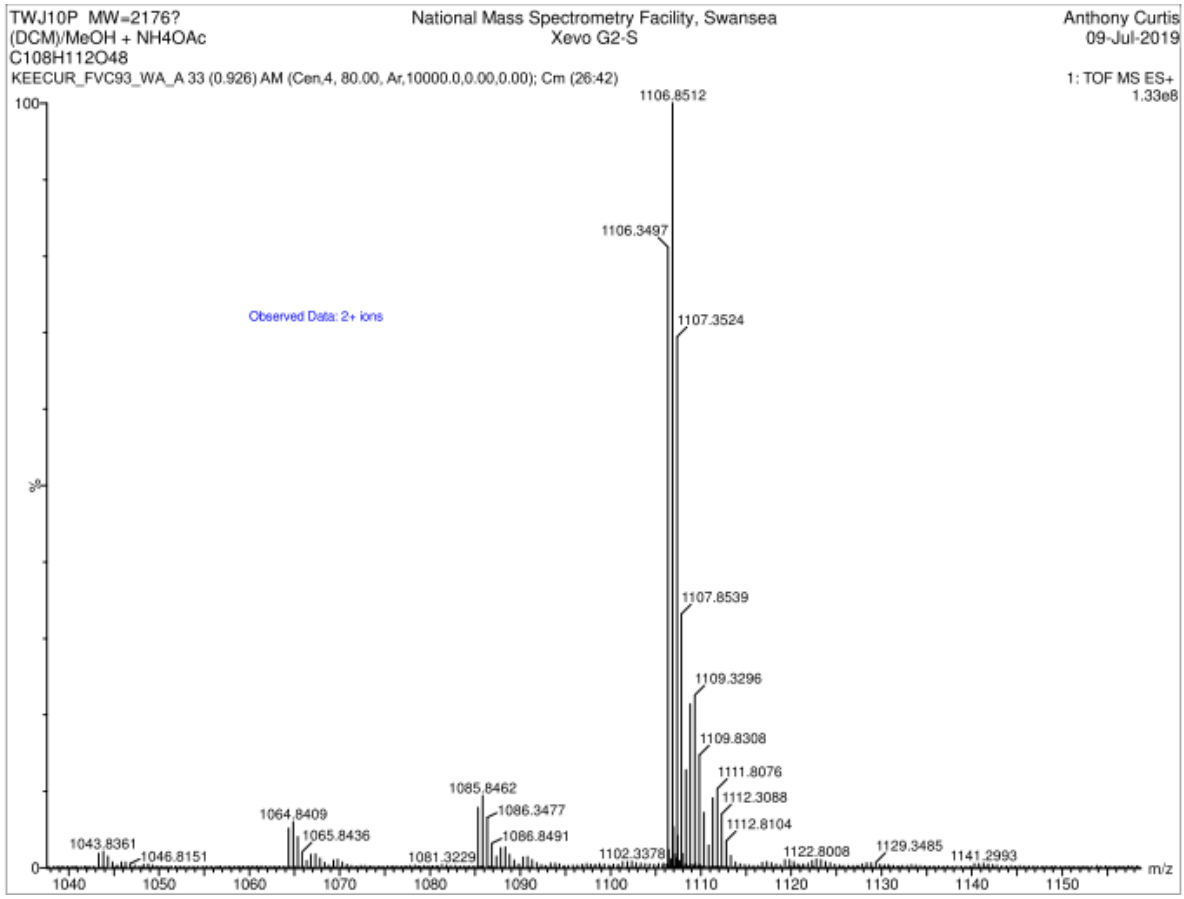
TWJ10P MW=2176?
(DCM)/MeOH + NH4OAc
C108H112O48
National Mass Spectrometry Facility, Swansea
Xevo G2-S
Anthony Curtis
09-Jul-2019
KEECUR_FVC93_WA_A 33 (0.926) AM (Cen,4, 80.00, Ar,10000.0,0.00,0.00); Cm (26:42)
1: TOF MS ES+
1.33e8
1106.8512
1106.3497
Obeserved Data: 2+ ions
1107.3524
1107.8539
1109.3296
1109.8308
1111.8076
1085.8462
1112.3088
1086.3477
1064.8409
1112.8104
1065.8436
1086.8491
1043.8361
1046.8151
1081.3229
1102.3378
1122.8008
1129.3485
1141.2993
%
m/z

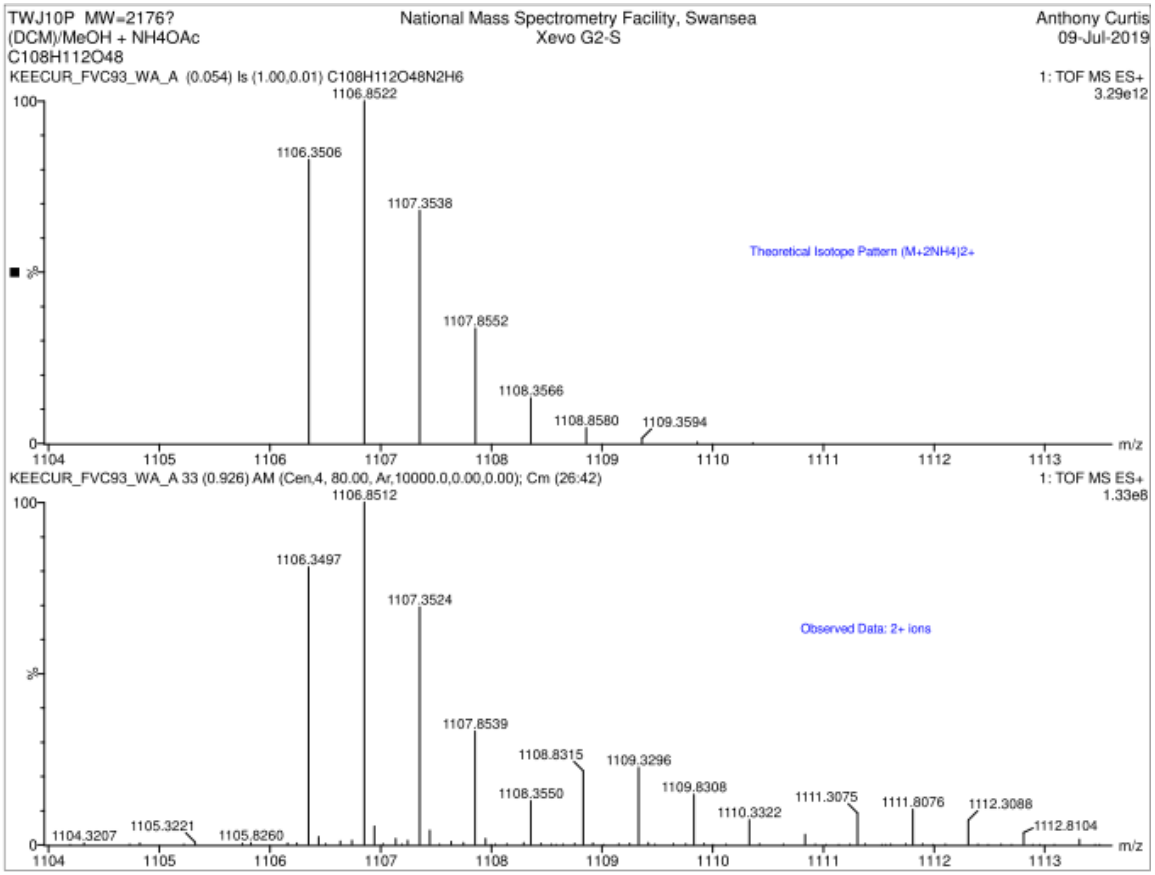

Appendix 3: Mass spectrum of **148**

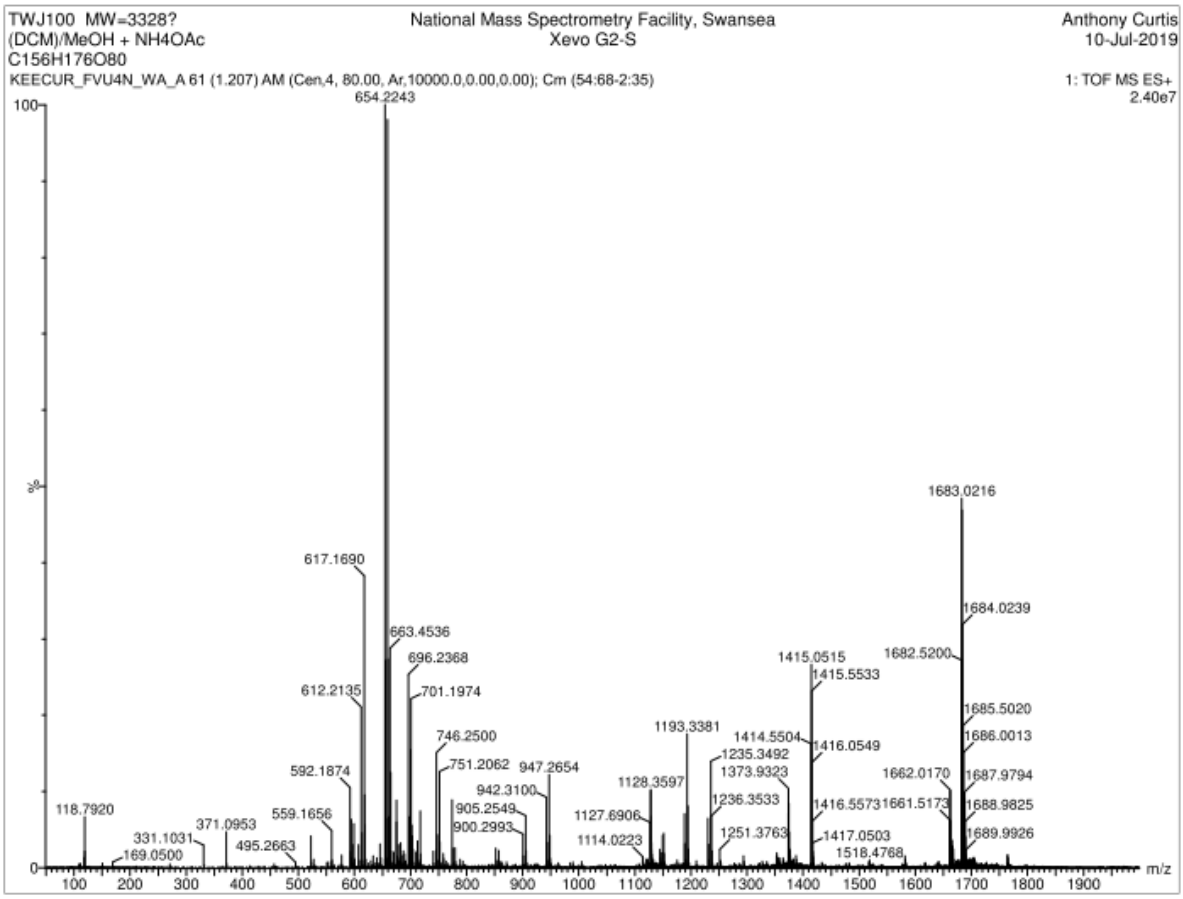
TWJ100 MW=3328?
(DCM)/MeOH + NH4OAc
C156H176O80
National Mass Spectrometry Facility, Swansea
Xevo G2-S
Anthony Curtis
10-Jul-2019
KEECUR_FVU4N_WA_A 61 (1.207) AM (Cen,4, 80.00, Ar,10000.0,0.00,0.00); Cm (54:68-2:35)
1: TOF MS ES+
2.40e7
654.2243
1683.0216
617.1690
1684.0239
663.4536
696.2368
1415.0515
1682.5200
1415.5533
612.2135
701.1974
1685.5020
1193.3381
1414.5504
746.2500
1686.0013
1416.0549
751.2062
947.2654
1235.3492
592.1874
1373.9323
1662.0170
1687.9794
1128.3597
942.3100
1236.3533
118.7920
559.1656
905.2549
1416.5573
1661.5173
1688.9825
371.0953
1127.6906
900.2993
1251.3763
331.1031
1417.0503
1689.9926
495.2663
1114.0223
169.0500
1518.4768
m/z

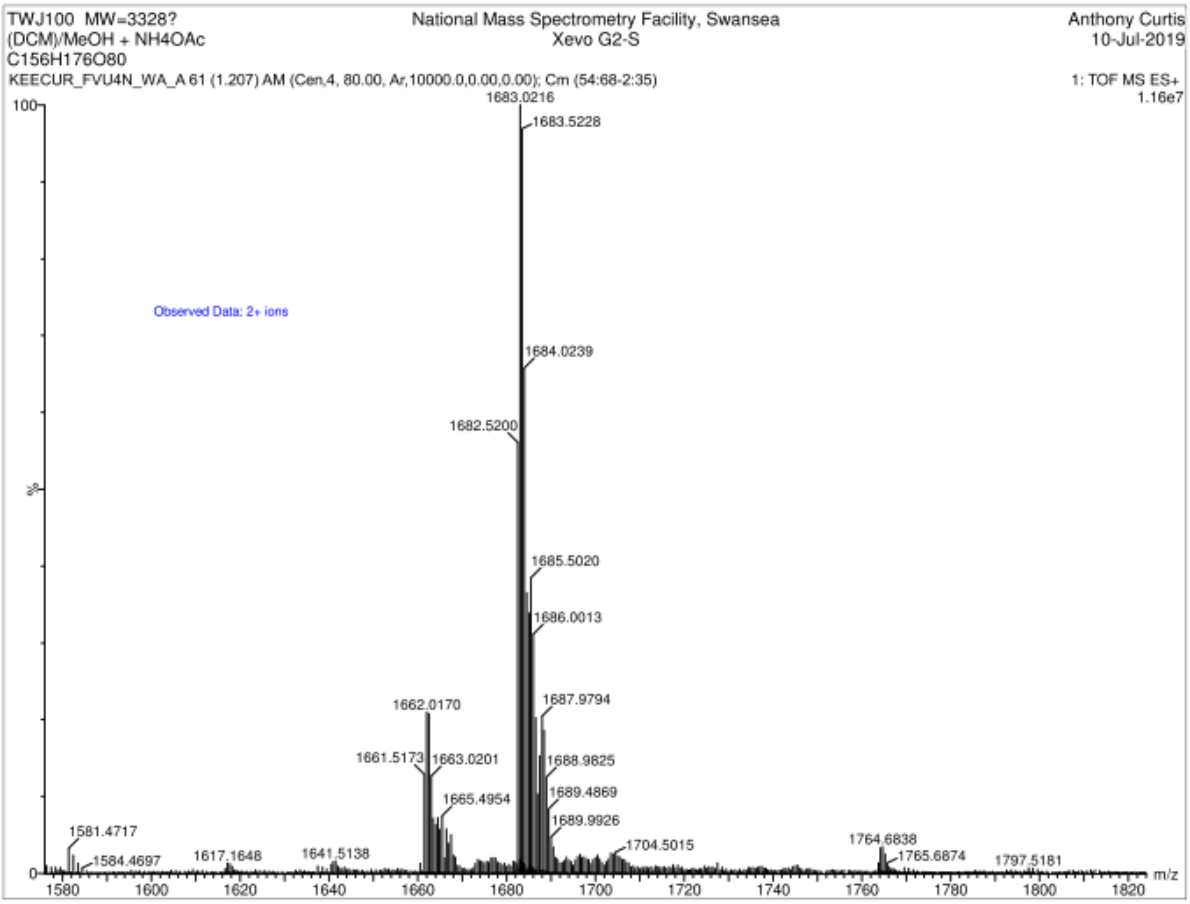
TWJ100 MW=3328?
(DCM)/MeOH + NH4OAc
C156H176O80
National Mass Spectrometry Facility, Swansea
Xevo G2-S
Anthony Curtis
10-Jul-2019
KEECUR_FVU4N_WA_A 61 (1.207) AM (Cen,4, 80.00, Ar,10000.0,0.00,0.00); Cm (54:68-2:35)
1: TOF MS ES+
1.16e7
1683.0216
1683.5228
Observed Data: 2+ ions
1684.0239
1682.5200
1685.5020
1686.0013
1662.0170
1687.9794
1661.5173
1663.0201
1688.9825
1665.4954
1689.4869
1581.4717
1689.9926
1704.5015
1764.6838
1584.4697
1617.1648
1641.5138
1765.6874
1797.5181
m/z

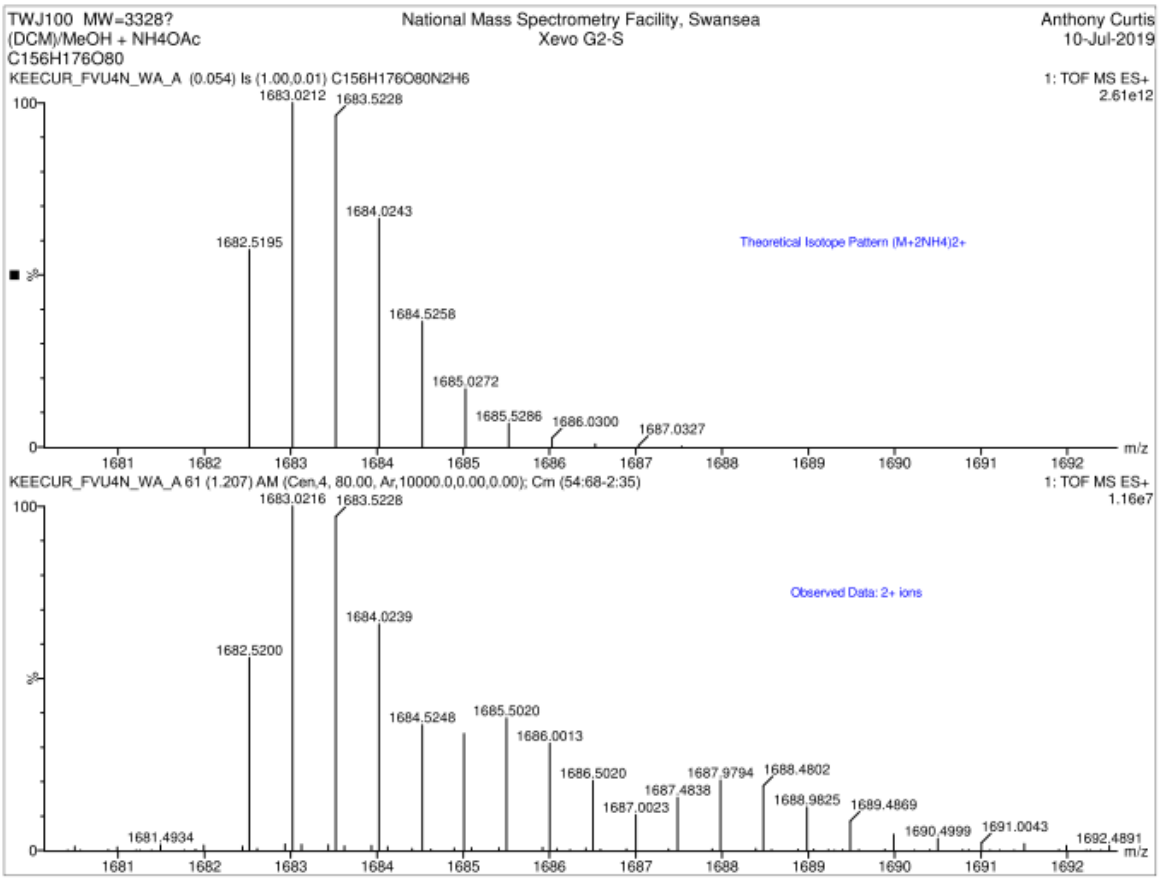

Appendix 4: Mass spectrum of **163**

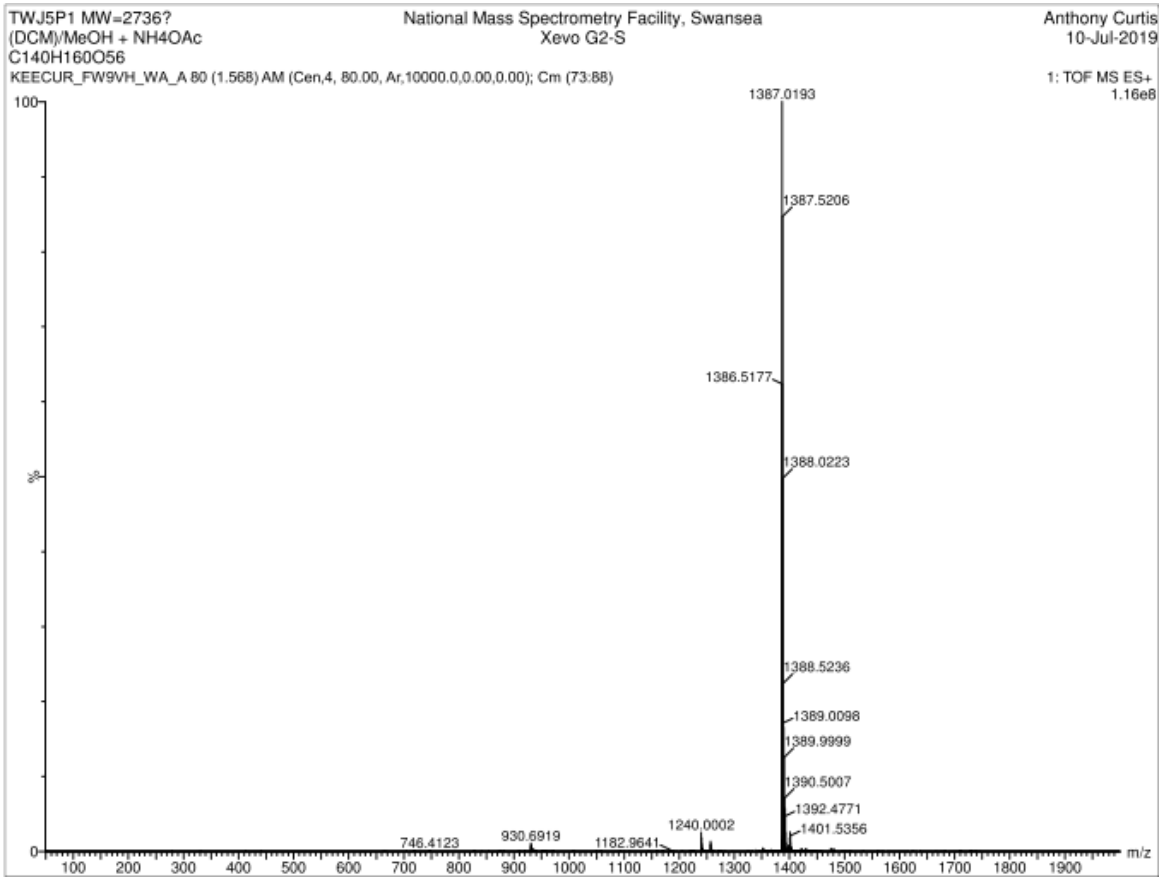
TWJ5P1 MW=2736?
(DCM)/MeOH + NH4OAc
C140H160O56
National Mass Spectrometry Facility, Swansea
Xevo G2-S
Anthony Curtis
10-Jul-2019
KEECUR_FW9VH_WA_A 80 (1.568) AM (Cen,4, 80.00, Ar,10000.0,0.00,0.00); Cm (73:88)
1: TOF MS ES+
1.16e8
1387.0193
1387.5206
1386.5177
1388.0223
1388.5236
1389.0098
1389.9999
1390.5007
1392.4771
1401.5356
1240.0002
746.4123
930.6919
1182.9641
%
m/z

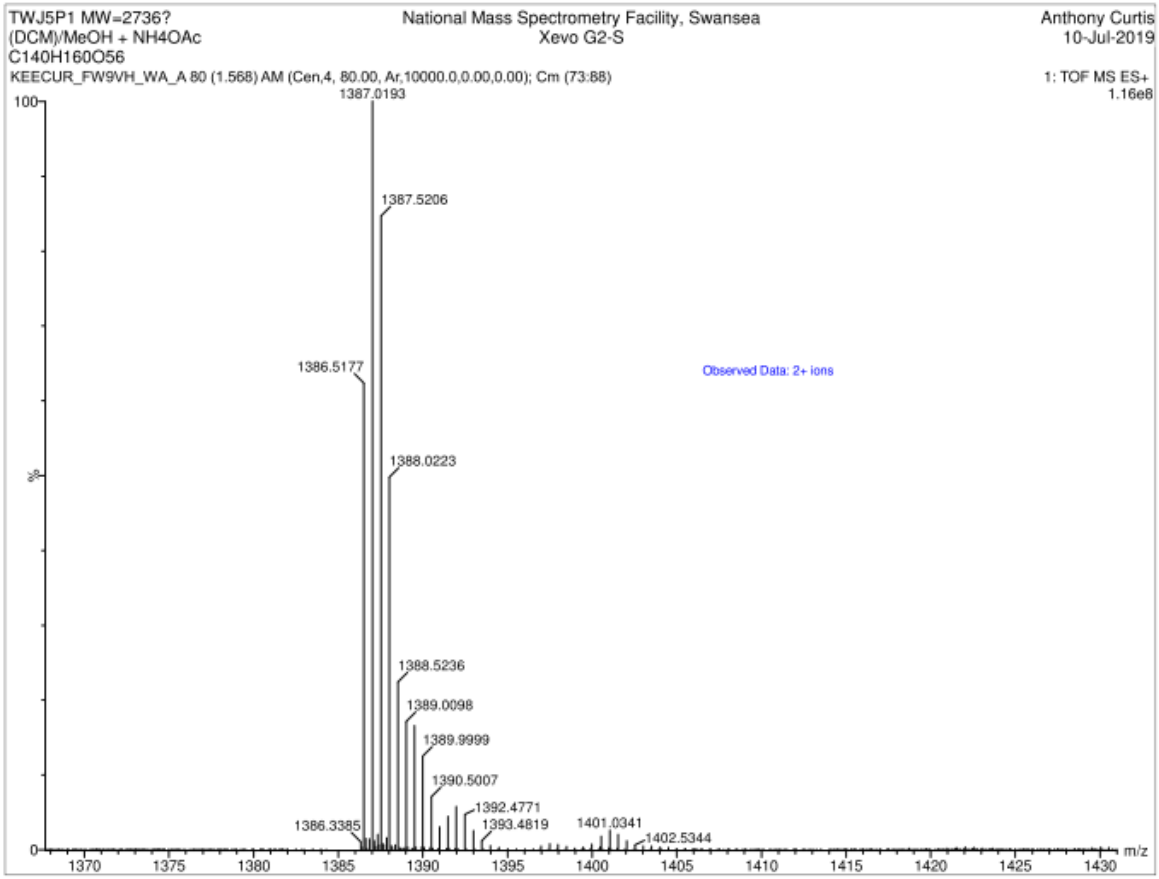
TWJ5P1 MW=2736?
(DCM)/MeOH + NH4OAc
C140H160O56
National Mass Spectrometry Facility, Swansea
Xevo G2-S
Anthony Curtis
10-Jul-2019
KEECUR_FW9VH_WA_A 80 (1.568) AM (Cen,4, 80.00, Ar,10000.0,0.00,0.00); Cm (73:88)
1: TOF MS ES+
1.16e8
1387.0193
1387.5206
1386.5177
Observed Data: 2+ ions
1388.0223
1388.5236
1389.0098
1389.9999
1390.5007
1392.4771
1393.4819
1401.0341
1402.5344
1386.3385
%
m/z

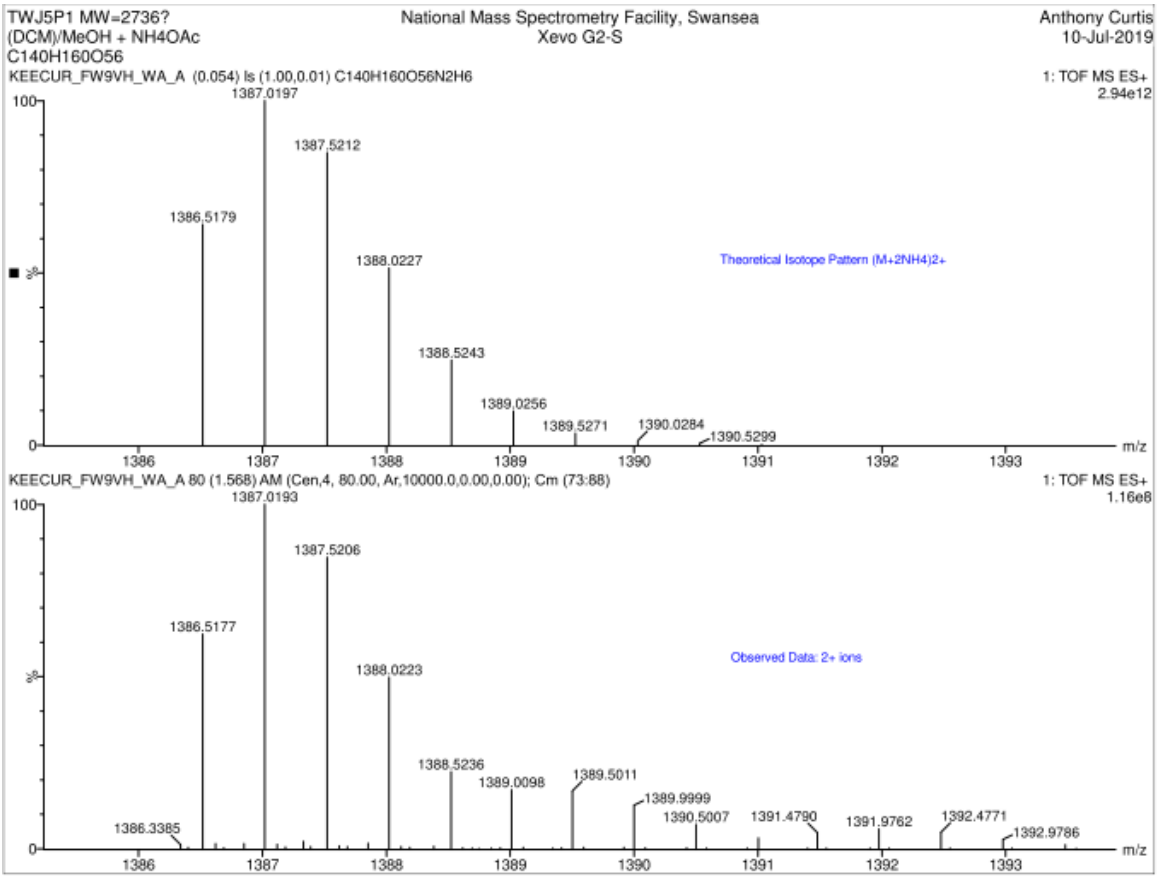

Appendix 5: Mass spectrum of **137a**

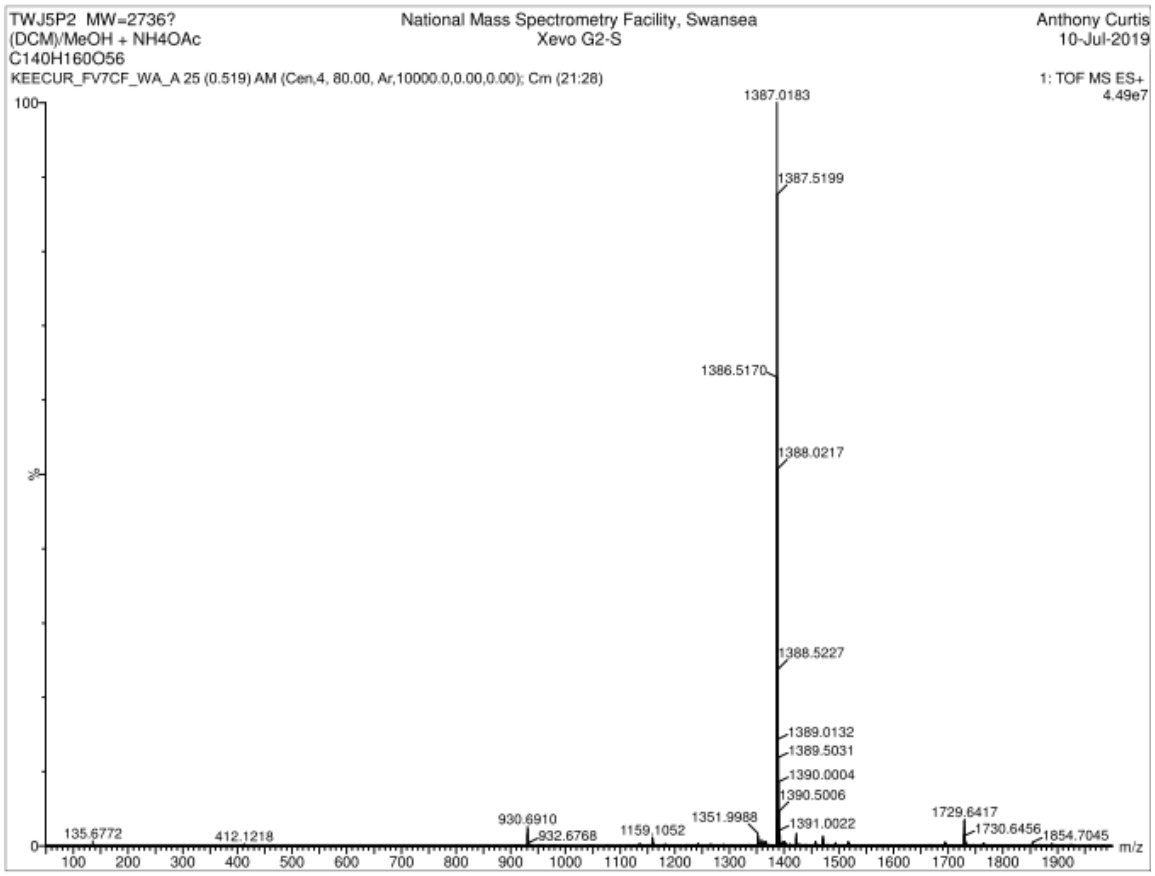
TWJ5P2 MW=2736?
(DCM)/MeOH + NH4OAc
C140H160O56
National Mass Spectrometry Facility, Swansea
Xevo G2-S
Anthony Curtis
10-Jul-2019
KEECUR_FV7CF_WA_A 25 (0.519) AM (Cen,4, 80.00, Ar,10000.0,0.00,0.00); Cm (21:28)
1: TOF MS ES+
4.49e7
1387.0183
1387.5199
1386.5170
1388.0217
1388.5227
1389.0132
1389.5031
1390.0004
1390.5006
1391.0022
1729.6417
1730.6456
1854.7045
930.6910
932.6768
1159.1052
1351.9988
135.6772
412.1218
%
m/z

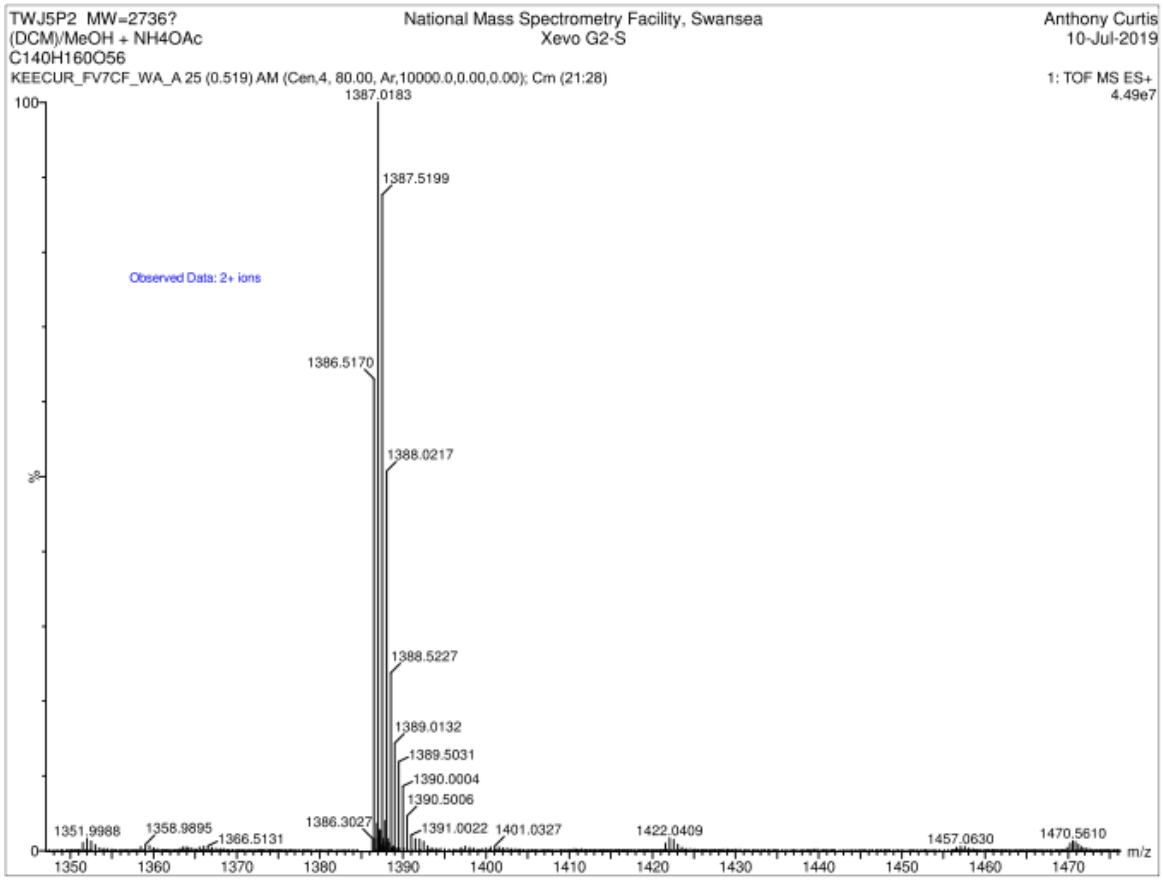
TWJ5P2 MW=2736?
(DCM)/MeOH + NH4OAc
C140H160O56
National Mass Spectrometry Facility, Swansea
Xevo G2-S
Anthony Curtis
10-Jul-2019
KEECUR_FV7CF_WA_A 25 (0.519) AM (Cen,4, 80.00, Ar,10000.0,0.00,0.00); Cm (21:28)
1: TOF MS ES+
4.49e7
Observed Data: 2+ ions
1387.0183
1387.5199
1386.5170
1388.0217
1388.5227
1389.0132
1389.5031
1390.0004
1390.5006
1391.0022
1386.3027
1351.9988
1358.9895
1366.5131
1401.0327
1422.0409
1457.0630
1470.5610
%
m/z

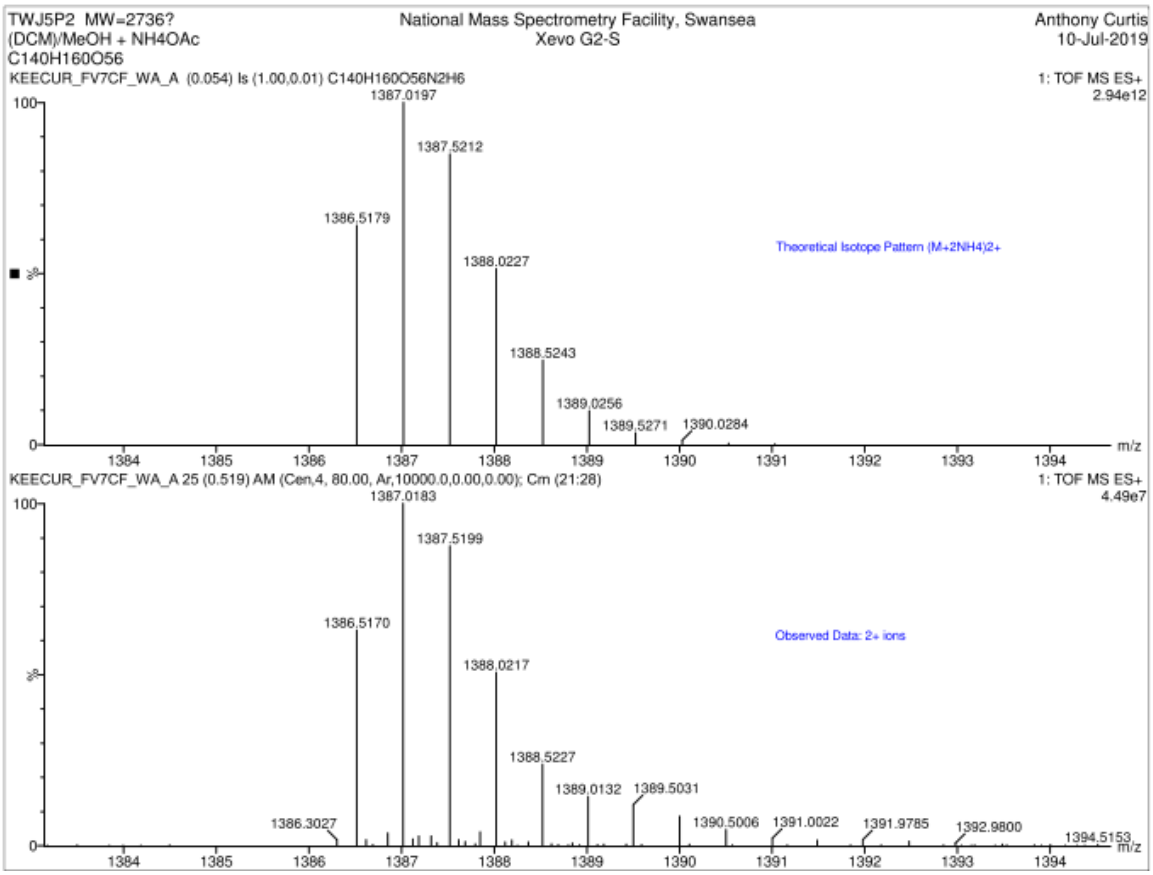

Appendix 6: Mass spectrum of **137b**

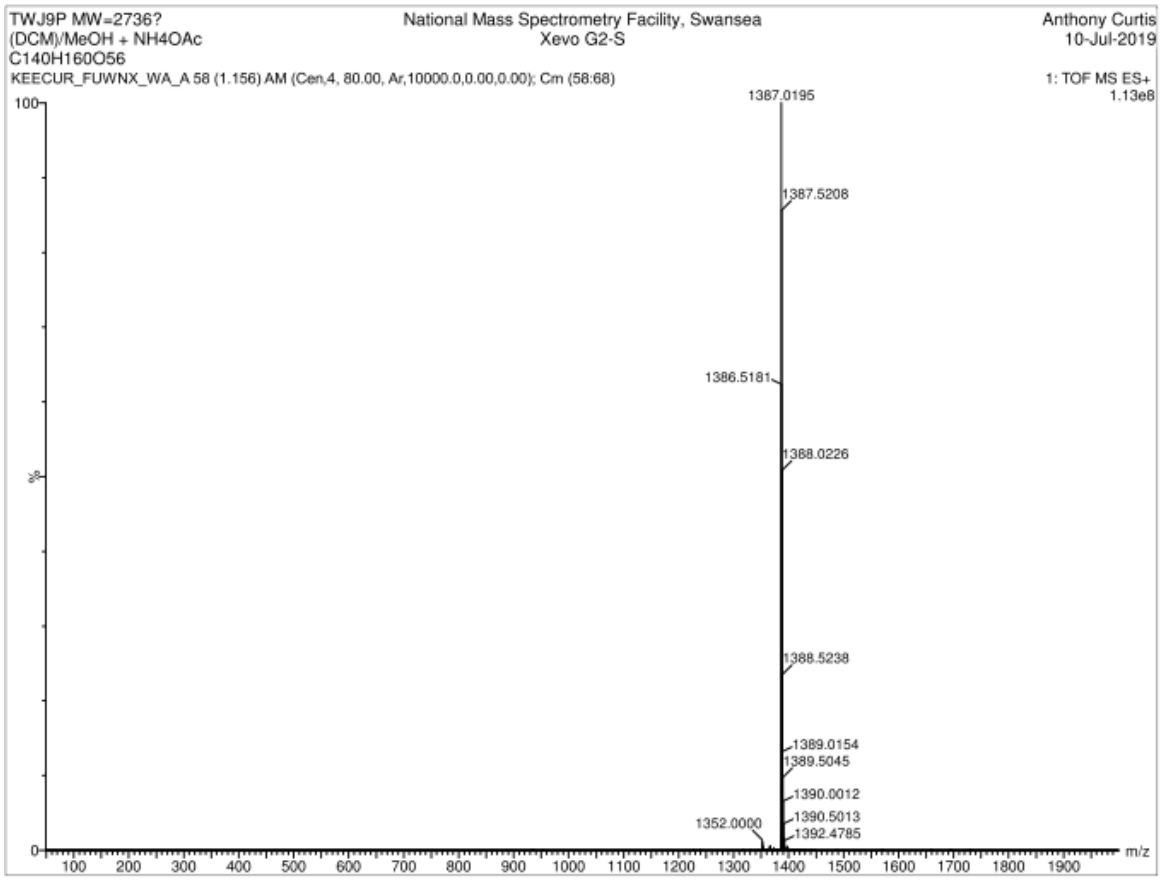
TWJ9P MW=2736?
(DCM)/MeOH + NH4OAc
C140H160O56
National Mass Spectrometry Facility, Swansea
Xevo G2-S
Anthony Curtis
10-Jul-2019
KEECUR_FUWNX_WA_A 58 (1.156) AM (Cen,4, 80.00, Ar,10000.0,0.00,0.00); Cm (58:68)
1: TOF MS ES+
1.13e8
1387.0195
1387.5208
1386.5181
1388.0226
1388.5238
1389.0154
1389.5045
1390.0012
1390.5013
1392.4785
1352.0000
%
m/z

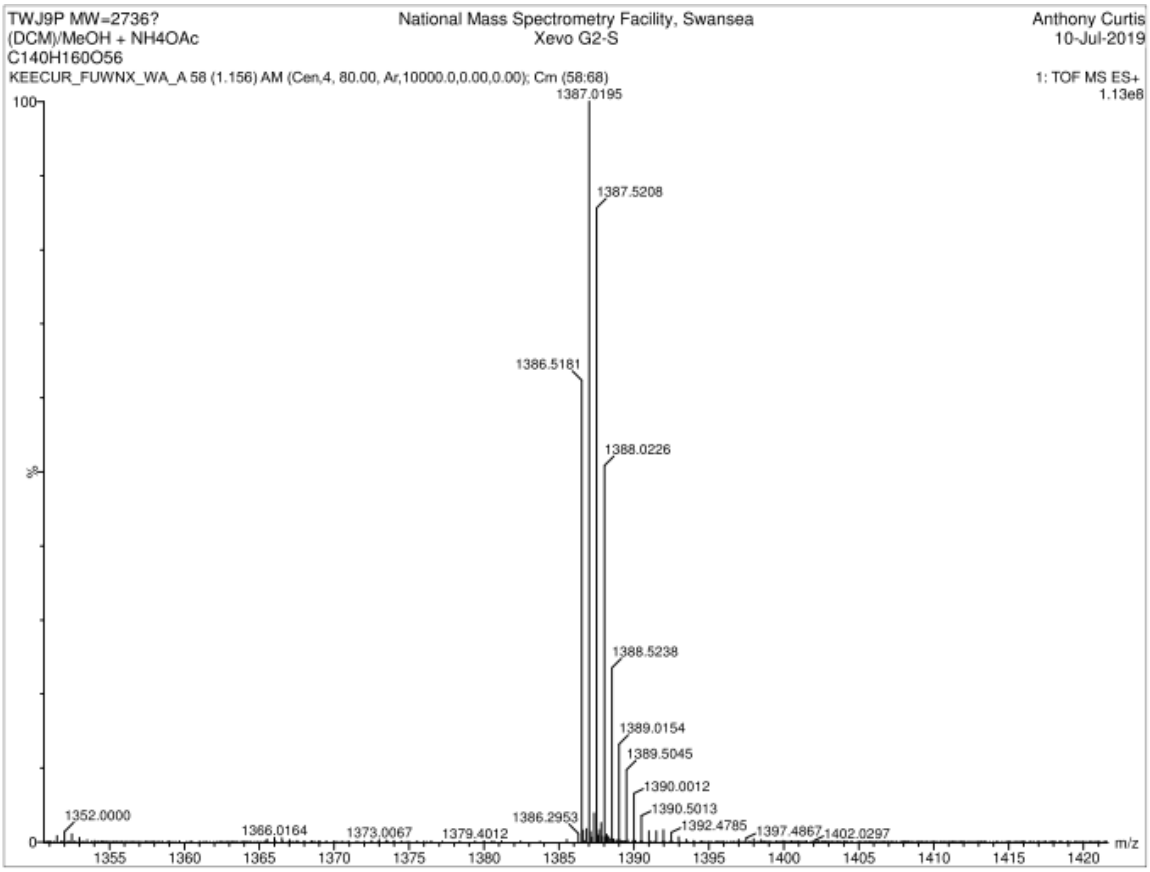
TWJ9P MW=2736?
(DCM)/MeOH + NH4OAc
C140H160O56
National Mass Spectrometry Facility, Swansea
Xevo G2-S
Anthony Curtis
10-Jul-2019
KEECUR_FUWNX_WA_A 58 (1.156) AM (Cen,4, 80.00, Ar,10000.0,0.00,0.00); Cm (58:68)
1: TOF MS ES+
1.13e8
1387.0195
1387.5208
1386.5181
1388.0226
1388.5238
1389.0154
1389.5045
1390.0012
1390.5013
1392.4785
1352.0000
1366.0164
1373.0067
1379.4012
1386.2953
1397.4867
1402.0297
%
m/z

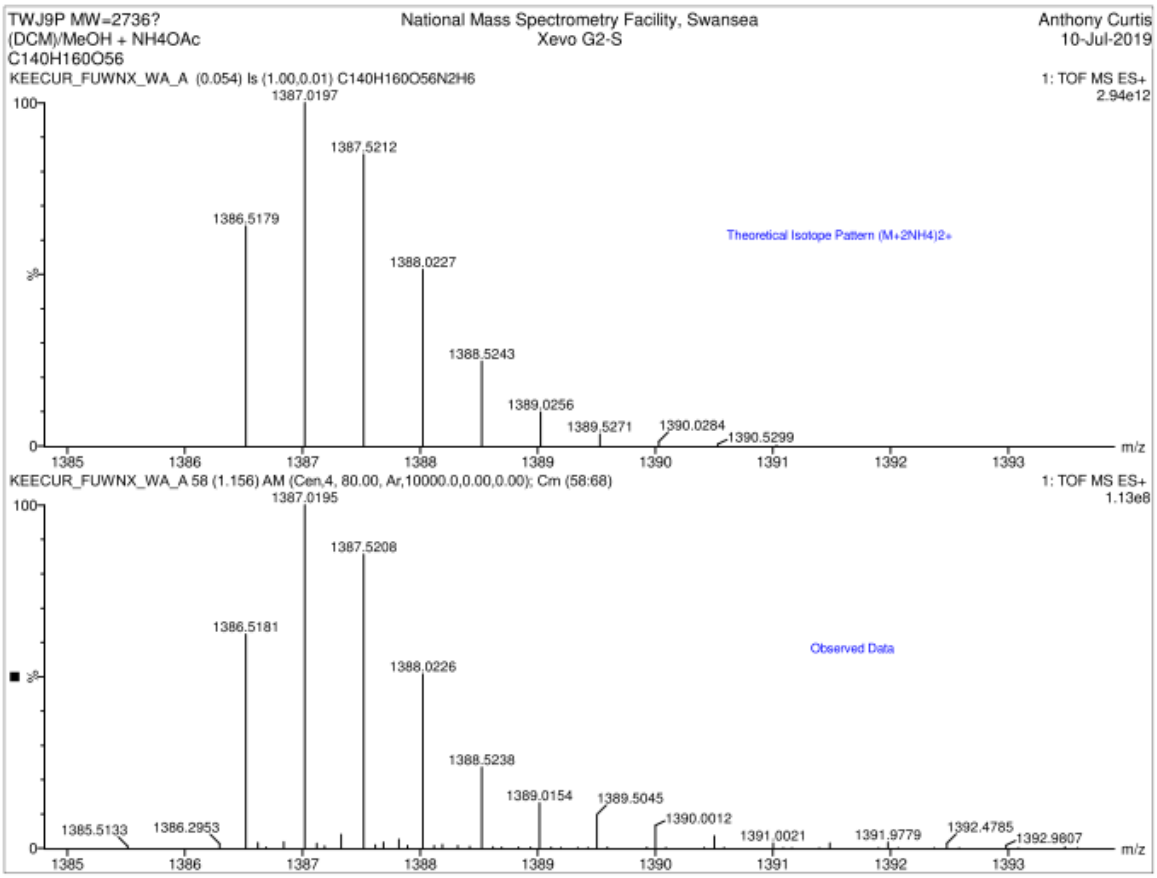

Appendix 7: Mass spectrum of **147**

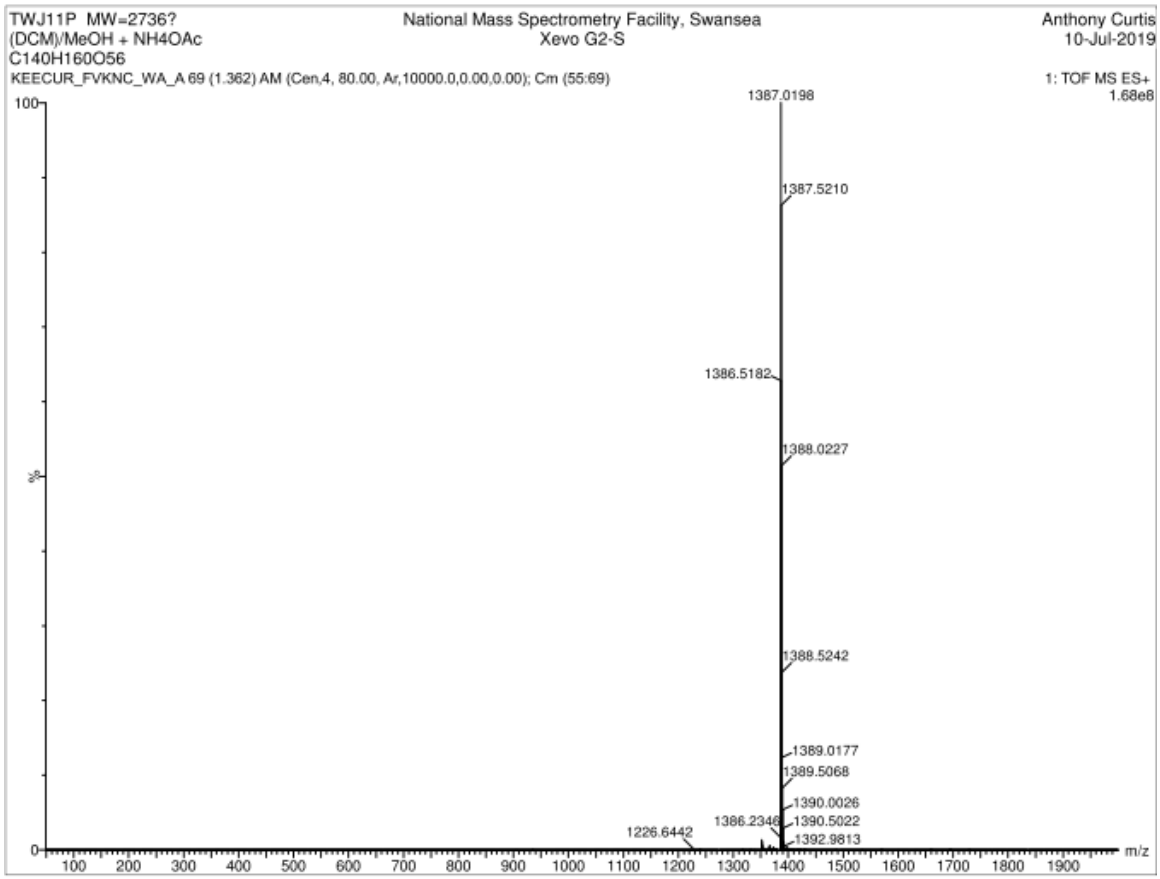
TWJ11P MW=2736?
(DCM)/MeOH + NH4OAc
C140H160O56
National Mass Spectrometry Facility, Swansea
Xevo G2-S
Anthony Curtis
10-Jul-2019
KEECUR_FVKNC_WA_A 69 (1.362) AM (Cen,4, 80.00, Ar,10000.0,0.00,0.00); Cm (55:69)
1: TOF MS ES+
1.68e8
1387.0198
1387.5210
1386.5182
1388.0227
1388.5242
1389.0177
1389.5068
1390.0026
1386.2346
1390.5022
1392.9813
1226.6442
%
m/z

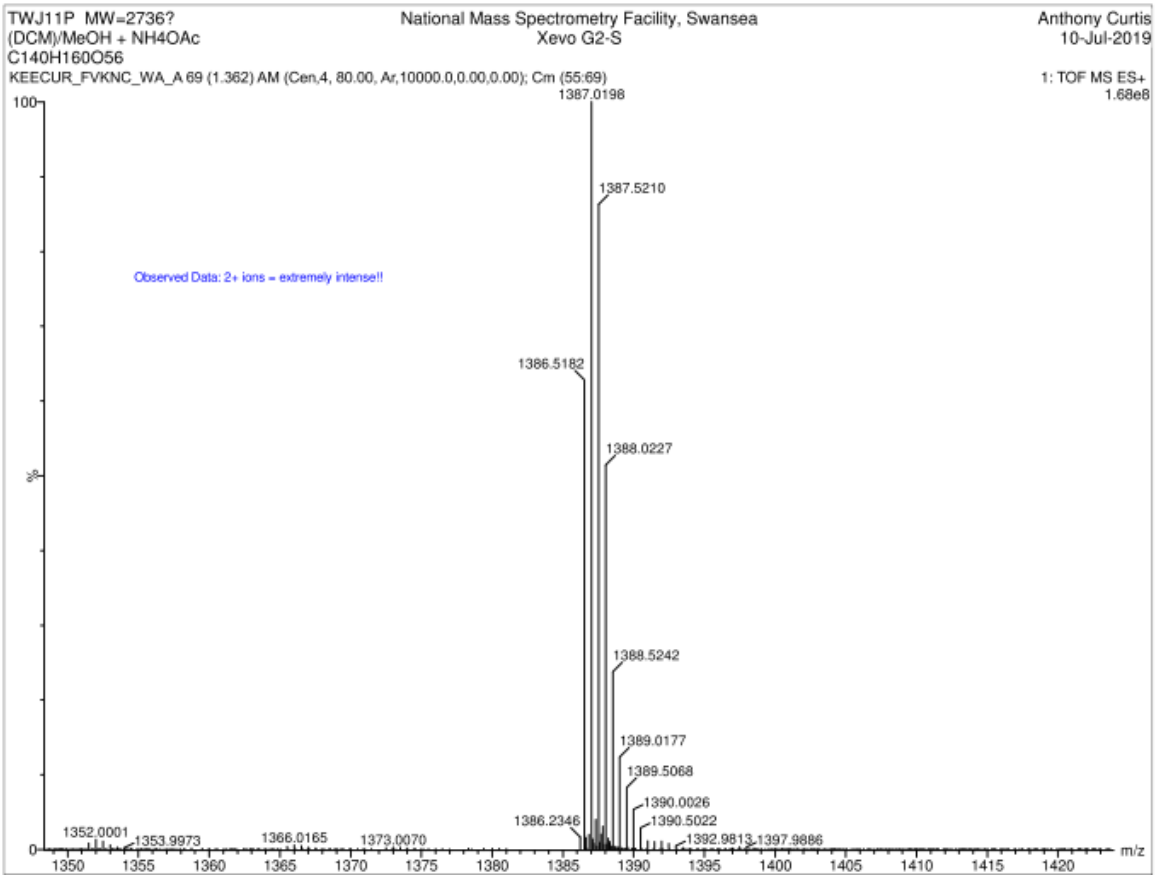
TWJ11P MW=2736?
(DCM)/MeOH + NH4OAc
C140H160O56
National Mass Spectrometry Facility, Swansea
Xevo G2-S
Anthony Curtis
10-Jul-2019
KEECUR_FVKNC_WA_A 69 (1.362) AM (Cen,4, 80.00, Ar,10000.0,0.00,0.00); Cm (55:69)
1: TOF MS ES+
1.68e8
Observed Data: 2+ ions = extremely intense!!
1387.0198
1387.5210
1386.5182
1388.0227
1388.5242
1389.0177
1389.5068
1390.0026
1386.2346
1390.5022
1392.9813
1397.9886
1352.0001
1353.9973
1366.0165
1373.0070
%
m/z

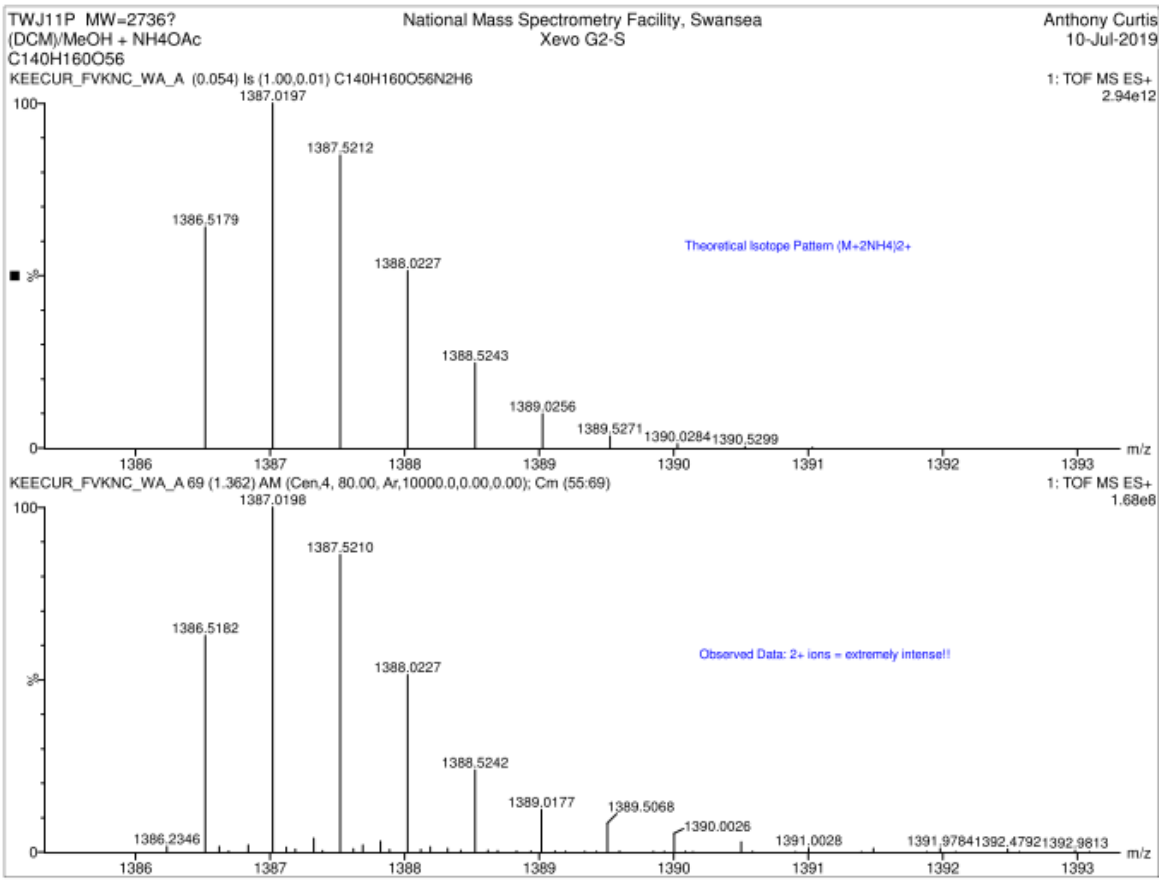

Appendix 8: Mass spectrum of **149**

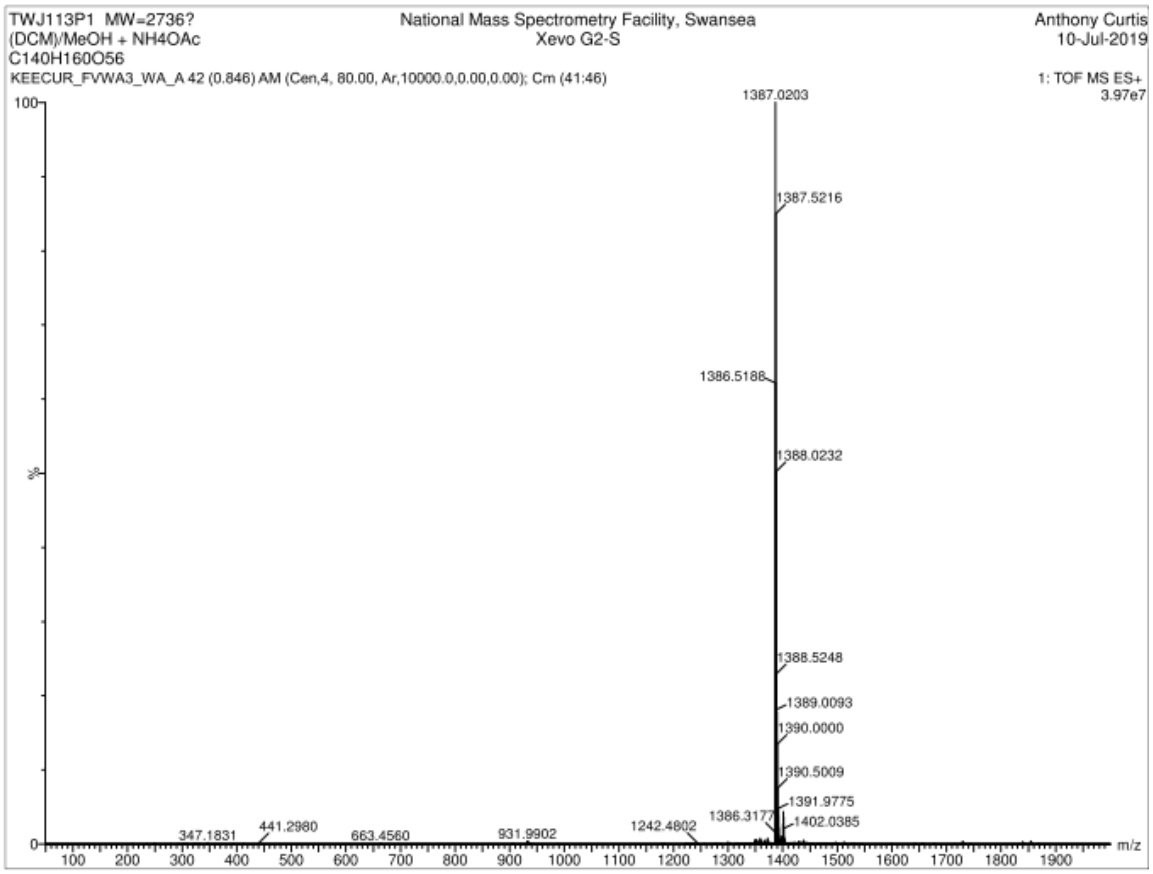
TWJ113P1 MW=2736?
(DCM)/MeOH + NH4OAc
C140H160O56
National Mass Spectrometry Facility, Swansea
Xevo G2-S
Anthony Curtis
10-Jul-2019
KEECUR_FVWA3_WA_A 42 (0.846) AM (Cen,4, 80.00, Ar,10000.0,0.00,0.00); Cm (41:46)
1: TOF MS ES+
3.97e7
1387.0203
1387.5216
1386.5188
1388.0232
1388.5248
1389.0093
1390.0000
1390.5009
1391.9775
1386.3177
1402.0385
347.1831
441.2980
663.4560
931.9902
1242.4802
%
m/z

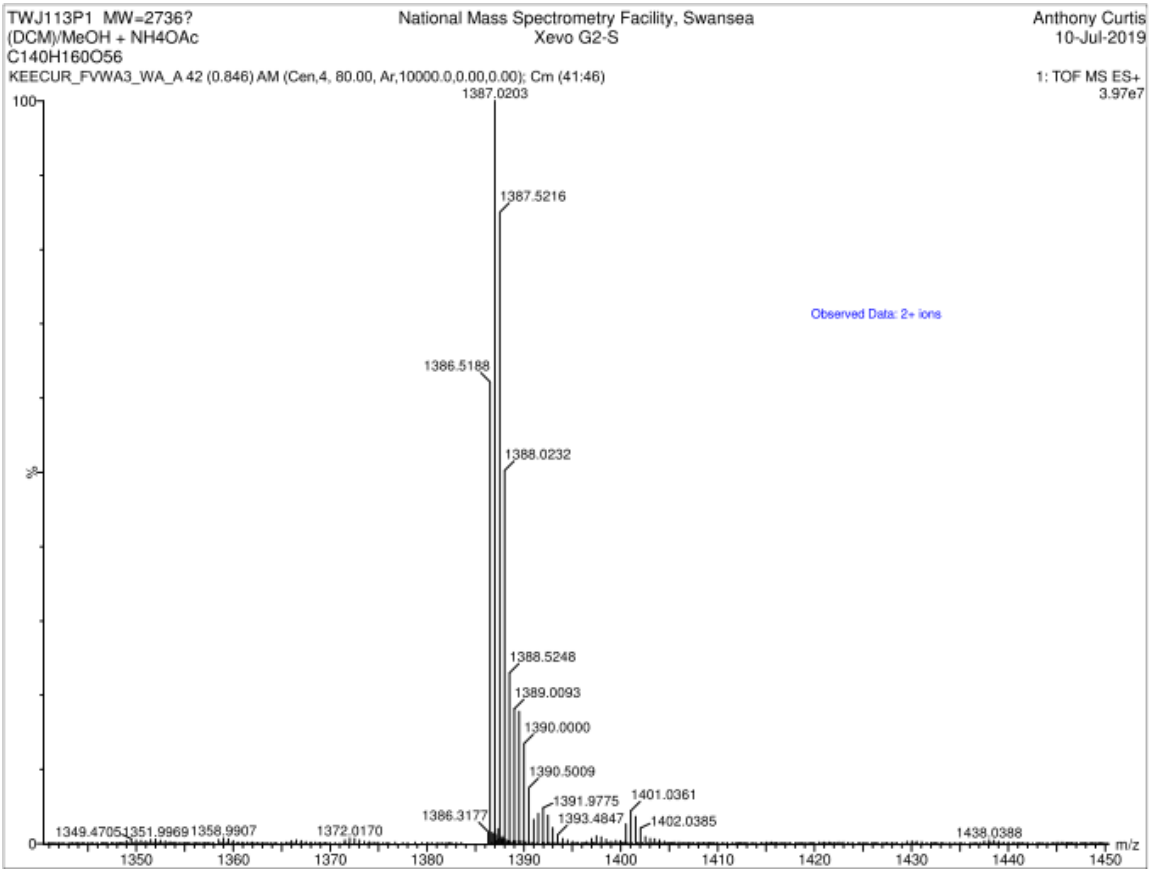
TWJ113P1 MW=2736?
(DCM)/MeOH + NH4OAc
C140H160O56
National Mass Spectrometry Facility, Swansea
Xevo G2-S
Anthony Curtis
10-Jul-2019
KEECUR_FVWA3_WA_A 42 (0.846) AM (Cen,4, 80.00, Ar,10000.0,0.00,0.00); Cm (41:46)
1: TOF MS ES+
3.97e7
Observed Data: 2+ ions
1387.0203
1387.5216
1386.5188
1388.0232
1388.5248
1389.0093
1390.0000
1390.5009
1391.9775
1401.0361
1386.3177
1393.4847
1402.0385
1349.4705
1351.9969
1358.9907
1372.0170
1438.0388
%
m/z

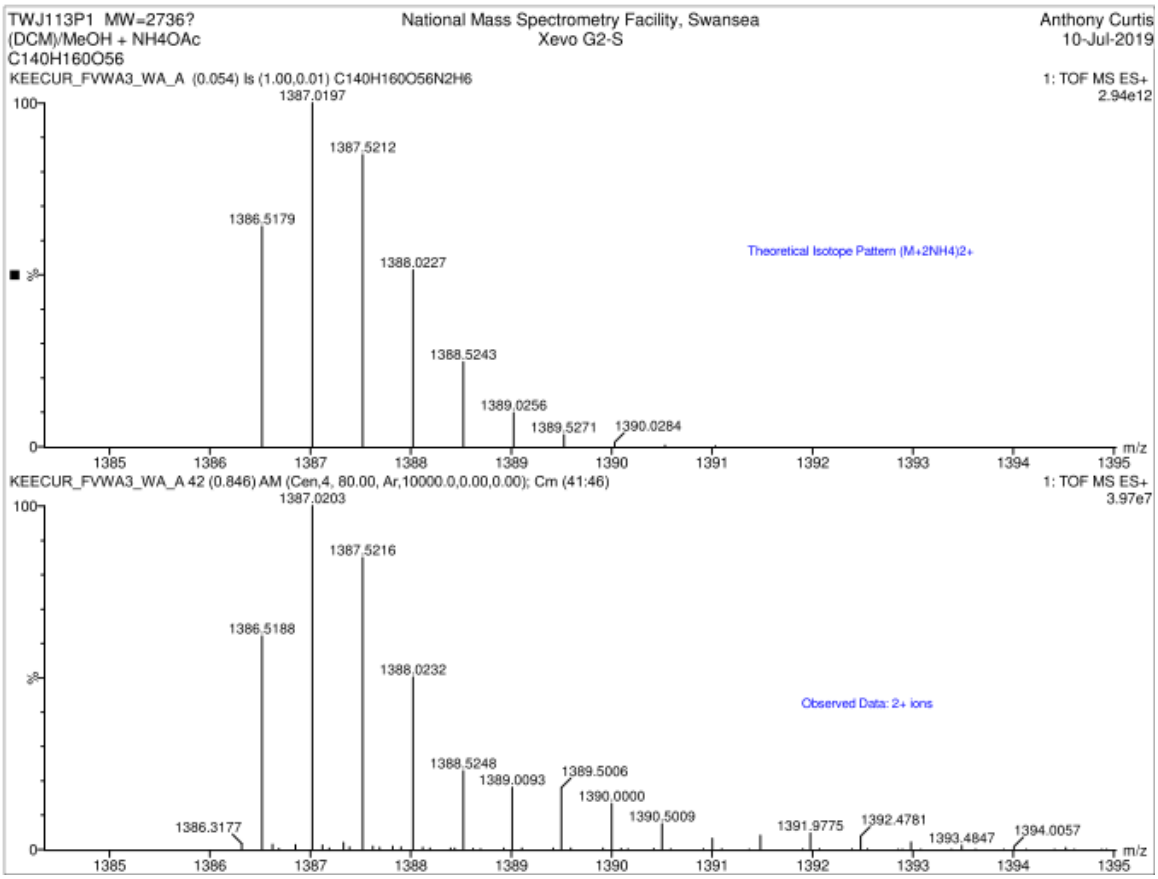

Appendix 9: Mass spectrum of **154a**

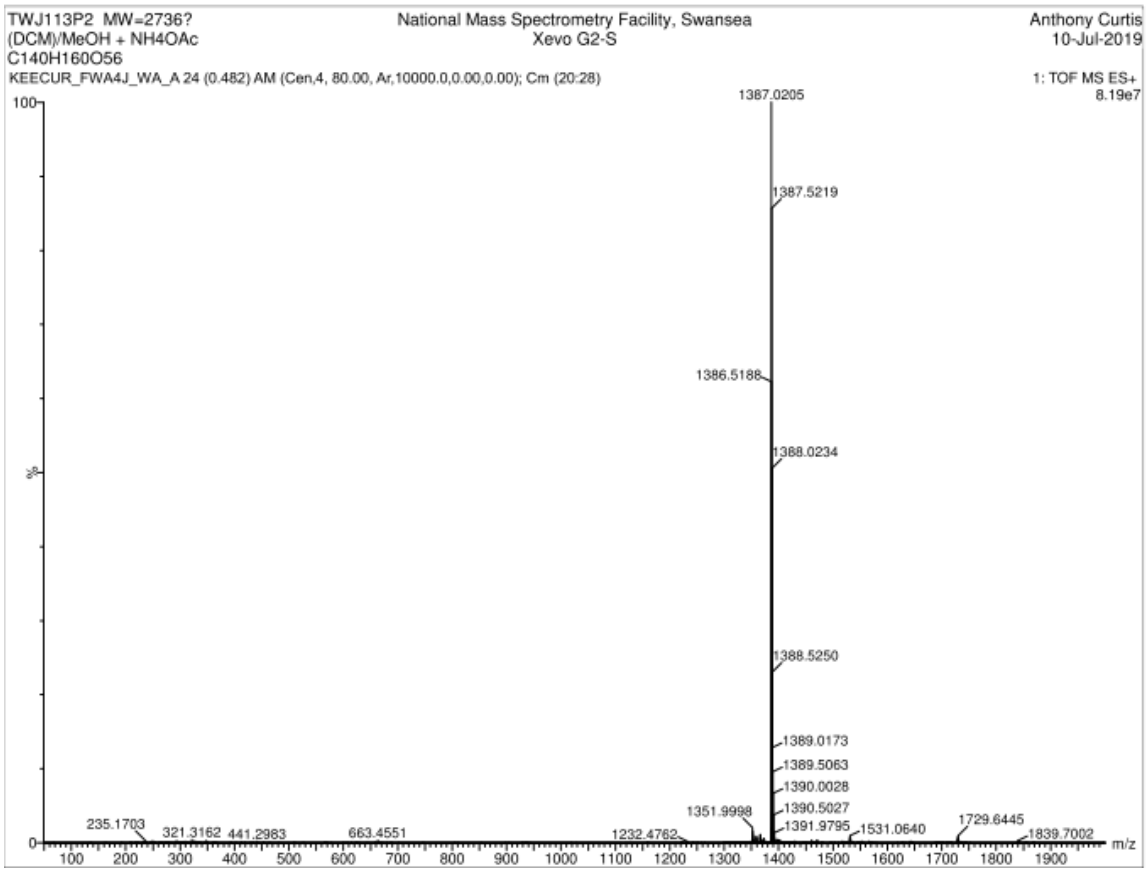
TWJ113P2 MW=2736?
(DCM)/MeOH + NH4OAc
C140H160O56
National Mass Spectrometry Facility, Swansea
Xevo G2-S
Anthony Curtis
10-Jul-2019
KEECUR_FWA4J_WA_A 24 (0.482) AM (Cen,4, 80.00, Ar,10000.0,0.00,0.00); Cm (20:28)
1: TOF MS ES+
8.19e7
1387.0205
1387.5219
1386.5188
1388.0234
1388.5250
1389.0173
1389.5063
1390.0028
1390.5027
1391.9795
1351.9998
1531.0640
1729.6445
1839.7002
1232.4762
235.1703
321.3162
441.2983
663.4551
%
m/z

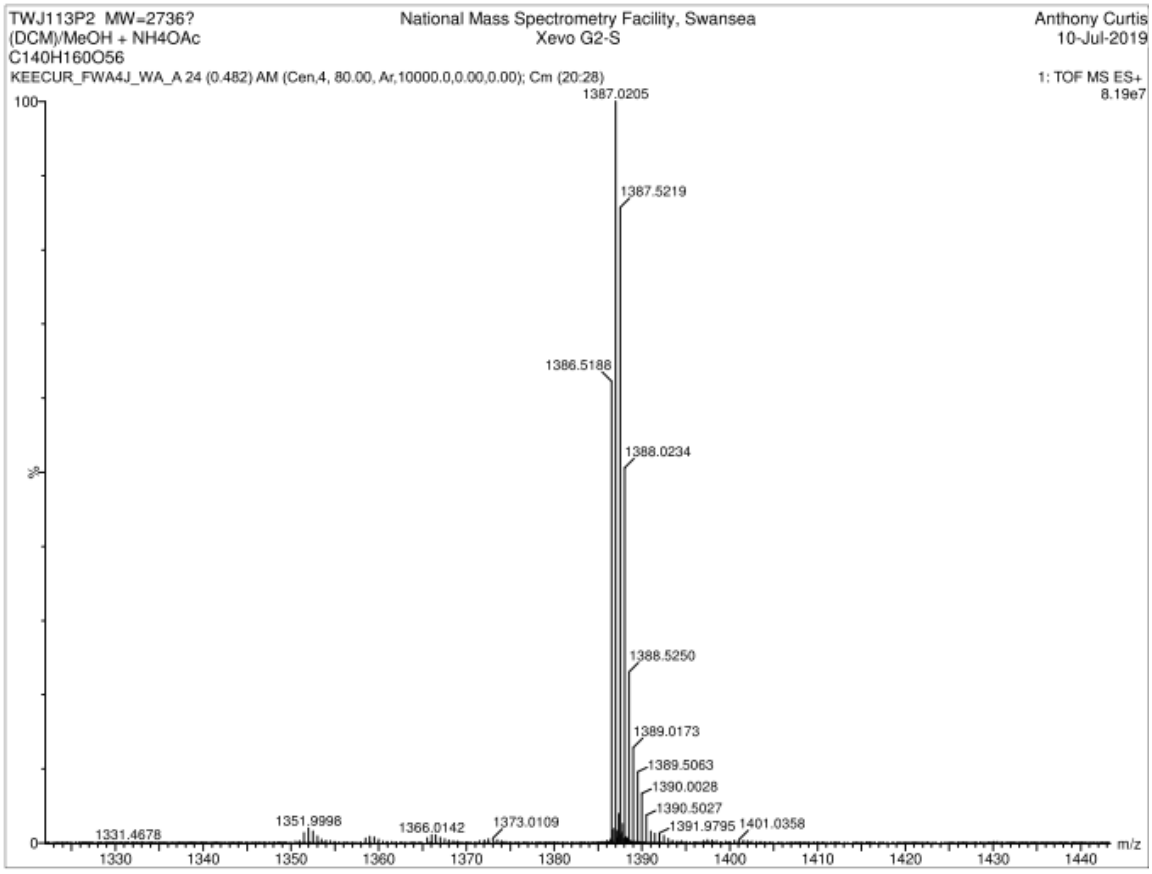
TWJ113P2 MW=2736?
(DCM)/MeOH + NH4OAc
C140H160O56
National Mass Spectrometry Facility, Swansea
Xevo G2-S
Anthony Curtis
10-Jul-2019
KEECUR_FWA4J_WA_A 24 (0.482) AM (Cen,4, 80.00, Ar,10000.0,0.00,0.00); Cm (20:28)
1: TOF MS ES+
8.19e7
1387.0205
1387.5219
1386.5188
1388.0234
1388.5250
1389.0173
1389.5063
1390.0028
1390.5027
1391.9795
1401.0358
1351.9998
1366.0142
1373.0109
1331.4678
%
m/z

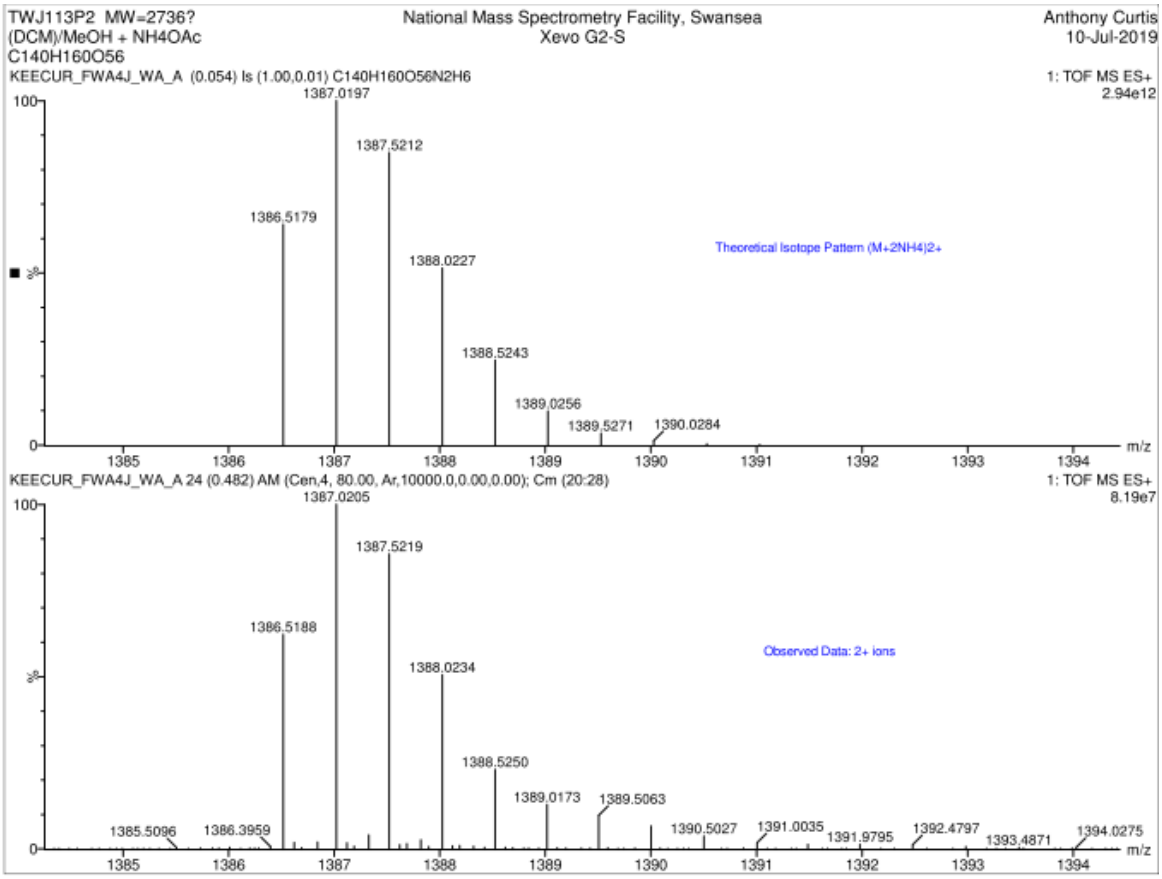

Appendix 10: Mass spectrum of **154b**

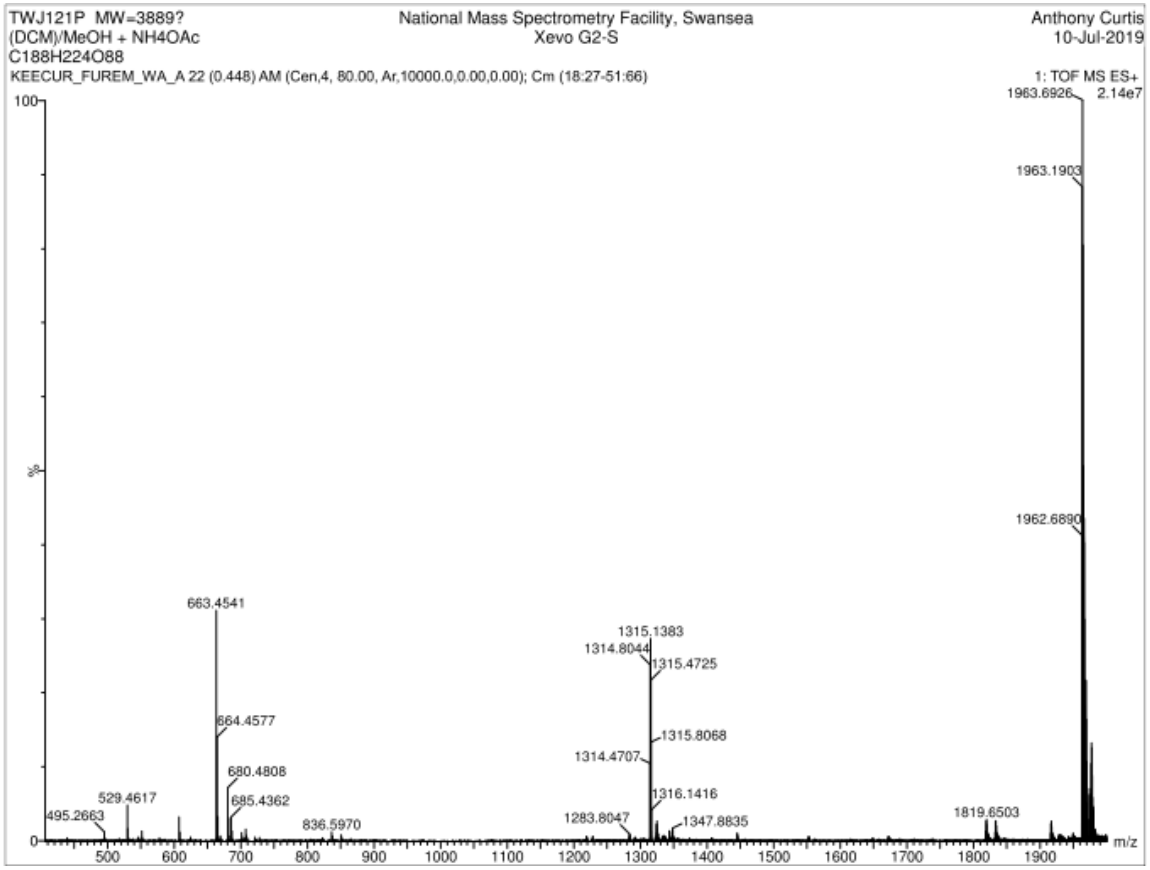
TWJ121P MW=3889?
(DCM)/MeOH + NH4OAc
C188H224O88
National Mass Spectrometry Facility, Swansea
Xevo G2-S
Anthony Curtis
10-Jul-2019
KEECUR_FUREM_WA_A 22 (0.448) AM (Cen,4, 80.00, Ar,10000.0,0.00,0.00); Cm (18:27-51:66)
1: TOF MS ES+
2.14e7
1963.6926
1963.1903
1962.6890
663.4541
1315.1383
1314.8044
1315.4725
664.4577
1315.8068
1314.4707
680.4808
1316.1416
529.4617
685.4362
495.2663
836.5970
1283.8047
1347.8835
1819.6503
%
m/z

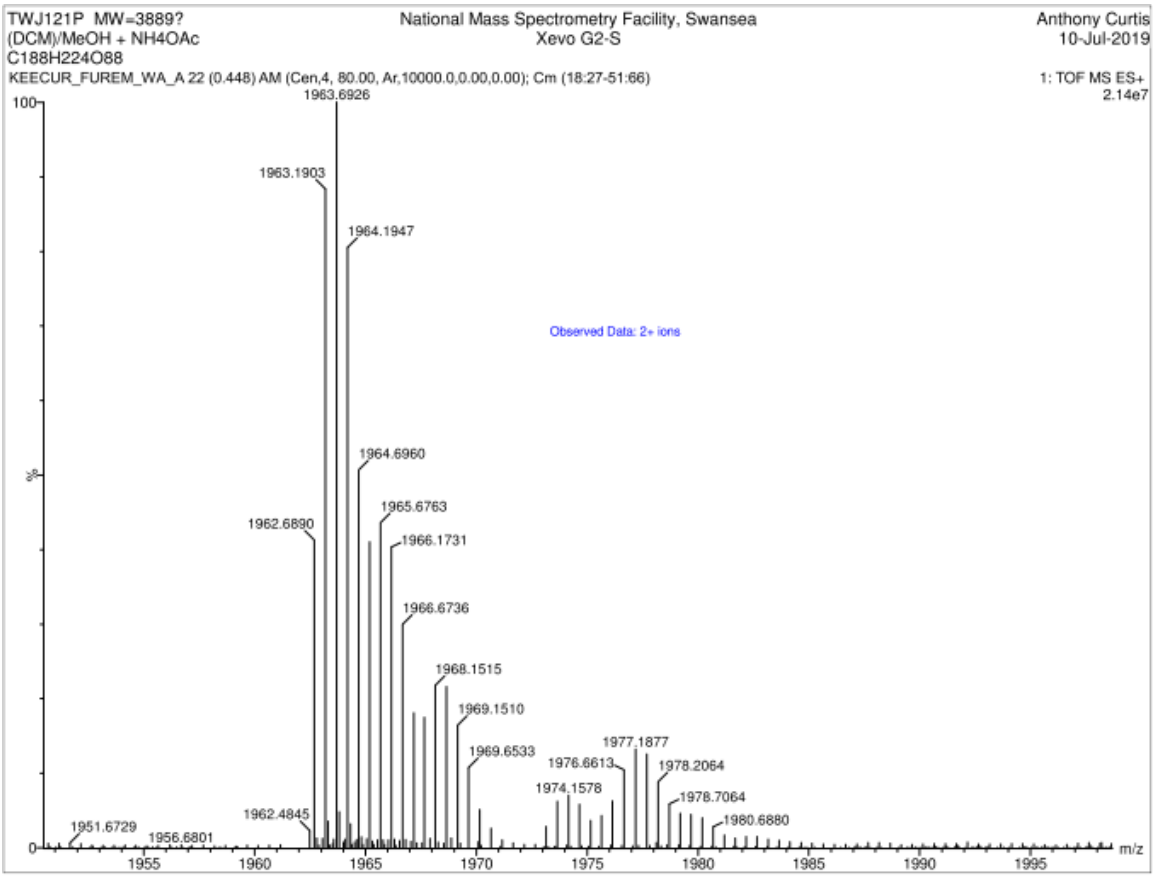
TWJ121P MW=3889?
(DCM)/MeOH + NH4OAc
C188H224O88
National Mass Spectrometry Facility, Swansea
Xevo G2-S
Anthony Curtis
10-Jul-2019
KEECUR_FUREM_WA_A 22 (0.448) AM (Cen,4, 80.00, Ar,10000.0,0.00,0.00); Cm (18:27-51:66)
1: TOF MS ES+
2.14e7
1963.6926
1963.1903
1964.1947
Observed Data: 2+ ions
1964.6960
1965.6763
1962.6890
1966.1731
1966.6736
1968.1515
1969.1510
1977.1877
1969.6533
1976.6613
1978.2064
1974.1578
1978.7064
1962.4845
1980.6880
1951.6729
1956.6801
%
m/z

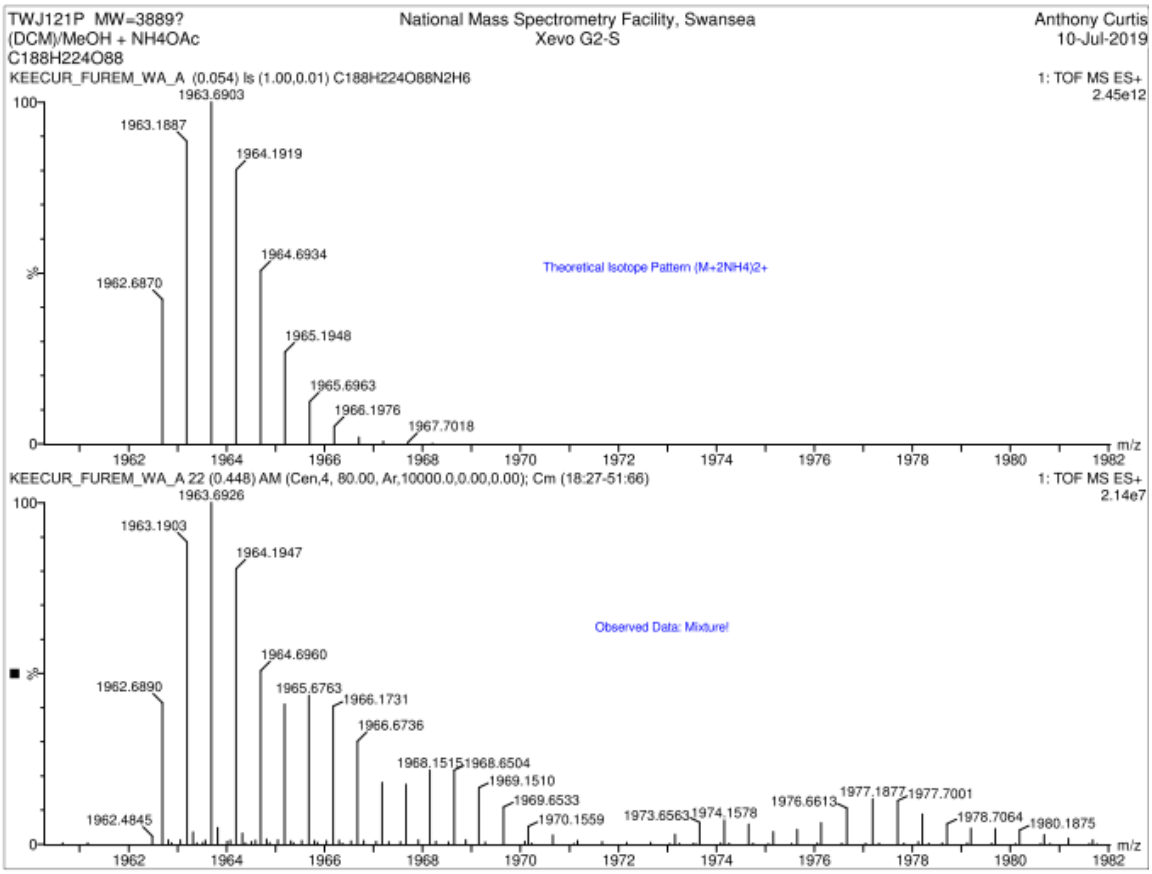

Appendix 11: Mass spectrum of **159**

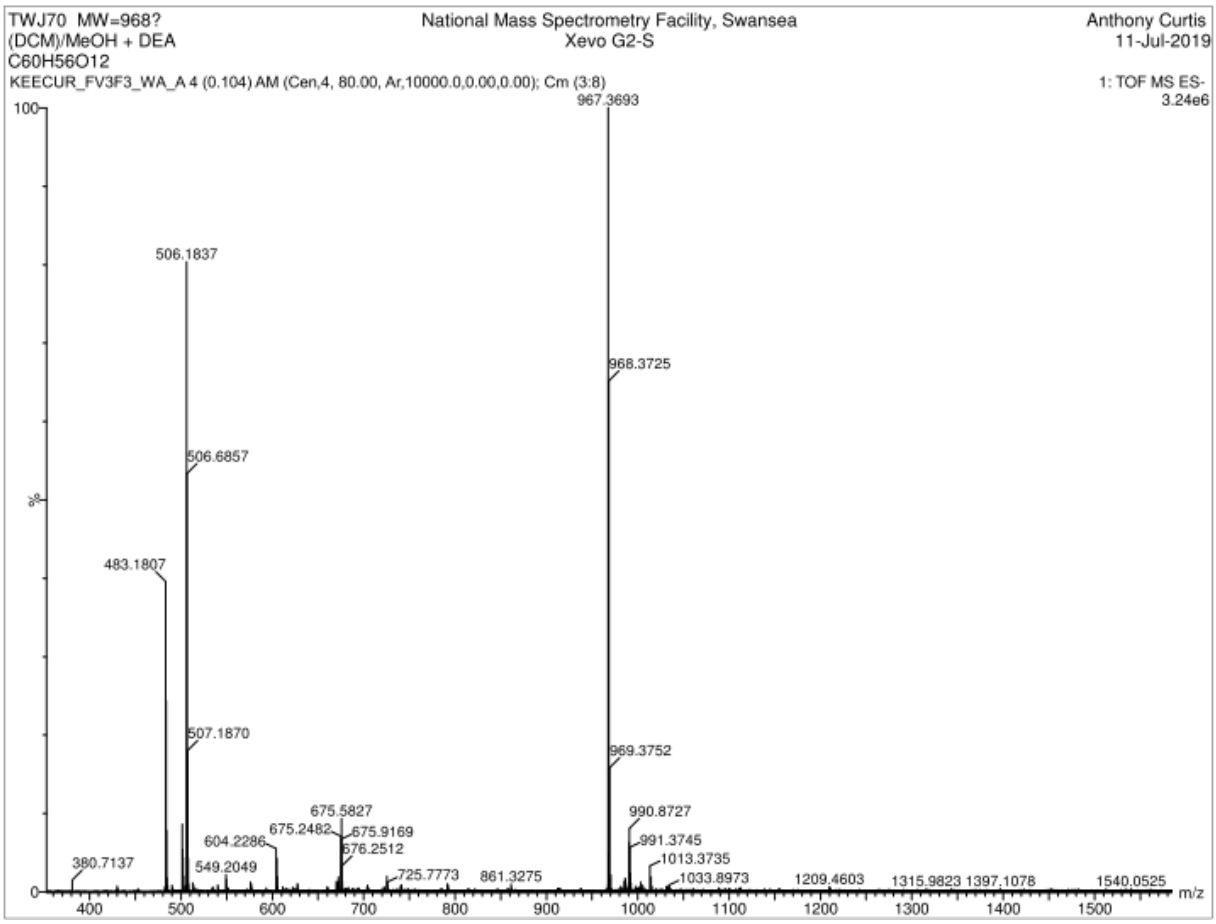
TWJ70 MW=968?
(DCM)/MeOH + DEA
C60H56O12
National Mass Spectrometry Facility, Swansea
Xevo G2-S
Anthony Curtis
11-Jul-2019
KEECUR_FV3F3_WA_A 4 (0.104) AM (Cen,4, 80.00, Ar,10000.0,0.00,0.00); Cm (3:8)
1: TOF MS ES-
3.24e6
967.3693
506.1837
968.3725
506.6857
483.1807
507.1870
969.3752
675.5827
990.8727
675.2482
675.9169
991.3745
604.2286
676.2512
1013.3735
380.7137
549.2049
725.7773
861.3275
1033.8973
1209.4603
1315.9823
1397.1078
1540.0525
m/z

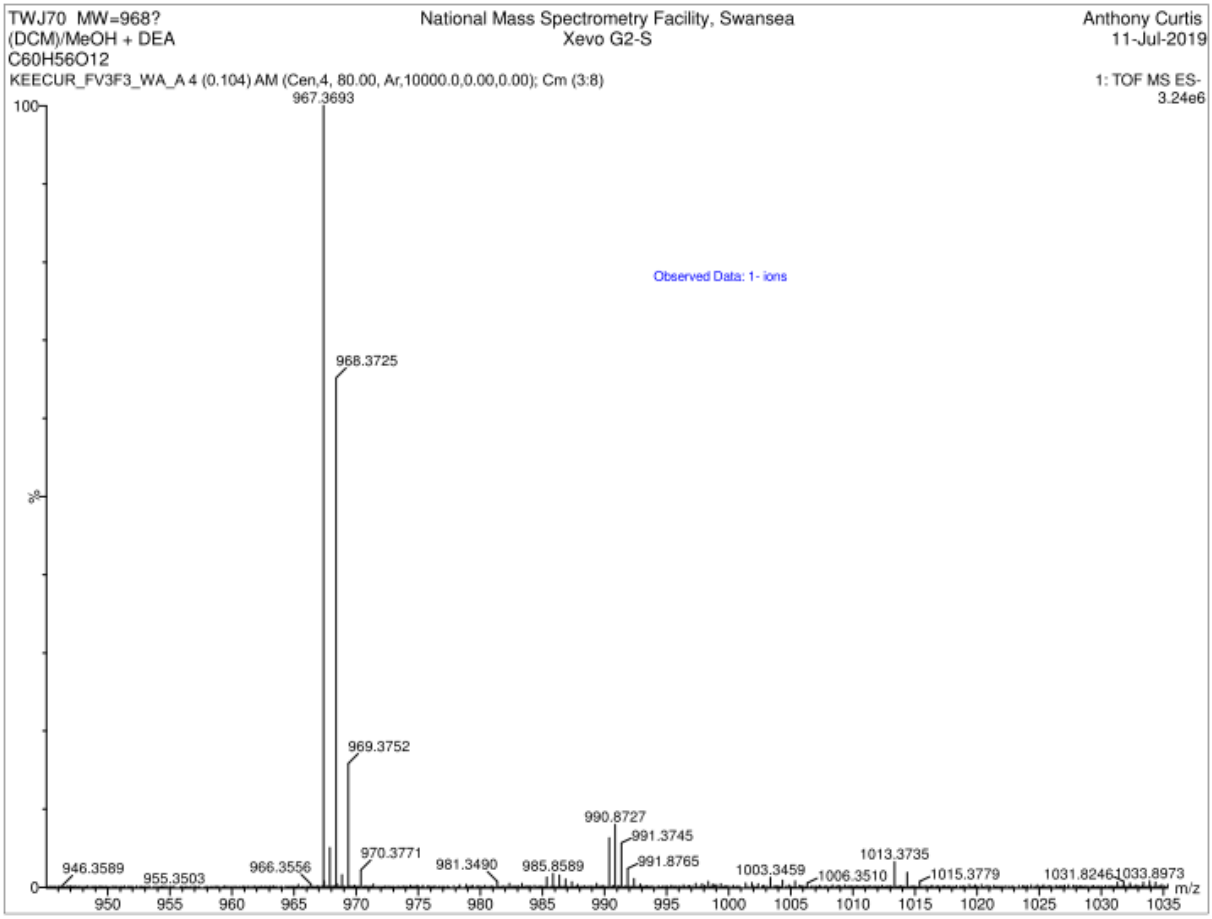
TWJ70 MW=968?
(DCM)/MeOH + DEA
C60H56O12
National Mass Spectrometry Facility, Swansea
Xevo G2-S
Anthony Curtis
11-Jul-2019
KEECUR_FV3F3_WA_A 4 (0.104) AM (Cen,4, 80.00, Ar,10000.0,0.00,0.00); Cm (3:8)
1: TOF MS ES-
3.24e6
967.3693
Observed Data: 1- ions
968.3725
969.3752
990.8727
991.3745
970.3771
1013.3735
946.3589
966.3556
981.3490
985.8589
991.8765
1003.3459
1006.3510
1015.3779
955.3503
1031.8246
1033.8973
m/z

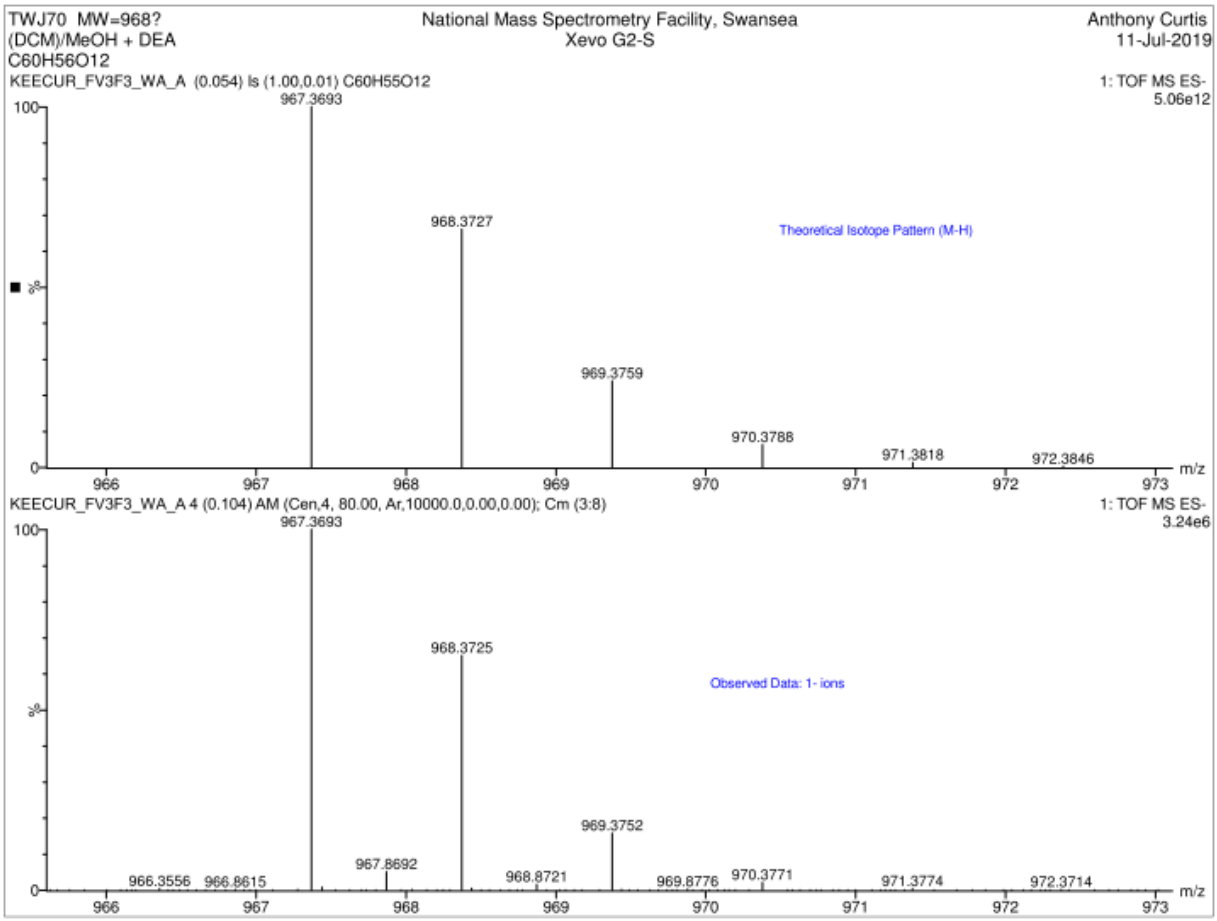

Appendix 12: Mass spectrum of **176**

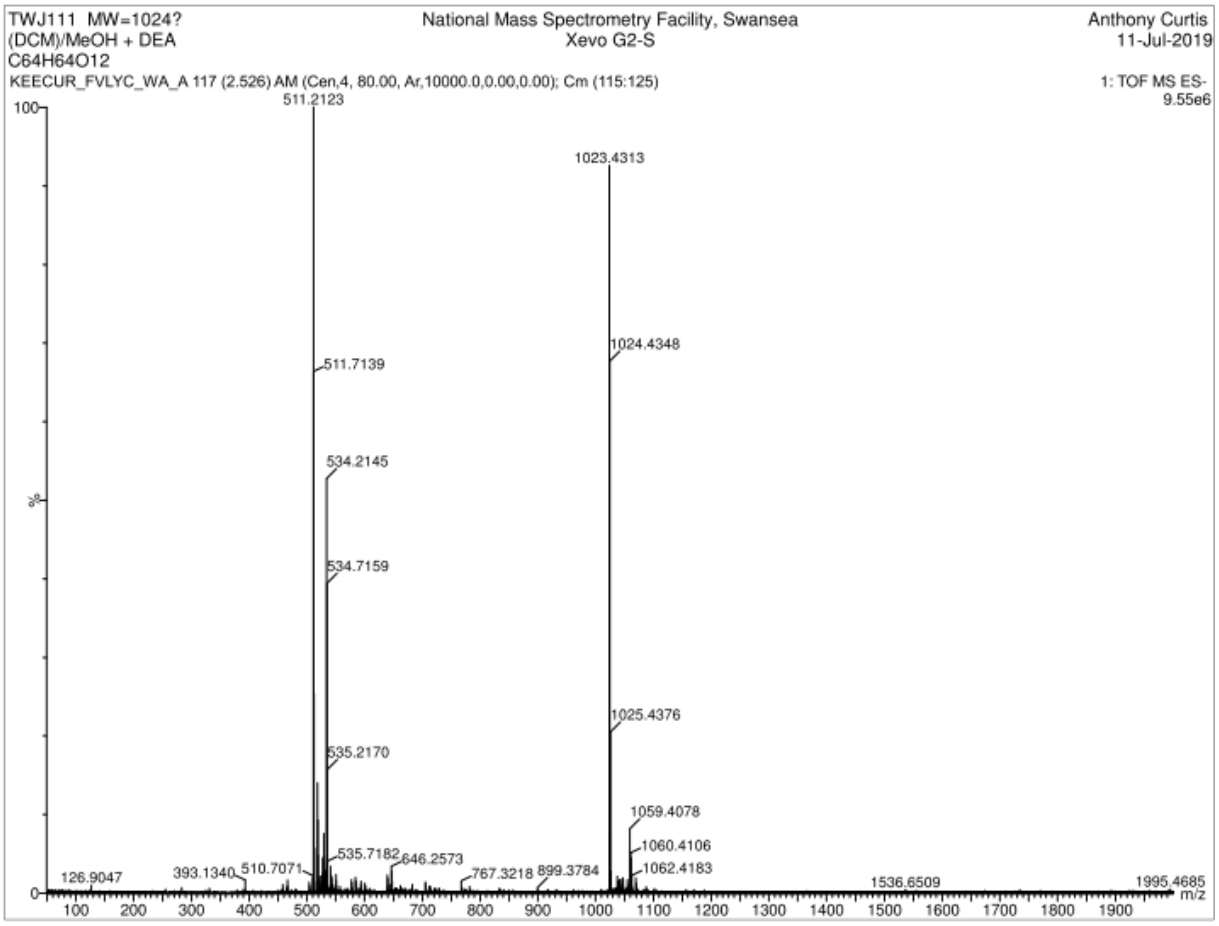
TWJ111 MW=1024?
(DCM)/MeOH + DEA
C64H64O12
National Mass Spectrometry Facility, Swansea
Xevo G2-S
Anthony Curtis
11-Jul-2019
KEECUR_FVLYC_WA_A 117 (2.526) AM (Cen,4, 80.00, Ar,10000.0,0.00,0.00); Cm (115:125)
1: TOF MS ES-
9.55e6
511.2123
1023.4313
1024.4348
511.7139
534.2145
534.7159
1025.4376
535.2170
1059.4078
1060.4106
1062.4183
535.7182
646.2573
126.9047
393.1340
510.7071
767.3218
899.3784
1536.6509
1995.4685
%
m/z

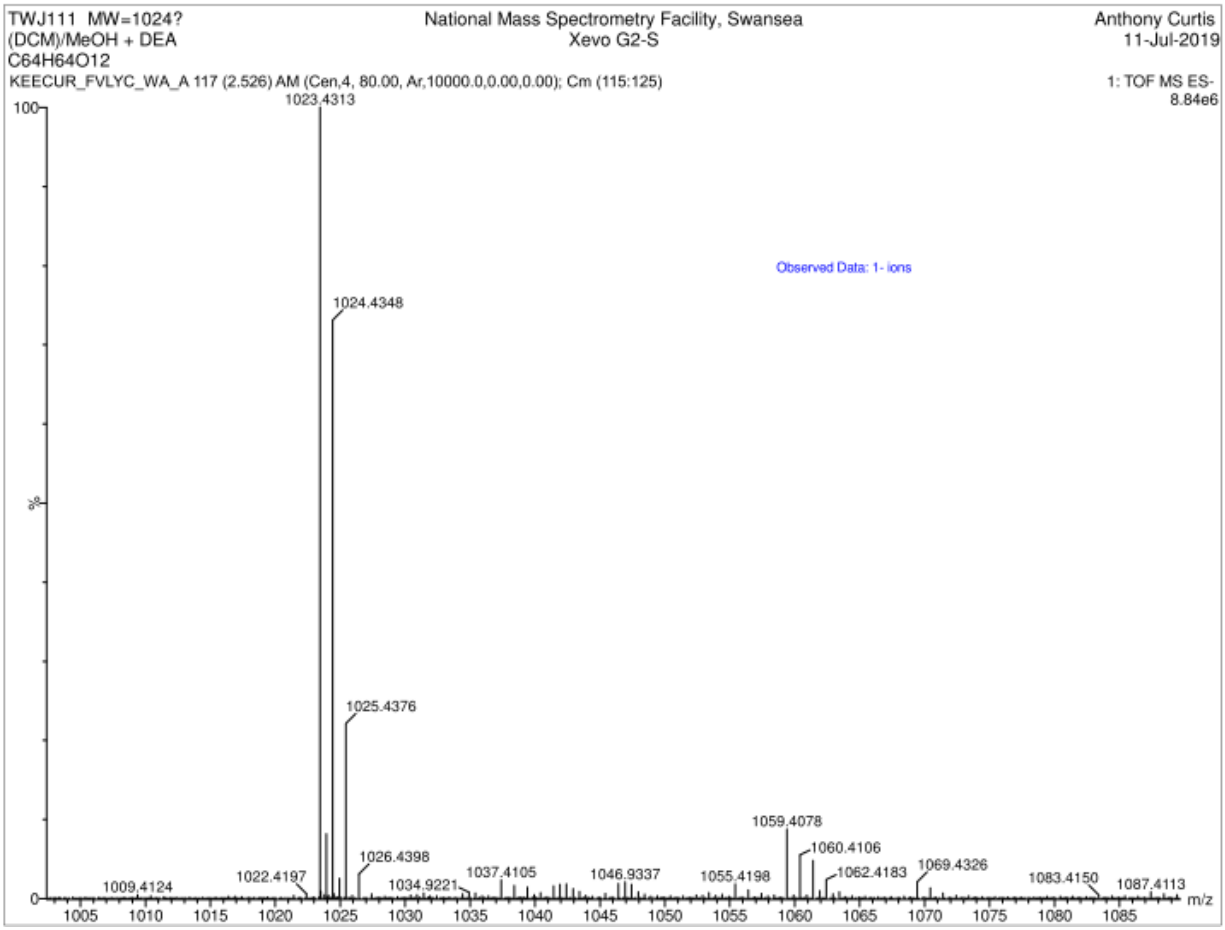
TWJ111 MW=1024?
(DCM)/MeOH + DEA
C64H64O12
National Mass Spectrometry Facility, Swansea
Xevo G2-S
Anthony Curtis
11-Jul-2019
KEECUR_FVLYC_WA_A 117 (2.526) AM (Cen,4, 80.00, Ar,10000.0,0.00,0.00); Cm (115:125)
1: TOF MS ES-
8.84e6
1023.4313
Observed Data: 1- ions
1024.4348
1025.4376
1059.4078
1060.4106
1062.4183
1069.4326
1026.4398
1037.4105
1009.4124
1022.4197
1034.9221
1046.9337
1055.4198
1083.4150
1087.4113
%
m/z

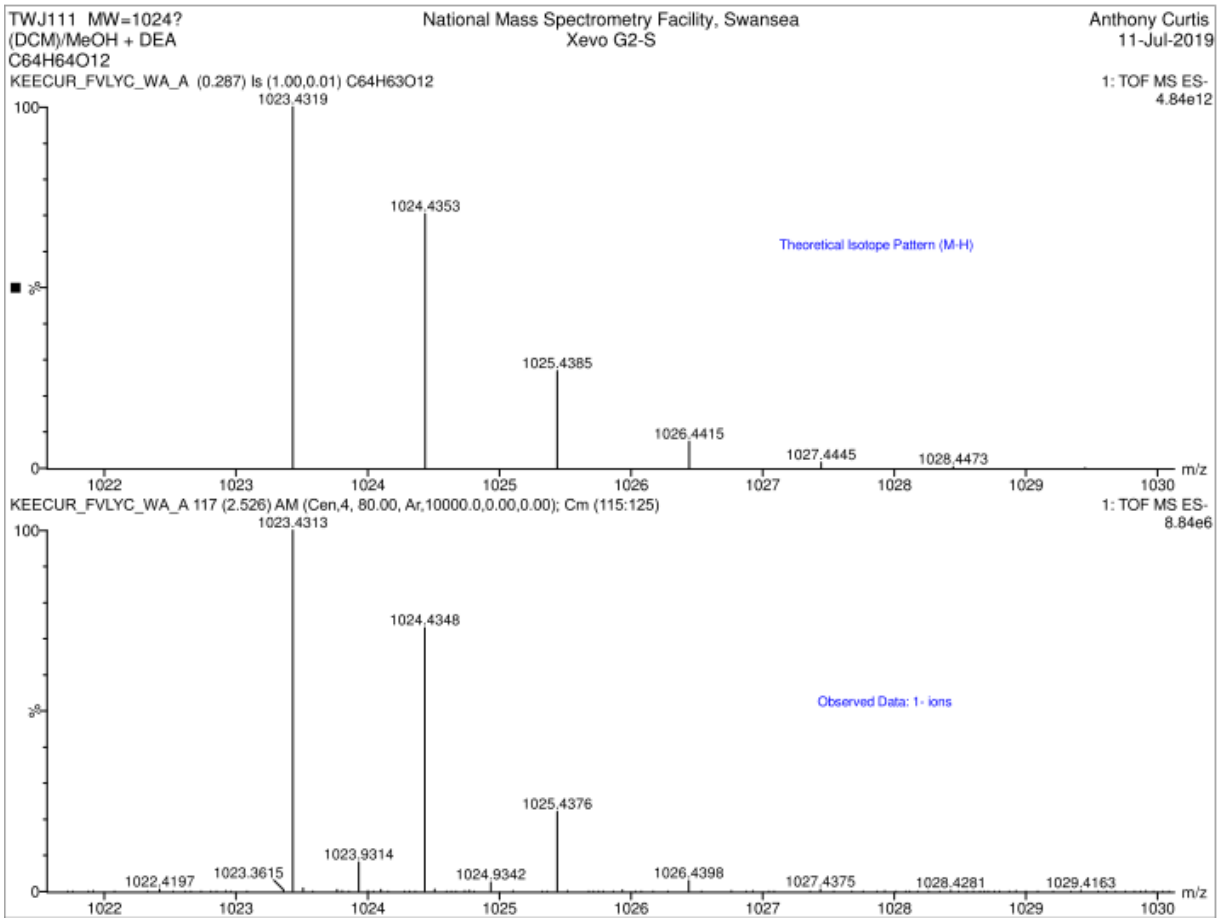

Appendix 13: Mass spectrum of **177**

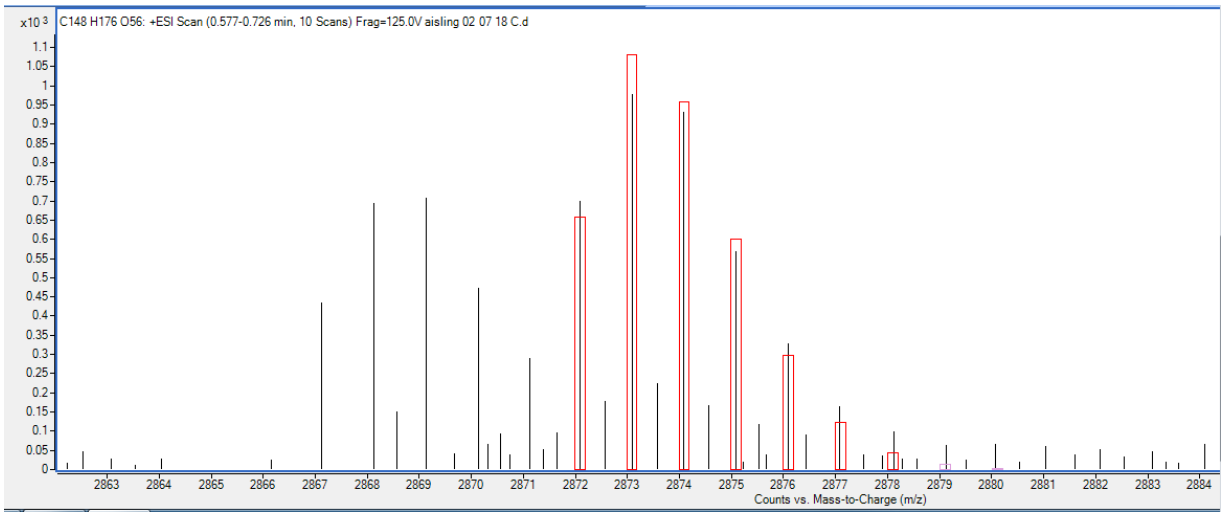

Appendix 14: Mass spectrum of **196**

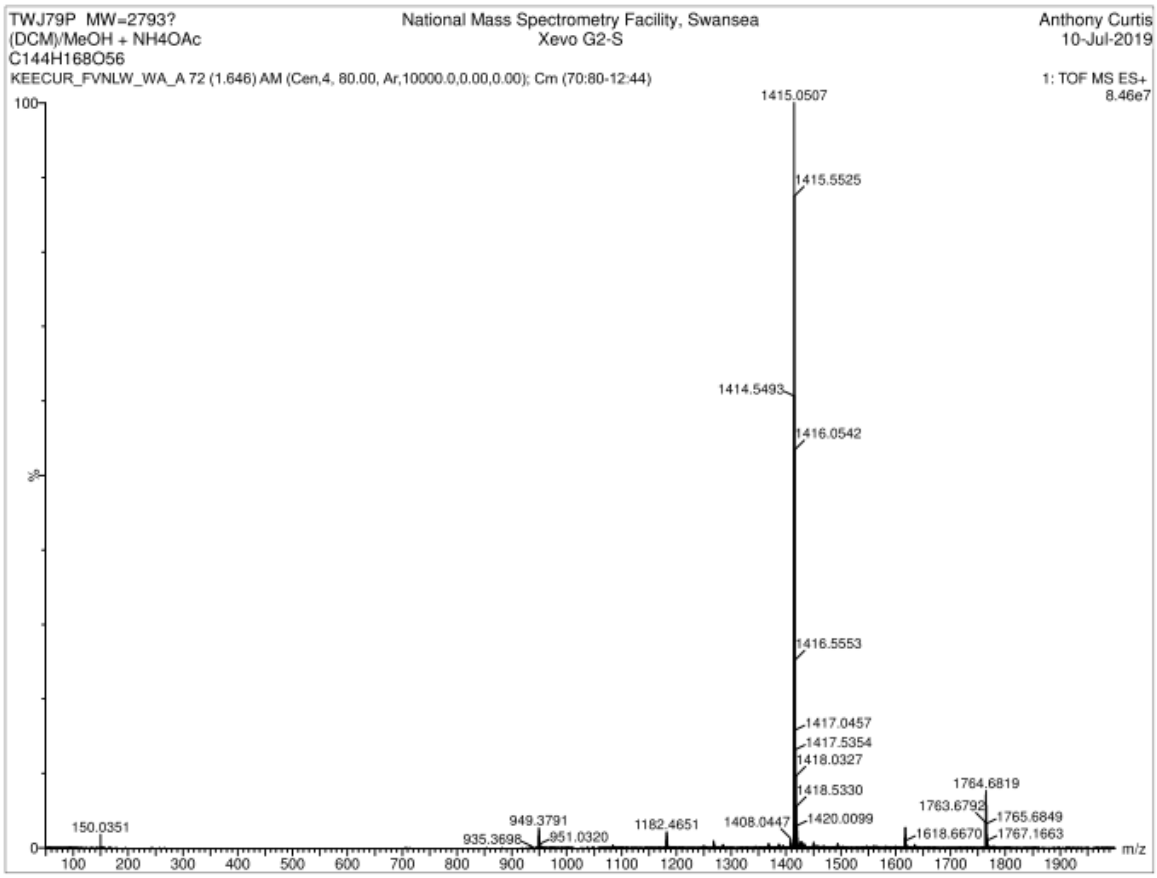
TWJ79P MW=2793?
(DCM)/MeOH + NH4OAc
C144H168O56
National Mass Spectrometry Facility, Swansea
Xevo G2-S
Anthony Curtis
10-Jul-2019
KEECUR_FVNLW_WA_A 72 (1.646) AM (Cen,4, 80.00, Ar,10000.0,0.00,0.00); Cm (70:80-12:44)
1: TOF MS ES+
8.46e7
1415.0507
1415.5525
1414.5493
1416.0542
1416.5553
1417.0457
1417.5354
1418.0327
1418.5330
1764.6819
1763.6792
1765.6849
1767.1663
1618.6670
1420.0099
1408.0447
1182.4651
949.3791
951.0320
935.3698
150.0351
%
m/z

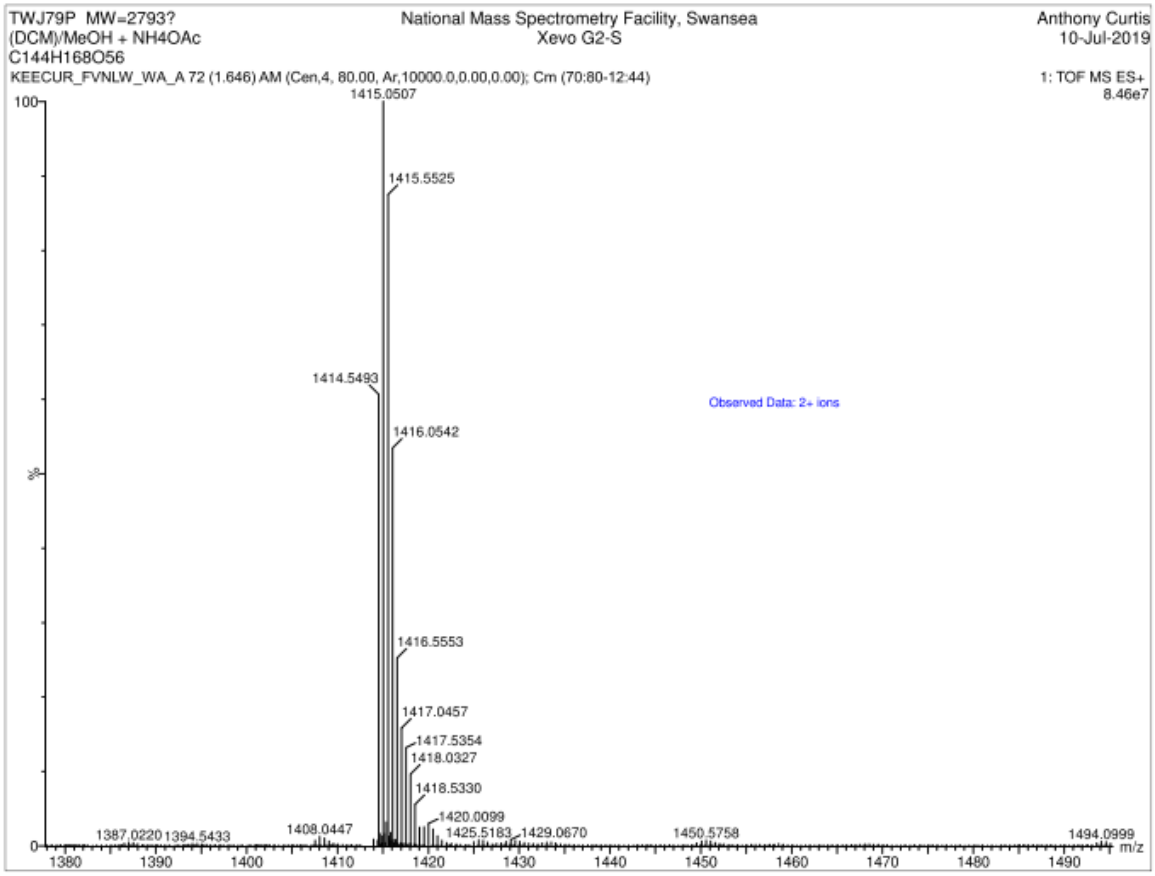
TWJ79P MW=2793?
(DCM)/MeOH + NH4OAc
C144H168O56
National Mass Spectrometry Facility, Swansea
Xevo G2-S
Anthony Curtis
10-Jul-2019
KEECUR_FVNLW_WA_A 72 (1.646) AM (Cen,4, 80.00, Ar,10000.0,0.00,0.00); Cm (70:80-12:44)
1: TOF MS ES+
8.46e7
1415.0507
1415.5525
1414.5493
Observed Data: 2+ ions
1416.0542
1416.5553
1417.0457
1417.5354
1418.0327
1418.5330
1420.0099
1387.0220
1394.5433
1408.0447
1425.5183
1429.0670
1450.5758
1494.0999
%
m/z

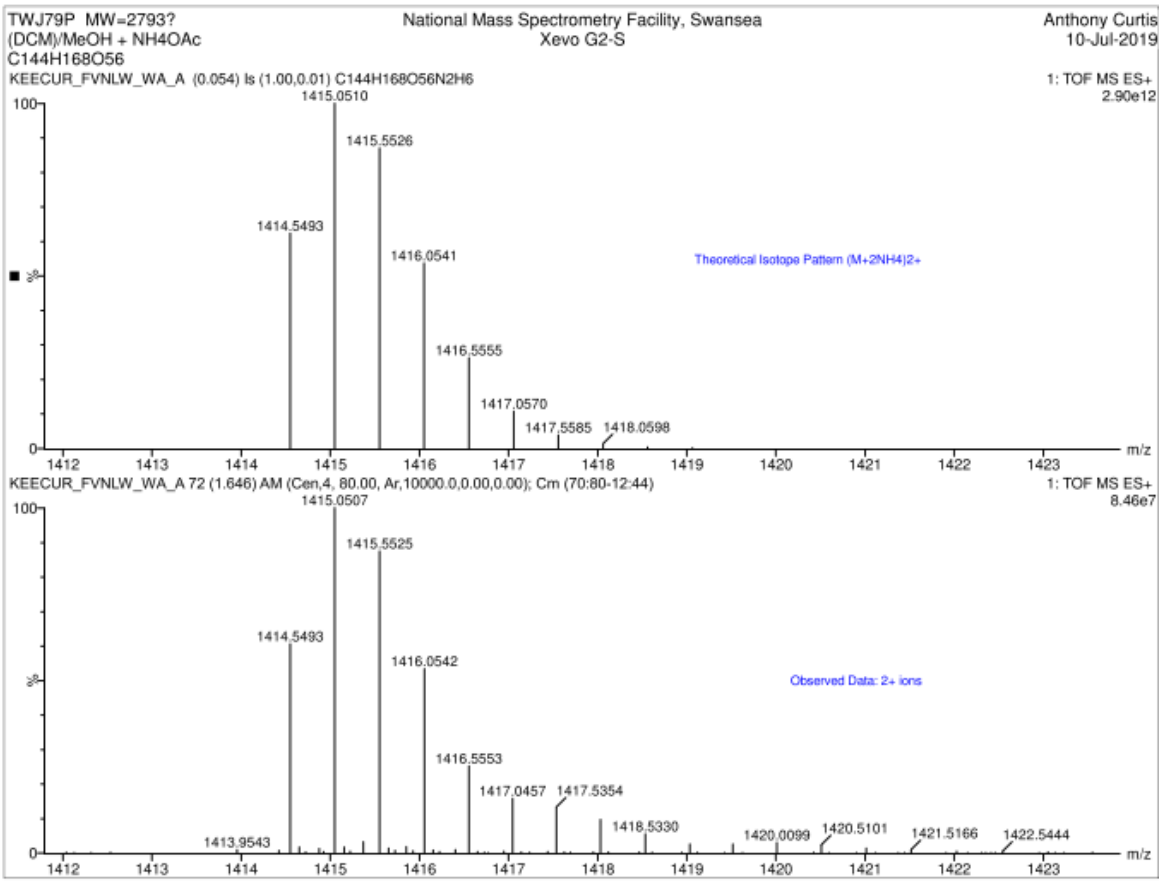

Appendix 15: Mass spectrum of **216**

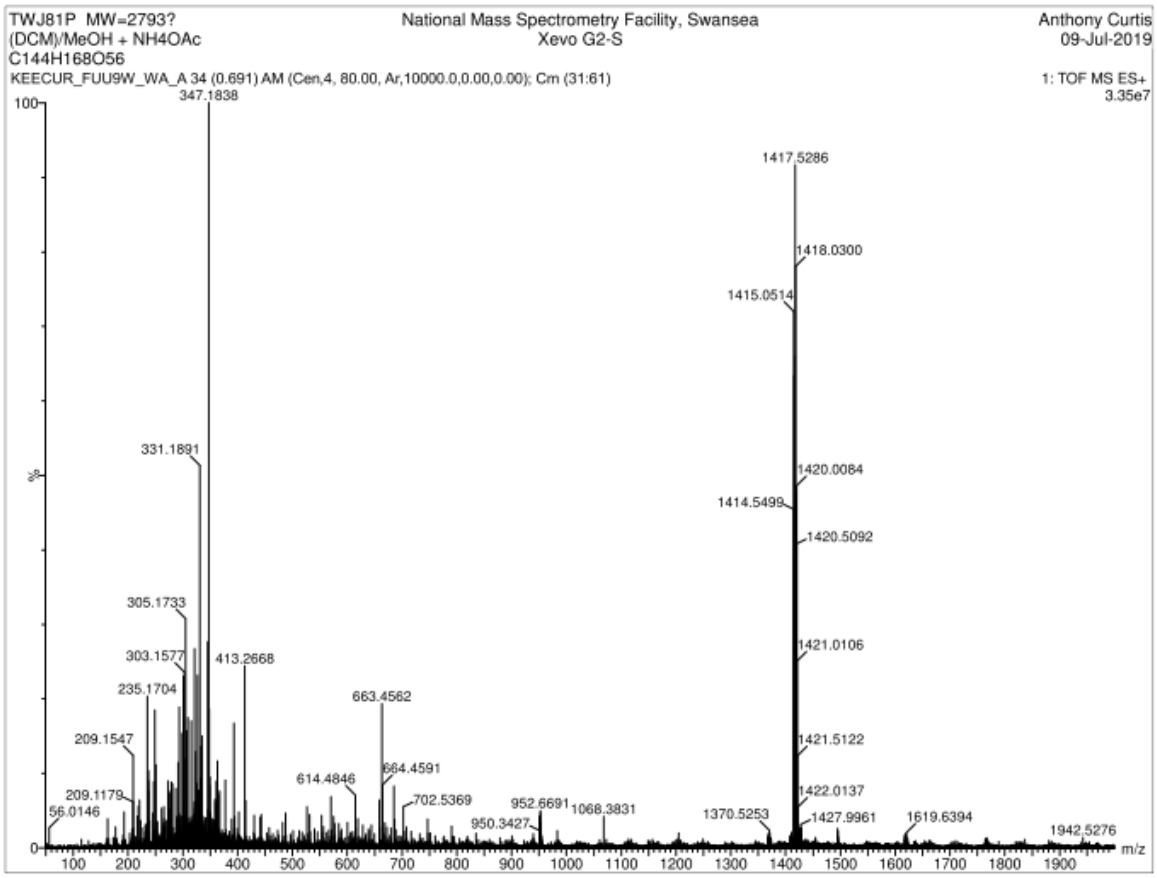
TWJ81P MW=2793?
(DCM)/MeOH + NH4OAc
C144H168O56
National Mass Spectrometry Facility, Swansea
Xevo G2-S
Anthony Curtis
09-Jul-2019
KEECUR_FUU9W_WA_A 34 (0.691) AM (Cen,4, 80.00, Ar,10000.0,0.00,0.00); Cm (31:61)
1: TOF MS ES+
3.35e7
347.1838
1417.5286
1418.0300
1415.0514
331.1891
1420.0084
1414.5499
1420.5092
305.1733
1421.0106
303.1577
413.2668
235.1704
663.4562
209.1547
1421.5122
664.4591
614.4846
1422.0137
209.1179
702.5369
952.6691
1068.3831
56.0146
950.3427
1370.5253
1427.9961
1619.6394
1942.5276
%
m/z

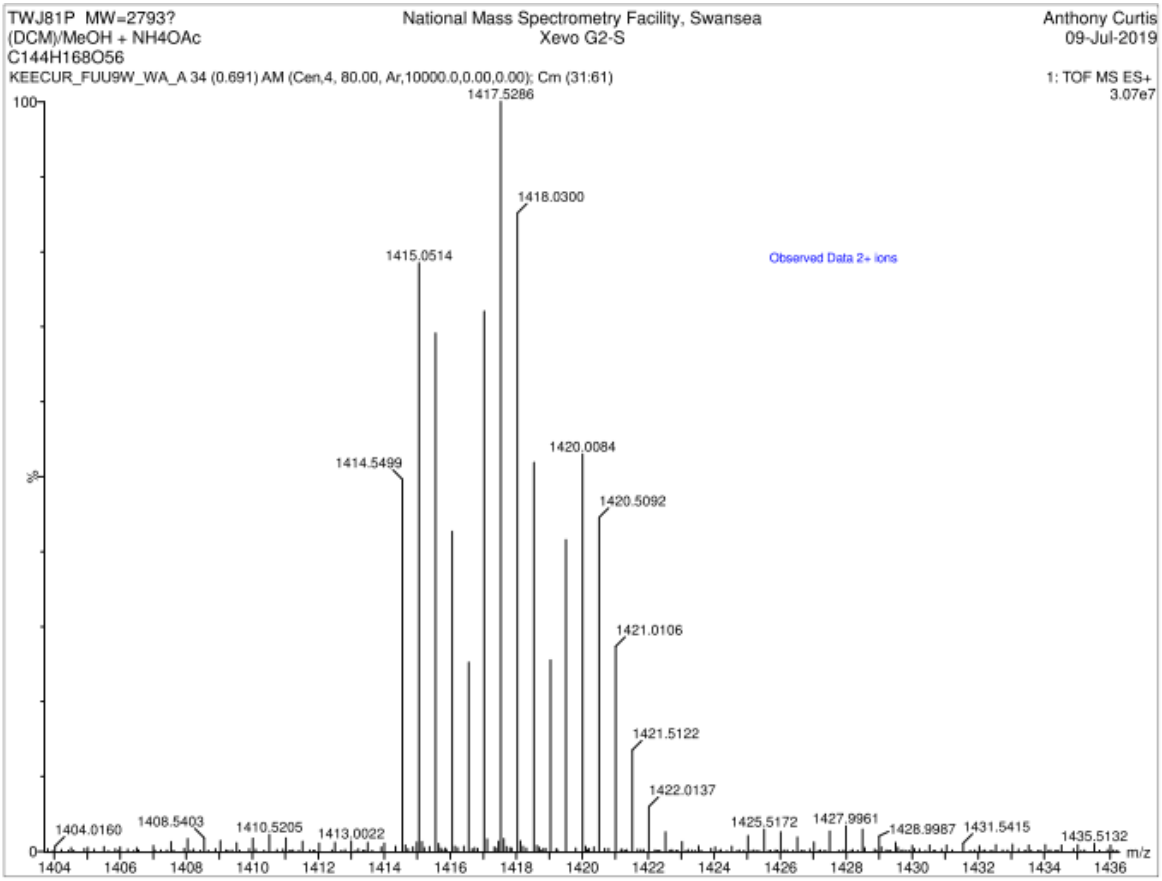
TWJ81P MW=2793?
(DCM)/MeOH + NH4OAc
C144H168O56
National Mass Spectrometry Facility, Swansea
Xevo G2-S
Anthony Curtis
09-Jul-2019
KEECUR_FUU9W_WA_A 34 (0.691) AM (Cen,4, 80.00, Ar,10000.0,0.00,0.00); Cm (31:61)
1: TOF MS ES+
3.07e7
1417.5286
1418.0300
1415.0514
Observed Data 2+ ions
1420.0084
1414.5499
1420.5092
1421.0106
1421.5122
1422.0137
1404.0160
1408.5403
1410.5205
1413.0022
1425.5172
1427.9961
1428.9987
1431.5415
1435.5132
%
m/z

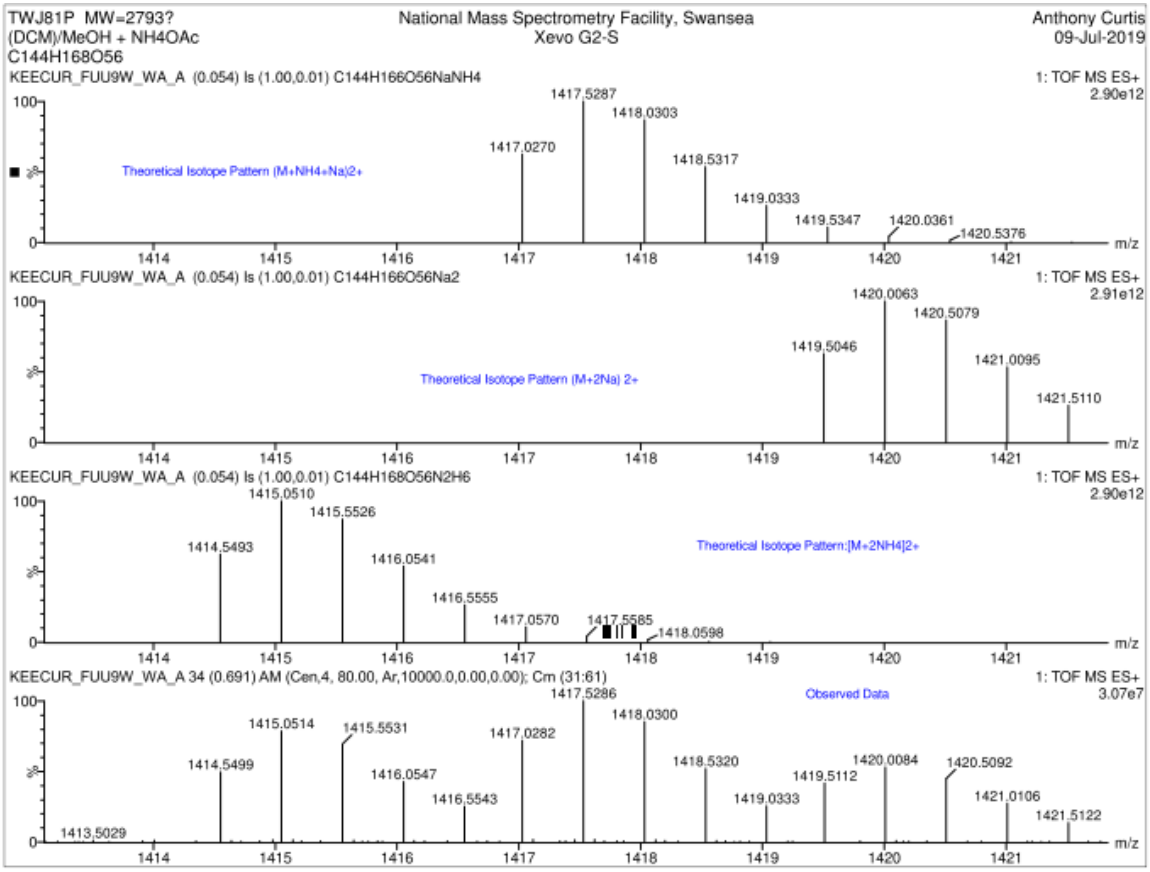

Appendix 16: Mass spectrum of **218**

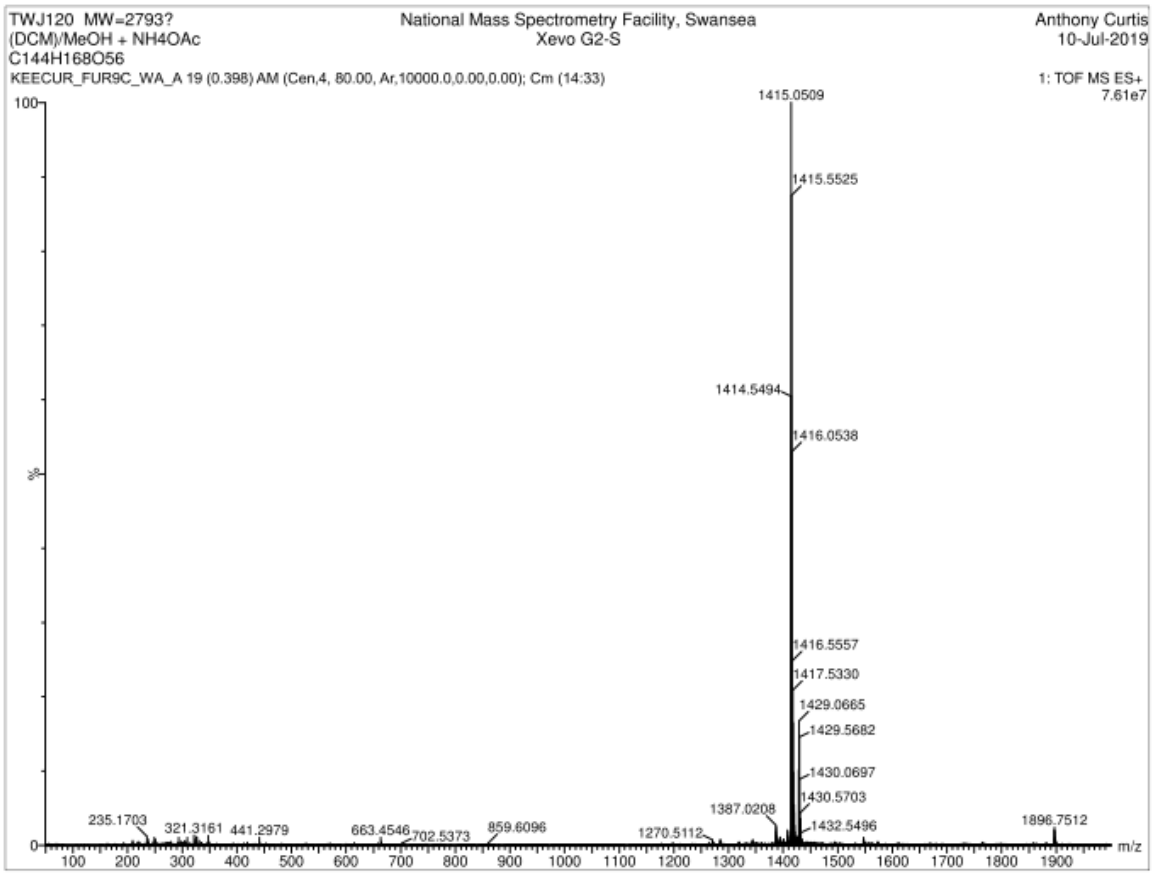
TWJ120 MW=2793?
(DCM)/MeOH + NH4OAc
C144H168O56
National Mass Spectrometry Facility, Swansea
Xevo G2-S
Anthony Curtis
10-Jul-2019
KEECUR_FUR9C_WA_A 19 (0.398) AM (Cen,4, 80.00, Ar,10000.0,0.00,0.00); Cm (14:33)
1: TOF MS ES+
7.61e7
1415.0509
1415.5525
1414.5494
1416.0538
1416.5557
1417.5330
1429.0665
1429.5682
1430.0697
1430.5703
1387.0208
1432.5496
1896.7512
235.1703
321.3161
441.2979
663.4546
702.5373
859.6096
1270.5112
m/z

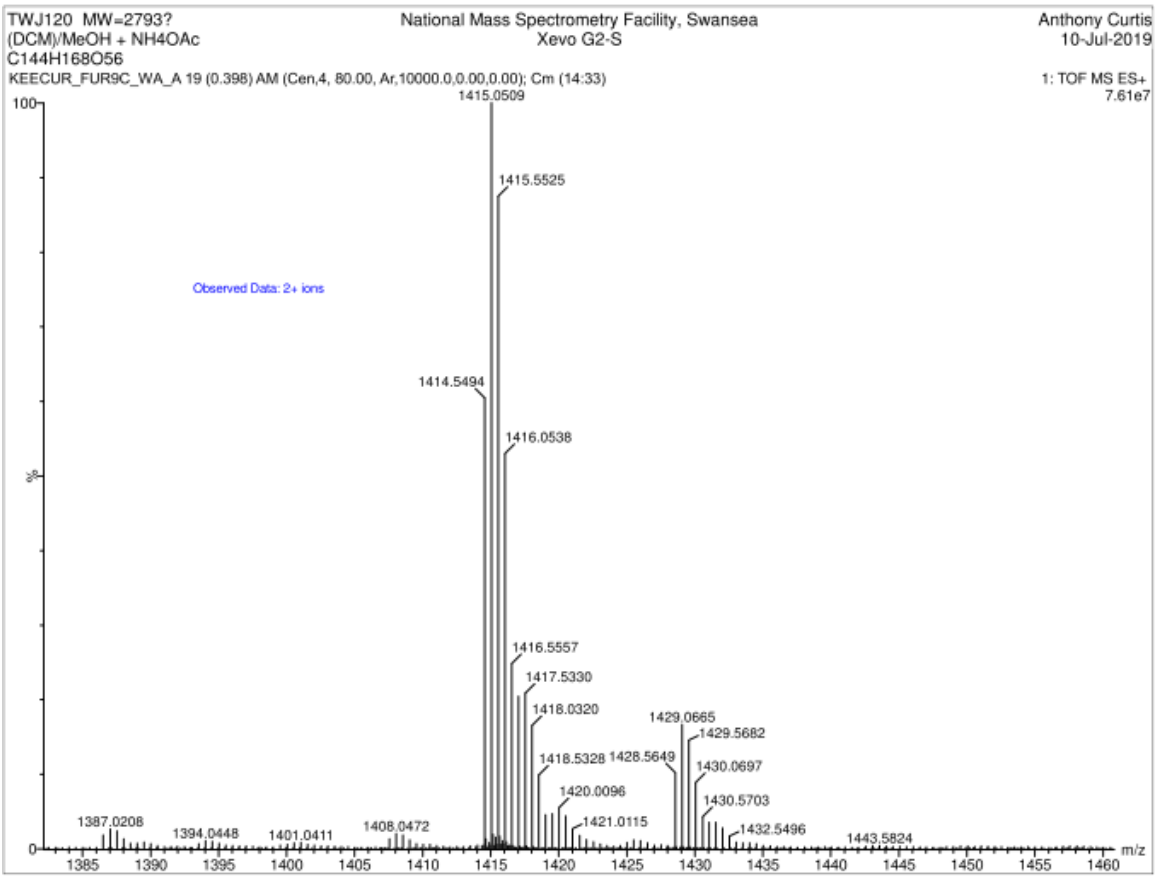
TWJ120 MW=2793?
(DCM)/MeOH + NH4OAc
C144H168O56
National Mass Spectrometry Facility, Swansea
Xevo G2-S
Anthony Curtis
10-Jul-2019
KEECUR_FUR9C_WA_A 19 (0.398) AM (Cen,4, 80.00, Ar,10000.0,0.00,0.00); Cm (14:33)
1: TOF MS ES+
7.61e7
Observed Data: 2+ ions
1415.0509
1415.5525
1414.5494
1416.0538
1416.5557
1417.5330
1418.0320
1429.0665
1429.5682
1418.5328
1428.5649
1430.0697
1420.0096
1430.5703
1387.0208
1421.0115
1394.0448
1401.0411
1408.0472
1432.5496
1443.5824
m/z

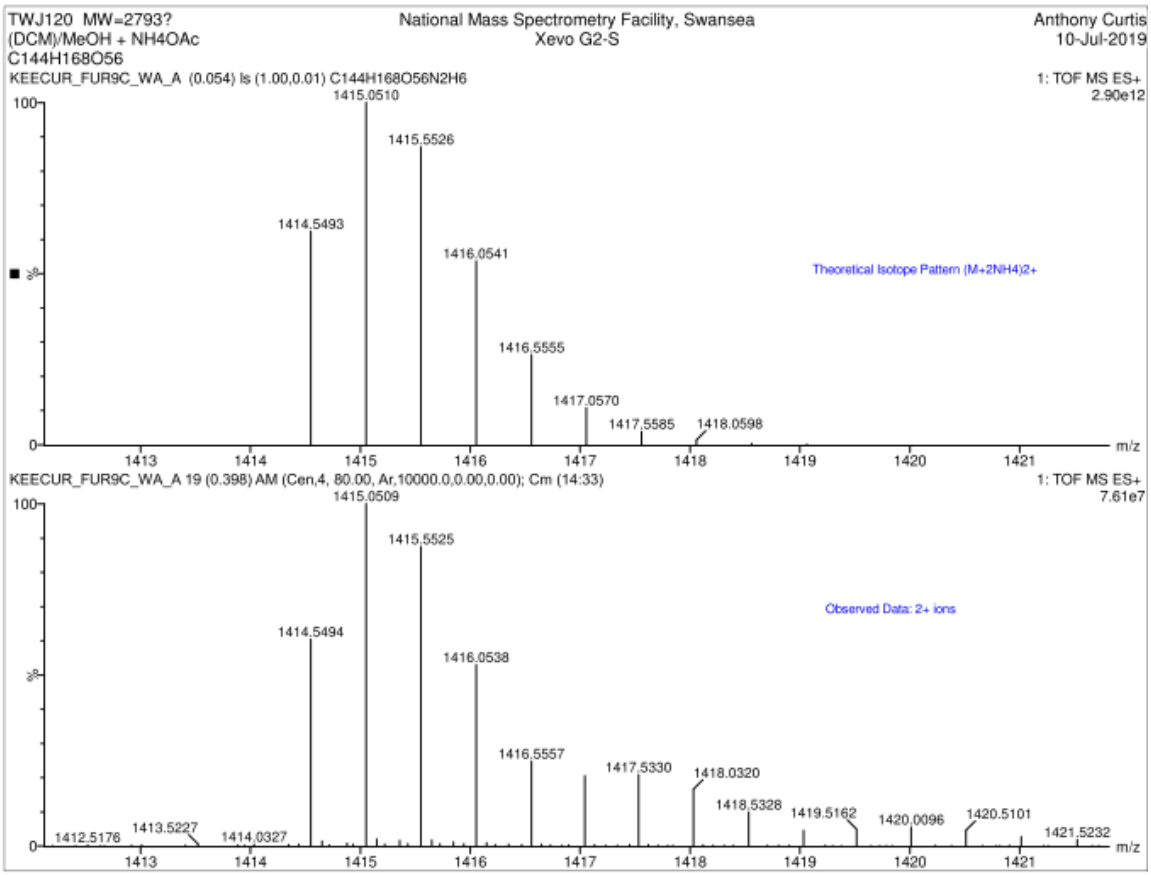

Appendix 17: Mass spectrum of **220**

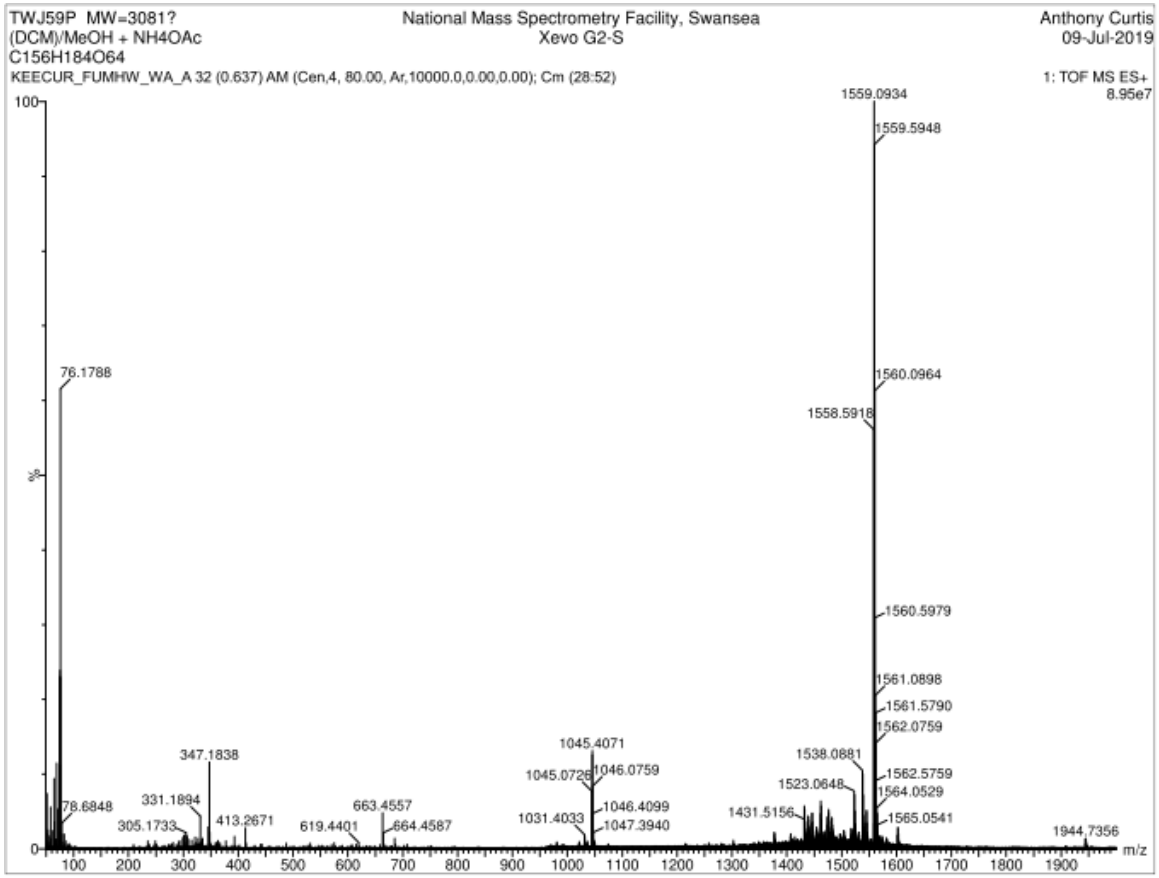
TWJ59P MW=3081?
(DCM)/MeOH + NH4OAc
C156H184O64
National Mass Spectrometry Facility, Swansea
Xevo G2-S
Anthony Curtis
09-Jul-2019
KEECUR_FUMHW_WA_A 32 (0.637) AM (Cen,4, 80.00, Ar,10000.0,0.00,0.00); Cm (28:52)
1: TOF MS ES+
8.95e7
1559.0934
1559.5948
76.1788
1560.0964
1558.5918
1560.5979
1561.0898
1561.5790
1562.0759
1045.4071
347.1838
1538.0881
1045.0726
1046.0759
1562.5759
1523.0648
1564.0529
331.1894
78.6848
663.4557
1046.4099
1565.0541
305.1733
413.2671
619.4401
664.4587
1031.4033
1047.3940
1431.5156
1944.7356
%
m/z

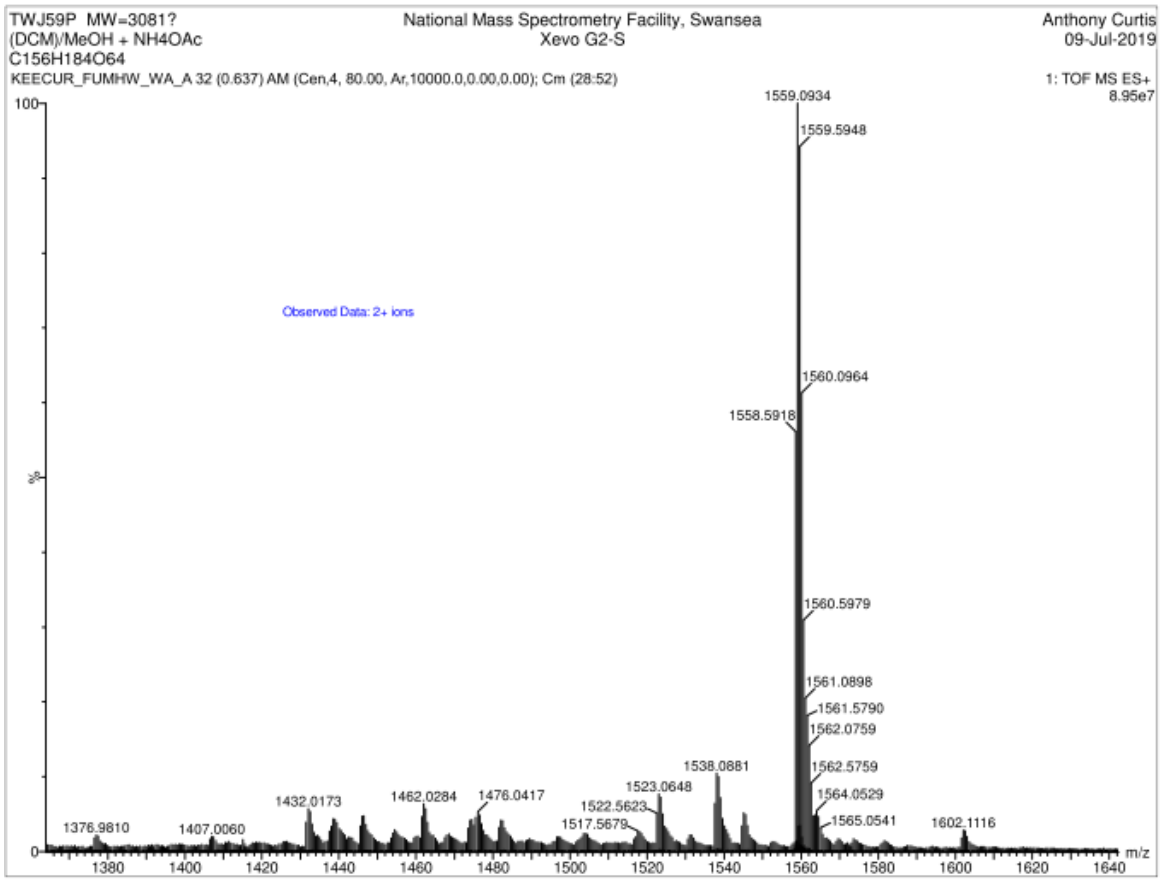
TWJ59P MW=3081?
(DCM)/MeOH + NH4OAc
C156H184O64
National Mass Spectrometry Facility, Swansea
Xevo G2-S
Anthony Curtis
09-Jul-2019
KEECUR_FUMHW_WA_A 32 (0.637) AM (Cen,4, 80.00, Ar,10000.0,0.00,0.00); Cm (28:52)
1: TOF MS ES+
8.95e7
1559.0934
1559.5948
Observed Data: 2+ ions
1560.0964
1558.5918
1560.5979
1561.0898
1561.5790
1562.0759
1538.0881
1562.5759
1523.0648
1564.0529
1432.0173
1462.0284
1476.0417
1522.5623
1565.0541
1376.9810
1407.0060
1517.5679
1602.1116
%
m/z

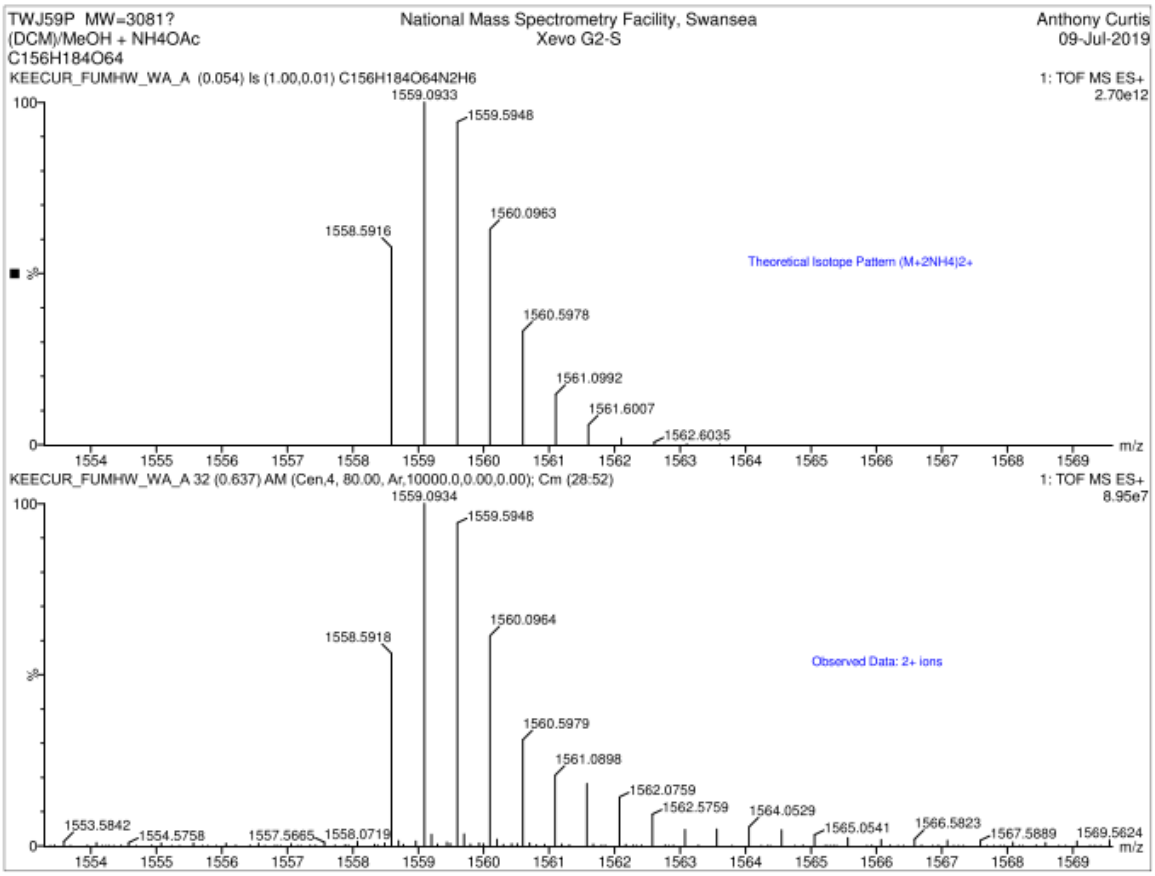

Appendix 18: Mass spectrum of **222**

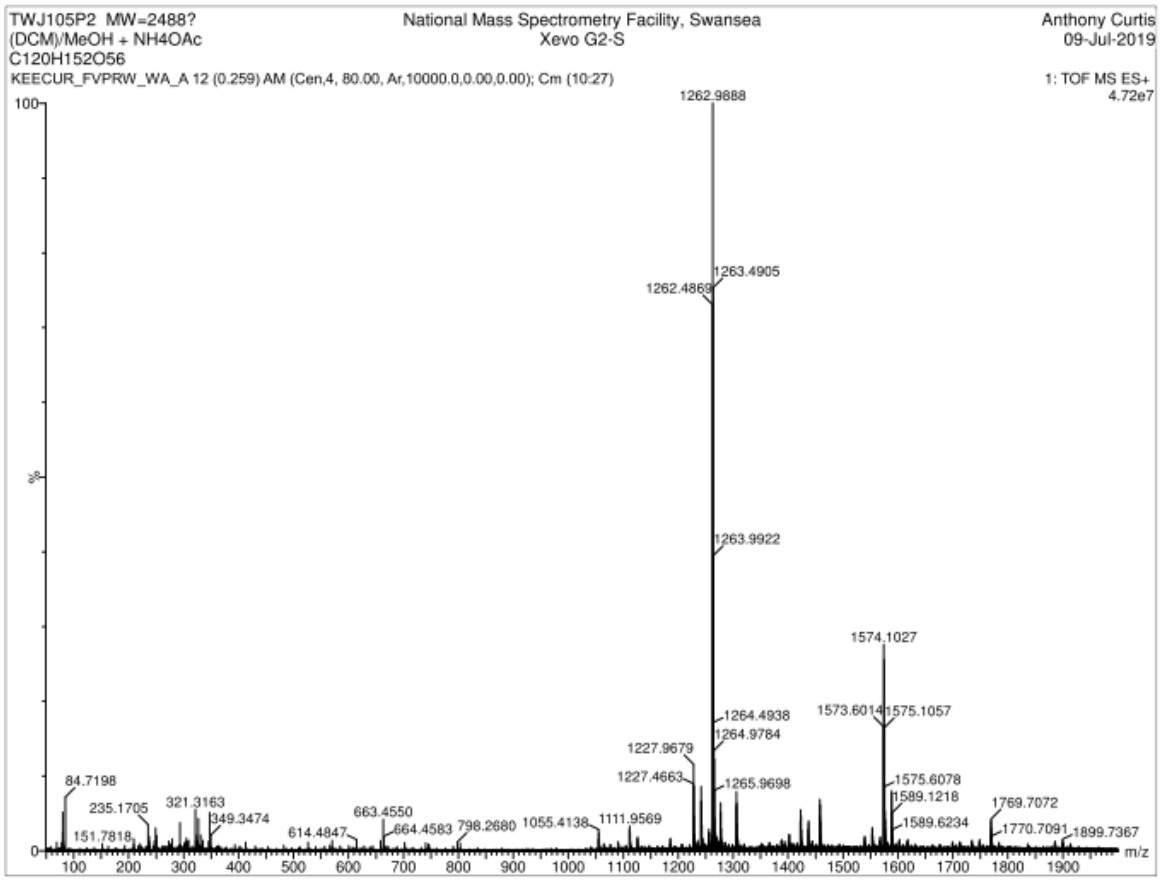
TWJ105P2 MW=2488?
(DCM)/MeOH + NH4OAc
C120H152O56
National Mass Spectrometry Facility, Swansea
Xevo G2-S
Anthony Curtis
09-Jul-2019
KEECUR_FVPRW_WA_A 12 (0.259) AM (Cen,4, 80.00, Ar,10000.0,0.00,0.00); Cm (10:27)
1: TOF MS ES+
4.72e7
1262.9888
1263.4905
1262.4869
1263.9922
1574.1027
1264.4938
1573.6014
1575.1057
1264.9784
1227.9679
1227.4663
1265.9698
84.7198
1575.6078
1589.1218
235.1705
321.3163
1769.7072
349.3474
663.4550
1589.6234
151.7818
614.4847
664.4583
798.2680
1055.4138
1111.9569
1770.7091
1899.7367
%
m/z

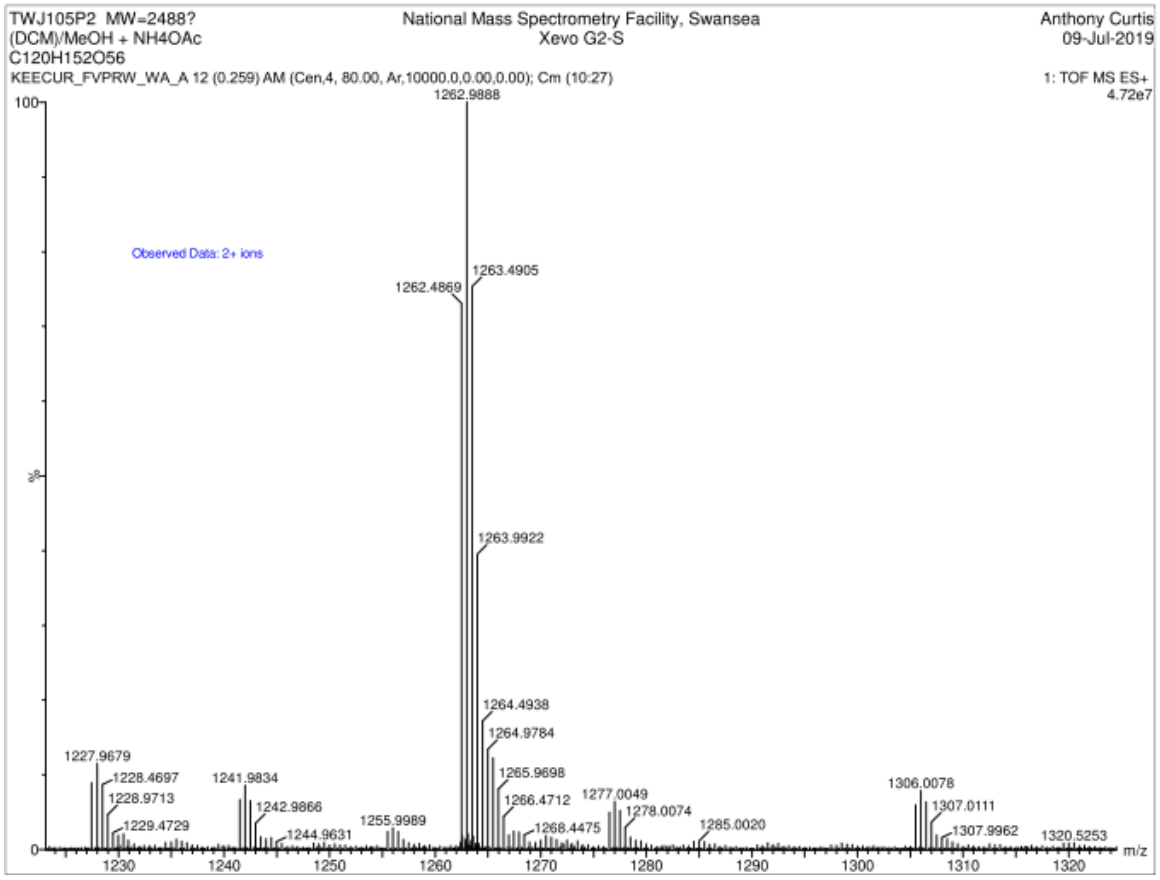
TWJ105P2 MW=2488?
(DCM)/MeOH + NH4OAc
C120H152O56
National Mass Spectrometry Facility, Swansea
Xevo G2-S
Anthony Curtis
09-Jul-2019
KEECUR_FVPRW_WA_A 12 (0.259) AM (Cen,4, 80.00, Ar,10000.0,0.00,0.00); Cm (10:27)
1: TOF MS ES+
4.72e7
1262.9888
Observed Data: 2+ ions
1263.4905
1262.4869
1263.9922
1264.4938
1264.9784
1227.9679
1265.9698
1228.4697
1241.9834
1228.9713
1242.9866
1266.4712
1277.0049
1306.0078
1229.4729
1255.9989
1278.0074
1307.0111
1244.9631
1268.4475
1285.0020
1307.9962
1320.5253
%
m/z

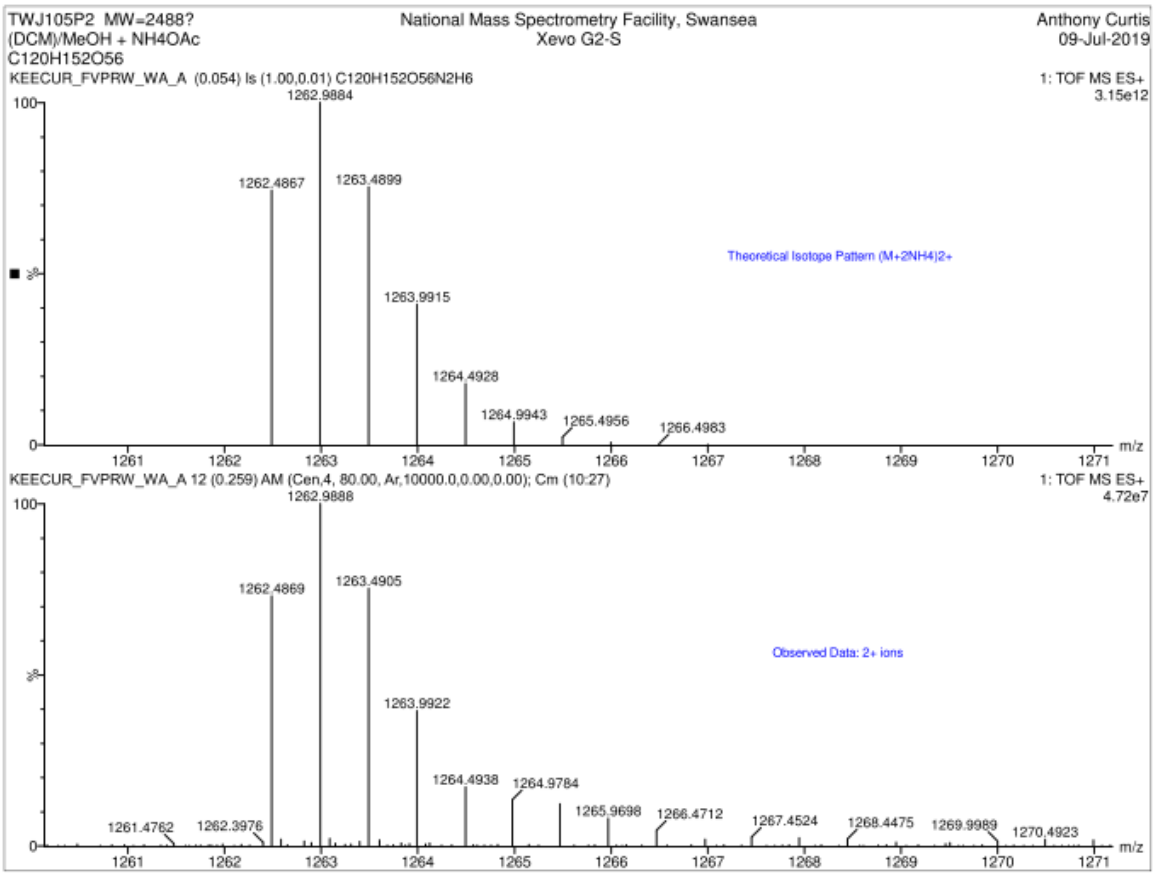

Appendix 19: Mass spectrum of **243**

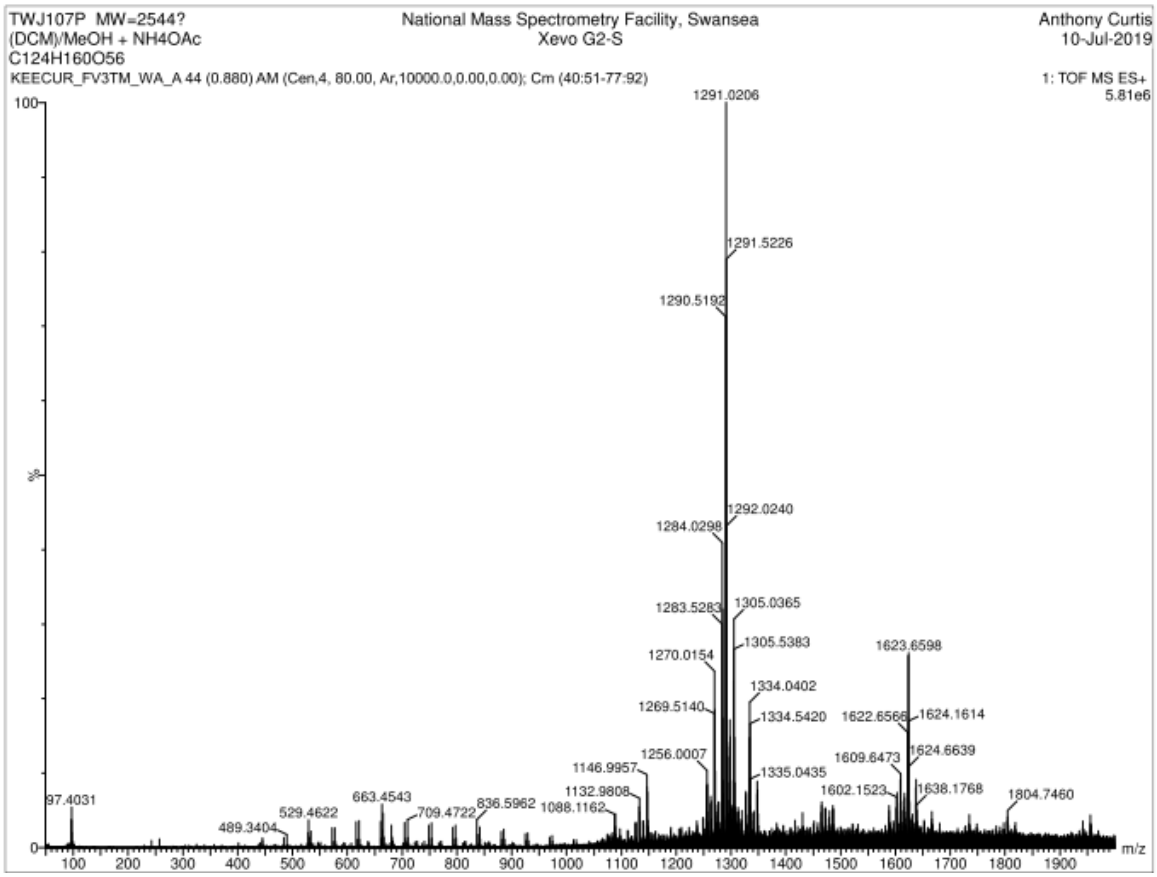
TWJ107P MW=2544?
(DCM)/MeOH + NH4OAc
C124H160O56
National Mass Spectrometry Facility, Swansea
Xevo G2-S
Anthony Curtis
10-Jul-2019
KEECUR_FV3TM_WA_A 44 (0.880) AM (Cen,4, 80.00, Ar,10000.0,0.00,0.00); Cm (40:51-77:92)
1: TOF MS ES+
5.81e6
1291.0206
1291.5226
1290.5192
1292.0240
1284.0298
1283.5283
1305.0365
1305.5383
1270.0154
1623.6598
1334.0402
1269.5140
1334.5420
1622.6566
1624.1614
1256.0007
1624.6639
1609.6473
1146.9957
1335.0435
1602.1523
1638.1768
1132.9808
1088.1162
1804.7460
97.4031
663.4543
529.4622
709.4722
836.5962
489.3404
%
m/z

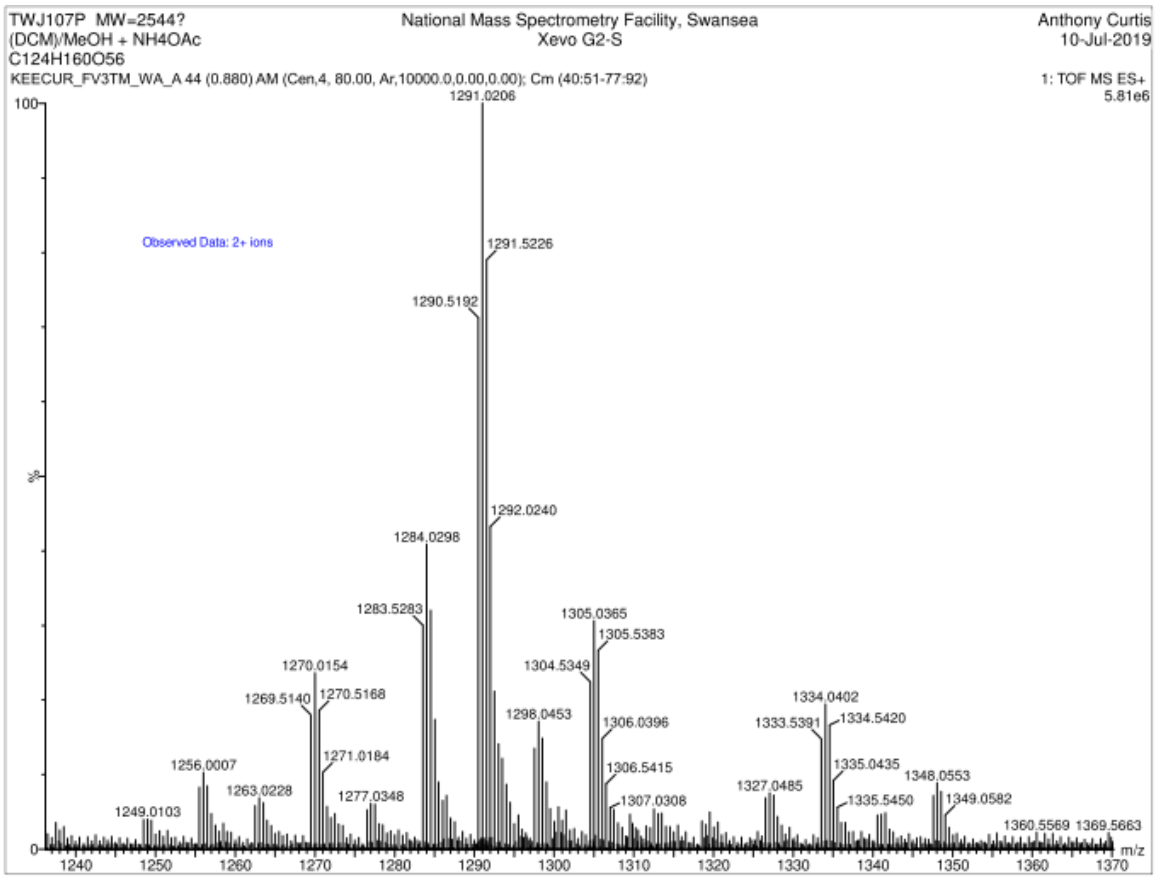
TWJ107P MW=2544?
(DCM)/MeOH + NH4OAc
C124H160O56
National Mass Spectrometry Facility, Swansea
Xevo G2-S
Anthony Curtis
10-Jul-2019
KEECUR_FV3TM_WA_A 44 (0.880) AM (Cen,4, 80.00, Ar,10000.0,0.00,0.00); Cm (40:51-77:92)
1: TOF MS ES+
5.81e6
Observed Data: 2+ ions
1291.0206
1291.5226
1290.5192
1292.0240
1284.0298
1283.5283
1305.0365
1305.5383
1304.5349
1270.0154
1269.5140
1270.5168
1334.0402
1333.5391
1334.5420
1298.0453
1306.0396
1256.0007
1271.0184
1306.5415
1335.0435
1348.0553
1263.0228
1277.0348
1327.0485
1307.0308
1335.5450
1349.0582
1249.0103
1360.5569
1369.5663
%
m/z

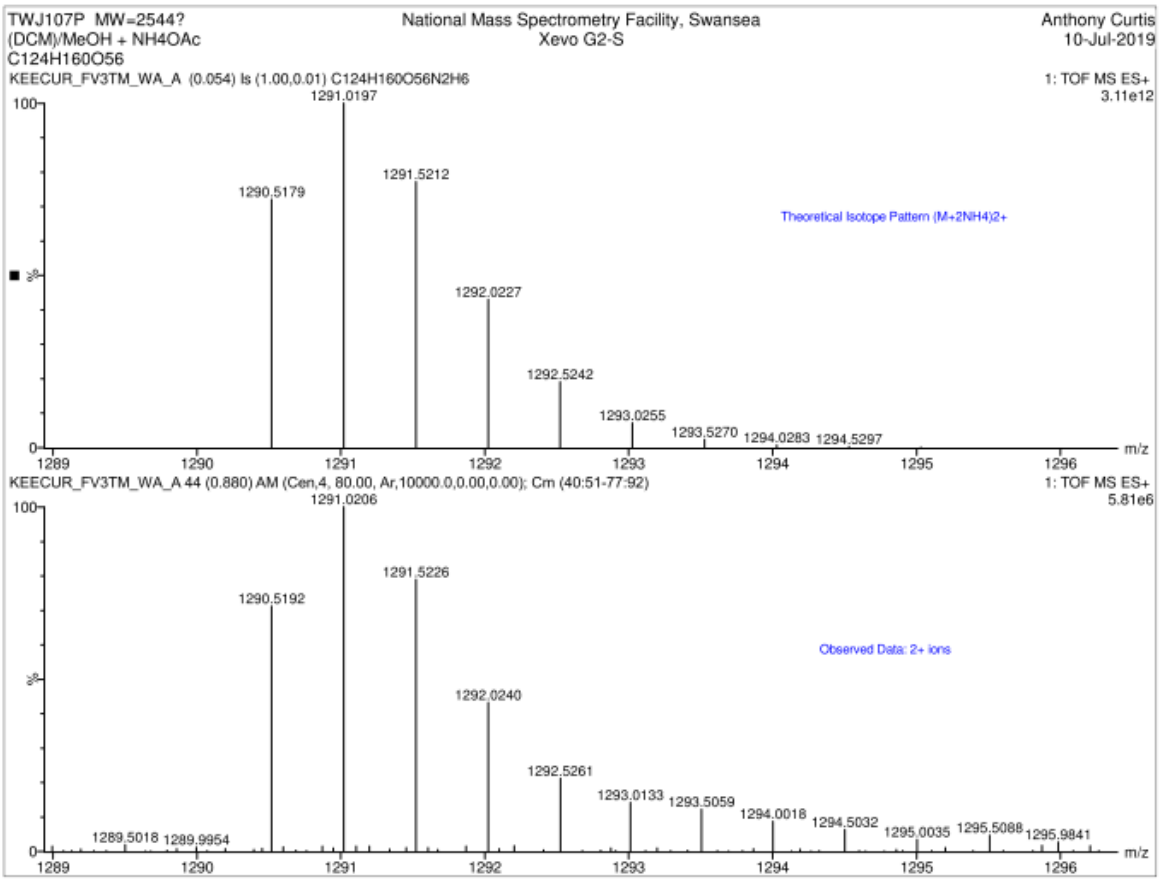

Appendix 20: Mass spectrum of **244**

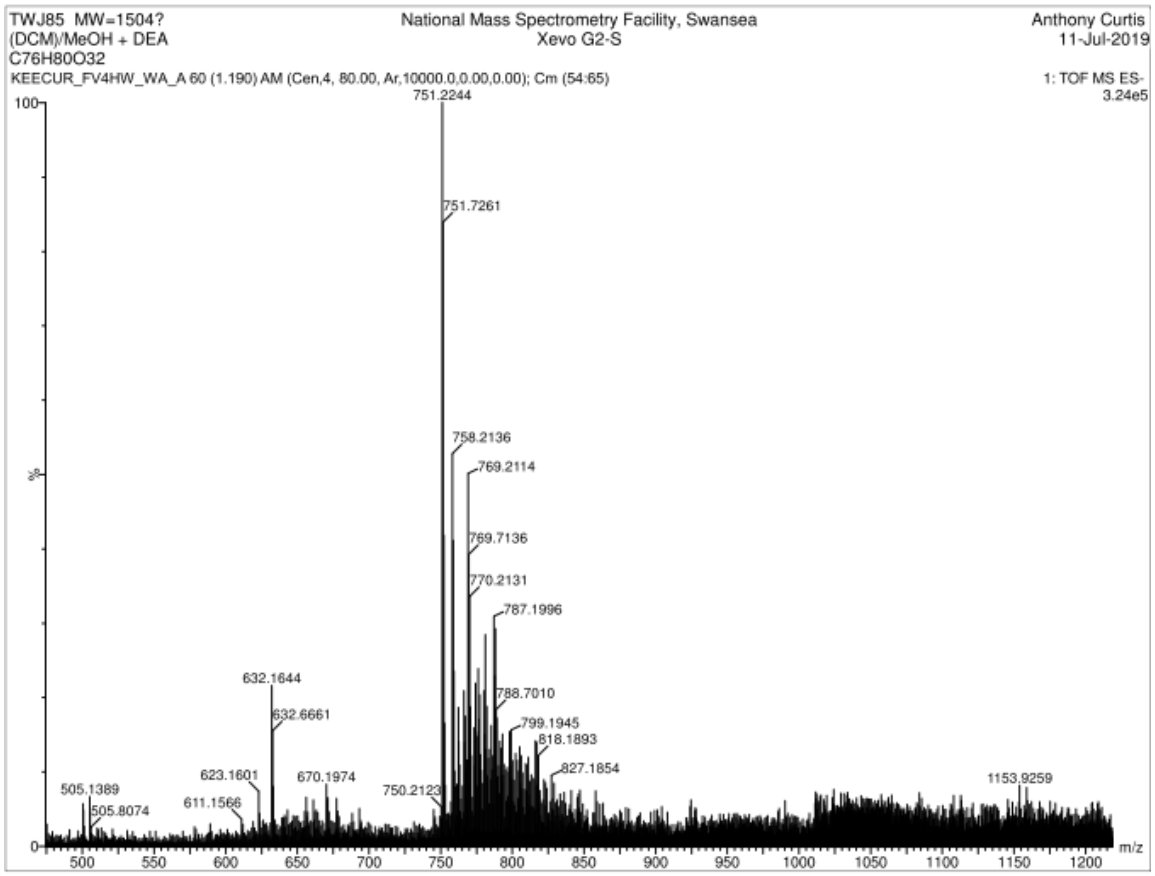
TWJ85 MW=1504?
(DCM)/MeOH + DEA
C76H80O32
National Mass Spectrometry Facility, Swansea
Xevo G2-S
Anthony Curtis
11-Jul-2019
KEECUR_FV4HW_WA_A 60 (1.190) AM (Cen,4, 80.00, Ar,10000.0,0.00,0.00); Cm (54:65)
1: TOF MS ES-
3.24e5
751.2244
751.7261
758.2136
769.2114
769.7136
770.2131
787.1996
788.7010
799.1945
818.1893
827.1854
632.1644
632.6661
623.1601
670.1974
611.1566
505.1389
505.8074
750.2123
1153.9259
%
m/z

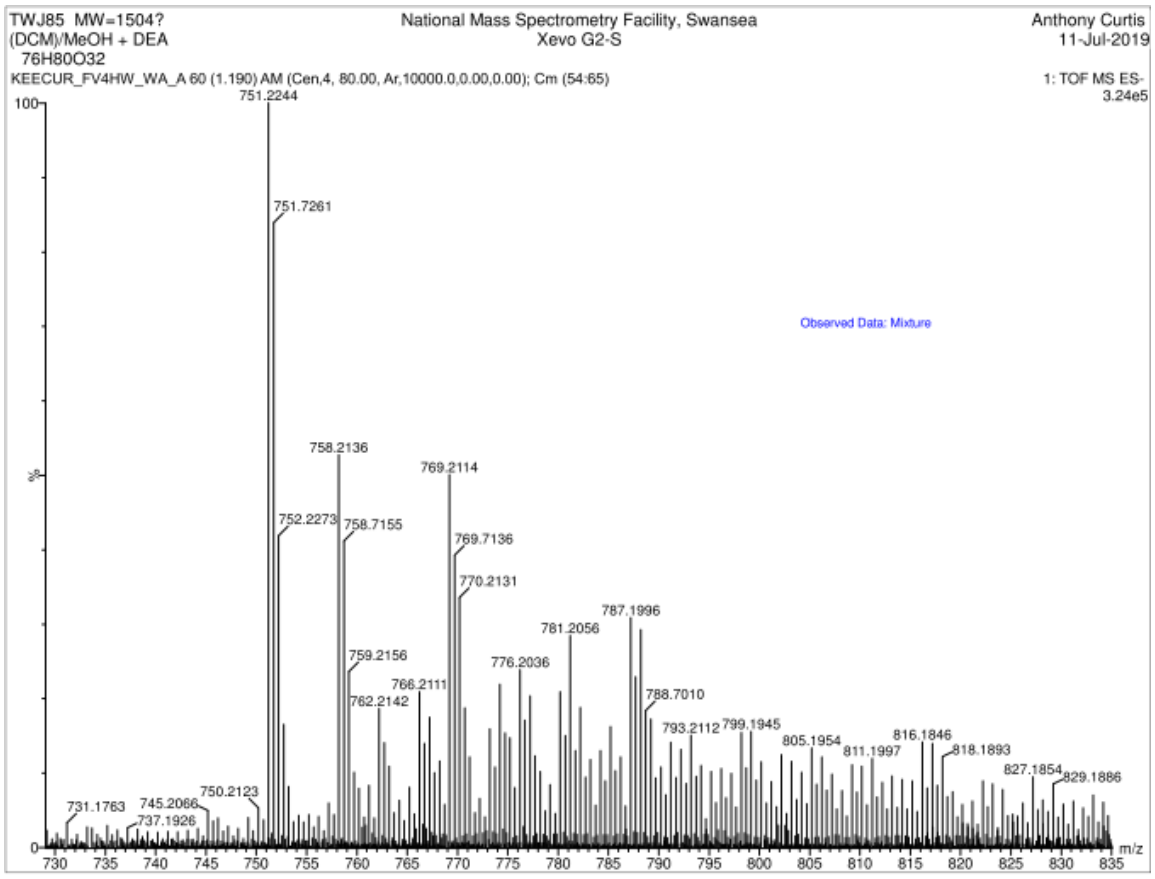
TWJ85 MW=1504?
(DCM)/MeOH + DEA
76H80O32
National Mass Spectrometry Facility, Swansea
Xevo G2-S
Anthony Curtis
11-Jul-2019
KEECUR_FV4HW_WA_A 60 (1.190) AM (Cen,4, 80.00, Ar,10000.0,0.00,0.00); Cm (54:65)
1: TOF MS ES-
3.24e5
751.2244
751.7261
Observed Data: Mixture
758.2136
769.2114
752.2273
758.7155
769.7136
770.2131
787.1996
781.2056
759.2156
776.2036
766.2111
762.2142
788.7010
793.2112
799.1945
805.1954
811.1997
816.1846
818.1893
827.1854
829.1886
750.2123
731.1763
745.2066
737.1926
%
m/z

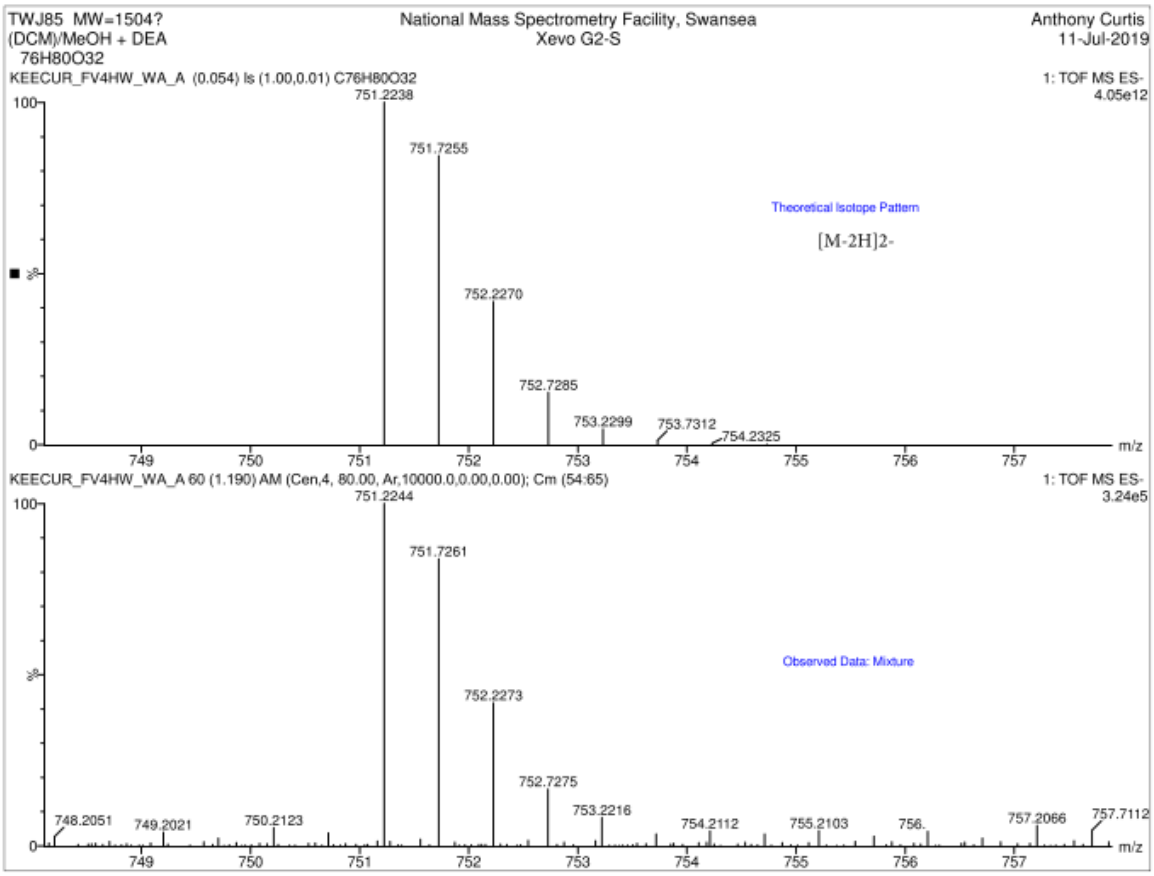

Appendix 21: Mass spectrum of **245**